

ANALYSIS OF HELIUM-RICH WHITE DWARFS POLLUTED BY HEAVY ELEMENTS IN THE GAIA ERA

S. COUTU,¹ P. DUFOUR,¹ P. BERGERON,¹ S. BLOUIN,¹ E. LORANGER,¹ N.F. ALLARD,^{2,3} AND B. H. DUNLAP^{4,5,6}

¹*Département de Physique, Université de Montréal, Montréal, QC H3C 3J7, Canada; coutu@astro.umontreal.ca, dufourpa@astro.umontreal.ca., bergeron@astro.umontreal.ca, sblouin@astro.umontreal.ca*

²*GEPI, Observatoire de Paris, Université PSL, CNRS, UMR 8111, 61 avenue de l'Observatoire, F-75014 Paris, France*

³*Sorbonne Université, CNRS, UMR 7095, Institut d'Astrophysique de Paris, 98bis boulevard Arago, F-75014 Paris, France*

⁴*Department of Physics and Astronomy, University of North Carolina at Chapel Hill, Chapel Hill, NC 27599, USA*

⁵*Department of Astronomy and McDonald Observatory, University of Texas at Austin, Austin, TX 78712, USA*

⁶*McDonald Observatory, Fort Davis, TX-79734, USA*

ABSTRACT

We present a homogeneous analysis of 1023 DBZ/DZ(A) and 319 DQ white dwarf stars taken from the Montreal White Dwarf Database. This represents a significant increase over the previous comprehensive studies on these types of objects. We use new trigonometric parallax measurements from the *Gaia* second data release, together with photometry from the Sloan Digital Sky Survey, Pan-STARRS, *Gaia*, or *BVRI* from the literature, which allow the determination of the mass for the majority of the objects in our sample. We use the photometric and spectroscopic techniques with the most recent model atmospheres available, which include high-density effects, to accurately determine the effective temperature, surface gravity, and heavy element abundances for each object. We study the abundance of hydrogen in DBZ/DZ white dwarfs and the properties of the accreted planetesimals. We explore the nature of the second sequence of DQ stars using proper motions from *Gaia*, and highlight evidence of crystallization in massive DQ stars. We also present mass distributions for both spectral types. Finally, we discuss the implications of our findings in the context of the spectral evolution of white dwarfs, and provide the atmospheric parameters for each star.

Keywords: stars: abundances – stars: atmospheres – stars: evolution – white dwarfs

1. INTRODUCTION

White dwarfs represent the final evolutionary phase of main sequence stars with initial mass below $\sim 8 M_{\odot}$ and are characterized by their high surface gravity, typically $g = 10^8 \text{ cm s}^{-2}$. Because of this, elements heavier than helium will sink below the photosphere in characteristic timescales that are many orders of magnitude smaller than the cooling age of the star (Paquette et al. 1986). This gravitational separation also explains why most white dwarfs — about 80% — have pure hydrogen atmospheres. The only absorption lines present in their spectra are those of hydrogen, and they are collectively known as DA stars. For a smaller fraction, practically no hydrogen survives the late phases of stellar evolution, and a thin opaque helium layer — the heaviest element remaining — will float on top and form the atmosphere. Depending on the effective temperature, they are classified as DO white dwarfs if they show ionized helium lines, and DB stars if only neutral helium lines can be observed. Below $T_{\text{eff}} \sim 12,000 \text{ K}$, spectra of pure helium atmosphere white dwarfs become featureless as there is not enough energy to populate the lower energy levels of He I line transitions. Such objects with continuous optical spectra are classified as DC white dwarfs. Note that a similar phenomenon also happens for hydrogen-rich white dwarfs cooler than about 5000 K as the electrons are mostly found in the ground state, preventing Balmer line transitions. In the absence of physical mechanisms competing with gravitational settling, the optical spectra of all white dwarfs should thus show only hydrogen lines, helium lines, or pure continuum. Nevertheless, white dwarfs with traces of heavy elements do exist, indicating that gravitational settling is not acting alone. These “contaminated” white dwarfs are found mainly in two categories: i) those with traces of heavy elements (other than carbon) in their optical spectra, and ii) those with primarily carbon absorption lines, either molecular or atomic.

1.1. Heavy Element Pollution

White dwarfs showing absorption lines from elements such as calcium, magnesium, or iron are collectively known as DZ stars if their spectra show only heavy element lines, DBZ stars if they show helium and heavy elements, and DAZ stars if they display hydrogen and metal features. Model atmospheres show that both the DZ and DBZ stars are helium dominated while the DAZs are hydrogen dominated. The presence of heavy elements in these objects is now understood as external accretion of matter from a disk of debris resulting from the destruction of a rocky object (asteroid or small planets) by the white dwarf’s tidal forces (see Jura & Young

2014, and references therein). These objects are thus temporarily imprinted (diffusion timescales range from a few hundred thousands to a few million years¹, much shorter than the cooling age) with the chemical composition of the polluting body, providing a unique opportunity to study the chemical composition of extra-solar bodies (Zuckerman et al. 2007; Klein et al. 2010, 2011; Dufour et al. 2012; Jura et al. 2012; Xu et al. 2014; Koester et al. 2014; Xu et al. 2016, 2017; Blouin et al. 2019b). High-resolution or UV spectroscopic observations of some samples have shown that 25 to 50% of all white dwarfs are contaminated by heavy elements at some level (Zuckerman et al. 2003, 2010; Koester et al. 2014).

Moreover, since observational evidence indicates that these white dwarfs had (or still have) at least some sort of planetary system around them, they can provide information about the correlation between stellar mass and planet occurrence, which can give insight into the planet formation process (Johnson et al. 2010). Indeed, most observational exoplanet surveys are biased towards lower mass stars. The Kepler mission prioritized G-type stars (Batalha et al. 2010), which have masses around $1 M_{\odot}$. More massive stars of type O and B are observed much less frequently by Kepler, mostly because of their scarcity (they spend a very short time on the main sequence), and the Kepler field of view was chosen to avoid young stellar populations (Batalha et al. 2010). Doppler surveys also favor Sun-like stars, as their spectral properties make their detection easier (Johnson et al. 2010). Thus, very little is known about the relation between planet occurrence and stellar mass above $M = 2-3 M_{\odot}$. While massive white dwarfs — which had massive main sequence progenitors — are fainter, the selection bias is much less important, especially with *Gaia* DR2, which is expected to be volume-complete within ~ 70 parsecs (Gentile Fusillo et al. 2019). Inferences of planetary systems around white dwarfs are thus not subjected to the same limitations.

1.2. Carbon Pollution

White dwarfs showing mainly carbon features are collectively known as DQ stars. They represent 9% of the white dwarfs in the local sample ($D < 20 \text{ pc}$, Giammichele et al. 2012). They show only atomic carbon lines when $T_{\text{eff}} \gtrsim 10,000 \text{ K}$, and molecular C_2 bands at lower effective temperatures, with a smooth transition around that temperature where both molec-

¹ Based on calculations by G. Fontaine, included in the MWDD and available at <http://www.montrealwhitedwarfdatabase.org/evolution.html>

ular bands and atomic carbon lines are simultaneously present. Model atmosphere analyses have shown that they are helium-dominated with carbon abundances ranging from $\log(\text{C}/\text{He}) = -7$ to -2 (Weidemann & Koester 1995; Dufour et al. 2005; Koester & Knist 2006), and effective temperatures between ~ 5000 K and $12,000$ K. A model where the deep helium convection zone catches up with the settling carbon in the core, and dredges it up to the surface, can successfully account for the observed abundances in most objects (Fontaine & Brassard 2005; Dufour et al. 2005). Dufour et al. (2005) showed, however, that several DQ stars had larger than average carbon abundances, forming a distinct sequence about 1 dex above the bulk of the sample in a $\log(\text{C}/\text{He})$ vs T_{eff} diagram (see also Koester & Knist 2006). Since the only object with a measured trigonometric parallax belonging to this second sequence was massive, Dufour et al. proposed that they could represent the high-mass tail of the white dwarf mass distribution. However, Brassard et al. (2007) showed that an evolutionary sequence at $1 M_{\odot}$ does not correctly predict the carbon abundance pattern that is empirically observed, indicating that another explanation to account for these stars must be sought.

While the cooler end of the DQ sequence is consistent with the expectations from the dredge-up model, very few stars were known at that time to test the theory on the hotter side ($T_{\text{eff}} \geq 13,000$ K). Many hot objects showing mainly ionized or neutral carbon lines (and also oxygen in a few cases) had been identified in the Sloan Digital Sky Survey (SDSS) by Liebert et al. (2003). The interpretation then was that these objects were a hotter version of the cool DQ white dwarfs, which had helium-dominated atmospheres with traces of carbon. However, when the hottest objects were analyzed using state-of-the-art model atmospheres, it was found in fact that the main atmospheric constituent was carbon, not helium (Dufour et al. 2007a, 2008). Dufour et al. (2013) then showed that, in a $u-g$ vs $g-r$ color-color diagram, the hot carbon-dominated atmosphere DQ stars ($T_{\text{eff}} \sim 18,000 - 24,000$ K with mainly ionized carbon lines) seem to form a sequence that connects with warm DQ white dwarfs with neutral atomic lines ($T_{\text{eff}} \sim 10,000 - 16,000$ K), followed by cooler DQ stars with strong molecular bands ($T_{\text{eff}} < 10,000$ K on the second sequence mentioned above). Unfortunately, very few trigonometric parallax measurements were available for these objects at that time, and thus the massive nature of the elusive sequence was somewhat speculative.

Since the studies of Dufour et al. (2005, 2007b) — the latest comprehensive analyses of large samples of DQ and DZ stars, respectively — there have been sev-

eral improvements in stellar atmosphere modeling (for example, Blouin et al. 2017, Blouin et al. 2018a). Simultaneously, several surveys have enlarged the sample of spectroscopically confirmed white dwarfs considerably, and consequently, the number of known DQ/DZ/DBZ white dwarfs has increased by more than a factor of five. Also, thanks to the second *Gaia* data release in April 2018, distances are now available, for the first time, for most of these objects, a quantity required to obtain precise measurements of their stellar masses.

The availability of improved model atmospheres and new data motivated us to perform an updated homogeneous analysis of all these metal-polluted white dwarfs. We describe the model atmospheres in Section 2, the observational data in Section 3, and the methodology in Section 4. We present the analysis for the DBZ/DZ stars in Section 5, and for the DQ stars in Section 6. We then discuss the implications of our results on our understanding of the spectral evolution of white dwarfs in Section 7. Our conclusions follow in Section 8.

2. MODEL ATMOSPHERES

Our DZ/DBZ/DQ model atmosphere code is similar to that outlined in Dufour et al. (2005, 2007b), but with several physical improvements described at length in Blouin et al. (2018a,b). Of particular importance for the study of DZ/DBZ stars are the new line profile calculations following the unified line shape theory of Allard et al. (1999) for strong transitions, the most important being Ca II H&K, Mg I $\lambda 2852$ and Mg II $\lambda 2795/2802$, the Mgb triplet, and Ca I $\lambda 4226$. Less important transitions use Lorentzian or quasistatic van der Waals broadening profiles (Walkup et al. 1984, D. Koester, private communication). For the DQ model atmospheres, one of the main improvements over Dufour et al. (2005) is the replacement of the “just overlapping line approximation” (Zeidler-K.T. & Koester 1982), to describe the C₂ Swan band opacity, with a complete linelist provided by J. O. Hornkohl (private communication; see Parigger et al. 2015 for details of the methodology). We find that the use of this new linelist provides a much better representation of the shape of the observed Swan bands in DQ white dwarfs, particularly in the region around 4300 \AA , which was poorly fitted in Dufour et al. (2005), compared to the prescription of Zeidler-K.T. & Koester (1982), Brooke et al. (2013), or Kurucz linelists². The atomic linelist of Kurucz has also been replaced by the compilation from the Vienna Atomic Line Database (VALD, Piskunov et al. 1995).

² <http://kurucz.harvard.edu/linelists.html>

For the DZ/DBZ(A) white dwarfs, we generated a 4-dimensional grid of model atmospheres and synthetic spectra with T_{eff} varying from 4000 K to 16,000 K by steps of 500 K, $\log g$ from 7.0 to 9.0 by steps of 0.5 dex, $\log \text{Ca/He}$ from -12 to -7 by steps of 0.5 dex, and $\log \text{H/He}$ from -7 to -3 by steps of 1 dex. We also generated a grid with no hydrogen. Metal-to-metal ratios have been fixed to that of chondrites (Lodders 2003) with respect to calcium. Calcium thus serves as a proxy for the abundances of all other heavy elements. While metal-to-metal ratios certainly differ from that of chondrites in many objects, our assumption provides a good first order approximation of the contribution of free electrons and opacity from heavy elements (see Dufour et al. 2007b, and also discussion below).

For the DQ model grid, since no DQ white dwarfs are found at high effective temperature and low carbon abundance, or at low effective temperature and high carbon abundance, we generated two separate 3-dimensional grids. The first grid is generated with T_{eff} from 8000 K to 16,000 K by steps of 500 K, $\log g$ from 7 to 9 by steps of 0.5 dex, and $\log \text{C/He}$ from -5 to -1 by steps of 0.5 dex. The second grid covers T_{eff} from 6000 K to 10,000 K by steps of 500 K, $\log g$ from 7 to 9 by steps of 0.5 dex, and $\log \text{C/He}$ from -8 to -4 by steps of 0.5 dex. No hydrogen is included in these models, but some smaller grids with hydrogen were generated to test its effects, as discussed in Section 6.3.

3. OBSERVATIONS

3.1. Note on Naming Convention

Some white dwarfs can have up to 20 different names. Here we decided to adopt names based on ICRS coordinates at epoch and equinox 2000 instead of mixing names from different catalogs. Stars will be named JHHMM \pm DDMM, where the first four digits correspond to the right ascension in hours and minutes, and the last four digits to the declination in degrees and minutes in sexagesimal notation. In some cases, a second relevant name will be written in parentheses. Table 5 provides cross-references for the names of the objects in our sample with *Gaia* source id, MWDD id, and the full coordinates.

3.2. Sample Selection

We first selected from the Montreal White Dwarf Database³ (Dufour et al. 2017, hereafter MWDD) all objects with either a Q or a Z in their spectral classification. This includes DZ, DZA, DBZ, DBZA, DQ,

etc. We did not include DAZ white dwarfs because they have hydrogen-rich atmospheres, and we are only interested here in helium-rich atmospheres. Most objects in our sample have previously been identified in various white dwarf catalogs from the Sloan Digital Sky Survey (SDSS; Kepler et al. 2015, 2016; Kleinman et al. 2004, 2013; Eisenstein et al. 2006). Many objects have also been classified as uncertain, such as DQ: or DC-DQ. We thus visually inspected every spectrum and rejected those that did not show the appropriate spectral lines, or were too noisy to make a reliable classification (spectra with better signal-to-noise will eventually confirm their spectral types). We rejected known unresolved binary systems as well as magnetic white dwarfs. In order to ensure a homogeneous analysis based exclusively on optical features, we also rejected some objects classified as DQ white dwarfs but with carbon features detected only in the ultraviolet. We also excluded stars that had carbon-dominated atmospheres, the so-called Hot DQ stars ($T_{\text{eff}} \gtrsim 18,000$ K), or any object for which our preliminary analysis gave atmospheric parameters outside of our model grid. Finally, DQpec white dwarfs with strong distorted Swan bands are also left out of our analysis because there are still large uncertainties regarding their modeling (see Blouin et al. 2019c).

All objects in our sample were then cross-matched with *Gaia* DR2 to retrieve photometric and astrometric data. For one object, J0739+0513 (Procyon B), we use the parallax from Hipparcos (284.56 ± 1.26 , van Leeuwen 2007). A few objects with negative parallaxes or very large uncertainties ($\sigma_{\pi}/\pi > 1$) were rejected; these are unlikely to be white dwarfs, and if they are, the data are too imprecise to allow any satisfactory analysis. Bailer-Jones (2015) demonstrated that inverting the parallax to estimate the distance might lead to unreliable distances when the uncertainty on the parallax is larger than 20%, and that it can lead to incorrect error estimates. Fortunately, 87% of our parallax sample have smaller uncertainties. In fact, the difference between a probabilistic analysis distance and the inverse of the parallax is less than 1% for the majority of objects when $\sigma_{\pi}/\pi < 0.1$.

With the availability of trigonometric parallaxes and broadband colors from *Gaia* for the majority of the objects in our sample, it is now possible to place them accurately in an observational Hertzsprung-Russell (HR) diagram (Gaia Collaboration et al. 2018). This is illustrated in Figure 1, where stars that have been erroneously classified as white dwarfs can easily be identified. Examples of such stars are the giant star SDSS J174618.94+262217.0 (Green 2013) and SDSS J192013.71+383917.7, two objects that have been er-

³ www.montrealwhitedwarfdatabase.org

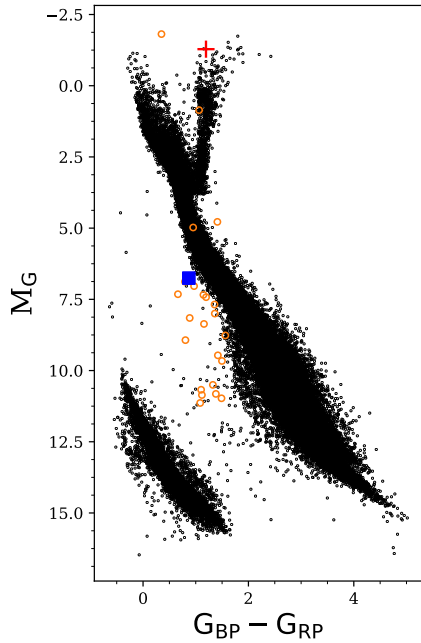


Figure 1. *Gaia* HR diagram for objects misclassified as white dwarfs (orange circles). SDSS J174618.94+262217.0 and SDSS J192013.71+383917.7, the two examples discussed in the text and displayed in Figure 2, are represented by a red cross and a blue square, respectively. Black dots are *Gaia* objects within 100 pc selected using the cuts proposed in [Gaia Collaboration et al. \(2018, Appendix B\)](#). White dwarf candidates are located in the bottom left portion of the diagram.

roneously classified as a DQ and a DZ white dwarf, respectively ([Kleinman et al. 2013](#)). The similarity of the spectra of these non-degenerate stars, displayed in Figure 2, with genuine DQ and DZ white dwarfs stresses the importance of using photometric and parallax measurements in combination to spectroscopic data during the classification process. Overall, 25 objects, listed in Table 1, previously classified as white dwarfs in various catalogs were rejected this way.

To constitute our final sample, we removed 63 stars that had parameters outside our model grids (these will be analyzed elsewhere) and 63 white dwarfs for which no optical spectroscopy was available. In the end, we are left with a sample of 1023 DZ (679 with parallax measurements) and 317 DQ (303 with parallax measurements) white dwarfs, which we analyze in a homogeneous fashion in the next sections.

3.3. Photometric and Spectroscopic Data

We cross-matched our sample with Pan-STARRS DR1 and SDSS DR14 to retrieve *grizy* and *ugriz* PSF magnitudes, respectively. Since SDSS photometry is available for 95% of our sample, while only 80% of our objects

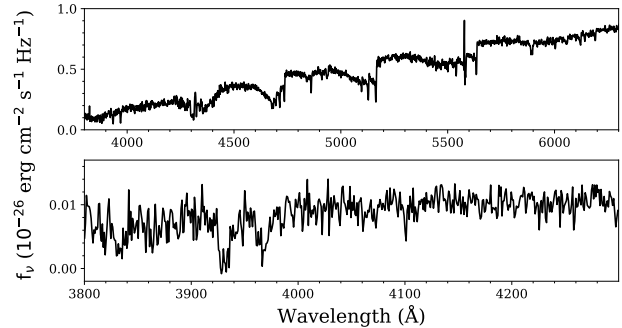


Figure 2. Optical spectra of SDSS J174618.94+262217.0 (top) and SDSS J192013.71+383917.7 (bottom), two objects that were previously misclassified as DQ and DZ white dwarfs, respectively.

have Pan-STARRS photometry, we decided to rely primarily on SDSS photometry for the sake of homogeneity. Note that although Pan-STARRS covers a much larger part of the sky than SDSS, most spectroscopically identified white dwarfs were discovered in the SDSS. Furthermore, SDSS has proven to be reliable many times (see [Genest-Beaulieu & Bergeron 2019](#)), while possible Pan-STARRS biases have not been fully explored yet. When SDSS *ugriz* is not available for an object, we rely on Pan-STARRS data, previously published *BVRI* photometry, or simply *Gaia* broadband photometry, in that order of priority. For J0739+0513 (Procyon B), we rely on HST photometry ([Provencal et al. 1997](#)).

The majority of the spectra used in this study are drawn from SDSS⁴. The spectra of 51 objects without SDSS spectroscopy are taken from [Limoges et al. \(2013, 2015\)](#), [Subasavage et al. \(2007, 2009\)](#), [Bergeron et al. \(1997, 2001\)](#), or archival data secured by the Montreal group in the last few decades. Finally, the spectroscopic data for Procyon B are from HST ([Provencal et al. 2002](#)).

4. ATMOSPHERIC PARAMETER DETERMINATION

Our fitting method is similar to that described in [Dufour et al. \(2005, 2007b\)](#) for DQ and DZ stars, respectively. Briefly, we first convert the observed magnitudes into average fluxes following the method described in [Holberg & Bergeron \(2006\)](#). The magnitudes on the AB system (SDSS, Pan-STARRS) are converted using the relation $m = -2.5 \log f_\nu^m - 48.60$, where f_ν^m is the stellar flux averaged over the bandpass response; the corrections from [Eisenstein et al. \(2006\)](#) are applied to put the SDSS photometry on the AB system. The magni-

⁴ https://www.sdss.org/dr14/spectro/spectro_basics/

Table 1. Objects rejected due to their location in the *Gaia* HR diagram

J Name	Gaia source id	MWDD id
J0205+0058	2508108382280944768	2MASS J02053812+0058354
J2112+0912	1743430270303257728	2MASS J21120843+0912019
J1642+3617	1328051961501737088	CI* NGC 6205 KAD 606
J0239-0003	2498734800840646400	SDSS J023955.79-000312.0
J0814+3508	902942352007933568	SDSS J081424.51+350822.9
J0815+1537	655412730925191808	SDSS J081502.24+153709.7
J0914-0022	3842424562164246656	SDSS J091455.49-002219.2
J1136+4702	787028812551381248	SDSS J113612.16+470206.8
J1208-0008	3698751446481826432	SDSS J120853.36-000847.3
J1228+2057	3952475922233611776	SDSS J122829.50+205747.0
J1336+1535	3742286441879709952	SDSS J133644.21+153554.2
J1357+1252	3727838511198756224	SDSS J135713.37+125230.9
J1507+1824	1211873229279489536	SDSS J150741.36+182406.8
J1549+0436	4426232766560567296	SDSS J154918.87+043651.0
J1610+0247	4412254439017190400	SDSS J161041.62+024706.2
J1714+2324	4568671714800327680	SDSS J171432.25+232423.0
J1746+2622	4582265290590354304	SDSS J174618.94+262217.0
J1920+3839	2052876071205883520	SDSS J192013.71+383917.7
J2105+0828	1744023628624108288	SDSS J210511.38+082853.7
J2106+0642	1736767710874927872	SDSS J210632.52+064233.5
J2111+0915	1743431683347518464	SDSS J211157.26+091554.2
J2153+2750	1800030173963458048	SDSS J215306.03+275057.3
J2259-1001	2606526522781415168	SDSS J225931.60-100146.9
J0124+0541	2563653437678125568	USNO-B1.0 0956-00013686
J0257+0111	339405495907200	WD 0255+009.1

tudes on the Vega system (*BVRI*, *Gaia*) are converted using the relation $m = -2.5 \log f_{\lambda}^m + c_m$, where c_m is the zero point in the corresponding bandpass. These zero points are calculated using the observed fluxes and magnitudes for Vega. For the *BVRI* bandpass response, we use Cohen et al. (2003), and for *Gaia*, we use the revised bandpasses⁵, while for the Vega flux, we use `alpha_lyr_stis_008.fits` from the CALSPEC Calibration Database⁶. Our results are summarized in Table 2.

Photometric data are also dereddened following the procedure described in Harris et al. (2006) using the extinction maps of Schlafly & Finkbeiner (2011). We

Table 2. Zero points derived for different bandpasses.

Bandpass	Zero point	Vega mag
<i>G</i>	-21.51572	0.00
<i>G</i> _{BP}	-20.99456	0.00
<i>G</i> _{RP}	-22.22677	0.00
<i>B</i>	-20.46331	0.024 ¹
<i>V</i>	-21.06662	0.026 ¹
<i>R</i>	-21.64524	0.033 ¹
<i>I</i>	-22.37877	0.029 ¹

(1)Holberg & Bergeron (2006)

thus consider the extinction to be negligible for stars with $D < 100$ pc, to be maximum for those located at $|z| > 250$ pc from the galactic plane (z is the distance from the galactic), and to vary linearly between these

⁵ https://www.cosmos.esa.int/web/gaia/iow_20180316

⁶ <http://www.stsci.edu/hst/observatory/crds/calspec.html>

two regimes. Genest-Beaulieu & Bergeron (2019) compared this method to that used by Gentile Fusillo et al. (2019) and came to the conclusion that they lead to similar results for white dwarfs in the SDSS. When no parallax measurement is available, we first obtain the photometric distance assuming $\log g = 8.0$, and then apply a dereddening correction using this distance, and repeat the process until the distance (and the reddening) converge to a single value.

Next we transform the monochromatic Eddington fluxes from our model grids into fluxes averaged over each bandpass. These synthetic average fluxes H_λ^m (or H_ν^m) are related to the observed fluxes by the equation:

$$f_\lambda^m = 4\pi \left(\frac{R}{D}\right)^2 H_\lambda^m \quad (1)$$

where R is the radius of the star, and D its distance from Earth. In the above equation, the average model fluxes depend on T_{eff} , $\log g$, and the atmospheric composition, which refers to the carbon abundance for DQ stars, and to the hydrogen and calcium abundances for DBZ/DZ stars. The best fit between observed photometry and synthetic fluxes is obtained using the nonlinear least square steepest decent method of Levenberg-Marquardt (Press et al. 1986), with the values of T_{eff} and the solid angle $\pi(R/D)^2$ left as free parameters, while $\log g$ and the atmospheric composition are kept fixed during the first iteration.

From the derived value of the solid angle and the distance given by the inverse of the parallax, we determine the radius R of the star. The values of $\log g$ and mass are then derived by interpolating in evolutionary models similar to those described in Fontaine et al. (2001) but with C/O cores, $\log q(\text{He}) \equiv \log M_{\text{He}}/M_\star = -2$ (where M_\star is the mass of the star) and $\log q(\text{H}) = -10$, which are representative of helium-rich atmosphere white dwarfs (Dufour et al. 2005). We repeat the process this time using the newly determined surface gravity until convergence is reached. If the parallax is unknown, we simply assume $\log g = 8$ and derive a radius R from the same evolutionary models, which yields a photometric distance when combined with the solid angle. The uncertainties on the effective temperature and the solid angle are obtained directly from the covariance matrix of the fitting procedure.

We next determine the chemical composition by fitting the spectroscopic data, again using the Levenberg-Marquardt method, keeping T_{eff} and $\log g$ fixed to the values obtained from the photometric fit. For cool DQ stars, we fit the Swan bands between 4000 and 6500 Å, while for hotter DQs, we use the atomic absorption lines between 4500 and 5500 Å. The carbon abundance, the

solid angle, and a first or second degree polynomial — to account for uncertainties in the flux calibration (see Dufour et al. 2005) — are considered free parameters during the fitting procedure. For DBZ/DZ stars, we begin by fixing the hydrogen abundance, either by fitting the H α spectral line if it is visible, or by fixing $\log \text{H}/\text{He}$ at the detection limit (we also fit stars not showing H α with our hydrogen-free grid; see Section 5 for a discussion of this matter). This detection limit was estimated by calculating, at each temperature and $\log g$ value in our grid, the amount of hydrogen required to reach a threshold of 500 mÅ for the equivalent width of the H α line. We then fit the Ca II H&K absorption lines to determine $\log \text{Ca}/\text{He}$. Then we repeat the photometric fit, but this time using the values of $\log g$, calcium abundance (or carbon abundance in the case of DQ white dwarfs), and hydrogen abundance obtained in this last iteration. We repeat the procedure, typically 3 to 5 iterations (or more in some cases), until the parameters have converged to a stable solution.

To obtain the uncertainty on the abundances measured from the spectroscopic fit, we rely on the same method described in Bergeron et al. (1992), where we first assume an arbitrary standard deviation $\sigma = 1$ for each data point, then calculate the root-mean-square deviation of the observed spectrum from the best-fit model spectrum. This is then propagated into the covariance matrix, from which the formal uncertainties of the fitted atmospheric parameters are obtained. This gives an uncertainty estimation that depends mostly on the signal-to-noise ratio of the observed spectra.

5. DZ/DBZ(A) WHITE DWARFS

5.1. Photometric and Spectroscopic Fits

Following the method described in Section 4, we determined the atmospheric parameters for all DZ/DBZ(A) white dwarfs in our sample. Figure 3 shows typical fits of the energy distribution and the Ca II H&K lines region (all our fits are available in Appendix I), while our final parameters are given in Table 6. The fit to the H α line, when present, is shown as an inset. Note that for stars that do not show hydrogen, we report a solution with the hydrogen abundance fixed at the detection limit (see explanation below).

We note that other lines, mostly Mg and Fe, are sometimes observed in addition to Ca II H&K. Since in our model grids, the abundances of these elements relative to calcium are fixed to the chondrite values, a visual inspection of the quality of the “fit” to these lines provides a quick assessment of the validity of this approximation, which appears to be adequate (or close enough) for most stars that show such lines in our sample. How-

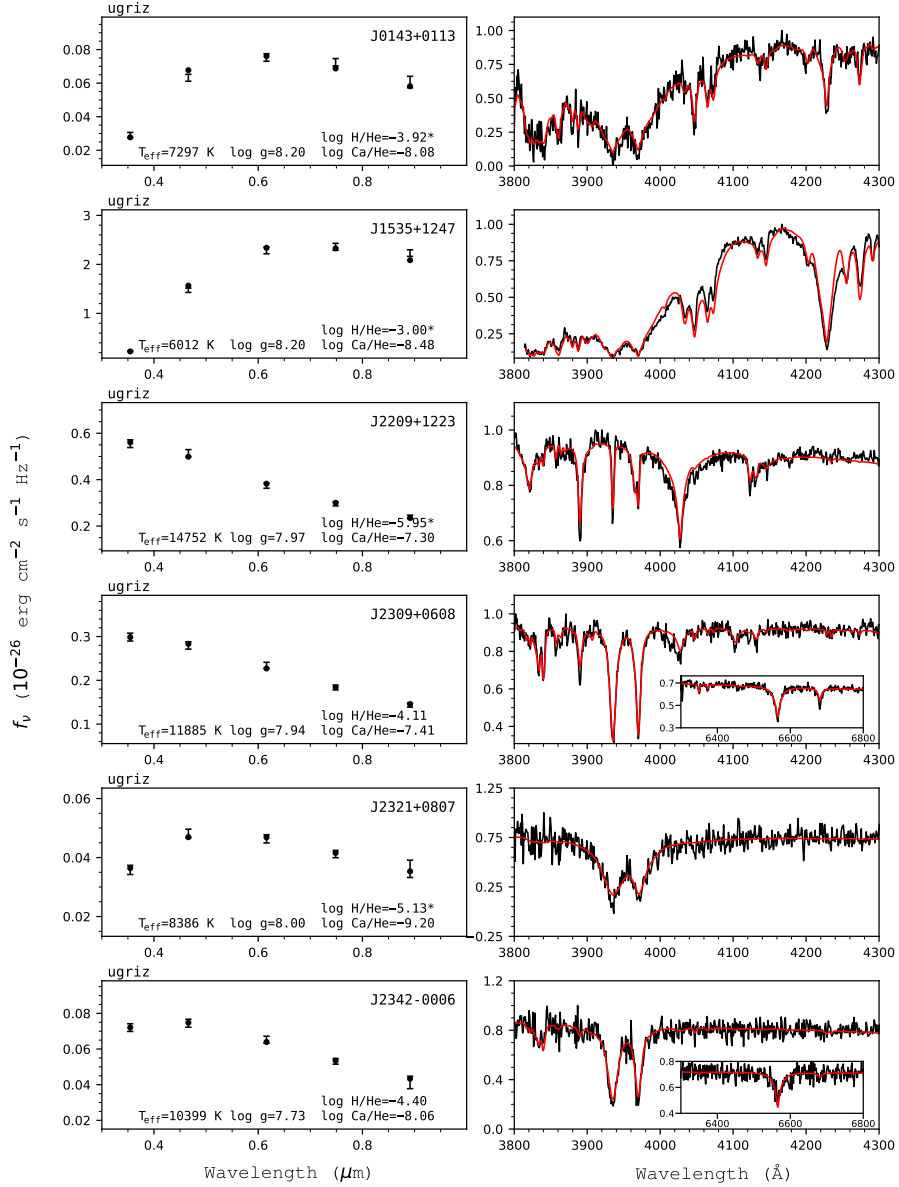


Figure 3. Examples of fits to our sample of DBZ/DZ(A) white dwarfs. Left panels: Photometric fits where error bars represent the observed data, while filled circles correspond to average model fluxes. A dagger symbol indicates that $\log g$ is fixed at 8.0 (no parallax measurement available), while a star symbol indicates a value of $\log H/He$ fixed at the visibility limit. Right panels: Spectroscopic fits (red) to the normalized observed spectra (black). The inset shows the fit to $H\alpha$ when present. A version of this figure with all our fits is available in Appendix I.

ever, it is certainly possible that some elements depart significantly from the chondrite values. Since what is most important, as far as the mass and effective temperature determinations are concerned, is the amount of free electrons in the photosphere (effects due to the redistribution of the flux absorbed in the UV can also play a role in some cases), small deviations should only have a minimal impact on those parameters, even more

so when hydrogen is present, because electrons from ionized hydrogen will dominate the free electron budget.

Recently, [Hollands et al. \(2017, 2018\)](#) analyzed a large sample of 230 cool DZ white dwarfs and determined abundances of individual elements. Their results indicate that to first order, objects are found with chemical compositions not too far from that of bulk Earth ratios, at least for the most visible elements, which are calcium, magnesium, and iron. Although their param-

eters were obtained using a different model atmosphere code that do not include all the improvements included in our code, a comparison of their results for 197 objects in common with our sample suggests that the exact metal-to-metal ratios used in their analysis has only a modest impact on the effective temperature determination. We find that the effective temperatures obtained with our approach are, on average, only 11 K lower than theirs, but with a somewhat large 330 K standard deviation. We find no correlation between the differences in effective temperature and the deviation to the chondrite abundances (relative to Ca) that they report. Instead, we find that these differences are correlated with $\log g$ values. Since the *Gaia* second data release was not available at the time the analyses of [Hollands et al. \(2017, 2018\)](#) were published, the authors assumed $\log g = 8$ for their whole sample, while our analysis makes use of the newly available parallax measurements to determine the surface gravities. This distinction seems to be the main explanation for the different atmospheric parameters derived in both studies. Indeed, we find a strong correlation between the differences in effective temperature and the departure from $\log g = 8$, our temperatures being higher (lower) for larger (smaller) $\log g$ values. Similarly, there is also a correlation between the differences in $\log \text{Ca}/\text{He}$ and $\log g$. This result is not surprising given that the difference in the strength of the calcium absorption features resulting from a change in surface gravity will need to be compensated by an appropriate change in calcium abundance, which in turn will affect the number of free electrons, and thus the effective temperature determination. We thus conclude that the atmospheric parameters derived using our approach should be reliable, and not significantly affected by our assumption of the metal-to-metal ratios.

Nevertheless, when better spectroscopic data (high-resolution or UV observations) for a given object indicate some departure from our approximation, atmospheric parameters should always be re-derived in a self-consistent way for better precision. For example, for the DZA white dwarf Ross 640 analyzed by [Blouin et al. \(2018a\)](#), changes in the abundances of Mg and Fe relative to Ca affected the UV flux level sufficiently to warrant the calculations of a specific grid with modified abundances in order to obtain atmospheric parameters in a self-consistent way. As a result, their final effective temperature was 250 K cooler, and the corresponding mass $0.04 M_{\odot}$ lower, than what we obtain here with our approach. Unfortunately, since high-resolution or ultraviolet spectroscopic data are not likely to become available for every object in our sample in a foreseeable future, we are forced to adopt this approximation, in

particular given the fact that most objects in our sample show only calcium lines. To conclude on this topic, while our approach provides the best atmospheric parameters that are possible to infer with the available data, the solutions for individual objects will always suffer from small intrinsic uncertainties related to our adopted metal abundances.

5.2. Hydrogen Abundance Measurements

While for most objects in our sample, the metal-to-metal ratio assumed in our analysis has only a modest impact on our atmospheric parameters, the abundance of hydrogen, on the other hand, has a deeper impact because it can be one of the main free electron donors, even when present below the visibility limit. For instance, [Bergeron et al. \(2019\)](#) recently showed that adding undetectable traces of hydrogen in the models had a non-negligible effect on the mass determination of helium-rich white dwarfs (this is also discussed in [Dufour et al. 2005](#) in a similar context, but with carbon as the main electron donor).

Only 105 of the 1023 (10%) white dwarfs in our sample show $\text{H}\alpha$ in their spectrum. This is much less than the 25% containing hydrogen reported by [Dufour et al. \(2007b\)](#) for two main reasons. The first one is that the presence of hydrogen for 7% of their objects was determined indirectly from the shape of the Ca II H&K absorption features, in the sense that much better fits to these lines could be achieved when hydrogen was included. However, the study of [Dufour et al.](#) was based on Lorentzian profiles, with $\log g$ fixed at 8.0, while here we use the unified line shape theory of [Allard et al. \(1999\)](#), with surface gravities constrained by parallax measurements. As a consequence, we no longer find objects with spectroscopic fits that are significantly improved by adding hydrogen, indicating that the need to add hydrogen in the [Dufour et al.](#) analysis was probably only a way to compensate sub-optimal line profiles and/or incorrect surface gravities. The second reason is that since [Dufour et al.](#), the proportion of DZ white dwarfs too cool to show hydrogen has increased substantially, thanks to the thorough search for metal-polluted white dwarfs near the main-sequence color space ([Koester et al. 2011; Hollands et al. 2017, 2018](#)).

Figure 4 shows the abundance of hydrogen as a function of effective temperature for all the DBZ/DZ(A) white dwarfs in our sample. For stars that do not show $\text{H}\alpha$, we determine the maximum amount of hydrogen that can be added without being detected (the scatter is explained by variations in $\log g$ for each object). While the hydrogen content, and thus its impact on the free electron budget, is well constrained for $T_{\text{eff}} \gtrsim 9000 \text{ K}$,

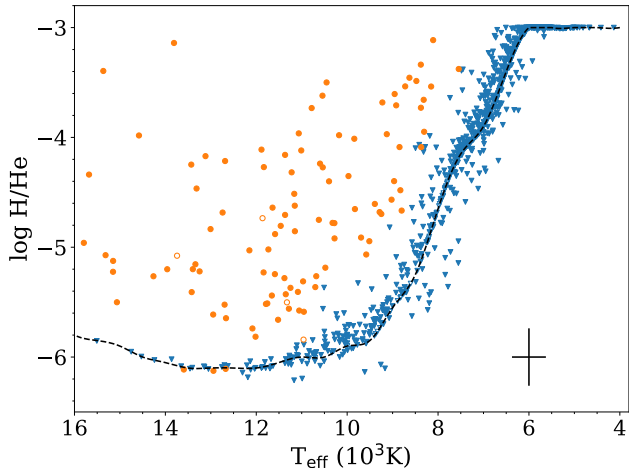


Figure 4. Hydrogen abundance as a function of effective temperature for our sample of DBZ/DZ(A) white dwarfs. Objects with parallax measurements are represented with filled symbols, while open symbols are used for stars for which we assumed $\log g = 8$. Orange circles are objects with hydrogen abundances determined from fitting $H\alpha$, while blue triangles correspond to upper limits. The dashed line represents the visibility limit, defined as an equivalent width of 0.5 \AA for $H\alpha$ at $\log g = 8$. The black error bars represent the average uncertainties.

increasingly large quantities of hydrogen can be hidden as the effective temperature decreases. To examine the impact of the unknown amount of hydrogen on our atmospheric parameter determinations, we fit each star in our sample with no detectable $H\alpha$ with both a hydrogen-free model grid, and with the abundance of hydrogen fixed at the detection limit. The results of this experiment are displayed in Figure 5.

Clearly, masses and effective temperatures are significantly reduced for the coolest stars when hydrogen is included. This reduction in both effective temperature and mass was recently explained by Bergeron et al. (2019, see their Figures 10 and 11). Briefly, adding hydrogen in the model increases the number of free electrons, which in turn increases the He^- free-free opacity. This has a quite dramatic effect on the continuum, as can be appreciated from Figure 6, where the energy distribution of two models that differ only by their hydrogen content are shown. As a result of the increased He^- free-free opacity, a lower temperature and a larger solid angle are required to match the observed fluxes, which translate into a larger radius, and thus a smaller mass. Note that this effect practically disappears for effective temperatures above $\sim 11,000 \text{ K}$, as the contribution from ionized helium starts to dominate the free electron budget.

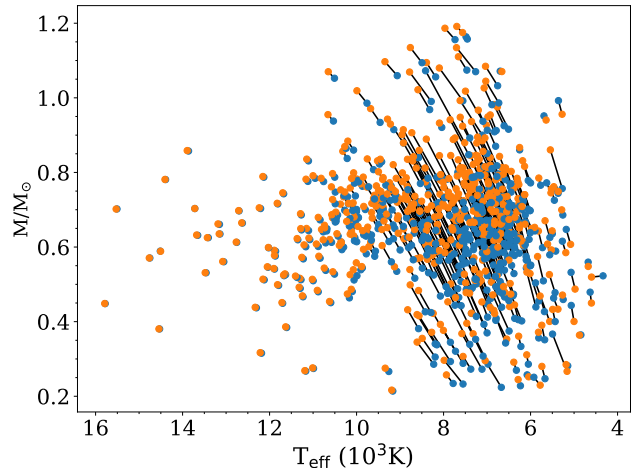


Figure 5. Comparison of masses and effective temperatures obtained with hydrogen-free models (orange dots) and with models where the hydrogen abundance was set at the visibility limit (blue dots). A black line connects the two solutions for each object.

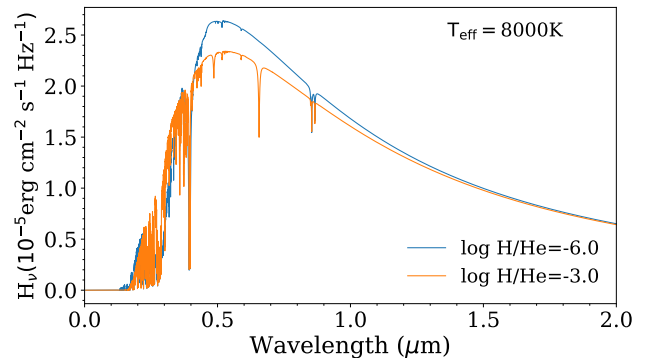


Figure 6. Synthetic spectra (Eddington fluxes) for models at $T_{\text{eff}} = 8000 \text{ K}$, $\log \text{Ca}/\text{He} = -9$, and $\log g = 8$, with two different hydrogen abundances indicated in the figure.

5.3. Mass Distributions

As discussed above, the parameters we derive depend intimately on the assumed amount of invisible hydrogen present in the star. It is certainly reasonable to expect at least some amount of hydrogen to be present in each object. After all, not only have these white dwarfs been traveling through the interstellar medium for billions of years, but potentially, they also have accreted bodies that may have contained large amounts of water and ice (Klein et al. 2010; Farihi 2011; Farihi et al. 2013; Raddi et al. 2015). While it is impossible to determine exactly the hydrogen abundance in each object, we know this abundance must lie within the two limiting cases explored here. We thus, in what follows, take a deeper look at the consequences this parameter has on the derived

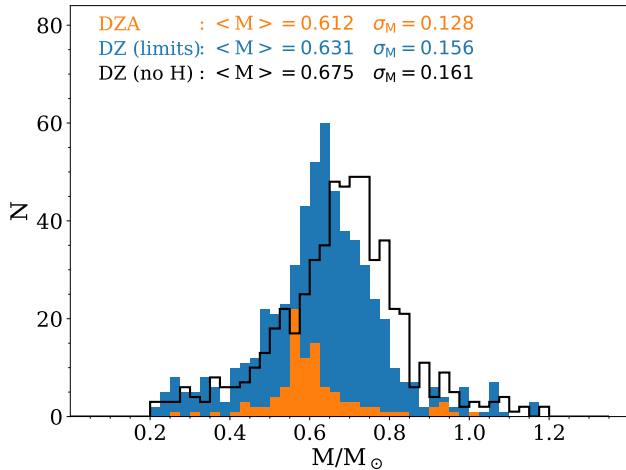


Figure 7. Mass distributions for DZ and DZA white dwarfs in our parallax sample. The DZA stars are shown in orange, while the DZ stars fitted with hydrogen-free models or with the hydrogen abundance set to the visibility limit are shown in black and blue, respectively.

global properties of the sample, and most importantly on the mass distribution.

Figure 7 compares the mass distributions of our parallax sample for stars with hydrogen abundances measured directly from $H\alpha$ (105 objects) with those with no detectable $H\alpha$ feature (918 objects) analyzed both with hydrogen-free models and with hydrogen abundances set to the visibility limit. We find that the mean mass for the DBZA/DZA stars is $0.612 M_{\odot}$, very close to the value recently reported by Genest-Beaulieu & Bergeron (2019) for DA ($0.617 M_{\odot}$) and DB ($0.620 M_{\odot}$) white dwarfs. However, the mean mass is significantly higher ($0.675 M_{\odot}$) for stars without $H\alpha$ if no hydrogen is included in our models. This indicates that the effective temperatures and masses obtained from hydrogen-free models are probably overestimated, most likely due to the presence of invisible traces of hydrogen in these stars. Adding the maximum amount of hydrogen pushes the mass distribution towards values that now become consistent (mean mass of $0.631 M_{\odot}$) with the mean mass of DA and DB white dwarfs, although the peak is still slightly shifted towards higher masses with respect to the DBZA/DZA stars.

Since there is no reason to believe that these objects represent a distinct massive population, this probably means that our effective temperatures and masses are still slightly overestimated for many objects using our approach, most likely due to small deviations of the abundances of some elements with respect to the chondrite values. For example, if the accretion episode responsible for the metal pollution in some of these stars

has stopped a long time ago, elements with different masses will start to settle with different timescales (photospheric abundances will be very close to that of the polluting body only during the early phase and steady state phase; Dupuis et al. 1993; Koester 2009), leading to abundances that can depart significantly from our assumed ratios. This will also affect, to a lesser extent, the relative strength of the absorption in the UV. Consequently, the uncertainties on the atmospheric parameters for these stars will be intrinsically larger than the statistical values reported here. Spectroscopic observations in the ultraviolet for every object in our sample would be required for a more accurate analysis, but unfortunately, such data will not become available anytime soon. Note that DZA white dwarfs are less affected by these uncertainties because when hydrogen is present in sufficient quantities to be detectable, it will also be the main free electron donor at the photosphere, diminishing the impact of small variations of heavy element abundance ratios with respect to chondrites.

Even though it is not possible to derive the exact photospheric hydrogen abundance for each object, the fact that the peak of the mass distribution appears more realistic when traces of hydrogen are included suggests that most of these objects probably have abundances close to the detection limit. As will be discussed in Section 7, this corresponds also approximately to the amount of hydrogen expected if such DZ stars are the results of convectively mixed DA white dwarfs. Consequently, our adopted atmospheric parameters reported in Table 6 are obtained with the hydrogen abundance set to the visibility limit, keeping in mind that the true solution for individual objects may be off by a few hundred degrees and a few hundredth solar mass, depending on their real hydrogen (and also metal) content.

Note finally that objects in Table 6 with $M \lesssim 0.47 M_{\odot}$ are most likely unresolved double degenerate binaries, because such low mass white dwarfs would have low mass progenitors on the main sequence, with lifetimes longer than the age of the Milky Way. Such binaries are more luminous, resulting in a larger solid angle for a given distance, and thus a larger radius (lower mass) is inferred when analyzed under the assumption of a single object.

5.4. Accreted Material

Figure 8 shows the abundance of calcium as a function of effective temperature for the 1023 DBZ/DZ(A) white dwarfs in our sample. The two gaps in the distribution reported by Dufour et al. (2007b), namely between 5000 and 6000 K as well as in the top right corner of the diagram, have been mostly filled, thanks to the re-

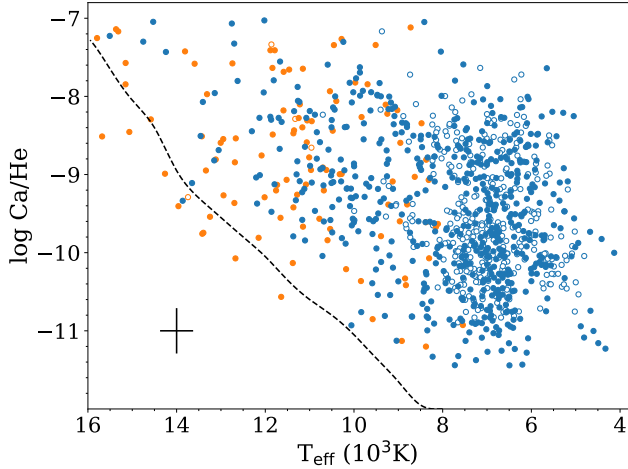


Figure 8. Calcium abundance as a function of effective temperature for all DZ white dwarfs in our sample. The black cross indicates the mean error bar. White dwarfs with a parallax measurement are shown with filled symbols, while $\log g = 8$ was assumed for objects with open symbols. Orange circles represent DZA stars with hydrogen abundances determined by fitting $H\alpha$, and blue circles represent DZ stars with the hydrogen abundance fixed at the detection limit. The dashed line indicates the detection limit of calcium, defined as an equivalent width of 0.5 \AA for the Ca II H line.

cent discovery of many new cool polluted white dwarfs (Kepler et al. 2015, 2016; Kleinman et al. 2013; Koester et al. 2011; Hollands et al. 2017, 2018). The absence of objects at high effective temperatures and low calcium abundances is still present, and is due to the detection limit of Ca II H\&K lines, as indicated in the figure. At the typical resolution of our spectroscopic observations, stars with such parameters would simply appear as DC white dwarfs below $T_{\text{eff}} \sim 12,000 \text{ K}$, and as DB stars above this temperature.

More interesting than the calcium-to-helium abundance ratio is the total mass of calcium contained in the convection zone of these white dwarfs. Using the derived effective temperature and surface gravity of each object, we can calculate the total mass of the helium convection zone using envelope models similar to those described in Fontaine et al. (2001, see Dufour et al. 2010 for further details) ranging from $T_{\text{eff}} = 7000 \text{ K}$ to $30,000 \text{ K}$, $\log g = 7.5$ to 9.0 , and with the $\text{ML2}/\alpha = 1.0$ version of the mixing-length theory (the effect of changing the mixing length is negligible below $T_{\text{eff}} \sim 16,000 \text{ K}$; see Figures 9 and 10 of Rolland et al. 2018). Our results are presented in Figure 9. Note that these values represent only lower limits to the total mass accreted since we do not know how much mass has already diffused at the bottom of the convection zone. Also shown for comparison in Figure 9 is the estimated mass of calcium present

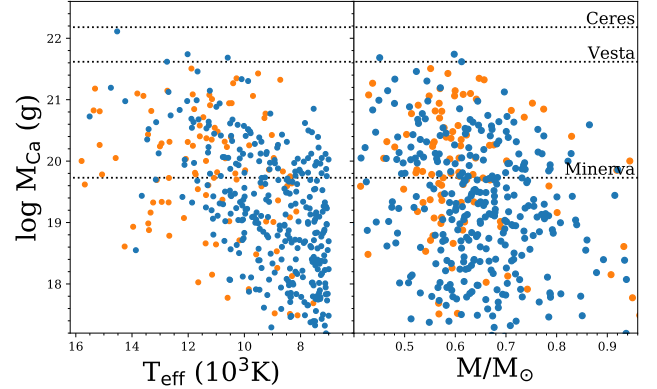


Figure 9. Total mass of calcium in the convection zone as a function of effective temperature (left) and mass (right). Orange circles are objects with hydrogen abundances determined by fitting $H\alpha$ and blue circles are objects with the hydrogen abundance fixed at the detection limit. We also show the estimated mass of calcium in Ceres, Vesta, and Minerva, assuming that calcium constitutes 1.6% of their total mass as in bulk Earth (Farihi 2011).

in well-known asteroids in the solar system, assuming that calcium accounts for 1.6% of the mass of a typical planetesimal (see Farihi 2011). Our results are similar to those presented in Farihi (2011), with masses ranging from 10^{18} g to 10^{22} g , with possibly smaller mass values at lower effective temperatures (the lack of low calcium mass values at high effective temperatures is simply a visibility limit effect; see Figure 8). Surprisingly, the total mass of calcium remains constant as a function of the white dwarf mass between $0.5 M_{\odot}$ and $0.75 M_{\odot}$, with a possible decrease in more massive white dwarfs, although we are probably dealing here with small number statistics.

5.5. Main Sequence Progenitors

It is also possible to estimate the mass of the white dwarf progenitors using the empirical initial-final mass relation (IFMR). While there are many different IFMR published (see Figure 8 of Williams et al. 2009 for a comparison), most of them rely on the observations of star clusters. El-Badry et al. (2018) propose an alternative way of calculating the relation using the *Gaia* color-magnitude diagram. Their results agree remarkably well with those of Williams et al. (2009), which we decided to use for simplicity. One must keep in mind that this relation includes many systematic errors, one being the possible dependence on initial metallicity (Marigo & Girardi 2007), information that is lost when evolving to the white dwarf phase. Because of this, it is difficult to determine accurate initial masses of individual objects, but we can obtain a good idea of the distribution. The

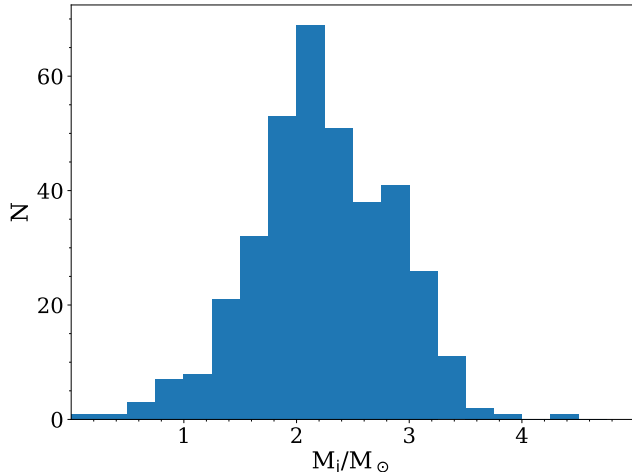


Figure 10. Mass distribution of white dwarf progenitors based on the IMFR of Williams et al. (2009) for the DBZ/DZ(A) stars in our sample with $\sigma_\pi/\pi < 0.1$.

result is shown in Figure 10 for stars with $\sigma_\pi/\pi < 0.1$. Note that below $M_i = 1 M_\odot$, the results are meaningless, since the white dwarfs in these bins have masses below $0.47 M_\odot$, and are most probably unresolved double degenerate binaries (single white dwarfs with such low mass have long main sequence lifetime, and are not expected to have evolved into white dwarfs within the age of the galactic disk yet).

On the basis of the results displayed in Figure 10, we find that 41 white dwarfs had main sequence progenitors with masses above $3 M_\odot$, indicating that the formation of rocky objects around massive stars may not be exceptional at all. Note that the *Extrasolar Planets Encyclopaedia*⁷ reports only 9 exoplanets (out of 3802 exoplanets with the mass of the host star determined) around 8 different stars with masses above $3 M_\odot$. The very small number of known planets around massive stars is mostly due to various selection effects, as the method used to find them (transit, radial velocity, direct imaging) are all less efficient around large, bright, and massive main sequence stars. Nevertheless, theoretical models of planet formation predict that planet occurrence around massive stars should be higher, and the presence of rocky material in the photosphere of many polluted white dwarfs with massive main sequence progenitors seems to confirm this hypothesis. However, to properly study planet occurrence and its correlation with stellar mass, an analysis of a large sample of DC and DB white dwarfs would be necessary, preferably for

a complete-volume sample, something that is outside the scope of this work.

5.6. Discussion of Individual Objects

J0005+7313 — The helium lines at 3889 and 4026 Å are deeper than those predicted by the model, indicating that the temperature determined from photometry, $T_{\text{eff}} = 12,673$ K, is probably underestimated. Using *Gaia* photometry, we find $T_{\text{eff}} = 13,152$ K, which is still too cool for a good spectroscopic fit. Bergeron et al. (2011) found $T_{\text{eff}} = 14,410$ K, $\log H/He = -5.97$, and no metals, using only spectroscopy. The absence of metals is not the explanation, since we obtain 12,715 K fitting photometry with our metal-free models. Because their technique is independent of photometry, one possible explanation is the reddening due to interstellar absorption. In this work, we use the procedure of Harris et al. (2006), and since the star is only at 34.7 parsecs, no correction for reddening is applied. If we use the procedure of Gentile Fusillo et al. (2019) instead, we need to apply 3.2% of the maximum absorption along the line of sight, and we now obtain $T_{\text{eff}} = 13,622$ K, which provides a much better agreement with the spectra. Three dimensional reddening maps made with *Gaia* should eventually allow better correction for reddening.

J0152+2418 — The Mg I lines at ~ 3830 Å and the red wing of the Ca II H&K lines are not well reproduced by our model. One possible explanation is that the abundance ratios differ significantly from that of chondrites. A deficiency in magnesium (and possibly Fe and other elements) may explain this discrepancy. More specific adjustments of the various abundances would be necessary to obtain a good fit.

J0209+2914, *J1242+0829*, and *J1424+5657* — All three white dwarfs have “flattened” Ca II lines, similar to those observed in J1249+6514, not analyzed here, which has been identified as magnetic by Hollands et al. (2017). The spectra do not show other lines that could be used to detect line splitting. We can only consider the values we found to be approximate, but if the presence of magnetism is confirmed, J1242+0829 would be the hottest known magnetic DZ star with $T_{\text{eff}} \sim 8123$ K.

J0302-0108 (GD 40) — Our effective temperature of $T_{\text{eff}} = 13,594$ K is much lower than that reported by Voss et al. (2007) — $T_{\text{eff}} = 15,316$ K (with $\log g$ fixed at 8) — obtained on the basis of metal-free models. They also relied on optical spectra rather than photometry to derive the temperature. Part of this large difference is probably attributable to the lack of heavy elements in their model atmosphere calculations, but since our predicted helium lines are a tiny bit too shallow compared to the observations, it is also possible that our effective

⁷ <http://exoplanet.eu/>

temperature is slightly underestimated, possibly due to our neglect of any reddening correction given that the distance is only 64 pc.

J0555-0410 (LP 658-2) and *J2201+0219* — While these objects do not show a clear H α absorption line, setting the hydrogen abundance at the detection limit leads to completely spurious fits, so we decided to adopt hydrogen-free models for these stars. J0555-0410 was also analyzed in Blouin et al. (2018a) who also found a lower hydrogen abundance of $\log \text{H}/\text{He} < -5$. The difference of 61 K in T_{eff} between both temperature estimates can be explained by the different sets of photometry used (*BVRI+JHK* instead of Pan-STARRS *grizy*). Blouin et al. were also able to constrain $\log \text{Mg}/\text{He}$ to -8.66 , a value much higher than the -9.92 we used here on the basis of the chondrite ratio.

J0801+5329, *J0842-1347*, and *J1428+4403* — These are objects similar to *J0152+2418* where the magnesium lines and the shape of the Ca II H&K lines are not well reproduced. Reducing $\log \text{H}/\text{He}$ improves the fit in one case (J1428+4403), but not to the point where the fit is satisfactory. Additional adjustments of individual metal abundances are most probably needed for these objects.

J0846+3538 and *J1356+4047* — Both stars seem to have an overabundance of magnesium and sharper than predicted Ca II H&K lines, as opposed to J0152+2418 and other similar objects discussed above. Again, a fit using a tailor-made grid with different abundance ratios would probably allow a better fit for these objects.

J1214+7822 — It was impossible to obtain a good spectroscopic fit for both the Ca II H&K lines and the Ca I line at 4226 Å simultaneously. We found the best agreement with H&K by using hydrogen-free models and ignoring the Ca I line. However, with a mass of only $0.31 M_{\odot}$, this star is most likely a double degenerate system, and a DZ+DC system could explain the unusually narrow H&K spectral lines at this temperature. Alternatively, Limoges et al. (2015) suggested that this object could have a hydrogen-rich atmosphere, with a lower atmospheric pressure and thus narrower absorption lines.

J1234+5606 — The SDSS magnitudes for this object are ~ 0.3 mag fainter than Pan-STARRS and *Gaia*, which leads to two different possible solutions. We could not reach a conclusion regarding this discrepancy, but the SDSS colors lead to a much better spectroscopic fit of the helium lines at 5876 and 6678 Å, indicating a good estimate of the effective temperature. We thus decided to adopt the SDSS photometric data set.

J2253-0646 (WD 2251-070) — Blouin et al. (2019a) found for this object $T_{\text{eff}} = 4170 \pm 90$ K, $\log g = 8.06 \pm 0.08$, and $\log \text{Ca}/\text{He} = -9.8 \pm 0.2$ from fitting *BVRI+JHK* and Pan-STARRS photometry, while we

find $T_{\text{eff}} = 4132 \pm 53$ K, $\log g = 8.03 \pm 0.07$, and $\log \text{Ca}/\text{He} = -10.00 \pm 0.05$. The values are very close, but Blouin et al. (2019a) show a much better fit in their Figure 9. This is not surprising because they relied on improved line profile calculations for the Ca I line at 4226 Å. These improved calculations are important only for objects with $T_{\text{eff}} \lesssim 4500$ K, and thus they have little impact on our analysis. Only 4 objects in our sample are in that temperature range; J1636+1619 and J0555-0410 do not show Ca I line, and J1214+7822 has already been discussed above.

6. DQ WHITE DWARFS

6.1. Carbon Abundances

Following the method described in Section 4, we obtained the atmospheric parameters for all 317 DQ stars in our sample by fitting simultaneously the spectral energy distribution and the carbon features (atomic and/or molecular). Figure 11 shows examples of spectroscopic and photometric fits for typical DQ white dwarfs (all our fits are available in Appendix I, and our final parameters are given in Table 7). The figures show the spectral region used for the fit, i.e. either the Swan bands between 4000 and 6500 Å, or the carbon lines between 4500 and 5500 Å for the hotter objects. Note that for some objects with weaker molecular absorption features, we used a smaller region centered on the observed bands to achieve a good fit.

Figure 12 shows the carbon abundance as a function of effective temperature, using a color scale to indicate the mass of each object. Two distinct populations are clearly present: one sequence with “normal” mass ($\sim 0.6 M_{\odot}$) DQ white dwarfs (bluish circles) at low effective temperature, and a second sequence (reddish circles) of massive white dwarfs ($M \geq 0.8 M_{\odot}$), with carbon abundances increasing with effective temperature. The first sequence follows nicely the expected evolutionary path for $0.6 M_{\odot}$ DQ stars with $\log q(\text{He}) = -2.0$ (Dantona & Mazzitelli 1979, Iben & MacDonald 1985, Fontaine & Brassard 2005). Note that in Dufour et al. (2005), the bulk of the stars was following the evolutionary sequence for $\log q(\text{He})$ closer to -3.0 . This is mainly due to the fact that in our improved models, the band strengths with our new line list are slightly higher than with the Zeidler-K.T. & Koester (1982) prescription, resulting in a systematic downward shift in carbon abundances compared to the values published in Dufour et al. (2005). Note also that the abrupt disappearance of normal mass DQ stars above ~ 9500 K is simply due to the visibility limit of carbon at these temperatures; in order to see carbon features in the optical at higher effective temperatures, the abundance must be at least $\log (\text{C}/\text{He}) =$

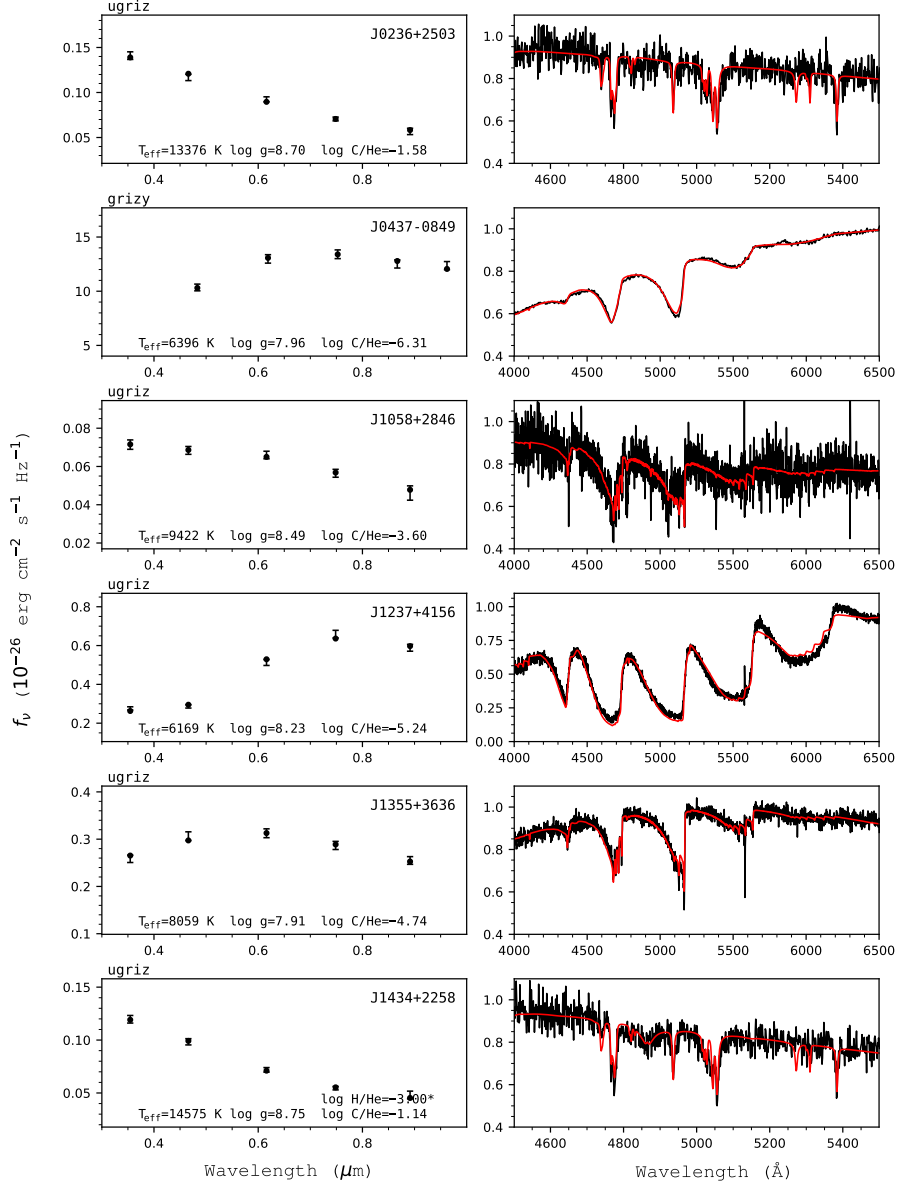


Figure 11. Examples of fits to DQ white dwarfs in our sample. In the left panels, error bars represent the observed data, while filled circles correspond to our best fit model, with the atmospheric parameters given in each panel. The photometry used in the fit is indicated at the top left of each panel. A dagger symbol indicates that the $\log g$ value has been fixed at 8.0, when no trigonometric parallax is available. A star symbol indicates that the value of $\log H/\text{He}$ has been fixed rather than fitted. The right panels show our spectroscopic fits (red) to the normalized observed spectra (black). The complete version of this figure is available in Appendix I.

–4.5. Unless an ultraviolet spectrum is available, objects following the predicted sequence in that range of effective temperature will simply be classified as DB white dwarfs. Also, the absence of stars below $T_{\text{eff}} \sim 6500$ K is artificial since these were not included in our sample due to the uncertainties in modeling the pressure-shifted Swan bands (the so-called peculiar DQ, or DQpec; see Kowalski 2010, Blouin et al. 2019c).

More importantly, our analysis confirms the presence of a second sequence (Dufour et al. 2005; Koester & Knist 2006) with an abundance about one dex higher than the bulk of DQ white dwarfs at $M \sim 0.6 M_{\odot}$. It appears that this second sequence is indeed composed of massive white dwarfs, as suggested by Dufour et al. (2005), at least for the hottest ones ($T_{\text{eff}} \gtrsim 9000$ K). In fact, almost all DQ white dwarfs with an effective

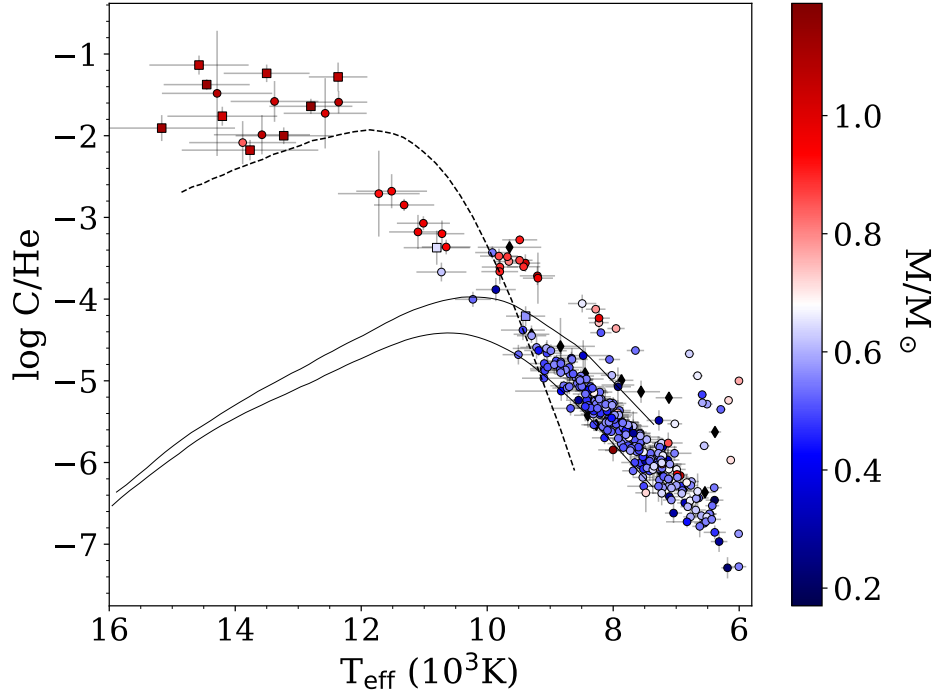


Figure 12. Carbon abundances as a function of effective temperature for DQ white dwarfs using a color scale for the mass of each object (objects without parallax measurements are shown as black diamonds). A square indicates an object fitted with models including a trace of hydrogen ($\log \text{H}/\text{He} = -3$, see text). Solid lines represent evolutionary models from Fontaine & Brassard (2005) at $0.6 M_{\odot}$ with, from top to bottom, $\log q(\text{He}) = -3$ and $\log q(\text{He}) = -2$, while the dashed line is for $1.0 M_{\odot}$ and $\log q(\text{He}) = -5$. The standard dredge-up scenario struggles to explain the observed abundance pattern for massive objects.

temperature above 10,000 K have masses higher than $0.8 M_{\odot}$. The coolest objects on the second sequence, however, do not appear to have larger masses. These massive DQ stars will be discussed in greater detail in Section 6.4.

6.2. Mass Distribution

The mass distribution of the DQ white dwarfs in our sample, displayed in Figure 13, reveals the two distinct populations very clearly, with the bulk of our sample centered around $0.55 M_{\odot}$, and a second bump centered around $1 M_{\odot}$ where all the hottest DQ stars in our sample are found. As stated before in the case of DBZ/DZ(A) white dwarfs, DQ stars with derived masses below $\sim 0.45 M_{\odot}$ are probably unresolved double degenerate binaries. Such low mass stars, if isolated, could not have been formed from single star evolution within the lifetime of the Galaxy. Moreover, these objects are usually interpreted as helium-core white dwarfs whose core mass was truncated by mass transfer with a companion. The presence of carbon in these apparently low-mass DQ stars indicates that at least one component has a carbon core. These binary are thus probably composed of two non-DA stars (e.g., DQ + DC), which

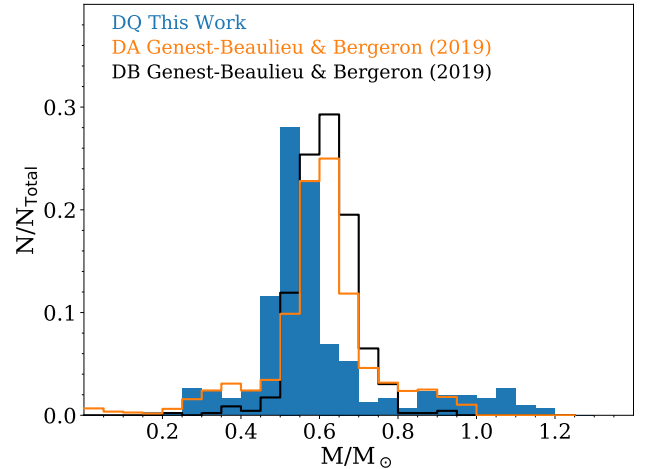


Figure 13. Mass distribution of DQ white dwarfs (blue), compared to the photometric mass distributions of DA and DB white dwarfs (orange and black lines, respectively) taken from Figure 21 of Genest-Beaulieu & Bergeron (2019).

means that the masses reported here are most likely underestimated.

Surprisingly, the main peak of the mass distribution for the DQ white dwarfs in our sample is shifted by $\sim 0.05 M_{\odot}$ relative to that obtained for the DA and

DB white dwarfs analyzed by [Genest-Beaulieu & Bergeron \(2019\)](#), see their Figure 21), raising suspicions about our mass determinations of DQ stars. A way to test the accuracy of our method for the mass determination is to look at the well-known DQ white dwarf Procyon B (J0739+0513), which has a very accurate dynamical mass determination of $0.592 \pm 0.006 M_{\odot}$ ([Bond et al. 2015](#)). Using our standard hybrid photometric/spectroscopic approach, we obtain a slightly lower mass of $0.554 \pm 0.013 M_{\odot}$ using HST photometry. This indicates we are probably dealing with a systematic shift in the mass determinations of DQ white dwarfs using our models⁸. Uncertainties related to our dereddening procedure for our T_{eff} and mass determinations should be irrelevant here given the proximity of Procyon B. In fact, if we take only objects within 100 pc, where reddening should be minimal along the line of sight for most stars, we still find that the peak of the mass distribution is too low. In order to identify the origin of this shift in mass, we performed several tests using various model grids where we replaced our treatment of the molecular band opacity with the old just overlapping line approximation ([Zeidler-K.T. & Koester 1982](#)). We also tried various treatments for the line broadening, and included undetectable traces of hydrogen or oxygen as well. In the end, similar mass distributions were always obtained, and we could not pinpoint the exact cause of this discrepancy.

We note, however, that several lines in the ultraviolet have wings that extend several hundreds of angstroms from the line center. This is probably not physically realistic, and the use of the impact approximation is certainly not appropriate for these lines. Unfortunately, the data required to compute line profiles with the unified line shape theory of [Allard et al. \(1999\)](#) are not available for these lines. For stars with available spectroscopic observations in the UV ([Holberg et al. 2003](#))⁹, the use of the quasistatic van der Waals broadening ([Walkup et al. 1984](#), [D. Koester, private communication](#)) provides a good fit to the asymmetric C I 1930 Å line, although the carbon abundance needed to reproduce the observations is different than that determined from the Swan bands. This problem is not new (see [Dufour 2011](#), for a detailed discussion), and the origin of this discrepancy still remains mysterious to this day, although it is most likely related to the uncertainties of the ultraviolet opacities. In fact, for DQ stars in the intermediate temperature regime where both atomic lines and molecular

bands are present (~ 9500 to $11,000$ K), the models also have difficulties reproducing both types of absorption features simultaneously. Examples of this problem are illustrated in Figure 14. While it is possible to obtain a good spectroscopic fit by increasing the effective temperature and carbon abundance for these objects, doing so would then produce an energy distribution completely at odds with the photometric observations (see right panel of Figure 14). A similar problem, based on an analysis using D. Koester’s model atmosphere code, was also reported by [Gänsicke et al. \(2010\)](#) for two DQ stars showing traces of oxygen. For these problematic DQ stars in our sample, we compare in Table 3 the results of our standard approach with the parameters obtained by fitting only the optical spectra, thus ignoring all photometric information. We note that even though the exact atmospheric parameters are somewhat uncertain because of this problem, the massive nature ($M > 0.8 M_{\odot}$) of these objects remains unquestionable, even when allowing for a conservative uncertainty of $0.15 M_{\odot}$.

While the problems mentioned above become apparent only for stars that show both atomic and molecular lines, it is likely, however, that the whole temperature, abundance, and mass scales for DQ white dwarfs are affected, which could perhaps also explain the $\sim 0.05 M_{\odot}$ shift of the peak of the DQ mass distribution relative to DA and DB white dwarfs. Until this problem is solved, the absolute values of the atmospheric parameters for all DQ white dwarfs should be considered uncertain, although the relative values between objects in the sample are probably reliable.

6.3. The Effects of Hydrogen

The presence of hydrogen is a rare phenomenon in DQ white dwarfs (see [Dufour 2011](#)). Hydrogen abundance measurements are reported only for two relatively hot and massive DQ stars in the literature, namely G35-26 ([Thejll et al. 1990](#)) and G227-5 ([Wegner & Koester 1985](#)), while its presence is also inferred from the detection of a CH molecular band in two other objects — G99-37 and GJ 841B, both magnetic white dwarfs ([Blouin et al. 2019c](#); [Vornanen et al. 2010](#)). Our sample of cool DQ white dwarfs with molecular carbon bands contains only six objects showing H α , three of which have masses below $0.47 M_{\odot}$, indicating they are most probably unresolved double degenerate binaries composed of a DQ and a DA white dwarf; these are listed in Table 4. [Leggett et al. \(2018\)](#) also identified two such DQ+DA unresolved binaries (see their Figure 7). Except for the hotter DQ J1243+1651, the other objects have an H α line that is too narrow to be reproduced by helium-rich models, and we believe they are also DQ + DA binaries. Hence, of

⁸ Note that a recent study by [Koester & Kepler \(2019\)](#) also finds a DQ mass distribution peaking near $0.55 M_{\odot}$.

⁹ <http://vega.lpl.arizona.edu/newsips/low/>

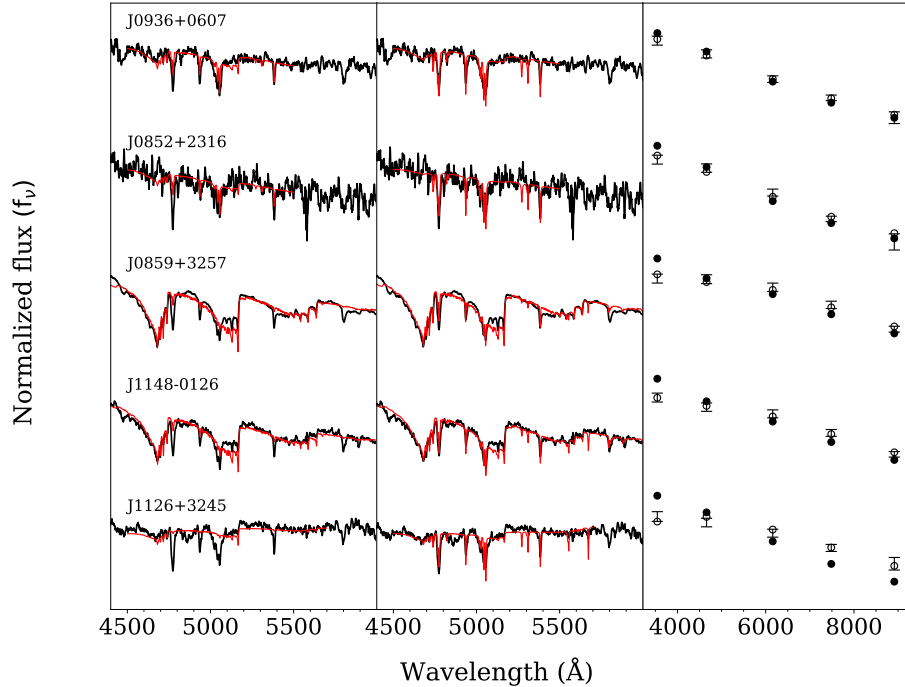


Figure 14. Left panel: best solutions when the effective temperature is obtained from fits to photometric data. Middle panel: best solutions when fitting only the optical spectra. Right panel: corresponding energy distributions for the two solutions. Open circles represent the best photometric/spectroscopic solutions (our standard approach), while filled circles correspond to the solutions with the effective temperature and carbon abundance determined solely from the optical spectra.

Table 3. Parameters of DQ white dwarfs with bad spectroscopic fits when the effective temperature is derived from photometry

Name	Photometric fits			Spectroscopic fits		
	T_{eff} (K)	$\log C/He$	M/M_{\odot}	T_{eff} (K)	$\log C/He$	M/M_{\odot}
J0852+2316	11099	-3.18	0.97	12733	-1.99	1.12
J0859+3257	9486	-3.52	0.87	10407	-2.87	0.97
J0936+0607	11013	-3.07	0.97	12109	-1.99	1.09
J1000+1005	7869	-4.99		10395	-2.87	
J1126+3245	9297	-4.43		11369	-2.73	
J1140+0735	10651	-3.36	0.94	12395	-1.60	1.12
J1140+1824	9656	-3.54	0.81	10921	-2.62	0.94
J1148-0126	9680	-3.48	0.88	10868	-2.62	1.00
J2248+2826	9390	-4.21	0.57	11920	-2.02	0.90

the 293 DQ white dwarfs with temperatures between ~ 6500 K and $10,500$ K in our sample, there is compelling evidence for the presence of hydrogen in only two objects, both hotter than 9000 K.

As mentioned in Section 5.1, undetectable traces of hydrogen can still have an impact on the atmospheric parameter determination of helium-atmosphere white

dwarfs, although in the case of DQ white dwarfs, the contribution of free electrons from carbon is usually much more important than that of heavy elements in DZ stars. To test the effect of hydrogen on the determination of the atmospheric parameters of cool DQ white dwarfs, we generated a small grid of models with $\log H/He = -3$, and refitted every object in our sample

Table 4. DQ white dwarfs showing hydrogen lines and Swan bands

Name	T_{eff} (K)	M/M_{\odot}
J0836+0437	8420	0.46
J0928+2638	7108	0.28
J0950+3238	8268	
J1243+1651	10227	0.53
J1406+3402	7042	0.30
J2310-0057	7647	0.54

with $T_{\text{eff}} < 10,000$ K. We find that by assuming such a hydrogen abundance, we could produce $H\alpha$ and $H\beta$ absorption features that would be easily detected above 8000 K, as well as a CH molecular band near 4300 Å for objects cooler than ~ 8500 K. Even by assuming an abundance that is clearly ruled out by the spectroscopic observations, we find that the presence of hydrogen has only a marginal impact on our atmospheric parameters, increasing the derived effective temperatures by 150 K and masses by $0.035 M_{\odot}$, on average. We can thus safely consider that the presence of undetectable traces of hydrogen does not affect significantly the parameters of cool DQ stars.

In the atomic lines regime ($T_{\text{eff}} \gtrsim 10,000$ K), however, spectroscopic observations tell a different story. Although $H\alpha$ is blended with the carbon lines near 6588 Å, $H\beta$ can be detected very clearly. These lines are observed in 40% of the objects (10/25). We thus generated additional grids with $\log H/He = -2, -3, \text{ and } -4$, with T_{eff} ranging from 10,000 K to 16,000K. We found that, surprisingly, the $\log H/He = -3$ grid best reproduces the observations for almost every star, suggesting that the hydrogen abundance appears relatively constant in the objects where hydrogen is detected. Therefore, the solutions with $\log H/He = -3$ are presented in Table 7 when the Balmer lines are observed. Note that it is possible that DQ stars with no detectable hydrogen features also contain some traces of hydrogen, since the Balmer lines are barely predicted for some objects with higher carbon abundance and lower effective temperature. The presence of hydrogen in these objects has a marginal impact on the measured effective temperature (265 K on average) and mass ($0.032 M_{\odot}$ on average), but the effect can be quite significant for the carbon abundance (around 0.5 dex in some cases). Since we do not know the exact hydrogen abundance for these objects, we provide the solutions without hydrogen in Table 7.

6.4. Massive DQ White Dwarfs

We now turn our attention to the population of massive ($M > 0.8 M_{\odot}$) DQ white dwarfs clearly distinguishable in Figures 12 and 13. First, the carbon abundance pattern observed for these objects indicates that they followed a different evolutionary path than their cooler normal mass counterparts, since the standard dredge-up prediction for massive white dwarfs completely fails to explain their chemical composition (see also [Brassard et al. 2007](#)). Second, such massive DQ stars could not have DB white dwarfs as progenitor because practically no massive helium-rich white dwarfs exist at higher effective temperatures ([Bergeron et al. 2011](#); [Genest-Beaulieu & Bergeron 2019](#); [Beauchamp et al. 1996](#)). Instead, the massive sequence connects nicely with the carbon-dominated atmosphere white dwarfs at higher effective temperature, the so-called Hot DQ stars ($T_{\text{eff}} \geq 18,000$ K and $\log(C/He) \geq 0$, see [Dufour et al. 2007a, 2008, 2013](#)). Note that *Gaia* trigonometric parallax measurements confirm that the carbon-dominated atmosphere white dwarfs are massive as well ([Dunlap et al., submitted](#)). We thus believe that our massive DQ stars represent cooler versions of the carbon-atmosphere white dwarfs.

The many unusual properties of Hot DQ white dwarfs — unique chemical composition, high mass, and high incidence of magnetism — recently prompted [Dunlap & Clemens \(2015\)](#) to propose that these hot carbon-atmosphere white dwarfs represent a population of merged white dwarfs (failed type Ia supernovae). The key piece of evidence for this proposed scenario comes from the kinematic properties of the sample, which provide an independent age indicator ([Dunlap & Clemens 2015](#)). Indeed, one interesting characteristic that stands out about the Hot DQ population is their very high tangential velocity, as a group, compared to other white dwarfs with the same age and mass. Over time, a population of stars is kinematically heated through gravitational interactions ([Wegg & Phinney 2012](#)). Hence, as a population gets older, its velocity dispersion increases. In particular, [Dunlap & Clemens](#) showed that there is a discrepancy between the young age inferred from the derived atmospheric parameters of carbon-atmosphere white dwarfs¹⁰, and the old age derived from the velocity dispersion. The merger scenario provides an elegant solution to this dilemma because the reheating induced by the merging event resets the cooling age clock, and consequently, the cooling age derived from the effective temperature and mass thus becomes meaningless. If the

¹⁰ Such hot massive white dwarfs should descend from massive, short-live main-sequence progenitors, and they should thus have a small total age if they evolved as single stars.

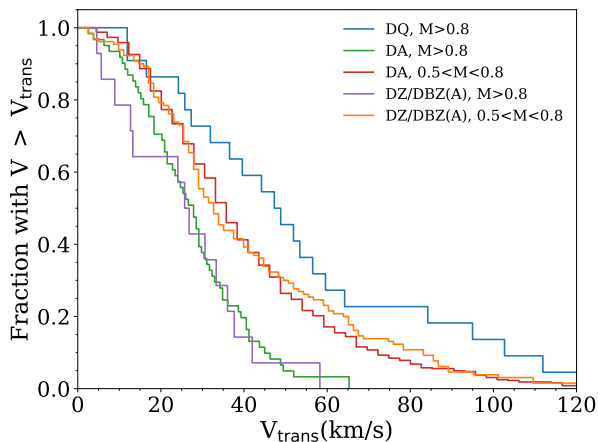


Figure 15. Cumulative distribution of transverse velocities for massive DQ, DBZ/DZ(A) (this paper) and DA (Genest-Beaulieu & Bergeron 2019) white dwarfs with T_{eff} between 10,000 and 16,000K.

massive DQ white dwarfs observed in Figures 12 and 13 are indeed cooled down versions of the Hot DQ stars, a kinematic analysis of the sample should then show the same discrepancy between the two age indicators.

We show in Figure 15 the cumulative distribution of transverse velocities, V_{trans} , for our sample of massive DQ white dwarfs, calculated using *Gaia* distances and proper motions. We selected DQ white dwarfs with $T_{\text{eff}} > 10,000$ K and $M > 0.8 M_{\odot}$, a point where there appears to be a clean separation between the two DQ populations. Since there is no DQ white dwarf with “normal” masses in this temperature range, we compare the properties of the massive DQ stars with those of our sample of DBZ/DZ(A) as well as DA white dwarfs with signal-to-noise ratio higher than 25 taken from Genest-Beaulieu & Bergeron (2019), a large and clean sample perfectly suited for this comparison. Also, in order to make a meaningful comparison, we selected only DBZ/DZ(A) and DA white dwarfs in the same range of effective temperature where the massive DQ stars are found, i.e. between 10,000 K and 16,000 K, and we compare the distributions of transverse velocities for stars with masses greater than $0.8 M_{\odot}$ and in the $0.5 - 0.8 M_{\odot}$ mass range.

First, we notice that the transverse velocity distribution for DBZ/DZ(A) and DA white dwarfs are very similar, and that those with $M > 0.8 M_{\odot}$ are much less dispersed than those with $0.5 < M < 0.8 M_{\odot}$. This is exactly what we expect, since massive white dwarfs have massive progenitors with shorter main sequence lifetimes, corresponding to a shorter total age, and thus a smaller velocity dispersion (Wegg & Phinney

2012). However, the velocity dispersion for the massive DQ stars displayed in Figure 15 is extremely broad, in sharp contrast with what is expected for a population of massive white dwarfs. We find indeed that 45% (10 out of 22) of the massive ($M > 0.8 M_{\odot}$) DQ population has $V_{\text{trans}} > 50 \text{ km s}^{-1}$, while the fractions are only 5% (3 out of 61) and 7% (1 out of 14) for DA and DBZ/DZ(A) with similar atmospheric parameters, respectively. The fact that the distribution is even larger than that of stars in the $0.5 - 0.8 M_{\odot}$ mass range strongly supports the idea that these objects are the descendants of the carbon-dominated atmosphere white dwarfs (the Hot DQ stars), and consequently, that they represent the outcome of the merging of two white dwarfs.

It is interesting to note, however, that very few massive DQ stars are found with a large magnetic field (J1040+0635 and J1036+6522 are the only two examples, Williams et al. 2013), in contrast with the very large fraction of magnetic Hot DQ white dwarfs (at least 70% are magnetic at some level, Dufour et al. 2013). Magnetic fields of a few MG would be easily detectable through line splitting in our spectra. It thus seems that as helium finds its way to the top of the photosphere, the strength of the magnetic field is also reduced significantly, as these stars cool down. If our hypothesis that the Hot DQ stars represent the progenitors of the massive DQ in our sample is correct, then the latter are probably still magnetic at some level. Unfortunately, the SDSS spectra used in our analysis lack the signal-to-noise ratio and spectral resolution required to properly identify weaker magnetic fields of a few 100 kG. We predict that a large fraction of these objects will eventually show magnetism when high-resolution spectroscopic observations become available. Also, at least one third of the Hot DQ stars are variable (Montgomery et al. 2008; Barlow et al. 2008; Dunlap et al. 2010; Lawrie et al. 2013; Dufour et al. 2011), presumably due to the presence of magnetic spots at the surface of a rapidly rotating star. If magnetism is indeed still present at some level, a large fraction of the massive DQ stars should also be variable.

Finally, we notice that there appears to be a correlation between the mass and the effective temperature, the hottest objects near 16,000 K being significantly more massive ($\sim 0.3 M_{\odot}$) than their cooler counterparts near 10,000 K. As it is expected that white dwarfs should evolve at constant masses, we first believed that some missing ingredient in our models was responsible for either an overestimation of the masses of the hottest stars, or an underestimation for the cooler ones. We experimented with many test grids incorporating traces of oxygen, hydrogen, as well as different treatments of line broadening, but none of these experiments affected the

relative masses of our object in a significant way. As mentioned in Section 6.2, we know there are some uncertainties concerning the absolute values of the atmospheric parameters of DQ white dwarfs that may explain the shifted position of the peak of the mass distribution and the difficulties in reproducing simultaneously the atomic and molecular features. However, it is unlikely that the shortcomings of our models translate into uncertainties on the masses much larger than $0.1 M_{\odot}$ (the radius of the star is tightly constrained from the measured energy distribution and distance), not enough to explain the clear correlation with effective temperature that we observe in our sample. We thus believe that the observed correlation is real and that it is most probably the manifestation of an observational bias due to the crystallization of the core of these white dwarfs (see next section).

6.5. The Crystallization Sequence

As a white dwarf cools off, thermal energy is gradually lost from the star in the form of radiation, until the kinetic motions of the ions lose amplitude and eventually become correlated. The ionic state then evolves from a gas to a fluid to a solid, a process referred to as crystallization (Fontaine et al. 2001). This liquid-to-solid transition, which begins in the center of the stellar core and slowly moves outwards, represents a first-order phase transition, and is thus accompanied by a release of latent heat, which contributes to slowing down the cooling process significantly. Over 50 years ago, van Horn (1968) predicted that this crystallization process would cause a decrease of the cooling rate during the transition, and would cause a pile-up of objects that could be detected in HR diagrams. The first direct observational evidence of this crystallization process was reported by Tremblay et al. (2019), in the form of a characteristic pile-up of white dwarfs forming a tight sequence in the *Gaia* M_G versus $G_{BP} - G_{RP}$ HR diagram, the so-called “Q branch” (see their Figure 2).

Our second, more massive sequence of DQ white dwarfs is particularly interesting in the context of crystallization, because for $\sim 0.6 M_{\odot}$ white dwarfs, crystallization occurs at the same time as another physical process referred to as convective coupling, which takes place when the base of the superficial convection zone reaches into the degenerate interior (Fontaine et al. 2001). Convective coupling also decreases the cooling process temporarily, and in $\sim 0.6 M_{\odot}$ white dwarfs, the effects of crystallization and convective coupling cannot be disentangled. Fortunately, crystallization occurs at much higher effective temperature for more massive white dwarfs, making the massive sequence of DQ white

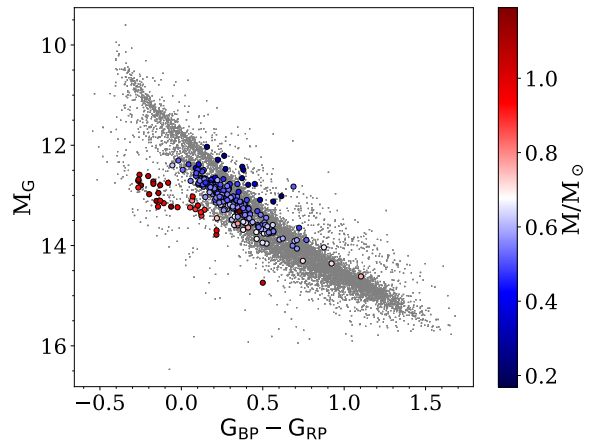


Figure 16. Absolute G magnitudes as a function of $G_{BP} - G_{RP}$. Filled circles represent DQ stars with $\sigma_{\pi}/\pi < 0.1$, using a color scale for the mass of each object. Black dots are white dwarf candidates within 100 pc selected from *Gaia* DR2 using the cuts proposed in Appendix B of *Gaia* Collaboration et al. (2018).

dwarfs ideal objects to examine the crystallization process.

Figure 16 shows the color-magnitude diagram for our sample of DQ white dwarfs with measured parallaxes and $\sigma_{\pi}/\pi < 0.1$. The lowest red point in this diagram is J0841+3329, for which the *Gaia* `phot_bp_rp_excess_factor` value is 1.34, indicating possibly a bad quality of magnitudes according to *Gaia* Collaboration et al. (2018). Our best fit based on SDSS photometry predicts a lower magnitude in the G bandpass. By removing this object, all our massive DQ stars fall in the region of the crystallization sequence reported by Tremblay et al. (2019).

Figure 17 shows the masses as a function of effective temperature for the same sample of DQ stars, together with the sample of DA white dwarfs analyzed by Bergeron et al. (2019, see their Figure 14). The black solid lines are also described at length in Bergeron et al. Briefly, the left line corresponds to the onset of crystallization at the center of an evolving model (the same as in Tremblay et al. 2019), while the right line indicates the location where 80% of the total mass of the star has solidified. Upon crystallization, latent heat is slowly released, and the white dwarf cooling is slowed down, a process that is well illustrated by the tightening of the isochrones (shown in red) between the two black lines. Figure 17 reveals that most of our massive DQ stars fall within these lines, indicating a possible pile-up due to crystallization.

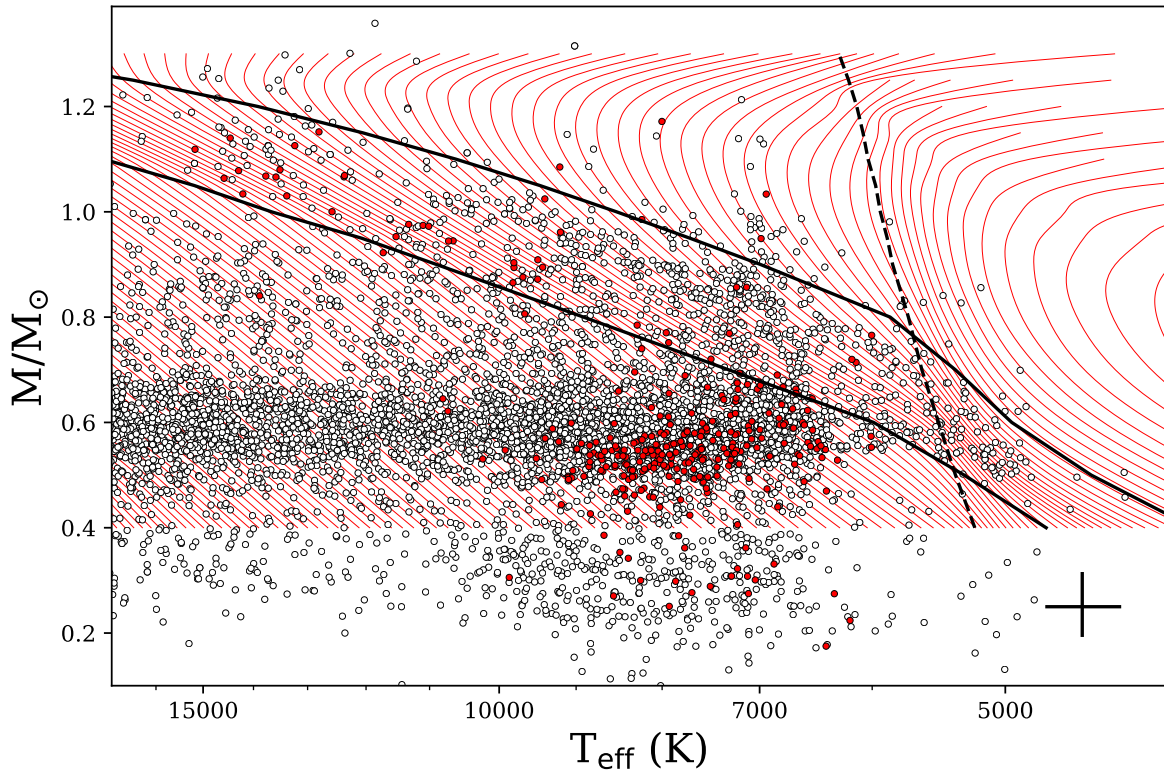


Figure 17. Mass as a function of T_{eff} for the DQ white dwarfs in our sample (red dots), and DA white dwarfs spectroscopically identified in the MWDD with $\sigma_{\pi}/\pi < 0.1$ (white dots), taken from Figure 14 of Bergeron et al. (2019). Also reproduced are their theoretical isochrones obtained from cooling sequences with C/O-core compositions, $q(\text{He}) = 10^{-2}$, and $q(\text{H}) = 10^{-4}$, equally spaced by $\Delta \log \tau_{\text{cool}} = 0.02$ (in years). The lower black solid curve indicates the onset of crystallization at the center of evolving models, while the upper one indicates the location where 80% of the total mass has solidified. The dashed curve indicates the onset of convective coupling. The black cross corresponds to the mean errors of each fitted parameter.

Figure 18 shows the masses of DBZ/DZ(A) white dwarfs in our sample as a function of effective temperature together with the same isochrones and crystallization sequences as before. The signature of crystallization cannot be seen, but this could be due to the fact that there are much less massive stars above $T_{\text{eff}} = 12,000$ K which is consistent with the idea that DBZ(A) white dwarfs belong to the same population as DB(A) stars. At high temperatures, it is also more difficult to see metal absorption lines (see the detection limit in Figure 8) and the diagram is thus much less populated in that range.

6.6. Discussion of Individual Objects

J0901+5751, *J0922+2928*, and *J1423+5729* — These stars show many O I lines, especially at 6156 and 7772 Å, and at 5330 and 5435 Å in the case of *J1423+5729*. For *J0922+2928*, Gänsicke et al. (2010) found $T_{\text{eff}} = 8270$ K and $\log \text{C}/\text{He} = -2.6$ using oxygen-rich models, while we found $T_{\text{eff}} = 8022$ K and $\log \text{C}/\text{He} = -4.93$. They also

found $\log \text{H}/\text{He} < -5.0$ and $\log \text{O}/\text{He} = -2.0$, which implies that oxygen is more abundant than carbon. White dwarfs with such a high amount of oxygen in their atmosphere must have followed a different evolutionary path, and the authors suggest that they could be O/Ne-core white dwarfs surrounded by a layer of carbon and oxygen. Such white dwarfs would be massive. According to our results, only one of these can be qualified as massive, but we determined the mass using evolutionary models with C/O cores and did not take atmospheric oxygen into account in our analysis. However, if we take the values of Gänsicke et al. (2010) for *J0922+2928*, all these objects fall above the first sequence in Figure 12, suggesting indeed a different evolutionary path. We also note that these objects are rare and have little impact on the conclusions of this work.

J1040+0635 — This star shows magnetic splitting, suggesting that our solution may be uncertain. To evaluate the influence of the magnetic field on our result,

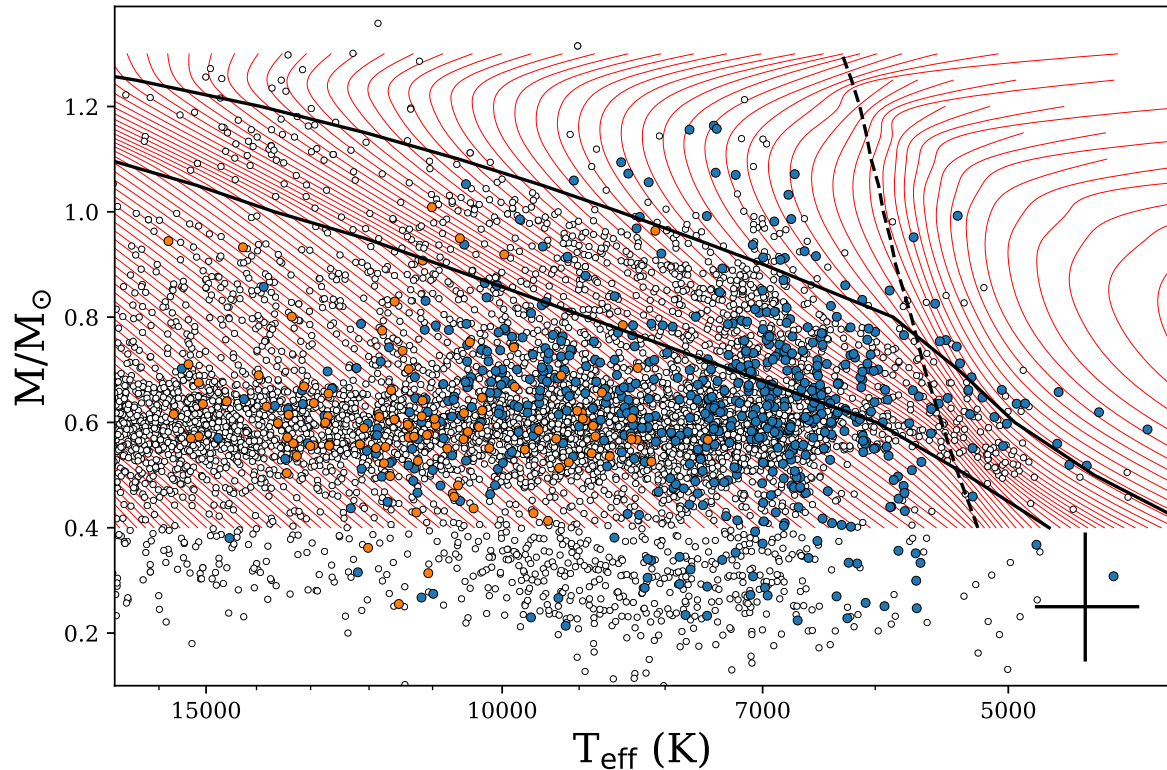


Figure 18. Same as Figure 17 but for DZ/DBZ white dwarfs. Blue circles correspond to DZ/DBZ stars, while orange circles represent DZA/DBZA stars.

we fitted the magnetic white dwarf J1036+6522 (not included in this analysis), which shows similar line splitting. We found $T_{\text{eff}} = 15,637$ K, $\log g = 8.8$, and $\log C/\text{He} = -1.87$, the carbon abundance being very approximate since we do not include splitting in this exercise. Williams et al. (2013) used magnetic synthetic spectra to fit this object and estimated $T_{\text{eff}} \sim 15,500$ K, $\log g \sim 9$, and $\log C/\text{He} = -1$, which is consistent with our solution.

J2101+3148 — This star shows a discrepancy for the Swan band at 4700 \AA . Dufour et al. (2005) also reported this problem without further explanation. With a larger sample, we can now compare this object with other stars with similar properties (for example J1424+0833 and J1118–0314), and this discrepancy is not observed anywhere else. A change in temperature of ± 500 K does not improve the situation. However, the finding chart on SIMBAD clearly shows a red object very near the white dwarf (potentially a companion or an object along the line of sight) that probably contaminates the spectra.

7. ON THE SPECTRAL EVOLUTION OF WHITE DWARFS

Thanks to the advent of *Gaia*, we now have, for the first time, detailed mass distributions for a large sample of DQ and DBZ/DZ(A) white dwarfs. Although there are still uncertainties regarding the individual mass determinations (see Sections 5.1 and 6.2), a lot of information can be extracted from the overall shape of these mass distributions, and in particular with respect to the spectral evolution of these white dwarfs.

The mass distribution of DQ white dwarfs shows two distinct peaks (see Figure 13), one centered around $0.55 M_{\odot}$ and another one centered around $1 M_{\odot}$. As discussed above, the location of the first peak is slightly shifted relative to that of DA and DB white dwarfs (see Figure 21 of Genest-Beaulieu & Bergeron 2019), most probably indicating a systematic error due to some unknown opacity source in the ultraviolet. Putting aside this problem, it is interesting to compare the overall shape of these mass distributions. The main difference between the mass distribution of DB stars and that of DA stars is the absence of a high-mass tail in the former. This difference was first noted by Beauchamp et al. (1996), and later confirmed by Bergeron et al. (2011) and Genest-Beaulieu & Bergeron (2019). The mass dis-

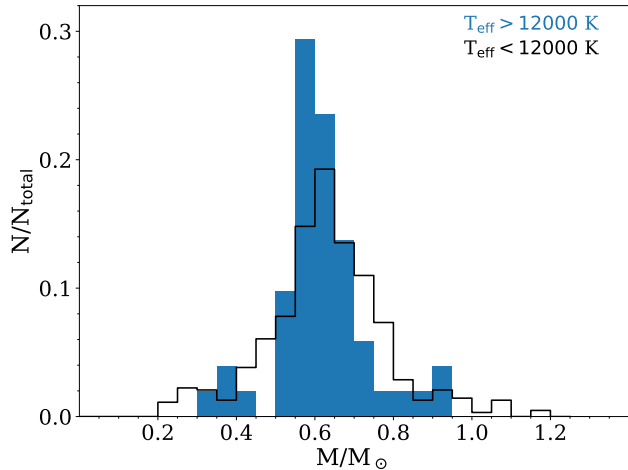


Figure 19. Comparison of the mass distributions of DBZ/DZ(A) white dwarfs for effective temperatures above and below 12,000 K.

tribution of our DQ sample does not show an extended tail extending to masses above $1 M_{\odot}$, but rather exhibits two distinct peaks with a clear separation near $0.8 M_{\odot}$. As discussed in Section 6.4, there is compelling evidence that the second peak represents a population of merged white dwarfs. Hence, the mass distribution of DQ stars with $T_{\text{eff}} < 10,000$ K — effectively removing practically all the massive objects — resemble much more that of DB white dwarfs than that of DA stars, reinforcing the belief that the progenitor of DQ white dwarfs are helium-rich DB stars.

In contrast, the mass distribution of DBZ/DZ(A) white dwarfs (see Figure 7) reveals a fair number of massive objects forming some sort of a tail similar to that observed in DA white dwarfs. The similitude is even more striking in Figure 19 where we show the mass distributions of our sample for effective temperatures above and below 12,000 K. We see that at low effective temperatures, the mass distribution — composed essentially of DZ(A) stars — clearly shows a high mass tail, which is barely present in the mass distribution of hotter white dwarfs, containing essentially only DBZ(A) white dwarfs.

The most logical explanation for this phenomenon is that the progenitors of a significant fraction of DZ(A) white dwarfs are DA stars that were convectively mixed, and transformed into helium-atmosphere white dwarfs. Indeed, it is well known that the ratio of non-DA to DA white dwarfs increases considerably with decreasing effective temperatures. This has been interpreted as the result of convective mixing, a process which becomes important below 12,000 K, as discussed at length in Rolland et al. (2018) and references therein. This is a

process where the thin hydrogen layer is mixed with the deeper and more massive helium layer through convection, effectively turning a hydrogen-rich white dwarf into a helium-rich one. Our results thus suggest that many DZ(A) stars, and certainly most of the massive ones, represent the outcome of mixed DA white dwarfs that have also accreted planetary material. In fact, Rolland et al. (2018) also demonstrated that most DZA stars below $T_{\text{eff}} \sim 12,000$ K could not be the descendants of DBA (or DBZA) stars, and that these objects must be the result of hydrogen-rich stars that turned helium-rich as a result of convective mixing. For the DBZ(A) white dwarfs, it is reasonable to consider these objects as being simply the metal-polluted version of DB(A) stars. These polluted DBZ(A) stars, when they cool off, will eventually become helium-rich white dwarfs, or DZ(A) stars if they also accrete material (they would not become DQ stars, however, see below).

Finally, the DQ white dwarfs with masses near the peak of the mass distribution — which rarely show any trace of hydrogen (see Section 6.3) — are most likely the descendants of the so-called “pure helium” DB stars that show no hydrogen feature. In these nearly hydrogen-free DB stars, hydrogen has probably been largely depleted during the earlier born-again post-AGB evolutionary phase (Rolland et al. 2018). This interpretation could simultaneously explain the rarity of DQZ objects¹¹ (i.e. DQ stars showing traces of metals), if the surroundings of the progenitor have been cleared of rocky debris during the active earlier post-AGB phases.

8. SUMMARY AND CONCLUSIONS

We presented a homogeneous analysis of 1023 DBZ/DZ(A) and 319 DQ white dwarfs based on state-of-the-art model atmospheres using new parallaxes, proper motions, and photometry from *Gaia* DR2, as well as photometry from SDSS, Pan-STARRS, previously published *BVRI*, and spectroscopy from various sources. This represents a significant increase over the previous comprehensive studies on these types of objects, namely those of Dufour et al. (2007b, 159 DZs) and Dufour et al. (2005, 56 DQs). Calcium abundance measurements for our large sample of DBZ/DZ(A) white dwarfs indicate that the rocky objects that polluted their photosphere had masses similar to those of large asteroids found in our solar system. We found several polluted white dwarfs with progenitor masses well above $3 M_{\odot}$, confirming that the formation of rocky material is also

¹¹ There are only 4 stars with Ca II H&K absorption lines in our sample: J0739+0513 (Procyon B), J0900+0331, J1332+2740, and J1534+4145.

common for early type stars. The availability of parallax measurements for nearly three quarters of our sample allowed us to determine, for the first time, meaningful mass distributions for these types of objects (the mass distributions for DQ and DZ stars of [Dufour et al. 2005, 2007b](#) contained only 11 and 16 objects, respectively). These mass distributions revealed several interesting aspects about the properties of our samples that we summarize here:

1. The mean mass for the DBZ/DZ white dwarfs (i.e. objects not showing H α) is significantly higher than that of DBZA/DZA stars. The two distributions are in much better agreement when undetectable traces of hydrogen are included in the model fits.
2. The mass distribution of DZ(A) white dwarfs cooler than $T_{\text{eff}} = 12,000$ K shows a high-mass tail similar to that observed for DA stars. This high-mass tail is absent for objects in our sample hotter than 12,000K. We interpret this as a signature that a significant fraction of the DZ(A) stars are convectively mixed DA white dwarfs that have accreted rocky material.
3. The mass distribution of DQ white dwarfs shows two distinct peaks, one centered at $0.55 M_{\odot}$, whose carbon abundances are well explained by the standard carbon dredge-up scenario, and another one centered at $\sim 1 M_{\odot}$, whose high kinematic properties are consistent with the idea that they represent a population of merged white dwarfs. We note that the location of the $0.55 M_{\odot}$ peak is slightly shifted towards smaller masses relative to that of DB white dwarfs, most probably due to some unknown opacity source in the ultraviolet in our DQ models.

While traces of hydrogen are detected (or needed) in nearly all DBZ/DZ(A) white dwarfs, its presence is extremely rare in cool DQ stars. This indicates that the nature of these two populations of helium-atmosphere white dwarfs are clearly distinct. The most logical way to explain the abundance pattern and mass distributions of these objects is to interpret hydrogen-free DB white dwarfs as progenitors of cool DQ stars, while the other types of cool helium-atmosphere white dwarfs, namely the DC and DZ(A) stars, would originate from both convectively mixed DA and cooled down DB(A) white dwarfs. Within this scenario, the rarity of both hydrogen and heavy elements in DQ white dwarfs is also naturally explained by invoking particularly active post-AGB

phases that would eliminate practically all the remaining hydrogen, as well as most nearby rocky objects in orbit.

The presence of hydrogen in 40% of the hotter DQ is, however, somewhat mysterious. We showed that this population of massive stars have much larger space velocities than what is expected for a relatively young star population. As originally proposed by [Dunlap & Clemens \(2015\)](#) in the case of Hot DQ white dwarfs, this indicates that the massive DQ stars in our sample, which are most likely cooled-down version of the Hot DQs, would also be the result of the merging of two C/O white dwarfs. [Dufour et al. \(2007a, 2008\)](#) proposed that the Hot DQ white dwarfs would disguise themselves as massive DB white dwarfs until the underlying convection zone completely dilutes the thin helium layer, effectively transforming the object into a C/O-dominated atmosphere when the star cools to about 24,000 K. However, such massive, and most probably magnetic, DB white dwarfs are very scarce. Another possibility is that these merger remnants could instead hide as DA stars with very thin hydrogen layers, or possibly as some of the massive magnetic white dwarfs that are often found at higher effective temperatures. We predict that spectropolarimetric or high-resolution spectroscopic observations of massive DQ white dwarfs should reveal that most of them are magnetic at some level.

Interestingly, we find there is a correlation between the stellar mass and the effective temperature for these massive DQ white dwarfs. Despite the uncertainties associated with the temperature, abundance, and mass scales for these objects (due most probably to some missing opacity in the ultraviolet), we believe the observed trend to be real, and that it represents a manifestation of an accumulation of stars at certain effective temperatures due to the slowing of the cooling process, when the stellar core eventually crystallizes. Future work should address the shortcomings in the modeling of DQ white dwarfs in order to reduce the uncertainties on the atmospheric parameters of these objects.

This work was supported in part by NSERC (Canada) and the Fund FRQNT (Québec). BHD acknowledges support from the Wootton Center for Astrophysical Plasma Properties under the United States Department of Energy collaborative agreement DE-FOA-0001634, from the United States Department of Energy grant under DE-SC0010623. This work has made use of the Montreal White Dwarf Database ([Dufour et al. 2017](#)), and also the VALD database, operated at Uppsala University, the Institute of Astronomy RAS in Moscow, and the University of Vienna, the SIMBAD database,

operated at CDS, Strasbourg, France (Wenger et al. 2000), data from the European Space Agency (ESA) mission *Gaia* (<https://www.cosmos.esa.int/gaia>), processed by the *Gaia* Data Processing and Analysis Consortium (DPAC, <https://www.cosmos.esa.int/web/gaia/dpac/consortium>). Funding for the DPAC has been provided by national institutions, in particular the institutions participating in the *Gaia* Multilateral Agreement (Gaia Collaboration et al. 2016, 2018). Funding for the Sloan Digital Sky Survey IV has been provided by the Alfred P. Sloan Foundation, the U.S. Department of Energy Office of Science, and the Participating Institutions. SDSS-IV acknowledges support and resources from the Center for High-Performance Computing at the University of Utah. The SDSS web site is www.sdss.org. SDSS-IV is managed by the Astrophysical Research Consortium for the Participating Institutions of the SDSS Collaboration including the Brazilian Participation Group, the Carnegie Institution for Science, Carnegie Mellon University, the Chilean Participation Group, the French Participation Group, Harvard-Smithsonian Center for Astrophysics, Instituto de Astrofísica de Canarias, The Johns Hopkins University, Kavli Institute for the Physics and Mathematics of the Universe (IPMU) / University of Tokyo, the Korean Participation Group, Lawrence Berkeley National Laboratory, Leibniz Institut für Astrophysik Potsdam (AIP), Max-Planck-Institut für Astronomie (MPIA Heidelberg), Max-Planck-Institut für Astrophysik (MPA Garching), Max-Planck-Institut für Extraterrestrische Physik (MPE), National Astronomical Observatories of China, New Mexico State University, New York University, University of Notre Dame, Observatório Nacional /

MCTI, The Ohio State University, Pennsylvania State University, Shanghai Astronomical Observatory, United Kingdom Participation Group, Universidad Nacional Autónoma de México, University of Arizona, University of Colorado Boulder, University of Oxford, University of Portsmouth, University of Utah, University of Virginia, University of Washington, University of Wisconsin, Vanderbilt University, and Yale University (Abolfathi et al. 2018). The Pan-STARRS1 Surveys (PS1) and the PS1 public science archive have been made possible through contributions by the Institute for Astronomy, the University of Hawaii, the Pan-STARRS Project Office, the Max-Planck Society and its participating institutes, the Max Planck Institute for Astronomy, Heidelberg and the Max Planck Institute for Extraterrestrial Physics, Garching, The Johns Hopkins University, Durham University, the University of Edinburgh, the Queen’s University Belfast, the Harvard-Smithsonian Center for Astrophysics, the Las Cumbres Observatory Global Telescope Network Incorporated, the National Central University of Taiwan, the Space Telescope Science Institute, the National Aeronautics and Space Administration under Grant No. NNX08AR22G issued through the Planetary Science Division of the NASA Science Mission Directorate, the National Science Foundation Grant No. AST-1238877, the University of Maryland, Eotvos Lorand University (ELTE), the Los Alamos National Laboratory, and the Gordon and Betty Moore Foundation (Chambers et al. 2016).

Softwares: Astropy (Astropy Collaboration et al. 2013, 2018), Matplotlib (Hunter 2007), NumPy (Oliphant 2006; van der Walt et al. 2011), PySpecKit (Ginsburg & Mirocha 2011).

REFERENCES

- Abolfathi, B., Aguado, D. S., Aguilar, G., et al. 2018, *ApJS*, 235, 42
- Allard, N. F., Royer, A., Kielkopf, J. F., & Feautrier, N. 1999, *PhRvA*, 60, 1021
- Astropy Collaboration, Robitaille, T. P., Tollerud, E. J., et al. 2013, *A&A*, 558, A33
- Astropy Collaboration, Price-Whelan, A. M., Sipőcz, B. M., et al. 2018, *AJ*, 156, 123
- Bailer-Jones, C. A. L. 2015, *PASP*, 127, 994
- Barlow, B. N., Dunlap, B. H., Rosen, R., & Clemens, J. C. 2008, *ApJL*, 688, L95
- Batalha, N. M., Borucki, W. J., Koch, D. G., et al. 2010, *ApJL*, 713, L109
- Beauchamp, A., Wesemael, F., Bergeron, P., Liebert, J., & Saffer, R. A. 1996, in *Astronomical Society of the Pacific Conference Series*, Vol. 96, *Hydrogen Deficient Stars*, ed. C. S. Jeffery & U. Heber, 295
- Bergeron, P., Dufour, P., Fontaine, G., et al. 2019, *ApJ*, 876, 67
- Bergeron, P., Leggett, S. K., & Ruiz, M. T. 2001, *ApJS*, 133, 413
- Bergeron, P., Ruiz, M. T., & Leggett, S. K. 1997, *ApJS*, 108, 339
- Bergeron, P., Saffer, R. A., & Liebert, J. 1992, *ApJ*, 394, 228
- Bergeron, P., Wesemael, F., Dufour, P., et al. 2011, *ApJ*, 737, 28

- Blouin, S., Allard, N. F., Leininger, T., Gad ea, F. X., & Dufour, P. 2019a, *ApJ*, 875, 137
- Blouin, S., Dufour, P., & Allard, N. F. 2018a, *ApJ*, 863, 184
- Blouin, S., Dufour, P., Allard, N. F., & Kilic, M. 2018b, *ApJ*, 867, 161
- Blouin, S., Dufour, P., Allard, N. F., et al. 2019b, *ApJ*, 872, 188
- Blouin, S., Dufour, P., Thibault, C., & Allard, N. F. 2019c, *ApJ*, 878, 63
- Blouin, S., Kowalski, P. M., & Dufour, P. 2017, *ApJ*, 848, 36
- Bond, H. E., Gilliland, R. L., Schaefer, G. H., et al. 2015, *ApJ*, 813, 106
- Brassard, P., Fontaine, G., Dufour, P., & Bergeron, P. 2007, in *Astronomical Society of the Pacific Conference Series*, Vol. 372, 15th European Workshop on White Dwarfs, ed. R. Napiwotzki & M. R. Burleigh, 19
- Brooke, J. S., Bernath, P. F., Schmidt, T. W., & Bacskey, G. B. 2013, *Journal of Quantitative Spectroscopy and Radiative Transfer*, 124, 11 .
<http://www.sciencedirect.com/science/article/pii/S0022407313000800>
- Chambers, K. C., Magnier, E. A., Metcalfe, N., et al. 2016, *arXiv e-prints*, arXiv:1612.05560
- Cohen, M., Megeath, S. T., Hammersley, P. L., Mart n-Luis, F., & Stauffer, J. 2003, *AJ*, 125, 2645
- Dantona, F., & Mazzitelli, I. 1979, *A&A*, 74, 161
- Dufour, P. 2011, *Stars with Unusual Compositions: Carbon and Oxygen in Cool White Dwarfs*, ed. D. W. Hoard, 53–88
- Dufour, P., B land, S., Fontaine, G., Chayer, P., & Bergeron, P. 2011, *ApJL*, 733, L19
- Dufour, P., Bergeron, P., & Fontaine, G. 2005, *ApJ*, 627, 404
- Dufour, P., Blouin, S., Coutu, S., et al. 2017, in *Astronomical Society of the Pacific Conference Series*, Vol. 509, 20th European White Dwarf Workshop, ed. P.-E. Tremblay, B. G nsicke, & T. Marsh, 3
- Dufour, P., Fontaine, G., Liebert, J., Schmidt, G. D., & Behara, N. 2008, *ApJ*, 683, 978
- Dufour, P., Kilic, M., Fontaine, G., et al. 2010, *ApJ*, 719, 803
- . 2012, *ApJ*, 749, 6
- Dufour, P., Liebert, J., Fontaine, G., & Behara, N. 2007a, *Nature*, 450, 522
- Dufour, P., Vornanen, T., Bergeron, P., & Fontaine, A., B. 2013, in *Astronomical Society of the Pacific Conference Series*, Vol. 469, 18th European White Dwarf Workshop., 167
- Dufour, P., Bergeron, P., Liebert, J., et al. 2007b, *ApJ*, 663, 1291
- Dunlap, B. H., Barlow, B. N., & Clemens, J. C. 2010, *ApJL*, 720, L159
- Dunlap, B. H., & Clemens, J. C. 2015, in *Astronomical Society of the Pacific Conference Series*, Vol. 493, 19th European Workshop on White Dwarfs, ed. P. Dufour, P. Bergeron, & G. Fontaine, 547
- Dupuis, J., Fontaine, G., & Wesemael, F. 1993, *ApJS*, 87, 345
- Eisenstein, D. J., Liebert, J., Koester, D., et al. 2006, *AJ*, 132, 676
- El-Badry, K., Rix, H.-W., & Weisz, D. R. 2018, *ApJL*, 860, L17
- Farihi, J. 2011, in *American Institute of Physics Conference Series*, Vol. 1331, American Institute of Physics Conference Series, ed. S. Schuh, H. Drechsel, & U. Heber, 193–210
- Farihi, J., G nsicke, B. T., & Koester, D. 2013, *Science*, 342, 218
- Fontaine, G., & Brassard, P. 2005, in *Astronomical Society of the Pacific Conference Series*, Vol. 334, 14th European Workshop on White Dwarfs, ed. D. Koester & S. Moehler, 49
- Fontaine, G., Brassard, P., & Bergeron, P. 2001, *PASP*, 113, 409
- Gaia Collaboration, Prusti, T., de Bruijne, J. H. J., et al. 2016, *A&A*, 595, A1
- Gaia Collaboration, Babusiaux, C., van Leeuwen, F., et al. 2018, *A&A*, 616, A10
- G nsicke, B. T., Koester, D., Girven, J., Marsh, T. R., & Steeghs, D. 2010, *Science*, 327, 188
- Genest-Beaulieu, C., & Bergeron, P. 2019, *ApJ*, 871, 169
- Gentile Fusillo, N. P., Tremblay, P.-E., G nsicke, B. T., et al. 2019, *MNRAS*, 482, 4570
- Giammichele, N., Bergeron, P., & Dufour, P. 2012, *ApJS*, 199, 29
- Ginsburg, A., & Mirocha, J. 2011, *PySpecKit: Python Spectroscopic Toolkit*, *Astrophysics Source Code Library*, , , ascl:1109.001
- Green, P. 2013, *ApJ*, 765, 12
- Harris, H. C., Munn, J. A., Kilic, M., et al. 2006, *AJ*, 131, 571
- Holberg, J. B., Barstow, M. A., & Burleigh, M. R. 2003, *ApJS*, 147, 145
- Holberg, J. B., & Bergeron, P. 2006, *AJ*, 132, 1221
- Hollands, M. A., G nsicke, B. T., & Koester, D. 2018, *MNRAS*, 477, 93
- Hollands, M. A., Koester, D., Alekseev, V., Herbert, E. L., & G nsicke, B. T. 2017, *MNRAS*, 467, 4970
- Hunter, J. D. 2007, *Computing In Science & Engineering*, 9, 90

- Iben, I. J., & MacDonald, J. 1985, *ApJ*, 296, 540
- Johnson, J. A., Aller, K. M., Howard, A. W., & Crepp, J. R. 2010, *PASP*, 122, 905
- Jura, M., Xu, S., Klein, B., Koester, D., & Zuckerman, B. 2012, *ApJ*, 750, 69
- Jura, M., & Young, E. D. 2014, *Annual Review of Earth and Planetary Sciences*, 42, 45
- Kepler, S. O., Pelisoli, I., Koester, D., et al. 2015, *MNRAS*, 446, 4078
- . 2016, *MNRAS*, 455, 3413
- Klein, B., Jura, M., Koester, D., & Zuckerman, B. 2011, *ApJ*, 741, 64
- Klein, B., Jura, M., Koester, D., Zuckerman, B., & Melis, C. 2010, *ApJ*, 709, 950
- Kleinman, S. J., Harris, H. C., Eisenstein, D. J., et al. 2004, *ApJ*, 607, 426
- Kleinman, S. J., Kepler, S. O., Koester, D., et al. 2013, *ApJS*, 204, 5
- Koester, D. 2009, *A&A*, 498, 517
- Koester, D., Gänsicke, B. T., & Farihi, J. 2014, *A&A*, 566, A34
- Koester, D., Girven, J., Gänsicke, B. T., & Dufour, P. 2011, *A&A*, 530, A114
- Koester, D., & Kepler, S. O. 2019, arXiv e-prints, arXiv:1905.11174
- Koester, D., & Knist, S. 2006, *A&A*, 454, 951
- Kowalski, P. M. 2010, *A&A*, 519, L8
- Lawrie, K. A., Burleigh, M. R., Dufour, P., & Hodgkin, S. T. 2013, *MNRAS*, 433, 1599
- Leggett, S. K., Bergeron, P., Subasavage, J. P., et al. 2018, *ApJS*, 239, 26
- Liebert, J., Harris, H. C., Dahn, C. C., et al. 2003, *AJ*, 126, 2521
- Limoges, M.-M., Bergeron, P., & Lépine, S. 2015, *ApJS*, 219, 19
- Limoges, M.-M., Lépine, S., & Bergeron, P. 2013, *AJ*, 145, 136
- Lodders, K. 2003, *ApJ*, 591, 1220
- Marigo, P., & Girardi, L. 2007, *A&A*, 469, 239
- Montgomery, M. H., Williams, K. A., Winget, D. E., et al. 2008, *ApJL*, 678, L51
- Oliphant, T. 2006, *NumPy: A guide to NumPy, USA*: Trelgol Publishing, . <http://www.numpy.org/>
- Paquette, C., Pelletier, C., Fontaine, G., & Michaud, G. 1986, *ApJS*, 61, 197
- Parigger, C. G., Woods, A. C., Surmick, D. M., et al. 2015, *Spectrochimica Acta Part B: Atomic Spectroscopy*, 107, 132 . <http://www.sciencedirect.com/science/article/pii/S058485471500066X>
- Piskunov, N. E., Kupka, F., Ryabchikova, T. A., Weiss, W. W., & Jeffery, C. S. 1995, *A&AS*, 112, 525
- Press, W. H., Flannery, B. P., & Teukolsky, S. A. 1986, *Numerical recipes. The art of scientific computing* (Cambridge University Press)
- Provencal, J. L., Shipman, H. L., Koester, D., Wesemael, F., & Bergeron, P. 2002, *ApJ*, 568, 324
- Provencal, J. L., Shipman, H. L., Wesemael, F., et al. 1997, *ApJ*, 480, 777
- Raddi, R., Gänsicke, B. T., Koester, D., et al. 2015, *MNRAS*, 450, 2083
- Rolland, B., Bergeron, P., & Fontaine, G. 2018, *ApJ*, 857, 56
- Schlafly, E. F., & Finkbeiner, D. P. 2011, *ApJ*, 737, 103
- Subasavage, J. P., Henry, T. J., Bergeron, P., et al. 2007, *AJ*, 134, 252
- Subasavage, J. P., Jao, W.-C., Henry, T. J., et al. 2009, *AJ*, 137, 4547
- Thejll, P., Shipman, H. L., MacDonald, J., & Macfarland, W. M. 1990, *ApJ*, 361, 197
- Tremblay, P.-E., Fontaine, G., Fusillo, N. P. G., et al. 2019, *Nature*, 565, 202
- van der Walt, S., Colbert, S. C., & Varoquaux, G. 2011, *Computing in Science Engineering*, 13, 22
- van Horn, H. M. 1968, *ApJ*, 151, 227
- van Leeuwen, F. 2007, *A&A*, 474, 653
- Vornanen, T., Berdyugina, S. V., Berdyugin, A. V., & Piirola, V. 2010, *ApJ*, 720, L52
- Voss, B., Koester, D., Napiwotzki, R., Christlieb, N., & Reimers, D. 2007, *A&A*, 470, 1079
- Walkup, R., Stewart, B., & Pritchard, D. E. 1984, *Phys. Rev. A*, 29, 169. <https://link.aps.org/doi/10.1103/PhysRevA.29.169>
- Wegg, C., & Phinney, E. S. 2012, *MNRAS*, 426, 427
- Wegner, G., & Koester, D. 1985, *ApJ*, 288, 746
- Weidemann, V., & Koester, D. 1995, *A&A*, 297, 216
- Wenger, M., Ochsenbein, F., Egret, D., et al. 2000, *A&AS*, 143, 9
- Williams, K. A., Bolte, M., & Koester, D. 2009, *ApJ*, 693, 355
- Williams, K. A., Winget, D. E., Montgomery, M. H., et al. 2013, *ApJ*, 769, 123
- Xu, S., Jura, M., Dufour, P., & Zuckerman, B. 2016, *ApJL*, 816, L22
- Xu, S., Jura, M., Koester, D., Klein, B., & Zuckerman, B. 2014, *ApJ*, 783, 79
- Xu, S., Zuckerman, B., Dufour, P., et al. 2017, *ApJL*, 836, L7
- Zeidler-K.T., E. M., & Koester, D. 1982, *A&A*, 113, 173

Zuckerman, B., Koester, D., Melis, C., Hansen, B. M., &

Jura, M. 2007, ApJ, 671, 872

Zuckerman, B., Koester, D., Reid, I. N., & Hüsch, M.
2003, ApJ, 596, 477

Zuckerman, B., Melis, C., Klein, B., Koester, D., & Jura,
M. 2010, ApJ, 722, 725

Table 5. Object names, spectral types, and coordinates

J Name	Gaia source id	MWDD id	Sp. type	R.A	Dec
J0000−0026	2449884942327523456	SDSS J000052.44−002610.5	DQ	0.21853	-0.43626
J0000−0850	2441060055844546816	WD 2357−091	DQ	0.04817	-8.83566
J0002+3209	2873769975034246272	SDSS J000215.65+320914.1	DZ	0.56522	32.15387
J0002−0627		SDSS J000232.35−062746.0	DZ	0.63479	-6.46278
J0003+2240		SDSS J000341.93+224043.7	DZ	0.92471	22.67881
J0004+0819		SDSS J000418.68+081929.9	DZ	1.07787	8.32499
J0004+2432	2849976676552398976	SDSS J000426.95+243258.9	DBZ	1.11226	24.54971
J0004+2531	2850199499454835968	SDSS J000439.38+253150.6	DZ	1.16411	25.53071
J0005+0018	2546096749538393600	WD 0003+000	DZ	1.48845	0.30924
J0005+4003	2881925666956510848	GD 1	DZA	1.25425	40.05996
J0005+7313	537563127588521600	GD 408	DBZA	1.27842	73.21927
J0006+0520	2742043289409950336	SDSS J000614.53+052039.0	DZ	1.56054	5.34418
J0006+1800	2773073470346643200	WD 0003+177	DQ	1.59557	18.00373
J0007+2821	2860138053779074560	SDSS J000705.02+282104.2	DQ	1.77087	28.35123
J0008+2507	2849930668862492544	GALEX 2667408659217122775	DQA	2.04310	25.13154
J0008−1034	2427847052815180544	WD 0005−108	DQ	2.03141	-10.56821
J0009+0152	2546743262376424064	SDSS J000950.09+015219.6	DZ	2.45871	1.87211
J0010−0430	2444911924250219648	SDSS J001052.56−043014.3	DZ	2.71886	-4.50390
J0010−0628		SDSS J001037.06−062857.7	DZ	2.65442	-6.48272
J0013+1109		SDSS J001309.43+110949.0	DZ	3.28929	11.16361
J0015+0309	2548437124462728704	SDSS J001523.91+030909.0	DQ	3.84950	3.15249
J0015+1830	2797320927258478464	SDSS J001557.38+183034.6	DZ	3.98905	18.50957
J0017+0230		SDSS J001703.79+023008.7	DZ	4.26579	2.50242
J0018−0012	2545263281069744512	PB 5858	DZ	4.70597	-0.20132
J0019+1848	2797345597551222656	SDSS J001910.66+184824.0	DZ	4.79449	18.80673
J0019+2209	2800362726177065984	SDSS J001949.26+220926.5	DZ	4.95519	22.15746
J0024−1107	2424780514884907648	WD 0022−114	DQ	6.22903	-11.12868
J0026−0006		SDSS J002639.47−000630.7	DBZ	6.66444	-0.10851
J0027+0102	2543967197379493120	SDSS J002758.56+010250.4	DZ	6.99400	1.04736
J0027+3350	2863148619694318208	SDSS J002755.88+335018.5	DZ	6.98276	33.83842
J0030−0254		SDSS J003058.58−025436.5	DZ	7.74408	-2.91014
J0031+2040	2796487909762143232	SDSS J003104.21+204033.6	DZ	7.76759	20.67601
J0031+3252		SDSS J003137.63+325215.5	DZ	7.90679	32.87099
J0032+0827	2749781068130558464	SDSS J003244.25+082720.1	DZ	8.18420	8.45562
J0033+0418	2554073392865462272	SDSS J003328.58+041834.6	DQ	8.36893	4.30958
J0033+2845	2857867974583987200	SDSS J003300.59+284504.8	DZ	8.25228	28.75131
J0036−1112	2425347347488993408	WD 0033−114	DZ	9.00572	-11.20389
J0038+1645	2782417115863764224	SDSS J003803.63+164504.4	DZ	9.51504	16.75136

Table 5. Object names, spectral types, and coordinates – continued

J Name	Gaia source id	MWDD id	Sp. type	R.A	Dec
J0039+1416		SDSS J003916.55+141623.4	DZ:	9.81896	14.27318
J0040+2349	2806346096656318208	SDSS J004038.99+234904.5	DZ	10.16250	23.81796
J0040+2723	2809357354062968704	SDSS J004011.38+272353.0	DZ	10.04719	27.39809
J0040+3016	2858528884154261120	SDSS J004015.15+301619.5	DZ	10.06312	30.27209
J0041+1511	2779758050071090688	WD 0038+149	DZ	10.34829	15.18586
J0041+7321	536979286914485760	WD 0038+730	DQ	10.44775	73.35407
J0042+2255	2803222521560799104	SDSS J004235.36+225536.5	DZ	10.64740	22.92686
J0044+0418	2551258990991085184	LSPM J0044+0418	DZ	11.21537	4.30535
J0044+1259	2776033626230867712	SDSS J004440.31+125923.3	DQ	11.16782	12.98991
J0046+0024	2549074978645621632	SDSS J004646.15+002430.9	DZ	11.69232	0.40859
J0046+0635	2556270869932443648	SDSS J004605.61+063513.6	DZ	11.52333	6.58730
J0046+2717	2808923867308433152	SDSS J004634.22+271737.6	DZ	11.64256	27.29386
J0049+0523	2552928187080872832	Wolf 28	DZ	12.29124	5.38861
J0050+1828		SDSS J005029.89+182816.2	DZ	12.62454	18.47117
J0050−0621	2523124962338002432	SDSS J005004.40−062104.1	DZ	12.51833	−6.35115
J0052+1846		SDSS J005247.16+184649.5	DZ	13.19650	18.78042
J0053+3115		SDSS J005304.15+311555.8	DZ	13.26729	31.26553
J0055+0850	2581058706745690752	SDSS J005505.42+085030.5	DQ	13.77256	8.84182
J0055+2413	2804037057813910272	SDSS J005537.21+241347.1	DZ	13.90504	24.22978
J0056+0005		SDSS J005651.25+000559.8	DZ	14.21354	0.09997
J0056+2453		SDSS J005649.27+245335.4	DZ	14.20529	24.89317
J0058+0507	2552263669740622720	SDSS J005818.82+050711.0	DZ	14.57842	5.11975
J0058+1102	2582516968401861632	LSPM J0058+1102	DZ	14.58887	11.04418
J0059+0017	2536491205505048960	WD 0056+000	DZ	14.77823	0.29035
J0100+0814		SDSS J010039.50+081401.0	DQ	15.16458	8.23364
J0102+1817		SDSS J010258.13+181733.3	DZ	15.74221	18.29261
J0102+3112		SDSS J010245.58+311216.5	DZ	15.68992	31.20461
J0103−0429	2525099577846697856	SDSS J010351.91−042913.7	DQ	15.96612	−4.48721
J0104−0030		SDSS J010425.85−003004.8	DZ	16.10771	−0.50136
J0106+2412		SDSS J010651.88+241258.5	DZ	16.71617	24.21625
J0106−0103	2533057533770551680	WD 0103−013	DZA	16.62438	−1.06233
J0107+0102	2537913801752406400	LSPM J0107+0102	DQ	16.95082	1.04461
J0107+2650	306779618349361920	LSPM J0107+2650	DZ	16.86880	26.83933
J0107+2905	308384183771218048	SDSS J010726.83+290557.1	DZ	16.86179	29.09931
J0108−0537	2476852079906496384	SDSS J010825.79−053755.6	DZ	17.10747	−5.63215
J0111+1501	2591195654198397696	GALEX 2418435336417843954	DZ	17.99707	15.02440
J0111+2848		SDSS J011100.82+284800.2	DZ	17.75342	28.80008
J0113−0006	2534630488233088256	SDSS J011338.36−000632.9	DZ	18.40984	−0.10913

Table 5. Object names, spectral types, and coordinates – continued

J Name	Gaia source id	MWDD id	Sp. type	R.A	Dec
J0113−0959	2471465301860389120	WD 0111−102	DZA	18.49577	−9.98704
J0114+3505	320947998199092992	SDSS J011421.17+350547.1	DZ	18.58831	35.09644
J0115−0542	2481890145264070400	SDSS J011512.11−054217.7	DZ	18.80047	−5.70483
J0116+0328	2562882748746769280	SDSS J011636.75+032823.9	DZ	19.15313	3.47331
J0116+0345	2562897214197044224	SDSS J011646.62+034504.0	DZ	19.19425	3.75111
J0116+1744	2785761314839472768	SDSS J011614.28+174425.6	DZ	19.05950	17.74047
J0116+2050	2787507098786135552	SDSS J011646.10+205001.9	DZ	19.19208	20.83386
J0116+2229		SDSS J011636.01+222935.2	DZ	19.15004	22.49311
J0116+2346	293138458619500800	SDSS J011639.84+234644.4	DQ	19.16600	23.77902
J0116+2402	293251570878605696	SDSS J011642.68+240223.8	DQ	19.17784	24.04001
J0117+0021	2534988314843345536	SDSS J011759.81+002138.1	DZ	19.49921	0.36057
J0117+0039		SDSS J011749.68+003900.5	DZ	19.45700	0.65014
J0118+1610	2591754107321120896	Wolf 1516	DQ	19.50031	16.17238
J0119+1758		SDSS J011908.15+175832.8	DZ	19.78396	17.97581
J0120−0041	2533741365578975744	[GMS97] NGC 450 121	DBZ	20.18653	−0.69975
J0121+1504		SDSS J012110.32+150433.3	DZ	20.29300	15.07594
J0121+3440	320029150076023808	2MASS J01213782+3440431	DZ	20.40748	34.67861
J0123+1324	2590150327877551616	WD 0120+131	DZ	20.91567	13.40932
J0125+2346		SDSS J012513.92+234638.8	DZ	21.30800	23.77744
J0126+2534	295286835620380032	SDSS J012620.48+253433.6	DZ	21.58533	25.57601
J0127+1545		SDSS J012755.15+154541.1	DZ	21.97979	15.76142
J0130+2218		SDSS J013013.30+221814.1	DZ	22.55542	22.30394
J0131+0250		SDSS J013121.28+025007.6	DZ	22.83867	2.83544
J0134+1857	95799314257405696	SDSS J013422.70+185704.6	DZ	23.59458	18.95131
J0135+1302	2586182156053386240	WD 0132+127	DZ	23.76715	13.04457
J0135−0027	2509739915804015232	SDSS J013557.23−002705.1	DZ	23.98846	−0.45144
J0136+0229		SDSS J013647.58+022953.7	DZ	24.19825	2.49828
J0136+2004	96167513213751936	SDSS J013655.67+200429.8	DQ	24.23200	20.07496
J0137+0047	2510118903716498816	SDSS J013719.01+004743.5	DQ	24.32920	0.79541
J0138+0031	2509910992940012416	SDSS J013831.12+003101.6	DZ	24.62970	0.51713
J0140+3125		SDSS J014031.53+312502.0	DZ	25.13137	31.41723
J0140+3357	317634168937635200	SDSS J014043.78+335723.7	DZ	25.18254	33.95644
J0141+2921	302222623688124800	SDSS J014135.06+292153.5	DZ	25.39614	29.36479
J0142+0118	2510436112821077760	SDSS J014213.26+011834.8	DZ	25.55525	1.30969
J0143+0113	2510420204262205312	SDSS J014300.52+011356.8	DZ	25.75218	1.23249
J0143+0424		SDSS J014331.92+042441.4	DZ	25.88300	4.41153
J0144+0305		SDSS J014441.64+030536.2	DZ	26.17350	3.09339
J0144+1920		SDSS J014415.12+192021.4	DZ	26.06300	19.33928

Table 5. Object names, spectral types, and coordinates – continued

J Name	Gaia source id	MWDD id	Sp. type	R.A	Dec
J0144−0757	2465432384637068672	SDSS J014405.93−075758.1	DQ	26.02473	-7.96612
J0145+2317	290678477446232960	G 34-49	DQ	26.33124	23.29825
J0145−0822	2465343629137442816	WD 0143−086	DQ	26.47522	-8.37268
J0147+1541		SDSS J014732.99+154104.6	DZ	26.88746	15.68461
J0147−0623		SDSS J014709.40−062349.9	DZ	26.78917	-6.39721
J0148−0112	2506055761575043456	SDSS J014834.00−011235.9	DZ	27.14167	-1.20997
J0150+1354	2576012498130773376	[VV2006] J015008.6+135433	DZ	27.53562	13.90944
J0150+1710	91408178348709376	SDSS J015048.48+171039.0	DZ	27.70200	17.17750
J0152+2418	99064833727036160	SDSS J015217.94+241850.6	DZ	28.07480	24.31413
J0153+0101		SDSS J015330.76+010135.9	DZ	28.37817	1.02664
J0154+1403	77986298173874176	WD 0151+138	DQ	28.67395	14.05221
J0154−0040	2506157672559170944	SDSS J015433.59−004047.1	DQ	28.63993	-0.67976
J0158−0942	2462572103921051648	SDSS J015849.02−094225.3	DZ	29.70411	-9.70698
J0200+0040	2507853291287991808	WD 0157+004	DZ	30.00837	0.67178
J0200+0715	2567842095943560448	LSPM J0200+0715	DQ	30.09463	7.25006
J0201+2015	94296969056387328	SDSS J020128.66+201521.8	DZ	30.36942	20.25606
J0201−0039	2506764706057099520	WD 0158−009	DZ	30.38433	-0.65903
J0202+2459		SDSS J020253.24+245921.4	DZ	30.72183	24.98928
J0208−0315		SDSS J020844.85−031535.4	DQ	32.18681	-3.25986
J0209+0558	2520139096777929344	SDSS J020942.37+055854.7	DZ	32.42649	5.98187
J0209+1425	77451939817925888	WD 0206+141	DQ	32.27529	14.42246
J0209+2914	300086341315084544	SDSS J020930.15+291423.8	DZ	32.37561	29.24007
J0211−0046	2494849302842058624	SDSS J021154.61−004607.2	DZA	32.97755	-0.76867
J0213+2848	107870405742373248	SDSS J021353.94+284855.5	DZ	33.47457	28.81548
J0214+0536	2519877790967868672	SDSS J021457.89+053653.6	DZ	33.74121	5.61489
J0218−0919	5176159517007960576	PHL 1255	DZ	34.65289	-9.32915
J0221−0445		SDSS J022141.04−044507.3	DZ	35.42100	-4.75203
J0225−0018	2500048030040892800	2SLAQ J022509.10−001854.6	DZ	36.28790	-0.31516
J0226−0444		VIPERS 116178525	DZ	36.72992	-4.73941
J0227+0018		SDSS J022751.36+001813.8	DQ	36.96400	0.30386
J0228−0009	2500373657281469056	SDSS J022851.97−000938.7	DZ	37.21655	-0.16077
J0231−0142		SDSS J023150.30−014204.5	DZ	37.95958	-1.70125
J0234−0510		SDSS J023407.46−051028.1	DZ	38.53108	-5.17448
J0236+2503	126173494772886144	SDSS J023633.74+250348.9	DQ	39.14059	25.06357
J0239+0027	2498791288251035520	2SLAQ J023945.02+002745.0	DQ	39.93753	0.46252
J0241−0533	5184841501339099008	SDSS J024142.65−053351.5	DZA	40.42773	-5.56418
J0243+0101	2498928486686282368	WD 0240+008	DQ	40.88657	1.01978
J0248+3408	139937559287208192	SDSS J024802.27+340802.4	DQ	42.00951	34.13424

Table 5. Object names, spectral types, and coordinates – continued

J Name	Gaia source id	MWDD id	Sp. type	R.A	Dec
J0251+7341	547501815051141248	EGGR 474	DZ	42.96365	73.69309
J0252+0054	2499087366116251392	SDSS J025253.20+005439.4	DZ	43.22167	0.91095
J0252-0401	5185475919548087808	SDSS J025206.06-040130.3	DZ	43.02506	-4.02508
J0253+3414	139799845455078912	SDSS J025357.12+341436.8	DQ	43.48792	34.24362
J0302-0108	5187830356195791488	GD 40	DBZA	45.72127	-1.14272
J0305+0557	3940546595098240	SDSS J030538.53+055734.4	DQ	46.41053	5.95946
J0308-0657	5179967194494422912	WD 0305-071	DZ	47.00165	-6.95002
J0314+0524	4081563256565120	GALEX 2691967329460291916	DZ	48.54539	5.41018
J0314-0827	5167512029854029184	SDSS J031448.24-082755.2	DZ	48.70109	-8.46535
J0319+3630	234469931207274112	PM J03196+3630	DZ	49.90945	36.50824
J0320-0716	5169190159475821312	WD 0318-074	DQ	50.22548	-7.27374
J0332-0037	3263359238612842880	WD 0329-007	DQ	53.07595	-0.62287
J0352-0605	3245199640146267264	SDSS J035222.85-060506.3	DQ	58.09523	-6.08509
J0411-0548	3197201731345817856	WD 0409-059	DZ	62.94123	-5.81348
J0416+0713	3297444373952016640	SDSS J041601.25+071308.9	DQ	64.00522	7.21911
J0437-0849	3186021141200137472	GJ 3306	DQ	69.44746	-8.81915
J0438+4109	203931163247581184	GD 61	DBZA	69.66406	41.15899
J0447+1124	3295565239861125888	SDSS J044751.21+112403.8	DZ	71.96337	11.40109
J0536+6154	286154360759650048	SDSS J053607.02+615409.8	DBZA	84.02918	61.90271
J0555-0410	3022956969731332096	NAME HL 4	DZ	88.78954	-4.16786
J0618+6413	1008292775881784192	SDSS J061844.92+641337.3	DZ	94.68737	64.22709
J0627+1002	3327488430402704000	WD 0625+10	DZ	96.90657	10.03718
J0649+3726	943713544541017088	SDSS J064912.36+372638.6	DZ	102.30144	37.44418
J0707+3825	946311759236089984	SDSS J070731.45+382531.0	DQ	106.88101	38.42534
J0710+3740	946030529073021440	GJ 3431 B	DQ	107.55900	37.67200
J0721+3928		SDSS J072144.23+392843.3	DZ	110.43433	39.47872
J0721+3955	948173369860748160	SDSS J072109.48+395539.6	DZ	110.28926	39.92783
J0723+3908	900040942684340608	SDSS J072339.09+390839.5	DQ	110.91285	39.14440
J0730+3456	893881581625207680	SDSS J073029.07+345613.4	DBZA	112.62115	34.93706
J0732+2746	872428494859607680	SDSS J073217.01+274641.5	DBZA	113.07087	27.77822
J0733+3727	898724140071904640	SDSS J073334.19+372735.8	DZ	113.39249	37.45998
J0734+4448	973522301201644416	SDSS J073416.91+444801.3	DBZ	113.57047	44.80037
J0736+4118	924478859922238720	SDSS J073635.22+411828.2	DZ	114.14675	41.30783
J0737+6455	1089540191183664768	SDSS J073703.83+645524.6	DQ	114.26592	64.92357
J0738+3844	899277915974764032	WD 0735+388	DZA	114.64991	38.74394
J0739+0513		* alf CMi B	DQZ	114.82449	5.22410
J0739+3024		SDSS J073957.64+302439.8	DZ	114.99017	30.41108
J0740+1810	671366580221327616	SDSS J074008.45+181047.2	DQ	115.03524	18.17983

Table 5. Object names, spectral types, and coordinates – continued

J Name	Gaia source id	MWDD id	Sp. type	R.A	Dec
J0740–1724	5717278911884258176	GJ 283 A	DZA	115.08662	-17.41365
J0741+3146	880328657704678016	SDSS J074153.45+314620.4	DZ	115.47275	31.77235
J0741+4829	981804273754602496	SDSS J074122.94+482925.9	DZ	115.34558	48.49053
J0742+2422		SDSS J074226.82+242229.0	DZ	115.61175	24.37472
J0742+4348	925185708460455936	SDSS J074204.79+434835.7	DQ	115.51993	43.80994
J0743+4240	924315311863541248	GALEX 2419490867580507837	DBZ	115.94924	42.67311
J0744+1640	667952729758500224	SDSS J074456.21+164041.8	DZ	116.23425	16.67829
J0744+2701	875121993405936640	SDSS J074450.24+270132.6	DZ	116.20933	27.02572
J0744+4408		SDSS J074444.03+440845.6	DZ	116.18350	44.14603
J0744+4649	927618687178189056	SDSS J074414.66+464912.5	DZ	116.06108	46.82017
J0747+3732	919872455957849984	WD 0744+376	DZ	116.96413	37.53805
J0747+4001	920780618202557312	WD 0744+401	DZ	116.93149	40.01945
J0747+4825	933721354665822720	SDSS J074729.50+482539.7	DZ	116.87292	48.42772
J0748+2544		SDSS J074847.45+254431.7	DZ	117.19771	25.74214
J0748+3506	894591148878550144	WD 0745+352	DZ	117.09114	35.11352
J0749+3124	880840789603989504	SDSS J074942.87+312424.6	DZ	117.42865	31.40686
J0749+4343	925919460672962816	WD 0746+438	DZ	117.49277	43.71835
J0750+1328	3152307739573943040	SDSS J075059.15+132855.4	DQ	117.74646	13.48206
J0750+2329	675367939256072704	SDSS J075000.55+232945.8	DQ	117.50230	23.49610
J0751+1310	3152283103641386112	SDSS J075156.89+131018.3	DBZ	117.98704	13.17175
J0753+2332	675220948295250560	SDSS J075333.61+233200.1	DBZA	118.39009	23.53339
J0753+2741		SDSS J075306.34+274146.7	DZ	118.27642	27.69633
J0753+6613	1094930963554291968	SDSS J075307.34+661354.0	DZ	118.28067	66.23172
J0755+2112	673563468875449344	SDSS J075543.97+211219.6	DZ	118.93321	21.20547
J0756+3353	881567910387854592	SDSS J075647.77+335314.6	DZ	119.19904	33.88742
J0758+1013		SDSS J075853.46+101347.4	DZ	119.72275	10.22985
J0758+3225	881133160914293888	SDSS J075846.91+322523.4	DZ	119.69545	32.42317
J0800+2242	674322750375093376	SDSS J080003.90+224210.1	DZ	120.01625	22.70281
J0801+1344	653532394243172736	SDSS J080132.37+134410.9	DZ	120.38487	13.73638
J0801+1414	654305389572962944	SDSS J080127.10+141455.0	DBZA	120.36291	14.24867
J0801+5329	936641833642799744	SDSS J080131.16+532900.9	DZ	120.37972	53.48352
J0802+3012	877285278237322496	SDSS J080211.41+301256.8	DZ	120.54762	30.21581
J0802+4050	921482450218605440	SDSS J080234.18+405015.2	DBZA	120.64244	40.83756
J0802+4257	922800562797653248	SDSS J080211.74+425747.8	DZ	120.54892	42.96328
J0803+4502	929208615347675776	WD 0759+451	DZA	120.88109	45.04934
J0804+0750	3145823678987592576	SDSS J080405.76+075055.1	DQ	121.02394	7.84869
J0805+3832	908957092928687104	EGGR 346	DZ	121.40687	38.53688
J0805+5406	1032748903780398592	SDSS J080513.13+540615.6	DBZA	121.30480	54.10434

Table 5. Object names, spectral types, and coordinates – continued

J Name	Gaia source id	MWDD id	Sp. type	R.A	Dec
J0806+3055		SDSS J080626.70+305555.7	DZ	121.61125	30.93216
J0806+3640	907059606440721024	SDSS J080615.26+364018.1	DZ	121.56359	36.67170
J0806+3702	907085926000534400	SDSS J080607.45+370209.1	DZ	121.53104	37.03589
J0806+3747	907379121944136832	SDSS J080602.91+374720.6	DZ	121.51218	37.78910
J0807+1949	669750259471847680	SDSS J080708.48+194950.7	DQA	121.78535	19.83062
J0807+4930	934631788948274304	SDSS J080740.69+493059.7	DZ	121.91954	49.51649
J0808+2118		SDSS J080858.40+211827.1	DZ	122.24333	21.30756
J0808+2809	683943477117809024	SDSS J080830.98+280915.8	DZ	122.12908	28.15439
J0809+1034	3146882852282366208	SDSS J080910.28+103449.2	DZ	122.29283	10.58033
J0809+3106	877057614905717760	SDSS J080949.93+310642.0	DBZA	122.45810	31.11170
J0812+0942	3146529359293906816	SDSS J081252.84+094228.2	DZ	123.22021	9.70787
J0812+3614		SDSS J081240.79+361427.8	DZ	123.16996	36.24108
J0813+3047	900818263045818880	SDSS J081323.31+304744.0	DQ	123.34715	30.79562
J0813+3453		SDSS J081341.18+345327.7	DZ	123.42158	34.89103
J0813+3506	902929806407158400	SDSS J081335.75+350620.2	DZ	123.39896	35.10564
J0814+2455	682315757527779584	WD 0811+250	DQ	123.70203	24.92825
J0816+2330		SDSS J081606.19+233030.1	DZ	124.02583	23.50839
J0818+1247		SDSS J081828.12+124717.2	DZ	124.61721	12.78812
J0818–3110	5548080118369905408	WD 0816–310	DZ	124.66775	–31.17231
J0819+0027	3077580153347317248	SDSS J081937.67+002716.7	DZA	124.90696	0.45463
J0819+5732	1035126803834023296	NLTT 19272	DZ	124.81237	57.54963
J0822+3910	908497870729287424	SDSS J082224.01+391028.9	DZ	125.60009	39.17472
J0822+5202	1028460327395772416	SDSS J082221.21+520248.1	DZ	125.58838	52.04672
J0822+5203	1028460670993157504	SDSS J082223.41+520308.4	DZ	125.63922	52.05234
J0823+2015	664002940394103808	SDSS J082346.00+201557.1	DZ	125.94176	20.26594
J0825+2009	663815301863336448	SDSS J082502.20+200921.1	DZ	126.25918	20.15586
J0825+2148	664271633551603328	SDSS J082535.44+214823.9	DZ	126.39767	21.80667
J0827+1731	662082918214070144	SDSS J082708.67+173120.6	DZA	126.78614	17.52237
J0827+2857	707499173712737408	SDSS J082723.78+285729.9	DZ	126.84908	28.95833
J0827+3304	902982754763873408	SDSS J082720.59+330438.0	DZ	126.83579	33.07725
J0827+5504		SDSS J082709.96+550413.5	DZ	126.79150	55.07042
J0827+6017	1041818603399415040	SDSS J082748.76+601738.3	DQ	126.95321	60.29391
J0829+0759	599123782896409984	SDSS J082927.85+075911.4	DZ	127.36615	7.98653
J0829+3551		SDSS J082903.99+355125.7	DZ	127.26662	35.85717
J0830–0319	3066599197577336960	SDSS J083033.66–031911.0	DZ	127.64013	–3.31969
J0831+1801	659207660948780160	SDSS J083151.29+180124.1	DZ	127.96371	18.02336
J0832–0408	3065744460430556032	SDSS J083231.57–040807.8	DQ	128.13145	–4.13527
J0833+0512	3092743556860766208	SDSS J083317.64+051201.4	DBZ	128.32353	5.20040

Table 5. Object names, spectral types, and coordinates – continued

J Name	Gaia source id	MWDD id	Sp. type	R.A	Dec
J0833+3638	904025332305851904	SDSS J083310.19+363846.9	DQ	128.29246	36.64636
J0834+2422	678517387234326528	SDSS J083421.14+242212.9	DBZA	128.58807	24.37026
J0834+3927		SDSS J083430.67+392721.0	DZ	128.62779	39.45583
J0834+4641	918504427269976192	WD 0831+468	DZ	128.64445	46.69187
J0835+0906	596684963026743936	SDSS J083556.32+090619.4	DZ	128.98463	9.10545
J0836+0437	3092463658136334208	SDSS J083608.54+043757.6	DQ+DA	129.03557	4.63272
J0836+4817	1014805114533282432	WD 0833+484	DQ	129.15747	48.29796
J0837+0321	3080032407874946560	SDSS J083728.83+032129.0	DQ	129.37012	3.35806
J0838+1121	601707227200568448	SDSS J083815.75+112118.8	DQ	129.56563	11.35533
J0838+2322	666207736086203648	SDSS J083858.56+232252.9	DZ	129.74400	23.38137
J0838+5455	1030661240436915072	SDSS J083844.36+545556.2	DZ	129.68483	54.93231
J0839+2158	665206291446423040	SDSS J083935.88+215844.7	DZ	129.89953	21.97904
J0839+2618	702830819140107904	SDSS J083930.08+261804.9	DBZA	129.87535	26.30137
J0840+0237	3079168604051593856	SDSS J084020.79+023733.4	DZ	130.08663	2.62597
J0840+1306	603090206670150400	SDSS J084023.21+130624.9	DZ	130.09671	13.10692
J0840+3202		SDSS J084036.32+320209.0	DZ	130.15133	32.03586
J0840+3812		SDSS J084043.88+381231.7	DZ	130.18283	38.20881
J0840+4529	917539532801552640	US 1431	DQ	130.00509	45.49275
J0841+3329	710392886455231360	SDSS J084131.55+332915.6	DQ	130.38147	33.48763
J0841+3723	909933248799545344	CBS 78	DBZ	130.47928	37.38666
J0841+5414	1030373477628554624	SDSS J084110.08+541453.6	DZ	130.29194	54.24822
J0842+1406	609236712891803264	SDSS J084223.14+140615.9	DZ	130.59642	14.10443
J0842+1536		SDSS J084239.85+153628.8	DZ	130.66604	15.60801
J0842+3625	717705287317984000	SDSS J084200.24+362540.0	DZA	130.50102	36.42781
J0842−1347	5734737438536674432	WD 0840−136	DZ	130.70194	−13.78700
J0843+1247	602283130775405056	SDSS J084353.36+124732.0	DZ	130.97233	12.79222
J0843+5614	1031206323326386432	SDSS J084300.23+561452.8	DZ	130.75102	56.24794
J0844+5446	1030783114428872704	SDSS J084415.68+544632.4	DZ	131.06533	54.77569
J0845+1258	608294087828806016	SDSS J084551.48+125810.4	DZ	131.46459	12.96954
J0845+4115	913170417190431488	SDSS J084502.72+411547.5	DZ	131.26134	41.26322
J0845+4802		SDSS J084500.85+480223.0	DZ	131.25354	48.03975
J0845+5352	1029607839578658560	WD 0841+540	DZ	131.35417	53.86910
J0845+6143	1042192506072573312	SDSS J084531.38+614336.4	DQ	131.38057	61.72684
J0846+1024	598707239788040448	SDSS J084624.72+102406.0	DQ	131.60308	10.40176
J0846+3538	717393648787722624	Ton 949	DZ	131.68506	35.64266
J0847+1830	660222170879118208	LB 8684	DQ	131.95512	18.50487
J0847+1919	661085768542888064	SDSS J084719.85+191906.2	DQ	131.83268	19.31836
J0847+4507	917238713292494080	SDSS J084709.12+450734.9	DZ	131.78802	45.12637

Table 5. Object names, spectral types, and coordinates – continued

J Name	Gaia source id	MWDD id	Sp. type	R.A	Dec
J0848+0028	3075425797751507840	WD 0846+006	DZ	132.24116	0.47636
J0848+3548	717762977319125632	SDSS J084849.42+354858.0	DZ	132.20596	35.81613
J0848+5214	1029230844528601472	WD 0844+524	DZ	132.11670	52.23955
J0849+0710	584716401001115392	SDSS J084906.69+071030.0	DZA	132.27788	7.17501
J0849+1827	660212752014880256	WD 0846+186	DZ	132.27167	18.45876
J0849+1836	660236219716267392	SDSS J084953.98+183633.9	DZ	132.47489	18.60945
J0849+4036	912415155781038464	SDSS J084911.86+403649.6	DZ	132.29947	40.61382
J0850+0709	584707506124191616	SDSS J085030.31+070937.0	DQ	132.62629	7.16028
J0851+0538	582802361711105152	SDSS J085141.72+053852.1	DZ	132.92387	5.64781
J0851+1543	609898313949732608	WD 0848+159	DZ	132.75101	15.71723
J0852+0428	581820218658061952	SDSS J085239.65+042804.4	DQ	133.16526	4.46791
J0852+1124		SDSS J085214.39+112403.7	DZ	133.05996	11.40103
J0852+2316	689246765295367808	SDSS J085235.43+231644.3	DQ	133.14759	23.27900
J0852+3402	716230640363477760	SDSS J085217.60+340211.3	DZ	133.07333	34.03649
J0852+5124		SDSS J085242.75+512435.3	DZ	133.17812	51.40981
J0852+5223	1017236379556868352	SDSS J085212.53+522336.2	DQ	133.05217	52.39337
J0853+1603	611387460714600064	SDSS J085329.09+160342.1	DZ	133.37121	16.06169
J0854+0603	583593696549710080	SDSS J085454.99+060345.7	DZ	133.72913	6.06272
J0854+1847	660375033059366400	SDSS J085423.47+184733.8	DZ	133.59777	18.79277
J0855+0639	584402318633098624	LSPM J0855+0639	DQ	133.77770	6.65127
J0855+5438		SDSS J085515.78+543848.3	DZ	133.81575	54.64675
J0856+4513	1010184519997258240	SDSS J085626.94+451336.9	DQ	134.11228	45.22695
J0857+0603	583604897824754688	SDSS J085709.01+060357.4	DQ	134.28755	6.06599
J0857+1438	608798110831521280	SDSS J085750.55+143812.9	DZ	134.46061	14.63697
J0857+2630	691813197233587712	SDSS J085749.95+263026.5	DZ	134.45812	26.50736
J0859+3257	712888090655562624	EGGR 182	DQ	134.81131	32.95338
J0859+5732	1037518722660955392	WD 0856+577	DBZ	134.98828	57.54723
J0859+6016	1038076351151065088	G 234–51	DQ	134.89893	60.27066
J0900+0331	578379365734698752	SDSS J090051.91+033149.3	DQZ	135.21635	3.53037
J0900+1020	603543888359619968	SDSS J090041.82+102047.5	DZ	135.17425	10.34653
J0901+0752	584968773279756032	SDSS J090146.87+075206.8	DZ	135.44529	7.86858
J0901+1113		SDSS J090159.01+111314.3	DZ	135.49587	11.22064
J0901+5337	1017732705977200640	SDSS J090108.41+533749.0	DZ	135.28504	53.63028
J0901+5751	1037553185478639360	WD 0858+580	DQ	135.49130	57.85997
J0902+5037	1016048043709449088	WD 0858+508	DQ	135.50152	50.62307
J0903–0120		SDSS J090322.57–012014.1	DZ	135.84404	-1.33728
J0904+3954	719439423313644672	SDSS J090449.72+395416.4	DQ	136.20724	39.90461
J0904–0029	3842783861947967232	2SLAQ J090451.98–002951.6	DZ	136.21636	-0.49764

Table 5. Object names, spectral types, and coordinates – continued

J Name	Gaia source id	MWDD id	Sp. type	R.A	Dec
J0905+0133	577045589410219904	WD 0902+017	DZ	136.32380	1.55211
J0905+0846	591125419920174976	SDSS J090522.38+084657.9	DZ	136.34325	8.78278
J0905+0904	591207406550605312	EGGR 532	DQ	136.31164	9.07396
J0905+5235	1017429511350062464	WD 0902+527	DZ	136.48424	52.59251
J0906+1141		SDSS J090652.19+114149.9	DZ	136.71750	11.69722
J0906+1628	610909070077557632	SDSS J090605.37+162835.5	DZ	136.52237	16.47653
J0906+5956	1039309620944640256	SDSS J090655.64+595654.1	DZ	136.73189	59.94849
J0907+2533	688417016269720704	SDSS J090707.34+253313.4	DZ	136.78049	25.55389
J0908+4119		SDSS J090814.52+411918.3	DZ	137.06050	41.32177
J0908+5136	1016558973019185664	SDSS J090803.35+513633.1	DZ	137.01403	51.60914
J0909−0045	3842065090580902144	2SLAQ J090945.07−004559.3	DZ	137.43779	−0.76648
J0910+1045	591988265964810112	SDSS J091056.79+104541.8	DZ	137.73662	10.76164
J0911+2433		SDSS J091142.33+243306.6	DZ	137.92637	24.55183
J0912−0128		SDSS J091211.80−012813.0	DZ	138.04917	−1.47028
J0913+2627	688954024621015040	SDSS J091322.38+262752.0	DZ	138.34321	26.46444
J0913+3116	699920381797443712	LP 313−27	DZ	138.42393	31.26954
J0913+4127		SDSS J091356.05+412728.6	DZ	138.48358	41.45797
J0915+2019	636095892172507264	SDSS J091500.58+201903.0	DQ	138.75242	20.31753
J0916+0110		WD 0914+013	DZ	139.16886	1.16844
J0916+1011	591040864898749312	PG 0913+104	DQ	139.01120	10.18630
J0916+2540	687914432080614528	SDSS J091621.36+254028.4	DZ	139.08878	25.67475
J0916−0212	3838621076566036736	SDSS J091633.07−021256.1	DZ	139.13779	−2.21558
J0917+2146		SDSS J091703.40+214602.4	DZ	139.26417	21.76733
J0917+2224		SDSS J091722.79+222437.2	DZ	139.34496	22.41033
J0918+4843	1012116705524378112	SDSS J091830.27+484323.0	DQ	139.62616	48.72318
J0919+0236	3845201035182583424	WD 0916+028	DQ	139.84244	2.60141
J0920+3603	714642425880664448	SDSS J092046.95+360353.5	DQ	140.19553	36.06497
J0921+1204	593551801563915520	SDSS J092110.80+120411.1	DBZA	140.29503	12.06977
J0921+3421	702332431134751360	SDSS J092153.46+342136.9	DQ	140.47275	34.36030
J0922+2007	637318274224686720	SDSS J092249.95+200747.1	DZA	140.70826	20.12975
J0922+2928	695775871499726208	WD J0922+2928	DQ	140.53417	29.46971
J0923+1842		[VV2010] J092356.5+184242	DQ	140.98545	18.71184
J0923+4823		SDSS J092326.28+482318.1	DZ	140.85950	48.38836
J0924+4301		SDSS J092450.03+430136.4	DZ	141.20846	43.02680
J0925+2256		SDSS J092515.41+225634.8	DZ	141.31421	22.94300
J0925+3130	700557819367554432	SDSS J092523.10+313019.0	DZ	141.34627	31.50545
J0925+5256	1019891219101344256	SDSS J092525.52+525651.9	DQ	141.35638	52.94780
J0926+0605		SDSS J092638.40+060532.3	DQ	141.66008	6.09208

Table 5. Object names, spectral types, and coordinates – continued

J Name	Gaia source id	MWDD id	Sp. type	R.A	Dec
J0926+4725	819574013135499776	SDSS J092613.45+472521.1	DQ	141.55608	47.42256
J0926+6212	1039978089654509952	SDSS J092627.59+621201.7	DQ	141.61507	62.20044
J0928+1801	631623697346239744	SDSS J092832.62+180149.0	DZ	142.13595	18.03035
J0928+2638	694176429973819520	SDSS J092825.16+263856.3	DQ+DA	142.10482	26.64904
J0928+6124	1039177168448595328	WD 0924+616	DZ	142.00745	61.40946
J0929+3310	701307621874580864	SDSS J092909.03+331011.7	DQ	142.28768	33.16993
J0929+4247	814515018401000064	SDSS J092932.50+424757.9	DZ	142.38542	42.79942
J0930+2601	646091930337657472	SDSS J093046.01+260136.2	DZA	142.69171	26.02675
J0930+2959	697155586793611648	SDSS J093017.14+295940.7	DQ	142.57157	29.99471
J0930+3013	697184758211607680	GALEX 2736932956989820904	DZA	142.62391	30.22338
J0931+0730	586292933172097408	SDSS J093130.31+073054.6	DBZ	142.87629	7.51517
J0931+1210		SDSS J093152.85+121022.1	DZ	142.97021	12.17281
J0931+1230		SDSS J093107.94+123020.4	DQ	142.78308	12.50567
J0932+4856	825789513712009216	SDSS J093210.54+485601.7	DZ	143.04397	48.93381
J0933+6334		SDSS J093320.01+633441.2	DZ	143.33350	63.57805
J0934+0822	587953535032442624	SDSS J093423.17+082225.3	DZ	143.59663	8.37373
J0934+1158	613987187238694144	SDSS J093448.86+115854.3	DQ	143.70375	11.98174
J0934+2626	646155255335699584	SDSS J093414.16+262641.2	DZ	143.55898	26.44475
J0934+5632	1025033665052512000	SDSS J093412.30+563232.8	DZ	143.55131	56.54237
J0935+0037	3841058384606465664	SDSS J093545.45+003750.8	DZ	143.93937	0.63080
J0935+2417	644881986510775680	SDSS J093537.57+241708.7	DQ	143.90640	24.28569
J0935+2420	644883773217189632	SDSS J093552.63+242042.8	DZ	143.96935	24.34527
J0935+4450	818151103353879808	US 739	DZ	143.78716	44.84049
J0936+0607	3852516395279467264	SDSS J093638.07+060710.0	DQ	144.15867	6.11948
J0936+1815	633002244409170688	SDSS J093635.96+181511.9	DBZA	144.14983	18.25333
J0937+2842	696007387416777856	SDSS J093708.92+284205.7	DBZA	144.28714	28.70152
J0937+3646	798980568368200320	SDSS J093704.99+364647.2	DZA	144.27087	36.77975
J0937+5228	1020417502917748096	WD 0933+526	DZ	144.32982	52.46731
J0938+6343	1064557259776082944	SDSS J093855.08+634314.4	DZ	144.72962	63.72057
J0939+4136	813599709331004288	SDSS J093916.04+413612.9	DZ	144.81683	41.60358
J0939+5019	826349066346658304	SDSS J093944.58+501917.6	DZ	144.93579	50.32156
J0939+5201	1020158400426591872	[VV98b] J093937.9+520146	DQ	144.90700	52.02873
J0939+5550	1022128244227188224	WD 0936+560	DZA	144.92632	55.84687
J0940+0210	3847322577227869952	WD 0937+023	DQ	145.01933	2.17295
J0940+6136	1063014099502601088	GALEX 2485743040223777830	DZ	145.10506	61.61359
J0940+6422	1064649481314008832	SDSS J094024.00+642201.9	DZ	145.10025	64.36723
J0941+0901	588332900903805824	2MASS J09411519+0901549	DQ	145.31326	9.03189
J0941+4414	820840165198320640	US 846	DQ	145.40866	44.24954

Table 5. Object names, spectral types, and coordinates – continued

J Name	Gaia source id	MWDD id	Sp. type	R.A	Dec
J0941+5022	826323257887507584	SDSS J094148.75+502214.5	DZ	145.45318	50.37072
J0942+0743	3854236409423135488	SDSS J094210.50+074354.8	DZ	145.54380	7.73189
J0942+5755	1025583077264885248	WD 0938+581	DZ	145.52589	57.93218
J0944+3939	801200997741011840	SDSS J094415.33+393943.0	DZ	146.06391	39.66195
J0944+4408	820167229722388864	SDSS J094451.59+440856.7	DZ	146.21500	44.14909
J0944−0039	3827999107046766720	WD 0941−004	DBZ	146.13033	−0.65938
J0945+0846	3854957448532256000	SDSS J094530.20+084624.8	DZ	146.37589	8.77356
J0945+5558	1022098175160994560	WD 0941+562	DQ	146.33656	55.97721
J0946+2024	639674321484637312	SDSS J094648.94+202423.2	DZ	146.70392	20.40647
J0947+1916	627435932433330048	SDSS J094757.96+191611.6	DZ	146.99150	19.26984
J0947+4238	819704575845347328	SDSS J094743.09+423841.3	DZ	146.92959	42.64483
J0948+1232	613553056239392768	LSPM J0948+1232	DQ	147.24135	12.54527
J0948+3008	744609512219878400	SDSS J094813.74+300851.2	DZ	147.05731	30.14761
J0950+3238	793334404360693632	CSO 20	DQA	147.51397	32.64153
J0950+4716	821800829123228544	SDSS J095023.70+471603.7	DZ	147.59875	47.26772
J0950+4848	826488184631550208	SDSS J095053.05+484811.8	DZ	147.72104	48.80328
J0950+5315	1020653077580086784	EGGR 251	DQ	147.57142	53.25412
J0951+4033	807280785942808320	SDSS J095119.85+403322.4	DZA	147.83278	40.55627
J0951+6243	1063462764670566016	WD 0947+629	DQ	147.90664	62.73020
J0953+1510	616712429888284288	SDSS J095339.13+151017.7	DZ	148.41304	15.17161
J0953+1719	620070750715749504	SDSS J095354.97+171953.1	DZ	148.47904	17.33142
J0954+1814	626343705070034432	SDSS J095449.30+181454.7	DBZA	148.70542	18.24853
J0954+3347	795177254568857600	SDSS J095406.43+334716.5	DZ	148.52687	33.78802
J0954+5635	1046044748139868544	SDSS J095435.86+563518.2	DZ	148.64941	56.58836
J0955+5233	828417999336648320	SDSS J095523.49+523350.3	DZ	148.84791	52.56391
J0956+5912	1049598202217308160	WD 0953+594	DZA	149.18811	59.21129
J0957+2822	743306350418730112	SDSS J095731.02+282232.4	DZ	149.37924	28.37571
J0958+0550	3850187217335099904	SDSS J095854.96+055021.3	DBAZ	149.72906	5.83906
J0959+2556	643650361688870656	SDSS J095934.77+255618.8	DZ	149.89489	25.93849
J0959+4537	821981423908534656	SDSS J095934.95+453725.4	DQ	149.89563	45.62374
J1000+1005		SDSS J100059.82+100531.7	DQ	150.24942	10.09192
J1000+3518	795577030124098304	GALEX 2684261956267803251	DBZA	150.15443	35.30611
J1000+4420	808316555959581568	US 1170	DBZA	150.00505	44.33787
J1000−0230		SDSS J100031.86−023050.0	DZ	150.13275	−2.51389
J1002+0313	3836479227914477184	SDSS J100237.36+031325.6	DZ	150.65568	3.22378
J1003+1421		SDSS J100309.89+142117.4	DZ	150.79121	14.35483
J1004+0451	3849136565255477760	SDSS J100421.25+045117.2	DZ	151.08856	4.85480
J1004+4231	807172995146946816	SDSS J100406.63+423151.5	DZ	151.02772	42.53097

Table 5. Object names, spectral types, and coordinates – continued

J Name	Gaia source id	MWDD id	Sp. type	R.A	Dec
J1005+1746		SDSS J100516.78+174635.3	DZ	151.31992	17.77647
J1005+2032	628573377212774656	SDSS J100553.03+203242.5	DZ	151.47096	20.54517
J1005+2244		SDSS J100537.43+224403.1	DZ	151.40596	22.73421
J1005+2655	739870788898835584	SDSS J100509.60+265524.0	DZ	151.29010	26.92341
J1005−0114	3830084537007178880	2QZ J100523.5−011429	DQ	151.34833	−1.24131
J1006+1752	623291048475264768	SDSS J100609.16+175221.3	DZ	151.53817	17.87261
J1006+6116	1050383902059149184	SDSS J100617.24+611613.3	DZ	151.57190	61.27027
J1008+0248	3836544614496629248	WD 1005+030	DZ	152.09894	2.81114
J1008+4349	808795706807426688	SDSS J100817.03+434931.7	DBZA	152.07106	43.82549
J1009+3337	747179998603216640	SDSS J100953.25+333754.4	DZ	152.47187	33.63181
J1010+2119		SDSS J101048.43+211944.2	DZ	152.70179	21.32897
J1010+2300	630102488648801024	SDSS J101009.54+230017.5	DQ	152.53967	23.00494
J1010+3948	803490735004698496	SDSS J101007.84+394852.2	DZA	152.53271	39.81453
J1012+0040	3831946697387407232	SDSS J101219.90+004019.7	DQ	153.08290	0.67214
J1012+4435	808936302560071040	SDSS J101217.24+443529.1	DZ	153.07190	44.59143
J1012−1843	5669427512997660800	WD 1009−184	DZ	153.00780	−18.72591
J1013+4350	808657370204219904	SDSS J101336.56+435054.7	DQ	153.40239	43.84851
J1013−0251		SDSS J101309.20−025105.4	DZ	153.28833	−2.85153
J1014+2827		SDSS J101451.15+282701.6	DZ	153.71312	28.45046
J1015+3518	753390452593714688	SDSS J101509.57+351813.8	DQ	153.78987	35.30393
J1015+4141	805192602906283520	SDSS J101558.21+414131.7	DZA	153.99258	41.69215
J1015+6327		SDSS J101506.59+632722.2	DZ	153.77746	63.45618
J1017+1948	625133520725582208	SDSS J101704.38+194848.3	DBZA	154.26827	19.81342
J1017+2419	725630326616623872	SDSS J101750.24+241911.6	DZ	154.45935	24.31999
J1017+3447	752599079099409408	SDSS J101711.54+344710.5	DZ	154.29818	34.78637
J1017+3736	754237557583214336	SDSS J101750.38+373637.5	DQ	154.45969	37.61052
J1018+0344	3860024719667494912	SDSS J101805.16+034435.6	DZ	154.52157	3.74324
J1018+0838	3875789001991057536	2MASS J10180002+0838206	DQ	154.50015	8.63904
J1018+3708	754117577672241920	SDSS J101800.81+370840.6	DBZ	154.50350	37.14464
J1018+3726	754220107131130624	CBS 127	DZA	154.66160	37.44956
J1019+2045		SDSS J101959.51+204553.4	DZ	154.99800	20.76486
J1019+3535		SDSS J101924.73+353527.6	DZ	154.85308	35.59103
J1019+3752	754266832080416512	SDSS J101929.78+375218.9	DBZA	154.87410	37.87193
J1022+2845	741044173964155136	USNO−B1.0 1187−00180823	DQ	155.54874	28.75244
J1023−0014		SDSS J102306.10−001434.8	DZ	155.77542	−0.24300
J1024+1014		SDSS J102438.05+101410.5	DZ	156.15854	10.23625
J1024+2227		SDSS J102421.89+222747.1	DZ	156.09121	22.46310
J1024+4531	833191803946601344	SDSS J102414.83+453109.9	DZ	156.06179	45.51942

Table 5. Object names, spectral types, and coordinates – continued

J Name	Gaia source id	MWDD id	Sp. type	R.A	Dec
J1024–0017		2SLAQ J102456.50–001732.4	DZ	156.23541	–0.29232
J1025+2016		SDSS J102540.75+201613.8	DZ	156.41979	20.27050
J1026+1948	624581428448988288	SDSS J102607.59+194808.0	DZ	156.53155	19.80217
J1026+2646		SDSS J102620.95+264611.6	DZ	156.58729	26.76991
J1026+2725	728685628908570240	SDSS J102635.07+272507.6	DQ	156.64610	27.41882
J1026+5807	1047132925349510784	LSPM J1026+5807	DQ	156.64922	58.12079
J1027+1218	3883495444630204672	SDSS J102705.07+121836.0	DQ	156.77130	12.31006
J1027+4532	830203606220330240	SDSS J102756.87+453223.3	DZ	156.98707	45.53980
J1028+2507		SDSS J102834.08+250724.6	DZ	157.14200	25.12352
J1028+2537	727648003464905728	SDSS J102836.21+253732.8	DQ	157.15092	25.62570
J1028–0135	3782563919332193792	2QZ J102807.8–013553	DBZA	157.03270	–1.59797
J1029+1227		SDSS J102956.06+122729.6	DZ	157.48358	12.45825
J1029+2013		SDSS J102930.40+201318.8	DZ	157.37667	20.22192
J1029+3103	747729754417122304	SDSS J102955.65+310353.6	DZ	157.48187	31.06489
J1030+0026	3855110692965549312	2QZ J103024.3+002613	DZ	157.60118	0.43729
J1031+0936	3870096319192789120	SDSS J103123.91+093657.8	DZ	157.84967	9.61602
J1031+1203	3883044266905679488	SDSS J103126.19+120340.4	DZ	157.85916	12.06126
J1031+2217	722275854075503616	SDSS J103102.52+221714.7	DQ	157.76050	22.28742
J1032+1338		SDSS J103205.15+133833.4	DZ	158.02150	13.64262
J1032+2101	720841884754600960	SDSS J103205.85+210131.1	DQ	158.02437	21.02531
J1032+3509	751262111614979328	SDSS J103242.42+350937.3	DQ	158.17683	35.16045
J1032+4519	830034079569393536	SDSS J103210.68+451929.9	DQ	158.04467	45.32518
J1032–0240	3781631086795267328	2QZ J103257.4–024012	DBZA	158.23946	–2.66978
J1033+1809	3890742944243942528	SDSS J103352.89+180935.3	DZ	158.47037	18.15980
J1033+2837	729218617173430784	SDSS J103310.69+283707.5	DZ	158.29454	28.61867
J1033+6247	1052295059426254208	SDSS J103300.12+624747.9	DZ	158.25054	62.79664
J1034+2245	721648380828681984	WD 1032+230	DZ	158.68095	22.76358
J1036+4837	834176141731355392	SDSS J103651.09+483754.0	DZA	159.21293	48.63169
J1037+0709	3862624171313960960	SDSS J103729.82+070902.7	DBZA	159.37429	7.15077
J1037+4341	828871861427262464	PB 424	DZ	159.48588	43.68460
J1038+0432	3858626690632865664	SDSS J103839.01+043223.8	DZ	159.66254	4.53997
J1038+1342	3884773386379596416	SDSS J103806.75+134225.3	DZ	159.52812	13.70706
J1038–0036		WD 1035–003	DZ	159.53837	–0.60617
J1039+2648	725041881733642112	SDSS J103923.87+264822.9	DBZA	159.84949	26.80636
J1039+4612	830469417454250496	SDSS J103941.85+461224.3	DZ	159.92458	46.20681
J1040+0635	3859527160591518464	SDSS J104052.40+063519.7	DQ	160.21833	6.58881
J1040+1349	3884858083134254848	SDSS J104028.33+134935.5	DZ	160.11804	13.82656
J1040+2408	723361209490895744	SDSS J104046.48+240759.5	DZ	160.19382	24.13338

Table 5. Object names, spectral types, and coordinates – continued

J Name	Gaia source id	MWDD id	Sp. type	R.A	Dec
J1041+2200	3989437719293787776	SDSS J104137.38+220032.4	DQ	160.40575	22.00897
J1041+2746	734116705248896128	SDSS J104119.39+274617.6	DZ	160.33073	27.77157
J1041+3432	750285088159627392	SDSS J104130.65+343240.7	DZ	160.37767	34.54469
J1041+4110	779606383212607104	SDSS J104156.42+411013.1	DZ	160.48508	41.17031
J1042+5833	855241272691342336	SDSS J104204.27+583347.7	DQ	160.51788	58.56326
J1043+0303	3857475197016034432	WD 1041+033	DQ	160.94469	3.05513
J1043+3516	750713313579071232	SDSS J104319.84+351641.6	DZ	160.83279	35.27836
J1044+2023	3987528623509801984	SDSS J104433.42+202313.0	DZ	161.13942	20.38692
J1044+2143	3989359653967394816	SDSS J104414.35+214337.3	DZ	161.05979	21.72706
J1045+2134	3989166483518724480	SDSS J104505.66+213447.2	DQ	161.27358	21.57978
J1045+5254	849175610638319616	SDSS J104504.99+525443.3	DBZ	161.27079	52.91203
J1045+6009	855674583352060544	SDSS J104552.51+600921.5	DZ	161.46886	60.15590
J1045+6254	1055070364214118272	SDSS J104511.21+625442.3	DZ	161.29676	62.91173
J1046+1329	3884925157638345856	SDSS J104658.12+132911.3	DZ	161.74217	13.48649
J1046+2424	723524383888419840	SDSS J104652.44+242438.6	DZ	161.71861	24.41086
J1047+5219	837084590505236864	SDSS J104708.84+521935.4	DZ	161.78688	52.32647
J1047+5912	855387061061127168	PSO J161.8956+59.2131	DQ	161.89590	59.21366
J1048+2623	729995971891636992	SDSS J104849.77+262333.6	DZ	162.20732	26.39267
J1049+1659	3982534641696914688	SDSS J104906.61+165923.6	DQA	162.27753	16.98992
J1049+2128		SDSS J104955.29+212832.6	DZ	162.48038	21.47574
J1049+5154	836823151552466304	USNO–B1.0 1419–00233520	DZ	162.29808	51.90662
J1049–0007	3806278083041021312	[VV2006] J104915.1–000707	DZA	162.31276	–0.11840
J1050+3138	736735600211990144	SDSS J105019.09+313820.1	DZ	162.57952	31.63895
J1051+2751		SDSS J105152.70+275118.7	DZ	162.96958	27.85519
J1051+5947		SDSS J105111.87+594735.2	DZ	162.79925	59.79287
J1051–0303		SDSS J105145.62–030359.3	DZ	162.94008	–3.06647
J1052+0659	3864644627009594368	SDSS J105221.56+065915.4	DZ	163.08985	6.98763
J1052+5911	861320712999661568	SBSS 1049+594	DQ	163.20250	59.19730
J1055+3509	762519594559623168	GALEX 2684543414064644977	DZ	163.93342	35.15739
J1055+3725	774872607698171392	SDSS J105533.73+372542.7	DZ	163.89058	37.42855
J1055+4115	778285113833405056	SDSS J105523.29+411550.1	DZ	163.84710	41.26391
J1056+0128	3808050667584060672	SDSS J105601.50+012825.0	DZA	164.00628	1.47358
J1056+5714	857165662854257792	PSO J164.1738+57.2466	DZ	164.17387	57.24697
J1056–0004	3804750723950984448	SDSS J105616.89–000449.5	DZA	164.07032	–0.08043
J1057+1053		SDSS J105741.62+105305.3	DZ	164.42342	10.88483
J1057–0413	3789156870225942656	G 163–28	DZ	164.44838	–4.22504
J1058+1124	3871463179649436544	SDSS J105855.32+112440.2	DZ	164.73050	11.41117
J1058+2846	732964137889540992	SDSS J105817.66+284609.3	DQ	164.57346	28.76942

Table 5. Object names, spectral types, and coordinates – continued

J Name	Gaia source id	MWDD id	Sp. type	R.A	Dec
J1058+3022	733397830802440704	SDSS J105815.65+302225.8	DZ	164.56530	30.37378
J1058+3143	736915954478557824	SDSS J105826.60+314358.3	DZ	164.61084	31.73290
J1058+3440	762250454729037440	SDSS J105854.34+344018.0	DQ	164.72642	34.67169
J1058+6041	861745571164680064	SDSS J105853.70+604136.8	DZ	164.72379	60.69358
J1059+5038		SDSS J105910.24+503827.5	DZ	164.79267	50.64099
J1100+1439		SDSS J110049.52+143915.4	DZ	165.20633	14.65428
J1100+1758	3983742627018262656	GALEX 2698265319179290502	DQA	165.24184	17.96865
J1101+2730		SDSS J110141.48+273017.9	DZ	165.42283	27.50499
J1101+5218	836517723541888000	SDSS J110140.41+521806.6	DQ	165.41809	52.30202
J1102+0214	3808536101967194368	SDSS J110234.21+021459.2	DZ	165.64254	2.24979
J1102+1755	3983562478910025728	SDSS J110251.37+175552.2	DZ	165.71404	17.93117
J1102+2653	730298028350540288	SDSS J110202.02+265335.5	DZ	165.50843	26.89324
J1102+2827		SDSS J110216.09+282730.7	DZ	165.56708	28.45854
J1103+4144	778183305928430592	SDSS J110304.15+414434.9	DZ	165.76735	41.74307
J1104+0711	3818299730867320704	SDSS J110438.38+071129.8	DZ	166.15996	7.19165
J1104+1657		SDSS J110426.37+165723.0	DZ	166.10987	16.95642
J1104+2439	3995629412866477696	SDSS J110446.03+243933.3	DZA	166.19186	24.65930
J1104+6426	1055640907669798272	SDSS J110456.77+642606.2	DZ	166.23663	64.43498
J1104−1607	3562462135495771648	SDSS J110424.47−160717.0	DZ	166.10201	−16.12136
J1105+0228		SDSS J110556.17+022849.0	DZ	166.48408	2.48029
J1105+1949		SDSS J110550.98+194938.7	DZ	166.46242	19.82744
J1105+3801	763282281967678848	SDSS J110502.99+380111.3	DZ	166.26249	38.01979
J1106+0104	3805152217493874304	SDSS J110608.27+010451.7	DZ	166.53446	1.08103
J1106−0039	3803570123340582400	2QZ J110644.2−003928	DZ	166.68450	−0.65767
J1107+4059	777512951728187392	SDSS J110759.46+405910.8	DQ	166.99806	40.98633
J1108+1349	3968318334306923264	SDSS J110831.47+134950.7	DQ	167.13112	13.83078
J1108+3033	732899545876664832	SDSS J110836.29+303304.6	DZ	167.15122	30.55134
J1109+2112		SDSS J110930.19+211241.0	DZ	167.37563	21.21136
J1109+4249	778707154499553792	SDSS J110912.21+424956.0	DQ	167.30078	42.83225
J1112+0700	3818095805815429760	SDSS J111215.06+070052.4	DZ	168.06275	7.01460
J1113+2228	3991951069730422784	SDSS J111349.33+222842.9	DZ	168.45558	22.47854
J1113+4455	785117341649573248	SDSS J111336.00+445505.1	DQ	168.40016	44.91819
J1113+4550	788216246452663040	SDSS J111350.59+455051.2	DZ	168.46073	45.84758
J1114+2957		SDSS J111409.30+295730.3	DZ	168.53871	29.95822
J1115+1720		SDSS J111549.85+172056.8	DZ	168.95771	17.34914
J1116−1228	3565086394873693184	SDSS J111639.67−122859.0	DQ	169.16537	−12.48307
J1117+0826		SDSS J111733.31+082605.3	DZ	169.38879	8.43483
J1117+3311	757581378601957376	SDSS J111741.76+331121.1	DZ	169.42405	33.18922

Table 5. Object names, spectral types, and coordinates – continued

J Name	Gaia source id	MWDD id	Sp. type	R.A	Dec
J1118+0838		SDSS J111817.14+083801.9	DZ	169.57142	8.63386
J1118-0314	3790040465258127616	LAWD 35	DQ	169.56277	-3.23488
J1120+1200	3964058791901412608	SDSS J112014.78+120053.3	DQ	170.06158	12.01481
J1120+4252	783773326123820928	SDSS J112023.61+425200.7	DQ	170.09848	42.86685
J1120-1102	3565714697049767936	SDSS J112010.61-110259.5	DQ	170.04430	-11.04992
J1121+1417	3966668139152301568	SDSS J112125.75+141713.6	DZA	170.35727	14.28716
J1122+5041	838344081075034240	WD 1120+509	DZA	170.74312	50.69632
J1123+3026	4023114386062671872	SDSS J112320.76+302634.3	DZ	170.83654	30.44270
J1123+3347	759151210623548672	SDSS J112348.02+334713.7	DQ	170.95008	33.78717
J1125+2853	4022064867854157696	SDSS J112505.92+285311.0	DZ	171.27473	28.88637
J1125+3823	761097999039664896	SDSS J112544.76+382316.0	DZ	171.43667	38.38782
J1126+3245		SDSS J112634.19+324530.2	DQ	171.64240	32.75822
J1126+4419	784290543265061504	SDSS J112604.28+441938.6	DQ	171.51805	44.32738
J1126+5241	839578798273255040	SDSS J112617.16+524155.1	DZA	171.57158	52.69865
J1127-0138	3796601418644353536	2QZ J112730.3-013801	DZ	171.87686	-1.63386
J1129+2917	4021995632981461760	SDSS J112909.12+291705.0	DZ	172.28806	29.28471
J1129-0152	3793667612383707904	SDSS J112956.98-015229.5	DZA	172.48745	-1.87490
J1130+1036	3915497520830530688	SDSS J113001.60+103614.8	DZ	172.50671	10.60415
J1130-0734	3592850369145726976	SDSS J113027.20-073451.8	DQ	172.61330	-7.58097
J1131+0736	3910703753212366080	SDSS J113127.45+073627.8	DQ	172.86443	7.60775
J1131+1845	3977321925788597504	SDSS J113104.23+184558.8	DQ	172.76778	18.76641
J1131+2315	3980618845764418432	SDSS J113146.45+231542.4	DZ	172.94345	23.26180
J1132+1002		SDSS J113238.95+100207.9	DZ	173.16229	10.03556
J1132+3323		SDSS J113209.59+332353.0	DZ	173.03996	33.39806
J1132+4705	785774510304049280	SDSS J113208.77+470523.3	DZ	173.03657	47.08982
J1132-0106	3794102366153078016	SDSS J113256.01-010622.7	DZ	173.23338	-1.10633
J1133+0610	3909508996390412032	SDSS J113300.18+061037.9	DZ	173.25102	6.17723
J1133+1804	3974222196351837056	SDSS J113319.76+180443.4	DZ	173.33233	18.07875
J1133+1900	3977309075246562944	SDSS J113300.58+190056.4	DQ	173.25242	19.01569
J1133+6331	863792964894515712	WD 1131+637	DQ	173.49982	63.52039
J1134+1236	3917474786334558976	SDSS J113426.79+123652.5	DZ	173.61162	12.61461
J1134+1542		SDSS J113410.85+154245.9	DZ	173.54525	15.71276
J1134+5928	858433945220510848	SDSS J113408.45+592846.1	DZ	173.53535	59.47945
J1137+0343	3800902265750001664	USNO-B1.0 0937-00210798	DZ	174.29715	3.72396
J1137-0023	3794254579793954688	2QZ J113728.3-002343	DZ	174.36813	-0.39533
J1138-0130		SDSS J113818.90-013044.4	DZ	174.57875	-1.51233
J1139+6239	862907411357721088	SDSS J113912.67+623908.9	DZ	174.80285	62.65242
J1139+6737	1058091311066785280	SDSS J113939.48+673737.4	DZ	174.91458	67.62708

Table 5. Object names, spectral types, and coordinates – continued

J Name	Gaia source id	MWDD id	Sp. type	R.A	Dec
J1139–0132		SDSS J113953.58–013240.8	DZ	174.97325	-1.54467
J1140+0735	3910091810567523456	SDSS J114059.85+073530.1	DQ	175.24938	7.59174
J1140+1540	3972370343892609280	SDSS J114056.78+154014.3	DQ	175.23668	15.67069
J1140+1824	3974116235214146432	SDSS J114006.35+182402.3	DQ	175.02664	18.40067
J1140+5328	840377937068042752	SDSS J114054.87+532827.4	DZA	175.22870	53.47426
J1141+3836	766499483055284864	SDSS J114136.53+383611.9	DQ	175.40208	38.60329
J1142+0352	3896760021627103360	SDSS J114256.66+035207.9	DQ	175.73608	3.86889
J1142+1104	3916465060998691328	SDSS J114209.56+110438.6	DZ	175.53983	11.07742
J1143+1928	3975786629599506816	SDSS J114339.16+192855.3	DZ	175.91311	19.48209
J1143–0145	3793121807939483776	2QZ J114310.2–014529	DZ	175.79281	-1.75797
J1144+1218	3916712206301454720	SDSS J114441.92+121829.2	DZ	176.17454	12.30815
J1144+3259	4024772621396103808	SDSS J114402.34+325911.7	DZ	176.00984	32.98665
J1144+3720	4032793627440382592	SDSS J114408.05+372007.8	DZ	176.03354	37.33550
J1145+6619	1056978016888546048	SDSS J114551.29+661923.5	DZ	176.46369	66.32313
J1145–6450	5332606522595645952	GJ 440	DQ	176.42882	-64.84152
J1147+4928	787923780658695680	USNO–B1.0 1394–00221747	DZ	176.80098	49.46696
J1147+5429		SDSS J114709.09+542940.8	DZ	176.78792	54.49463
J1148+4109	768373570560162176	SDSS J114804.59+410928.5	DZ	177.01898	41.15797
J1148+4124	768406070577604864	SDSS J114850.37+412429.0	DZ	177.20990	41.40807
J1148+5708	845306291781647360	SDSS J114830.05+570840.6	DZ	177.12539	57.14472
J1148–0126	3794415245931016320	WD 1146–011	DQ	177.21536	-1.43686
J1149+0519	3897357571836998784	SDSS J114944.95+051947.7	DZ	177.43729	5.32994
J1149+4943	787933057786712960	SDSS J114901.99+494328.2	DZ	177.25829	49.72440
J1150+4928	787888523268272000	SDSS J115015.74+492843.7	DZ	177.56554	49.47872
J1151+4527	773341881353587968	SDSS J115149.92+452729.8	DQ	177.95822	45.45820
J1151–2732	3487220772397809536	WD 1149–272	DQ	177.90044	-27.53920
J1152+2834	4019646766906456448	SDSS J115243.92+283419.8	DZ	178.18297	28.57224
J1152+5101		SDSS J115207.15+510126.2	DZ	178.02983	51.02389
J1155+4327	769790390076725376	CSO 1241	DZ	178.94766	43.46428
J1156+2212	4000563990987070592	LSPM J1156+2212	DQ	179.01444	22.20827
J1157+6138		SDSS J115748.35+613845.9	DZ	179.45146	61.64610
J1158+0454	3896383782491848192	SDSS J115818.76+045447.5	DZ	179.57817	4.91321
J1158+1845	3927086888783407616	SDSS J115809.38+184557.3	DZ	179.53908	18.76592
J1158+4712	774517602881392256	SDSS J115822.32+471214.9	DZ	179.59309	47.20416
J1158+5942	846585951516974976	SDSS J115809.88+594210.3	DZ	179.54125	59.70279
J1159+2059		SDSS J115934.82+205903.1	DZ	179.89508	20.98421
J1159+4045	4035112669261814912	SDSS J115958.93+404541.7	DZ	179.99557	40.76163
J1159–4629	5377861592235273856	WD 1157–462	DQ	179.99246	-46.48483

Table 5. Object names, spectral types, and coordinates – continued

J Name	Gaia source id	MWDD id	Sp. type	R.A	Dec
J1201+3400	4028120776036373760	SDSS J120154.70+340055.9	DQ	180.47795	34.01537
J1203+0834	3899809757644549632	WD 1200+088	DZ	180.85067	8.56937
J1203+2323		SDSS J120324.42+232350.7	DZ	180.85175	23.39742
J1203+2439	4002914643768684288	SDSS J120319.78+243955.7	DBZA	180.83255	24.66546
J1203+6451	1585063422960992256	WD 1200+651	DQ	180.88292	64.85039
J1204+1030		SDSS J120435.35+103044.8	DZ	181.14729	10.51244
J1204+5007	1546867312429206656	SDSS J120436.40+500730.9	DZ	181.15162	50.12517
J1205+3536	4029735271423173248	SDSS J120548.97+353642.4	DZ	181.45408	35.61180
J1205+4312	1537735902720638720	SDSS J120543.74+431226.6	DZ	181.43224	43.20739
J1206+1310		SDSS J120646.49+131020.1	DZ	181.69371	13.17225
J1206+1454	3921972269928228096	SDSS J120630.63+145435.6	DZ	181.62762	14.90992
J1206+2650	4006630542098974464	SDSS J120603.74+265026.6	DZ	181.51558	26.84075
J1208+1907	3950937048336547840	SDSS J120840.86+190710.2	DZ	182.17028	19.11951
J1209+3026	4014467830917382912	SDSS J120943.03+302629.1	DZ	182.42933	30.44134
J1209+5355	1573002085346485888	SDSS J120936.50+535525.7	DQ	182.40215	53.92382
J1210+0553	3895376870362295680	SDSS J121048.44+055348.2	DBZA	182.70194	5.89676
J1210+3136	4014824794238339840	SDSS J121051.66+313659.9	DZ	182.71535	31.61664
J1210+4332		SDSS J121050.42+433214.1	DZ	182.71008	43.53725
J1210+4751	1546026289113665792	SDSS J121011.79+475132.8	DZ	182.54916	47.85908
J1211+2326	4001872474248647936	SDSS J121106.43+232623.0	DZ	182.77694	23.43964
J1212+5409	1573053006478894464	SDSS J121218.68+540938.7	DZ	183.07791	54.16074
J1212+5452	1573476112296657408	SDSS J121211.03+545222.6	DQ	183.04591	54.87302
J1212+6351	1584414053970166784	SDSS J121231.65+635157.4	DZ	183.13194	63.86588
J1214+2216	3953431908939316096	SDSS J121437.07+221628.3	DZ	183.65461	22.27447
J1214+7822	1717341818608187648	LP 20–214	DZ	183.63264	78.38237
J1215+3953	1532901560546248320	SDSS J121543.40+395348.8	DZ	183.93088	39.89687
J1215+4700	1545134482103819136	SDSS J121510.64+470011.0	DQA	183.79437	47.00313
J1216+6208		SDSS J121632.42+620838.3	DZ	184.13508	62.14400
J1217+1157	3908228546380210432	SDSS J121731.31+115715.9	DZ	184.38050	11.95443
J1217+6420	1584767615678182272	SDSS J121701.53+642000.1	DZ	184.25635	64.33336
J1218+0023	3698477839885075200	SDSS J121837.12+002304.0	DZ	184.65466	0.38441
J1218+6023		SDSS J121843.28+602304.2	DZ	184.68033	60.38451
J1219+0848	3902219234298271488	SDSS J121905.53+084840.1	DZ	184.77304	8.81117
J1219+3018		SDSS J121927.94+301842.2	DZ	184.86642	30.31174
J1219+5720		SDSS J121952.80+572004.1	DZ	184.97000	57.33449
J1220+0929		SDSS J122035.76+092948.1	DZ	185.14900	9.49672
J1220+2700	4009486184250297344	SDSS J122021.63+270007.8	DQ	185.09023	27.00212
J1222+6343	1583984114858734720	SDSS J122204.47+634354.6	DZ	185.51878	63.73189

Table 5. Object names, spectral types, and coordinates – continued

J Name	Gaia source id	MWDD id	Sp. type	R.A	Dec
J1223+1600		SDSS J122303.79+160036.5	DZ	185.76579	16.01017
J1223+1935		SDSS J122335.34+193531.9	DZ	185.89725	19.59219
J1224+2838	4010119017615780608	SDSS J122437.07+283853.0	DZ	186.15446	28.64805
J1225+4706	1542337839923130624	PSO J186.4406+47.1036	DQ	186.44143	47.10363
J1225–0245	3693806156714162816	2QZ J122555.3–024547	DZ	186.48067	-2.76261
J1226+4445	1541711569263906944	GALEX 2686197079552822523	DBZ	186.70841	44.75394
J1227+4434		SDSS J122713.08+443431.8	DZ	186.80450	44.57552
J1227+6330	1583921850718408960	WD 1225+637	DZ	186.88939	63.50818
J1229+0743	3901145183236527872	SDSS J122943.92+074311.8	DZ	187.43300	7.71994
J1229+1606		SDSS J122948.48+160640.4	DZ	187.45200	16.11125
J1229+3021	4012015915692131456	SDSS J122906.01+302108.8	DZ	187.27511	30.35263
J1229+4254	1535265643690386816	SDSS J122929.04+425414.4	DZ	187.37100	42.90402
J1229+5129	1568771851797540736	SDSS J122953.17+512925.2	DZ	187.47158	51.49034
J1230+0813		SDSS J123013.19+081317.8	DZ	187.55496	8.22161
J1230+3143	4012552339927419520	SDSS J123024.04+314339.7	DZ	187.60017	31.72773
J1232+3232		SDSS J123216.13+323240.4	DZ	188.06721	32.54456
J1232+3729		SDSS J123229.31+372954.0	DZ	188.12212	37.49836
J1233+1253	3931756484602030848	2MASS J12334759+1253454	DQ	188.44831	12.89606
J1234+3051	4012252894807339264	SDSS J123412.27+305123.1	DZ	188.55117	30.85644
J1234+5208	1568852322304497280	SDSS J123415.21+520808.1	DZ	188.56333	52.13564
J1234+5606	1571584539980588544	SBSS 1232+563	DBZA	188.63615	56.11195
J1234–0330	3681368652978824960	WD 1232–032	DZ	188.73315	-3.51310
J1235+3918	1533514911941019008	SDSS J123534.86+391820.4	DQ	188.89516	39.30573
J1236+2144		SDSS J123645.05+214419.8	DZ	189.18771	21.73883
J1236+3502	1518558259563900416	SDSS J123646.98+350246.8	DQ	189.19582	35.04632
J1237+4156	1534384148897669248	WD 1235+422	DQ	189.46763	41.94019
J1238+1328	3932223532230002944	SDSS J123838.90+132815.3	DZ	189.66208	13.47094
J1238+2149	3955605402909063552	SDSS J123826.93+214937.7	DZ	189.61221	21.82714
J1239+0756	3710371635120188288	SDSS J123927.94+075611.1	DZ	189.86642	7.93644
J1239+3522		SDSS J123941.79+352210.2	DZ	189.92412	35.36950
J1240+1603	3935035773736441216	SDSS J124006.86+160357.9	DZ	190.02858	16.06608
J1240+1911	3948086603096305664	SDSS J124020.22+191157.9	DZ	190.08425	19.19944
J1240+2748	3962505117546749696	SDSS J124018.47+274835.3	DQ	190.07693	27.80989
J1240–0037	3695821316713228032	SDSS J124006.35–003700.8	DZ	190.02647	-0.61693
J1240–0144	3683297604395370240	[VV2003b] J124035.0–014500	DQ	190.14537	-1.74991
J1241+3010	4011269965771874688	SDSS J124159.86+301024.4	DZ	190.49942	30.17344
J1242+0829	3710792163957803648	SDSS J124201.80+082945.7	DZ	190.50750	8.49603
J1243+1651	393521427257795712	WD 1240+171	DQA	190.78028	16.85953

Table 5. Object names, spectral types, and coordinates – continued

J Name	Gaia source id	MWDD id	Sp. type	R.A	Dec
J1243+3607	1520035689658571264	SDSS J124338.97+360729.0	DQ	190.91237	36.12468
J1244+2709	3961476455699563136	SDSS J124433.81+270923.9	DQ	191.14082	27.15663
J1244+3724	1520393997305175424	SDSS J124456.83+372415.5	DZ	191.23679	37.40431
J1244+5732	1577634018596346624	SDSS J124420.37+573239.6	DZ	191.08483	57.54425
J1244–0118	3683519637024466176	SDSS J124437.69–011838.4	DZ	191.15702	–1.31066
J1245+0822	3710635414832030976	SDSS J124547.11+082231.4	DZ	191.44629	8.37542
J1245+6700	1682132737571666560	SDSS J124522.69+670036.2	DZ	191.34458	67.00999
J1246+1155	3928060510626899200	WD 1243+121	DZ	191.62548	11.92240
J1246–0236		SDSS J124644.88–023619.1	DZ	191.68700	–2.60531
J1247+4113	1522140502806435456	LSPM J1247+4113	DQ	191.75815	41.22808
J1247+4934	1567391625404274304	WD 1244+498	DBZA	191.76365	49.57320
J1248+1411	3930813172345263872	SDSS J124805.39+141140.4	DBZ	192.02248	14.19454
J1249+0806	3709828029699575808	USNO–B1.0 0981–00259963	DZ	192.42920	8.10377
J1249+2800	3961998375830065152	SDSS J124926.17+280058.3	DQ	192.35904	28.01617
J1249+3407	1515081328918440064	WIRED J124911.87+340705.5	DQ	192.29950	34.11820
J1250+0205	3702648596727152768	2QZ J125004.5+020517	DQ	192.51896	2.08844
J1250+5249	1569926755619671040	SDSS J125014.58+524931.8	DZ	192.56065	52.82546
J1251+4646	1531053247143615488	PB 10	DQ	192.96487	46.77426
J1252+1943	3942041105914664832	LSPM J1252+1943	DQ	193.18958	19.71999
J1252+3327		SDSS J125228.96+332756.4	DZ	193.12067	33.46567
J1252+3330		SDSS J125238.85+333008.3	DZ	193.16188	33.50231
J1252+6401		SDSS J125200.11+640104.9	DZ	193.00046	64.01804
J1253+0139	3690553556505229312	WD 1251+019	DQ	193.49839	1.65712
J1253+1808	3940985407247934848	SDSS J125353.84+180837.9	DBZ	193.47446	18.14384
J1253+3842		SDSS J125350.98+384225.7	DZ	193.46242	38.70714
J1254+2233	3956500645892257408	GALEX 2695907992019142607	DBZA	193.53623	22.56331
J1254+3551	1516793058069558784	SDSS J125454.93+355145.7	DZ	193.72888	35.86269
J1254–0236	3682412703692940032	WD 1251–023	DZ	193.55745	–2.60237
J1255+4001		SDSS J125515.83+400133.2	DZ	193.81596	40.02592
J1257+3238		SDSS J125710.13+323848.5	DZ	194.29221	32.64682
J1257+5938	1578968688278446080	SDSS J125724.77+593818.7	DQ	194.35333	59.63848
J1257–0310		SDSS J125720.87–031025.1	DZ	194.33696	–3.17365
J1259+3112	1465529324856790656	SDSS J125922.03+311215.2	DZ	194.84179	31.20424
J1259+4729	1554975145532543744	SDSS J125945.32+472953.6	DZ	194.93887	47.49828
J1302+0923	3734180047591687936	SDSS J130201.30+092351.6	DQ	195.50536	9.39777
J1302+2215	3944459138142121728	SDSS J130247.76+221551.0	DZ	195.69900	22.26419
J1303+4055	1527325967146769664	SDSS J130328.07+405545.5	DZ	195.86696	40.92933
J1303+4418	1529446512759983616	SDSS J130355.87+441815.8	DZ	195.98277	44.30442

Table 5. Object names, spectral types, and coordinates – continued

J Name	Gaia source id	MWDD id	Sp. type	R.A	Dec
J1307+0307	3692497733580887040	WD 1305+033	DZA	196.94308	3.12832
J1308+0258		SDSS J130830.03+025844.5	DZ	197.12517	2.97903
J1308+0957	3735751868182285312	SDSS J130826.36+095724.0	DZ	197.10983	9.95669
J1309+3812		SDSS J130902.65+381210.3	DZ	197.26104	38.20289
J1309+4445	1529705447748085376	SDSS J130945.62+444540.9	DQ	197.44023	44.76139
J1309+4913	1554843655110340992	PB 85	DZ	197.27188	49.23329
J1310+0645		SDSS J131021.96+064556.5	DZ	197.59150	6.76572
J1310+1323		SDSS J131049.65+132354.3	DZ	197.70687	13.39842
J1310+3149	1466195014723444480	SDSS J131028.90+314901.5	DZ	197.62041	31.81710
J1311+1019	3732881936675288192	SDSS J131116.29+101903.1	DZ	197.81788	10.31753
J1313+3811	1522894419890933504	SDSS J131352.32+381111.3	DQ	198.46807	38.18644
J1313+5738	1566553007268519168	LB 2597	DZA	198.40429	57.63378
J1313+5813	1566610796052681728	SDSS J131308.79+581321.9	DZ	198.28671	58.22271
J1314+3748	1522822577973910016	SDSS J131420.49+374806.5	DZ	198.58542	37.80181
J1314+5223	1557096756297688704	SBSS 1312+526	DBZA	198.52814	52.39741
J1315+4711	1551346520939849728	NLTT 33455	DQ	198.89459	47.18593
J1316+0810	3731530843043705216	SDSS J131640.71+081058.6	DQ	199.16970	8.18298
J1316+1916	3939691969258025216	SDSS J131606.82+191602.9	DZA	199.02843	19.26748
J1316+1918	3939694335783773696	SDSS J131612.87+191806.5	DZ	199.05362	19.30183
J1316+5117	1556792019777662208	SDSS J131655.06+511747.3	DZ	199.22924	51.29641
J1316−2007	3506567328028533120	LHS 2710	DZ	199.08156	−20.12557
J1318+2022	3940212274480243072	SDSS J131826.64+202234.9	DZ	199.61100	20.37639
J1319+0844	3731667388643923840	SDSS J131953.50+084422.8	DZ	199.97292	8.73972
J1319+1401	3742980950976788352	SDSS J131930.66+140137.1	DQ	199.87764	14.02705
J1319+3025	1463122974939958528	OMHR 10489	DZ	199.90127	30.42227
J1319+3641	1474478765391306368	SDSS J131900.19+364149.8	DZ	199.75079	36.69717
J1320+0204	3688377657353004032	SDSS J132005.53+020419.0	DZ	200.02304	2.07197
J1320+4332	1526350322380366720	SDSS J132020.95+433201.1	DZ	200.08729	43.53366
J1321+1614	3744460000274429312	SDSS J132147.12+161446.4	DZ	200.44642	16.24627
J1321+2019	3940245740865078656	SDSS J132108.28+201957.6	DZ	200.28450	20.33267
J1321−0237	3638091080740030336	SDSS J132144.04−023751.4	DZ	200.43346	−2.63099
J1322+1224		SDSS J132251.72+122459.0	DZ	200.71550	12.41639
J1322+3730	1474623595985489664	[VV2010] J132232.1+373033	DQ	200.63362	37.50919
J1322+6707	1684435806410554368	SDSS J132236.35+670704.9	DZA	200.65149	67.11804
J1323+2112		SDSS J132351.98+211225.7	DZ	200.96658	21.20714
J1323+3849	1476388823247556608	SDSS J132330.45+384929.1	DBZA	200.87690	38.82489
J1325+6521	1678166558611938944	WD 1323+656	DZA	201.27895	65.35893
J1326+1854	3939012569855670144	SDSS J132615.67+185416.6	DZ	201.56535	18.90458

Table 5. Object names, spectral types, and coordinates – continued

J Name	Gaia source id	MWDD id	Sp. type	R.A	Dec
J1326+4235		SDSS J132649.53+423513.1	DZ	201.70638	42.58699
J1327+4508	1550148770522625024	SDSS J132751.98+450805.4	DZ	201.96674	45.13487
J1327+5519		SDSS J132720.10+551927.7	DZ	201.83375	55.32438
J1328+3640	1475033331568894080	SDSS J132825.33+364016.9	DQ	202.10570	36.67143
J1329+0746	3719493011785709056	USNO–B1.0 0977–00289412	DQ	202.37961	7.78118
J1329+1301	3739809925082831104	SDSS J132941.79+130131.9	DZ	202.42412	13.02553
J1329+6459		SDSS J132933.78+645917.7	DZ	202.39075	64.98826
J1331+6704	1684391409332966400	WD 1329+673	DQ	202.86259	67.07209
J1332+1522	3744903481417287552	SDSS J133205.52+152248.3	DZ	203.02317	15.38020
J1332+2355	1443309397450725376	SDSS J133221.56+235502.1	DQA	203.08983	23.91728
J1332+2740	1448881864114808448	SDSS J133205.63+274003.9	DQZ	203.02355	27.66770
J1332+5446		SDSS J133242.19+544644.3	DZ	203.17579	54.77897
J1333+2357	1444622768385439104	SDSS J133313.73+235721.9	DQ	203.30730	23.95598
J1333+3254	1469124246843402624	GALEX 2699672702652776758	DBZ	203.27224	32.90003
J1333+6349	1665473315344805760	WD 1331+640	DBZA	203.27912	63.82677
J1334+1622	3745402968934425216	SDSS J133420.09+162235.8	DQ	203.58353	16.37695
J1335+2254		SDSS J133555.81+225422.2	DZ	203.98254	22.90617
J1336+3012		SDSS J133620.04+301200.7	DZ	204.08350	30.20020
J1336+3547	1471788161655374080	SDSS J133624.26+354751.2	DZ	204.10113	35.79770
J1338+1334	3740641224592907904	SDSS J133836.18+133400.0	DBZA	204.65076	13.56667
J1338+3255	1468984471427930496	SDSS J133826.43+325540.8	DZ	204.61012	32.92800
J1338–0130	3661716738057880320	WD 1335–012	DZ	204.60410	–1.50473
J1339+2643	1445611018884630912	SDSS J133905.98+264322.9	DZ	204.77492	26.72303
J1339+6401	1665809972061825408	SDSS J133938.04+640128.1	DZ	204.90842	64.02442
J1340+0835	3724917864718061056	SDSS J134019.55+083520.1	DZ	205.08152	8.58892
J1340+2702	1445645279839722368	SDSS J134050.31+270219.0	DZ	205.20962	27.03864
J1341+0346	3713647252057777536	SDSS J134124.28+034628.7	DQA	205.35117	3.77464
J1341+1338	3740678745426551296	SDSS J134156.63+133845.3	DZ	205.48594	13.64595
J1341+2216	1443411828126496512	SDSS J134107.38+221644.4	DZ	205.28075	22.27903
J1341+3024	1456378364457038208	SDSS J134116.56+302448.8	DZ	205.31897	30.41355
J1341–0112	3661660211993375360	WD 1339–009	DZ	205.43375	–1.21064
J1341–3124	6174669289396761088	WD 1338–311	DZ	205.35804	–31.41408
J1342+0522	3714962577202183168	SDSS J134226.93+052248.6	DZ	205.61222	5.38018
J1342+1813		SDSS J134203.60+181332.8	DZ	205.51500	18.22578
J1343+2941	1455527965227944064	SDSS J134353.14+294114.1	DZ	205.97140	29.68723
J1343+4641	1503980964467235584	SDSS J134317.31+464104.7	DZ	205.82221	46.68464
J1344+1849	1248152852388496896	PB 4069	DQ	206.11017	18.82532
J1344+6505	1671965931506508288	WD 1343+653	DZ	206.24730	65.08681

Table 5. Object names, spectral types, and coordinates – continued

J Name	Gaia source id	MWDD id	Sp. type	R.A	Dec
J1345+1153	3728178127148086784	SDSS J134520.99+115357.6	DZ	206.33746	11.89935
J1345+5854	1659379924983087488	SDSS J134508.12+585421.3	DZ	206.28376	58.90588
J1347+0720	3721524466892038656	SDSS J134721.36+072017.6	DZ	206.83900	7.33825
J1347+1415	3740936580903900160	SDSS J134711.47+141528.0	DZ	206.79779	14.25781
J1347+1528	3741346355143254272	SDSS J134747.94+152851.0	DQ	206.94975	15.48083
J1347+1733	1244597066144718336	SDSS J134751.54+173343.0	DZ	206.96475	17.56197
J1347+3817	1496440964697320576	SDSS J134707.57+381749.7	DQ	206.78154	38.29714
J1347+5019	1558850305545116928	SDSS J134716.07+501941.9	DQ	206.81686	50.32829
J1349+0209		SDSS J134955.76+020931.2	DZ	207.48233	2.15867
J1349+0243	3665065605662377088	WD 1347+029	DBZ	207.48426	2.71927
J1350+1058	3727077099396496000	SDSS J135054.02+105808.0	DZ	207.72508	10.96892
J1350+2148		SDSS J135024.97+214814.8	DZ	207.60404	21.80414
J1351+1900	1245205027355144064	SDSS J135116.60+190006.3	DBZ	207.81914	19.00180
J1351+2645	1450680729561299840	SDSS J135123.86+264546.5	DZ	207.84942	26.76292
J1351+4253	1502063317405058304	LSPM J1351+4253	DZ	207.82669	42.88803
J1351+6136	1664233581625001856	SDSS J135137.07+613607.1	DZ	207.90446	61.60199
J1351+6623	1672147149062665472	WD 1350+666	DQ	207.89347	66.38730
J1352+2218	1251457881262355456	SDSS J135201.98+221811.4	DQ	208.00825	22.30317
J1352+2658	1450701860800499712	[CCH92] 1350.7+2713	DQ	208.24451	26.98175
J1353+1347	3728893389526098432	SDSS J135320.79+134720.7	DZ	208.33663	13.78908
J1353+3239	1457834740625970560	SDSS J135343.13+323925.0	DZ	208.42970	32.65701
J1354+1217	3727701007821059072	SDSS J135409.79+121732.1	DQ	208.54079	12.29228
J1355+0810	3721831501224246272	SDSS J135543.54+081029.5	DZ	208.93142	8.17486
J1355+3636	1495340933377121792	CSO 1025	DQ	208.81924	36.60353
J1356+0236	3664591647431946240	SDSS J135654.01+023641.5	DZ	209.22504	2.61153
J1356+2416	1257923215792065152	[VV2010] J135632.7+241605	DZ	209.13583	24.26841
J1356+4047	1498645171976598144	SDSS J135637.78+404703.4	DZ	209.15752	40.78429
J1356+4342		SDSS J135609.74+434220.8	DZ	209.04058	43.70579
J1356–0009	3660622479174640640	WD 1353+000	DQ	209.11767	-0.16148
J1357+2949	1453674429141463936	SDSS J135739.52+294921.5	DQ	209.41475	29.82261
J1357+5727		SDSS J135702.22+572709.1	DZ	209.25925	57.45254
J1358+0552	3672120793821311744	SDSS J135810.42+055237.6	DQ	209.54342	5.87711
J1359+3810		SDSS J135953.17+381057.6	DZ	209.97154	38.18267
J1400+4507	1505711149093085184	SDSS J140048.98+450758.7	DZ	210.20404	45.13299
J1400–0154	3657765432570156160	2QZ J140051.6–015413	DQ	210.21494	-1.90396
J1401+2840	1452751492209135616	SDSS J140115.38+284048.8	DZ	210.31407	28.68019
J1401+3009	1453786643751444352	SDSS J140101.13+300943.3	DZ	210.25469	30.16204
J1401+3659	1483683911099065088	SDSS J140137.31+365909.9	DZ	210.40546	36.98607

Table 5. Object names, spectral types, and coordinates – continued

J Name	Gaia source id	MWDD id	Sp. type	R.A	Dec
J1402+1113	3724362336470991488	SDSS J140256.39+111332.3	DQ	210.73492	11.22577
J1402+2506	1258268604177744256	SDSS J140216.29+250643.0	DZ	210.56791	25.11192
J1402+2518	1258284336642384768	SDSS J140207.62+251827.4	DZ	210.53175	25.30761
J1402+4742	1509394551702059392	SDSS J140210.98+474245.3	DZ	210.54573	47.71263
J1403+1954	1246965487205372672	SDSS J140336.35+195455.2	DBZA	210.90153	19.91530
J1404+3620	1483427385588999936	SDSS J140410.72+362056.8	DZ	211.04486	36.34920
J1404−0232	3647147315636540032	SDSS J140445.10−023237.2	DZ	211.18797	−2.54369
J1405+1549	1231399834234447488	SDSS J140557.10+154940.5	DZ	211.48805	15.82794
J1405+2542		SDSS J140525.20+254212.4	DZ	211.35500	25.70344
J1406+0148	3667337544578212736	WD 1403+020	DQ	211.63511	1.81065
J1406+0204	3667357915607541632	WD 1403+023	DQ	211.60707	2.07972
J1406+1814	1245445167566647936	SDSS J140653.67+181444.8	DZ	211.72362	18.24578
J1406+3402	1481854770426696704	SDSS J140641.03+340200.3	DQ+DA	211.67090	34.03353
J1406−0037	3659643535868664832	2QZ J140615.9−003715	DZ	211.56660	−0.62081
J1407+2039	1247128489804218368	SDSS J140723.04+203918.6	DQ	211.84613	20.65518
J1407+3218	1478409656899499392	SDSS J140730.28+321812.9	DZ	211.87617	32.30361
J1408+1535	1231351421362931584	SDSS J140820.04+153507.3	DZ	212.08357	15.58531
J1408+1750		SDSS J140838.48+175058.5	DZ	212.16033	17.84961
J1409+1254		SDSS J140935.97+125415.3	DZ	212.39988	12.90428
J1409+1511	1230575131794474752	SDSS J140918.87+151136.3	DZ	212.32875	15.19360
J1410+1445	1230479444218162432	SDSS J141037.54+144544.7	DBZ	212.65644	14.76234
J1411+3410	1479231236900790144	SDSS J141140.27+341039.4	DZ	212.91779	34.17764
J1412+1343	1227084358469891328	SDSS J141248.87+134324.1	DZ	213.20362	13.72339
J1412+4011		SDSS J141215.36+401138.2	DZ	213.06400	40.19397
J1413+1659		SDSS J141334.88+165941.1	DZ	213.39533	16.99478
J1413+1820		SDSS J141333.27+182030.1	DZ	213.38863	18.34172
J1414−0113	3647680024725171968	WD 1411−009	DZ	213.61061	−1.23184
J1416+0230	3666876265090396672	SDSS J141615.25+023050.6	DZ	214.06354	2.51406
J1416+3016	1285060846393119360	SDSS J141648.86+301653.9	DQ	214.20359	30.28167
J1417+2412	1255667705126644224	SDSS J141745.42+241222.6	DQ	214.43935	24.20630
J1417+2931		SDSS J141706.52+293105.2	DZ	214.27717	29.51813
J1419+4400	1504806251022988160	SDSS J141936.11+440019.9	DZ	214.90046	44.00553
J1420+4405		SDSS J142055.12+440507.0	DZ	215.22967	44.08528
J1420+4759	1507764869311437568	SDSS J142055.87+475917.5	DZ	215.23278	47.98817
J1421+1843	1239668986308981632	SDSS J142120.11+184351.6	DZ	215.33387	18.73104
J1421+5703	1611374216521821952	SDSS J142119.93+570329.9	DZ	215.33307	57.05834
J1422+5229	1604959219009055360	SDSS J142258.01+522925.8	DBZA	215.74177	52.49048
J1423+5729	1611364359572790016	WD 1422+577	DQ	215.92766	57.49703

Table 5. Object names, spectral types, and coordinates – continued

J Name	Gaia source id	MWDD id	Sp. type	R.A	Dec
J1424+0833	1175788425887673728	SDSS J142413.37+083316.4	DQ	216.05573	8.55448
J1424+5657	1611313365425136384	SDSS J142456.64+565720.8	DZ	216.23598	56.95570
J1425+1801	1238621701484033664	SDSS J142531.98+180116.2	DQ	216.38327	18.02127
J1425+2302	1254382616552890496	SDSS J142525.77+230245.3	DBZA	216.35740	23.04602
J1425−0050	3652865390281317120	WD 1422−006	DZ	216.31844	−0.84690
J1427+4825	1507446659477664512	SDSS J142744.98+482527.3	DZ	216.93736	48.42424
J1427+6110	1666378698746614528	EGGR 362	DQ	216.86790	61.17402
J1428+3238	1287258636998635008	SDSS J142812.54+323817.7	DQ	217.05217	32.63829
J1428+4210	1491662379787040896	SDSS J142820.31+421051.5	DZ	217.08463	42.18097
J1428+4403	1494157691363079168	WD 1426+442	DZ	217.14056	44.06304
J1429+3841	1487653182435218048	SDSS J142939.38+384113.2	DZ	217.41413	38.68701
J1429+5839	1611891639821969408	SDSS J142931.17+583927.9	DZ	217.37998	58.65776
J1430+3245		SDSS J143022.06+324521.7	DZ	217.59192	32.75603
J1430−0151	3649553970495586432	SDSS J143007.15−015129.5	DZ	217.52983	−1.85824
J1431+3750	1487348067958833536	SDSS J143144.83+375011.8	DQ	217.93686	37.83661
J1432+0354	3668760342689186048	WD 1430+041	DZA	218.14925	3.90645
J1432+1522	1228332918347939968	SDSS J143253.37+152222.1	DZ	218.22235	15.37280
J1432+3542	1480227871175119616	SDSS J143247.94+354202.0	DZ	218.19975	35.70058
J1433+0714	1172289608089050496	SDSS J143350.83+071452.2	DBZA	218.46183	7.24785
J1433+6139		SDSS J143351.85+613931.7	DZ	218.46604	61.65881
J1434+2258	1242732500581829632	SDSS J143437.82+225859.5	DQA	218.65765	22.98324
J1435+2120	1241254207198151168	SDSS J143550.13+212014.5	DQ	218.95887	21.33736
J1435+4554	1494738469724112512	SDSS J143548.73+455419.1	DQ	218.95313	45.90526
J1435+5318	1605233036060102144	SDSS J143534.01+531815.0	DQA	218.89174	53.30418
J1436+2152		SDSS J143637.94+215231.3	DZ	219.15808	21.87539
J1438+1046		SDSS J143810.86+104639.6	DZ	219.54525	10.77767
J1438+2234	1242472569161161472	SDSS J143859.38+223402.4	DQ	219.74742	22.56733
J1440+0958	1174728432253334784	SDSS J144006.80+095835.4	DQ	220.02836	9.97659
J1440+1227		SDSS J144026.02+122720.9	DZ	220.10842	12.45581
J1440−0232	3648790157806712448	SDSS J144022.52−023222.2	DZ	220.09384	−2.53951
J1441+0831	1172831907840206848	SDSS J144124.34+083104.6	DZ	220.35151	8.51797
J1441+2347	1266711131199577216	SDSS J144152.14+234704.2	DQ	220.46734	23.78444
J1441+4714	1590927320335127424	SDSS J144129.56+471452.6	DZ	220.37300	47.24799
J1441+5215	1605820896823841536	SDSS J144147.78+521531.4	DZ	220.44881	52.25872
J1442+4202	1490005484484145280	SDSS J144221.53+420250.1	DQ	220.58971	42.04728
J1442+5833	1616918538265393536	SDSS J144237.91+583321.4	DZ	220.65798	58.55590
J1443+2054		SDSS J144326.39+205422.1	DZ	220.85996	20.90614
J1443+3014		SDSS J144354.13+301413.3	DZ	220.97554	30.23706

Table 5. Object names, spectral types, and coordinates – continued

J Name	Gaia source id	MWDD id	Sp. type	R.A	Dec
J1443+3810	1486866348722547072	SDSS J144337.01+381025.7	DQ	220.90413	38.17387
J1443+5833		SDSS J144301.55+583301.6	DZ	220.75646	58.55046
J1444+0434	1158766577140118144	WD 1441+047	DQ	221.03024	4.57966
J1444+1151		SDSS J144449.31+115124.7	DZ	221.20546	11.85689
J1444+2059		SDSS J144416.52+205946.7	DZ	221.06883	20.99633
J1444+4741		SDSS J144416.62+474104.3	DZ	221.06925	47.68455
J1444+5741	1616801852593079040	SDSS J144453.67+574147.3	DZ	221.22369	57.69648
J1445+0913		SDSS J144535.03+091340.4	DZ	221.39600	9.22791
J1445+5850	1617010931601618432	WD 1443+590	DBZ	221.32512	58.84227
J1445−0208	3648744214542134912	SDSS J144516.24−020849.6	DZ	221.31766	−2.14710
J1446+0111		SDSS J144612.30+011139.1	DZ	221.55125	1.19422
J1446+0112		SDSS J144604.69+011209.7	DZ	221.51954	1.20272
J1447+1340		SDSS J144722.94+134038.3	DZ	221.84558	13.67731
J1448+1047	1175204104176381696	SDSS J144804.49+104709.1	DZ	222.01871	10.78586
J1448+2946		SDSS J144820.62+294629.5	DZ	222.08592	29.77486
J1448+2958	1282587151389251968	SDSS J144830.61+295817.2	DZ	222.12754	29.97147
J1448−0047	3650615686411758080	WD 1445−005	DQ	222.03361	−0.79886
J1449+2916	1281751453832480128	SDSS J144954.84+291633.7	DQ	222.47850	29.27603
J1452+1346	1185098132573773184	SDSS J145213.98+134633.5	DBZ	223.05827	13.77596
J1452+4544		SDSS J145216.86+454448.6	DZ	223.07025	45.74684
J1452+6020	1617584636152648448	WD 1451+605	DQ	223.15241	60.34342
J1453+2452		SDSS J145351.49+245244.0	DZ	223.46454	24.87889
J1453+3003		SDSS J145304.75+300311.5	DZ	223.26979	30.05322
J1453+3241	1289479302593197056	SDSS J145309.32+324145.1	DZ	223.28883	32.69589
J1453+4719	1590415360233819776	SDSS J145312.96+471910.5	DQ	223.30403	47.31958
J1455+2010	1237285592992374784	SDSS J145558.75+201057.6	DZ	223.99479	20.18267
J1455+4209	1489435937460963712	SDSS J145524.89+420910.8	DQ	223.85373	42.15300
J1458+4719	1587462866571138048	SDSS J145832.11+471955.8	DBZA	224.63386	47.33219
J1500+2315		SDSS J150028.02+231554.0	DZ	225.11679	23.26501
J1501+0627	1160138114816313472	SDSS J150136.90+062720.5	DQ	225.40373	6.45582
J1501+3807	1295272393132844288	SDSS J150134.65+380747.2	DZ	225.39437	38.12978
J1501+5609	1612720366646956928	SDSS J150119.76+560914.5	DZ	225.33233	56.15403
J1502+3744	1295063619067459712	SDSS J150228.71+374452.9	DZ	225.61962	37.74803
J1503+4414		SDSS J150302.85+441423.2	DZ	225.76187	44.23978
J1503+4642		SDSS J150351.94+464243.6	DZ	225.96642	46.71214
J1506+4152	1392973720770987392	BSO 24	DZ	226.60932	41.87949
J1506+5844	1614158871454061696	SDSS J150603.62+584449.2	DZ	226.51518	58.74693
J1507+2633	1268369057294713472	SDSS J150710.20+263312.5	DZ	226.79250	26.55350

Table 5. Object names, spectral types, and coordinates – continued

J Name	Gaia source id	MWDD id	Sp. type	R.A	Dec
J1507+4034		SDSS J150739.03+403408.9	DZ	226.91267	40.56916
J1508+0622	1157277288640874496	SDSS J150822.60+062242.1	DZ	227.09417	6.37836
J1509+1620	1184399079402015616	SDSS J150901.11+162012.3	DQ	227.25481	16.33653
J1509+1838	1211965588257187840	SDSS J150926.04+183825.4	DZ	227.35850	18.64039
J1510+3814	1292517802972365952	SDSS J151054.85+381450.2	DZA	227.72857	38.24729
J1511+2654	1265489814296750592	SDSS J151133.87+265437.9	DZ	227.89112	26.91053
J1511+5008	1589607700223131264	SDSS J151118.19+500800.7	DQ	227.82576	50.13355
J1512+5304		SDSS J151221.62+530426.3	DZ	228.09008	53.07398
J1514+1423	1183073068378187776	SDSS J151417.00+142354.1	DQ	228.57084	14.39839
J1514+5012	1589669582111773312	SDSS J151441.86+501209.7	DZ	228.67448	50.20273
J1515+1348	1182836742097801600	SDSS J151522.04+134836.5	DZ	228.84183	13.81014
J1515+4532	1395405256376599552	SDSS J151514.54+453211.1	DZ	228.81058	45.53642
J1516+2118	1214926813587984768	SDSS J151610.57+211824.4	DZ	229.04421	21.30685
J1516–0040	4418628372344562048	SDSS J151642.97–004042.7	DBZA	229.17903	-0.67847
J1517+2256	1215384313505335424	SDSS J151734.42+225618.7	DQ	229.39359	22.93847
J1518+0506	1156006287558141056	SDSS J151835.63+050627.5	DZ	229.64845	5.10763
J1518+5619	1600924702825302784	SDSS J151806.55+561935.1	DZ	229.52720	56.32644
J1519+3856	1388487923784151168	SDSS J151942.66+385658.7	DQ	229.92776	38.94961
J1520+2703	1271298912183099520	SDSS J152030.30+270321.5	DQ	230.12625	27.05597
J1520+2718	1271338327098920704	SDSS J152033.66+271839.7	DZ	230.14025	27.31103
J1523+5601		SDSS J152345.85+560135.0	DZ	230.94104	56.02641
J1524+4049	1389075921987168512	SDSS J152449.58+404938.1	DZ	231.20658	40.82724
J1524+4052		SDSS J152418.19+405252.1	DZ	231.07579	40.88114
J1525+1625	1207623754277319040	SDSS J152554.24+162547.0	DZ	231.47600	16.42972
J1525+4258	1394025712881244928	SDSS J152521.94+425805.8	DZ	231.34123	42.96834
J1526+1308		SDSS J152615.36+130846.8	DZ	231.56400	13.14633
J1527+2752	1271077944705755904	SDSS J152702.59+275213.6	DQ	231.76079	27.87050
J1528+0442	4428393925389673344	SDSS J152854.10+044226.6	DQ	232.22541	4.70746
J1528+0753	1163021962017933312	SDSS J152819.04+075346.2	DZ	232.07933	7.89617
J1528+4003	1388228984500678016	SDSS J152840.08+400336.0	DQ	232.16704	40.06006
J1528+5134	1595970711451752192	SDSS J152812.03+513445.2	DQ	232.05018	51.57925
J1531+2505		SDSS J153100.63+250546.2	DZ	232.75262	25.09617
J1531+4240	1391331222197901696	SDSS J153129.26+424015.7	DZ	232.87198	42.67105
J1532+1006		SDSS J153226.52+100629.4	DZ	233.11050	10.10817
J1532+1611		SDSS J153233.08+161140.5	DZ	233.13783	16.19458
J1532+2748		SDSS J153240.34+274818.3	DZ	233.16808	27.80508
J1533+5301	1596218239007316608	SDSS J153333.95+530107.8	DZ	233.39151	53.01877
J1534+1242		SDSS J153407.58+124254.4	DZ	233.53162	12.71511

Table 5. Object names, spectral types, and coordinates – continued

J Name	Gaia source id	MWDD id	Sp. type	R.A	Dec
J1534+1345	1193929989788210944	SDSS J153417.60+134515.6	DBZ	233.57340	13.75431
J1534+4145	1390295486540598656	LSPM J1534+4145	DQZ	233.69828	41.76643
J1535+1247	1193520666521113344	WD 1532+12	DZ	233.77421	12.79589
J1537+1337	1194088628700386432	SDSS J153746.05+133733.5	DQ	234.44184	13.62610
J1537+3608		SDSS J153745.52+360818.6	DZ	234.43967	36.13851
J1537+4625	1400755548676988544	SDSS J153724.24+462521.1	DZ	234.35103	46.42251
J1539+1930	1210014401793691264	SDSS J153946.30+193055.4	DZ	234.94292	19.51539
J1539+5248		SDSS J153930.32+524819.3	DZ	234.87633	52.80537
J1540+2109	1217134048821424384	SDSS J154057.43+210944.6	DZ	235.23929	21.16239
J1540+3737	1377011285837278080	SDSS J154045.28+373747.8	DZ	235.18868	37.62994
J1540+5149	1596598601310586368	SDSS J154025.18+514921.6	DZ	235.10491	51.82271
J1540+5352		SDSS J154022.80+535239.8	DZ	235.09519	53.87753
J1541+0715		SDSS J154152.58+071549.2	DZ	235.46908	7.26367
J1542+1314	1190978660061347584	SDSS J154238.98+131455.7	DQ	235.66258	13.24876
J1542+2544	1223037571566004992	SDSS J154234.73+254438.7	DQ	235.64474	25.74419
J1542+4329	1396483602405444352	SDSS J154248.67+432902.4	DQ	235.70274	43.48404
J1542+4650	1400829525199398912	SDSS J154201.75+465020.2	DZ	235.50733	46.83897
J1543+2024		SDSS J154349.79+202442.9	DZ	235.95746	20.41192
J1544+2345	1218155666922071552	SDSS J154403.30+234516.6	DZ	236.01364	23.75466
J1545+2854	1224851624015623680	SDSS J154518.44+285412.9	DQ	236.32697	28.90363
J1545+4921	1401734938659475456	SDSS J154540.21+492145.1	DZ	236.41756	49.36258
J1545+5236	1596740644469446656	SDSS J154510.31+523618.4	DZ	236.29299	52.60505
J1546+1750		SDSS J154630.17+175034.5	DZ	236.62571	17.84294
J1546+3927	1377594233157992704	SDSS J154623.07+392723.6	DZ	236.59614	39.45656
J1547+0659	4430165650933432576	SDSS J154729.96+065909.5	DZ	236.87495	6.98600
J1548+0222	4423437704923843968	SDSS J154807.93+022257.1	DZ	237.03304	2.38256
J1548+2135	1216820413129873280	SDSS J154815.23+213528.4	DBZA	237.06350	21.59122
J1548+5626	1598666993137041280	WD 1547+565	DQ	237.04443	56.44659
J1549+0239	4423539654567531136	WD 1547+028	DZ	237.47203	2.65824
J1549+1906		SDSS J154933.23+190646.7	DZ	237.38846	19.11299
J1549+2020	1204133766931561344	SDSS J154941.55+202023.8	DZ	237.42312	20.33997
J1549+2633	1223368966945806848	SDSS J154913.46+263301.1	DZ	237.30608	26.55033
J1549+4422	1396603002496338432	SDSS J154907.11+442257.9	DZ	237.27962	44.38275
J1550+2013		SDSS J155030.78+201309.6	DZ	237.62825	20.21933
J1550+5214		SDSS J155033.47+521438.4	DZ	237.63946	52.24401
J1551+0824	4454432667131057792	SDSS J155155.26+082431.7	DQ	237.98022	8.40887
J1551+1529		SDSS J155106.77+152955.3	DZ	237.77821	15.49872
J1551+2547		SDSS J155113.05+254752.1	DZ	237.80437	25.79783

Table 5. Object names, spectral types, and coordinates – continued

J Name	Gaia source id	MWDD id	Sp. type	R.A	Dec
J1552+0815	4454420740003558528	SDSS J155240.07+081516.8	DZ	238.16698	8.25469
J1552+1148	1189726007080211200	SDSS J155202.39+114829.1	DQ	238.00999	11.80812
J1552+3910	1376870960665371136	SDSS J155206.42+391017.6	DQ	238.02713	39.17135
J1554+0336	4425127624234553984	WD 1551+037	DQ	238.55633	3.60965
J1554+1735	1202552914026910976	SDSS J155429.01+173545.9	DZ	238.62085	17.59626
J1555+3123	1321574115723174144	SDSS J155530.18+312310.4	DQ	238.87579	31.38624
J1555+3219	1321789143262245248	SDSS J155539.51+321914.1	DQ	238.91469	32.32054
J1557+2157	1206198821567293056	SDSS J155724.87+215746.4	DZA	239.35360	21.96288
J1558+0312	4424935480278206976	WD 1556+033	DZ	239.71916	3.21193
J1558+1507	1192938917495381504	SDSS J155847.89+150735.4	DZ	239.69962	15.12641
J1558+2512	1219957873855946240	USNO–B1.0 1152–00234632	DZ	239.57211	25.21415
J1559+0445	4425689367298237312	SDSS J155917.21+044549.4	DZ	239.82173	4.76371
J1600+1833	1203094762803715712	SDSS J160020.65+183325.6	DZ	240.08604	18.55711
J1600+3819	1379356410995780480	SDSS J160032.88+381904.5	DZ	240.13700	38.31794
J1600+4120		SDSS J160000.12+412033.4	DZ	240.00050	41.34264
J1600–0009		WD 1557–000B	DZ	240.05225	-0.15147
J1601+1824		SDSS J160143.58+182437.9	DZ	240.43158	18.41053
J1602+1923		SDSS J160221.46+192351.6	DZ	240.58942	19.39769
J1603+4140		SDSS J160359.58+414047.8	DZ	240.99825	41.67997
J1604+0831	4451614618828537216	SDSS J160401.31+083109.0	DBZA	241.00544	8.51917
J1604+1830	1200053822878445056	SDSS J160429.80+183035.4	DZ	241.12421	18.50983
J1606+1908		SDSS J160612.76+190801.3	DZ	241.55317	19.13369
J1606+4712	1399018870061627520	SDSS J160646.32+471207.7	DZ	241.69300	47.20213
J1607+3950	1379917024487277056	SDSS J160702.05+395058.6	DZ	241.75854	39.84964
J1607+5321	1428807010879180672	GALEX 2432438716509192504	DZ	241.79941	53.36601
J1608+1342	4458463884776394880	SDSS J160819.44+134204.3	DZ	242.08103	13.70116
J1608+3831	1379023018454640256	SDSS J160859.59+383146.3	DZ	242.24829	38.52953
J1609+0655	4450425359563998720	SDSS J160935.86+065511.9	DQ	242.39945	6.91999
J1610+3036	1318849697708771584	SDSS J161018.94+303618.9	DQ	242.57900	30.60522
J1610+3714	1378301463949155200	SDSS J161038.92+371403.0	DBZA	242.66219	37.23415
J1610+4006		SDSS J161026.10+400619.7	DZ	242.60879	40.10547
J1611+1117	4456951094215638016	SDSS J161114.32+111708.3	DZ	242.80963	11.28563
J1612+1845		SDSS J161216.54+184512.3	DZ	243.06892	18.75342
J1612+3534		SDSS J161248.17+353434.8	DZ	243.20071	35.57635
J1613+5116	1424602959450847872	WD 1611+513	DQ	243.31400	51.26899
J1615+1746	1200496999080913920	SDSS J161544.48+174627.4	DZ	243.93539	17.77426
J1616+3303	1322623152896019328	SDSS J161603.00+330301.2	DZ	244.01254	33.05031
J1616+3924	1380443823700583552	SDSS J161653.36+392444.4	DQ	244.22240	39.41232

Table 5. Object names, spectral types, and coordinates – continued

J Name	Gaia source id	MWDD id	Sp. type	R.A	Dec
J1618+4452	1385558957951613952	SDSS J161801.33+445220.7	DZ	244.50558	44.87243
J1619+4745		SDSS J161922.43+474553.7	DZ	244.84346	47.76493
J1620+1809	1200428928142394496	SDSS J162004.03+180912.6	DQ	245.01692	18.15366
J1621+2253	1301685290406051072	SDSS J162153.82+225309.5	DQ	245.47431	22.88597
J1622+4731		SDSS J162247.25+473146.8	DZ	245.69688	47.52968
J1622+6319	1628970289513198976	SDSS J162236.76+631908.9	DZA	245.65316	63.31918
J1624+3310		SDSS J162408.57+331019.0	DZ	246.03571	33.17194
J1626+3303		SDSS J162612.73+330308.2	DZ	246.55308	33.05228
J1627+1443	4463884614540773632	SDSS J162702.24+144324.7	DZ	246.75938	14.72350
J1627+4646	1410054324670763904	SDSS J162703.34+464658.2	DZ	246.76392	46.78286
J1628+3646	1331106782752978688	Ross 640	DZA	247.10418	36.77107
J1629+1758	4467141230543287808	SDSS J162946.94+175805.2	DZ	247.44559	17.96811
J1633+1840	4467283273702508800	SDSS J163310.02+184011.7	DZ	248.29185	18.66986
J1634+5710	1431176943768691328	WD 1633+572	DQ	248.58980	57.16913
J1636+1619	4465939601772584448	SDSS J163601.33+161907.1	DZ	249.00558	16.31866
J1638+1244	4460911603818614272	SDSS J163857.94+124420.6	DQ	249.74131	12.73905
J1638+3837	1331552115026136448	SDSS J163827.68+383726.5	DZ	249.61533	38.62403
J1640+3154	1312731877573336448	SDSS J164026.65+315453.9	DZ	250.11106	31.91493
J1640+7310	1654560662439820416	WD 1641+732	DQ	250.10153	73.17614
J1641+1856	4562675699936729216	SDSS J164104.95+185602.1	DZ	250.27062	18.93392
J1641+4833	1410448259071414528	SDSS J164143.31+483301.6	DQ	250.43058	48.55041
J1642+3211	1312718893887366784	SDSS J164208.47+321136.6	DZ	250.53529	32.19350
J1642+3749		SDSS J164211.83+374954.9	DZ	250.54929	37.83192
J1642+4529		SDSS J164224.39+452911.8	DZ	250.60163	45.48664
J1643+1422	4461739604794187520	SDSS J164336.31+142250.2	DZ	250.90126	14.38067
J1643+4002	1355756420402482688	WD 1641+401	DQ	250.86892	40.03450
J1643+4129	1356453338975443840	SDSS J164317.39+412959.2	DQ	250.82246	41.49978
J1644+3853	1352596698862254208	SDSS J164427.54+385357.7	DZ	251.11475	38.89936
J1646+2742	1307617155638441344	GALEX 2680180581990401605	DBZA	251.59259	27.71011
J1647+2636	1307226283551364224	SDSS J164744.70+263646.7	DZ	251.93592	26.61258
J1647+4156		SDSS J164723.80+415644.5	DZ	251.84917	41.94569
J1647+4350	1357729871975804160	SDSS J164701.52+435047.9	DQ	251.75643	43.84661
J1647+5119	1413228614740924032	SDSS J164700.05+511922.3	DQ:	251.75009	51.32270
J1648+5241	1413937593584775168	SDSS J164842.83+524131.5	DZ	252.17858	52.69192
J1649+2238	4565805356705582976	SDSS J164939.23+223807.2	DZ	252.41346	22.63536
J1649+4152		SDSS J164912.04+415241.8	DZ	252.30017	41.87828
J1650+4055		SDSS J165020.80+405550.2	DZ	252.58667	40.93061
J1653+1113	4447744196162611200	SDSS J165309.19+111345.1	DQ:	253.28830	11.22931

Table 5. Object names, spectral types, and coordinates – continued

J Name	Gaia source id	MWDD id	Sp. type	R.A	Dec
J1654+3157	1313265900922425856	SDSS J165436.86+315754.4	DQ	253.65361	31.96510
J1655+2134	4565249351715525888	SDSS J165518.49+213428.2	DZ	253.82704	21.57450
J1655+3722	1351330100122743040	WD 1653+374	DQ	253.91046	37.37976
J1657+3738	1351667753271611264	SDSS J165741.58+373824.2	DZ	254.42331	37.64005
J1657+4759	1408298645123645824	SDSS J165751.23+475911.6	DZ	254.46337	47.98644
J1700+2047		SDSS J170029.59+204704.3	DZ	255.12329	20.78456
J1703+2541	4572969916208600704	SDSS J170326.57+254103.8	DZA	255.86069	25.68437
J1706+2541		SDSS J170638.11+254111.7	DZ	256.65879	25.68661
J1707+4250	1355088432729232384	SDSS J170715.38+425043.1	DZ	256.81408	42.84533
J1708+0257	4388138816124225792	GJ 1211	DZ	257.03319	2.96030
J1711+2201	4567999535238106880	SDSS J171139.82+220152.9	DZ	257.91594	22.03137
J1712+3406	1335069349644072064	SDSS J171221.94+340609.8	DQ	258.09142	34.10275
J1713+3240	1334374153353733888	LSPM J1713+3240	DQ	258.42396	32.66922
J1714+3658	1340140572149710336	SDSS J171403.75+365810.5	DBZA	258.51553	36.96963
J1714+5501	1420411964723649408	WD 1713+550	DZ	258.65175	55.02010
J1715+2804	4575202298472648576	SDSS J171513.63+280403.9	DZ	258.80683	28.06774
J1719+5623	1420738111655252992	SDSS J171900.63+562350.5	DZ	259.75263	56.39736
J1722+2723	4574208168163608832	SDSS J172223.31+272326.2	DZA	260.59709	27.39064
J1724+5333	1416339274870578176	WD 1723+536	DQ	261.23076	53.56494
J1728+0815	4490308833894507008	SDSS J172822.61+081549.3	DBZA	262.09425	8.26367
J1728+3250	4601940290956951424	GALEX 2680391675338031787	DBZ	262.23419	32.84605
J1728+5558	1422012892308493568	GD 524	DQA	262.23425	55.97295
J1833+1945	4525569007873380736	WD 1831+19	DQ	278.49312	19.76472
J1838+4046	2110571565187233152	SDSS J183806.18+404629.8	DQ	279.52583	40.77487
J2007–1208	6880697900670837632	SDSS J200757.10–120832.0	DBZA	301.98789	-12.14222
J2046–0715	6907027901322999552	WD 2043–074	DQ	311.60188	-7.25526
J2050–0110	4226851932184135552	SDSS J205059.11–011021.9	DZ	312.74631	-1.17276
J2053–0702	6909994246262080000	WD 2050–072	DQ	313.31806	-7.03449
J2101+3148	1864760695541016832	EGGR 262	DQ	315.43652	31.81073
J2103–0108	6917166017006522368	SDSS J210303.47–010842.5	DZ	315.76450	-1.14510
J2107–0055	2689055590685508864	SDSS J210733.93–005557.7	DZ	316.89132	-0.93269
J2109–0039	2689160181727792512	SDSS J210916.51–003921.6	DZ	317.31883	-0.65602
J2110+0512		SDSS J211045.34+051214.8	DZ	317.68892	5.20411
J2110–0001	2689964337045144704	SDSS J211003.74–000152.9	DBZA	317.51554	-0.03130
J2111–0036	2689129601561746560	SDSS J211130.04–003628.7	DQ	317.87516	-0.60796
J2114–0051	2688921828223018496	SDSS J211412.77–005125.5	DZ	318.55321	-0.85708
J2123+0016	2690911738111175936	SDSS J212312.20+001653.5	DZ	320.80083	0.28154
J2124–0114	2686055710647408128	2SLAQ J212424.69–011452.5	DZ	321.10293	-1.24790

Table 5. Object names, spectral types, and coordinates – continued

J Name	Gaia source id	MWDD id	Sp. type	R.A	Dec
J2127+0319	2692018980680713856	SDSS J212757.26+031939.6	DZ	321.98858	3.32767
J2130-0243	2684869956075600640	SDSS J213024.38-024302.2	DZ	322.60158	-2.71728
J2132-0203		SDSS J213254.64-020309.0	DZ	323.22767	-2.05253
J2135+0003	2687339493552038400	SDSS J213503.32+000318.4	DQ	323.76378	0.05515
J2136+1137	1766826194114406656	SDSS J213621.56+113726.8	DZA	324.08984	11.62413
J2139+0354		SDSS J213954.44+035403.7	DZ	324.97683	3.90103
J2140-0045	2686998713666980992	2SLAQ J214058.24-004528.8	DQ	325.24271	-0.75800
J2141+0225		SDSS J214105.26+022543.7	DZ	325.27192	2.42883
J2141-3300	6592315723192176896	WD 2138-332	DZ	325.48985	-33.00828
J2142+0908	1741347932717756928	SDSS J214247.87+090858.8	DQ	325.69946	9.14967
J2142+2059	1792830060723673472	GJ 836.5	DQ	325.67086	20.99948
J2142+2252	1794409921493969792	2MASS J21420390+2252290	DZ	325.51622	22.87484
J2143-0019		SDSS J214323.03-001934.6	DZ	325.84596	-0.32631
J2149+2039	1792618572237988608	SDSS J214944.06+203921.7	DQ	327.43353	20.65606
J2150-0113	2674012072593383168	6dFGS gJ215027.8-011348	DQ	327.61591	-1.23055
J2151-0112	2680013864187927168	2SLAQ J215144.77-011247.4	DZ	327.93641	-1.21320
J2155+4103	1959573541696236032	2MASS J21550637+4103067	DZ	328.77654	41.05186
J2156+0559	2697327113581223936	SDSS J215652.94+055925.1	DQ	329.22050	5.99043
J2157+1137	2726854738863780992	SDSS J215759.09+113730.1	DQ	329.49622	11.62510
J2157+1206	2728434462194932352	SDSS J215752.30+120603.1	DZ	329.46792	12.10089
J2201+0219	2683345934175922176	LSPM J2201+0219	DZ	330.34661	2.32685
J2202+0013		SDSS J220242.32+001336.1	DZ	330.67633	0.22672
J2202+0320		SDSS J220251.46+032039.3	DZ	330.71442	3.34425
J2206+1007	2727009632564240384	SDSS J220651.57+100744.2	DZ	331.71488	10.12897
J2207+0135	2682344450881423360	VIPERS 403166921	DQ	331.94253	1.58604
J2207+2319		SDSS J220750.08+231955.6	DZ	331.95867	23.33211
J2209+1223	2727904257071365760	WD J2209+1223	DBZ	332.39521	12.39349
J2211+2145	1782054361439384960	SDSS J221132.37+214526.8	DZ	332.88488	21.75747
J2213+0103		SDSS J221353.85+010334.1	DZ	333.47437	1.05947
J2218+2123	1778839767397091200	SDSS J221850.23+212303.7	DQ	334.70948	21.38478
J2218+3908	1956838712683591296	GD 401	DZ	334.50476	39.14552
J2220+0140		SDSS J222057.35+014001.0	DZ	335.23896	1.66697
J2220+1420	2734603650138728448	SDSS J222032.10+142033.4	DQ	335.13379	14.34263
J2225+1251	2730798480916011648	SDSS J222552.64+125116.8	DQ	336.46933	12.85467
J2225+2338	1878579387730218112	SDSS J222503.71+233855.1	DZ	336.26546	23.64864
J2228+1207	2730508416002618752	2MASS J22280206+1207334	DZ	337.00857	12.12594
J2230+1905		SDSS J223014.70+190514.4	DZ	337.56125	19.08736
J2230+3052	1900628306721576064	SDSS J223010.83+305240.9	DZ	337.54512	30.87805

Table 5. Object names, spectral types, and coordinates – continued

J Name	Gaia source id	MWDD id	Sp. type	R.A	Dec
J2231+0040	2702211693987574400	SDSS J223159.94+004046.4	DZ	337.99974	0.67956
J2231+0906	2711092621203766912	LSPM J2231+0906	DZ	337.75415	9.11086
J2232+0109	2702382156944616832	SDSS J223222.32+010920.7	DZ	338.09301	1.15577
J2235−0056		SDSS J223507.65−005607.7	DZ	338.78188	−0.93549
J2236+0109	2654669468332355584	USNO−A2.0 0900−20178217	DBAZ	339.22070	1.16064
J2236+0413		SDSS J223601.38+041324.7	DZ	339.00575	4.22356
J2238+0101	2654620329611594496	SDSS J223841.06+010150.1	DZ	339.67106	1.03068
J2238+0213		SDSS J223811.10+021352.9	DZ	339.54629	2.23137
J2238−0113	2652983573409260800	SDSS J223815.97−011336.9	DZ	339.56661	−1.22690
J2239+2303	1876067076676460800	SDSS J223937.63+230328.9	DQ	339.90665	23.05808
J2239+2932		SDSS J223956.24+293225.7	DZ	339.98433	29.54048
J2243+3210	1890668861674532224	SDSS J224346.29+321027.1	DBZ	340.94300	32.17422
J2245+2748	1884129791148258304	SDSS J224524.71+274827.8	DZ	341.35301	27.80781
J2248+1318	2719990109813842688	SDSS J224828.65+131838.5	DBZ	342.11940	13.31071
J2248+2826	1884548739436672640	SDSS J224827.82+282637.2	DQA	342.11606	28.44385
J2248−0153	2649709841962009088	SDSS J224847.11−015301.8	DZ	342.19629	−1.88386
J2250+1240	2719705542461133568	SDSS J225000.22+124019.8	DQ	342.50088	12.67219
J2253−0646	2611561706216413696	GJ 1276	DZ	343.47244	−6.78180
J2258−0006		SDSS J225833.44−000614.8	DZ	344.63933	−0.10411
J2258−0829	2607019447587739008	SDSS J225809.37−082920.1	DBZA	344.53907	−8.48893
J2259+1251	2718973478170263808	SDSS J225950.66+125119.3	DZ	344.96096	12.85542
J2259+1748		SDSS J225935.37+174825.6	DZ	344.89738	17.80713
J2300+2204	2835805586577740288	LP 401−31	DZ	345.09152	22.07111
J2302+1626	2816958617248201984	SDSS J230227.96+162602.6	DZ	345.61651	16.43408
J2302+2430	2843077206728009472	SDSS J230249.37+243027.9	DQ	345.70583	24.50797
J2304+2415	2842312874347797632	SDSS J230414.49+241554.0	DZ	346.06044	24.26513
J2305+2307	2841985288602442752	GALEX 2665262369570030960	DZA	346.40428	23.13154
J2306+2111	2832478464391764480	SDSS J230620.01+211118.5	DBZA	346.58340	21.18850
J2309+0608	2665008240592600704	PB 5274	DBZA	347.47097	6.13894
J2310+2203	2838626486737671040	SDSS J231019.68+220323.3	DZ	347.58191	22.05649
J2310−0057	2638932738224859776	WD 2307−012	DQA	347.62609	−0.96271
J2311+1042	2810602344823007872	SDSS J231106.56+104251.7	DZ	347.77733	10.71447
J2311+1510		SDSS J231129.04+151022.1	DZ	347.87100	15.17281
J2311+3343		SDSS J231143.15+334334.2	DZ	347.92979	33.72618
J2311−0041	2650975899537545728	USNO−A2.0 0825−19880842	DBZ	347.92326	−0.68351
J2314−0632	2631876970245863552	GJ 893.1	DQ	348.60494	−6.54663
J2315−0209	2638553754605793408	EGGR 554	DZ	348.82836	−2.16128
J2316+0041		2SLAQ J231601.88+004131.2	DZ	349.00788	0.69201

Table 5. Object names, spectral types, and coordinates – continued

J Name	Gaia source id	MWDD id	Sp. type	R.A	Dec
J2318+2916		SDSS J231820.78+291617.3	DZ	349.58658	29.27149
J2318–0320	2637115142424897536	SDSS J231847.23–032013.0	DZ	349.69679	-3.33697
J2319+3018	2870363305758068480	SDSS J231937.39+301848.4	DZ	349.90564	30.31348
J2321+0807	2664985631884840704	SDSS J232112.68+080715.3	DZ	350.30287	8.12096
J2324+1135	2762920717413900416	SDSS J232423.50+113542.6	DZ	351.09797	11.59513
J2324+1207	2811012462660275968	PG 2322+119	DZA	351.24155	12.12760
J2328+0711		SDSS J232828.78+071119.4	DZ	352.11992	7.18873
J2328+0830		SDSS J232833.31+083028.4	DZ	352.13883	8.50790
J2330+1015	2761789865409701760	SDSS J233011.79+101541.4	DZ	352.54921	10.26146
J2330+2620	2865440826559975296	SDSS J233056.20+262048.4	DZ	352.73416	26.34677
J2330+2805	2865936671944556160	SDSS J233054.31+280517.4	DZ	352.72617	28.08821
J2333+1058		SDSS J233320.38+105830.2	DZ	353.33492	10.97505
J2336+1657		SDSS J233625.13+165751.4	DZ	354.10471	16.96428
J2336+2021	2826113047981744896	SDSS J233610.58+202126.1	DZ	354.04411	20.35727
J2337+2607		SDSS J233719.10+260708.6	DZ	354.32958	26.11906
J2339+4631	1939136468100337536	SDSS J233911.63+463142.4	DZA	354.79837	46.52845
J2340+0124	2646118355949741440	SDSS J234034.61+012416.6	DZ	355.14421	1.40461
J2340+0817	2758086538448464512	SDSS J234048.74+081753.3	DZ	355.20284	8.29811
J2340+1621		SDSS J234000.97+162127.0	DZ	355.00404	16.35751
J2341+0059	2646042317848350464	SDSS J234131.41+005957.9	DZ	355.38088	0.99942
J2341+2448	2852254177449825152	SDSS J234141.51+244854.3	DZ	355.42284	24.81501
J2341–0101	2641006004837594752	SDSS J234132.82–010104.5	DQ	355.38677	-1.01794
J2342–0006	2642625482386020224	SDSS J234245.90–000632.4	DZA	355.69129	-0.10902
J2343+2242	2827053439660604544	SDSS J234355.80+224223.2	DZ	355.98244	22.70644
J2343+3155		SDSS J234315.21+315556.7	DZ	355.81338	31.93244
J2343–0010	2642621084339810560	SDSS J234307.67–001016.3	DZ	355.78196	-0.17120
J2344+1343	2770878737762658816	SDSS J234457.13+134342.1	DZ	356.23805	13.72838
J2344+1813		SDSS J234444.70+181343.5	DZ	356.18625	18.22876
J2345+2857		SDSS J234530.32+285739.8	DZ	356.37633	28.96108
J2346+2816		SDSS J234644.52+281601.0	DZ	356.68550	28.26696
J2348+1341	2770165738831638784	GALEX 2665121662146448800	DBZA	357.21916	13.69466
J2348–4428	6531195177474061824	WD 2345–447	DZ	357.06986	-44.46993
J2349+0325		SDSS J234909.76+032535.2	DZ	357.29067	3.42647
J2351+0633	2744849968934530304	SDSS J235125.70+063305.3	DZ	357.85711	6.55154
J2351+3612	2878778418002027648	SDSS J235139.39+361203.1	DBZ	357.91413	36.20087
J2352+1922		SDSS J235224.26+192247.3	DZ	358.10108	19.37982
J2352+3344		SDSS J235249.13+334439.2	DZ	358.20471	33.74423
J2352–0146	2449345460075810048	SDSS J235254.92–014651.9	DZ	358.22883	-1.78111

Table 5. Object names, spectral types, and coordinates – continued

J Name	Gaia source id	MWDD id	Sp. type	R.A	Dec
J2353+0415	2743352635960001792	SDSS J235313.49+041525.4	DZ	358.30621	4.25706
J2353+3720	2879694208111191168	SDSS J235336.08+372055.3	DBZA	358.40036	37.34868
J2354+4027	1921351390779081600	EGGR 507	DQ	358.73449	40.45821
J2355+1431	2770512570327553408	SDSS J235516.61+143136.1	DZ	358.81910	14.52674
J2356−0320		SDSS J235625.20−032020.5	DZ	359.10500	−3.33906
J2357+2348		SDSS J235715.03+234848.9	DZ	359.31263	23.81360
J2357−0324	2448097411298706560	SDSS J235737.37−032408.7	DZ	359.40571	−3.40244
J2358+0445		SDSS J235810.49+044517.8	DZ	359.54371	4.75497
J2359+0243	2739899276095504640	SDSS J235937.33+024357.0	DZ	359.90554	2.73250
J2359+0347	2740318086946217472	SDSS J235926.15+034758.5	DZ	359.85896	3.79961

Table 6. Atmospheric parameters for DZ stars. A dagger indicates that the distance is a photometric distance based on the value of $\log g = 8$ in the absence of a parallax.

J Name	T_{eff} (K)	$\log g$	M/M_{\odot}	$\log \text{Ca/He}$	$\log \text{H/He}$	D (pc)
J0002+3209	6447(121)	8.30($^{+0.23}_{-0.22}$)	0.77($^{+0.16}_{-0.14}$)	-9.00(0.18)	<-3.08	180.6(28.7)
J0002-0627	7306(428)	8.00		-9.62(0.31)	<-4.05	343.6(28.3)
J0003+2240	5493(269)	8.00		-10.27(0.22)	<-3.00	229.1(22.4)
J0004+0819	5896(234)	8.00		-8.86(0.16)	<-3.00	337.4(27.7)
J0004+2432	10490(614)	8.26($^{+0.28}_{-0.25}$)	0.75($^{+0.18}_{-0.16}$)	-9.74(0.18)	<-5.82	287.9(49.8)
J0004+2531	12132(1141)	8.32($^{+0.81}_{-0.62}$)	0.79($^{+0.45}_{-0.36}$)	-8.27(0.35)	<-6.04	431.5(214.5)
J0005+0018	8073(208)	7.81($^{+0.14}_{-0.14}$)	0.47($^{+0.08}_{-0.07}$)	-10.05(0.09)	<-5.01	156.4(11.6)
J0005+4003	8829(427)	8.03($^{+0.09}_{-0.09}$)	0.59($^{+0.06}_{-0.05}$)	-10.42(0.04)	-4.48(0.21)	64.3(0.3)
J0005+7313	12673(759)	7.95($^{+0.08}_{-0.08}$)	0.56($^{+0.05}_{-0.04}$)	-10.07(0.36)	-6.11(0.00)	34.7(0.0)
J0006+0520	5906(160)	7.97($^{+0.27}_{-0.25}$)	0.55($^{+0.17}_{-0.14}$)	-9.78(0.10)	<-3.00	178.3(27.0)
J0009+0152	7159(212)	8.25($^{+0.32}_{-0.30}$)	0.73($^{+0.22}_{-0.19}$)	-9.45(0.12)	<-3.81	180.4(38.1)
J0010-0430	7089(160)	8.25($^{+0.29}_{-0.27}$)	0.73($^{+0.19}_{-0.17}$)	-8.04(0.09)	<-3.77	204.1(38.4)
J0010-0628	7883(1189)	8.00		-9.87(0.29)	<-4.51	488.1(105.7)
J0013+1109	5939(283)	8.00		-9.96(0.67)	<-3.00	275.2(24.9)
J0015+1830	7346(417)	8.00		-8.86(0.30)	<-4.07	320.0(26.3)
J0017+0230	7477(495)	8.00		-9.06(0.68)	<-4.14	448.5(42.1)
J0018-0012	9958(331)	8.16($^{+0.08}_{-0.08}$)	0.68($^{+0.05}_{-0.05}$)	-9.28(0.04)	<-5.81	151.4(5.3)
J0019+1848	6977(312)	7.39($^{+0.63}_{-0.51}$)	0.29($^{+0.30}_{-0.14}$)	-10.34(0.12)	<-4.28	307.7(91.8)
J0019+2209	5676(152)	7.58($^{+0.34}_{-0.30}$)	0.35($^{+0.17}_{-0.11}$)	-10.18(0.16)	<-3.00	187.7(31.5)
J0026-0006	5020(1185)	8.00		-10.75(0.11)	<-3.00	324.9(154.2)
J0027+0102	8573(374)	8.23($^{+0.34}_{-0.31}$)	0.72($^{+0.22}_{-0.19}$)	-9.25(0.14)	<-4.95	246.8(52.9)
J0027+3350	7114(384)	8.00		-9.62(0.21)	<-3.97	297.0(22.3)
J0030-0254	7011(904)	8.00		-9.99(0.61)	<-3.91	451.8(87.1)
J0031+2040	7853(584)	8.00		-8.87(0.42)	<-4.47	373.8(40.4)
J0031+3252	6537(332)	8.00		-10.01(0.23)	<-3.44	287.6(23.8)
J0032+0827	5771(320)	7.84($^{+0.20}_{-0.20}$)	0.48($^{+0.12}_{-0.10}$)	-10.16(0.10)	<-3.00	133.6(8.5)
J0033+2845	7117(353)	7.35($^{+1.24}_{-1.47}$)	0.27($^{+0.69}_{-0.25}$)	-11.09(0.18)	<-4.47	401.2(218.5)
J0036-1112	7513(108)	8.20($^{+0.04}_{-0.04}$)	0.70($^{+0.02}_{-0.02}$)	-9.06(0.08)	<-4.02	52.3(0.3)
J0038+1645	6609(313)	8.54($^{+0.46}_{-0.40}$)	0.93($^{+0.26}_{-0.26}$)	-10.06(0.19)	<-3.05	170.3(55.3)
J0039+1416	6557(327)	8.00		-8.77(0.24)	<-3.46	327.0(29.2)
J0040+2349	8170(231)	8.22($^{+0.11}_{-0.11}$)	0.72($^{+0.07}_{-0.07}$)	-9.73(0.06)	<-4.54	158.6(10.0)
J0040+2723	6448(375)	7.71($^{+1.14}_{-0.86}$)	0.42($^{+0.70}_{-0.28}$)	-10.39(0.22)	<-3.61	280.0(154.9)
J0040+3016	7411(658)	8.00		-10.25(0.12)	<-4.10	302.8(39.2)
J0041+1511	8259(278)	8.02($^{+0.16}_{-0.16}$)	0.59($^{+0.10}_{-0.09}$)	-10.62(0.08)	<-4.95	187.7(16.5)
J0042+2255	7726(495)	7.48($^{+1.05}_{-0.77}$)	0.32($^{+0.60}_{-0.20}$)	-11.44(0.23)	<-5.04	373.8(180.4)
J0044+0418	6058(54)	8.20($^{+0.04}_{-0.04}$)	0.70($^{+0.03}_{-0.03}$)	-9.76(0.05)	<-3.00	74.1(1.3)
J0046+0024	9866(266)	8.29($^{+0.26}_{-0.24}$)	0.76($^{+0.17}_{-0.15}$)	-7.70(0.18)	<-5.72	230.9(39.8)

Table 6. Atmospheric parameters for DZ stars – continued.

J Name	T_{eff} (K)	$\log g$	M/M_{\odot}	$\log \text{Ca/He}$	$\log \text{H/He}$	D (pc)
J0046+0635	6738(134)	8.04($^{+0.07}_{-0.07}$)	0.60($^{+0.05}_{-0.04}$)	-11.05(0.05)	<-3.63	101.9(3.0)
J0046+2717	8041(262)	8.53($^{+0.26}_{-0.24}$)	0.92($^{+0.16}_{-0.16}$)	-7.43(0.23)	<-4.09	219.9(42.3)
J0049+0523	6106(211)	8.20($^{+0.08}_{-0.08}$)	0.70($^{+0.06}_{-0.05}$)	-9.92(0.03)	<-3.01	4.3(0.0)
J0050+1828	7029(372)	8.00		-9.33(0.26)	<-3.92	323.6(25.2)
J0050-0621	6466(234)	8.29($^{+0.34}_{-0.31}$)	0.76($^{+0.22}_{-0.20}$)	-9.21(0.16)	<-3.10	194.4(43.0)
J0052+1846	5021(138)	8.00		-9.73(0.37)	<-3.00	198.3(13.6)
J0053+3115	6290(374)	8.00		-9.71(0.71)	<-3.19	282.8(28.2)
J0055+2413	7652(412)	8.00		-9.10(0.86)	<-4.27	353.4(26.7)
J0056+0005	6567(306)	8.00		-9.85(0.39)	<-3.47	346.3(26.4)
J0056+2453	5206(153)	8.00		-10.10(0.31)	<-3.01	203.1(13.3)
J0058+0507	8817(759)	8.00		-9.69(0.27)	<-5.45	426.1(50.8)
J0058+1102	6366(93)	8.04($^{+0.09}_{-0.09}$)	0.60($^{+0.06}_{-0.05}$)	-9.67(0.09)	<-3.23	113.3(5.5)
J0059+0017	10839(415)	8.15($^{+0.19}_{-0.18}$)	0.67($^{+0.13}_{-0.11}$)	-8.80(0.12)	<-5.94	242.6(29.0)
J0102+1817	6374(245)	8.00		-9.18(0.25)	<-3.27	293.1(19.6)
J0102+3112	7001(566)	8.00		-9.61(0.34)	<-3.90	331.6(39.0)
J0104-0030	7615(931)	8.00		-9.37(0.77)	<-4.23	592.6(105.9)
J0106+2412	5590(4814)	8.00		-10.40(0.07)	<-3.00	349.3(419.7)
J0106-0103	11222(493)	7.90($^{+0.15}_{-0.14}$)	0.53($^{+0.09}_{-0.07}$)	-8.10(0.09)	-4.32(0.12)	226.1(17.8)
J0107+2650	5258(80)	8.18($^{+0.06}_{-0.06}$)	0.69($^{+0.04}_{-0.04}$)	-9.47(0.17)	<-3.00	68.3(1.6)
J0107+2905	6904(111)	7.88($^{+0.19}_{-0.18}$)	0.51($^{+0.11}_{-0.09}$)	-9.38(0.14)	<-3.90	171.9(18.5)
J0108-0537	6326(160)	7.35($^{+0.48}_{-0.42}$)	0.27($^{+0.21}_{-0.11}$)	-9.10(0.14)	<-3.75	260.3(60.4)
J0111+1501	10838(413)	7.98($^{+0.18}_{-0.17}$)	0.57($^{+0.11}_{-0.09}$)	-8.46(0.12)	<-6.01	275.7(28.3)
J0111+2848	7217(964)	8.00		-9.47(0.48)	<-4.02	399.8(75.4)
J0113-0006	7617(202)	7.92($^{+0.15}_{-0.15}$)	0.53($^{+0.09}_{-0.08}$)	-10.17(0.08)	<-4.32	176.9(14.6)
J0113-0959	10480(384)	8.00($^{+0.07}_{-0.07}$)	0.58($^{+0.04}_{-0.04}$)	-8.44(0.09)	-5.19(0.13)	129.9(2.3)
J0114+3505	6233(165)	8.00		-8.46(0.15)	<-3.14	242.1(12.8)
J0115-0542	7739(417)	7.76($^{+0.81}_{-0.62}$)	0.44($^{+0.50}_{-0.23}$)	-10.14(0.12)	<-4.67	324.7(135.3)
J0116+0328	7204(368)	8.00		-9.64(0.22)	<-4.01	281.5(21.5)
J0116+0345	7377(500)	8.00		-9.61(0.29)	<-4.08	301.5(30.6)
J0116+1744	7122(215)	8.20($^{+0.21}_{-0.20}$)	0.70($^{+0.14}_{-0.13}$)	-10.02(0.15)	<-3.83	193.2(25.7)
J0116+2050	6258(33)	8.02($^{+0.03}_{-0.03}$)	0.58($^{+0.02}_{-0.02}$)	-8.81(0.05)	<-3.15	73.6(1.0)
J0116+2229	8603(394)	8.00		-8.10(0.83)	<-5.33	444.2(30.4)
J0117+0021	7068(86)	8.08($^{+0.09}_{-0.08}$)	0.63($^{+0.06}_{-0.05}$)	-8.57(0.06)	<-3.89	141.3(7.0)
J0117+0039	6135(510)	8.00		-10.06(0.35)	<-3.07	388.3(57.7)
J0119+1758	5327(143)	8.00		-9.79(0.25)	<-3.01	238.5(17.1)
J0120-0041	11792(423)	7.84($^{+0.12}_{-0.11}$)	0.50($^{+0.07}_{-0.06}$)	-9.12(0.24)	<-6.10	227.4(13.9)
J0121+1504	8149(836)	8.00		-8.56(0.52)	<-4.84	579.2(92.6)
J0121+3440	6906(134)	8.13($^{+0.05}_{-0.05}$)	0.65($^{+0.03}_{-0.03}$)	-10.80(0.06)	<-3.72	38.9(0.2)

Table 6. Atmospheric parameters for DZ stars – continued.

J Name	T_{eff} (K)	$\log g$	M/M_{\odot}	$\log \text{Ca/He}$	$\log \text{H/He}$	D (pc)
J0123+1324	7341(239)	8.33($^{+0.19}_{-0.18}$)	0.79($^{+0.12}_{-0.12}$)	-9.85(0.25)	<-3.86	178.8(22.0)
J0125+2346	7009(477)	8.00		-10.19(0.27)	<-3.91	347.8(36.1)
J0126+2534	5692(162)	8.58($^{+0.19}_{-0.18}$)	0.95($^{+0.12}_{-0.12}$)	-9.11(0.20)	<-3.01	113.0(15.5)
J0127+1545	6576(307)	8.00		-8.95(0.29)	<-3.48	329.7(26.2)
J0130+2218	6568(677)	8.00		-9.26(0.55)	<-3.48	385.9(59.4)
J0131+0250	4808(139)	8.00		-10.04(0.21)	<-3.00	164.1(11.8)
J0134+1857	6525(253)	8.15($^{+0.32}_{-0.29}$)	0.67($^{+0.21}_{-0.18}$)	-10.22(0.13)	<-3.28	210.5(40.8)
J0135+1302	6005(63)	8.11($^{+0.07}_{-0.07}$)	0.64($^{+0.05}_{-0.04}$)	-9.23(0.14)	<-3.00	98.9(4.0)
J0135-0027	4811(127)	7.62($^{+0.23}_{-0.22}$)	0.37($^{+0.11}_{-0.09}$)	-11.09(0.11)	<-3.00	108.5(11.7)
J0136+0229	7032(422)	8.00		-9.19(0.47)	<-3.92	408.2(36.1)
J0138+0031	9494(329)	8.13($^{+0.26}_{-0.24}$)	0.66($^{+0.17}_{-0.14}$)	-9.95(0.14)	<-5.77	216.2(34.4)
J0140+3125	6741(674)	8.00		-9.67(0.24)	<-3.67	343.3(54.6)
J0140+3357	6473(133)	8.09($^{+0.08}_{-0.08}$)	0.63($^{+0.05}_{-0.05}$)	-10.95(0.10)	<-3.28	101.5(4.1)
J0141+2921	6647(189)	7.87($^{+0.21}_{-0.19}$)	0.50($^{+0.12}_{-0.10}$)	-10.54(0.07)	<-3.69	184.2(20.3)
J0142+0118	6727(244)	7.84($^{+0.28}_{-0.26}$)	0.48($^{+0.17}_{-0.13}$)	-11.00(0.11)	<-3.79	219.4(32.8)
J0143+0113	7297(95)	8.20($^{+0.09}_{-0.09}$)	0.70($^{+0.06}_{-0.06}$)	-8.08(0.05)	<-3.92	145.1(8.0)
J0143+0424	7403(393)	8.00		-8.61(0.34)	<-4.10	359.5(29.3)
J0144+0305	6272(280)	8.00		-9.96(0.37)	<-3.17	288.8(22.6)
J0144+1920	5863(198)	8.00		-9.06(0.11)	<-3.00	190.4(12.6)
J0147+1541	8762(1288)	8.00		-8.58(1.43)	<-5.42	660.0(137.1)
J0147-0623	7330(557)	8.00		-9.56(0.43)	<-4.06	372.7(40.5)
J0148-0112	6791(166)	7.69($^{+1.17}_{-0.87}$)	0.41($^{+0.71}_{-0.27}$)	-9.04(0.17)	<-3.94	312.5(177.7)
J0150+1354	6996(124)	8.32($^{+0.15}_{-0.14}$)	0.78($^{+0.10}_{-0.09}$)	-8.34(0.15)	<-3.63	170.0(16.8)
J0150+1710	8422(598)	7.72($^{+0.66}_{-0.52}$)	0.43($^{+0.40}_{-0.19}$)	-10.39(0.16)	<-5.47	374.5(126.0)
J0152+2418	7465(115)	8.08($^{+0.04}_{-0.04}$)	0.62($^{+0.03}_{-0.03}$)	-9.24(0.07)	<-4.07	52.9(0.3)
J0153+0101	7480(774)	8.00		-9.95(0.35)	<-4.14	478.2(73.6)
J0158-0942	6126(177)	8.06($^{+0.30}_{-0.28}$)	0.61($^{+0.20}_{-0.16}$)	-10.07(0.13)	<-3.04	176.8(31.9)
J0200+0040	10467(359)	8.16($^{+0.10}_{-0.10}$)	0.68($^{+0.06}_{-0.06}$)	-9.10(0.14)	<-5.90	169.4(8.4)
J0201+2015	6306(194)	8.16($^{+0.23}_{-0.21}$)	0.67($^{+0.15}_{-0.13}$)	-8.99(0.13)	<-3.10	170.2(23.2)
J0201-0039	9863(261)	8.15($^{+0.06}_{-0.06}$)	0.67($^{+0.04}_{-0.04}$)	-7.99(0.05)	<-5.81	111.2(2.0)
J0202+2459	6248(353)	8.00		-9.19(0.47)	<-3.15	359.4(40.1)
J0209+0558	8575(464)	7.62($^{+0.79}_{-0.57}$)	0.38($^{+0.46}_{-0.18}$)	-9.91(0.22)	<-5.63	382.1(150.4)
J0209+2914	6790(226)	8.52($^{+0.16}_{-0.15}$)	0.91($^{+0.10}_{-0.10}$)	-9.27(0.10)	<-3.22	146.3(16.3)
J0211-0046	10701(454)	7.79($^{+0.37}_{-0.31}$)	0.46($^{+0.21}_{-0.14}$)	-8.91(0.50)	-5.36(0.57)	354.5(71.9)
J0213+2848	6920(316)	7.80($^{+0.25}_{-0.23}$)	0.46($^{+0.14}_{-0.11}$)	-10.69(0.08)	<-3.96	207.7(25.1)
J0214+0536	7492(355)	8.01($^{+0.40}_{-0.36}$)	0.58($^{+0.26}_{-0.19}$)	-10.16(0.13)	<-4.13	269.1(63.0)
J0218-0919	10273(321)	8.19($^{+0.06}_{-0.06}$)	0.70($^{+0.04}_{-0.04}$)	-9.81(0.04)	<-5.84	96.2(1.1)
J0221-0445	7719(873)	8.00		-10.45(0.30)	<-4.33	423.8(70.4)

Table 6. Atmospheric parameters for DZ stars – continued.

J Name	T_{eff} (K)	$\log g$	M/M_{\odot}	$\log \text{Ca/He}$	$\log \text{H/He}$	D (pc)
J0225–0018	6207(101)	8.24($^{+0.15}_{-0.14}$)	0.73($^{+0.10}_{-0.09}$)	-10.01(0.12)	<-3.02	135.4(13.1)
J0226–0444	7247(757)	8.00		-10.37(0.20)	<-4.03	405.8(64.3)
J0228–0009	8573(312)	8.41($^{+0.30}_{-0.27}$)	0.84($^{+0.19}_{-0.18}$)	-8.79(0.79)	<-4.64	227.1(47.1)
J0231–0142	7037(736)	8.00		-10.17(0.23)	<-3.92	397.6(65.2)
J0234–0510	6696(245)	8.00		-8.55(0.18)	<-3.62	303.9(19.3)
J0241–0533	8379(226)	7.99($^{+0.09}_{-0.09}$)	0.57($^{+0.05}_{-0.05}$)	-9.61(0.07)	-3.34(0.11)	143.3(5.6)
J0251+7341	7531(155)	8.07($^{+0.05}_{-0.05}$)	0.62($^{+0.03}_{-0.03}$)	-9.97(0.08)	<-4.12	61.4(0.3)
J0252+0054	7433(130)	8.01($^{+0.18}_{-0.17}$)	0.58($^{+0.11}_{-0.10}$)	-8.55(0.21)	<-4.10	205.3(21.8)
J0252–0401	6936(150)	8.03($^{+0.29}_{-0.27}$)	0.59($^{+0.19}_{-0.15}$)	-8.59(0.10)	<-3.83	220.4(37.9)
J0302–0108	13594(1735)	8.02($^{+0.19}_{-0.18}$)	0.60($^{+0.12}_{-0.10}$)	-7.58(0.10)	-6.11(0.16)	64.4(0.3)
J0308–0657	10049(487)	8.30($^{+0.28}_{-0.26}$)	0.77($^{+0.18}_{-0.16}$)	-8.08(0.54)	<-5.72	289.0(52.3)
J0314+0524	14241(1314)	8.09($^{+0.23}_{-0.21}$)	0.64($^{+0.14}_{-0.12}$)	-7.43(0.32)	<-6.03	277.0(31.4)
J0314–0827	11810(625)	8.21($^{+0.57}_{-0.48}$)	0.72($^{+0.36}_{-0.27}$)	-7.79(0.78)	<-6.05	353.2(126.4)
J0319+3630	6335(307)	8.12($^{+0.12}_{-0.11}$)	0.64($^{+0.08}_{-0.07}$)	-9.37(0.14)	<-3.15	32.0(0.1)
J0411–0548	10069(652)	8.43($^{+0.33}_{-0.30}$)	0.86($^{+0.21}_{-0.20}$)	-9.18(0.43)	<-5.60	291.7(65.6)
J0438+4109	15680(1633)	8.04($^{+0.16}_{-0.15}$)	0.62($^{+0.10}_{-0.09}$)	-8.51(0.56)	-4.34(0.06)	53.7(0.2)
J0447+1124	6598(141)	7.81($^{+0.29}_{-0.27}$)	0.47($^{+0.17}_{-0.13}$)	-9.28(0.17)	<-3.69	206.6(33.6)
J0536+6154	10953(398)	8.02($^{+0.07}_{-0.06}$)	0.59($^{+0.04}_{-0.04}$)	-8.32(0.06)	-5.59(0.13)	132.7(2.1)
J0555–0410	4491(67)	7.92($^{+0.06}_{-0.06}$)	0.52($^{+0.03}_{-0.03}$)	-11.16(0.02)	<-30.00	6.4(0.0)
J0618+6413	9000(289)	8.02($^{+0.11}_{-0.11}$)	0.59($^{+0.07}_{-0.06}$)	-10.37(0.06)	<-5.54	186.1(9.1)
J0627+1002	8429(411)	8.07($^{+0.09}_{-0.09}$)	0.62($^{+0.06}_{-0.05}$)	-10.50(0.03)	<-5.08	52.8(0.2)
J0649+3726	6627(124)	8.25($^{+0.14}_{-0.13}$)	0.74($^{+0.09}_{-0.09}$)	-9.98(0.11)	<-3.28	142.6(12.8)
J0721+3928	5997(164)	8.00		-9.47(0.15)	<-3.00	189.1(9.9)
J0721+3955	6731(90)	7.92($^{+0.05}_{-0.05}$)	0.53($^{+0.03}_{-0.03}$)	-9.73(0.07)	<-3.72	96.1(1.9)
J0730+3456	10970(420)	8.04($^{+0.07}_{-0.07}$)	0.61($^{+0.04}_{-0.04}$)	-8.94(0.06)	-5.31(0.09)	98.0(1.2)
J0732+2746	12084(553)	8.01($^{+0.16}_{-0.15}$)	0.59($^{+0.10}_{-0.08}$)	-8.76(0.15)	-5.74(0.33)	238.0(21.3)
J0733+3727	7599(291)	7.88($^{+0.42}_{-0.37}$)	0.51($^{+0.26}_{-0.18}$)	-10.84(0.21)	<-4.35	252.0(59.2)
J0734+4448	13863(822)	8.42($^{+0.20}_{-0.19}$)	0.86($^{+0.13}_{-0.12}$)	-9.34(0.56)	<-6.02	288.5(38.4)
J0736+4118	4676(70)	7.99($^{+0.11}_{-0.11}$)	0.56($^{+0.07}_{-0.06}$)	-9.73(0.24)	<-3.00	80.3(3.9)
J0738+3844	10280(279)	8.11($^{+0.24}_{-0.22}$)	0.65($^{+0.16}_{-0.13}$)	-7.27(0.21)	-4.78(0.51)	300.5(45.4)
J0739+3024	7106(624)	8.00		-9.75(0.32)	<-3.96	427.7(56.1)
J0740–1724	7545(587)	7.99($^{+0.16}_{-0.16}$)	0.57($^{+0.10}_{-0.09}$)	-10.93(0.05)	-3.38(0.04)	9.2(0.0)
J0741+3146	6065(113)	8.29($^{+0.20}_{-0.19}$)	0.76($^{+0.13}_{-0.12}$)	-8.63(0.12)	<-3.00	154.5(20.5)
J0741+4829	6741(217)	8.34($^{+0.20}_{-0.19}$)	0.80($^{+0.14}_{-0.13}$)	-10.59(0.15)	<-3.32	174.9(23.7)
J0742+2422	7106(469)	8.00		-10.13(0.27)	<-3.96	332.4(33.3)
J0743+4240	12303(728)	7.72($^{+0.63}_{-0.47}$)	0.44($^{+0.37}_{-0.17}$)	-8.45(0.86)	<-6.14	511.7(172.1)
J0744+1640	4943(85)	8.11($^{+0.24}_{-0.23}$)	0.64($^{+0.16}_{-0.14}$)	-9.88(0.27)	<-3.00	118.5(16.8)
J0744+2701	7735(189)	8.20($^{+0.33}_{-0.30}$)	0.70($^{+0.22}_{-0.19}$)	-8.30(0.19)	<-4.17	246.0(52.1)

Table 6. Atmospheric parameters for DZ stars – continued.

J Name	T_{eff} (K)	$\log g$	M/M_{\odot}	$\log \text{Ca/He}$	$\log \text{H/He}$	D (pc)
J0744+4408	6655(246)	8.00		-8.69(0.24)	<-3.57	310.2(21.0)
J0744+4649	5045(61)	8.15($^{+0.05}_{-0.05}$)	0.66($^{+0.03}_{-0.03}$)	-8.25(0.03)	<-3.00	56.0(0.9)
J0747+3732	10165(373)	7.79($^{+0.27}_{-0.24}$)	0.46($^{+0.15}_{-0.11}$)	-9.18(0.24)	<-6.00	322.4(47.3)
J0747+4001	8688(268)	8.14($^{+0.09}_{-0.09}$)	0.66($^{+0.06}_{-0.06}$)	-10.82(0.18)	<-5.21	150.6(5.9)
J0747+4825	6647(185)	7.83($^{+0.34}_{-0.31}$)	0.48($^{+0.20}_{-0.14}$)	-10.45(0.08)	<-3.72	198.1(36.5)
J0748+2544	6497(512)	8.00		-10.60(0.43)	<-3.40	383.1(49.5)
J0748+3506	11168(481)	7.27($^{+1.26}_{-0.71}$)	0.27($^{+0.65}_{-0.14}$)	-9.23(0.40)	<-6.21	600.7(337.0)
J0749+3124	6678(90)	8.12($^{+0.05}_{-0.05}$)	0.65($^{+0.03}_{-0.03}$)	-9.97(0.04)	<-3.47	91.7(2.1)
J0749+4343	9459(477)	8.55($^{+0.30}_{-0.27}$)	0.93($^{+0.18}_{-0.18}$)	-9.18(0.25)	<-5.38	253.3(54.6)
J0751+1310	11886(458)	7.92($^{+0.10}_{-0.10}$)	0.54($^{+0.06}_{-0.05}$)	-8.26(0.19)	<-6.10	227.9(10.7)
J0753+2332	11150(914)	8.50($^{+0.82}_{-0.61}$)	0.91($^{+0.39}_{-0.39}$)	-9.67(0.34)	-4.85(0.79)	340.3(178.2)
J0753+2741	6548(369)	8.00		-9.41(0.47)	<-3.45	388.1(36.3)
J0753+6613	7485(179)	8.03($^{+0.15}_{-0.14}$)	0.59($^{+0.09}_{-0.08}$)	-9.45(0.17)	<-4.12	198.5(17.0)
J0755+2112	6843(131)	8.25($^{+0.12}_{-0.11}$)	0.73($^{+0.08}_{-0.07}$)	-9.46(0.10)	<-3.53	148.3(10.9)
J0756+3353	7909(256)	7.82($^{+0.26}_{-0.24}$)	0.48($^{+0.15}_{-0.12}$)	-9.69(0.10)	<-4.78	262.8(37.7)
J0758+1013	5600(144)	8.00		-8.50(0.14)	<-3.00	219.3(13.0)
J0758+3225	10532(467)	8.55($^{+0.26}_{-0.24}$)	0.94($^{+0.16}_{-0.16}$)	-9.58(0.24)	<-5.56	236.2(44.7)
J0800+2242	6153(172)	8.05($^{+0.58}_{-0.51}$)	0.60($^{+0.38}_{-0.26}$)	-9.82(0.17)	<-3.06	210.6(71.8)
J0801+1344	10073(523)	8.12($^{+0.56}_{-0.47}$)	0.66($^{+0.36}_{-0.26}$)	-9.30(0.36)	<-5.85	367.6(124.7)
J0801+1414	15066(1062)	8.08($^{+0.11}_{-0.11}$)	0.64($^{+0.07}_{-0.06}$)	-8.46(0.32)	-5.50(0.21)	177.9(5.0)
J0801+5329	8805(210)	8.22($^{+0.06}_{-0.05}$)	0.72($^{+0.04}_{-0.04}$)	-8.36(0.16)	<-5.21	82.4(0.9)
J0802+3012	10471(544)	8.14($^{+0.97}_{-0.71}$)	0.67($^{+0.56}_{-0.35}$)	-8.14(0.35)	<-5.91	419.8(231.2)
J0802+4050	13247(794)	7.91($^{+0.13}_{-0.12}$)	0.54($^{+0.07}_{-0.06}$)	-9.54(0.26)	-5.22(0.14)	196.7(7.0)
J0802+4257	6705(230)	7.83($^{+0.66}_{-0.55}$)	0.48($^{+0.42}_{-0.23}$)	-9.85(0.13)	<-3.77	250.8(88.9)
J0803+4502	9225(327)	8.18($^{+0.22}_{-0.21}$)	0.69($^{+0.15}_{-0.13}$)	-9.38(0.23)	-3.68(0.37)	238.5(33.2)
J0805+3832	10680(354)	8.11($^{+0.06}_{-0.06}$)	0.65($^{+0.04}_{-0.04}$)	-9.60(0.02)	<-5.95	45.3(0.1)
J0805+5406	12942(535)	8.08($^{+0.07}_{-0.07}$)	0.64($^{+0.05}_{-0.04}$)	-9.27(0.19)	-6.13(0.37)	154.6(3.7)
J0806+3055	6708(153)	8.00		-8.72(0.14)	<-3.63	255.0(10.0)
J0806+3640	10881(533)	7.81($^{+0.73}_{-0.55}$)	0.48($^{+0.46}_{-0.21}$)	-8.23(0.47)	<-6.06	459.9(182.2)
J0806+3702	6751(229)	8.02($^{+0.31}_{-0.29}$)	0.59($^{+0.20}_{-0.16}$)	-10.48(0.13)	<-3.66	209.4(37.6)
J0806+3747	9800(263)	8.19($^{+0.14}_{-0.13}$)	0.70($^{+0.09}_{-0.08}$)	-7.93(0.13)	<-5.78	236.0(20.3)
J0807+4930	5281(138)	8.15($^{+0.29}_{-0.27}$)	0.66($^{+0.19}_{-0.16}$)	-8.21(0.14)	<-3.00	153.7(26.2)
J0808+2118	9048(1059)	8.00		-9.38(0.40)	<-5.58	577.7(99.0)
J0808+2809	6878(155)	8.24($^{+0.27}_{-0.25}$)	0.73($^{+0.18}_{-0.16}$)	-8.21(0.13)	<-3.58	214.5(37.6)
J0809+1034	6842(138)	8.27($^{+0.07}_{-0.07}$)	0.75($^{+0.05}_{-0.05}$)	-10.18(0.06)	<-3.51	109.0(4.1)
J0809+3106	11657(434)	7.85($^{+0.11}_{-0.10}$)	0.50($^{+0.06}_{-0.05}$)	-9.55(0.24)	-5.44(0.26)	230.0(11.8)
J0812+0942	10593(332)	7.76($^{+0.17}_{-0.15}$)	0.45($^{+0.09}_{-0.07}$)	-7.59(0.16)	<-6.08	293.0(26.5)
J0812+3614	7612(388)	8.00		-9.79(0.23)	<-4.23	360.7(27.3)

Table 6. Atmospheric parameters for DZ stars – continued.

J Name	T_{eff} (K)	$\log g$	M/M_{\odot}	$\log \text{Ca/He}$	$\log \text{H/He}$	D (pc)
J0813+3453	6753(300)	8.00		-9.61(0.35)	<-3.68	331.4(22.3)
J0813+3506	7094(172)	8.06($^{+0.45}_{-0.40}$)	0.61($^{+0.30}_{-0.22}$)	-9.12(0.25)	<-3.91	247.4(67.6)
J0816+2330	7143(415)	8.00		-9.81(0.35)	<-3.98	310.9(25.6)
J0818+1247	6872(264)	8.00		-9.03(0.36)	<-3.80	310.6(19.3)
J0818-3110	6535(645)	8.28($^{+0.19}_{-0.18}$)	0.75($^{+0.13}_{-0.12}$)	-8.99(0.04)	<-3.17	19.4(0.0)
J0819+0027	11366(567)	8.19($^{+0.23}_{-0.21}$)	0.70($^{+0.15}_{-0.13}$)	-8.47(0.21)	-4.16(0.56)	250.3(34.8)
J0819+5732	6074(80)	7.99($^{+0.04}_{-0.04}$)	0.56($^{+0.03}_{-0.03}$)	-11.10(0.10)	<-3.04	54.5(0.3)
J0822+3910	11277(765)	7.87($^{+0.81}_{-0.59}$)	0.51($^{+0.51}_{-0.24}$)	-8.83(0.37)	<-6.05	440.1(191.2)
J0822+5202	6639(346)	8.00		-10.28(0.13)	<-3.55	262.3(22.8)
J0822+5203	10039(369)	8.07($^{+0.20}_{-0.19}$)	0.62($^{+0.13}_{-0.11}$)	-9.30(0.09)	<-5.87	237.6(27.7)
J0823+2015	10575(374)	8.05($^{+0.12}_{-0.12}$)	0.61($^{+0.08}_{-0.07}$)	-8.68(0.07)	<-5.98	220.3(14.4)
J0825+2009	8457(397)	8.00($^{+0.28}_{-0.26}$)	0.58($^{+0.18}_{-0.14}$)	-9.89(0.24)	<-5.21	271.6(43.7)
J0825+2148	6411(147)	8.22($^{+0.10}_{-0.10}$)	0.71($^{+0.07}_{-0.07}$)	-10.96(0.19)	<-3.12	126.7(7.2)
J0827+1731	10537(382)	8.06($^{+0.08}_{-0.08}$)	0.62($^{+0.05}_{-0.05}$)	-9.70(0.04)	-4.27(0.07)	129.1(2.7)
J0827+2857	7465(277)	8.78($^{+0.35}_{-0.30}$)	1.07($^{+0.17}_{-0.19}$)	-8.68(0.57)	<-3.57	183.4(51.3)
J0827+3304	8489(203)	7.94($^{+0.23}_{-0.21}$)	0.54($^{+0.14}_{-0.11}$)	-8.50(0.36)	<-5.32	259.1(33.9)
J0827+5504	7371(511)	8.00		-10.14(0.30)	<-4.08	341.2(35.5)
J0829+0759	10016(287)	8.15($^{+0.09}_{-0.09}$)	0.67($^{+0.06}_{-0.06}$)	-7.95(0.10)	<-5.83	176.1(8.7)
J0829+3551	6682(678)	8.00		-10.28(0.45)	<-3.60	390.4(62.5)
J0830-0319	6365(105)	7.70($^{+0.13}_{-0.12}$)	0.41($^{+0.06}_{-0.06}$)	-9.51(0.13)	<-3.52	174.4(11.3)
J0831+1801	7103(436)	8.00		-10.50(0.17)	<-3.96	284.8(26.6)
J0833+0512	12185(555)	7.42($^{+0.41}_{-0.30}$)	0.32($^{+0.17}_{-0.08}$)	-9.37(0.30)	<-6.18	424.0(91.5)
J0834+2422	11590(456)	8.04($^{+0.12}_{-0.11}$)	0.61($^{+0.07}_{-0.06}$)	-8.18(0.15)	-5.25(0.14)	214.2(13.0)
J0834+3927	8117(673)	8.00		-8.42(0.37)	<-4.80	532.6(66.0)
J0834+4641	7065(84)	8.04($^{+0.07}_{-0.07}$)	0.60($^{+0.04}_{-0.04}$)	-9.20(0.13)	<-3.91	123.1(4.4)
J0835+0906	8546(315)	8.18($^{+0.13}_{-0.13}$)	0.69($^{+0.09}_{-0.08}$)	-9.60(0.11)	<-5.00	155.7(11.3)
J0838+2322	6037(61)	8.25($^{+0.05}_{-0.05}$)	0.73($^{+0.03}_{-0.03}$)	-9.84(0.13)	<-3.00	84.4(2.2)
J0838+5455	6795(315)	8.25($^{+0.53}_{-0.47}$)	0.73($^{+0.34}_{-0.28}$)	-10.51(0.27)	<-3.47	205.8(69.3)
J0839+2158	8340(265)	8.26($^{+0.14}_{-0.14}$)	0.74($^{+0.09}_{-0.09}$)	-8.78(0.31)	<-4.63	162.3(14.0)
J0839+2618	14581(1486)	8.09($^{+0.27}_{-0.24}$)	0.64($^{+0.17}_{-0.14}$)	-8.29(0.67)	-3.98(0.28)	315.8(39.2)
J0840+0237	7398(302)	7.53($^{+0.51}_{-0.41}$)	0.34($^{+0.26}_{-0.13}$)	-11.02(0.10)	<-4.59	318.1(80.7)
J0840+1306	6854(216)	7.96($^{+0.35}_{-0.32}$)	0.55($^{+0.22}_{-0.17}$)	-11.03(0.16)	<-3.81	198.5(39.7)
J0840+3202	7535(886)	8.00		-10.07(0.38)	<-4.17	453.9(78.8)
J0840+3812	7421(760)	8.00		-9.96(0.26)	<-4.11	478.6(68.9)
J0841+3723	12036(493)	7.93($^{+0.08}_{-0.08}$)	0.55($^{+0.05}_{-0.04}$)	-7.95(0.08)	<-6.11	171.3(5.2)
J0841+5414	7884(304)	7.83($^{+0.21}_{-0.20}$)	0.48($^{+0.12}_{-0.10}$)	-10.33(0.07)	<-4.73	220.5(24.1)
J0842+1406	7111(55)	7.99($^{+0.04}_{-0.04}$)	0.57($^{+0.03}_{-0.03}$)	-8.45(0.06)	<-3.97	99.1(2.1)
J0842+1536	5932(137)	8.00		-9.88(0.23)	<-3.00	198.7(9.1)

Table 6. Atmospheric parameters for DZ stars – continued.

J Name	T_{eff} (K)	$\log g$	M/M_{\odot}	$\log \text{Ca/He}$	$\log \text{H/He}$	D (pc)
J0842+3625	10322(424)	$8.02^{(+0.13)}_{(-0.13)}$	$0.59^{(+0.08)}_{(-0.07)}$	-9.00(0.15)	-4.78(0.21)	213.7(14.2)
J0842-1347	5010(89)	$8.05^{(+0.06)}_{(-0.06)}$	$0.60^{(+0.04)}_{(-0.04)}$	-9.93(0.13)	<-3.00	14.8(0.0)
J0843+1247	6507(163)	$8.52^{(+0.16)}_{(-0.15)}$	$0.92^{(+0.10)}_{(-0.10)}$	-10.23(0.13)	<-3.00	134.9(15.4)
J0843+5614	6581(183)	$8.32^{(+0.25)}_{(-0.24)}$	$0.78^{(+0.17)}_{(-0.16)}$	-8.78(0.15)	<-3.17	183.9(31.4)
J0844+5446	7033(412)	$8.36^{(+0.39)}_{(-0.35)}$	$0.81^{(+0.25)}_{(-0.23)}$	-9.77(0.16)	<-3.62	216.9(55.3)
J0845+1258	9473(329)	$8.38^{(+0.42)}_{(-0.37)}$	$0.82^{(+0.26)}_{(-0.24)}$	-7.98(0.37)	<-5.57	275.4(79.2)
J0845+4115	8194(248)	$7.43^{(+0.32)}_{(-0.26)}$	$0.31^{(+0.13)}_{(-0.08)}$	-9.62(0.25)	<-5.51	297.3(47.2)
J0845+4802	8145(871)	8.00		-8.46(0.50)	<-4.84	608.1(103.0)
J0845+5352	7138(167)	$8.21^{(+0.09)}_{(-0.09)}$	$0.71^{(+0.06)}_{(-0.06)}$	-10.68(0.14)	<-3.83	125.4(5.7)
J0846+3538	8791(204)	$8.16^{(+0.05)}_{(-0.05)}$	$0.68^{(+0.03)}_{(-0.03)}$	-8.69(0.10)	<-5.27	24.6(0.0)
J0847+4507	8921(394)	$8.46^{(+0.18)}_{(-0.17)}$	$0.88^{(+0.12)}_{(-0.12)}$	-9.51(0.22)	<-5.09	210.6(26.0)
J0848+0028	11667(380)	$7.89^{(+0.11)}_{(-0.10)}$	$0.52^{(+0.06)}_{(-0.05)}$	-7.55(0.08)	<-6.09	236.4(12.9)
J0848+3548	7864(189)	$8.17^{(+0.06)}_{(-0.06)}$	$0.68^{(+0.04)}_{(-0.04)}$	-10.49(0.04)	<-4.30	89.3(1.8)
J0848+5214	8349(221)	$8.07^{(+0.07)}_{(-0.07)}$	$0.62^{(+0.04)}_{(-0.04)}$	-10.72(0.06)	<-4.98	106.1(2.4)
J0849+0710	8477(218)	$8.32^{(+0.18)}_{(-0.17)}$	$0.78^{(+0.12)}_{(-0.11)}$	-8.34(0.29)	-3.49(0.55)	198.6(24.3)
J0849+1827	6127(67)	$8.06^{(+0.05)}_{(-0.05)}$	$0.61^{(+0.03)}_{(-0.03)}$	-10.50(0.09)	<-3.05	88.4(2.0)
J0849+1836	8805(287)	$8.03^{(+0.41)}_{(-0.37)}$	$0.60^{(+0.27)}_{(-0.20)}$	-8.39(0.38)	<-5.41	309.6(76.2)
J0849+4036	9388(295)	$8.20^{(+0.08)}_{(-0.08)}$	$0.70^{(+0.05)}_{(-0.05)}$	-10.12(0.09)	<-5.69	123.2(3.5)
J0851+0538	7415(183)	$8.09^{(+0.19)}_{(-0.18)}$	$0.63^{(+0.12)}_{(-0.11)}$	-9.50(0.31)	<-4.04	195.0(22.6)
J0851+1543	6495(63)	$8.21^{(+0.05)}_{(-0.05)}$	$0.71^{(+0.03)}_{(-0.03)}$	-8.71(0.09)	<-3.19	96.1(2.4)
J0852+1124	6656(476)	8.00		-10.21(0.30)	<-3.57	392.3(45.3)
J0852+3402	5036(100)	$7.98^{(+0.31)}_{(-0.29)}$	$0.56^{(+0.20)}_{(-0.16)}$	-9.56(0.25)	<-3.00	154.8(27.4)
J0852+5124	7827(721)	8.00		-9.63(0.42)	<-4.44	432.7(60.4)
J0853+1603	7538(526)	$8.11^{(+1.88)}_{(-1.02)}$	$0.64^{(+1.05)}_{(-0.44)}$	-10.32(0.18)	<-4.09	307.6(248.6)
J0854+0603	7340(345)	$7.85^{(+0.43)}_{(-0.38)}$	$0.49^{(+0.26)}_{(-0.17)}$	-10.90(0.17)	<-4.19	282.9(65.2)
J0854+1847	8119(243)	$8.23^{(+0.14)}_{(-0.13)}$	$0.72^{(+0.09)}_{(-0.09)}$	-9.94(0.09)	<-4.48	170.7(14.5)
J0855+5438	7903(936)	8.00		-8.50(1.25)	<-4.53	615.5(111.4)
J0857+1438	8180(201)	$8.11^{(+0.15)}_{(-0.14)}$	$0.64^{(+0.10)}_{(-0.09)}$	-9.09(0.42)	<-4.72	184.7(16.2)
J0857+2630	6402(127)	$7.82^{(+0.24)}_{(-0.22)}$	$0.47^{(+0.14)}_{(-0.11)}$	-10.86(0.11)	<-3.46	144.0(18.9)
J0859+5732	13140(903)	$8.08^{(+0.21)}_{(-0.20)}$	$0.63^{(+0.13)}_{(-0.11)}$	-7.96(0.37)	<-6.09	301.8(36.1)
J0900+1020	7301(378)	8.00		-10.61(0.18)	<-4.05	316.7(24.7)
J0901+0752	6995(117)	$7.91^{(+0.31)}_{(-0.29)}$	$0.52^{(+0.19)}_{(-0.15)}$	-7.87(0.08)	<-3.95	216.7(38.8)
J0901+1113	7545(465)	8.00		-10.51(0.23)	<-4.18	378.7(35.8)
J0901+5337	5802(284)	8.00		-10.71(0.65)	<-3.00	253.0(23.9)
J0903-0120	8731(1234)	8.00		-9.80(0.26)	<-5.41	536.4(107.7)
J0904-0029	7933(421)	8.00		-10.35(0.12)	<-4.57	329.5(25.2)
J0905+0133	7977(227)	$8.25^{(+0.13)}_{(-0.12)}$	$0.73^{(+0.08)}_{(-0.08)}$	-10.24(0.12)	<-4.33	157.9(11.9)
J0905+0846	6152(201)	8.00		-10.09(0.28)	<-3.08	242.2(14.0)

Table 6. Atmospheric parameters for DZ stars – continued.

J Name	T_{eff} (K)	$\log g$	M/M_{\odot}	$\log \text{Ca/He}$	$\log \text{H/He}$	D (pc)
J0905+5235	7650(126)	8.15($^{+0.09}_{-0.09}$)	0.67($^{+0.06}_{-0.06}$)	-9.07(0.22)	<-4.14	143.4(7.8)
J0906+1141	6592(161)	8.00		-8.50(0.19)	<-3.50	282.9(12.5)
J0906+1628	7099(340)	8.00		-10.60(0.22)	<-3.96	270.7(19.7)
J0906+5956	9953(277)	8.31($^{+0.12}_{-0.11}$)	0.77($^{+0.08}_{-0.07}$)	-7.77(0.16)	<-5.71	214.3(15.5)
J0907+2533	8745(286)	8.22($^{+0.15}_{-0.15}$)	0.71($^{+0.10}_{-0.09}$)	-9.30(0.09)	<-5.16	184.2(17.0)
J0908+4119	6268(206)	8.00		-9.87(0.46)	<-3.17	268.7(15.3)
J0908+5136	5811(62)	7.80($^{+0.09}_{-0.09}$)	0.46($^{+0.05}_{-0.04}$)	-10.12(0.10)	<-3.00	125.2(5.6)
J0909-0045	9160(293)	8.13($^{+0.13}_{-0.13}$)	0.66($^{+0.09}_{-0.08}$)	-9.40(0.08)	<-5.59	196.4(14.3)
J0910+1045	9425(270)	8.26($^{+0.11}_{-0.11}$)	0.74($^{+0.08}_{-0.07}$)	-8.60(0.10)	<-5.66	202.0(13.7)
J0911+2433	6731(655)	8.00		-10.06(0.44)	<-3.66	433.2(70.9)
J0912-0128	7509(409)	8.00		-9.33(0.28)	<-4.16	323.5(26.3)
J0913+2627	5342(96)	8.22($^{+0.14}_{-0.13}$)	0.71($^{+0.09}_{-0.09}$)	-9.69(0.18)	<-3.00	106.8(9.0)
J0913+3116	5446(45)	8.29($^{+0.05}_{-0.05}$)	0.76($^{+0.03}_{-0.03}$)	-10.06(0.06)	<-3.00	55.0(1.3)
J0913+4127	5932(126)	8.00		-8.77(0.32)	<-3.00	229.2(10.0)
J0916+0110	7527(339)	8.00		-10.34(0.08)	<-4.17	238.8(15.5)
J0916+2540	5652(57)	8.13($^{+0.04}_{-0.04}$)	0.65($^{+0.03}_{-0.03}$)	-7.64(0.04)	<-3.00	46.3(0.4)
J0916-0212	6672(300)	7.19($^{+0.57}_{-0.59}$)	0.22($^{+0.22}_{-0.13}$)	-11.25(0.09)	<-4.21	326.1(84.9)
J0917+2146	6674(319)	8.00		-9.29(0.33)	<-3.59	357.8(28.1)
J0917+2224	6771(432)	8.00		-10.64(0.27)	<-3.70	311.6(31.9)
J0921+1204	13314(898)	7.95($^{+0.34}_{-0.30}$)	0.56($^{+0.21}_{-0.15}$)	-7.97(0.55)	-4.47(0.44)	406.3(79.9)
J0922+2007	8377(218)	7.98($^{+0.08}_{-0.08}$)	0.57($^{+0.05}_{-0.04}$)	-11.20(0.20)	-3.73(0.16)	120.0(3.7)
J0923+4823	9334(1365)	8.00		-9.09(0.60)	<-5.77	705.1(138.0)
J0924+4301	5537(117)	8.00		-10.08(0.20)	<-3.00	209.6(9.1)
J0925+2256	6748(297)	8.00		-9.74(0.35)	<-3.67	303.5(21.0)
J0925+3130	5901(58)	8.00		-8.97(0.12)	<-3.00	88.9(2.0)
J0928+1801	10189(364)	8.22($^{+0.15}_{-0.14}$)	0.72($^{+0.10}_{-0.09}$)	-9.88(0.11)	<-5.81	210.8(18.7)
J0928+6124	9167(303)	7.08($^{+1.55}_{-1.46}$)	0.21($^{+0.77}_{-0.19}$)	-8.08(0.40)	<-6.10	582.6(370.6)
J0929+4247	6683(88)	7.86($^{+0.24}_{-0.22}$)	0.50($^{+0.14}_{-0.11}$)	-8.26(0.15)	<-3.72	217.7(29.1)
J0930+2601	9843(636)	8.26($^{+0.33}_{-0.30}$)	0.74($^{+0.22}_{-0.19}$)	-10.36(0.29)	-4.01(0.46)	259.5(54.2)
J0930+3013	11366(508)	7.98($^{+0.19}_{-0.17}$)	0.57($^{+0.11}_{-0.09}$)	-9.42(0.09)	-4.71(0.12)	242.7(24.7)
J0931+0730	11699(537)	7.75($^{+0.68}_{-0.50}$)	0.45($^{+0.41}_{-0.19}$)	-8.28(0.27)	<-6.10	445.6(162.6)
J0931+1210	7431(424)	8.00		-9.11(0.34)	<-4.11	378.1(31.0)
J0932+4856	8831(257)	8.08($^{+0.30}_{-0.28}$)	0.63($^{+0.20}_{-0.16}$)	-8.34(0.47)	<-5.39	288.8(53.7)
J0933+6334	6265(165)	8.00		-8.55(0.33)	<-3.17	265.1(14.6)
J0934+0822	9453(291)	8.19($^{+0.08}_{-0.07}$)	0.70($^{+0.05}_{-0.05}$)	-9.50(0.03)	<-5.72	110.6(3.2)
J0934+2626	8367(354)	8.30($^{+0.37}_{-0.33}$)	0.77($^{+0.24}_{-0.21}$)	-10.28(0.16)	<-4.60	236.4(56.9)
J0934+5632	6494(92)	8.23($^{+0.06}_{-0.06}$)	0.72($^{+0.04}_{-0.04}$)	-9.55(0.41)	<-3.18	108.7(3.3)
J0935+0037	10098(490)	7.82($^{+0.85}_{-0.61}$)	0.48($^{+0.53}_{-0.23}$)	-7.83(0.44)	<-5.98	492.7(222.6)

Table 6. Atmospheric parameters for DZ stars – continued.

J Name	T_{eff} (K)	$\log g$	M/M_{\odot}	$\log \text{Ca/He}$	$\log \text{H/He}$	D (pc)
J0935+2420	8289(284)	$7.72^{(+0.45)}_{(-0.38)}$	$0.42^{(+0.26)}_{(-0.15)}$	-9.60(0.33)	<-5.35	294.0(71.2)
J0935+4450	7484(170)	$8.02^{(+0.07)}_{(-0.07)}$	$0.59^{(+0.04)}_{(-0.04)}$	-11.13(0.14)	<-4.12	109.6(2.9)
J0936+1815	11520(641)	$7.21^{(+0.70)}_{(-0.44)}$	$0.26^{(+0.28)}_{(-0.09)}$	-9.07(0.82)	-5.66(0.61)	548.1(190.5)
J0937+2842	13743(865)	8.00		-9.29(0.61)	-5.08(0.31)	365.1(25.5)
J0937+3646	11733(565)	$7.95^{(+0.16)}_{(-0.15)}$	$0.55^{(+0.10)}_{(-0.08)}$	-9.13(0.37)	-5.02(0.32)	286.0(23.4)
J0937+5228	6621(80)	$7.97^{(+0.09)}_{(-0.09)}$	$0.56^{(+0.06)}_{(-0.05)}$	-8.59(0.07)	<-3.56	142.2(7.3)
J0938+6343	7980(743)	8.00		-10.09(0.22)	<-4.63	392.4(52.7)
J0939+4136	6251(124)	$8.44^{(+0.25)}_{(-0.23)}$	$0.86^{(+0.16)}_{(-0.16)}$	-8.14(0.16)	<-3.00	152.0(27.3)
J0939+5019	6086(97)	$7.98^{(+0.11)}_{(-0.11)}$	$0.56^{(+0.07)}_{(-0.06)}$	-8.01(0.26)	<-3.04	145.6(8.8)
J0939+5550	9023(186)	$8.07^{(+0.05)}_{(-0.05)}$	$0.62^{(+0.03)}_{(-0.03)}$	-8.18(0.05)	-4.57(0.06)	68.4(0.4)
J0940+6136	9205(202)	$8.29^{(+0.05)}_{(-0.05)}$	$0.76^{(+0.03)}_{(-0.03)}$	-8.00(0.05)	<-5.53	113.9(1.7)
J0940+6422	6875(177)	$7.74^{(+0.11)}_{(-0.11)}$	$0.43^{(+0.06)}_{(-0.05)}$	-10.87(0.08)	<-3.97	155.2(7.6)
J0941+5022	11230(437)	$7.79^{(+0.20)}_{(-0.19)}$	$0.47^{(+0.11)}_{(-0.09)}$	-8.07(0.18)	<-6.07	354.3(39.6)
J0942+0743	9777(299)	$8.00^{(+0.20)}_{(-0.19)}$	$0.58^{(+0.13)}_{(-0.11)}$	-8.35(0.16)	<-5.89	214.9(25.9)
J0942+5755	11264(454)	$8.10^{(+0.18)}_{(-0.17)}$	$0.65^{(+0.11)}_{(-0.10)}$	-8.06(0.44)	<-6.00	292.4(30.8)
J0944+3939	11106(862)	$8.39^{(+0.23)}_{(-0.21)}$	$0.83^{(+0.15)}_{(-0.14)}$	-8.64(0.24)	<-5.89	235.3(34.1)
J0944+4408	10997(425)	$7.87^{(+0.25)}_{(-0.23)}$	$0.51^{(+0.15)}_{(-0.11)}$	-8.19(0.34)	<-6.04	346.6(50.0)
J0944-0039	12625(604)	$8.13^{(+0.08)}_{(-0.07)}$	$0.66^{(+0.05)}_{(-0.05)}$	-7.80(0.08)	<-6.08	160.3(4.5)
J0945+0846	10880(409)	$8.03^{(+0.16)}_{(-0.15)}$	$0.60^{(+0.10)}_{(-0.09)}$	-9.47(0.21)	<-5.99	227.0(20.5)
J0946+2024	7557(191)	8.00		-8.05(0.22)	<-4.19	338.2(14.2)
J0947+1916	9996(359)	8.00		-9.47(0.27)	<-5.90	297.5(14.1)
J0947+4238	9611(335)	$8.36^{(+0.23)}_{(-0.22)}$	$0.81^{(+0.15)}_{(-0.14)}$	-9.05(0.25)	<-5.62	216.2(34.2)
J0948+3008	6233(137)	$7.22^{(+0.39)}_{(-0.38)}$	$0.23^{(+0.14)}_{(-0.09)}$	-9.52(0.15)	<-3.75	278.4(52.1)
J0950+4716	6803(172)	$8.45^{(+0.24)}_{(-0.22)}$	$0.87^{(+0.15)}_{(-0.15)}$	-9.39(0.18)	<-3.28	164.6(28.0)
J0950+4848	6995(230)	$8.52^{(+0.23)}_{(-0.21)}$	$0.91^{(+0.14)}_{(-0.14)}$	-8.84(0.26)	<-3.43	174.3(28.9)
J0951+4033	8306(218)	$8.20^{(+0.06)}_{(-0.05)}$	$0.70^{(+0.04)}_{(-0.04)}$	-10.07(0.03)	-3.95(0.09)	72.3(0.6)
J0953+1510	6933(220)	$8.11^{(+0.28)}_{(-0.26)}$	$0.65^{(+0.19)}_{(-0.16)}$	-10.83(0.20)	<-3.76	181.7(31.3)
J0953+1719	7072(305)	$7.66^{(+0.95)}_{(-0.72)}$	$0.39^{(+0.58)}_{(-0.23)}$	-10.35(0.15)	<-4.14	315.2(148.3)
J0954+1814	11325(445)	8.00		-8.29(0.12)	-5.50(0.19)	217.1(9.4)
J0954+3347	10290(345)	$8.25^{(+0.07)}_{(-0.07)}$	$0.74^{(+0.05)}_{(-0.05)}$	-9.09(0.08)	<-5.80	143.4(4.1)
J0954+5635	9404(314)	$8.16^{(+0.16)}_{(-0.15)}$	$0.68^{(+0.10)}_{(-0.09)}$	-9.35(0.22)	<-5.72	216.1(20.2)
J0955+5233	7620(175)	$7.92^{(+0.23)}_{(-0.22)}$	$0.53^{(+0.14)}_{(-0.11)}$	-8.65(0.15)	<-4.32	245.8(32.9)
J0956+5912	8723(105)	$8.13^{(+0.05)}_{(-0.05)}$	$0.66^{(+0.03)}_{(-0.03)}$	-7.12(0.09)	-3.54(0.18)	138.8(3.1)
J0957+2822	6494(218)	$7.62^{(+0.37)}_{(-0.32)}$	$0.37^{(+0.19)}_{(-0.12)}$	-11.44(0.33)	<-3.75	240.4(44.6)
J0958+0550	10960(402)	8.00		-8.66(0.09)	-5.84(0.25)	179.9(7.2)
J0959+2556	9304(284)	$8.17^{(+0.07)}_{(-0.07)}$	$0.68^{(+0.04)}_{(-0.04)}$	-10.81(0.04)	<-5.66	57.1(0.5)
J1000+3518	12666(640)	$7.95^{(+0.11)}_{(-0.11)}$	$0.56^{(+0.06)}_{(-0.06)}$	-8.54(0.15)	-5.65(0.16)	212.4(10.0)
J1000+4420	13430(909)	$7.85^{(+0.20)}_{(-0.18)}$	$0.50^{(+0.11)}_{(-0.09)}$	-8.51(0.24)	-4.25(0.14)	255.2(23.4)

Table 6. Atmospheric parameters for DZ stars – continued.

J Name	T_{eff} (K)	$\log g$	M/M_{\odot}	$\log \text{Ca/He}$	$\log \text{H/He}$	D (pc)
J1000–0230	5318(203)	8.00		-10.16(0.24)	<-3.01	188.4(15.1)
J1002+0313	9997(333)	8.06($^{+0.15}_{-0.14}$)	0.61($^{+0.09}_{-0.08}$)	-8.89(0.11)	<-5.87	214.0(18.3)
J1003+1421	5725(312)	8.00		-10.46(0.73)	<-3.00	298.2(30.5)
J1004+0451	7797(194)	7.82($^{+0.24}_{-0.22}$)	0.47($^{+0.14}_{-0.11}$)	-9.77(0.19)	<-4.65	211.5(28.0)
J1004+4231	8152(356)	8.33($^{+0.19}_{-0.18}$)	0.79($^{+0.12}_{-0.12}$)	-10.01(0.15)	<-4.36	189.9(22.2)
J1005+1746	5749(214)	8.00		-10.39(0.47)	<-3.00	229.9(16.3)
J1005+2032	6522(281)	8.00		-10.44(0.29)	<-3.43	266.1(19.0)
J1005+2244	6006(224)	8.00		-9.60(0.25)	<-3.00	267.1(19.1)
J1005+2655	8038(206)	8.01($^{+0.10}_{-0.10}$)	0.58($^{+0.06}_{-0.06}$)	-9.90(0.04)	<-4.69	141.5(6.8)
J1006+1752	5883(127)	8.43($^{+0.17}_{-0.16}$)	0.85($^{+0.11}_{-0.11}$)	-8.82(0.24)	<-3.00	135.8(15.6)
J1006+6116	6935(229)	8.10($^{+0.19}_{-0.18}$)	0.63($^{+0.12}_{-0.11}$)	-10.74(0.12)	<-3.77	183.0(19.6)
J1008+0248	7648(184)	7.95($^{+0.10}_{-0.10}$)	0.55($^{+0.06}_{-0.06}$)	-11.32(0.13)	<-4.31	118.2(6.0)
J1008+4349	11380(444)	8.02($^{+0.09}_{-0.09}$)	0.60($^{+0.06}_{-0.05}$)	-10.13(0.09)	-5.28(0.10)	146.1(5.4)
J1009+3337	6543(244)	8.00		-10.11(0.30)	<-3.45	238.8(14.7)
J1010+2119	6968(408)	8.00		-9.64(0.37)	<-3.88	401.8(35.2)
J1010+3948	8371(170)	8.05($^{+0.06}_{-0.06}$)	0.61($^{+0.04}_{-0.04}$)	-8.81(0.06)	-4.09(0.12)	122.8(2.9)
J1012+4435	9065(483)	8.75($^{+1.43}_{-0.74}$)	1.06($^{+0.86}_{-0.47}$)	-8.48(0.73)	<-4.82	219.4(161.8)
J1012–1843	5938(213)	8.05($^{+0.09}_{-0.08}$)	0.60($^{+0.05}_{-0.05}$)	-10.19(0.05)	<-3.00	18.1(0.0)
J1013–0251	7065(631)	8.00		-9.84(0.33)	<-3.94	385.0(53.1)
J1014+2827	6243(196)	8.00		-8.04(0.41)	<-3.15	264.1(18.0)
J1015+4141	9694(241)	7.95($^{+0.15}_{-0.14}$)	0.55($^{+0.09}_{-0.08}$)	-7.84(0.09)	-4.91(0.20)	236.6(20.3)
J1015+6327	8230(595)	8.00		-8.82(0.48)	<-4.95	494.5(55.2)
J1017+1948	15794(1718)	8.56($^{+0.36}_{-0.32}$)	0.94($^{+0.21}_{-0.21}$)	-7.25(0.62)	-4.96(0.71)	291.1(74.6)
J1017+2419	6831(97)	8.51($^{+0.27}_{-0.25}$)	0.91($^{+0.17}_{-0.17}$)	-8.37(0.08)	<-3.26	132.4(27.1)
J1017+3447	5995(143)	7.97($^{+0.23}_{-0.22}$)	0.55($^{+0.14}_{-0.12}$)	-10.27(0.23)	<-3.00	182.8(23.8)
J1018+0344	9264(370)	8.17($^{+0.40}_{-0.36}$)	0.68($^{+0.26}_{-0.21}$)	-8.69(0.44)	<-5.64	275.4(68.7)
J1018+3708	15508(1643)	8.18($^{+0.18}_{-0.17}$)	0.70($^{+0.11}_{-0.10}$)	-7.23(0.28)	<-5.85	272.3(20.3)
J1018+3726	10543(361)	7.98($^{+0.07}_{-0.07}$)	0.57($^{+0.04}_{-0.04}$)	-7.93(0.22)	-3.62(1.83)	137.7(2.9)
J1019+2045	5552(133)	8.00		-9.45(0.44)	<-3.00	191.7(9.6)
J1019+3535	6079(227)	8.00		-9.45(0.50)	<-3.04	261.2(17.6)
J1019+3752	12697(593)	8.04($^{+0.18}_{-0.17}$)	0.61($^{+0.11}_{-0.10}$)	-9.36(0.19)	-5.52(0.19)	243.9(25.7)
J1023–0014	7549(603)	8.00		-9.42(0.45)	<-4.18	397.9(46.7)
J1024+1014	6226(129)	8.00		-7.72(0.10)	<-3.13	195.1(9.4)
J1024+2227	7517(434)	8.00		-10.41(0.17)	<-4.16	367.2(30.9)
J1024+4531	6375(134)	8.38($^{+0.16}_{-0.16}$)	0.82($^{+0.11}_{-0.10}$)	-8.68(0.16)	<-3.01	148.7(16.5)
J1024–0017	7370(390)	8.00		-8.84(0.29)	<-4.08	355.4(27.5)
J1025+2016	7612(680)	8.00		-9.95(0.58)	<-4.23	461.7(59.5)
J1026+1948	10703(387)	8.00		-8.23(0.09)	<-6.01	246.9(10.3)

Table 6. Atmospheric parameters for DZ stars – continued.

J Name	T_{eff} (K)	$\log g$	M/M_{\odot}	$\log \text{Ca/He}$	$\log \text{H/He}$	D (pc)
J1026+2646	6803(371)	8.00		-10.56(0.24)	<-3.73	305.3(26.8)
J1027+4532	9076(202)	7.92($^{+0.23}_{-0.21}$)	0.53($^{+0.14}_{-0.11}$)	-8.13(0.07)	<-5.65	195.8(25.9)
J1028+2507	5847(214)	8.00		-9.47(0.41)	<-3.00	273.8(20.0)
J1028-0135	12948(776)	7.95($^{+0.21}_{-0.19}$)	0.56($^{+0.12}_{-0.10}$)	-8.55(0.27)	-5.61(0.23)	304.3(34.1)
J1029+1227	7158(401)	8.00		-10.33(0.24)	<-3.99	304.9(26.4)
J1029+2013	6281(232)	8.00		-10.75(0.28)	<-3.18	226.8(14.0)
J1029+3103	9423(335)	8.39($^{+0.43}_{-0.38}$)	0.83($^{+0.27}_{-0.25}$)	-7.83(0.39)	<-5.55	268.3(79.9)
J1030+0026	6747(161)	8.02($^{+0.12}_{-0.12}$)	0.58($^{+0.08}_{-0.07}$)	-10.37(0.08)	<-3.66	148.5(9.8)
J1031+0936	11104(423)	8.10($^{+0.13}_{-0.12}$)	0.64($^{+0.08}_{-0.07}$)	-9.84(0.14)	<-5.98	200.9(14.0)
J1031+1203	8486(177)	8.12($^{+0.06}_{-0.06}$)	0.65($^{+0.04}_{-0.04}$)	-8.94(0.12)	<-5.05	100.5(2.6)
J1032+1338	5588(131)	8.00		-8.99(0.23)	<-3.00	208.8(11.5)
J1032-0240	11010(518)	8.66($^{+0.36}_{-0.31}$)	1.01($^{+0.19}_{-0.20}$)	-8.78(0.12)	-4.12(0.21)	173.9(47.1)
J1033+1809	6324(94)	8.35($^{+0.10}_{-0.09}$)	0.80($^{+0.06}_{-0.06}$)	-8.46(0.36)	<-3.01	117.1(7.3)
J1033+2837	6681(240)	8.00		-9.05(0.27)	<-3.60	291.2(17.5)
J1033+6247	7474(171)	8.09($^{+0.07}_{-0.07}$)	0.63($^{+0.05}_{-0.05}$)	-10.04(0.09)	<-4.07	127.5(4.1)
J1034+2245	7214(75)	8.21($^{+0.03}_{-0.03}$)	0.71($^{+0.02}_{-0.02}$)	-8.85(0.04)	<-3.88	40.8(0.2)
J1036+4837	11247(470)	7.71($^{+0.24}_{-0.21}$)	0.43($^{+0.12}_{-0.09}$)	-8.28(0.19)	-5.37(0.30)	346.0(44.4)
J1037+0709	11153(462)	8.10($^{+0.18}_{-0.17}$)	0.64($^{+0.12}_{-0.10}$)	-7.65(0.11)	-4.62(0.32)	258.3(28.4)
J1037+4341	11075(425)	8.06($^{+0.13}_{-0.12}$)	0.62($^{+0.08}_{-0.07}$)	-8.28(0.11)	<-5.99	242.9(17.1)
J1038+0432	6319(139)	8.00		-8.37(0.26)	<-3.22	216.2(9.0)
J1038+1342	9088(211)	8.25($^{+0.12}_{-0.11}$)	0.74($^{+0.08}_{-0.07}$)	-8.25(0.09)	<-5.46	172.7(12.7)
J1038-0036	7795(82)	8.00		-8.14(0.06)	<-4.41	65.0(1.4)
J1039+2648	13421(637)	7.97($^{+0.11}_{-0.11}$)	0.57($^{+0.07}_{-0.06}$)	-9.76(0.32)	-5.41(0.14)	183.8(9.4)
J1039+4612	6994(91)	7.77($^{+0.14}_{-0.13}$)	0.45($^{+0.07}_{-0.06}$)	-9.45(0.14)	<-4.02	134.7(10.1)
J1040+1349	7605(339)	8.00		-10.24(0.14)	<-4.23	293.2(19.0)
J1040+2408	5899(67)	8.12($^{+0.06}_{-0.06}$)	0.64($^{+0.04}_{-0.04}$)	-8.63(0.14)	<-3.00	93.3(2.5)
J1041+2746	7480(222)	7.84($^{+0.40}_{-0.35}$)	0.49($^{+0.24}_{-0.16}$)	-10.12(0.08)	<-4.30	220.9(49.0)
J1041+3432	7672(249)	8.35($^{+0.36}_{-0.33}$)	0.80($^{+0.24}_{-0.21}$)	-8.28(0.21)	<-4.04	254.8(62.7)
J1041+4110	7204(150)	8.34($^{+0.33}_{-0.30}$)	0.79($^{+0.22}_{-0.20}$)	-8.84(0.25)	<-3.77	204.4(46.5)
J1043+3516	6115(58)	8.15($^{+0.05}_{-0.05}$)	0.67($^{+0.03}_{-0.03}$)	-8.84(0.07)	<-3.02	85.5(2.3)
J1044+2023	8411(293)	8.11($^{+0.08}_{-0.08}$)	0.64($^{+0.05}_{-0.05}$)	-10.46(0.03)	<-4.99	89.2(1.6)
J1044+2143	10000(401)	8.19($^{+0.16}_{-0.15}$)	0.70($^{+0.11}_{-0.10}$)	-8.86(0.15)	<-5.80	210.1(20.2)
J1045+5254	10990(641)	7.30($^{+1.61}_{-0.90}$)	0.27($^{+0.87}_{-0.18}$)	-8.89(0.55)	<-6.20	684.9(464.3)
J1045+6009	7651(387)	7.80($^{+0.45}_{-0.39}$)	0.47($^{+0.27}_{-0.17}$)	-10.43(0.13)	<-4.51	313.2(74.3)
J1045+6254	9566(574)	8.02($^{+0.41}_{-0.36}$)	0.59($^{+0.26}_{-0.19}$)	-9.60(0.38)	<-5.86	378.3(87.9)
J1046+1329	5251(88)	7.97($^{+0.21}_{-0.20}$)	0.55($^{+0.13}_{-0.11}$)	-9.47(0.21)	<-3.01	140.2(16.6)
J1046+2424	6252(87)	8.09($^{+0.05}_{-0.05}$)	0.63($^{+0.03}_{-0.03}$)	-10.85(0.06)	<-3.11	59.1(0.7)
J1047+5219	7095(254)	8.56($^{+0.24}_{-0.22}$)	0.94($^{+0.15}_{-0.15}$)	-9.87(0.15)	<-3.49	165.2(28.8)

Table 6. Atmospheric parameters for DZ stars – continued.

J Name	T_{eff} (K)	$\log g$	M/M_{\odot}	$\log \text{Ca/He}$	$\log \text{H/He}$	D (pc)
J1048+2623	6911(182)	8.00		-9.10(0.32)	<-3.83	274.7(12.2)
J1049+2128	6850(452)	8.00		-9.83(0.31)	<-3.78	368.7(39.1)
J1049+5154	7224(73)	8.10($^{+0.04}_{-0.04}$)	0.64($^{+0.02}_{-0.02}$)	-8.77(0.05)	<-3.95	79.7(1.0)
J1049-0007	9286(221)	7.98($^{+0.14}_{-0.13}$)	0.57($^{+0.08}_{-0.07}$)	-8.11(0.08)	-4.68(0.16)	197.9(15.1)
J1050+3138	9394(324)	8.22($^{+0.12}_{-0.11}$)	0.72($^{+0.08}_{-0.07}$)	-8.00(0.21)	<-5.67	187.5(12.5)
J1051+2751	8735(591)	8.00		-7.72(0.32)	<-5.41	633.4(66.7)
J1051+5947	6995(521)	8.00		-10.33(0.33)	<-3.90	332.2(39.0)
J1051-0303	7241(539)	8.00		-9.27(1.34)	<-4.03	349.6(37.3)
J1052+0659	11224(469)	7.97($^{+0.22}_{-0.20}$)	0.57($^{+0.13}_{-0.11}$)	-9.09(0.50)	<-6.02	320.3(40.3)
J1055+3509	10767(397)	8.10($^{+0.11}_{-0.10}$)	0.64($^{+0.07}_{-0.06}$)	-8.59(0.07)	<-5.96	197.4(11.1)
J1055+3725	5869(104)	7.76($^{+0.20}_{-0.19}$)	0.44($^{+0.11}_{-0.09}$)	-8.49(0.11)	<-3.00	177.0(19.0)
J1055+4115	10058(395)	7.88($^{+0.17}_{-0.16}$)	0.51($^{+0.10}_{-0.08}$)	-10.93(0.24)	<-5.95	245.2(22.3)
J1056+0128	10278(378)	8.07($^{+0.07}_{-0.07}$)	0.62($^{+0.05}_{-0.04}$)	-8.99(0.06)	-4.92(0.10)	118.7(2.0)
J1056+5714	7300(181)	8.05($^{+0.07}_{-0.07}$)	0.60($^{+0.04}_{-0.04}$)	-10.69(0.09)	<-4.02	94.3(1.2)
J1056-0004	11862(494)	8.00		-7.34(0.35)	-4.74(0.79)	402.1(18.4)
J1057+1053	5947(252)	8.00		-9.49(0.28)	<-3.00	280.0(23.8)
J1057-0413	6529(375)	8.05($^{+0.14}_{-0.14}$)	0.60($^{+0.09}_{-0.08}$)	-10.28(0.02)	<-3.38	36.3(0.1)
J1058+1124	10153(358)	8.16($^{+0.14}_{-0.13}$)	0.68($^{+0.09}_{-0.08}$)	-9.18(0.11)	<-5.84	229.5(18.5)
J1058+3022	10216(397)	8.40($^{+0.31}_{-0.28}$)	0.84($^{+0.20}_{-0.19}$)	-8.95(0.24)	<-5.65	238.0(51.8)
J1058+3143	7135(91)	8.14($^{+0.07}_{-0.07}$)	0.66($^{+0.05}_{-0.05}$)	-8.87(0.06)	<-3.88	125.4(5.2)
J1058+6041	9327(515)	8.29($^{+0.29}_{-0.27}$)	0.77($^{+0.19}_{-0.17}$)	-9.31(0.45)	<-5.59	287.9(53.7)
J1059+5038	6922(288)	8.00		-9.57(0.29)	<-3.84	302.5(18.9)
J1100+1439	7146(478)	8.00		-10.01(0.31)	<-3.98	359.8(37.3)
J1101+2730	7735(629)	8.00		-9.02(0.59)	<-4.35	470.1(55.0)
J1102+0214	5699(58)	8.14($^{+0.08}_{-0.08}$)	0.66($^{+0.06}_{-0.05}$)	-9.78(0.14)	<-3.00	96.5(4.8)
J1102+1755	6949(159)	8.30($^{+0.19}_{-0.18}$)	0.77($^{+0.13}_{-0.12}$)	-9.60(0.15)	<-3.60	166.8(20.8)
J1102+2653	6938(140)	8.27($^{+0.19}_{-0.18}$)	0.75($^{+0.13}_{-0.12}$)	-9.36(0.12)	<-3.61	177.5(22.0)
J1102+2827	6324(222)	8.00		-8.24(0.44)	<-3.22	278.6(19.5)
J1103+4144	5812(92)	7.59($^{+0.20}_{-0.18}$)	0.36($^{+0.09}_{-0.07}$)	-9.36(0.08)	<-3.03	153.7(15.2)
J1104+0711	11167(399)	8.03($^{+0.08}_{-0.08}$)	0.60($^{+0.05}_{-0.04}$)	-9.58(0.09)	<-6.00	166.6(4.7)
J1104+1657	6959(339)	8.00		-9.40(0.56)	<-3.87	303.0(22.1)
J1104+2439	10453(305)	8.27($^{+0.11}_{-0.10}$)	0.75($^{+0.07}_{-0.07}$)	-7.34(0.09)	-3.50(0.26)	164.6(11.0)
J1104+6426	5668(148)	7.29($^{+0.62}_{-0.61}$)	0.25($^{+0.27}_{-0.15}$)	-10.75(0.26)	<-3.09	272.2(77.1)
J1104-1607	8182(559)	8.75($^{+0.34}_{-0.29}$)	1.06($^{+0.17}_{-0.18}$)	-8.52(0.52)	<-3.99	189.2(48.6)
J1105+0228	5848(143)	8.00		-9.51(0.40)	<-3.00	170.9(8.0)
J1105+1949	6616(498)	8.00		-10.13(0.43)	<-3.53	370.0(46.1)
J1105+3801	7843(280)	7.54($^{+1.83}_{-1.46}$)	0.34($^{+0.97}_{-0.31}$)	-8.97(0.41)	<-5.10	411.4(312.9)
J1106+0104	6989(218)	8.15($^{+0.16}_{-0.16}$)	0.67($^{+0.11}_{-0.10}$)	-11.27(0.29)	<-3.77	172.1(16.5)

Table 6. Atmospheric parameters for DZ stars – continued.

J Name	T_{eff} (K)	$\log g$	M/M_{\odot}	$\log \text{Ca/He}$	$\log \text{H/He}$	D (pc)
J1106–0039	11350(457)	8.06($^{+0.27}_{-0.25}$)	0.62($^{+0.18}_{-0.14}$)	-8.19(0.13)	<-6.02	285.8(48.1)
J1108+3033	6530(207)	8.00($^{+0.27}_{-0.25}$)	0.57($^{+0.17}_{-0.14}$)	-10.37(0.09)	<-3.44	188.7(28.8)
J1109+2112	6684(268)	8.00		-10.83(0.20)	<-3.60	228.9(15.2)
J1112+0700	6664(120)	7.76($^{+0.15}_{-0.15}$)	0.44($^{+0.08}_{-0.07}$)	-10.00(0.17)	<-3.80	156.3(12.7)
J1113+2228	6631(196)	8.00		-10.76(0.13)	<-3.55	199.9(9.9)
J1113+4550	9836(315)	8.09($^{+0.09}_{-0.09}$)	0.63($^{+0.06}_{-0.05}$)	-10.76(0.18)	<-5.85	138.4(5.1)
J1114+2957	6689(167)	8.00		-9.95(0.09)	<-3.61	179.8(7.4)
J1115+1720	8112(792)	8.00		-10.45(0.24)	<-4.80	433.2(62.3)
J1117+0826	8657(667)	8.00		-9.93(0.24)	<-5.37	412.0(45.5)
J1117+3311	7918(432)	8.32($^{+0.44}_{-0.39}$)	0.78($^{+0.28}_{-0.25}$)	-9.71(0.15)	<-4.21	253.3(72.5)
J1118+0838	9058(876)	8.00		-9.40(0.32)	<-5.59	468.7(67.1)
J1121+1417	8921(352)	8.04($^{+0.13}_{-0.13}$)	0.60($^{+0.08}_{-0.07}$)	-11.13(0.19)	-3.71(0.15)	164.5(8.4)
J1122+5041	9512(181)	8.01($^{+0.18}_{-0.17}$)	0.59($^{+0.11}_{-0.09}$)	-7.34(0.23)	-4.95(0.39)	257.8(27.4)
J1123+3026	9215(377)	8.00		-9.15(0.20)	<-5.69	270.9(15.0)
J1125+2853	10952(431)	8.32($^{+0.15}_{-0.14}$)	0.78($^{+0.10}_{-0.09}$)	-9.10(0.14)	<-5.89	222.8(20.8)
J1125+3823	10437(330)	8.17($^{+0.07}_{-0.07}$)	0.69($^{+0.05}_{-0.04}$)	-8.17(0.07)	<-5.88	131.2(3.8)
J1126+5241	8967(266)	8.07($^{+0.08}_{-0.08}$)	0.62($^{+0.05}_{-0.05}$)	-9.60(0.04)	-4.40(0.17)	140.1(3.8)
J1127–0138	7655(95)	8.11($^{+0.05}_{-0.05}$)	0.64($^{+0.03}_{-0.03}$)	-8.63(0.22)	<-4.17	95.0(2.0)
J1129+2917	8346(440)	7.92($^{+0.46}_{-0.40}$)	0.53($^{+0.29}_{-0.19}$)	-10.99(0.25)	<-5.20	256.8(65.0)
J1129–0152	8955(266)	8.05($^{+0.14}_{-0.14}$)	0.61($^{+0.09}_{-0.08}$)	-8.59(0.08)	-3.60(0.14)	202.0(16.5)
J1130+1036	9144(214)	8.52($^{+0.09}_{-0.08}$)	0.91($^{+0.06}_{-0.05}$)	-8.16(0.11)	<-5.27	133.6(7.5)
J1131+2315	7656(529)	8.00		-10.89(0.18)	<-4.27	353.4(37.0)
J1132+1002	7239(479)	8.00		-9.69(0.33)	<-4.02	314.4(30.5)
J1132+3323	6168(170)	8.00		-8.26(0.20)	<-3.09	256.1(14.1)
J1132+4705	7553(372)	7.21($^{+1.39}_{-1.47}$)	0.23($^{+0.73}_{-0.21}$)	-10.17(0.23)	<-5.14	434.0(252.9)
J1132–0106	7755(417)	8.01($^{+0.55}_{-0.48}$)	0.58($^{+0.36}_{-0.24}$)	-10.93(0.19)	<-4.35	272.2(85.9)
J1133+0610	10711(364)	8.05($^{+0.09}_{-0.08}$)	0.61($^{+0.05}_{-0.05}$)	-10.04(0.07)	<-5.99	158.6(5.7)
J1133+1804	7780(356)	7.21($^{+1.38}_{-1.47}$)	0.23($^{+0.72}_{-0.21}$)	-9.04(0.20)	<-5.36	422.8(246.6)
J1134+1236	6960(172)	8.36($^{+0.13}_{-0.12}$)	0.81($^{+0.09}_{-0.08}$)	-9.58(0.10)	<-3.54	144.7(12.2)
J1134+1542	6850(223)	8.00		-8.52(0.20)	<-3.78	317.2(18.7)
J1134+5928	8378(274)	8.08($^{+0.11}_{-0.11}$)	0.63($^{+0.07}_{-0.07}$)	-10.25(0.14)	<-5.00	195.1(10.8)
J1137+0343	6793(126)	8.09($^{+0.05}_{-0.05}$)	0.63($^{+0.03}_{-0.03}$)	-10.95(0.10)	<-3.64	65.0(0.9)
J1137–0023	10003(359)	8.18($^{+0.16}_{-0.15}$)	0.69($^{+0.10}_{-0.09}$)	-9.61(0.07)	<-5.80	214.4(20.2)
J1138–0130	5493(231)	8.00		-10.18(0.18)	<-3.00	229.4(19.2)
J1139+6239	7252(198)	7.87($^{+0.32}_{-0.29}$)	0.50($^{+0.19}_{-0.14}$)	-9.06(0.28)	<-4.12	270.7(48.6)
J1139+6737	6600(196)	7.94($^{+0.22}_{-0.21}$)	0.54($^{+0.14}_{-0.11}$)	-10.05(0.14)	<-3.57	206.6(25.6)
J1139–0132	5204(152)	8.00		-10.46(0.20)	<-3.01	200.8(12.5)
J1140+5328	9829(323)	8.14($^{+0.12}_{-0.12}$)	0.67($^{+0.08}_{-0.07}$)	-8.26(0.12)	-4.65(0.39)	219.4(15.0)

Table 6. Atmospheric parameters for DZ stars – continued.

J Name	T_{eff} (K)	$\log g$	M/M_{\odot}	$\log \text{Ca/He}$	$\log \text{H/He}$	D (pc)
J1142+1104	10424(341)	8.08($^{+0.19}_{-0.18}$)	0.63($^{+0.12}_{-0.11}$)	-8.00(0.10)	<-5.94	242.1(28.2)
J1143+1928	7845(198)	8.11($^{+0.11}_{-0.10}$)	0.64($^{+0.07}_{-0.06}$)	-10.86(0.06)	<-4.34	115.7(6.7)
J1143-0145	9583(342)	7.99($^{+0.16}_{-0.15}$)	0.58($^{+0.10}_{-0.09}$)	-9.76(0.06)	<-5.88	208.1(18.1)
J1144+1218	5500(47)	8.11($^{+0.04}_{-0.04}$)	0.64($^{+0.02}_{-0.02}$)	-9.25(0.09)	<-3.00	50.5(0.6)
J1144+3259	7324(289)	7.98($^{+0.13}_{-0.12}$)	0.56($^{+0.08}_{-0.07}$)	-10.28(0.08)	<-4.08	142.5(8.1)
J1144+3720	7379(165)	7.84($^{+0.35}_{-0.32}$)	0.49($^{+0.21}_{-0.15}$)	-8.54(0.17)	<-4.22	279.6(55.5)
J1145+6619	7556(480)	8.64($^{+0.57}_{-0.46}$)	0.99($^{+0.28}_{-0.30}$)	-10.04(0.32)	<-3.78	220.9(88.9)
J1147+4928	7573(174)	8.07($^{+0.06}_{-0.06}$)	0.62($^{+0.04}_{-0.04}$)	-10.06(0.05)	<-4.14	102.0(1.8)
J1147+5429	5178(117)	8.00		-9.19(0.64)	<-3.01	204.4(12.3)
J1148+4109	6698(98)	7.89($^{+0.07}_{-0.07}$)	0.51($^{+0.04}_{-0.04}$)	-10.03(0.05)	<-3.72	117.9(3.4)
J1148+4124	11119(433)	8.31($^{+0.15}_{-0.15}$)	0.78($^{+0.10}_{-0.10}$)	-9.18(0.29)	<-5.93	249.4(24.6)
J1148+5708	10207(337)	8.25($^{+0.08}_{-0.07}$)	0.73($^{+0.05}_{-0.05}$)	-8.39(0.09)	<-5.79	170.7(5.4)
J1149+0519	7004(94)	7.84($^{+0.20}_{-0.19}$)	0.48($^{+0.12}_{-0.10}$)	-8.88(0.15)	<-3.99	189.4(21.9)
J1149+4943	7597(464)	8.00		-10.41(0.19)	<-4.22	372.0(33.8)
J1150+4928	7261(227)	8.11($^{+0.17}_{-0.16}$)	0.64($^{+0.11}_{-0.10}$)	-9.51(0.17)	<-3.96	192.0(19.1)
J1152+2834	6844(232)	8.02($^{+0.26}_{-0.25}$)	0.58($^{+0.17}_{-0.14}$)	-10.32(0.10)	<-3.76	187.5(28.4)
J1152+5101	5080(132)	8.00		-9.92(0.32)	<-3.00	178.5(11.0)
J1155+4327	9902(339)	7.93($^{+0.10}_{-0.10}$)	0.54($^{+0.06}_{-0.05}$)	-9.73(0.09)	<-5.92	174.9(8.0)
J1157+6138	7008(477)	8.00		-8.54(0.23)	<-3.91	378.0(42.8)
J1158+0454	5433(100)	8.12($^{+0.29}_{-0.28}$)	0.65($^{+0.20}_{-0.17}$)	-8.51(0.08)	<-3.00	149.6(27.0)
J1158+1845	6910(117)	8.16($^{+0.22}_{-0.20}$)	0.67($^{+0.14}_{-0.13}$)	-8.12(0.09)	<-3.70	185.9(25.5)
J1158+4712	8026(242)	8.32($^{+0.47}_{-0.41}$)	0.78($^{+0.30}_{-0.26}$)	-7.99(0.17)	<-4.28	284.5(88.2)
J1158+5942	5816(129)	7.87($^{+0.20}_{-0.19}$)	0.50($^{+0.12}_{-0.10}$)	-10.04(0.34)	<-3.00	190.7(21.0)
J1159+2059	7407(659)	8.00		-10.56(0.23)	<-4.10	398.3(54.3)
J1159+4045	7839(186)	8.00($^{+0.08}_{-0.08}$)	0.58($^{+0.05}_{-0.05}$)	-9.92(0.09)	<-4.46	137.7(4.7)
J1203+0834	6009(54)	7.96($^{+0.05}_{-0.05}$)	0.55($^{+0.03}_{-0.03}$)	-10.21(0.05)	<-3.01	62.7(1.2)
J1203+2323	6559(316)	8.00		-8.92(0.27)	<-3.47	312.6(25.5)
J1203+2439	13959(1027)	8.17($^{+0.13}_{-0.12}$)	0.69($^{+0.08}_{-0.08}$)	-9.40(0.17)	-5.20(0.07)	99.2(1.1)
J1204+1030	5630(212)	8.00		-10.08(0.35)	<-3.00	242.1(17.6)
J1204+5007	8496(498)	8.81($^{+0.30}_{-0.26}$)	1.09($^{+0.14}_{-0.16}$)	-8.55(0.44)	<-4.10	206.8(49.6)
J1205+3536	5918(133)	8.14($^{+0.18}_{-0.18}$)	0.66($^{+0.12}_{-0.11}$)	-8.94(0.06)	<-3.00	157.7(17.2)
J1205+4312	7000(311)	7.61($^{+0.61}_{-0.49}$)	0.37($^{+0.34}_{-0.16}$)	-10.73(0.16)	<-4.12	331.9(101.7)
J1206+1310	6644(519)	8.00		-10.17(0.34)	<-3.56	332.6(42.0)
J1206+1454	6774(226)	8.38($^{+0.65}_{-0.54}$)	0.82($^{+0.38}_{-0.34}$)	-9.80(0.16)	<-3.32	216.3(92.2)
J1206+2650	6322(169)	8.00		-10.02(0.20)	<-3.22	203.5(9.9)
J1208+1907	7375(176)	8.14($^{+0.09}_{-0.09}$)	0.66($^{+0.06}_{-0.06}$)	-10.47(0.07)	<-3.99	120.6(5.5)
J1209+3026	6850(97)	8.01($^{+0.12}_{-0.12}$)	0.58($^{+0.08}_{-0.07}$)	-9.42(0.17)	<-3.77	161.7(11.5)
J1210+0553	9391(558)	7.69($^{+0.16}_{-0.15}$)	0.41($^{+0.08}_{-0.06}$)	-9.79(0.06)	-4.61(0.16)	194.9(11.7)

Table 6. Atmospheric parameters for DZ stars – continued.

J Name	T_{eff} (K)	$\log g$	M/M_{\odot}	$\log \text{Ca/He}$	$\log \text{H/He}$	D (pc)
J1210+3136	9121(275)	8.12($^{+0.10}_{-0.10}$)	0.65($^{+0.06}_{-0.06}$)	-9.18(0.13)	<-5.57	175.0(8.3)
J1210+4332	7926(783)	8.00		-10.28(0.25)	<-4.56	474.1(67.2)
J1210+4751	7263(348)	8.77($^{+0.46}_{-0.38}$)	1.07($^{+0.20}_{-0.24}$)	-9.90(0.22)	<-3.41	177.8(62.8)
J1211+2326	6699(199)	8.77($^{+0.27}_{-0.24}$)	1.07($^{+0.13}_{-0.15}$)	-8.04(0.16)	<-3.02	149.8(31.6)
J1212+5409	8388(241)	8.14($^{+0.07}_{-0.07}$)	0.67($^{+0.04}_{-0.04}$)	-9.61(0.04)	<-4.90	123.7(2.5)
J1212+6351	7596(140)	7.76($^{+0.16}_{-0.15}$)	0.44($^{+0.09}_{-0.07}$)	-8.67(0.09)	<-4.51	241.1(20.8)
J1214+2216	7575(194)	7.99($^{+0.11}_{-0.11}$)	0.57($^{+0.07}_{-0.06}$)	-10.58(0.10)	<-4.21	146.1(8.4)
J1214+7822	4329(61)	7.48($^{+0.07}_{-0.07}$)	0.31($^{+0.03}_{-0.02}$)	-11.23(0.13)	<-30.00	32.7(0.1)
J1215+3953	9971(436)	8.31($^{+0.29}_{-0.27}$)	0.78($^{+0.19}_{-0.17}$)	-9.02(0.35)	<-5.71	257.6(49.6)
J1216+6208	7624(439)	8.00		-8.89(0.52)	<-4.24	421.8(35.5)
J1217+1157	6149(155)	7.53($^{+0.33}_{-0.29}$)	0.33($^{+0.16}_{-0.10}$)	-9.48(0.07)	<-3.36	230.0(37.7)
J1217+6420	10688(402)	8.10($^{+0.13}_{-0.13}$)	0.64($^{+0.09}_{-0.08}$)	-9.14(0.10)	<-5.96	245.2(18.1)
J1218+0023	6456(77)	8.31($^{+0.08}_{-0.07}$)	0.77($^{+0.05}_{-0.05}$)	-9.51(0.13)	<-3.09	112.3(5.3)
J1218+6023	6700(416)	8.00		-9.70(0.41)	<-3.62	337.9(32.6)
J1219+0848	7964(520)	8.00		-8.71(0.16)	<-4.61	390.2(35.9)
J1219+3018	8193(383)	8.00		-8.62(0.34)	<-4.90	415.6(29.9)
J1219+5720	7249(510)	8.00		-10.26(0.24)	<-4.03	341.8(36.6)
J1220+0929	6842(239)	8.00		-8.31(0.10)	<-3.77	285.7(17.5)
J1222+6343	10027(410)	8.25($^{+0.16}_{-0.15}$)	0.74($^{+0.10}_{-0.10}$)	-9.56(0.24)	<-5.76	254.9(23.9)
J1223+1600	7695(663)	8.00		-8.57(0.56)	<-4.31	479.3(63.2)
J1223+1935	5313(207)	8.00		-10.44(0.30)	<-3.01	232.5(18.1)
J1224+2838	5096(84)	8.07($^{+0.08}_{-0.07}$)	0.61($^{+0.05}_{-0.05}$)	-10.05(0.13)	<-3.00	81.7(2.4)
J1225-0245	6934(245)	8.16($^{+0.46}_{-0.41}$)	0.67($^{+0.30}_{-0.24}$)	-10.22(0.12)	<-3.72	209.5(59.1)
J1226+4445	11861(1068)	8.01($^{+0.21}_{-0.20}$)	0.59($^{+0.13}_{-0.11}$)	-9.48(0.18)	<-6.09	222.7(9.3)
J1227+4434	6231(218)	8.00		-9.92(0.30)	<-3.14	277.4(16.6)
J1227+6330	7418(82)	8.07($^{+0.04}_{-0.04}$)	0.62($^{+0.02}_{-0.02}$)	-8.71(0.09)	<-4.05	96.8(1.3)
J1229+0743	6079(141)	7.32($^{+0.54}_{-0.49}$)	0.26($^{+0.23}_{-0.13}$)	-8.62(0.12)	<-3.47	263.5(67.2)
J1229+1606	8025(562)	8.00		-8.79(0.71)	<-4.68	498.9(51.4)
J1229+3021	6000(138)	8.31($^{+0.18}_{-0.17}$)	0.77($^{+0.12}_{-0.11}$)	-10.36(0.21)	<-3.00	142.0(16.7)
J1229+4254	11868(692)	7.99($^{+0.64}_{-0.51}$)	0.58($^{+0.41}_{-0.24}$)	-8.30(0.55)	<-6.09	470.0(172.3)
J1229+5129	9660(388)	8.06($^{+0.13}_{-0.13}$)	0.62($^{+0.08}_{-0.08}$)	-9.57(0.12)	<-5.85	227.6(15.1)
J1230+0813	7133(941)	8.00		-10.71(0.30)	<-3.98	449.5(93.7)
J1230+3143	6282(149)	7.69($^{+0.35}_{-0.31}$)	0.41($^{+0.19}_{-0.13}$)	-9.64(0.17)	<-3.41	228.6(42.2)
J1232+3232	7682(862)	8.00		-10.24(0.22)	<-4.29	468.1(77.8)
J1232+3729	7000(535)	8.00		-9.33(1.54)	<-3.90	478.0(55.8)
J1234+3051	7552(380)	7.39($^{+0.71}_{-0.56}$)	0.29($^{+0.35}_{-0.14}$)	-10.58(0.23)	<-4.95	371.0(125.0)
J1234+5208	7534(63)	8.05($^{+0.04}_{-0.04}$)	0.61($^{+0.03}_{-0.02}$)	-7.59(0.07)	<-4.13	115.1(2.1)
J1234+5606	11787(423)	8.30($^{+0.06}_{-0.06}$)	0.77($^{+0.04}_{-0.04}$)	-7.41(0.06)	-5.52(0.14)	173.8(3.6)

Table 6. Atmospheric parameters for DZ stars – continued.

J Name	T_{eff} (K)	$\log g$	M/M_{\odot}	$\log \text{Ca/He}$	$\log \text{H/He}$	D (pc)
J1234–0330	9184(287)	8.19($^{+0.08}_{-0.07}$)	0.70($^{+0.05}_{-0.05}$)	-10.54(0.07)	<-5.57	107.1(2.6)
J1236+2144	6660(612)	8.00		-9.79(0.40)	<-3.58	405.5(60.7)
J1238+1328	6785(147)	8.23($^{+0.15}_{-0.15}$)	0.72($^{+0.10}_{-0.09}$)	-9.69(0.22)	<-3.49	141.6(13.6)
J1238+2149	5768(128)	8.30($^{+0.20}_{-0.19}$)	0.77($^{+0.13}_{-0.12}$)	-8.26(0.32)	<-3.00	150.6(19.1)
J1239+0756	6962(182)	8.29($^{+0.24}_{-0.23}$)	0.76($^{+0.16}_{-0.15}$)	-9.38(0.41)	<-3.62	204.0(33.3)
J1239+3522	7717(719)	8.00		-10.05(0.36)	<-4.33	470.6(63.2)
J1240+1603	6499(158)	8.19($^{+0.18}_{-0.18}$)	0.70($^{+0.12}_{-0.11}$)	-10.56(0.12)	<-3.21	150.8(17.3)
J1240+1911	7137(437)	8.00		-10.03(0.32)	<-3.98	340.6(30.7)
J1240–0037	8514(177)	8.13($^{+0.06}_{-0.06}$)	0.66($^{+0.04}_{-0.04}$)	-8.91(0.20)	<-5.05	114.5(2.6)
J1241+3010	7525(233)	8.08($^{+0.23}_{-0.22}$)	0.63($^{+0.15}_{-0.13}$)	-9.66(0.22)	<-4.10	217.7(30.3)
J1242+0829	8123(161)	8.17($^{+0.14}_{-0.13}$)	0.68($^{+0.09}_{-0.08}$)	-8.62(0.12)	<-4.57	183.5(15.5)
J1244+3724	6637(87)	8.14($^{+0.10}_{-0.10}$)	0.66($^{+0.07}_{-0.06}$)	-9.37(0.10)	<-3.41	142.2(8.7)
J1244+5732	6973(496)	8.00		-10.36(0.17)	<-3.88	310.6(35.5)
J1244–0118	8466(185)	8.14($^{+0.10}_{-0.10}$)	0.67($^{+0.07}_{-0.06}$)	-8.65(0.17)	<-4.98	164.7(9.5)
J1245+0822	5924(159)	7.30($^{+0.96}_{-1.25}$)	0.25($^{+0.48}_{-0.22}$)	-9.16(0.19)	<-3.31	308.1(131.7)
J1245+6700	7842(338)	7.40($^{+0.50}_{-0.39}$)	0.29($^{+0.23}_{-0.11}$)	-10.49(0.14)	<-5.25	363.6(89.1)
J1246+1155	8182(142)	8.05($^{+0.05}_{-0.05}$)	0.61($^{+0.03}_{-0.03}$)	-8.77(0.10)	<-4.81	79.9(0.8)
J1246–0236	5540(1292)	8.00		-10.27(0.21)	<-3.00	459.2(210.8)
J1247+4934	15150(1357)	7.97($^{+0.13}_{-0.12}$)	0.57($^{+0.07}_{-0.07}$)	-7.57(0.14)	-5.12(0.11)	120.4(1.1)
J1248+1411	12755(802)	8.05($^{+0.27}_{-0.24}$)	0.61($^{+0.17}_{-0.13}$)	-7.07(0.40)	<-6.09	366.5(57.9)
J1249+0806	7016(166)	8.16($^{+0.08}_{-0.08}$)	0.67($^{+0.05}_{-0.05}$)	-10.98(0.14)	<-3.79	116.2(4.1)
J1250+5249	6889(270)	8.62($^{+0.64}_{-0.50}$)	0.98($^{+0.30}_{-0.33}$)	-9.17(0.24)	<-3.23	197.6(88.4)
J1252+3327	7283(461)	8.00		-10.83(0.19)	<-4.04	337.1(32.6)
J1252+3330	6922(699)	8.00		-9.77(0.42)	<-3.84	457.7(69.4)
J1252+6401	6394(414)	8.00		-10.26(0.27)	<-3.29	327.9(37.3)
J1253+1808	13459(741)	7.90($^{+0.35}_{-0.30}$)	0.53($^{+0.21}_{-0.15}$)	-8.51(0.31)	<-6.11	312.5(63.1)
J1253+3842	7367(540)	8.00		-10.19(0.26)	<-4.08	435.9(48.7)
J1254+2233	15366(1585)	8.20($^{+0.21}_{-0.19}$)	0.71($^{+0.13}_{-0.12}$)	-7.14(0.22)	-3.40(0.13)	277.5(26.5)
J1254+3551	6685(174)	8.20($^{+0.30}_{-0.28}$)	0.70($^{+0.20}_{-0.17}$)	-8.79(0.15)	<-3.40	213.8(40.7)
J1254–0236	6903(123)	8.23($^{+0.05}_{-0.05}$)	0.72($^{+0.03}_{-0.03}$)	-10.27(0.08)	<-3.62	78.7(1.2)
J1255+4001	6297(326)	8.00		-10.19(0.33)	<-3.20	372.1(34.4)
J1257+3238	5531(209)	8.00		-8.63(0.17)	<-3.00	230.5(21.9)
J1257–0310	6471(166)	8.00		-8.34(0.10)	<-3.37	226.9(10.7)
J1259+3112	5976(82)	8.20($^{+0.08}_{-0.08}$)	0.70($^{+0.05}_{-0.05}$)	-9.13(0.24)	<-3.00	115.3(5.5)
J1259+4729	5706(207)	7.90($^{+0.38}_{-0.35}$)	0.51($^{+0.24}_{-0.17}$)	-9.83(0.37)	<-3.00	210.7(42.9)
J1302+2215	7092(310)	7.45($^{+0.84}_{-0.67}$)	0.31($^{+0.46}_{-0.18}$)	-10.38(0.24)	<-4.33	365.8(145.7)
J1303+4055	6542(115)	8.09($^{+0.09}_{-0.09}$)	0.63($^{+0.06}_{-0.05}$)	-8.81(0.08)	<-3.36	147.0(7.0)
J1303+4418	6849(449)	8.00		-10.83(0.26)	<-3.77	294.2(31.2)

Table 6. Atmospheric parameters for DZ stars – continued.

J Name	T_{eff} (K)	$\log g$	M/M_{\odot}	$\log \text{Ca/He}$	$\log \text{H/He}$	D (pc)
J1307+0307	8152(208)	7.91($^{+0.08}_{-0.08}$)	0.53($^{+0.05}_{-0.04}$)	-9.67(0.07)	-3.54(0.11)	134.5(4.7)
J1308+0258	6075(160)	8.00		-9.00(0.11)	<-3.03	214.0(11.1)
J1308+0957	7946(373)	8.00		-8.00(0.28)	<-4.58	417.2(30.2)
J1309+3812	8234(650)	8.00		-8.36(0.44)	<-4.95	545.0(65.9)
J1309+4913	8677(243)	8.10($^{+0.06}_{-0.06}$)	0.64($^{+0.04}_{-0.04}$)	-10.11(0.03)	<-5.26	78.9(0.5)
J1310+0645	7935(662)	8.00		-8.45(0.25)	<-4.57	469.5(59.8)
J1310+1323	7701(675)	8.00		-9.98(0.33)	<-4.31	394.5(50.4)
J1310+3149	6925(449)	8.00		-10.04(0.27)	<-3.84	375.2(37.5)
J1311+1019	7359(152)	7.72($^{+0.26}_{-0.24}$)	0.42($^{+0.14}_{-0.10}$)	-8.99(0.14)	<-4.33	251.6(35.0)
J1313+5738	8801(227)	7.99($^{+0.06}_{-0.06}$)	0.57($^{+0.04}_{-0.03}$)	-9.38(0.03)	-4.67(0.17)	68.0(0.3)
J1313+5813	6808(136)	7.91($^{+0.12}_{-0.12}$)	0.52($^{+0.07}_{-0.06}$)	-9.75(0.20)	<-3.81	189.9(12.6)
J1314+3748	6107(147)	8.40($^{+0.27}_{-0.25}$)	0.83($^{+0.18}_{-0.17}$)	-8.64(0.49)	<-3.00	168.3(31.6)
J1314+5223	11351(434)	8.01($^{+0.07}_{-0.07}$)	0.59($^{+0.04}_{-0.04}$)	-8.43(0.08)	-5.43(0.15)	143.6(2.6)
J1316+1916	12686(674)	8.11($^{+0.13}_{-0.12}$)	0.65($^{+0.08}_{-0.07}$)	-8.84(0.16)	-4.22(0.15)	230.0(13.4)
J1316+1918	5250(129)	7.81($^{+0.38}_{-0.35}$)	0.46($^{+0.23}_{-0.16}$)	-10.33(0.30)	<-3.01	185.0(37.4)
J1316+5117	6465(195)	8.00		-9.20(0.36)	<-3.36	282.7(14.6)
J1316-2007	4667(103)	8.14($^{+0.06}_{-0.06}$)	0.66($^{+0.04}_{-0.04}$)	-10.74(0.09)	<-3.00	23.2(0.1)
J1318+2022	6167(166)	8.24($^{+0.24}_{-0.23}$)	0.72($^{+0.16}_{-0.15}$)	-9.49(0.29)	<-3.01	181.8(28.2)
J1319+0844	9040(273)	8.16($^{+0.07}_{-0.07}$)	0.68($^{+0.05}_{-0.05}$)	-11.13(0.08)	<-5.48	108.5(2.1)
J1319+3025	9506(302)	8.11($^{+0.08}_{-0.08}$)	0.65($^{+0.05}_{-0.05}$)	-9.57(0.05)	<-5.79	160.6(5.3)
J1319+3641	7335(165)	8.24($^{+0.17}_{-0.17}$)	0.73($^{+0.12}_{-0.11}$)	-8.85(0.18)	<-3.91	209.3(23.8)
J1320+0204	7070(349)	8.22($^{+0.95}_{-0.73}$)	0.71($^{+0.54}_{-0.39}$)	-9.02(0.39)	<-3.78	282.0(155.0)
J1320+4332	6649(262)	7.83($^{+0.26}_{-0.24}$)	0.48($^{+0.15}_{-0.12}$)	-10.32(0.13)	<-3.72	215.6(28.2)
J1321+1614	6659(101)	8.18($^{+0.06}_{-0.06}$)	0.69($^{+0.04}_{-0.04}$)	-9.98(0.08)	<-3.39	103.3(3.2)
J1321+2019	7484(273)	8.95($^{+0.26}_{-0.23}$)	1.16($^{+0.10}_{-0.12}$)	-8.61(0.32)	<-3.39	156.3(34.9)
J1321-0237	5632(117)	7.92($^{+0.31}_{-0.29}$)	0.53($^{+0.19}_{-0.15}$)	-8.59(0.27)	<-3.00	171.2(29.7)
J1322+1224	6824(372)	8.00		-9.42(0.44)	<-3.75	367.7(31.2)
J1322+6707	9971(435)	8.52($^{+0.29}_{-0.27}$)	0.92($^{+0.18}_{-0.18}$)	-7.82(0.27)	-4.35(0.46)	287.1(61.4)
J1323+2112	6871(525)	8.00		-10.03(0.31)	<-3.80	417.3(50.0)
J1323+3849	10623(454)	7.82($^{+0.11}_{-0.11}$)	0.48($^{+0.06}_{-0.05}$)	-8.94(0.09)	-4.75(0.19)	229.2(10.3)
J1325+6521	11833(601)	8.04($^{+0.14}_{-0.13}$)	0.61($^{+0.09}_{-0.08}$)	-8.49(0.15)	-4.27(0.27)	260.2(17.2)
J1326+1854	9259(423)	7.29($^{+0.82}_{-0.56}$)	0.27($^{+0.38}_{-0.12}$)	-8.86(0.48)	<-6.07	547.5(213.5)
J1326+4235	6948(418)	8.00		-10.09(0.20)	<-3.86	360.9(34.4)
J1327+4508	7073(292)	8.37($^{+0.19}_{-0.18}$)	0.81($^{+0.12}_{-0.12}$)	-10.48(0.32)	<-3.64	185.3(22.1)
J1327+5519	6941(450)	8.00		-9.33(0.59)	<-3.86	387.3(38.3)
J1329+1301	6800(129)	7.68($^{+0.24}_{-0.22}$)	0.40($^{+0.12}_{-0.09}$)	-8.83(0.10)	<-3.95	228.0(28.9)
J1329+6459	6904(499)	8.00		-9.44(0.58)	<-3.82	399.0(44.0)
J1332+1522	7313(161)	8.03($^{+0.07}_{-0.07}$)	0.59($^{+0.05}_{-0.04}$)	-10.58(0.08)	<-4.03	116.4(3.4)

Table 6. Atmospheric parameters for DZ stars – continued.

J Name	T_{eff} (K)	$\log g$	M/M_{\odot}	$\log \text{Ca/He}$	$\log \text{H/He}$	D (pc)
J1332+5446	9279(1339)	8.00		-9.54(0.32)	<-5.73	632.1(134.6)
J1333+3254	12021(492)	8.02($^{+0.14}_{-0.13}$)	0.60($^{+0.08}_{-0.07}$)	-7.03(0.09)	<-6.10	296.8(22.5)
J1333+6349	15316(1559)	7.96($^{+0.17}_{-0.16}$)	0.57($^{+0.10}_{-0.08}$)	-7.17(0.19)	-5.07(0.18)	292.7(17.4)
J1335+2254	6388(332)	8.00		-9.97(0.43)	<-3.28	346.3(31.4)
J1336+3012	9400(786)	8.00		-8.17(0.39)	<-5.81	560.1(63.3)
J1336+3547	6247(31)	8.08($^{+0.03}_{-0.03}$)	0.62($^{+0.02}_{-0.02}$)	-8.85(0.03)	<-3.11	59.7(0.4)
J1338+1334	13396(634)	8.05($^{+0.13}_{-0.13}$)	0.61($^{+0.08}_{-0.07}$)	-9.75(0.49)	-5.20(0.21)	252.4(17.4)
J1338+3255	7104(286)	8.19($^{+0.31}_{-0.29}$)	0.69($^{+0.21}_{-0.18}$)	-10.23(0.12)	<-3.83	230.5(45.3)
J1338-0130	10338(322)	8.02($^{+0.07}_{-0.07}$)	0.59($^{+0.04}_{-0.04}$)	-9.32(0.08)	<-5.96	138.6(3.5)
J1339+2643	6456(53)	8.07($^{+0.06}_{-0.06}$)	0.62($^{+0.04}_{-0.04}$)	-9.28(0.09)	<-3.29	103.8(3.3)
J1339+6401	8070(616)	8.00		-9.84(0.18)	<-4.74	387.7(42.4)
J1340+0835	7546(180)	8.23($^{+0.08}_{-0.08}$)	0.72($^{+0.06}_{-0.05}$)	-10.60(0.14)	<-4.03	112.4(4.9)
J1340+2702	8414(277)	8.78($^{+0.48}_{-0.39}$)	1.07($^{+0.21}_{-0.25}$)	-7.05(0.22)	<-4.07	246.9(91.1)
J1341+1338	10507(368)	7.91($^{+0.18}_{-0.17}$)	0.53($^{+0.11}_{-0.09}$)	-8.40(0.16)	<-6.04	271.9(27.7)
J1341+2216	8102(214)	7.98($^{+0.15}_{-0.14}$)	0.56($^{+0.09}_{-0.08}$)	-8.66(0.15)	<-4.81	214.6(17.3)
J1341+3024	6436(183)	7.96($^{+0.21}_{-0.20}$)	0.55($^{+0.13}_{-0.11}$)	-10.76(0.13)	<-3.37	166.5(19.5)
J1341-0112	8533(242)	8.30($^{+0.17}_{-0.16}$)	0.77($^{+0.11}_{-0.10}$)	-8.87(0.41)	<-4.77	196.4(21.3)
J1341-3124	7935(463)	8.01($^{+0.12}_{-0.12}$)	0.58($^{+0.08}_{-0.07}$)	-10.39(0.05)	<-4.56	67.8(0.9)
J1342+0522	8189(150)	8.02($^{+0.12}_{-0.12}$)	0.59($^{+0.08}_{-0.07}$)	-8.77(0.25)	<-4.86	154.8(10.9)
J1342+1813	5635(133)	8.00		-8.88(0.55)	<-3.00	201.4(10.7)
J1343+2941	11271(616)	8.17($^{+0.17}_{-0.16}$)	0.69($^{+0.11}_{-0.10}$)	-7.88(0.11)	<-5.99	249.9(25.0)
J1343+4641	6531(182)	8.05($^{+0.17}_{-0.16}$)	0.60($^{+0.11}_{-0.10}$)	-10.92(0.16)	<-3.39	167.8(16.1)
J1344+6505	10516(429)	8.15($^{+0.21}_{-0.19}$)	0.68($^{+0.13}_{-0.12}$)	-9.01(0.39)	<-5.91	311.1(39.0)
J1345+1153	6064(102)	8.22($^{+0.11}_{-0.11}$)	0.71($^{+0.07}_{-0.07}$)	-8.03(0.10)	<-3.00	120.1(7.8)
J1345+5854	7258(270)	8.22($^{+0.21}_{-0.20}$)	0.71($^{+0.14}_{-0.13}$)	-9.63(0.18)	<-3.89	219.0(28.2)
J1347+0720	6787(232)	8.00		-9.76(0.23)	<-3.71	237.6(12.2)
J1347+1415	6489(76)	8.18($^{+0.10}_{-0.10}$)	0.69($^{+0.07}_{-0.06}$)	-8.56(0.07)	<-3.21	136.8(8.9)
J1347+1733	6953(208)	8.22($^{+0.27}_{-0.25}$)	0.71($^{+0.18}_{-0.16}$)	-9.53(0.13)	<-3.68	183.3(32.0)
J1349+0209	5935(164)	8.00		-9.51(0.22)	<-3.00	198.8(10.4)
J1349+0243	13408(863)	8.06($^{+0.12}_{-0.12}$)	0.63($^{+0.08}_{-0.07}$)	-8.07(0.20)	<-6.10	228.0(10.9)
J1350+1058	5359(117)	8.64($^{+0.18}_{-0.17}$)	0.99($^{+0.11}_{-0.11}$)	-9.10(0.23)	<-3.00	105.3(14.6)
J1350+2148	6997(725)	8.00		-9.70(0.45)	<-3.90	427.5(66.9)
J1351+1900	14528(1593)	7.58($^{+0.88}_{-0.54}$)	0.38($^{+0.50}_{-0.15}$)	-7.05(0.39)	<-6.00	709.1(311.6)
J1351+2645	5850(109)	7.86($^{+0.16}_{-0.16}$)	0.49($^{+0.09}_{-0.08}$)	-8.48(0.09)	<-3.00	171.2(14.7)
J1351+4253	6506(104)	8.12($^{+0.05}_{-0.04}$)	0.65($^{+0.03}_{-0.03}$)	-11.16(0.09)	<-3.29	39.4(0.1)
J1351+6136	6858(171)	8.14($^{+0.09}_{-0.08}$)	0.66($^{+0.06}_{-0.05}$)	-10.45(0.14)	<-3.66	141.9(5.4)
J1353+1347	8319(258)	8.60($^{+0.28}_{-0.25}$)	0.97($^{+0.16}_{-0.17}$)	-8.49(0.22)	<-4.13	202.9(43.5)
J1353+3239	8360(234)	8.03($^{+0.07}_{-0.07}$)	0.60($^{+0.05}_{-0.04}$)	-10.82(0.04)	<-5.06	112.9(1.9)

Table 6. Atmospheric parameters for DZ stars – continued.

J Name	T_{eff} (K)	$\log g$	M/M_{\odot}	$\log \text{Ca/He}$	$\log \text{H/He}$	D (pc)
J1355+0810	7160(146)	8.25($^{+0.14}_{-0.14}$)	0.74($^{+0.09}_{-0.09}$)	-9.04(0.17)	<-3.81	160.5(14.6)
J1356+0236	7722(114)	8.12($^{+0.28}_{-0.26}$)	0.65($^{+0.19}_{-0.16}$)	-7.80(0.09)	<-4.22	189.7(33.8)
J1356+2416	6317(54)	8.08($^{+0.05}_{-0.05}$)	0.62($^{+0.03}_{-0.03}$)	-8.95(0.13)	<-3.16	100.6(2.5)
J1356+4047	6792(145)	8.11($^{+0.06}_{-0.06}$)	0.64($^{+0.04}_{-0.04}$)	-10.08(0.07)	<-3.62	109.0(2.5)
J1356+4342	6942(610)	8.00		-9.65(0.29)	<-3.86	394.5(53.0)
J1357+5727	6976(456)	8.00		-9.78(0.41)	<-3.88	345.1(35.4)
J1359+3810	6552(301)	8.00		-10.47(0.11)	<-3.46	181.4(17.7)
J1400+4507	7238(294)	8.16($^{+0.23}_{-0.22}$)	0.67($^{+0.15}_{-0.13}$)	-9.97(0.09)	<-3.92	221.0(30.1)
J1401+2840	9200(293)	7.97($^{+0.11}_{-0.10}$)	0.56($^{+0.06}_{-0.06}$)	-10.04(0.05)	<-5.70	180.1(8.2)
J1401+3009	8283(510)	8.64($^{+0.30}_{-0.27}$)	0.99($^{+0.17}_{-0.18}$)	-9.04(0.28)	<-4.09	229.5(51.1)
J1401+3659	5891(42)	7.94($^{+0.04}_{-0.04}$)	0.54($^{+0.03}_{-0.02}$)	-10.14(0.09)	<-3.00	84.3(1.4)
J1402+2506	9224(286)	8.28($^{+0.07}_{-0.07}$)	0.75($^{+0.05}_{-0.05}$)	-8.81(0.08)	<-5.55	131.8(3.3)
J1402+2518	6777(143)	8.26($^{+0.09}_{-0.09}$)	0.74($^{+0.06}_{-0.06}$)	-9.67(0.09)	<-3.44	132.0(6.7)
J1402+4742	7847(354)	8.00		-8.37(0.24)	<-4.47	407.1(29.0)
J1403+1954	13117(867)	8.14($^{+0.19}_{-0.18}$)	0.67($^{+0.12}_{-0.11}$)	-8.81(0.41)	-4.17(0.30)	274.6(27.3)
J1404+3620	6448(45)	8.27($^{+0.03}_{-0.03}$)	0.75($^{+0.02}_{-0.02}$)	-8.85(0.08)	<-3.11	81.7(1.2)
J1404-0232	7597(164)	8.17($^{+0.08}_{-0.08}$)	0.68($^{+0.05}_{-0.05}$)	-9.76(0.13)	<-4.09	128.1(4.8)
J1405+1549	6952(61)	8.02($^{+0.09}_{-0.09}$)	0.59($^{+0.06}_{-0.05}$)	-8.60(0.08)	<-3.85	124.7(6.7)
J1405+2542	5653(150)	8.00		-10.28(0.35)	<-3.00	201.8(10.3)
J1406+1814	8664(267)	8.12($^{+0.11}_{-0.11}$)	0.65($^{+0.07}_{-0.07}$)	-9.86(0.06)	<-5.22	168.0(9.3)
J1406-0037	7522(197)	8.10($^{+0.51}_{-0.45}$)	0.64($^{+0.34}_{-0.25}$)	-8.78(0.24)	<-4.09	253.4(79.1)
J1407+3218	6988(162)	7.70($^{+0.24}_{-0.22}$)	0.41($^{+0.13}_{-0.09}$)	-9.24(0.22)	<-4.06	244.2(30.9)
J1408+1535	10502(370)	8.32($^{+0.11}_{-0.11}$)	0.79($^{+0.07}_{-0.07}$)	-8.30(0.09)	<-5.77	184.3(12.1)
J1408+1750	7484(472)	8.00		-9.58(0.49)	<-4.14	413.1(38.4)
J1409+1254	6215(334)	8.00		-9.83(0.56)	<-3.13	316.2(30.3)
J1409+1511	6542(112)	8.14($^{+0.06}_{-0.06}$)	0.66($^{+0.04}_{-0.04}$)	-10.75(0.10)	<-3.31	87.2(1.8)
J1410+1445	13152(674)	8.12($^{+0.18}_{-0.17}$)	0.66($^{+0.12}_{-0.10}$)	-8.82(0.32)	<-6.08	321.4(35.2)
J1411+3410	5527(93)	8.39($^{+0.14}_{-0.13}$)	0.83($^{+0.09}_{-0.09}$)	-8.20(0.88)	<-3.00	120.1(11.1)
J1412+1343	10166(382)	8.12($^{+0.13}_{-0.12}$)	0.66($^{+0.08}_{-0.08}$)	-8.39(0.09)	<-5.86	232.5(16.4)
J1412+4011	9370(797)	8.00		-7.17(0.48)	<-5.79	818.8(106.2)
J1413+1659	7946(1078)	8.00		-9.88(0.36)	<-4.58	553.7(104.5)
J1413+1820	7034(412)	8.00		-9.99(16.68)	<-3.92	303.4(27.1)
J1414-0113	8697(238)	7.98($^{+0.07}_{-0.07}$)	0.57($^{+0.04}_{-0.04}$)	-10.82(0.07)	<-5.41	108.4(1.9)
J1416+0230	7003(401)	8.00		-10.07(0.24)	<-3.90	288.5(26.2)
J1417+2931	5887(325)	8.00		-9.56(0.19)	<-3.00	328.5(36.0)
J1419+4400	7292(273)	8.33($^{+0.15}_{-0.15}$)	0.79($^{+0.10}_{-0.10}$)	-9.91(0.13)	<-3.83	197.9(18.0)
J1420+4405	5780(227)	8.00		-10.03(0.41)	<-3.00	315.6(25.1)
J1420+4759	11369(412)	7.89($^{+0.11}_{-0.11}$)	0.52($^{+0.06}_{-0.06}$)	-9.79(0.17)	<-6.06	250.1(13.6)

Table 6. Atmospheric parameters for DZ stars – continued.

J Name	T_{eff} (K)	$\log g$	M/M_{\odot}	$\log \text{Ca/He}$	$\log \text{H/He}$	D (pc)
J1421+1843	6610(117)	$8.06^{(+0.27)}_{(-0.26)}$	$0.61^{(+0.18)}_{(-0.15)}$	-8.27(0.11)	<-3.46	204.4(34.1)
J1421+5703	6980(255)	$8.14^{(+0.20)}_{(-0.19)}$	$0.66^{(+0.13)}_{(-0.12)}$	-9.94(0.12)	<-3.78	215.8(25.5)
J1422+5229	12016(531)	$7.55^{(+0.23)}_{(-0.20)}$	$0.36^{(+0.10)}_{(-0.07)}$	-9.29(0.32)	-5.81(0.51)	443.7(53.1)
J1424+5657	6723(206)	$8.25^{(+0.11)}_{(-0.10)}$	$0.73^{(+0.07)}_{(-0.07)}$	-9.95(0.11)	<-3.40	148.8(8.0)
J1425+2302	11839(514)	$8.05^{(+0.15)}_{(-0.14)}$	$0.62^{(+0.09)}_{(-0.08)}$	-7.64(0.14)	-5.23(0.22)	248.8(20.9)
J1425-0050	7116(149)	$8.19^{(+0.05)}_{(-0.05)}$	$0.70^{(+0.04)}_{(-0.03)}$	-10.90(0.07)	<-3.83	70.8(1.0)
J1427+4825	7561(174)	$7.96^{(+0.07)}_{(-0.06)}$	$0.55^{(+0.04)}_{(-0.04)}$	-10.87(0.08)	<-4.23	116.7(2.2)
J1428+4210	7422(311)	$8.42^{(+0.39)}_{(-0.35)}$	$0.85^{(+0.24)}_{(-0.23)}$	-9.66(0.21)	<-3.85	246.8(65.9)
J1428+4403	6602(59)	$8.06^{(+0.03)}_{(-0.03)}$	$0.61^{(+0.02)}_{(-0.02)}$	-9.44(0.11)	<-3.45	44.9(0.1)
J1429+3841	5761(112)	$7.75^{(+0.25)}_{(-0.23)}$	$0.43^{(+0.14)}_{(-0.11)}$	-10.07(0.22)	<-3.00	208.7(27.2)
J1429+5839	9382(301)	$8.24^{(+0.11)}_{(-0.11)}$	$0.73^{(+0.07)}_{(-0.07)}$	-8.55(0.33)	<-5.65	217.0(13.3)
J1430+3245	7294(669)	8.00		-9.73(0.49)	<-4.05	491.2(66.8)
J1430-0151	6098(88)	$7.95^{(+0.08)}_{(-0.08)}$	$0.54^{(+0.05)}_{(-0.05)}$	-8.34(0.25)	<-3.06	118.9(4.8)
J1432+0354	11164(532)	$8.05^{(+0.17)}_{(-0.16)}$	$0.61^{(+0.11)}_{(-0.09)}$	-8.40(0.12)	-4.51(0.17)	238.2(22.5)
J1432+1522	10489(406)	$8.14^{(+0.16)}_{(-0.15)}$	$0.67^{(+0.10)}_{(-0.09)}$	-9.42(0.20)	<-5.92	244.1(23.0)
J1432+3542	6800(193)	$7.86^{(+0.37)}_{(-0.33)}$	$0.49^{(+0.22)}_{(-0.16)}$	-9.87(0.17)	<-3.83	260.4(53.3)
J1433+0714	11282(418)	$7.98^{(+0.07)}_{(-0.07)}$	$0.57^{(+0.04)}_{(-0.04)}$	-9.26(0.05)	-5.56(0.09)	97.6(1.3)
J1433+6139	7843(464)	8.00		-8.35(0.36)	<-4.46	499.5(46.0)
J1436+2152	7286(429)	8.00		-9.88(0.47)	<-4.04	338.2(28.8)
J1438+1046	6971(708)	8.00		-10.17(0.42)	<-3.88	461.0(74.3)
J1440+1227	7763(1062)	8.00		-9.74(0.38)	<-4.37	528.4(105.5)
J1440-0232	6719(173)	$7.96^{(+0.10)}_{(-0.09)}$	$0.55^{(+0.06)}_{(-0.05)}$	-10.56(0.09)	<-3.68	100.2(2.2)
J1441+0831	7056(146)	$7.99^{(+0.08)}_{(-0.08)}$	$0.57^{(+0.05)}_{(-0.05)}$	-10.83(0.04)	<-3.94	100.9(3.6)
J1441+4714	7176(345)	8.00		-10.26(0.15)	<-4.00	308.5(22.2)
J1441+5215	7839(414)	8.00		-9.48(0.37)	<-4.46	358.7(27.3)
J1442+5833	6774(225)	$8.33^{(+0.25)}_{(-0.24)}$	$0.79^{(+0.17)}_{(-0.16)}$	-9.20(0.19)	<-3.37	208.7(35.3)
J1443+2054	6582(700)	8.00		-10.73(0.44)	<-3.49	380.6(67.6)
J1443+3014	7001(302)	8.00		-8.23(0.29)	<-30.00	405.7(32.4)
J1443+5833	7056(402)	8.00		-8.49(0.23)	<-3.94	398.7(38.7)
J1444+1151	4937(185)	8.00		-10.53(0.23)	<-3.00	188.1(15.1)
J1444+2059	7636(827)	8.00		-9.53(0.71)	<-4.25	539.1(87.2)
J1444+4741	5431(167)	8.00		-10.07(0.29)	<-3.00	257.8(17.5)
J1444+5741	9105(412)	$8.25^{(+0.29)}_{(-0.27)}$	$0.74^{(+0.19)}_{(-0.17)}$	-8.36(1.00)	<-5.48	316.7(57.9)
J1445+0913	7154(309)	8.00		-7.64(0.23)	<-3.99	380.4(29.1)
J1445+5850	13052(673)	$7.96^{(+0.09)}_{(-0.09)}$	$0.56^{(+0.05)}_{(-0.05)}$	-8.69(0.17)	<-6.11	179.0(3.9)
J1445-0208	6467(86)	$8.14^{(+0.05)}_{(-0.05)}$	$0.66^{(+0.03)}_{(-0.03)}$	-10.27(0.05)	<-3.23	87.3(1.6)
J1446+0111	6391(632)	8.00		-10.81(0.54)	<-3.29	333.7(55.0)
J1446+0112	7293(556)	8.00		-10.21(0.22)	<-4.05	326.5(36.2)

Table 6. Atmospheric parameters for DZ stars – continued.

J Name	T_{eff} (K)	$\log g$	M/M_{\odot}	$\log \text{Ca/He}$	$\log \text{H/He}$	D (pc)
J1447+1340	4999(175)	8.00		-10.38(0.30)	<-3.00	209.7(16.8)
J1448+1047	6316(47)	8.16($^{+0.04}_{-0.04}$)	0.67($^{+0.03}_{-0.03}$)	-9.06(0.06)	<-3.10	88.9(2.1)
J1448+2946	7678(612)	8.00		-9.99(0.25)	<-4.29	409.9(48.2)
J1448+2958	8819(268)	8.28($^{+0.10}_{-0.10}$)	0.75($^{+0.07}_{-0.06}$)	-9.33(0.08)	<-5.17	162.3(9.1)
J1452+1346	12206(546)	8.19($^{+0.19}_{-0.18}$)	0.70($^{+0.12}_{-0.11}$)	-9.04(0.19)	<-6.07	256.4(29.9)
J1452+4544	8678(650)	8.00		-9.38(0.27)	<-5.38	470.4(51.3)
J1453+2452	5907(171)	8.00		-9.73(0.28)	<-3.00	240.4(14.1)
J1453+3003	7644(539)	8.00		-9.37(40.72)	<-4.26	475.9(50.3)
J1453+3241	6371(123)	8.01($^{+0.10}_{-0.09}$)	0.58($^{+0.06}_{-0.06}$)	-10.74(0.11)	<-3.26	128.2(6.1)
J1455+2010	7737(285)	8.93($^{+0.49}_{-0.37}$)	1.16($^{+0.17}_{-0.21}$)	-8.38(0.24)	<-3.64	171.3(65.7)
J1458+4719	12741(854)	8.02($^{+0.19}_{-0.18}$)	0.60($^{+0.12}_{-0.10}$)	-7.58(0.29)	-4.68(0.47)	322.6(33.0)
J1500+2315	6682(304)	8.00		-8.29(0.33)	<-3.60	371.4(31.9)
J1501+3807	7206(483)	8.00		-10.73(0.24)	<-4.01	342.2(35.8)
J1501+5609	9471(266)	8.20($^{+0.07}_{-0.07}$)	0.70($^{+0.05}_{-0.04}$)	-7.99(0.06)	<-5.72	104.9(1.2)
J1502+3744	5556(62)	8.09($^{+0.07}_{-0.06}$)	0.63($^{+0.04}_{-0.04}$)	-10.05(0.15)	<-3.00	106.2(3.5)
J1503+4414	8682(916)	8.00		-9.52(0.73)	<-5.38	570.7(85.4)
J1503+4642	7089(724)	8.00		-9.91(0.88)	<-3.95	406.8(62.8)
J1506+4152	9463(295)	8.17($^{+0.07}_{-0.07}$)	0.68($^{+0.04}_{-0.04}$)	-10.54(0.04)	<-5.74	95.7(0.8)
J1506+5844	7107(197)	8.01($^{+0.10}_{-0.10}$)	0.58($^{+0.06}_{-0.06}$)	-10.56(0.08)	<-3.95	164.6(7.4)
J1507+2633	7249(249)	7.89($^{+0.13}_{-0.13}$)	0.51($^{+0.08}_{-0.07}$)	-11.38(0.09)	<-4.10	145.0(6.8)
J1507+4034	7352(290)	8.00		-7.97(0.22)	<-4.07	371.3(25.7)
J1508+0622	9991(352)	7.90($^{+0.23}_{-0.22}$)	0.52($^{+0.14}_{-0.11}$)	-9.59(0.15)	<-5.94	261.0(34.7)
J1509+1838	7943(282)	7.86($^{+0.31}_{-0.28}$)	0.49($^{+0.19}_{-0.14}$)	-9.16(0.22)	<-4.78	262.8(45.5)
J1510+3814	9248(230)	7.89($^{+0.15}_{-0.14}$)	0.51($^{+0.09}_{-0.07}$)	-8.22(0.24)	-4.70(0.37)	259.5(21.4)
J1511+2654	6381(172)	8.10($^{+0.24}_{-0.23}$)	0.64($^{+0.16}_{-0.14}$)	-10.49(0.12)	<-3.19	176.3(25.9)
J1512+5304	8221(593)	8.00		-8.25(0.28)	<-4.94	542.6(58.5)
J1514+5012	10508(559)	8.74($^{+0.26}_{-0.23}$)	1.05($^{+0.14}_{-0.15}$)	-9.11(0.43)	<-5.37	239.7(49.2)
J1515+1348	6736(202)	8.03($^{+0.23}_{-0.22}$)	0.59($^{+0.15}_{-0.12}$)	-10.53(0.12)	<-3.63	194.0(25.9)
J1515+4532	7476(218)	7.97($^{+0.18}_{-0.17}$)	0.56($^{+0.11}_{-0.09}$)	-9.10(0.21)	<-4.16	235.4(23.4)
J1516+2118	9588(302)	8.24($^{+0.07}_{-0.07}$)	0.73($^{+0.04}_{-0.04}$)	-10.39(0.06)	<-5.72	107.6(1.8)
J1516-0040	13006(735)	7.95($^{+0.10}_{-0.10}$)	0.56($^{+0.06}_{-0.05}$)	-8.59(0.14)	-4.83(0.08)	141.9(2.4)
J1518+0506	5366(76)	8.27($^{+0.07}_{-0.07}$)	0.74($^{+0.04}_{-0.04}$)	-9.33(0.22)	<-3.00	69.2(2.2)
J1518+5619	7373(550)	8.00		-9.90(0.26)	<-4.08	369.1(39.5)
J1520+2718	7414(568)	8.00		-9.75(0.17)	<-4.10	416.4(49.5)
J1523+5601	7520(485)	8.00		-10.05(0.26)	<-4.16	386.1(36.3)
J1524+4049	6250(93)	8.22($^{+0.09}_{-0.09}$)	0.71($^{+0.06}_{-0.06}$)	-8.57(0.09)	<-3.04	146.4(7.7)
J1524+4052	5777(485)	8.00		-10.11(0.44)	<-3.00	357.4(57.0)
J1525+1625	6757(221)	8.71($^{+0.21}_{-0.19}$)	1.03($^{+0.11}_{-0.12}$)	-9.81(0.14)	<-3.08	153.1(24.8)

Table 6. Atmospheric parameters for DZ stars – continued.

J Name	T_{eff} (K)	$\log g$	M/M_{\odot}	$\log \text{Ca/He}$	$\log \text{H/He}$	D (pc)
J1525+4258	10491(378)	8.22($^{+0.11}_{-0.10}$)	0.72($^{+0.07}_{-0.07}$)	-8.96(0.12)	<-5.86	226.7(13.1)
J1526+1308	7373(630)	8.00		-10.20(0.33)	<-4.08	403.2(50.1)
J1528+0753	7480(125)	8.09($^{+0.14}_{-0.14}$)	0.63($^{+0.09}_{-0.08}$)	-8.43(0.11)	<-4.07	190.3(16.7)
J1531+2505	7591(587)	8.00		-9.71(0.59)	<-4.22	410.5(46.2)
J1531+4240	6998(126)	8.00($^{+0.05}_{-0.05}$)	0.57($^{+0.03}_{-0.03}$)	-10.05(0.06)	<-3.90	86.7(1.0)
J1532+1006	5085(178)	8.00		-10.01(0.30)	<-3.00	254.3(21.0)
J1532+1611	7167(680)	8.00		-10.22(0.31)	<-3.99	449.2(63.8)
J1532+2748	6871(452)	8.00		-9.12(0.44)	<-3.80	450.5(55.6)
J1533+5301	11632(459)	7.90($^{+0.14}_{-0.13}$)	0.53($^{+0.08}_{-0.07}$)	-8.33(0.14)	<-6.08	321.4(24.1)
J1534+1242	6386(265)	8.00		-7.78(0.18)	<-3.28	324.6(27.5)
J1534+1345	13652(720)	8.07($^{+0.19}_{-0.18}$)	0.63($^{+0.12}_{-0.10}$)	-9.11(1.04)	<-6.08	302.6(32.9)
J1535+1247	6012(28)	8.20($^{+0.02}_{-0.02}$)	0.70($^{+0.02}_{-0.02}$)	-8.48(0.03)	<-3.00	19.3(0.0)
J1537+3608	5564(128)	8.00		-9.81(0.35)	<-3.00	198.8(9.5)
J1537+4625	7445(173)	8.16($^{+0.22}_{-0.21}$)	0.68($^{+0.15}_{-0.13}$)	-8.99(0.35)	<-4.01	230.7(32.4)
J1539+1930	7140(203)	8.15($^{+0.13}_{-0.13}$)	0.67($^{+0.09}_{-0.08}$)	-9.80(0.21)	<-3.88	166.2(12.9)
J1539+5248	6995(422)	8.00		-10.45(0.20)	<-3.90	331.0(31.5)
J1540+2109	7001(293)	8.42($^{+0.42}_{-0.37}$)	0.85($^{+0.26}_{-0.24}$)	-9.96(0.15)	<-3.52	199.3(57.2)
J1540+3737	8226(310)	7.91($^{+0.29}_{-0.27}$)	0.52($^{+0.18}_{-0.14}$)	-8.89(1.01)	<-5.07	327.2(53.8)
J1540+5149	8107(289)	8.06($^{+0.19}_{-0.19}$)	0.61($^{+0.13}_{-0.11}$)	-9.92(0.20)	<-4.70	228.1(25.5)
J1540+5352	6486(189)	8.00		-8.71(0.28)	<-3.39	296.1(15.8)
J1541+0715	7461(770)	8.00		-10.24(0.29)	<-4.13	444.3(67.0)
J1542+4650	6206(185)	8.32($^{+0.19}_{-0.18}$)	0.78($^{+0.13}_{-0.12}$)	-8.14(0.24)	<-3.00	183.2(22.3)
J1543+2024	6341(255)	8.00		-8.65(0.19)	<-3.24	304.1(23.2)
J1544+2345	6693(141)	7.97($^{+0.13}_{-0.13}$)	0.56($^{+0.08}_{-0.07}$)	-10.27(0.08)	<-3.64	151.5(10.9)
J1545+4921	9628(453)	8.17($^{+0.32}_{-0.29}$)	0.68($^{+0.21}_{-0.17}$)	-8.18(0.70)	<-5.78	339.0(66.6)
J1545+5236	6034(85)	8.08($^{+0.10}_{-0.10}$)	0.62($^{+0.06}_{-0.06}$)	-9.18(0.12)	<-3.00	142.9(8.2)
J1546+1750	8206(595)	8.00		-8.99(0.62)	<-4.92	491.0(52.4)
J1546+3927	8924(216)	8.13($^{+0.09}_{-0.09}$)	0.66($^{+0.06}_{-0.06}$)	-8.46(0.22)	<-5.41	191.6(9.4)
J1547+0659	8737(244)	8.04($^{+0.06}_{-0.06}$)	0.60($^{+0.04}_{-0.04}$)	-9.74(0.03)	<-5.36	87.8(0.9)
J1548+0222	8359(277)	8.32($^{+0.11}_{-0.11}$)	0.78($^{+0.08}_{-0.07}$)	-10.45(0.07)	<-4.54	156.0(10.1)
J1548+2135	11084(442)	7.99($^{+0.09}_{-0.08}$)	0.58($^{+0.05}_{-0.05}$)	-9.13(0.07)	-5.41(0.11)	167.1(4.9)
J1549+0239	8684(487)	8.00		-9.60(0.50)	<-5.38	300.8(23.2)
J1549+1906	6331(249)	8.00		-8.60(0.28)	<-3.23	286.6(21.2)
J1549+2020	7150(251)	8.34($^{+0.68}_{-0.56}$)	0.79($^{+0.40}_{-0.34}$)	-8.79(0.29)	<-3.74	240.5(104.6)
J1549+2633	7178(184)	8.28($^{+0.28}_{-0.26}$)	0.76($^{+0.19}_{-0.17}$)	-8.56(0.13)	<-3.80	225.9(41.7)
J1549+4422	6428(158)	8.01($^{+0.12}_{-0.11}$)	0.58($^{+0.07}_{-0.07}$)	-10.49(0.13)	<-3.31	163.7(9.4)
J1550+2013	5944(334)	8.00		-9.77(0.56)	<-3.00	309.9(32.4)
J1550+5214	7531(384)	8.00		-9.49(0.35)	<-4.17	388.1(29.9)

Table 6. Atmospheric parameters for DZ stars – continued.

J Name	T_{eff} (K)	$\log g$	M/M_{\odot}	$\log \text{Ca/He}$	$\log \text{H/He}$	D (pc)
J1551+1529	7501(1032)	8.00		-10.17(0.28)	<-4.15	520.9(106.1)
J1551+2547	7677(671)	8.00		-8.46(0.47)	<-4.29	590.4(78.5)
J1552+0815	10758(550)	8.31($^{+0.54}_{-0.46}$)	0.78($^{+0.34}_{-0.28}$)	-8.93(0.49)	<-5.85	333.1(116.7)
J1554+1735	6768(46)	8.20($^{+0.03}_{-0.03}$)	0.70($^{+0.02}_{-0.02}$)	-8.71(0.05)	<-3.50	56.4(0.4)
J1557+2157	8630(223)	7.93($^{+0.10}_{-0.09}$)	0.54($^{+0.06}_{-0.05}$)	-9.03(0.11)	-3.46(0.19)	171.5(7.8)
J1558+0312	7734(122)	7.91($^{+0.11}_{-0.10}$)	0.52($^{+0.06}_{-0.06}$)	-8.77(0.17)	<-4.46	161.4(9.4)
J1558+1507	10090(592)	8.19($^{+0.13}_{-0.12}$)	0.70($^{+0.08}_{-0.08}$)	-9.40(0.10)	<-5.81	150.7(5.5)
J1558+2512	7201(155)	8.06($^{+0.05}_{-0.05}$)	0.61($^{+0.03}_{-0.03}$)	-10.89(0.05)	<-3.97	54.0(0.2)
J1559+0445	7389(225)	8.07($^{+0.18}_{-0.17}$)	0.62($^{+0.11}_{-0.10}$)	-10.14(0.12)	<-4.04	171.0(17.5)
J1600+1833	8154(435)	7.52($^{+0.81}_{-0.58}$)	0.34($^{+0.45}_{-0.16}$)	-10.14(0.27)	<-5.41	405.3(158.2)
J1600+3819	7101(328)	8.00		-8.75(0.30)	<-3.96	365.2(26.3)
J1600+4120	7765(639)	8.00		-9.88(0.36)	<-4.38	404.4(49.1)
J1600-0009	6544(138)	8.00		-10.58(0.15)	<-3.45	117.0(4.4)
J1601+1824	5240(196)	8.00		-10.04(0.25)	<-3.01	219.1(18.1)
J1602+1923	5267(324)	8.00		-10.41(0.28)	<-3.01	249.1(31.5)
J1603+4140	7673(706)	8.00		-9.56(0.41)	<-4.29	453.7(63.7)
J1604+0831	11757(452)	7.89($^{+0.13}_{-0.12}$)	0.52($^{+0.07}_{-0.06}$)	-9.20(0.14)	-5.51(0.17)	234.9(15.8)
J1604+1830	6459(104)	8.13($^{+0.10}_{-0.10}$)	0.65($^{+0.07}_{-0.06}$)	-9.61(0.12)	<-3.24	139.1(8.3)
J1606+1908	7788(563)	8.00		-10.37(0.19)	<-4.40	384.3(40.8)
J1606+4712	8227(488)	7.37($^{+1.28}_{-1.01}$)	0.29($^{+0.72}_{-0.22}$)	-11.33(0.28)	<-5.57	518.2(292.2)
J1607+3950	7397(239)	8.49($^{+0.44}_{-0.38}$)	0.89($^{+0.26}_{-0.25}$)	-8.88(0.32)	<-3.79	212.7(66.1)
J1607+5321	9657(441)	8.09($^{+0.21}_{-0.20}$)	0.63($^{+0.14}_{-0.12}$)	-9.16(0.17)	<-5.84	300.2(36.3)
J1608+1342	9223(219)	8.23($^{+0.09}_{-0.09}$)	0.73($^{+0.06}_{-0.06}$)	-8.16(0.25)	<-5.57	168.8(8.2)
J1608+3831	6507(170)	8.05($^{+0.11}_{-0.11}$)	0.61($^{+0.07}_{-0.07}$)	-10.39(0.08)	<-3.35	158.9(9.1)
J1610+3714	11462(464)	8.24($^{+0.12}_{-0.12}$)	0.74($^{+0.08}_{-0.08}$)	-7.66(0.11)	-4.81(0.25)	262.8(18.6)
J1610+4006	6053(158)	8.00		-9.83(0.39)	<-3.02	238.7(11.6)
J1611+1117	7676(169)	7.85($^{+0.10}_{-0.10}$)	0.49($^{+0.06}_{-0.05}$)	-9.72(0.24)	<-4.48	168.2(8.0)
J1612+1845	7376(531)	8.00		-10.06(0.18)	<-4.08	363.0(38.8)
J1612+3534	7058(320)	8.00		-8.90(0.53)	<-3.94	379.1(27.0)
J1615+1746	9613(456)	7.14($^{+2.49}_{-1.60}$)	0.23($^{+1.18}_{-0.21}$)	-7.95(0.60)	<-6.14	740.2(633.9)
J1616+3303	6382(72)	7.93($^{+0.06}_{-0.06}$)	0.53($^{+0.04}_{-0.03}$)	-8.49(0.05)	<-3.34	127.3(3.6)
J1618+4452	9867(261)	7.94($^{+0.13}_{-0.12}$)	0.54($^{+0.07}_{-0.07}$)	-7.63(0.18)	<-5.92	266.0(18.2)
J1619+4745	8888(603)	8.00		-8.25(0.39)	<-5.49	555.0(53.8)
J1622+4731	7716(279)	8.00		-8.20(0.22)	<-4.33	408.5(24.0)
J1622+6319	11586(785)	8.39($^{+0.20}_{-0.19}$)	0.83($^{+0.13}_{-0.12}$)	-7.69(0.33)	-4.88(0.43)	325.5(40.9)
J1624+3310	6628(216)	8.00		-9.16(0.36)	<-3.54	300.0(16.4)
J1626+3303	6918(261)	8.00		-8.34(0.21)	<-3.84	309.1(20.2)
J1627+1443	9121(435)	8.24($^{+0.26}_{-0.24}$)	0.73($^{+0.17}_{-0.15}$)	-10.19(0.20)	<-5.50	267.2(42.3)

Table 6. Atmospheric parameters for DZ stars – continued.

J Name	T_{eff} (K)	$\log g$	M/M_{\odot}	$\log \text{Ca/He}$	$\log \text{H/He}$	D (pc)
J1627+4646	5639(114)	$7.54^{(+0.21)}_{(-0.19)}$	$0.33^{(+0.10)}_{(-0.07)}$	-10.59(0.36)	<-3.01	201.1(20.6)
J1628+3646	8316(435)	$7.98^{(+0.09)}_{(-0.09)}$	$0.57^{(+0.06)}_{(-0.05)}$	-9.07(0.08)	-3.66(0.03)	15.9(0.0)
J1629+1758	10709(465)	$7.92^{(+0.26)}_{(-0.23)}$	$0.54^{(+0.15)}_{(-0.12)}$	-8.91(0.37)	<-6.04	342.6(50.0)
J1633+1840	10298(325)	$8.03^{(+0.07)}_{(-0.07)}$	$0.60^{(+0.04)}_{(-0.04)}$	-8.81(0.06)	<-5.95	165.2(4.3)
J1636+1619	4416(66)	$8.08^{(+0.09)}_{(-0.09)}$	$0.62^{(+0.06)}_{(-0.05)}$	-9.83(0.20)	<-3.00	69.1(2.4)
J1638+3837	7247(179)	$7.70^{(+0.27)}_{(-0.25)}$	$0.41^{(+0.15)}_{(-0.10)}$	-9.19(0.25)	<-4.25	271.3(39.3)
J1640+3154	6857(108)	$8.04^{(+0.06)}_{(-0.06)}$	$0.60^{(+0.04)}_{(-0.03)}$	-9.98(0.06)	<-3.75	111.6(2.6)
J1641+1856	5559(90)	$8.01^{(+0.11)}_{(-0.11)}$	$0.58^{(+0.07)}_{(-0.06)}$	-10.16(0.08)	<-3.00	131.2(8.0)
J1642+3211	7278(341)	8.00		-10.30(0.22)	<-4.04	297.9(20.8)
J1642+3749	6706(592)	8.00		-9.65(0.68)	<-3.63	473.6(66.6)
J1642+4529	7649(431)	8.00		-9.98(0.20)	<-4.26	353.3(29.2)
J1643+1422	6374(98)	$8.05^{(+0.05)}_{(-0.05)}$	$0.60^{(+0.03)}_{(-0.03)}$	-11.23(0.08)	<-3.23	75.7(1.1)
J1644+3853	6054(158)	$8.32^{(+0.47)}_{(-0.41)}$	$0.78^{(+0.30)}_{(-0.26)}$	-9.75(0.22)	<-3.00	182.3(56.4)
J1646+2742	13810(1412)	$8.07^{(+0.27)}_{(-0.25)}$	$0.63^{(+0.17)}_{(-0.14)}$	-7.42(0.31)	-3.14(0.23)	378.3(50.1)
J1647+2636	7034(120)	$8.00^{(+0.05)}_{(-0.05)}$	$0.57^{(+0.03)}_{(-0.03)}$	-9.99(0.05)	<-3.93	50.5(0.2)
J1647+4156	6876(395)	8.00		-9.65(0.45)	<-3.80	359.7(32.0)
J1648+5241	6934(225)	$8.29^{(+0.17)}_{(-0.17)}$	$0.76^{(+0.12)}_{(-0.11)}$	-9.73(0.19)	<-3.59	185.5(20.5)
J1649+2238	5180(86)	$8.12^{(+0.17)}_{(-0.17)}$	$0.65^{(+0.12)}_{(-0.10)}$	-9.09(0.20)	<-3.00	137.1(14.2)
J1649+4152	5678(293)	8.00		-10.01(0.24)	<-3.00	266.5(27.4)
J1650+4055	7113(766)	8.00		-9.65(0.44)	<-3.97	433.8(67.9)
J1655+2134	7040(460)	8.00		-10.05(0.18)	<-3.93	354.6(35.6)
J1657+3738	7503(175)	$8.12^{(+0.10)}_{(-0.09)}$	$0.65^{(+0.06)}_{(-0.06)}$	-9.91(0.12)	<-4.06	163.7(8.3)
J1657+4759	7377(285)	8.00		-8.75(0.23)	<-4.08	359.1(22.3)
J1700+2047	7156(473)	8.00		-8.84(0.74)	<-3.99	474.1(47.7)
J1703+2541	8848(244)	$7.94^{(+0.07)}_{(-0.06)}$	$0.54^{(+0.04)}_{(-0.04)}$	-10.33(0.03)	-4.09(0.10)	109.6(1.4)
J1706+2541	5397(152)	8.00		-10.27(0.20)	<-3.01	193.0(12.4)
J1707+4250	6574(335)	$7.55^{(+0.66)}_{(-0.53)}$	$0.34^{(+0.36)}_{(-0.17)}$	-10.67(0.17)	<-3.89	340.0(109.1)
J1708+0257	6396(262)	$8.11^{(+0.09)}_{(-0.08)}$	$0.64^{(+0.06)}_{(-0.05)}$	-9.93(0.02)	<-3.20	17.9(0.0)
J1711+2201	9256(340)	$8.06^{(+0.23)}_{(-0.21)}$	$0.61^{(+0.15)}_{(-0.12)}$	-9.02(0.29)	<-5.69	286.4(38.8)
J1714+3658	10680(429)	$7.77^{(+0.12)}_{(-0.12)}$	$0.46^{(+0.07)}_{(-0.06)}$	-9.20(0.11)	-5.26(0.19)	244.6(13.6)
J1714+5501	9761(589)	$8.63^{(+0.26)}_{(-0.24)}$	$0.99^{(+0.15)}_{(-0.16)}$	-9.29(0.31)	<-5.33	266.0(50.3)
J1715+2804	8328(238)	$8.16^{(+0.07)}_{(-0.07)}$	$0.67^{(+0.05)}_{(-0.05)}$	-10.83(0.12)	<-4.81	127.0(2.6)
J1719+5623	9783(309)	$8.08^{(+0.09)}_{(-0.08)}$	$0.63^{(+0.05)}_{(-0.05)}$	-8.55(0.09)	<-5.85	203.4(7.6)
J1722+2723	8108(367)	$8.60^{(+0.19)}_{(-0.18)}$	$0.96^{(+0.12)}_{(-0.12)}$	-9.63(0.31)	-3.11(0.27)	208.8(29.2)
J1728+0815	10597(628)	$8.57^{(+0.35)}_{(-0.31)}$	$0.95^{(+0.20)}_{(-0.20)}$	-9.84(0.29)	-4.24(0.39)	255.0(64.1)
J1728+3250	12123(496)	$7.87^{(+0.09)}_{(-0.09)}$	$0.51^{(+0.05)}_{(-0.04)}$	-9.01(0.19)	<-6.12	230.8(8.0)
J2007–1208	12151(506)	$7.95^{(+0.08)}_{(-0.07)}$	$0.56^{(+0.04)}_{(-0.04)}$	-9.81(0.17)	-5.03(0.07)	111.2(1.2)
J2050–0110	10240(306)	$8.44^{(+0.22)}_{(-0.20)}$	$0.86^{(+0.14)}_{(-0.14)}$	-7.30(0.22)	<-5.61	249.4(39.2)

Table 6. Atmospheric parameters for DZ stars – continued.

J Name	T_{eff} (K)	$\log g$	M/M_{\odot}	$\log \text{Ca/He}$	$\log \text{H/He}$	D (pc)
J2103–0108	8496(195)	8.07($^{+0.13}_{-0.12}$)	0.62($^{+0.08}_{-0.07}$)	-8.85(0.52)	<-5.15	188.8(13.6)
J2107–0055	7276(167)	7.90($^{+0.10}_{-0.09}$)	0.51($^{+0.06}_{-0.05}$)	-10.66(0.10)	<-4.11	125.3(5.5)
J2109–0039	5764(92)	7.82($^{+0.16}_{-0.15}$)	0.47($^{+0.09}_{-0.08}$)	-9.78(0.60)	<-3.00	153.0(12.9)
J2110+0512	5704(197)	8.00		-10.01(0.48)	<-3.00	242.6(16.1)
J2110–0001	10781(400)	7.95($^{+0.09}_{-0.09}$)	0.55($^{+0.05}_{-0.05}$)	-9.57(0.07)	-3.73(0.12)	149.4(4.7)
J2114–0051	6952(2067)	7.35($^{+0.96}_{-0.88}$)	0.27($^{+0.50}_{-0.20}$)	-10.05(0.10)	<-4.31	238.7(33.5)
J2123+0016	5492(90)	8.29($^{+0.27}_{-0.25}$)	0.75($^{+0.18}_{-0.16}$)	-9.65(0.23)	<-3.00	112.1(20.0)
J2124–0114	7732(153)	8.05($^{+0.07}_{-0.07}$)	0.61($^{+0.04}_{-0.04}$)	-9.49(0.14)	<-4.29	121.1(3.4)
J2127+0319	6957(132)	8.09($^{+0.17}_{-0.16}$)	0.63($^{+0.11}_{-0.10}$)	-9.30(0.12)	<-3.80	159.7(16.7)
J2130–0243	7234(402)	8.00		-9.96(0.23)	<-4.02	300.7(24.3)
J2132–0203	5562(244)	8.00		-10.40(0.44)	<-3.00	239.2(20.8)
J2136+1137	11642(523)	8.13($^{+0.11}_{-0.11}$)	0.66($^{+0.07}_{-0.06}$)	-10.57(0.22)	-4.64(0.10)	175.0(7.8)
J2139+0354	7688(889)	8.00		-9.69(0.47)	<-4.30	490.8(83.1)
J2141+0225	6809(488)	8.00		-9.20(0.45)	<-3.74	446.6(51.6)
J2141–3300	6908(760)	8.05($^{+0.23}_{-0.21}$)	0.60($^{+0.15}_{-0.12}$)	-8.80(0.08)	<-3.79	16.1(0.0)
J2142+2252	9505(297)	8.09($^{+0.07}_{-0.07}$)	0.64($^{+0.04}_{-0.04}$)	-10.22(0.03)	<-5.80	46.6(0.2)
J2143–0019	6638(381)	8.00		-9.63(0.44)	<-3.55	348.9(31.2)
J2151–0112	6930(254)	8.00		-8.58(0.18)	<-3.85	286.6(17.3)
J2155+4103	6106(317)	8.17($^{+0.13}_{-0.12}$)	0.68($^{+0.08}_{-0.08}$)	-11.28(0.07)	<-3.01	59.0(0.5)
J2157+1206	6103(82)	8.00($^{+0.14}_{-0.13}$)	0.57($^{+0.08}_{-0.08}$)	-9.03(0.06)	<-3.05	131.4(10.4)
J2201+0219	4599(66)	7.92($^{+0.08}_{-0.08}$)	0.52($^{+0.05}_{-0.04}$)	-11.00(0.16)	<-30.00	63.8(1.6)
J2202+0013	7458(636)	8.00		-9.80(0.28)	<-4.13	431.7(54.3)
J2202+0320	6421(407)	8.00		-9.68(0.29)	<-3.32	328.4(33.6)
J2206+1007	5878(142)	7.76($^{+0.46}_{-0.41}$)	0.44($^{+0.28}_{-0.17}$)	-10.27(0.19)	<-3.00	210.5(51.8)
J2207+2319	7238(1143)	8.00		-9.73(0.65)	<-4.02	469.4(111.2)
J2209+1223	14752(1192)	7.97($^{+0.12}_{-0.11}$)	0.57($^{+0.07}_{-0.06}$)	-7.30(0.12)	<-5.95	165.8(3.8)
J2211+2145	6731(239)	8.63($^{+0.16}_{-0.15}$)	0.99($^{+0.10}_{-0.10}$)	-10.27(0.16)	<-3.09	131.2(15.6)
J2213+0103	6706(256)	8.00		-9.19(0.25)	<-3.63	322.9(19.8)
J2218+3908	8914(199)	8.21($^{+0.05}_{-0.05}$)	0.71($^{+0.03}_{-0.03}$)	-8.34(0.15)	<-5.34	48.3(0.1)
J2220+0140	6996(484)	8.00		-9.05(0.32)	<-3.90	376.7(39.1)
J2225+2338	6100(114)	7.99($^{+0.11}_{-0.10}$)	0.57($^{+0.06}_{-0.06}$)	-9.31(0.08)	<-3.05	123.9(6.8)
J2228+1207	6887(92)	8.09($^{+0.04}_{-0.04}$)	0.63($^{+0.02}_{-0.02}$)	-9.68(0.03)	<-3.74	33.9(0.1)
J2230+1905	5593(134)	8.00		-8.57(0.48)	<-3.00	171.0(9.7)
J2230+3052	6719(223)	8.30($^{+0.17}_{-0.17}$)	0.76($^{+0.12}_{-0.11}$)	-10.70(0.24)	<-3.34	163.4(17.5)
J2231+0040	8456(319)	8.08($^{+0.25}_{-0.24}$)	0.63($^{+0.17}_{-0.14}$)	-10.66(0.26)	<-5.08	223.6(33.8)
J2231+0906	5726(72)	8.05($^{+0.08}_{-0.08}$)	0.60($^{+0.05}_{-0.05}$)	-9.84(0.07)	<-3.00	90.0(3.9)
J2232+0109	6886(156)	8.01($^{+0.12}_{-0.11}$)	0.58($^{+0.07}_{-0.07}$)	-10.55(0.15)	<-3.80	134.6(8.2)
J2235–0056	6486(144)	8.00		-8.54(0.15)	<-3.38	214.3(8.5)

Table 6. Atmospheric parameters for DZ stars – continued.

J Name	T_{eff} (K)	$\log g$	M/M_{\odot}	$\log \text{Ca/He}$	$\log \text{H/He}$	D (pc)
J2236+0109	13339(708)	8.34($^{+0.26}_{-0.24}$)	0.80($^{+0.17}_{-0.15}$)	-8.95(0.37)	-5.16(0.25)	253.6(44.4)
J2236+0413	7145(577)	8.00		-10.32(0.22)	<-3.98	341.3(40.5)
J2238+0101	7135(158)	8.15($^{+0.10}_{-0.10}$)	0.67($^{+0.07}_{-0.06}$)	-9.93(0.11)	<-3.87	121.0(7.3)
J2238+0213	7096(224)	8.00		-8.65(0.19)	<-3.96	268.5(13.1)
J2238-0113	6222(198)	7.53($^{+0.87}_{-0.71}$)	0.33($^{+0.50}_{-0.20}$)	-9.54(0.21)	<-3.46	290.8(121.1)
J2239+2932	6595(451)	8.00		-9.41(0.69)	<-3.51	335.1(37.6)
J2243+3210	11295(447)	7.83($^{+0.14}_{-0.13}$)	0.49($^{+0.07}_{-0.06}$)	-9.00(0.17)	<-6.06	252.6(17.4)
J2245+2748	6607(276)	8.16($^{+0.19}_{-0.18}$)	0.68($^{+0.13}_{-0.11}$)	-10.27(0.08)	<-3.35	157.5(11.1)
J2248+1318	11676(465)	8.25($^{+0.13}_{-0.13}$)	0.74($^{+0.09}_{-0.08}$)	-8.67(0.13)	<-6.02	228.2(18.4)
J2248-0153	7493(350)	8.00		-10.60(0.22)	<-4.15	262.9(18.1)
J2253-0646	4132(53)	8.03($^{+0.07}_{-0.07}$)	0.59($^{+0.05}_{-0.04}$)	-10.00(0.05)	<-3.00	8.5(0.0)
J2258-0006	8832(1006)	8.00		-9.64(0.33)	<-5.46	530.2(84.2)
J2258-0829	14262(1391)	8.54($^{+0.33}_{-0.29}$)	0.93($^{+0.19}_{-0.19}$)	-8.99(0.94)	-5.26(0.68)	354.8(78.6)
J2259+1251	6748(261)	7.94($^{+0.34}_{-0.31}$)	0.54($^{+0.22}_{-0.16}$)	-10.53(0.11)	<-3.72	191.4(36.7)
J2259+1748	7476(842)	8.00		-10.76(0.24)	<-4.14	317.9(54.5)
J2300+2204	7000(122)	8.06($^{+0.05}_{-0.05}$)	0.61($^{+0.03}_{-0.03}$)	-10.15(0.04)	<-3.86	60.8(0.4)
J2302+1626	7311(299)	8.00		-8.93(0.39)	<-4.05	301.5(17.7)
J2304+2415	5269(80)	8.07($^{+0.08}_{-0.07}$)	0.62($^{+0.05}_{-0.05}$)	-8.92(0.16)	<-3.01	87.1(2.5)
J2305+2307	11055(427)	7.99($^{+0.10}_{-0.10}$)	0.58($^{+0.06}_{-0.05}$)	-8.31(0.08)	-5.58(0.16)	198.0(9.5)
J2306+2111	9580(433)	7.72($^{+0.28}_{-0.25}$)	0.43($^{+0.15}_{-0.10}$)	-10.85(0.21)	-5.07(0.82)	267.8(38.8)
J2309+0608	11885(490)	7.94($^{+0.09}_{-0.09}$)	0.55($^{+0.05}_{-0.05}$)	-7.41(0.06)	-4.11(0.12)	176.9(5.5)
J2310+2203	10049(444)	8.06($^{+0.29}_{-0.26}$)	0.62($^{+0.19}_{-0.15}$)	-9.65(0.19)	<-5.88	300.6(51.6)
J2311+1042	6180(142)	8.25($^{+0.22}_{-0.21}$)	0.73($^{+0.15}_{-0.13}$)	-9.72(0.10)	<-3.01	151.2(21.2)
J2311+1510	7073(472)	8.00		-10.17(0.16)	<-3.95	310.0(31.6)
J2311+3343	6605(553)	8.00		-10.23(0.25)	<-3.52	353.2(48.5)
J2311-0041	12701(746)	8.18($^{+0.12}_{-0.11}$)	0.70($^{+0.08}_{-0.07}$)	-7.32(0.24)	<-6.07	234.4(13.7)
J2315-0209	6389(60)	8.10($^{+0.03}_{-0.03}$)	0.64($^{+0.02}_{-0.02}$)	-9.80(0.03)	<-3.20	29.7(0.1)
J2316+0041	7696(565)	8.00		-8.69(0.41)	<-4.31	460.1(48.9)
J2318+2916	6635(295)	8.00		-9.93(0.20)	<-3.55	298.8(21.3)
J2318-0320	6935(542)	8.00		-10.27(0.15)	<-3.85	308.7(37.1)
J2319+3018	7454(269)	8.94($^{+0.43}_{-0.34}$)	1.16($^{+0.16}_{-0.19}$)	-8.41(0.34)	<-3.38	164.1(57.1)
J2321+0807	8386(258)	8.00($^{+0.26}_{-0.25}$)	0.58($^{+0.17}_{-0.13}$)	-9.20(0.15)	<-5.13	240.3(37.4)
J2324+1135	7685(504)	8.00		-10.49(0.15)	<-4.30	304.0(29.3)
J2324+1207	9128(246)	7.91($^{+0.06}_{-0.06}$)	0.52($^{+0.03}_{-0.03}$)	-9.09(0.10)	-3.97(0.18)	50.3(0.2)
J2328+0711	8735(758)	8.00		-9.56(0.29)	<-5.41	417.7(50.0)
J2328+0830	5663(230)	8.00		-9.02(0.37)	<-3.00	242.0(22.0)
J2330+1015	8661(447)	7.89($^{+1.34}_{-0.86}$)	0.52($^{+0.76}_{-0.32}$)	-8.50(0.26)	<-5.48	360.3(237.9)
J2330+2620	7263(384)	7.57($^{+0.91}_{-0.69}$)	0.35($^{+0.54}_{-0.20}$)	-10.91(0.13)	<-4.39	324.4(142.3)

Table 6. Atmospheric parameters for DZ stars – continued.

J Name	T_{eff} (K)	$\log g$	M/M_{\odot}	$\log \text{Ca/He}$	$\log \text{H/He}$	D (pc)
J2330+2805	6470(228)	$8.16^{(+0.50)}_{(-0.44)}$	$0.67^{(+0.33)}_{(-0.25)}$	-9.02(0.18)	<-3.22	215.8(65.8)
J2333+1058	6971(343)	8.00		-8.30(0.28)	<-3.88	349.3(29.0)
J2336+1657	7284(738)	8.00		-9.28(0.90)	<-4.04	455.2(65.6)
J2336+2021	7311(534)	8.00		-9.80(0.25)	<-4.05	321.2(34.5)
J2337+2607	7179(810)	8.00		-10.38(0.28)	<-4.00	393.2(69.5)
J2339+4631	10178(372)	$7.95^{(+0.14)}_{(-0.13)}$	$0.55^{(+0.08)}_{(-0.07)}$	-10.21(0.15)	-3.98(0.22)	226.3(15.8)
J2340+0124	6167(63)	$8.06^{(+0.09)}_{(-0.08)}$	$0.61^{(+0.05)}_{(-0.05)}$	-8.84(0.09)	<-3.06	115.0(5.7)
J2340+0817	6123(146)	$8.18^{(+0.21)}_{(-0.20)}$	$0.69^{(+0.14)}_{(-0.12)}$	-8.65(0.22)	<-3.01	146.0(19.0)
J2340+1621	7637(773)	8.00		-10.14(0.08)	<-4.25	413.1(60.1)
J2341+0059	6325(145)	$8.07^{(+0.26)}_{(-0.24)}$	$0.62^{(+0.17)}_{(-0.14)}$	-10.00(0.16)	<-3.17	180.6(28.0)
J2341+2448	6203(203)	$7.68^{(+0.20)}_{(-0.19)}$	$0.40^{(+0.10)}_{(-0.08)}$	-11.43(0.18)	<-3.31	190.4(18.2)
J2342-0006	10399(376)	$7.73^{(+0.24)}_{(-0.21)}$	$0.44^{(+0.13)}_{(-0.09)}$	-8.06(0.09)	-4.40(0.18)	322.3(41.5)
J2343+2242	8193(513)	$7.53^{(+1.57)}_{(-1.10)}$	$0.34^{(+0.89)}_{(-0.26)}$	-10.91(0.18)	<-5.43	432.1(294.7)
J2343+3155	7578(495)	8.00		-9.29(0.57)	<-4.21	436.6(42.9)
J2343-0010	5672(112)	$7.45^{(+0.35)}_{(-0.31)}$	$0.30^{(+0.16)}_{(-0.10)}$	-10.15(0.30)	<-3.03	210.6(35.9)
J2344+1343	7886(248)	$7.98^{(+0.55)}_{(-0.48)}$	$0.56^{(+0.36)}_{(-0.23)}$	-8.67(0.40)	<-4.53	313.9(100.5)
J2344+1813	7805(992)	8.00		-8.90(0.60)	<-4.42	539.3(95.9)
J2345+2857	7548(458)	8.00		-9.83(0.40)	<-4.18	354.4(31.1)
J2346+2816	8363(1646)	8.00		-9.89(0.26)	<-5.11	477.5(131.9)
J2348+1341	11065(568)	$7.42^{(+0.26)}_{(-0.21)}$	$0.31^{(+0.10)}_{(-0.06)}$	-8.59(0.17)	-3.96(0.24)	354.5(46.8)
J2348-4428	4886(125)	$8.11^{(+0.08)}_{(-0.08)}$	$0.64^{(+0.05)}_{(-0.05)}$	-10.94(0.39)	<-3.00	36.3(0.2)
J2349+0325	7564(794)	8.00		-8.54(0.32)	<-4.19	557.2(85.6)
J2351+0633	9724(328)	$8.29^{(+0.12)}_{(-0.12)}$	$0.76^{(+0.08)}_{(-0.08)}$	-9.12(0.07)	<-5.70	174.3(12.3)
J2351+3612	11311(803)	$7.94^{(+0.33)}_{(-0.30)}$	$0.55^{(+0.21)}_{(-0.15)}$	-9.33(0.27)	<-6.04	344.7(65.5)
J2352+1922	6126(209)	8.00		-8.38(0.28)	<-3.06	266.1(19.2)
J2352+3344	6629(212)	8.00		-9.69(0.26)	<-3.54	270.0(13.7)
J2352-0146	6568(182)	$8.05^{(+0.17)}_{(-0.17)}$	$0.60^{(+0.11)}_{(-0.10)}$	-10.76(0.09)	<-3.42	154.0(15.2)
J2353+0415	6551(330)	8.00		-10.01(0.23)	<-3.46	260.7(20.7)
J2353+3720	15152(6173)	$8.14^{(+0.84)}_{(-0.63)}$	$0.68^{(+0.51)}_{(-0.32)}$	-7.85(0.73)	-5.22(0.47)	422.2(94.8)
J2355+1431	6523(113)	$8.10^{(+0.08)}_{(-0.08)}$	$0.64^{(+0.05)}_{(-0.05)}$	-10.58(0.10)	<-3.32	111.3(4.6)
J2356-0320	8219(854)	8.00		-9.65(0.39)	<-4.94	508.9(71.9)
J2357+2348	6314(285)	8.00		-8.76(0.10)	<-3.21	270.0(21.8)
J2357-0324	9152(358)	$8.07^{(+0.19)}_{(-0.18)}$	$0.62^{(+0.12)}_{(-0.11)}$	-9.86(0.08)	<-5.61	199.2(21.7)
J2358+0445	8065(724)	8.00		-8.68(0.48)	<-4.73	482.0(65.6)
J2359+0243	7902(558)	8.00		-9.46(0.28)	<-4.53	387.4(38.8)
J2359+0347	6886(203)	$8.36^{(+0.16)}_{(-0.16)}$	$0.81^{(+0.11)}_{(-0.11)}$	-9.78(0.10)	<-3.46	153.9(16.7)

Table 7. Atmospheric parameters for DQ stars. A star indicate that the value of $\log H/He$ have been fixed rather than fitted. A dagger indicates that the distance is a photometric distance based on the value of $\log g = 8$ in the absence of a parallax.

J Name	T_{eff} (K)	$\log g$	M/M_{\odot}	$\log C/He$	$\log H/He$	D (pc)
J0000-0026	7420(163)	$7.87^{(+0.09)}_{(-0.08)}$	$0.50^{(+0.05)}_{(-0.04)}$	-6.11(0.12)		125.9(4.5)
J0000-0850	7853(226)	$7.42^{(+0.19)}_{(-0.17)}$	$0.30^{(+0.07)}_{(-0.05)}$	-5.51(0.09)		207.3(18.4)
J0006+1800	7422(155)	$7.90^{(+0.06)}_{(-0.06)}$	$0.52^{(+0.03)}_{(-0.03)}$	-5.98(0.03)		57.9(0.4)
J0007+2821	7409(195)	$7.92^{(+0.15)}_{(-0.15)}$	$0.53^{(+0.09)}_{(-0.08)}$	-5.89(0.10)		184.5(15.1)
J0008+2507	10801(525)	$8.10^{(+0.28)}_{(-0.26)}$	$0.64^{(+0.18)}_{(-0.15)}$	-3.37(0.21)	-3.00*	311.1(53.6)
J0008-1034	7587(543)	$7.86^{(+0.26)}_{(-0.24)}$	$0.50^{(+0.15)}_{(-0.12)}$	-5.85(0.14)		145.0(7.5)
J0015+0309	7261(217)	$7.98^{(+0.21)}_{(-0.20)}$	$0.56^{(+0.13)}_{(-0.11)}$	-6.03(0.12)		199.2(23.0)
J0024-1107	8330(202)	$7.88^{(+0.07)}_{(-0.07)}$	$0.51^{(+0.04)}_{(-0.04)}$	-5.09(0.06)		108.1(2.1)
J0033+0418	7658(214)	$7.86^{(+0.10)}_{(-0.10)}$	$0.49^{(+0.06)}_{(-0.05)}$	-6.00(0.07)		133.4(5.0)
J0041+7321	9433(349)	$7.84^{(+0.07)}_{(-0.06)}$	$0.49^{(+0.04)}_{(-0.03)}$	-4.38(0.12)		55.8(0.1)
J0044+1259	7109(195)	$8.03^{(+0.18)}_{(-0.17)}$	$0.59^{(+0.12)}_{(-0.10)}$	-6.28(0.10)		174.5(18.2)
J0055+0850	6552(160)	$7.98^{(+0.08)}_{(-0.08)}$	$0.56^{(+0.05)}_{(-0.05)}$	-6.74(0.06)		88.1(2.2)
J0100+0814	6384(98)	8.00		-5.63(0.04)		165.9(5.2)
J0103-0429	7215(227)	$7.49^{(+0.40)}_{(-0.33)}$	$0.32^{(+0.19)}_{(-0.10)}$	-5.81(0.11)		269.7(53.3)
J0107+0102	6600(108)	$8.04^{(+0.06)}_{(-0.06)}$	$0.60^{(+0.04)}_{(-0.04)}$	-6.65(0.05)		93.3(2.2)
J0116+2346	8047(189)	$7.93^{(+0.06)}_{(-0.06)}$	$0.54^{(+0.04)}_{(-0.03)}$	-5.46(0.04)		89.4(1.1)
J0116+2402	9217(258)	$7.97^{(+0.14)}_{(-0.13)}$	$0.56^{(+0.08)}_{(-0.07)}$	-4.59(0.14)		175.8(13.5)
J0118+1610	8833(218)	$7.96^{(+0.06)}_{(-0.06)}$	$0.56^{(+0.03)}_{(-0.03)}$	-4.90(0.06)		16.8(0.0)
J0136+2004	7115(211)	8.00		-5.21(0.07)		289.1(16.3)
J0137+0047	8127(216)	$7.95^{(+0.24)}_{(-0.23)}$	$0.55^{(+0.15)}_{(-0.12)}$	-5.28(0.19)		187.7(26.2)
J0144-0757	7296(240)	$8.30^{(+0.18)}_{(-0.17)}$	$0.77^{(+0.12)}_{(-0.11)}$	-6.06(0.11)		140.4(15.6)
J0145+2317	7731(188)	$8.02^{(+0.06)}_{(-0.06)}$	$0.58^{(+0.04)}_{(-0.04)}$	-5.55(0.02)		61.0(0.4)
J0145-0822	8002(236)	$8.97^{(+0.05)}_{(-0.05)}$	$1.17^{(+0.02)}_{(-0.02)}$	-5.85(0.14)		71.6(0.8)
J0154+1403	6529(100)	$7.97^{(+0.05)}_{(-0.05)}$	$0.55^{(+0.03)}_{(-0.03)}$	-6.72(0.05)		61.7(0.7)
J0154-0040	7321(147)	$7.94^{(+0.07)}_{(-0.07)}$	$0.54^{(+0.04)}_{(-0.04)}$	-6.01(0.09)		113.5(3.0)
J0200+0715	6758(120)	$8.04^{(+0.07)}_{(-0.07)}$	$0.60^{(+0.04)}_{(-0.04)}$	-6.23(0.04)		98.0(2.5)
J0208-0315	7233(253)	8.00		-6.13(0.26)		235.2(13.5)
J0209+1425	7117(192)	$7.45^{(+0.23)}_{(-0.21)}$	$0.31^{(+0.10)}_{(-0.07)}$	-6.20(0.12)		184.3(21.0)
J0227+0018	9646(504)	8.00		-3.37(0.10)		511.5(38.3)
J0236+2503	13376(697)	$8.70^{(+0.12)}_{(-0.11)}$	$1.03^{(+0.07)}_{(-0.07)}$	-1.58(0.25)		175.6(13.0)
J0239+0027	7134(185)	$7.59^{(+0.22)}_{(-0.20)}$	$0.36^{(+0.11)}_{(-0.08)}$	-5.97(0.14)		212.2(23.6)
J0243+0101	8225(172)	$8.63^{(+0.17)}_{(-0.16)}$	$0.99^{(+0.10)}_{(-0.11)}$	-4.23(0.15)		174.9(23.6)
J0248+3408	6009(68)	$8.00^{(+0.05)}_{(-0.05)}$	$0.57^{(+0.03)}_{(-0.03)}$	-6.87(0.03)		76.7(1.5)
J0253+3414	7489(234)	$7.39^{(+0.34)}_{(-0.28)}$	$0.29^{(+0.14)}_{(-0.08)}$	-5.98(0.20)		255.4(42.9)
J0305+0557	8446(365)	8.00		-4.91(0.32)		305.7(20.3)
J0320-0716	6510(89)	$8.02^{(+0.09)}_{(-0.09)}$	$0.59^{(+0.05)}_{(-0.05)}$	-5.29(0.03)		125.4(5.9)

Table 7. Atmospheric parameters for DQ stars – continued.

J Name	T_{eff} (K)	$\log g$	M/M_{\odot}	$\log \text{C/He}$	$\log \text{H/He}$	D (pc)
J0332–0037	8017(190)	$8.01^{(+0.07)}_{(-0.07)}$	$0.58^{(+0.04)}_{(-0.04)}$	-5.30(0.05)		110.6(2.5)
J0352–0605	7519(179)	$7.81^{(+0.09)}_{(-0.09)}$	$0.47^{(+0.05)}_{(-0.05)}$	-6.08(0.15)		132.8(4.8)
J0416+0713	7266(213)	$7.96^{(+0.14)}_{(-0.14)}$	$0.55^{(+0.09)}_{(-0.08)}$	-6.21(0.11)		153.5(11.0)
J0437–0849	6396(121)	$7.96^{(+0.05)}_{(-0.05)}$	$0.55^{(+0.03)}_{(-0.03)}$	-6.31(0.01)		9.4(0.0)
J0707+3825	6929(191)	$7.82^{(+0.27)}_{(-0.25)}$	$0.47^{(+0.16)}_{(-0.12)}$	-6.29(0.11)		219.8(31.8)
J0710+3740	6643(159)	$7.94^{(+0.06)}_{(-0.06)}$	$0.54^{(+0.03)}_{(-0.03)}$	-6.43(0.02)		24.4(0.0)
J0723+3908	9086(230)	$7.84^{(+0.07)}_{(-0.07)}$	$0.49^{(+0.04)}_{(-0.03)}$	-4.88(0.11)		118.0(2.3)
J0737+6455	7215(176)	$7.69^{(+0.17)}_{(-0.16)}$	$0.41^{(+0.09)}_{(-0.07)}$	-5.95(0.10)		196.2(16.8)
J0739+0513	7585(33)	$7.96^{(+0.02)}_{(-0.02)}$	$0.55^{(+0.01)}_{(-0.01)}$	-5.86(0.03)		3.5(0.0)
J0740+1810	6993(144)	$8.15^{(+0.13)}_{(-0.13)}$	$0.67^{(+0.09)}_{(-0.08)}$	-6.08(0.06)		138.1(10.9)
J0742+4348	8042(208)	$7.95^{(+0.09)}_{(-0.08)}$	$0.55^{(+0.05)}_{(-0.05)}$	-5.33(0.11)		139.6(4.5)
J0750+1328	8085(210)	$7.91^{(+0.10)}_{(-0.09)}$	$0.52^{(+0.06)}_{(-0.05)}$	-5.47(0.09)		162.4(6.6)
J0750+2329	7194(218)	$8.19^{(+0.20)}_{(-0.19)}$	$0.69^{(+0.13)}_{(-0.12)}$	-6.04(0.12)		187.0(23.0)
J0804+0750	7828(236)	$7.84^{(+0.25)}_{(-0.23)}$	$0.49^{(+0.15)}_{(-0.11)}$	-5.59(0.15)		214.2(29.2)
J0807+1949	13501(682)	$8.78^{(+0.10)}_{(-0.09)}$	$1.08^{(+0.05)}_{(-0.05)}$	-1.24(0.11)	-3.00*	176.6(10.4)
J0813+3047	7570(177)	$7.92^{(+0.09)}_{(-0.09)}$	$0.53^{(+0.05)}_{(-0.05)}$	-5.75(0.09)		138.0(5.5)
J0814+2455	7919(186)	$7.94^{(+0.06)}_{(-0.06)}$	$0.54^{(+0.04)}_{(-0.03)}$	-5.71(0.05)		58.9(0.3)
J0827+6017	6391(141)	$7.01^{(+0.33)}_{(-0.43)}$	$0.18^{(+0.09)}_{(-0.09)}$	-6.46(0.05)		270.5(41.5)
J0832–0408	6791(77)	$8.10^{(+0.04)}_{(-0.04)}$	$0.63^{(+0.03)}_{(-0.03)}$	-4.67(0.01)		82.1(1.3)
J0833+3638	7699(196)	$7.97^{(+0.11)}_{(-0.10)}$	$0.56^{(+0.06)}_{(-0.06)}$	-5.65(0.12)		142.1(7.1)
J0836+0437	8420(226)	$7.79^{(+0.11)}_{(-0.11)}$	$0.46^{(+0.06)}_{(-0.05)}$	-5.28(0.10)		172.8(8.6)
J0836+4817	7281(157)	$7.92^{(+0.08)}_{(-0.08)}$	$0.53^{(+0.05)}_{(-0.05)}$	-6.29(0.19)		121.2(4.1)
J0837+0321	8168(229)	$7.94^{(+0.13)}_{(-0.12)}$	$0.54^{(+0.08)}_{(-0.07)}$	-5.56(0.12)		172.8(10.7)
J0838+1121	7467(181)	$8.04^{(+0.11)}_{(-0.11)}$	$0.60^{(+0.07)}_{(-0.06)}$	-5.72(0.06)		141.9(7.7)
J0840+4529	7798(185)	$7.98^{(+0.07)}_{(-0.07)}$	$0.56^{(+0.04)}_{(-0.04)}$	-5.66(0.05)		105.1(2.3)
J0841+3329	6937(110)	$8.71^{(+0.07)}_{(-0.06)}$	$1.03^{(+0.04)}_{(-0.04)}$	-6.16(0.07)		53.2(2.6)
J0845+6143	7900(180)	$7.93^{(+0.06)}_{(-0.06)}$	$0.53^{(+0.04)}_{(-0.03)}$	-5.36(0.03)		76.4(0.6)
J0846+1024	8825(732)	$7.72^{(+0.29)}_{(-0.26)}$	$0.43^{(+0.15)}_{(-0.11)}$	-5.13(0.12)		129.5(3.5)
J0847+1830	8307(199)	$7.86^{(+0.06)}_{(-0.06)}$	$0.50^{(+0.04)}_{(-0.03)}$	-5.54(0.07)		73.1(0.6)
J0847+1919	7558(302)	8.00		-5.13(0.14)		361.8(26.2)
J0850+0709	8379(230)	$7.53^{(+0.19)}_{(-0.17)}$	$0.34^{(+0.08)}_{(-0.06)}$	-5.25(0.13)		240.3(22.1)
J0852+0428	9918(273)	$7.94^{(+0.13)}_{(-0.12)}$	$0.55^{(+0.08)}_{(-0.07)}$	-3.43(0.08)		209.8(14.7)
J0852+2316	11099(458)	$8.61^{(+0.13)}_{(-0.12)}$	$0.97^{(+0.08)}_{(-0.08)}$	-3.18(0.21)		190.7(17.4)
J0852+5223	8837(547)	8.00		-4.58(0.35)		402.2(38.4)
J0855+0639	7273(142)	$7.96^{(+0.06)}_{(-0.06)}$	$0.55^{(+0.03)}_{(-0.03)}$	-6.08(0.05)		76.4(1.1)
J0856+4513	9484(278)	$8.51^{(+0.18)}_{(-0.17)}$	$0.91^{(+0.11)}_{(-0.11)}$	-3.27(0.06)		208.2(27.1)
J0857+0603	8290(218)	$7.98^{(+0.08)}_{(-0.08)}$	$0.56^{(+0.05)}_{(-0.05)}$	-5.25(0.13)		123.2(3.6)
J0859+3257	9486(206)	$8.45^{(+0.04)}_{(-0.04)}$	$0.87^{(+0.03)}_{(-0.03)}$	-3.52(0.02)		23.1(0.0)

Table 7. Atmospheric parameters for DQ stars – continued.

J Name	T_{eff} (K)	$\log g$	M/M_{\odot}	$\log \text{C/He}$	$\log \text{H/He}$	D (pc)
J0859+6016	7572(167)	$7.96^{(+0.06)}_{(-0.06)}$	$0.55^{(+0.03)}_{(-0.03)}$	-5.64(0.05)		41.8(0.1)
J0900+0331	7627(178)	$7.94^{(+0.08)}_{(-0.08)}$	$0.54^{(+0.05)}_{(-0.04)}$	-5.87(0.07)		116.2(3.4)
J0901+5751	13576(763)	$8.76^{(+0.09)}_{(-0.09)}$	$1.07^{(+0.05)}_{(-0.05)}$	-1.99(0.24)		152.9(5.1)
J0902+5037	7599(215)	$7.86^{(+0.13)}_{(-0.13)}$	$0.50^{(+0.08)}_{(-0.07)}$	-5.81(0.19)		164.3(10.4)
J0904+3954	7284(171)	$8.06^{(+0.14)}_{(-0.14)}$	$0.61^{(+0.09)}_{(-0.08)}$	-5.79(0.11)		156.4(12.3)
J0905+0904	8216(192)	$7.88^{(+0.06)}_{(-0.06)}$	$0.51^{(+0.03)}_{(-0.03)}$	-5.41(0.04)		59.6(0.3)
J0915+2019	8731(234)	$7.93^{(+0.17)}_{(-0.16)}$	$0.54^{(+0.10)}_{(-0.09)}$	-5.09(0.14)		193.5(18.4)
J0916+1011	8406(201)	$7.93^{(+0.06)}_{(-0.06)}$	$0.53^{(+0.03)}_{(-0.03)}$	-5.21(0.03)		38.8(0.1)
J0918+4843	9203(280)	$8.80^{(+0.15)}_{(-0.14)}$	$1.09^{(+0.08)}_{(-0.08)}$	-3.72(0.11)		176.4(21.6)
J0919+0236	11319(478)	$8.61^{(+0.10)}_{(-0.10)}$	$0.98^{(+0.06)}_{(-0.06)}$	-2.85(0.07)		156.3(9.2)
J0920+3603	7795(203)	$7.98^{(+0.12)}_{(-0.11)}$	$0.56^{(+0.07)}_{(-0.06)}$	-5.72(0.10)		154.2(8.9)
J0921+3421	8239(202)	$7.42^{(+0.12)}_{(-0.11)}$	$0.30^{(+0.05)}_{(-0.04)}$	-5.20(0.06)		181.4(10.3)
J0922+2928	8022(175)	$8.06^{(+0.09)}_{(-0.09)}$	$0.61^{(+0.06)}_{(-0.05)}$	-4.93(0.04)		114.6(5.1)
J0923+1842	6879(118)	8.00		-6.33(0.06)		89.9(2.8)
J0925+5256	9505(251)	$7.92^{(+0.07)}_{(-0.06)}$	$0.53^{(+0.04)}_{(-0.03)}$	-4.68(0.12)		126.0(2.2)
J0926+0605	8404(217)	8.00		-5.42(0.15)		134.1(5.5)
J0926+4725	7215(139)	$8.01^{(+0.06)}_{(-0.06)}$	$0.58^{(+0.04)}_{(-0.04)}$	-6.31(0.09)		93.4(2.1)
J0926+6212	7026(269)	$7.96^{(+0.63)}_{(-0.53)}$	$0.55^{(+0.41)}_{(-0.25)}$	-5.89(0.09)		272.6(96.5)
J0928+2638	7108(144)	$7.36^{(+0.07)}_{(-0.07)}$	$0.28^{(+0.03)}_{(-0.02)}$	-6.42(0.07)		101.4(2.2)
J0929+3310	6587(76)	$7.85^{(+0.06)}_{(-0.06)}$	$0.49^{(+0.04)}_{(-0.03)}$	-5.17(0.02)		90.8(2.6)
J0930+2959	8233(200)	$7.81^{(+0.15)}_{(-0.14)}$	$0.47^{(+0.08)}_{(-0.07)}$	-5.28(0.07)		157.5(12.2)
J0931+1230	6544(172)	8.00		-6.37(0.08)		177.2(8.3)
J0934+1158	8421(217)	$7.81^{(+0.11)}_{(-0.11)}$	$0.47^{(+0.06)}_{(-0.05)}$	-5.24(0.07)		159.7(8.7)
J0935+2417	8697(224)	$7.93^{(+0.09)}_{(-0.09)}$	$0.54^{(+0.05)}_{(-0.05)}$	-5.07(0.09)		126.6(4.7)
J0936+0607	11013(421)	$8.61^{(+0.11)}_{(-0.11)}$	$0.97^{(+0.07)}_{(-0.07)}$	-3.07(0.09)		162.0(12.1)
J0939+5201	8527(201)	$7.96^{(+0.06)}_{(-0.06)}$	$0.56^{(+0.03)}_{(-0.03)}$	-5.00(0.03)		73.6(0.6)
J0940+0210	7229(134)	$8.12^{(+0.05)}_{(-0.05)}$	$0.65^{(+0.03)}_{(-0.03)}$	-6.00(0.03)		52.0(0.3)
J0941+0901	8550(200)	$7.32^{(+0.06)}_{(-0.06)}$	$0.27^{(+0.02)}_{(-0.02)}$	-5.24(0.08)		89.5(1.0)
J0941+4414	8222(203)	$7.98^{(+0.08)}_{(-0.08)}$	$0.57^{(+0.05)}_{(-0.05)}$	-5.22(0.07)		134.5(4.6)
J0945+5558	7371(212)	$8.12^{(+0.12)}_{(-0.12)}$	$0.65^{(+0.08)}_{(-0.07)}$	-6.09(0.30)		168.2(10.4)
J0948+1232	7218(146)	$8.16^{(+0.06)}_{(-0.06)}$	$0.67^{(+0.04)}_{(-0.04)}$	-6.29(0.11)		80.5(1.3)
J0950+3238	8268(199)	8.00		-5.54(0.06)		77.8(2.9)
J0950+5315	8031(188)	$7.91^{(+0.06)}_{(-0.06)}$	$0.52^{(+0.04)}_{(-0.03)}$	-5.62(0.04)		27.5(0.0)
J0951+6243	9060(535)	$8.03^{(+0.19)}_{(-0.18)}$	$0.60^{(+0.12)}_{(-0.10)}$	-4.60(0.08)		168.9(8.1)
J0959+4537	7274(196)	$7.45^{(+0.35)}_{(-0.29)}$	$0.31^{(+0.15)}_{(-0.09)}$	-5.48(0.12)		256.2(44.2)
J1000+1005	7869(190)	8.00		-4.99(0.04)		155.4(6.4)
J1005-0114	8376(233)	$7.85^{(+0.20)}_{(-0.19)}$	$0.49^{(+0.12)}_{(-0.09)}$	-5.13(0.11)		196.5(21.4)
J1010+2300	8534(204)	$7.89^{(+0.09)}_{(-0.09)}$	$0.51^{(+0.05)}_{(-0.05)}$	-5.02(0.06)		137.3(5.4)

Table 7. Atmospheric parameters for DQ stars – continued.

J Name	T_{eff} (K)	$\log g$	M/M_{\odot}	$\log \text{C/He}$	$\log \text{H/He}$	D (pc)
J1012+0040	9184(229)	$7.75^{(+0.07)}_{(-0.07)}$	$0.44^{(+0.04)}_{(-0.03)}$	-4.63(0.07)		119.2(3.3)
J1013+4350	8569(263)	$7.95^{(+0.10)}_{(-0.09)}$	$0.55^{(+0.06)}_{(-0.05)}$	-5.03(0.09)		144.1(5.5)
J1015+3518	8097(208)	$7.79^{(+0.15)}_{(-0.14)}$	$0.46^{(+0.08)}_{(-0.07)}$	-5.37(0.11)		173.0(12.7)
J1017+3736	7184(137)	$7.95^{(+0.09)}_{(-0.09)}$	$0.54^{(+0.05)}_{(-0.05)}$	-6.02(0.06)		124.0(5.3)
J1018+0838	7576(164)	$7.93^{(+0.06)}_{(-0.06)}$	$0.53^{(+0.03)}_{(-0.03)}$	-6.03(0.06)		43.8(0.2)
J1022+2845	7244(162)	$7.94^{(+0.10)}_{(-0.09)}$	$0.54^{(+0.06)}_{(-0.05)}$	-5.97(0.09)		139.7(6.1)
J1026+2725	8270(223)	$7.95^{(+0.12)}_{(-0.12)}$	$0.55^{(+0.07)}_{(-0.07)}$	-5.28(0.10)		150.9(9.5)
J1026+5807	8133(189)	$7.90^{(+0.06)}_{(-0.06)}$	$0.52^{(+0.03)}_{(-0.03)}$	-5.35(0.06)		69.1(0.5)
J1027+1218	7230(146)	$8.11^{(+0.07)}_{(-0.07)}$	$0.64^{(+0.05)}_{(-0.04)}$	-6.38(0.15)		97.1(3.0)
J1028+2537	6672(115)	$7.91^{(+0.07)}_{(-0.07)}$	$0.52^{(+0.04)}_{(-0.04)}$	-6.44(0.06)		109.7(2.8)
J1031+2217	6986(172)	$8.57^{(+0.18)}_{(-0.17)}$	$0.95^{(+0.11)}_{(-0.11)}$	-6.15(0.14)		135.9(18.2)
J1032+2101	8193(212)	$8.00^{(+0.11)}_{(-0.10)}$	$0.57^{(+0.07)}_{(-0.06)}$	-5.22(0.08)		166.9(8.7)
J1032+3509	8332(223)	$7.86^{(+0.10)}_{(-0.10)}$	$0.50^{(+0.06)}_{(-0.05)}$	-5.12(0.11)		146.8(6.0)
J1032+4519	8905(227)	$7.86^{(+0.08)}_{(-0.08)}$	$0.50^{(+0.04)}_{(-0.04)}$	-4.76(0.07)		126.1(3.6)
J1040+0635	13882(849)	$8.40^{(+0.24)}_{(-0.22)}$	$0.84^{(+0.15)}_{(-0.14)}$	-2.08(0.26)		277.3(42.8)
J1041+2200	7608(347)	8.00		-5.69(0.19)		335.5(25.3)
J1042+5833	7236(145)	$8.07^{(+0.08)}_{(-0.08)}$	$0.62^{(+0.05)}_{(-0.05)}$	-5.88(0.07)		125.8(4.8)
J1043+0303	6833(128)	$8.18^{(+0.11)}_{(-0.11)}$	$0.69^{(+0.07)}_{(-0.07)}$	-6.25(0.10)		115.5(7.4)
J1045+2134	7662(196)	$7.89^{(+0.12)}_{(-0.11)}$	$0.51^{(+0.07)}_{(-0.06)}$	-5.72(0.10)		153.9(8.4)
J1047+5912	8201(192)	$7.82^{(+0.07)}_{(-0.06)}$	$0.48^{(+0.04)}_{(-0.03)}$	-5.39(0.08)		101.3(1.4)
J1049+1659	12799(659)	$8.92^{(+0.12)}_{(-0.11)}$	$1.15^{(+0.05)}_{(-0.06)}$	-1.64(0.09)	-3.00*	173.6(14.9)
J1052+5911	7903(204)	$7.90^{(+0.08)}_{(-0.07)}$	$0.52^{(+0.04)}_{(-0.04)}$	-5.62(0.04)		113.8(2.0)
J1058+2846	9422(265)	$8.49^{(+0.09)}_{(-0.09)}$	$0.89^{(+0.06)}_{(-0.06)}$	-3.60(0.04)		154.3(8.9)
J1058+3440	6779(161)	$8.15^{(+0.17)}_{(-0.16)}$	$0.67^{(+0.11)}_{(-0.10)}$	-6.47(0.08)		165.7(16.9)
J1100+1758	12367(465)	$8.76^{(+0.10)}_{(-0.09)}$	$1.07^{(+0.05)}_{(-0.05)}$	-1.28(0.18)	-3.00*	141.6(9.8)
J1101+5218	8431(235)	$7.86^{(+0.12)}_{(-0.12)}$	$0.50^{(+0.07)}_{(-0.06)}$	-5.11(0.10)		191.6(11.3)
J1107+4059	7077(132)	$7.99^{(+0.06)}_{(-0.05)}$	$0.57^{(+0.03)}_{(-0.03)}$	-6.46(0.04)		54.3(0.6)
J1108+1349	7530(162)	$8.02^{(+0.06)}_{(-0.06)}$	$0.59^{(+0.04)}_{(-0.04)}$	-6.18(0.07)		89.8(1.6)
J1109+4249	8677(316)	$7.88^{(+0.09)}_{(-0.09)}$	$0.51^{(+0.05)}_{(-0.05)}$	-5.34(0.09)		88.0(1.6)
J1113+4455	8023(207)	$7.92^{(+0.13)}_{(-0.12)}$	$0.53^{(+0.08)}_{(-0.07)}$	-5.52(0.09)		149.7(9.8)
J1116–1228	8476(434)	$7.56^{(+0.89)}_{(-0.62)}$	$0.35^{(+0.51)}_{(-0.18)}$	-4.69(0.19)		385.3(166.0)
J1118–0314	9095(226)	$7.85^{(+0.06)}_{(-0.06)}$	$0.50^{(+0.03)}_{(-0.03)}$	-4.85(0.05)		36.6(0.1)
J1120+1200	8416(213)	$7.90^{(+0.09)}_{(-0.09)}$	$0.52^{(+0.05)}_{(-0.05)}$	-5.33(0.12)		124.2(4.5)
J1120+4252	7404(153)	$8.01^{(+0.08)}_{(-0.08)}$	$0.58^{(+0.05)}_{(-0.04)}$	-5.96(0.10)		109.4(3.7)
J1120–1102	9863(317)	$7.41^{(+0.50)}_{(-0.36)}$	$0.31^{(+0.22)}_{(-0.09)}$	-3.88(0.14)		349.6(89.6)
J1123+3347	7752(192)	$8.18^{(+0.14)}_{(-0.13)}$	$0.69^{(+0.09)}_{(-0.08)}$	-5.69(0.09)		129.4(10.7)
J1126+3245	9297(284)	8.00		-4.43(0.11)		165.1(7.1)
J1126+4419	6997(134)	$8.02^{(+0.08)}_{(-0.08)}$	$0.59^{(+0.05)}_{(-0.05)}$	-6.28(0.07)		121.4(4.5)

Table 7. Atmospheric parameters for DQ stars – continued.

J Name	T_{eff} (K)	$\log g$	M/M_{\odot}	$\log \text{C/He}$	$\log \text{H/He}$	D (pc)
J1130–0734	7925(260)	$8.13^{(+0.42)}_{(-0.37)}$	$0.66^{(+0.27)}_{(-0.21)}$	-5.05(0.22)		234.9(60.1)
J1131+0736	7530(170)	$7.82^{(+0.08)}_{(-0.07)}$	$0.47^{(+0.04)}_{(-0.04)}$	-5.93(0.09)		116.5(2.7)
J1131+1845	8396(252)	$7.90^{(+0.16)}_{(-0.16)}$	$0.52^{(+0.10)}_{(-0.08)}$	-5.30(0.10)		153.9(13.0)
J1133+1900	7821(196)	$7.64^{(+0.16)}_{(-0.15)}$	$0.38^{(+0.08)}_{(-0.06)}$	-5.59(0.07)		184.1(14.8)
J1133+6331	11517(562)	$8.57^{(+0.11)}_{(-0.11)}$	$0.95^{(+0.07)}_{(-0.07)}$	-2.68(0.21)		193.6(11.0)
J1140+0735	10651(387)	$8.56^{(+0.09)}_{(-0.09)}$	$0.94^{(+0.06)}_{(-0.06)}$	-3.36(0.09)		160.9(9.6)
J1140+1540	6472(116)	$7.96^{(+0.09)}_{(-0.09)}$	$0.55^{(+0.06)}_{(-0.05)}$	-6.63(0.08)		115.9(5.1)
J1140+1824	9656(228)	$8.35^{(+0.05)}_{(-0.05)}$	$0.81^{(+0.03)}_{(-0.03)}$	-3.54(0.03)		94.8(1.4)
J1141+3836	6004(48)	$8.30^{(+0.06)}_{(-0.06)}$	$0.77^{(+0.04)}_{(-0.04)}$	-5.00(0.03)		79.1(2.6)
J1142+0352	7702(234)	$7.72^{(+0.16)}_{(-0.15)}$	$0.42^{(+0.08)}_{(-0.07)}$	-5.63(0.09)		182.4(14.2)
J1145–6450	7951(351)	$8.01^{(+0.10)}_{(-0.10)}$	$0.58^{(+0.06)}_{(-0.06)}$	-5.50(0.03)		4.6(0.0)
J1148–0126	9680(222)	$8.46^{(+0.04)}_{(-0.04)}$	$0.88^{(+0.03)}_{(-0.03)}$	-3.48(0.03)		68.1(0.7)
J1151+4527	8698(208)	$7.88^{(+0.06)}_{(-0.06)}$	$0.51^{(+0.04)}_{(-0.03)}$	-4.84(0.06)		106.4(1.6)
J1151–2732	6436(148)	$7.97^{(+0.06)}_{(-0.05)}$	$0.56^{(+0.03)}_{(-0.03)}$	-6.70(0.04)		25.2(0.0)
J1156+2212	7022(117)	$8.14^{(+0.08)}_{(-0.08)}$	$0.66^{(+0.05)}_{(-0.05)}$	-5.53(0.03)		110.0(4.9)
J1159–4629	7101(249)	$8.02^{(+0.09)}_{(-0.08)}$	$0.58^{(+0.05)}_{(-0.05)}$	-6.02(0.03)		63.1(0.5)
J1201+3400	6134(62)	$8.22^{(+0.03)}_{(-0.03)}$	$0.71^{(+0.02)}_{(-0.02)}$	-5.97(0.01)		40.5(0.2)
J1203+6451	12359(455)	$8.77^{(+0.05)}_{(-0.05)}$	$1.07^{(+0.03)}_{(-0.03)}$	-1.59(0.14)		87.3(0.8)
J1209+5355	11721(649)	$8.53^{(+0.16)}_{(-0.15)}$	$0.92^{(+0.10)}_{(-0.10)}$	-2.71(0.53)		225.9(20.8)
J1212+5452	8186(195)	$7.95^{(+0.06)}_{(-0.06)}$	$0.55^{(+0.04)}_{(-0.03)}$	-5.29(0.04)		94.5(1.0)
J1215+4700	13230(764)	$8.87^{(+0.09)}_{(-0.09)}$	$1.13^{(+0.05)}_{(-0.05)}$	-2.00(0.10)	-3.00*	148.1(6.7)
J1220+2700	6185(98)	$7.20^{(+0.09)}_{(-0.09)}$	$0.22^{(+0.03)}_{(-0.02)}$	-7.29(0.13)		135.8(4.7)
J1225+4706	6292(79)	$7.92^{(+0.07)}_{(-0.07)}$	$0.53^{(+0.04)}_{(-0.04)}$	-5.35(0.05)		112.6(4.0)
J1233+1253	6807(112)	$8.04^{(+0.05)}_{(-0.05)}$	$0.60^{(+0.03)}_{(-0.03)}$	-6.52(0.04)		50.4(0.3)
J1235+3918	9295(233)	$8.02^{(+0.06)}_{(-0.05)}$	$0.59^{(+0.03)}_{(-0.03)}$	-4.45(0.05)		79.6(0.7)
J1236+3502	9052(238)	$7.85^{(+0.09)}_{(-0.08)}$	$0.49^{(+0.05)}_{(-0.04)}$	-4.66(0.16)		157.5(5.7)
J1237+4156	6169(53)	$8.23^{(+0.03)}_{(-0.03)}$	$0.72^{(+0.02)}_{(-0.02)}$	-5.24(0.01)		36.2(0.1)
J1240+2748	8492(224)	$8.13^{(+0.42)}_{(-0.38)}$	$0.66^{(+0.28)}_{(-0.22)}$	-4.05(0.11)		252.7(66.6)
J1240–0144	8443(241)	$7.82^{(+0.18)}_{(-0.17)}$	$0.47^{(+0.10)}_{(-0.08)}$	-5.32(0.18)		209.8(19.5)
J1243+1651	10227(286)	$7.91^{(+0.07)}_{(-0.07)}$	$0.53^{(+0.04)}_{(-0.04)}$	-4.00(0.09)		140.1(3.5)
J1243+3607	8513(209)	$7.95^{(+0.07)}_{(-0.07)}$	$0.55^{(+0.04)}_{(-0.04)}$	-4.94(0.08)		116.8(2.4)
J1244+2709	7922(205)	$7.26^{(+0.09)}_{(-0.08)}$	$0.25^{(+0.03)}_{(-0.02)}$	-5.07(0.05)		162.9(5.2)
J1247+4113	8590(212)	$7.99^{(+0.07)}_{(-0.06)}$	$0.57^{(+0.04)}_{(-0.04)}$	-4.96(0.06)		119.2(2.0)
J1249+2800	7482(167)	$8.23^{(+0.07)}_{(-0.07)}$	$0.72^{(+0.05)}_{(-0.04)}$	-6.37(0.24)		93.3(2.6)
J1249+3407	8441(201)	$7.93^{(+0.06)}_{(-0.06)}$	$0.54^{(+0.04)}_{(-0.03)}$	-5.16(0.04)		71.7(0.5)
J1250+0205	7103(184)	$7.86^{(+0.16)}_{(-0.16)}$	$0.49^{(+0.10)}_{(-0.08)}$	-6.04(0.07)		187.2(16.1)
J1251+4646	8687(244)	$7.92^{(+0.08)}_{(-0.07)}$	$0.53^{(+0.04)}_{(-0.04)}$	-4.92(0.09)		106.7(1.4)
J1252+1943	6863(122)	$7.52^{(+0.08)}_{(-0.08)}$	$0.33^{(+0.03)}_{(-0.03)}$	-6.49(0.04)		84.1(2.5)

Table 7. Atmospheric parameters for DQ stars – continued.

J Name	T_{eff} (K)	$\log g$	M/M_{\odot}	$\log \text{C/He}$	$\log \text{H/He}$	D (pc)
J1253+0139	8655(254)	$7.94^{(+0.12)}_{(-0.12)}$	$0.55^{(+0.07)}_{(-0.06)}$	-4.74(0.14)		177.8(10.6)
J1257+5938	7682(238)	$8.07^{(+0.15)}_{(-0.15)}$	$0.62^{(+0.10)}_{(-0.09)}$	-5.56(0.18)		204.2(17.0)
J1302+0923	7279(156)	$7.92^{(+0.08)}_{(-0.07)}$	$0.53^{(+0.04)}_{(-0.04)}$	-5.91(0.05)		113.6(3.1)
J1309+4445	7955(137)	$8.30^{(+0.05)}_{(-0.05)}$	$0.77^{(+0.03)}_{(-0.03)}$	-4.36(0.03)		109.4(2.2)
J1313+3811	6903(161)	$7.93^{(+0.19)}_{(-0.18)}$	$0.54^{(+0.12)}_{(-0.10)}$	-6.34(0.15)		196.2(20.7)
J1315+4711	7562(165)	$7.84^{(+0.06)}_{(-0.06)}$	$0.49^{(+0.03)}_{(-0.03)}$	-6.01(0.05)		84.5(0.7)
J1316+0810	6773(113)	$8.04^{(+0.06)}_{(-0.06)}$	$0.60^{(+0.04)}_{(-0.04)}$	-6.66(0.07)		87.7(2.0)
J1319+1401	7753(197)	$7.91^{(+0.09)}_{(-0.09)}$	$0.52^{(+0.05)}_{(-0.05)}$	-5.57(0.09)		144.9(5.5)
J1322+3730	7729(219)	$8.01^{(+0.09)}_{(-0.09)}$	$0.58^{(+0.06)}_{(-0.05)}$	-5.85(0.12)		138.7(5.2)
J1328+3640	8213(199)	$7.93^{(+0.07)}_{(-0.07)}$	$0.54^{(+0.04)}_{(-0.04)}$	-5.14(0.03)		126.1(2.8)
J1329+0746	8067(186)	$7.97^{(+0.06)}_{(-0.06)}$	$0.56^{(+0.04)}_{(-0.03)}$	-5.51(0.05)		70.2(0.5)
J1331+6704	8990(253)	$7.95^{(+0.09)}_{(-0.08)}$	$0.55^{(+0.05)}_{(-0.05)}$	-4.63(0.08)		172.7(5.9)
J1332+2355	14205(872)	$8.70^{(+0.13)}_{(-0.13)}$	$1.03^{(+0.08)}_{(-0.08)}$	-1.76(0.12)	-3.00*	226.8(19.4)
J1332+2740	8316(200)	$7.97^{(+0.06)}_{(-0.06)}$	$0.56^{(+0.04)}_{(-0.03)}$	-5.41(0.08)		71.8(0.6)
J1333+2357	7847(199)	$7.97^{(+0.09)}_{(-0.08)}$	$0.56^{(+0.05)}_{(-0.05)}$	-5.57(0.08)		131.7(4.4)
J1334+1622	8757(216)	$7.97^{(+0.07)}_{(-0.07)}$	$0.56^{(+0.04)}_{(-0.04)}$	-4.87(0.06)		118.4(2.4)
J1341+0346	13765(1084)	$8.76^{(+0.22)}_{(-0.20)}$	$1.07^{(+0.11)}_{(-0.12)}$	-2.18(0.13)	-3.00*	215.5(33.9)
J1344+1849	8137(201)	$7.79^{(+0.08)}_{(-0.07)}$	$0.46^{(+0.04)}_{(-0.04)}$	-5.70(0.08)		115.3(2.2)
J1347+1528	8306(228)	$8.19^{(+0.10)}_{(-0.10)}$	$0.70^{(+0.07)}_{(-0.06)}$	-5.14(0.07)		147.3(7.7)
J1347+3817	8118(213)	$8.08^{(+0.09)}_{(-0.09)}$	$0.63^{(+0.06)}_{(-0.06)}$	-5.32(0.08)		156.3(6.7)
J1347+5019	8195(169)	$7.89^{(+0.09)}_{(-0.09)}$	$0.51^{(+0.05)}_{(-0.05)}$	-4.41(0.04)		154.2(6.2)
J1351+6623	8935(219)	$7.97^{(+0.06)}_{(-0.06)}$	$0.56^{(+0.03)}_{(-0.03)}$	-4.80(0.11)		100.2(0.9)
J1352+2218	8000(208)	$7.94^{(+0.11)}_{(-0.11)}$	$0.54^{(+0.07)}_{(-0.06)}$	-5.28(0.08)		169.6(9.2)
J1352+2658	7849(265)	$7.94^{(+0.10)}_{(-0.10)}$	$0.54^{(+0.06)}_{(-0.06)}$	-5.51(0.09)		154.0(6.6)
J1354+1217	7756(219)	$7.58^{(+0.26)}_{(-0.23)}$	$0.36^{(+0.12)}_{(-0.09)}$	-5.59(0.09)		215.9(28.5)
J1355+3636	8059(169)	$7.91^{(+0.06)}_{(-0.06)}$	$0.53^{(+0.03)}_{(-0.03)}$	-4.74(0.01)		85.7(0.8)
J1356-0009	6555(85)	$8.08^{(+0.05)}_{(-0.05)}$	$0.62^{(+0.03)}_{(-0.03)}$	-5.80(0.02)		78.1(1.3)
J1357+2949	7581(185)	$7.96^{(+0.08)}_{(-0.07)}$	$0.55^{(+0.05)}_{(-0.04)}$	-5.83(0.10)		119.1(2.7)
J1358+0552	8360(223)	$7.88^{(+0.12)}_{(-0.12)}$	$0.51^{(+0.07)}_{(-0.06)}$	-5.07(0.09)		170.6(10.3)
J1400-0154	9394(237)	$8.69^{(+0.12)}_{(-0.12)}$	$1.02^{(+0.07)}_{(-0.07)}$	-3.56(0.11)		146.0(13.6)
J1402+1113	7238(250)	$8.00^{(+0.12)}_{(-0.12)}$	$0.58^{(+0.08)}_{(-0.07)}$	-5.90(0.06)		114.7(3.4)
J1406+0148	7713(186)	$7.91^{(+0.08)}_{(-0.08)}$	$0.52^{(+0.04)}_{(-0.04)}$	-5.83(0.13)		112.9(2.8)
J1406+0204	7680(186)	$7.35^{(+0.11)}_{(-0.10)}$	$0.28^{(+0.04)}_{(-0.03)}$	-5.64(0.17)		177.1(7.8)
J1406+3402	7042(137)	$7.43^{(+0.07)}_{(-0.06)}$	$0.30^{(+0.03)}_{(-0.02)}$	-6.62(0.12)		99.5(1.3)
J1407+2039	8387(209)	$7.73^{(+0.11)}_{(-0.11)}$	$0.43^{(+0.06)}_{(-0.05)}$	-5.11(0.08)		157.9(8.3)
J1416+3016	7518(253)	$8.15^{(+0.28)}_{(-0.26)}$	$0.67^{(+0.19)}_{(-0.16)}$	-5.87(0.10)		224.4(38.6)
J1417+2412	7930(194)	$8.06^{(+0.07)}_{(-0.07)}$	$0.61^{(+0.05)}_{(-0.04)}$	-5.48(0.09)		119.9(3.2)
J1423+5729	10727(397)	$8.07^{(+0.09)}_{(-0.09)}$	$0.62^{(+0.06)}_{(-0.05)}$	-3.67(0.12)		174.7(5.9)

Table 7. Atmospheric parameters for DQ stars – continued.

J Name	T_{eff} (K)	$\log g$	M/M_{\odot}	$\log \text{C/He}$	$\log \text{H/He}$	D (pc)
J1424+0833	9094(226)	$7.85^{(+0.07)}_{(-0.06)}$	$0.49^{(+0.04)}_{(-0.03)}$	-4.79(0.07)		112.8(2.1)
J1425+1801	7924(204)	$7.86^{(+0.09)}_{(-0.09)}$	$0.50^{(+0.05)}_{(-0.05)}$	-5.44(0.07)		132.0(4.5)
J1427+6110	6461(96)	$7.98^{(+0.05)}_{(-0.05)}$	$0.56^{(+0.03)}_{(-0.03)}$	-6.63(0.02)		43.0(0.1)
J1428+3238	10718(355)	$8.56^{(+0.08)}_{(-0.08)}$	$0.94^{(+0.05)}_{(-0.05)}$	-3.20(0.16)		159.0(7.3)
J1431+3750	6319(132)	$7.37^{(+0.12)}_{(-0.11)}$	$0.27^{(+0.04)}_{(-0.04)}$	-6.97(0.13)		158.2(7.9)
J1434+2258	14575(788)	$8.75^{(+0.11)}_{(-0.10)}$	$1.06^{(+0.06)}_{(-0.06)}$	-1.14(0.12)	-3.00*	206.8(14.4)
J1435+2120	8832(275)	$7.93^{(+0.14)}_{(-0.14)}$	$0.54^{(+0.09)}_{(-0.07)}$	-4.77(0.13)		200.0(14.9)
J1435+4554	6980(181)	$7.99^{(+0.13)}_{(-0.13)}$	$0.57^{(+0.08)}_{(-0.07)}$	-6.18(0.12)		180.3(11.9)
J1435+5318	15167(1164)	$8.85^{(+0.12)}_{(-0.11)}$	$1.12^{(+0.06)}_{(-0.06)}$	-1.91(0.16)	-3.00*	199.8(10.0)
J1438+2234	8310(221)	$7.79^{(+0.14)}_{(-0.14)}$	$0.46^{(+0.08)}_{(-0.07)}$	-5.37(0.14)		190.4(13.6)
J1440+0958	8100(189)	$7.93^{(+0.06)}_{(-0.06)}$	$0.54^{(+0.04)}_{(-0.03)}$	-5.49(0.06)		72.6(0.8)
J1441+2347	7233(150)	$8.11^{(+0.11)}_{(-0.11)}$	$0.64^{(+0.07)}_{(-0.07)}$	-5.76(0.07)		128.8(8.0)
J1442+4202	8636(231)	$7.89^{(+0.12)}_{(-0.12)}$	$0.52^{(+0.07)}_{(-0.06)}$	-4.91(0.09)		189.8(11.4)
J1443+3810	8843(216)	$7.89^{(+0.07)}_{(-0.06)}$	$0.52^{(+0.04)}_{(-0.03)}$	-4.86(0.09)		137.4(2.5)
J1444+0434	9813(301)	$8.44^{(+0.19)}_{(-0.18)}$	$0.87^{(+0.12)}_{(-0.12)}$	-3.47(0.09)		191.8(25.3)
J1448-0047	7075(129)	$8.05^{(+0.06)}_{(-0.06)}$	$0.60^{(+0.04)}_{(-0.04)}$	-6.31(0.08)		89.5(2.0)
J1449+2916	7873(217)	$7.97^{(+0.12)}_{(-0.12)}$	$0.56^{(+0.07)}_{(-0.07)}$	-5.77(0.12)		159.5(9.3)
J1452+6020	12572(659)	$8.65^{(+0.13)}_{(-0.12)}$	$1.00^{(+0.08)}_{(-0.08)}$	-1.73(0.43)		239.2(19.7)
J1453+4719	7928(313)	$8.28^{(+0.19)}_{(-0.18)}$	$0.75^{(+0.13)}_{(-0.12)}$	-5.39(0.16)		216.1(25.1)
J1455+4209	14288(876)	$8.78^{(+0.14)}_{(-0.13)}$	$1.08^{(+0.07)}_{(-0.08)}$	-1.48(0.77)		266.1(25.4)
J1501+0627	7116(133)	$8.16^{(+0.08)}_{(-0.07)}$	$0.67^{(+0.05)}_{(-0.05)}$	-6.08(0.07)		107.8(4.2)
J1509+1620	8356(221)	$7.88^{(+0.14)}_{(-0.14)}$	$0.51^{(+0.08)}_{(-0.07)}$	-5.33(0.12)		160.3(12.1)
J1511+5008	7779(197)	$7.96^{(+0.08)}_{(-0.08)}$	$0.55^{(+0.05)}_{(-0.05)}$	-5.62(0.15)		146.7(4.3)
J1514+1423	6661(84)	$8.14^{(+0.07)}_{(-0.07)}$	$0.66^{(+0.05)}_{(-0.04)}$	-4.94(0.05)		115.2(4.3)
J1517+2256	7464(154)	$7.98^{(+0.06)}_{(-0.06)}$	$0.57^{(+0.03)}_{(-0.03)}$	-6.07(0.06)		79.3(0.8)
J1519+3856	8250(213)	$7.91^{(+0.09)}_{(-0.09)}$	$0.53^{(+0.05)}_{(-0.05)}$	-5.34(0.10)		169.0(5.9)
J1520+2703	7800(219)	$7.78^{(+0.13)}_{(-0.12)}$	$0.45^{(+0.07)}_{(-0.06)}$	-5.61(0.07)		173.1(9.6)
J1527+2752	8278(156)	$8.32^{(+0.07)}_{(-0.07)}$	$0.78^{(+0.05)}_{(-0.05)}$	-4.12(0.04)		133.0(5.0)
J1528+0442	7303(166)	$7.90^{(+0.13)}_{(-0.12)}$	$0.52^{(+0.07)}_{(-0.06)}$	-6.03(0.17)		142.0(9.0)
J1528+4003	7588(198)	$8.00^{(+0.08)}_{(-0.08)}$	$0.57^{(+0.05)}_{(-0.05)}$	-5.83(0.09)		139.4(4.2)
J1528+5134	7578(167)	$8.01^{(+0.06)}_{(-0.06)}$	$0.58^{(+0.04)}_{(-0.04)}$	-5.65(0.04)		103.8(1.5)
J1534+4145	7684(172)	$7.92^{(+0.06)}_{(-0.06)}$	$0.53^{(+0.04)}_{(-0.03)}$	-6.10(0.07)		65.8(0.3)
J1537+1337	7952(192)	$7.89^{(+0.08)}_{(-0.08)}$	$0.52^{(+0.05)}_{(-0.04)}$	-5.53(0.08)		117.6(3.4)
J1542+1314	7952(191)	$7.96^{(+0.08)}_{(-0.07)}$	$0.55^{(+0.05)}_{(-0.04)}$	-5.44(0.04)		116.9(3.1)
J1542+2544	6682(121)	$8.03^{(+0.08)}_{(-0.08)}$	$0.59^{(+0.05)}_{(-0.05)}$	-6.44(0.07)		121.4(4.3)
J1542+4329	9799(287)	$8.49^{(+0.09)}_{(-0.08)}$	$0.89^{(+0.06)}_{(-0.06)}$	-3.61(0.16)		175.2(9.1)
J1545+2854	7260(156)	$7.94^{(+0.10)}_{(-0.09)}$	$0.54^{(+0.06)}_{(-0.05)}$	-5.81(0.13)		158.4(7.2)
J1548+5626	7911(208)	$8.03^{(+0.08)}_{(-0.08)}$	$0.60^{(+0.05)}_{(-0.05)}$	-5.42(0.12)		145.9(4.3)

Table 7. Atmospheric parameters for DQ stars – continued.

J Name	T_{eff} (K)	$\log g$	M/M_{\odot}	$\log \text{C/He}$	$\log \text{H/He}$	D (pc)
J1551+0824	6768(109)	$7.98^{(+0.05)}_{(-0.05)}$	$0.56^{(+0.03)}_{(-0.03)}$	-6.28(0.03)		71.9(0.7)
J1552+1148	7764(205)	$8.00^{(+0.10)}_{(-0.10)}$	$0.58^{(+0.06)}_{(-0.06)}$	-5.54(0.10)		140.0(6.3)
J1552+3910	7570(169)	$8.04^{(+0.07)}_{(-0.06)}$	$0.60^{(+0.04)}_{(-0.04)}$	-5.67(0.08)		113.7(2.3)
J1554+0336	6626(117)	$7.94^{(+0.07)}_{(-0.07)}$	$0.54^{(+0.04)}_{(-0.04)}$	-6.78(0.13)		102.5(2.7)
J1555+3123	8227(156)	$8.26^{(+0.06)}_{(-0.06)}$	$0.74^{(+0.04)}_{(-0.04)}$	-4.29(0.04)		128.6(3.7)
J1555+3219	9195(239)	$8.59^{(+0.11)}_{(-0.11)}$	$0.96^{(+0.07)}_{(-0.07)}$	-3.74(0.31)		184.2(15.1)
J1609+0655	6828(333)	$7.76^{(+0.11)}_{(-0.11)}$	$0.44^{(+0.06)}_{(-0.05)}$	-6.73(0.07)		85.6(0.9)
J1610+3036	8054(207)	$7.97^{(+0.09)}_{(-0.09)}$	$0.56^{(+0.05)}_{(-0.05)}$	-5.27(0.06)		159.5(5.8)
J1613+5116	7979(226)	$8.00^{(+0.10)}_{(-0.10)}$	$0.58^{(+0.06)}_{(-0.06)}$	-5.42(0.13)		161.3(6.8)
J1616+3924	7225(139)	$7.95^{(+0.06)}_{(-0.05)}$	$0.55^{(+0.03)}_{(-0.03)}$	-6.07(0.05)		93.6(1.0)
J1620+1809	7763(180)	$7.88^{(+0.07)}_{(-0.07)}$	$0.51^{(+0.04)}_{(-0.04)}$	-5.79(0.06)		100.8(1.6)
J1621+2253	7839(209)	$7.89^{(+0.08)}_{(-0.08)}$	$0.51^{(+0.05)}_{(-0.04)}$	-5.82(0.10)		123.3(2.5)
J1634+5710	6006(119)	$7.97^{(+0.06)}_{(-0.06)}$	$0.55^{(+0.03)}_{(-0.03)}$	-7.28(0.03)		14.9(0.0)
J1638+1244	8532(204)	$7.90^{(+0.06)}_{(-0.06)}$	$0.52^{(+0.04)}_{(-0.03)}$	-5.07(0.04)		101.4(1.4)
J1640+7310	8426(275)	$7.95^{(+0.07)}_{(-0.07)}$	$0.55^{(+0.04)}_{(-0.04)}$	-4.98(0.05)		53.7(0.1)
J1641+4833	7652(172)	$8.01^{(+0.06)}_{(-0.06)}$	$0.58^{(+0.04)}_{(-0.03)}$	-5.80(0.04)		91.4(1.0)
J1643+4002	7352(169)	$8.11^{(+0.09)}_{(-0.08)}$	$0.64^{(+0.06)}_{(-0.05)}$	-6.05(0.17)		137.4(5.3)
J1643+4129	7224(310)	$8.43^{(+0.40)}_{(-0.36)}$	$0.86^{(+0.25)}_{(-0.23)}$	-6.02(0.14)		219.6(60.1)
J1647+4350	9041(238)	$7.88^{(+0.07)}_{(-0.07)}$	$0.51^{(+0.04)}_{(-0.04)}$	-4.83(0.11)		157.5(3.6)
J1647+5119	8091(222)	$7.89^{(+0.09)}_{(-0.09)}$	$0.51^{(+0.05)}_{(-0.05)}$	-5.61(0.11)		150.5(4.6)
J1653+1113	6690(160)	$8.08^{(+0.12)}_{(-0.12)}$	$0.63^{(+0.08)}_{(-0.07)}$	-6.58(0.10)		143.0(9.6)
J1654+3157	7281(140)	$8.01^{(+0.05)}_{(-0.05)}$	$0.58^{(+0.03)}_{(-0.03)}$	-5.89(0.03)		63.4(0.3)
J1655+3722	8831(220)	$7.91^{(+0.07)}_{(-0.07)}$	$0.53^{(+0.04)}_{(-0.04)}$	-4.79(0.07)		147.3(3.5)
J1712+3406	7982(213)	$7.90^{(+0.11)}_{(-0.10)}$	$0.52^{(+0.06)}_{(-0.06)}$	-5.47(0.10)		180.5(8.4)
J1713+3240	7908(182)	$7.97^{(+0.06)}_{(-0.06)}$	$0.56^{(+0.04)}_{(-0.03)}$	-5.38(0.03)		69.6(0.3)
J1724+5333	6660(164)	$8.13^{(+0.16)}_{(-0.15)}$	$0.66^{(+0.10)}_{(-0.09)}$	-6.35(0.22)		178.2(16.4)
J1728+5558	14453(683)	$8.90^{(+0.06)}_{(-0.06)}$	$1.14^{(+0.03)}_{(-0.03)}$	-1.37(0.07)	-3.00*	47.2(0.1)
J1833+1945	7124(133)	$7.97^{(+0.05)}_{(-0.05)}$	$0.56^{(+0.03)}_{(-0.03)}$	-6.20(0.03)		39.3(0.1)
J1838+4046	7126(229)	$8.43^{(+0.31)}_{(-0.29)}$	$0.86^{(+0.20)}_{(-0.19)}$	-5.76(0.13)		199.5(43.6)
J2046–0715	8025(210)	$7.75^{(+0.10)}_{(-0.10)}$	$0.44^{(+0.05)}_{(-0.05)}$	-5.45(0.16)		162.7(6.6)
J2053–0702	6584(80)	$8.04^{(+0.06)}_{(-0.06)}$	$0.60^{(+0.04)}_{(-0.04)}$	-5.27(0.04)		98.1(2.9)
J2101+3148	9100(348)	$7.86^{(+0.07)}_{(-0.07)}$	$0.50^{(+0.04)}_{(-0.04)}$	-4.97(0.08)		32.2(0.0)
J2111–0036	7199(141)	$7.91^{(+0.06)}_{(-0.06)}$	$0.52^{(+0.04)}_{(-0.04)}$	-6.17(0.08)		94.5(1.9)
J2135+0003	6427(110)	$7.93^{(+0.21)}_{(-0.20)}$	$0.53^{(+0.13)}_{(-0.11)}$	-6.53(0.08)		120.7(14.5)
J2140–0045	7524(192)	$8.02^{(+0.12)}_{(-0.12)}$	$0.58^{(+0.08)}_{(-0.07)}$	-5.90(0.07)		154.3(9.9)
J2142+0908	7211(169)	$8.14^{(+0.18)}_{(-0.17)}$	$0.66^{(+0.12)}_{(-0.11)}$	-5.92(0.06)		131.0(14.6)
J2142+2059	7515(262)	$7.86^{(+0.08)}_{(-0.08)}$	$0.50^{(+0.04)}_{(-0.04)}$	-6.29(0.06)		11.0(0.0)
J2149+2039	8663(238)	$7.63^{(+0.20)}_{(-0.18)}$	$0.39^{(+0.10)}_{(-0.07)}$	-4.72(0.08)		211.5(22.0)

Table 7. Atmospheric parameters for DQ stars – continued.

J Name	T_{eff} (K)	$\log g$	M/M_{\odot}	$\log \text{C/He}$	$\log \text{H/He}$	D (pc)
J2150–0113	8785(213)	$7.94^{(+0.06)}_{(-0.06)}$	$0.54^{(+0.04)}_{(-0.04)}$	-5.06(0.06)		90.4(1.5)
J2156+0559	6911(127)	$8.07^{(+0.06)}_{(-0.06)}$	$0.62^{(+0.04)}_{(-0.04)}$	-6.38(0.06)		97.2(2.3)
J2157+1137	8522(206)	$7.80^{(+0.10)}_{(-0.09)}$	$0.47^{(+0.05)}_{(-0.05)}$	-4.99(0.06)		151.9(6.7)
J2207+0135	6514(131)	$8.12^{(+0.09)}_{(-0.09)}$	$0.65^{(+0.06)}_{(-0.05)}$	-6.67(0.08)		115.6(5.1)
J2218+2123	8120(188)	$7.95^{(+0.06)}_{(-0.06)}$	$0.55^{(+0.04)}_{(-0.04)}$	-5.29(0.04)		96.5(1.5)
J2220+1420	8542(228)	$8.03^{(+0.09)}_{(-0.09)}$	$0.60^{(+0.06)}_{(-0.05)}$	-4.98(0.05)		134.6(5.6)
J2225+1251	6388(176)	$7.82^{(+0.24)}_{(-0.22)}$	$0.47^{(+0.14)}_{(-0.11)}$	-6.86(0.08)		155.6(19.5)
J2239+2303	8116(239)	$7.99^{(+0.14)}_{(-0.13)}$	$0.57^{(+0.09)}_{(-0.08)}$	-5.51(0.14)		177.6(12.9)
J2248+2826	9390(311)	$7.98^{(+0.16)}_{(-0.16)}$	$0.57^{(+0.10)}_{(-0.09)}$	-4.21(0.12)	-3.00*	233.7(21.1)
J2250+1240	9801(292)	$8.50^{(+0.13)}_{(-0.13)}$	$0.90^{(+0.08)}_{(-0.08)}$	-3.66(0.15)		173.1(15.9)
J2302+2430	6816(116)	$8.06^{(+0.05)}_{(-0.05)}$	$0.61^{(+0.03)}_{(-0.03)}$	-6.54(0.04)		72.5(0.9)
J2310–0057	7647(138)	$7.94^{(+0.12)}_{(-0.11)}$	$0.54^{(+0.07)}_{(-0.06)}$	-4.63(0.02)		143.9(9.2)
J2314–0632	7352(197)	$7.96^{(+0.07)}_{(-0.06)}$	$0.55^{(+0.04)}_{(-0.04)}$	-6.06(0.03)		25.9(0.0)
J2341–0101	8499(220)	$7.93^{(+0.08)}_{(-0.08)}$	$0.54^{(+0.05)}_{(-0.04)}$	-5.07(0.10)		122.6(3.6)
J2354+4027	7555(232)	$7.93^{(+0.07)}_{(-0.07)}$	$0.53^{(+0.04)}_{(-0.04)}$	-5.75(0.04)		22.1(0.0)

9. APPENDIX I

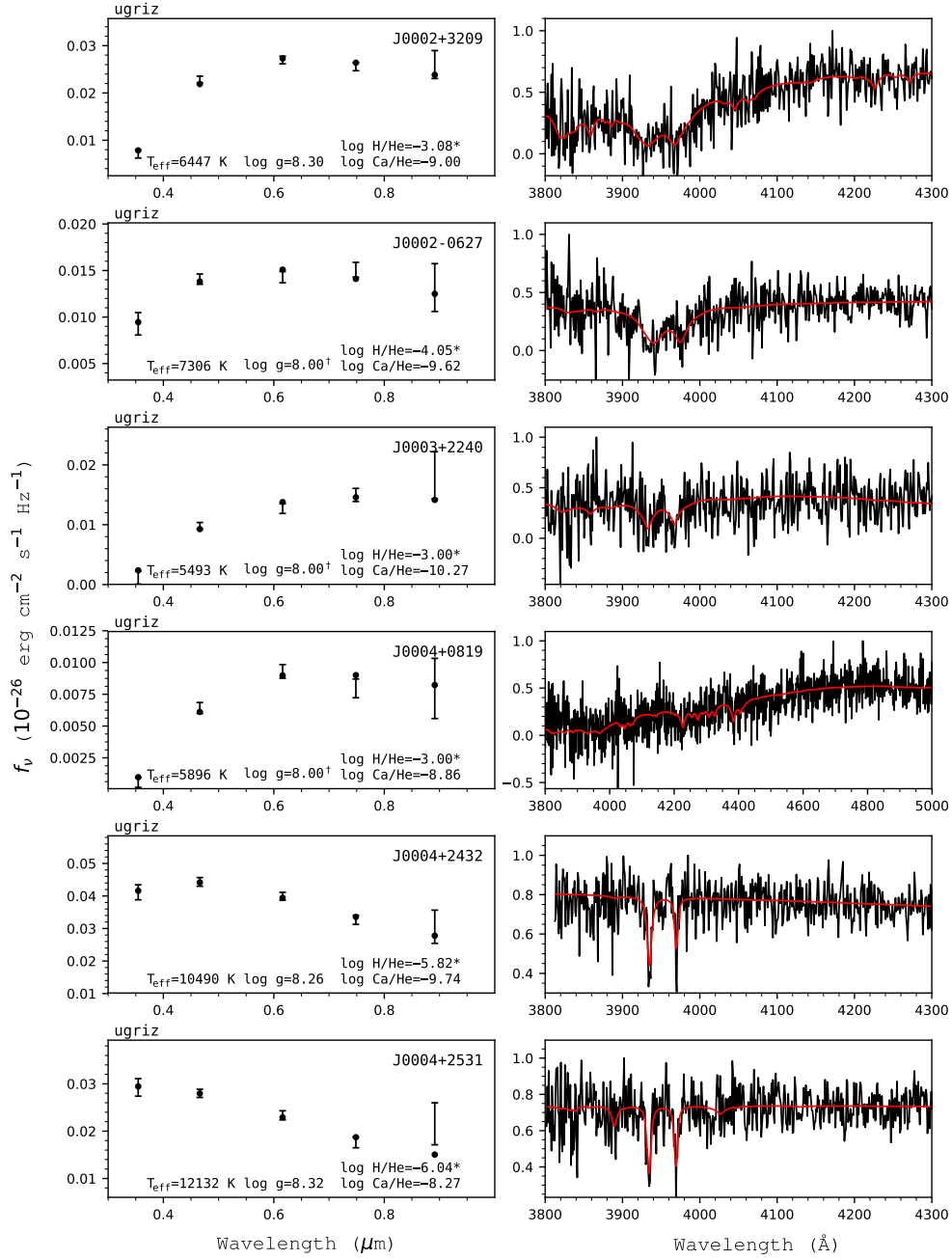


Figure 20. Fits to our sample of DBZ/DZ(A) white dwarfs. Left panels: Photometric fits where error bars represent the observed data, while filled circles correspond to average model fluxes. A dagger symbol indicates that $\log g$ is fixed at 8.0 (no parallax measurement available), while a star symbol indicates a value of $\log \text{H/He}$ fixed at the visibility limit. Right panels: Spectroscopic fits (red) to the normalized observed spectra (black). The inset shows the fit to $\text{H}\alpha$ when present.

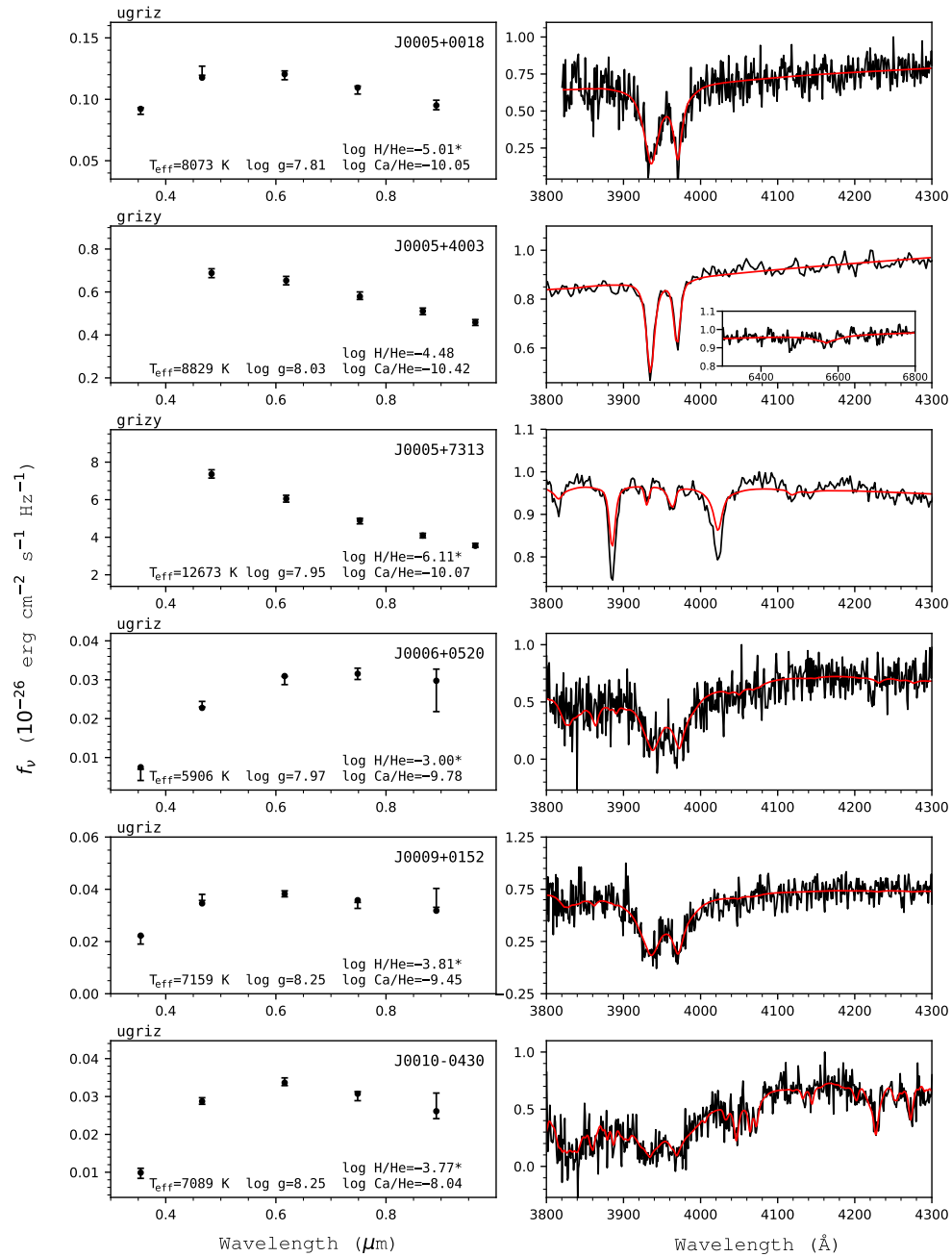


Figure 21. Fits to the DBZ/DZ(A) white dwarfs - continued.

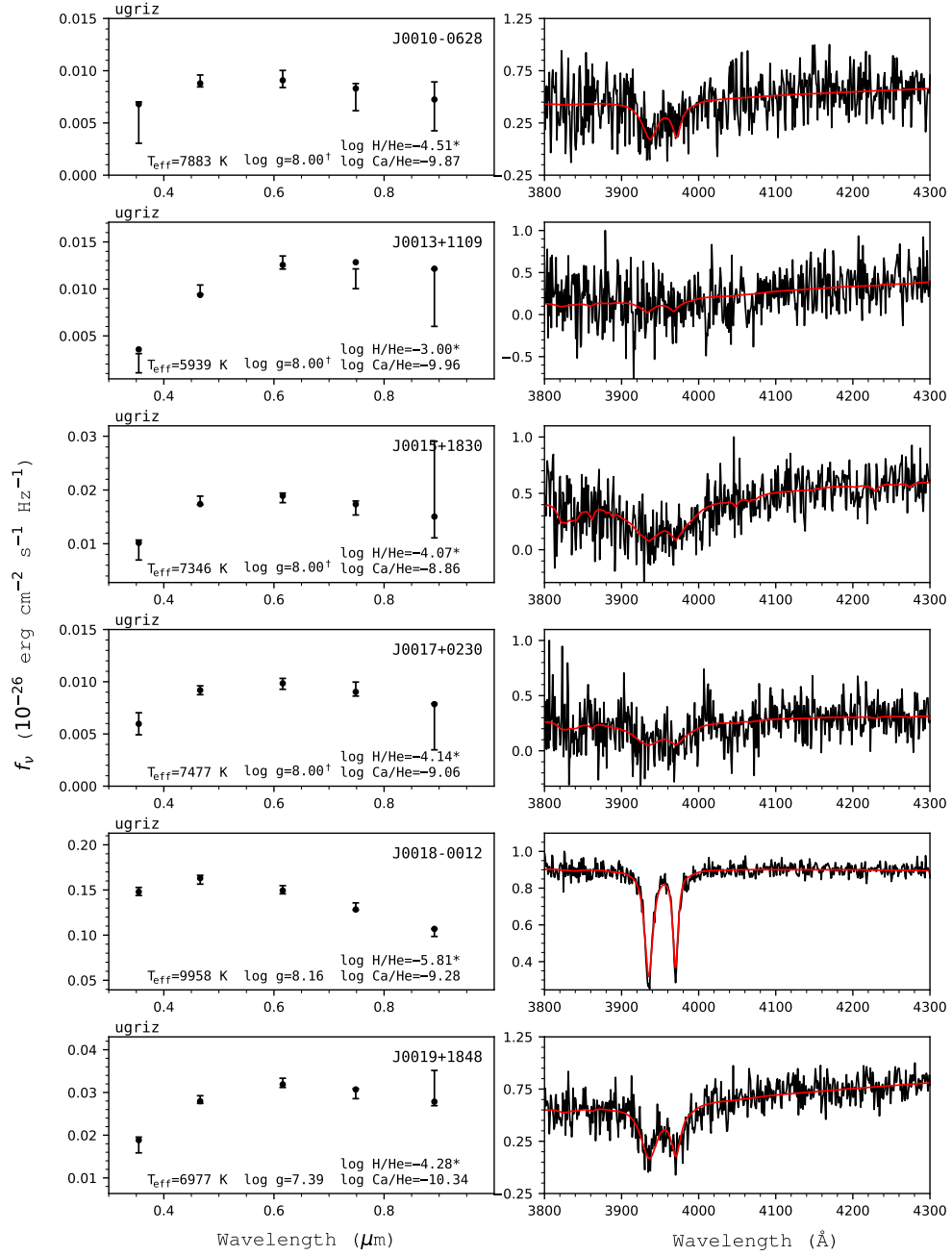


Figure 22. Fits to the DBZ/DZ(A) white dwarfs - continued.

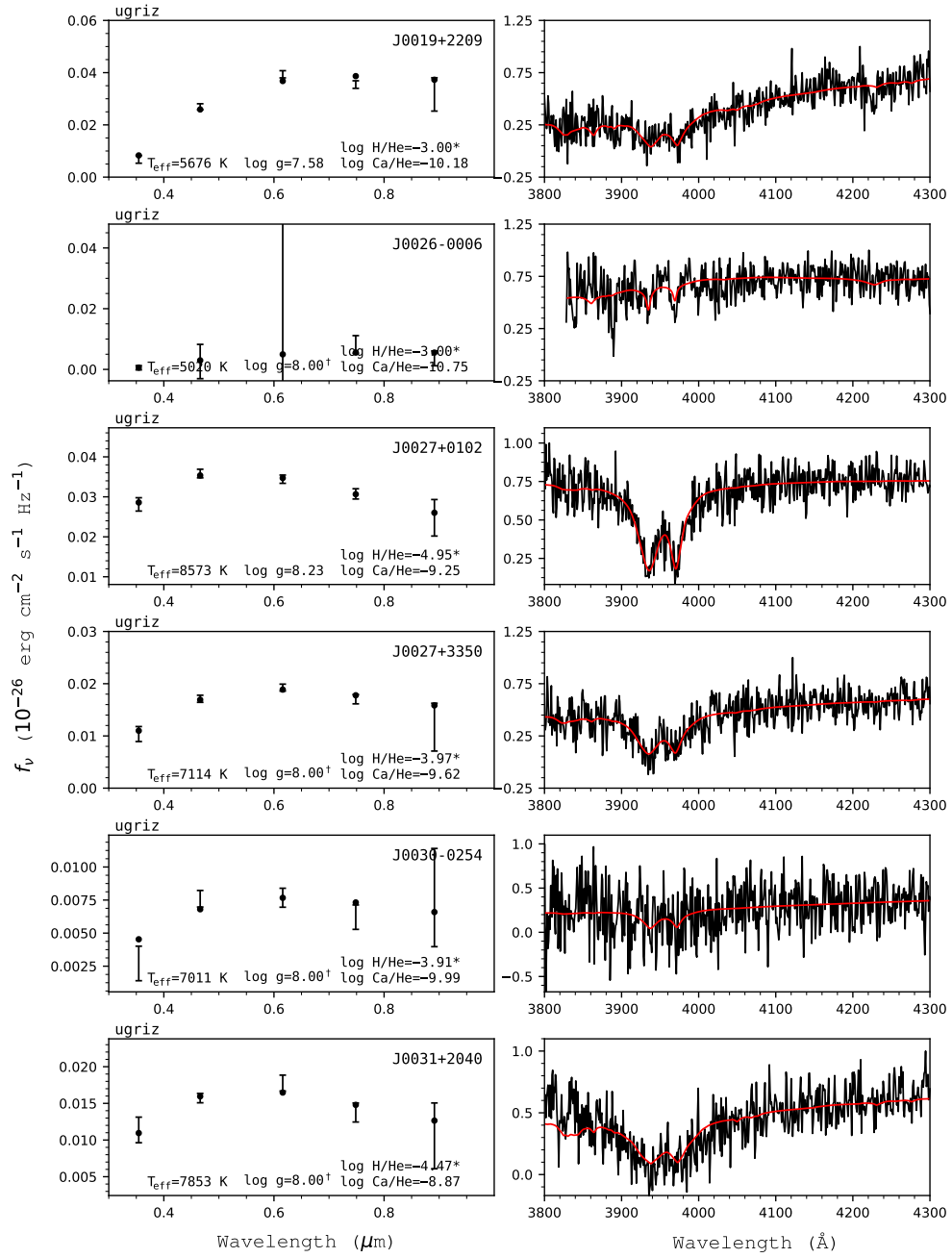


Figure 23. Fits to the DBZ/DZ(A) white dwarfs - continued.

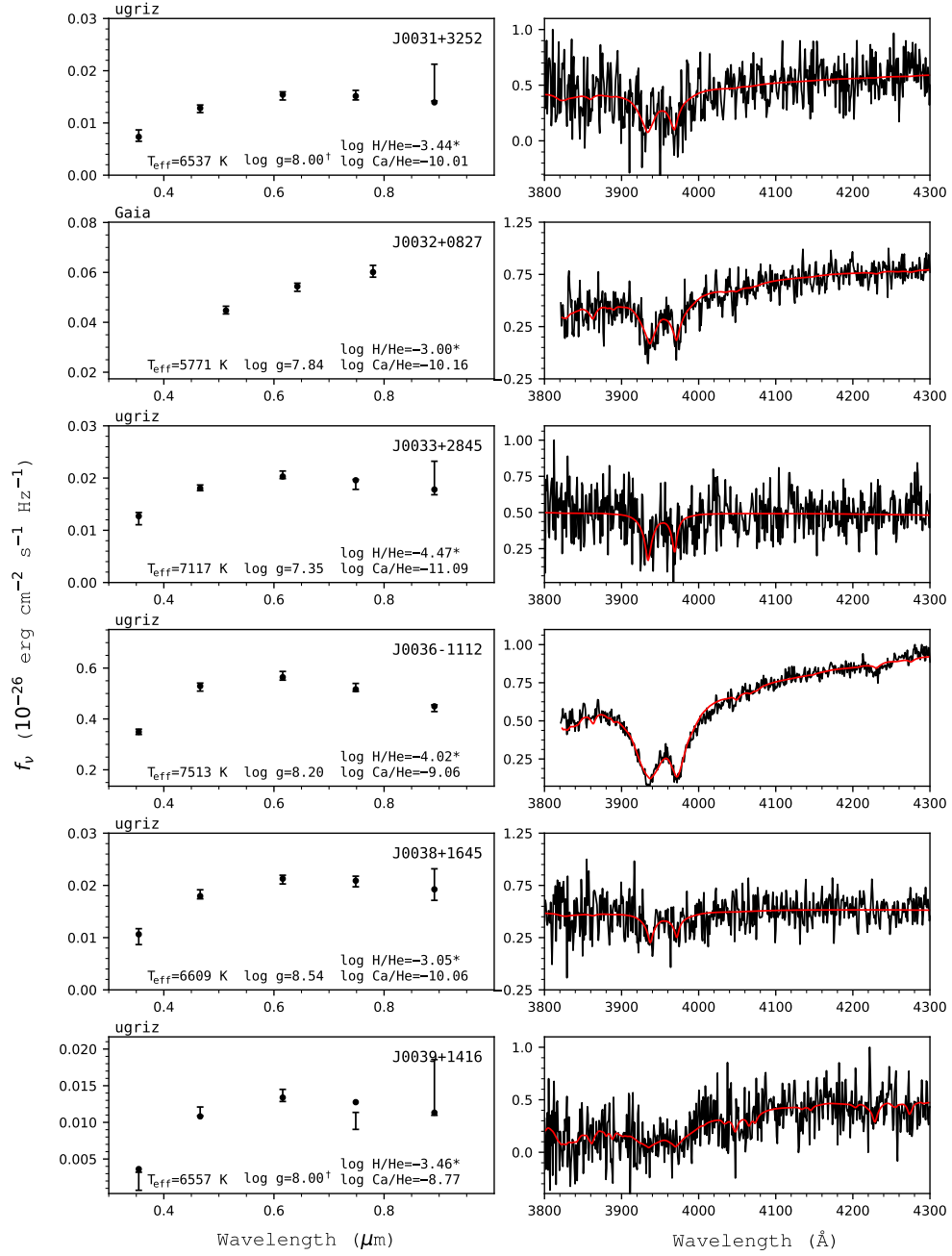


Figure 24. Fits to the DBZ/DZ(A) white dwarfs - continued.

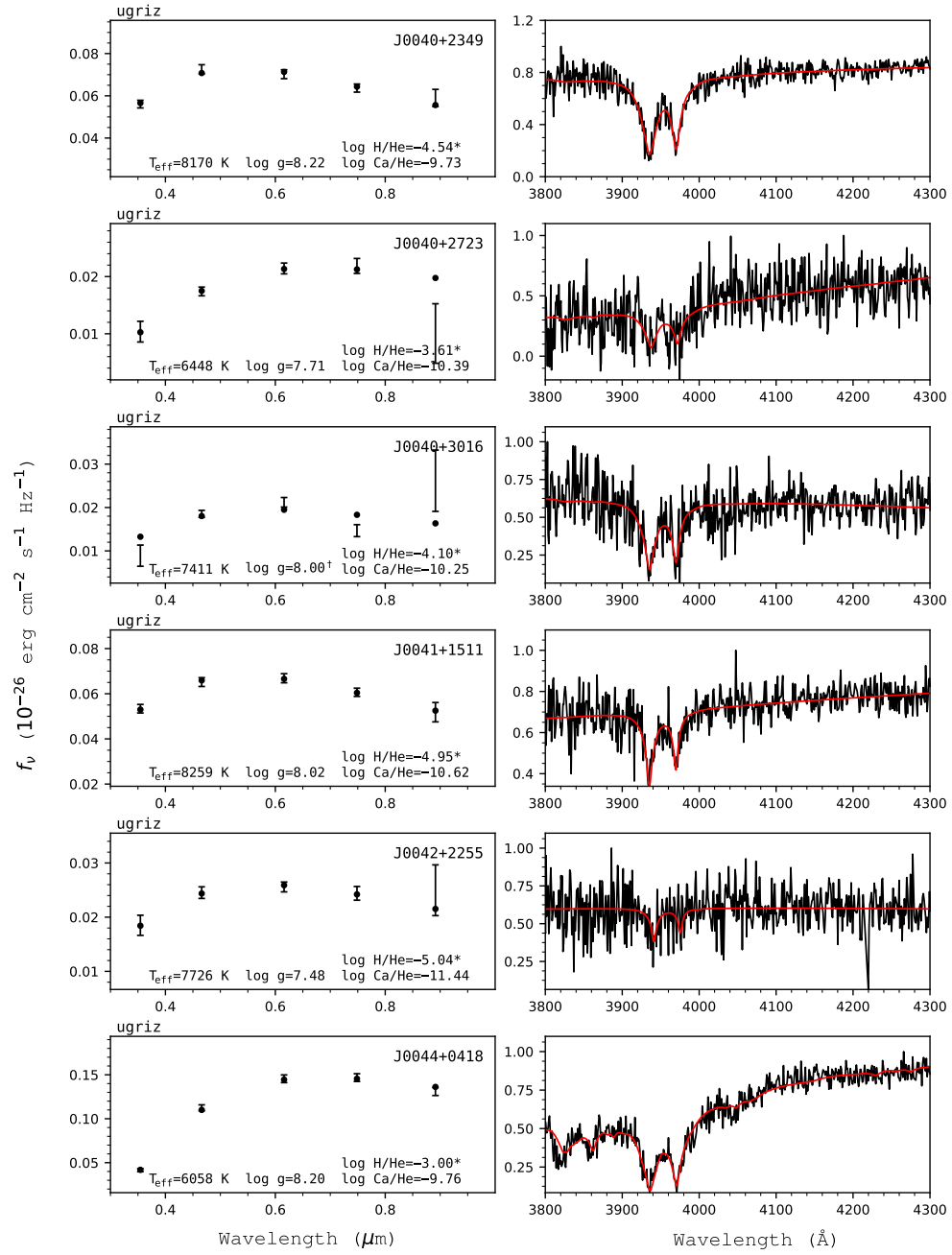


Figure 25. Fits to the DBZ/DZ(A) white dwarfs - continued.

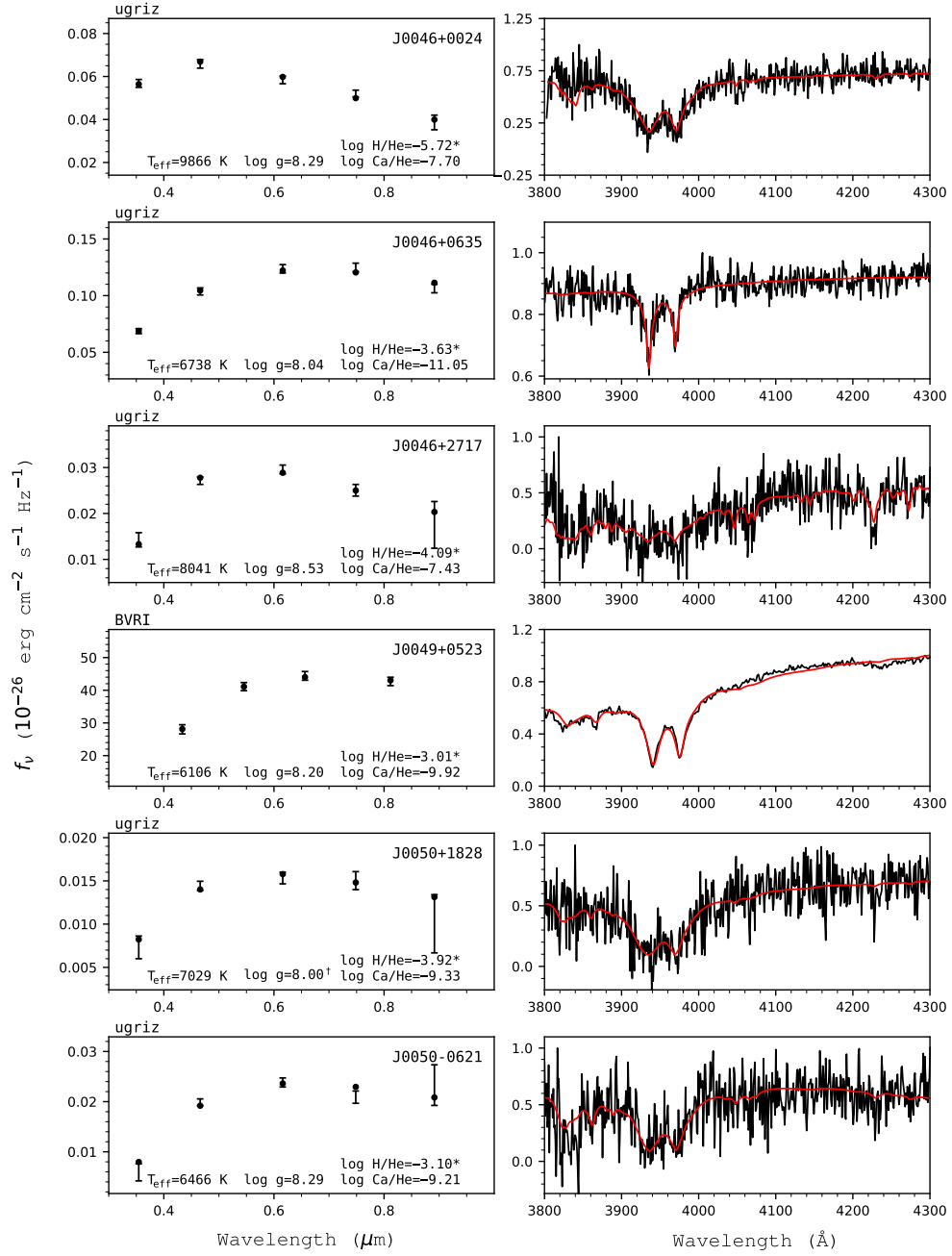


Figure 26. Fits to the DBZ/DZ(A) white dwarfs - continued.

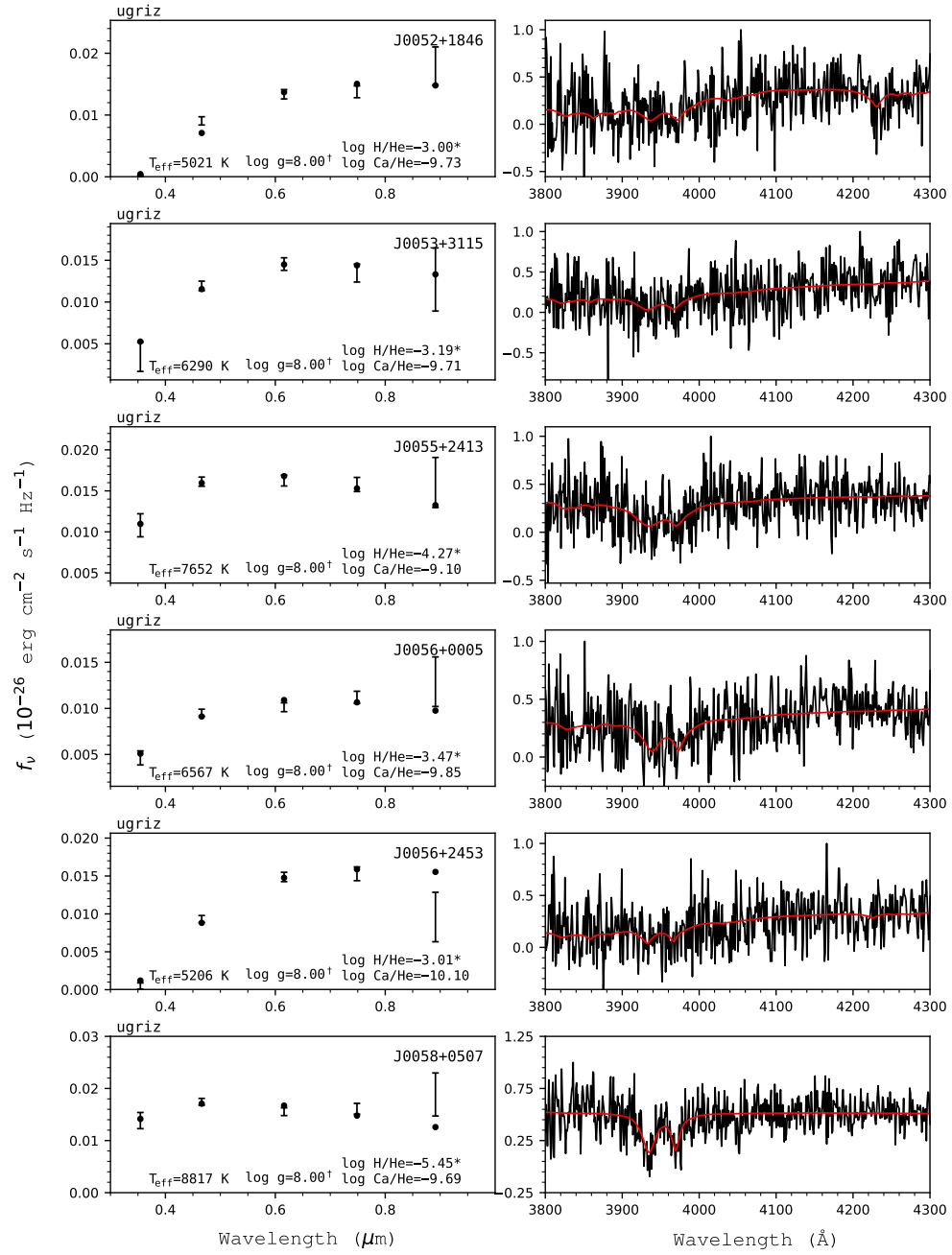


Figure 27. Fits to the DBZ/DZ(A) white dwarfs - continued.

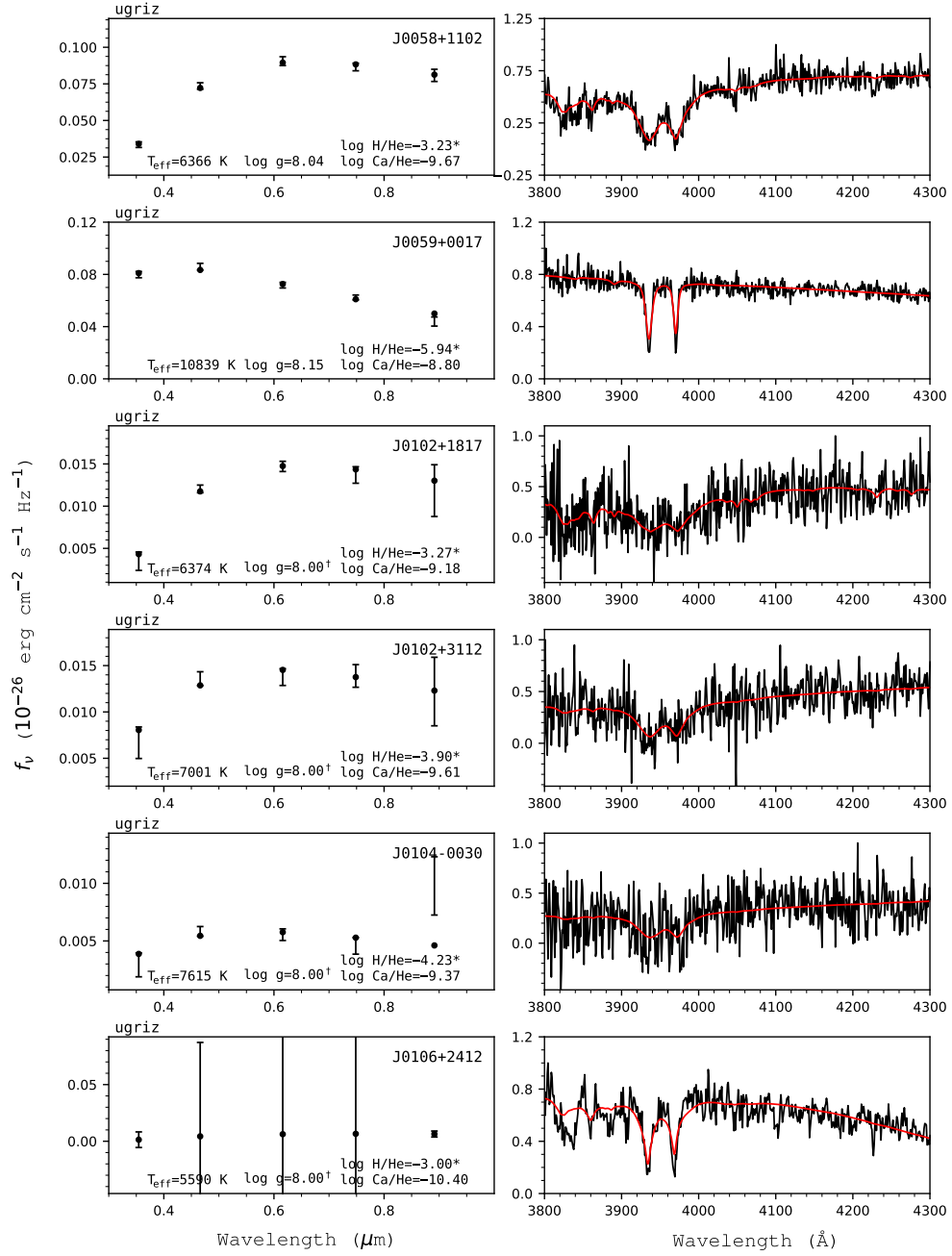


Figure 28. Fits to the DBZ/DZ(A) white dwarfs - continued.

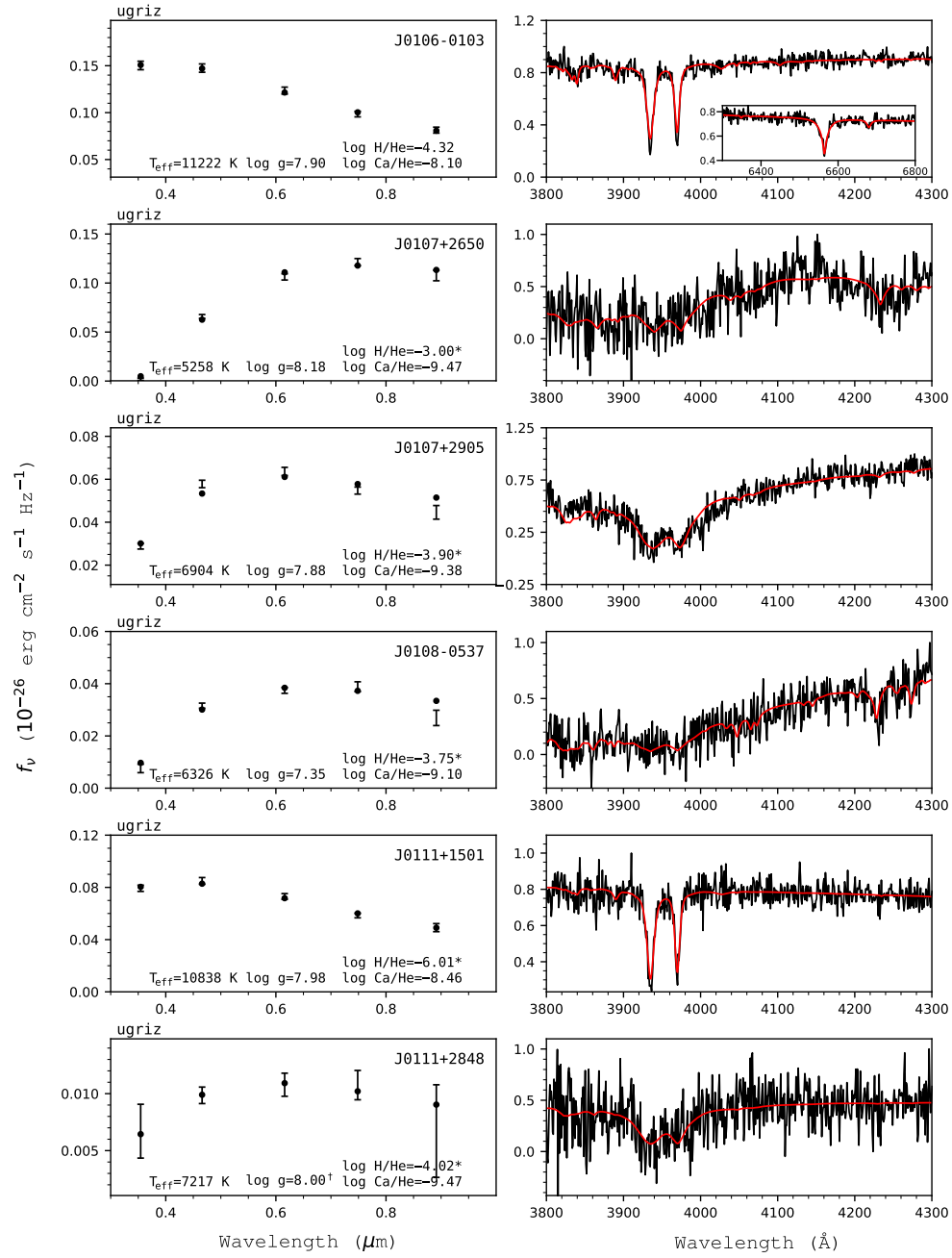


Figure 29. Fits to the DBZ/DZ(A) white dwarfs - continued.

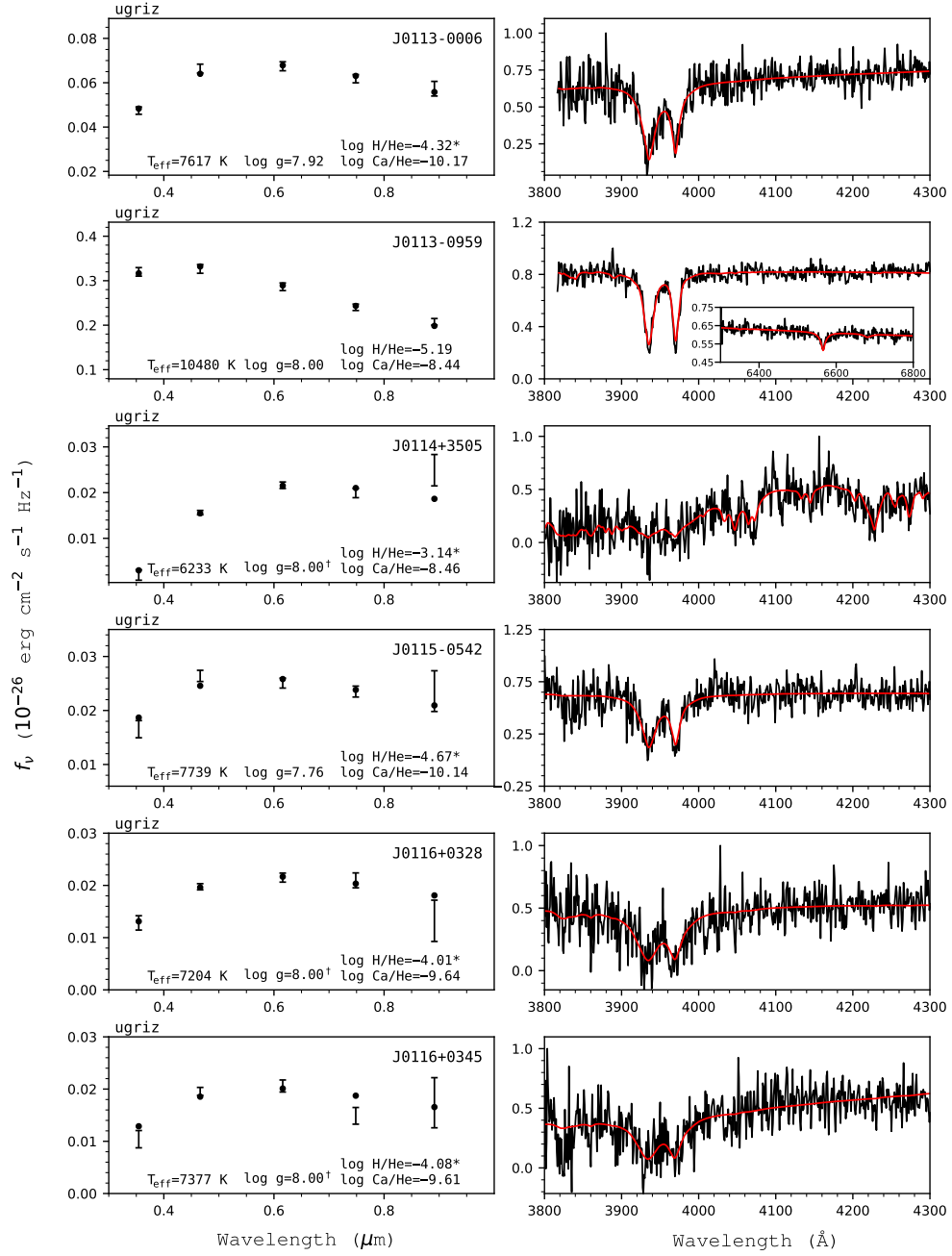


Figure 30. Fits to the DBZ/DZ(A) white dwarfs - continued.

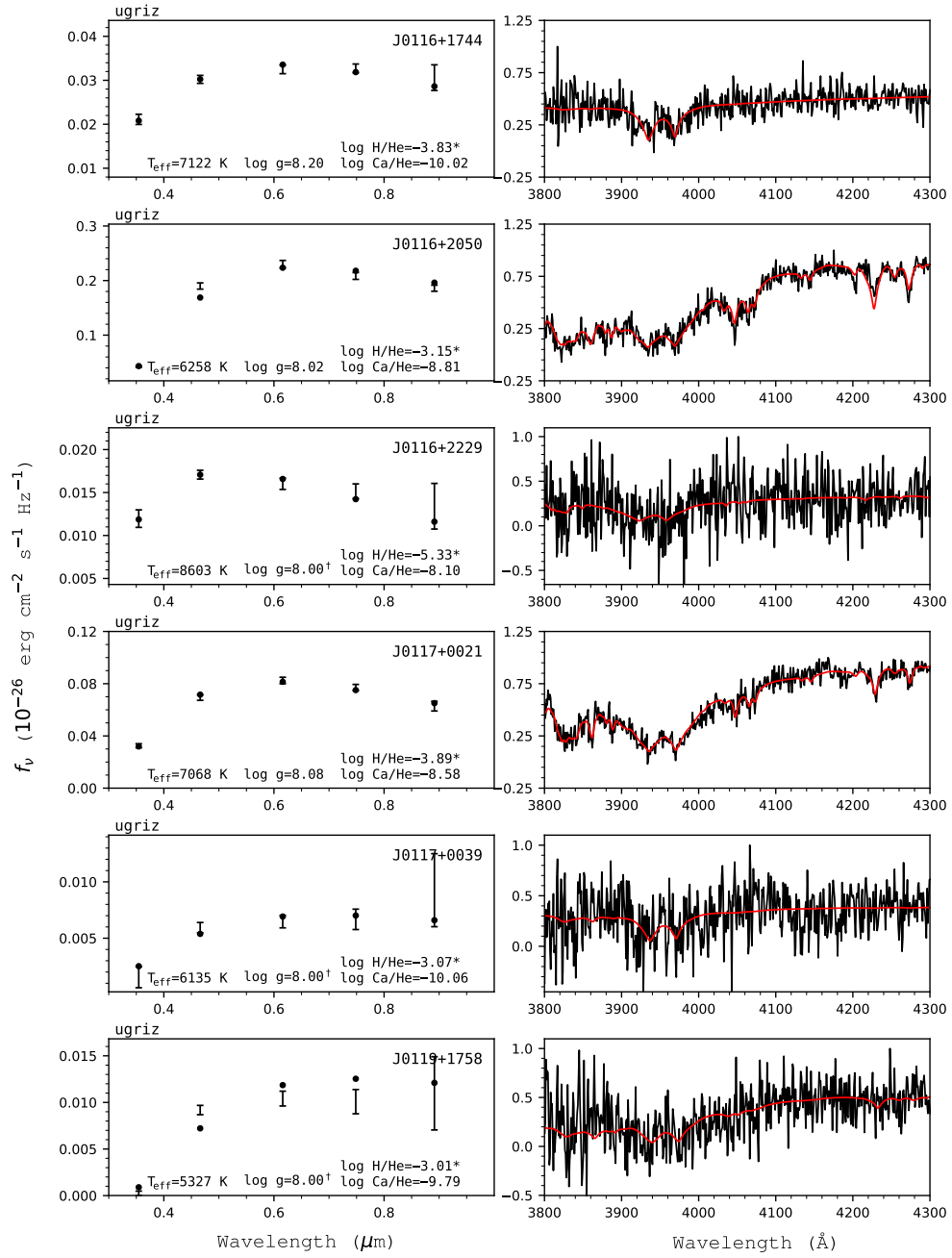


Figure 31. Fits to the DBZ/DZ(A) white dwarfs - continued.

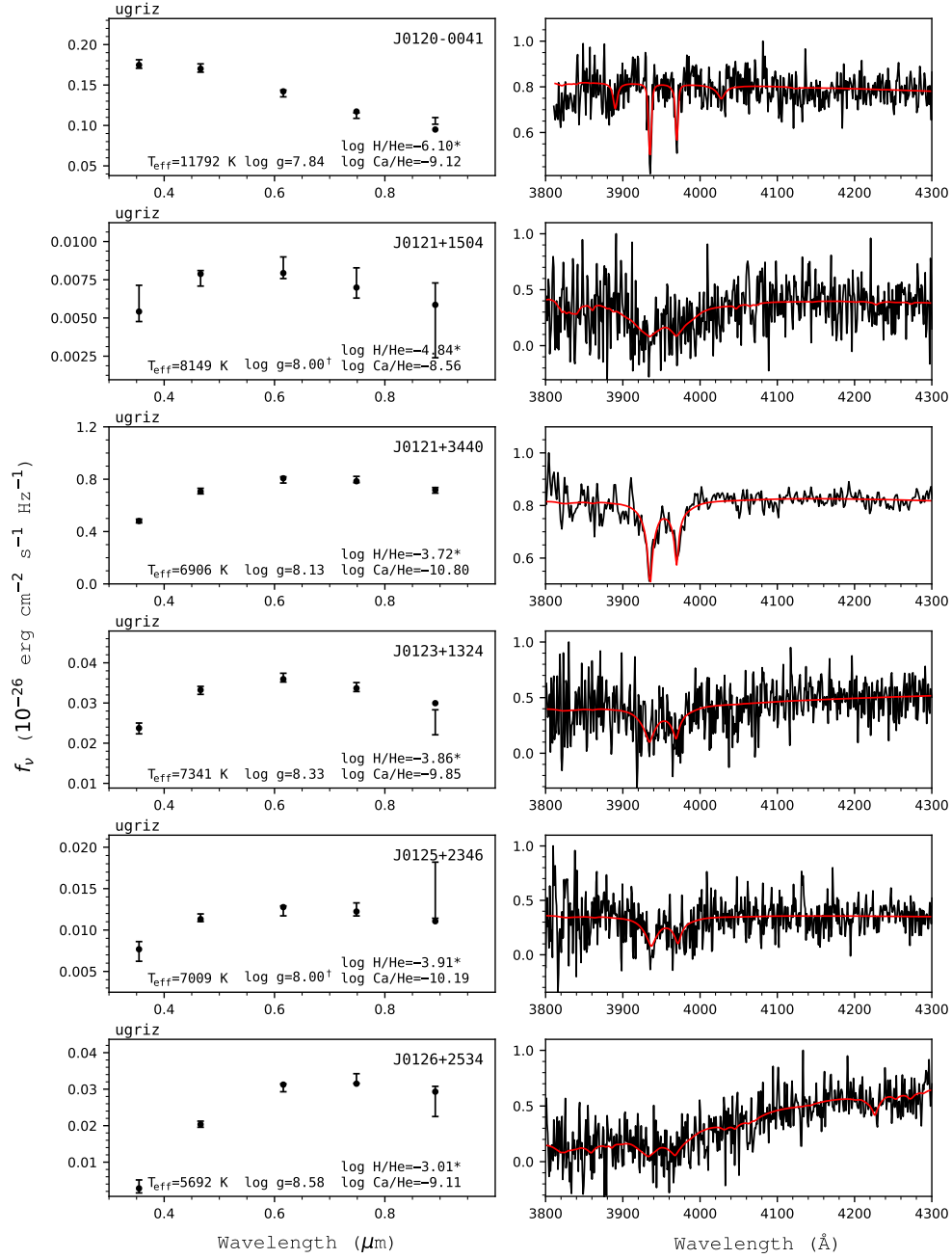


Figure 32. Fits to the DBZ/DZ(A) white dwarfs - continued.

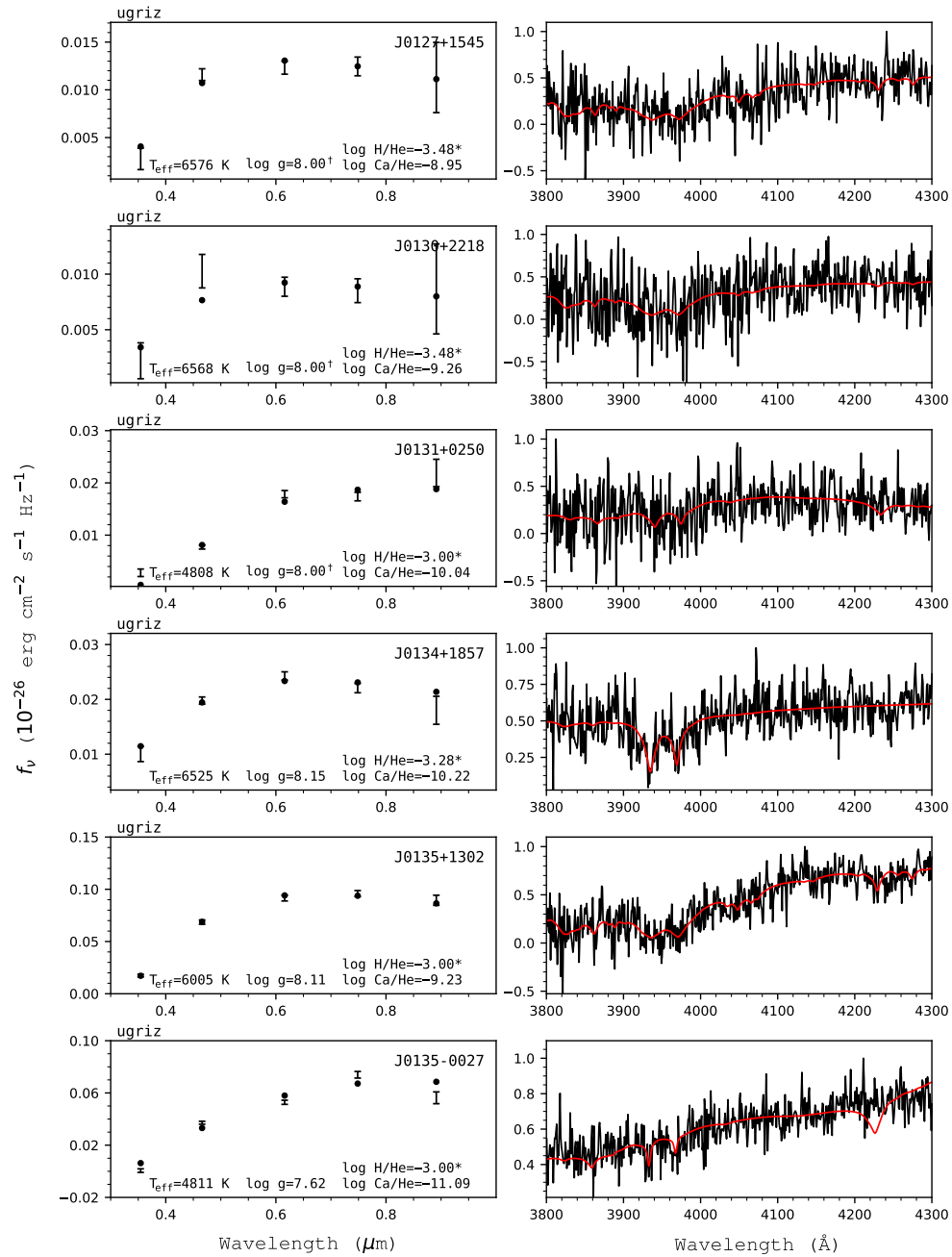


Figure 33. Fits to the DBZ/DZ(A) white dwarfs - continued.

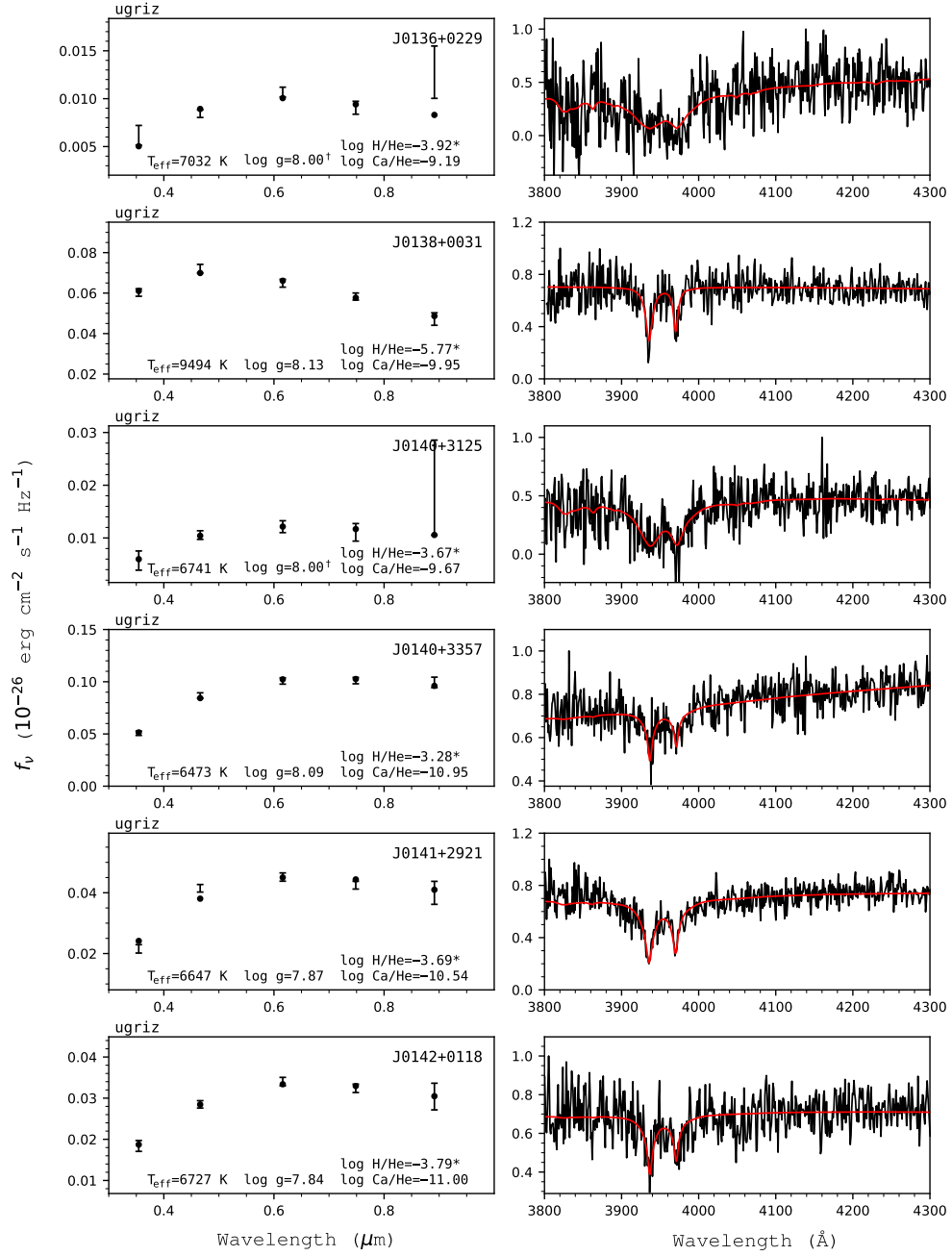


Figure 34. Fits to the DBZ/DZ(A) white dwarfs - continued.

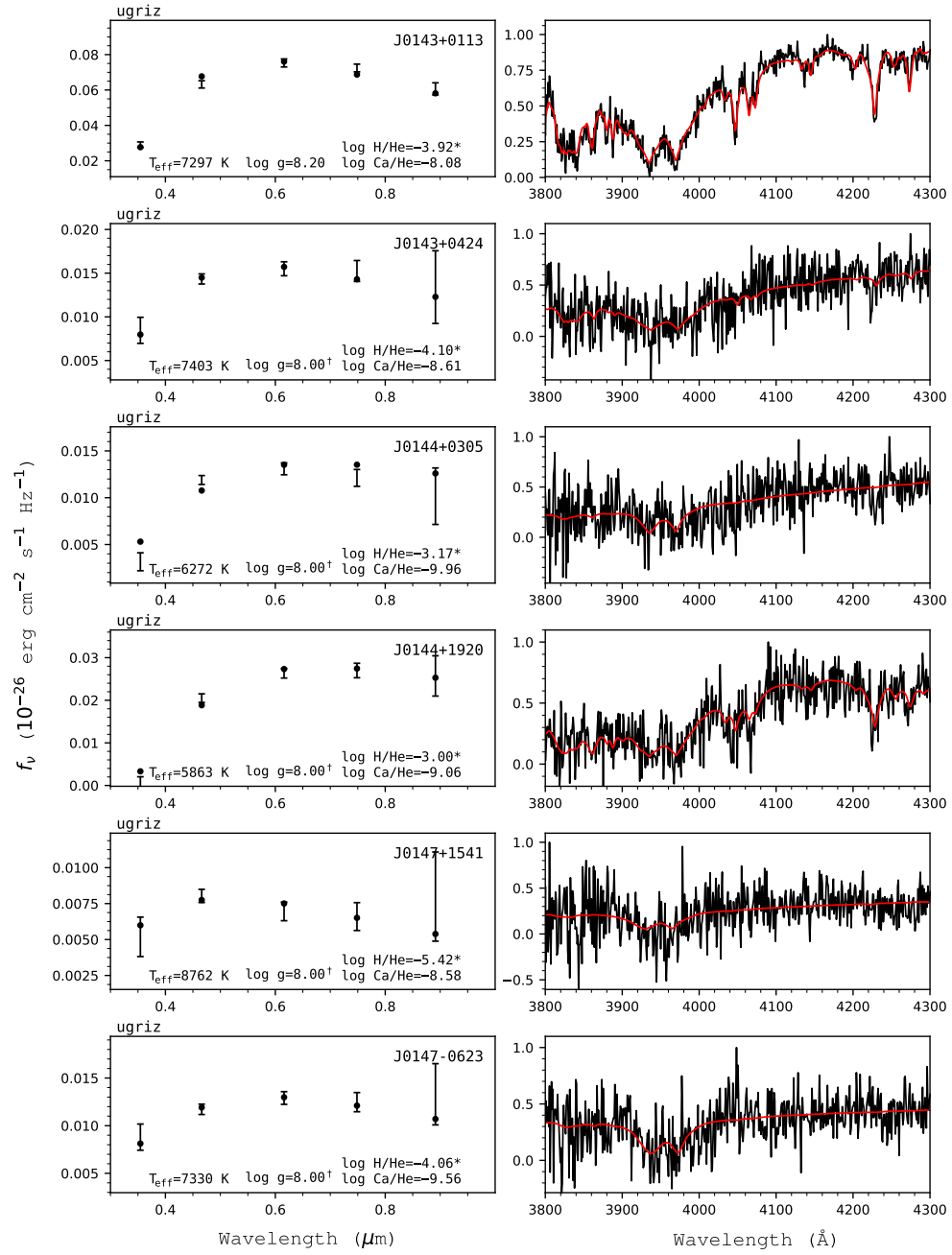


Figure 35. Fits to the DBZ/DZ(A) white dwarfs - continued.

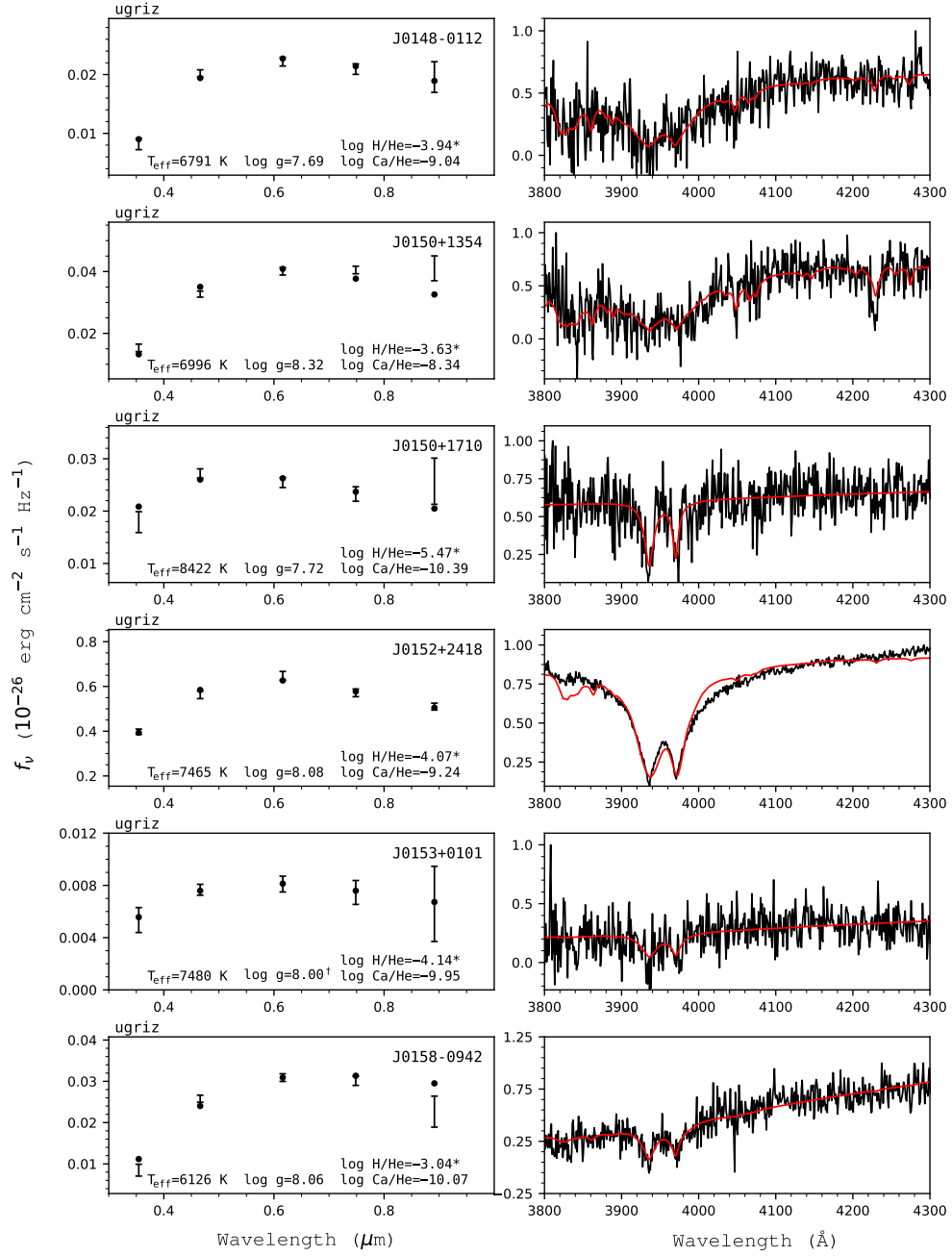


Figure 36. Fits to the DBZ/DZ(A) white dwarfs - continued.

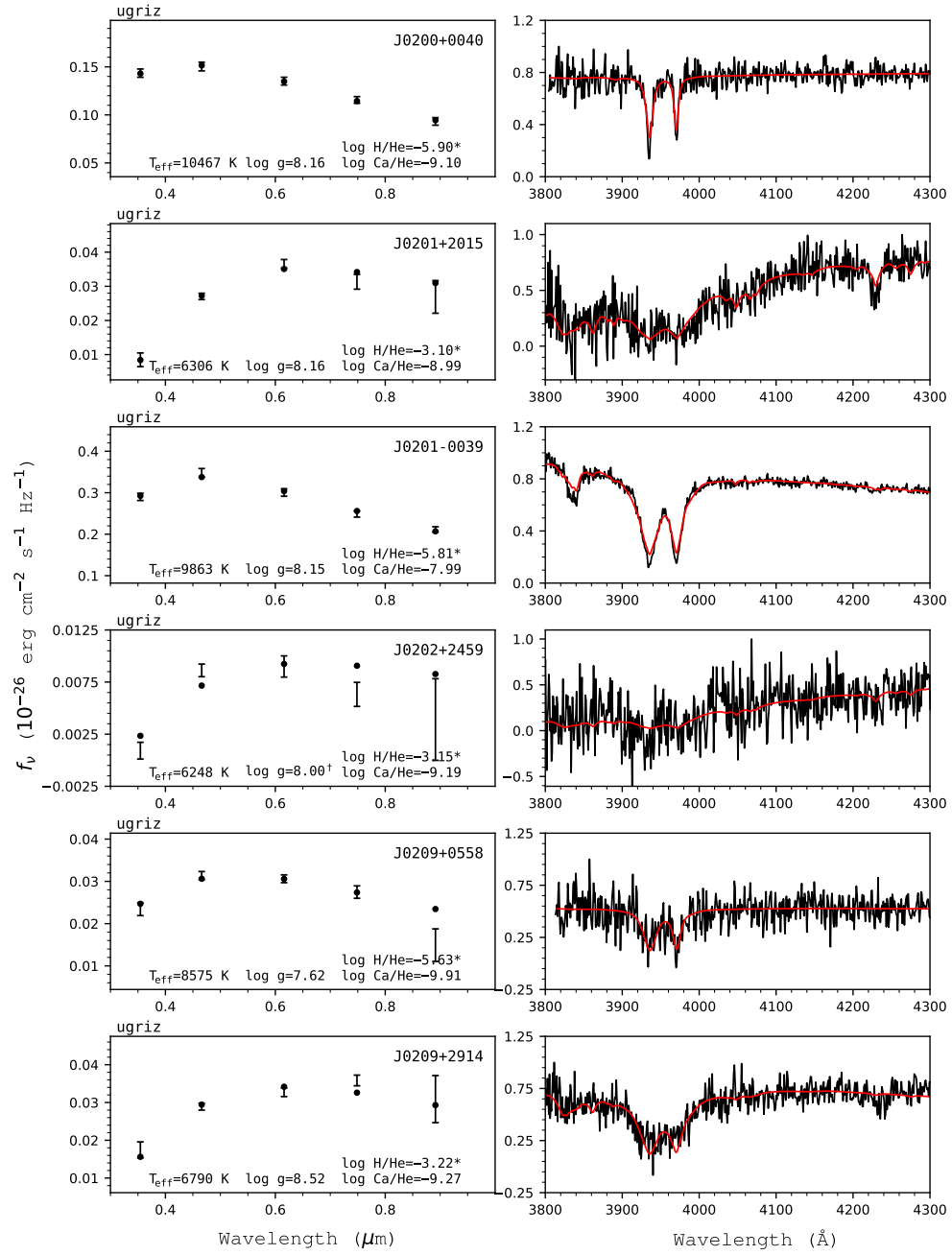


Figure 37. Fits to the DBZ/DZ(A) white dwarfs - continued.

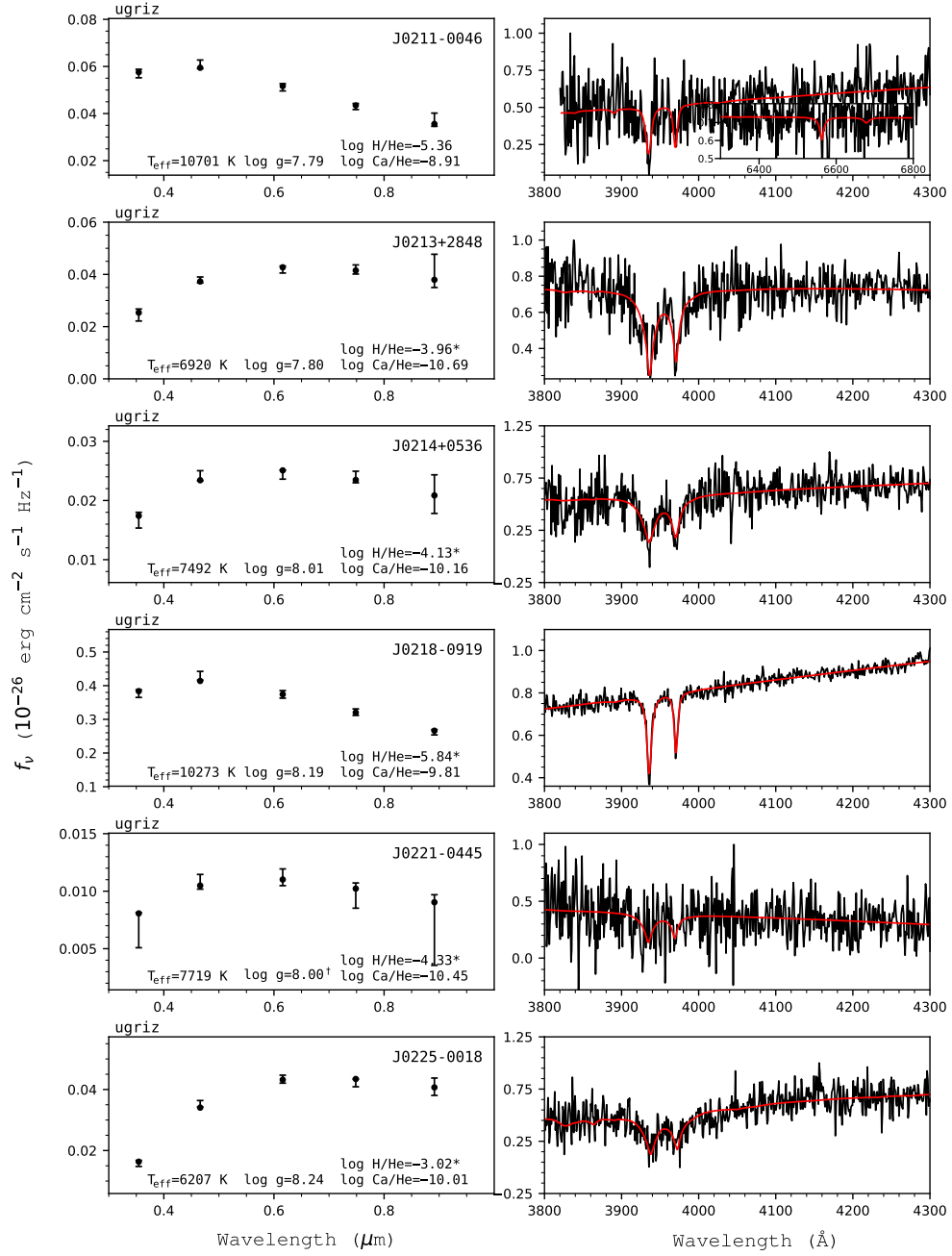


Figure 38. Fits to the DBZ/DZ(A) white dwarfs - continued.

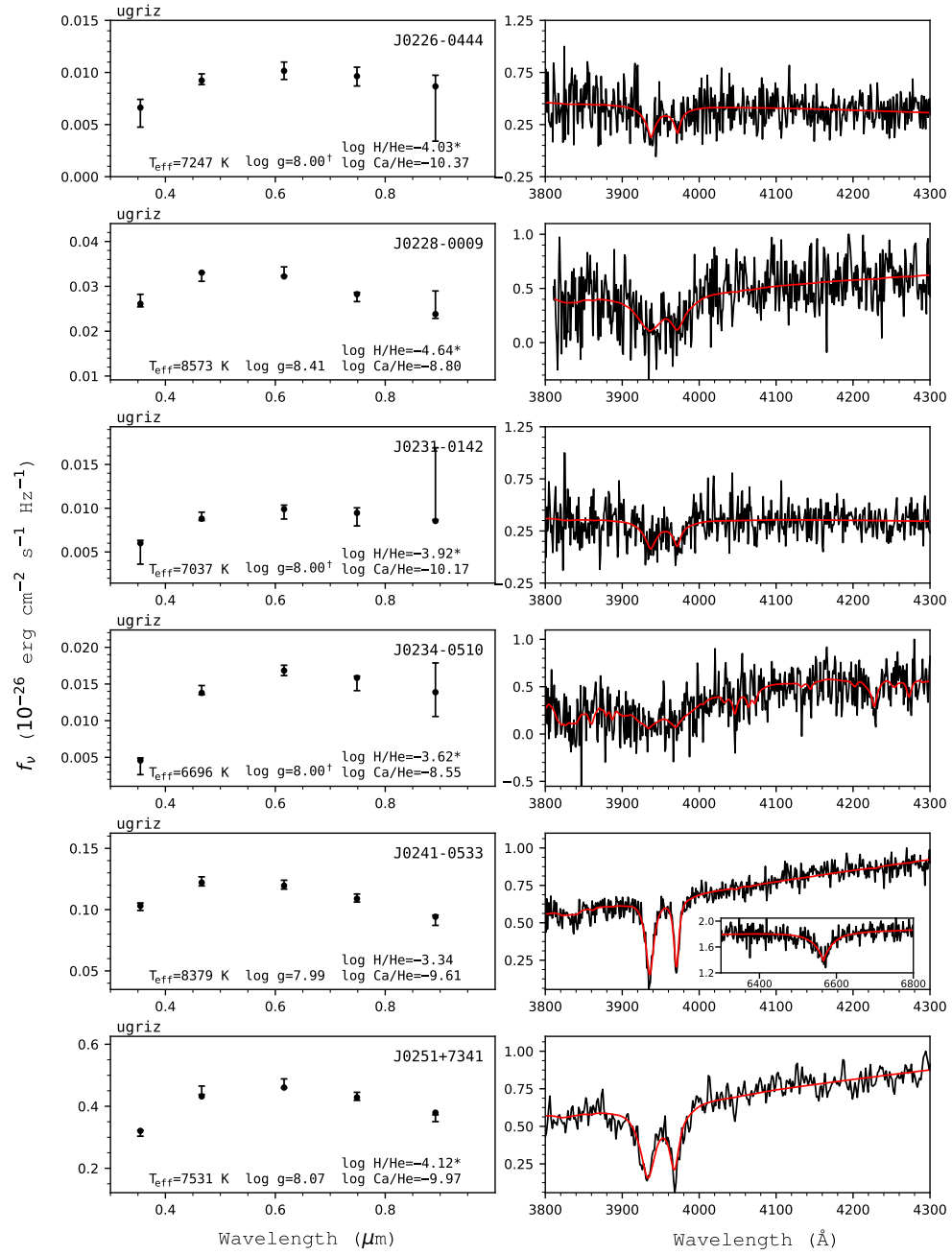


Figure 39. Fits to the DBZ/DZ(A) white dwarfs - continued.

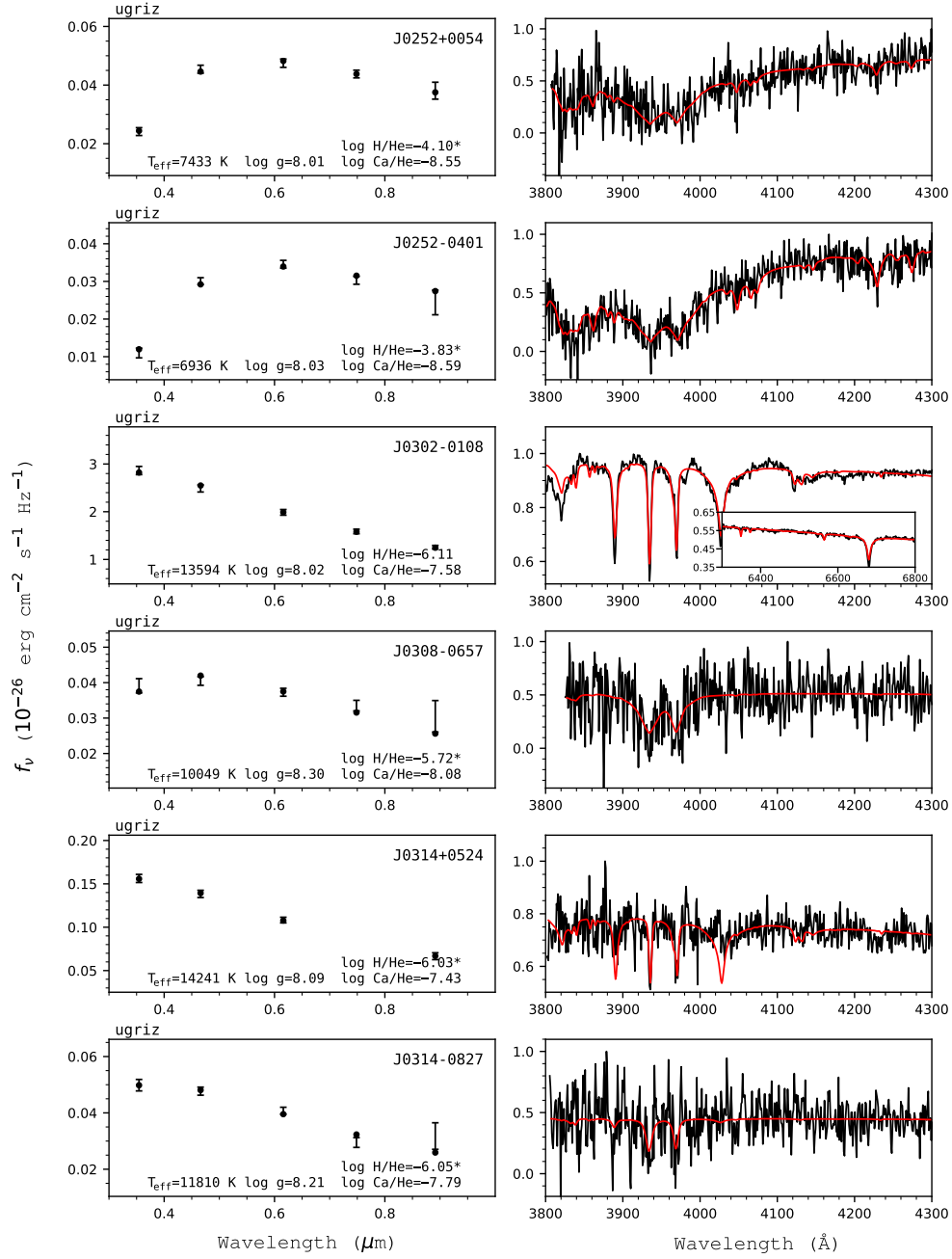


Figure 40. Fits to the DBZ/DZ(A) white dwarfs - continued.

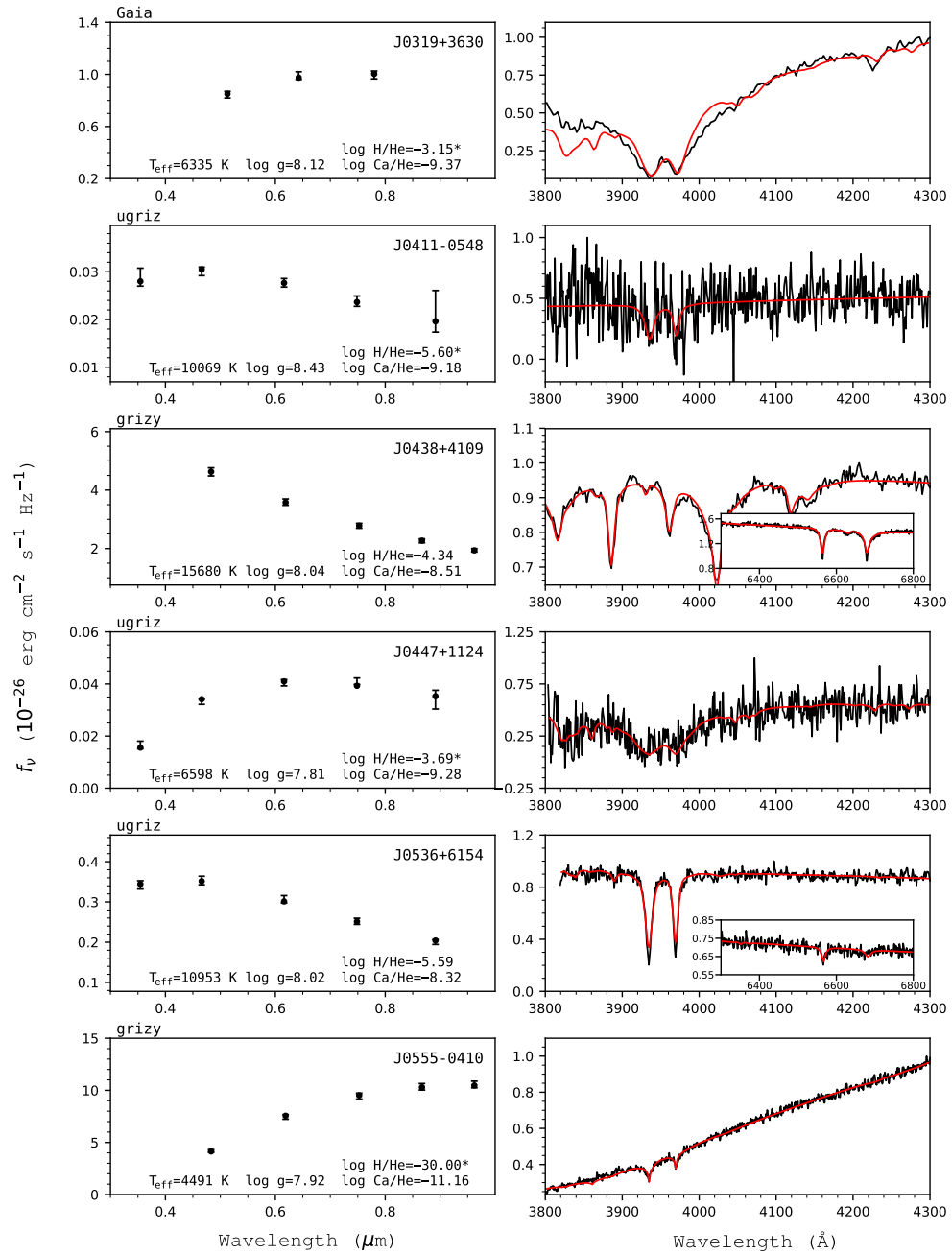


Figure 41. Fits to the DBZ/DZ(A) white dwarfs - continued.

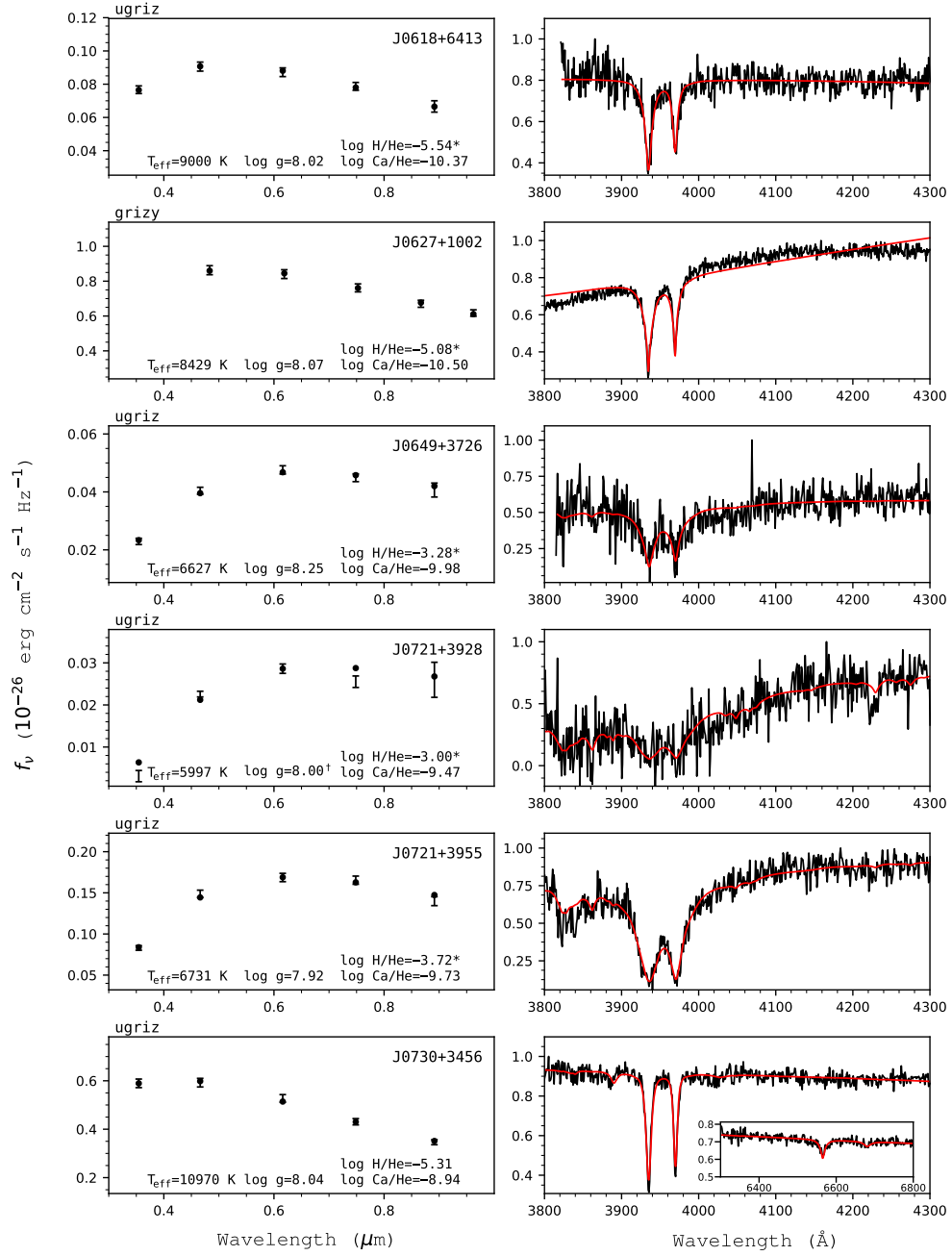


Figure 42. Fits to the DBZ/DZ(A) white dwarfs - continued.

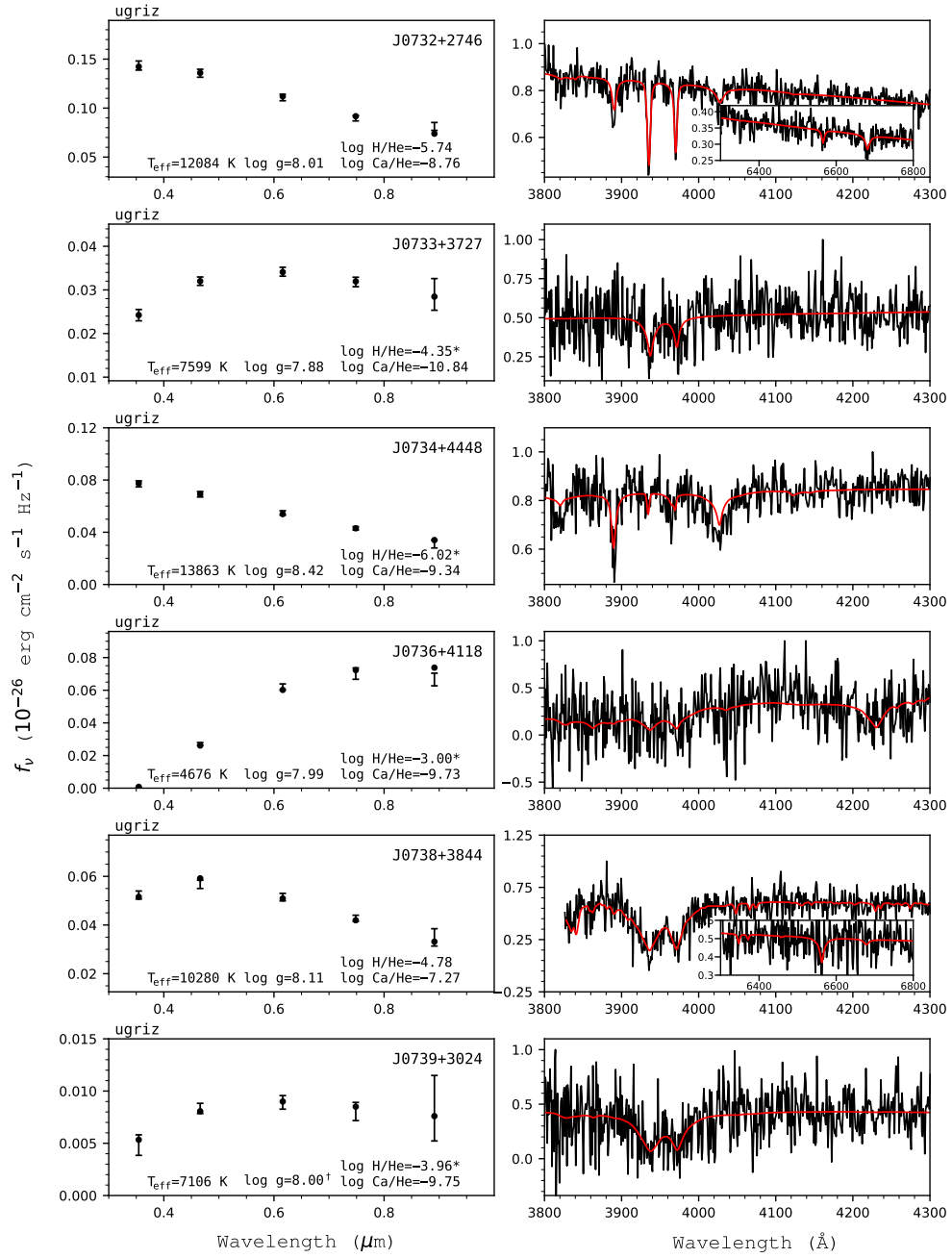


Figure 43. Fits to the DBZ/DZ(A) white dwarfs - continued.

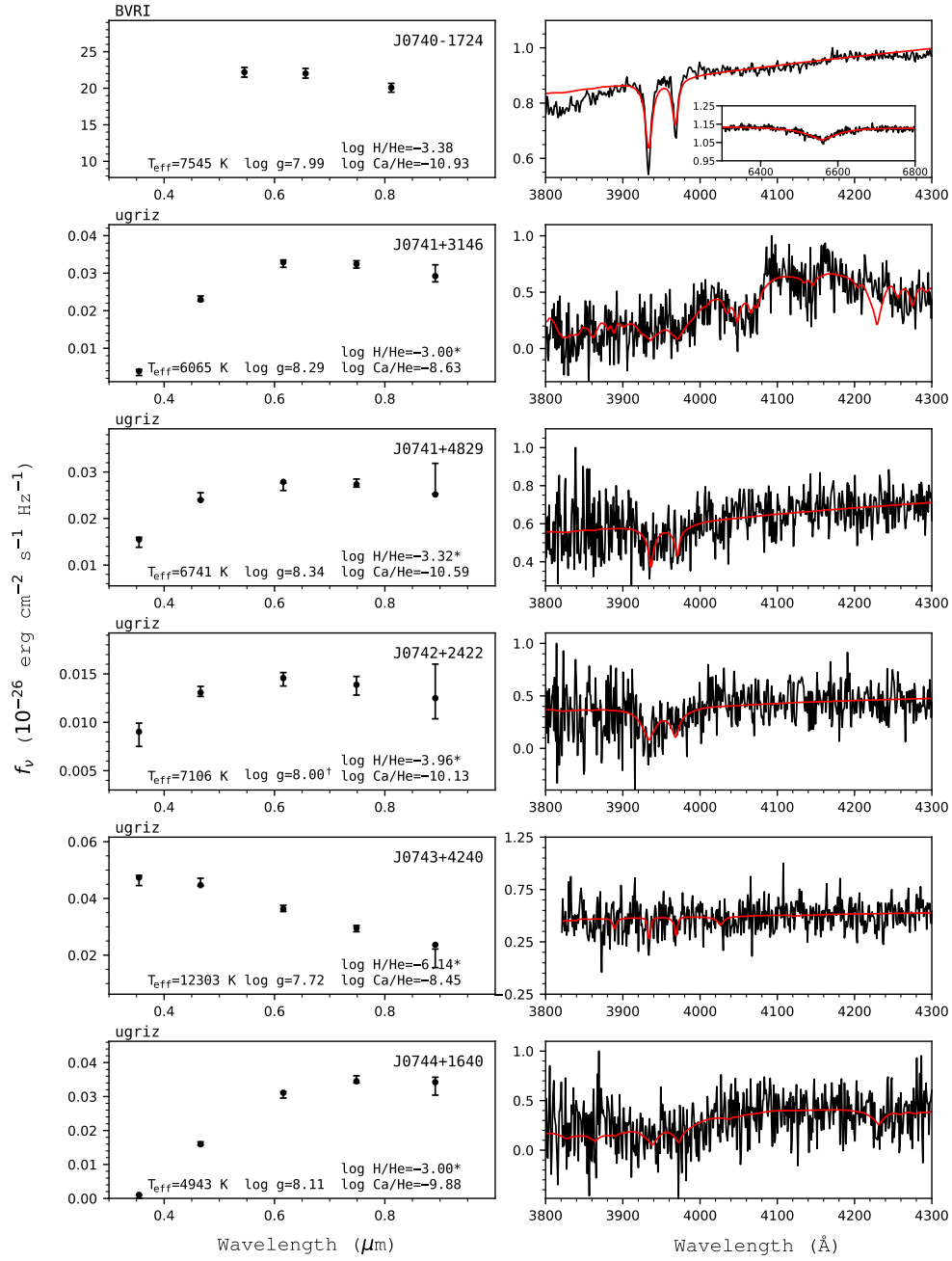


Figure 44. Fits to the DBZ/DZ(A) white dwarfs - continued.

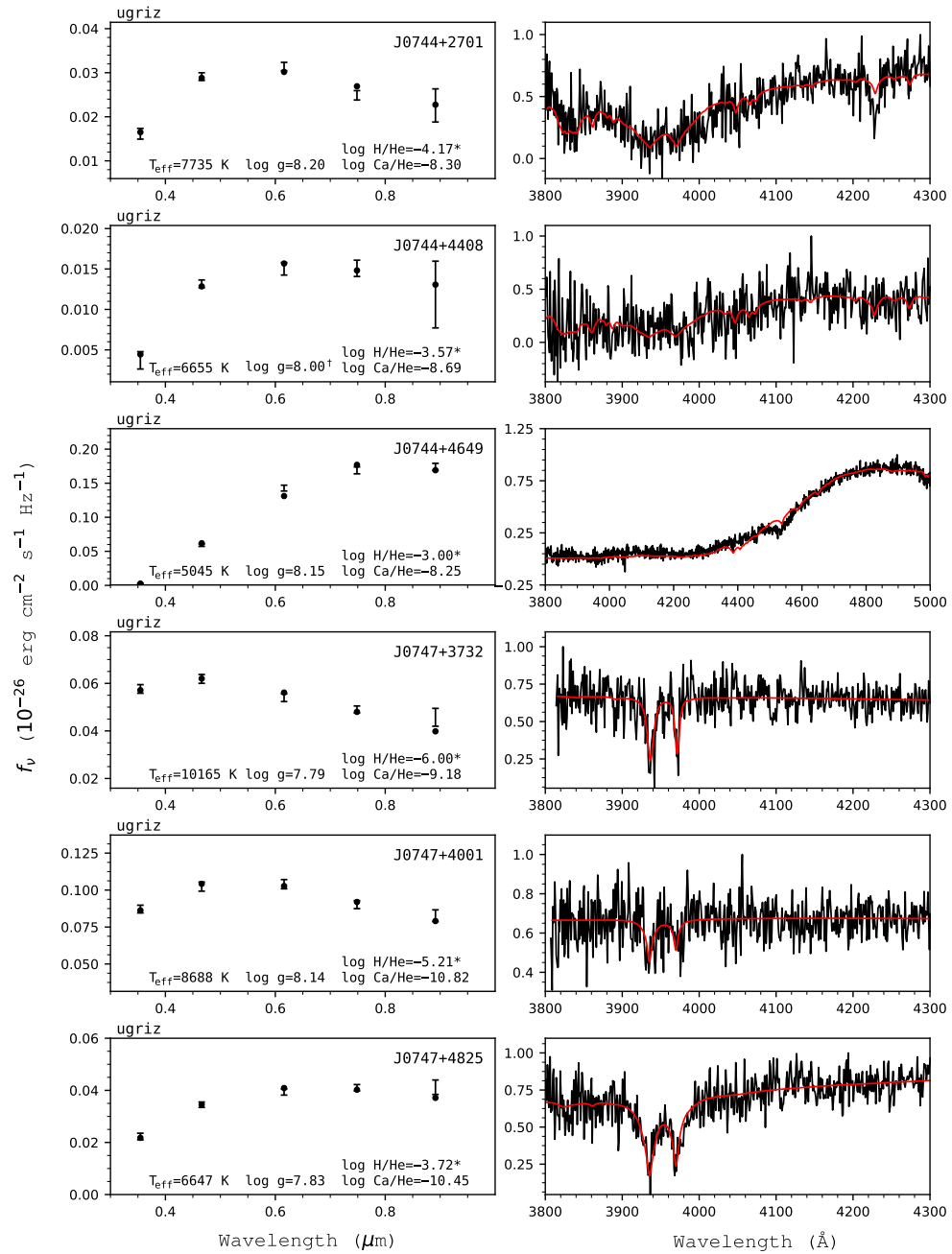


Figure 45. Fits to the DBZ/DZ(A) white dwarfs - continued.

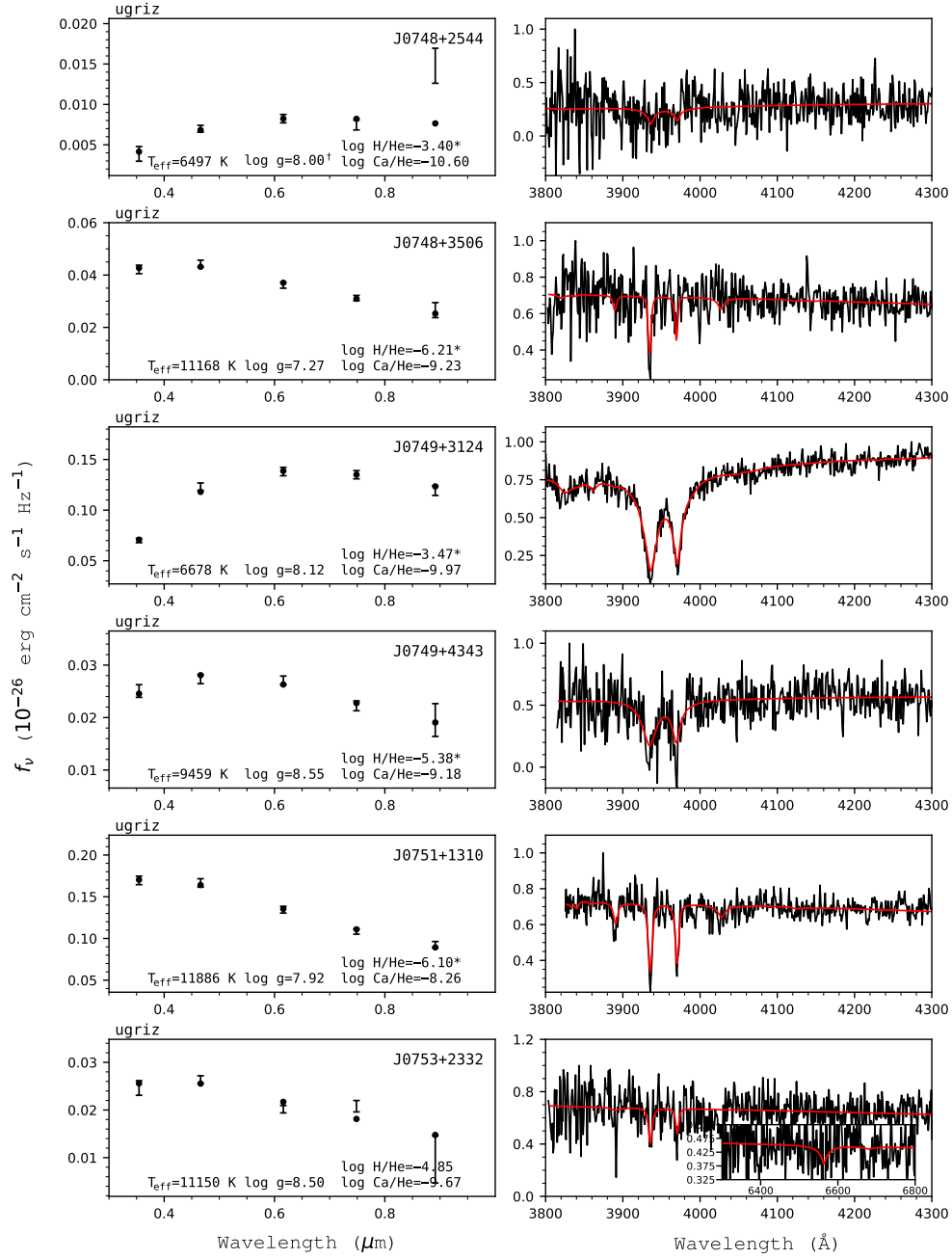


Figure 46. Fits to the DBZ/DZ(A) white dwarfs - continued.

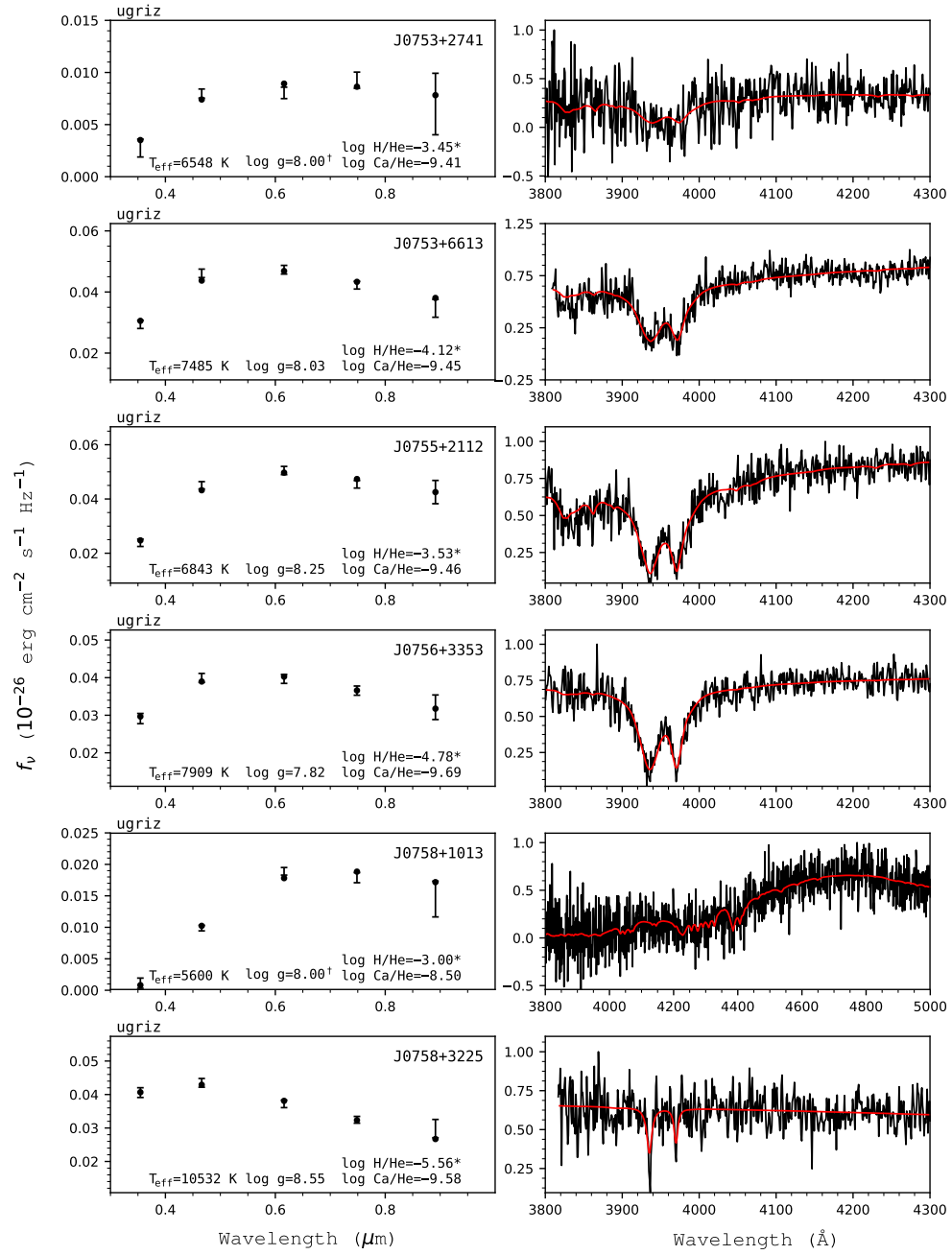


Figure 47. Fits to the DBZ/DZ(A) white dwarfs - continued.

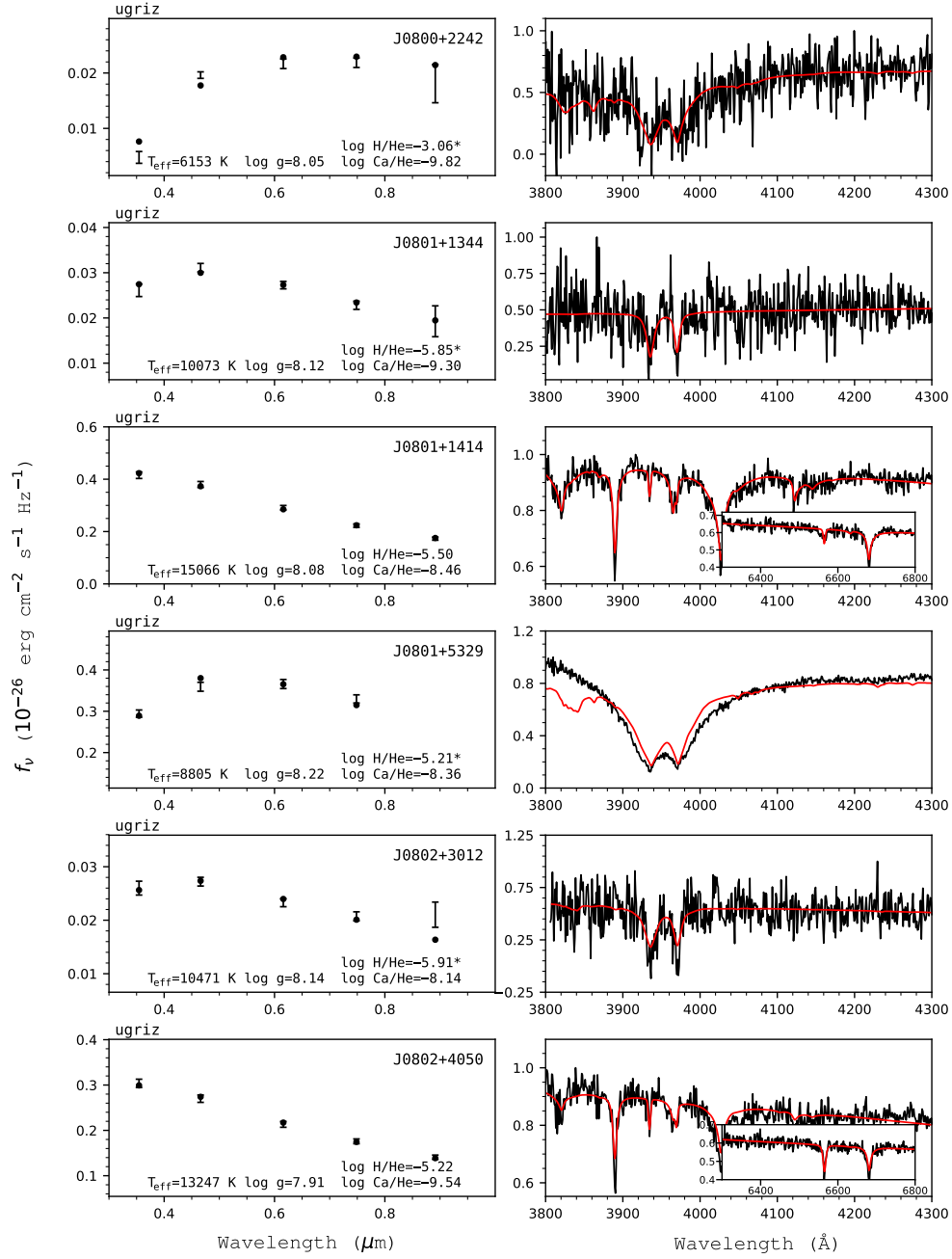


Figure 48. Fits to the DBZ/DZ(A) white dwarfs - continued.

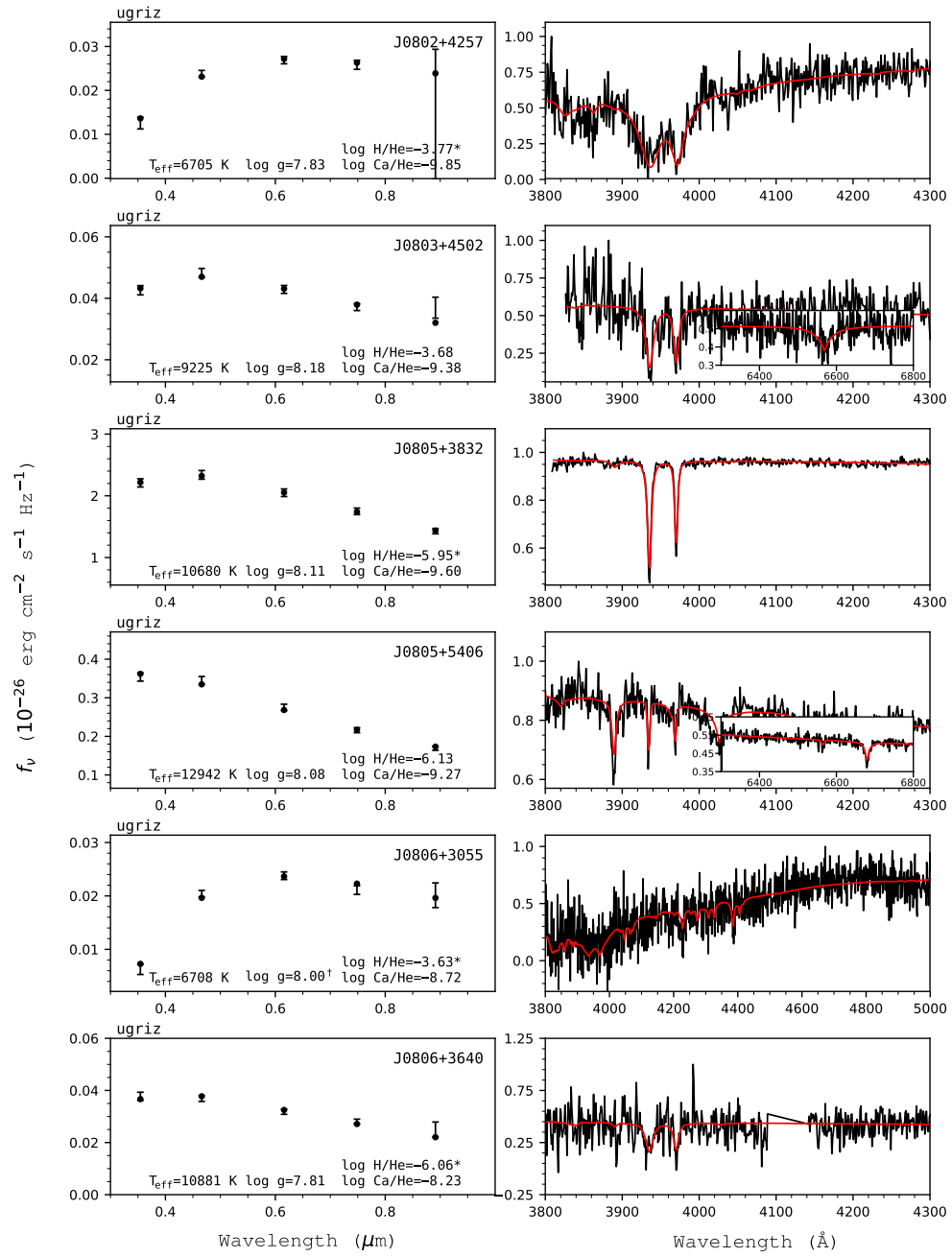


Figure 49. Fits to the DBZ/DZ(A) white dwarfs - continued.

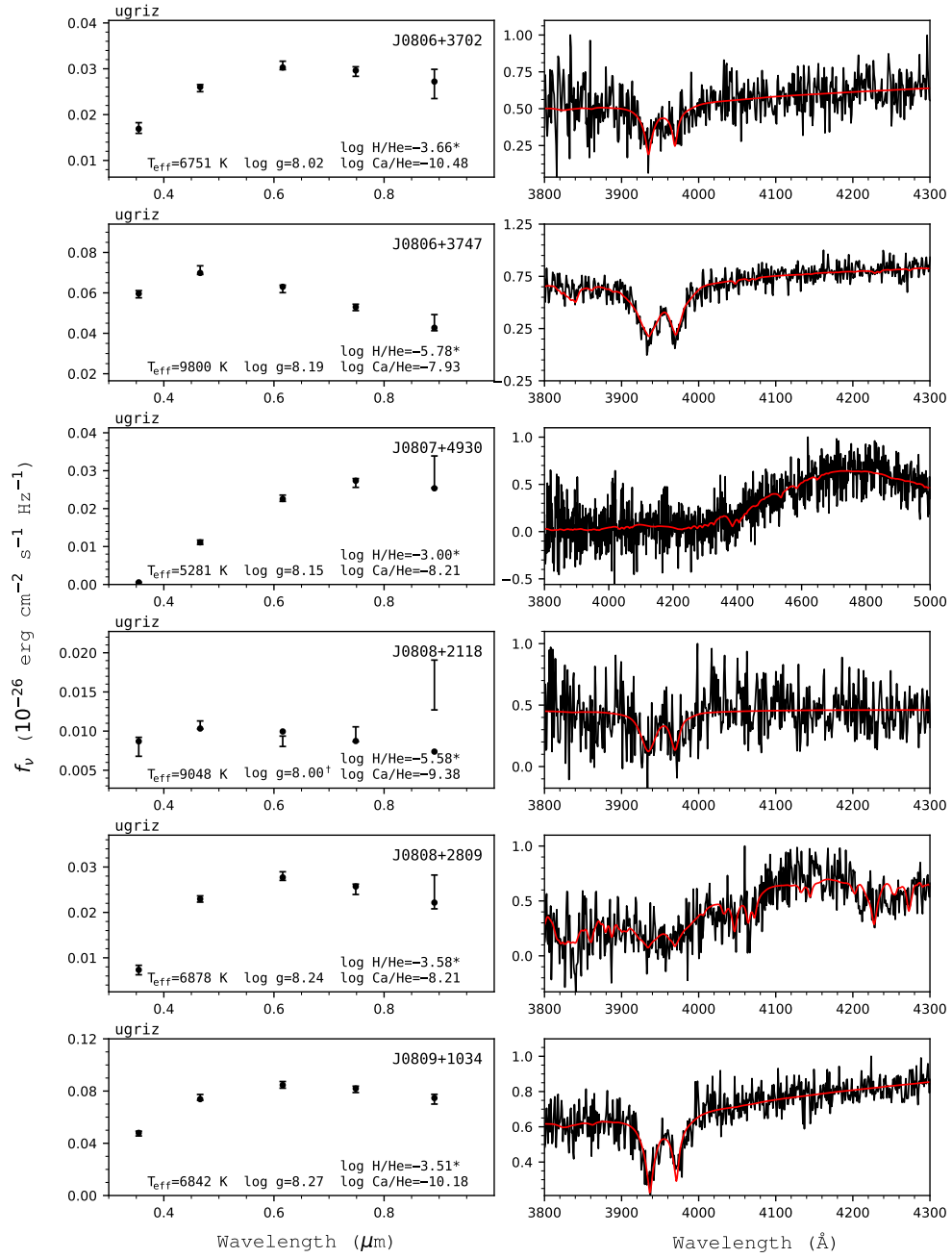


Figure 50. Fits to the DBZ/DZ(A) white dwarfs - continued.

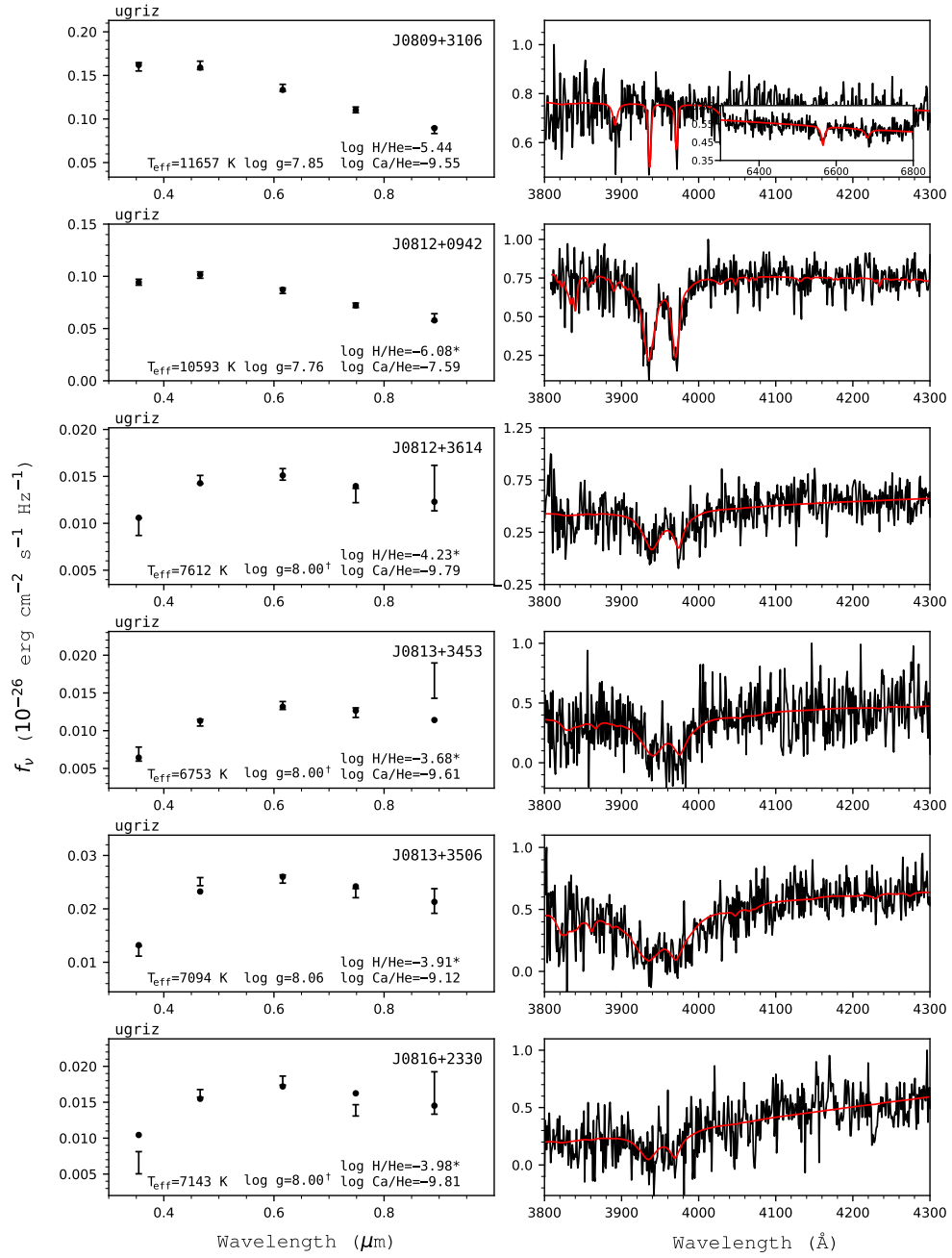


Figure 51. Fits to the DBZ/DZ(A) white dwarfs - continued.

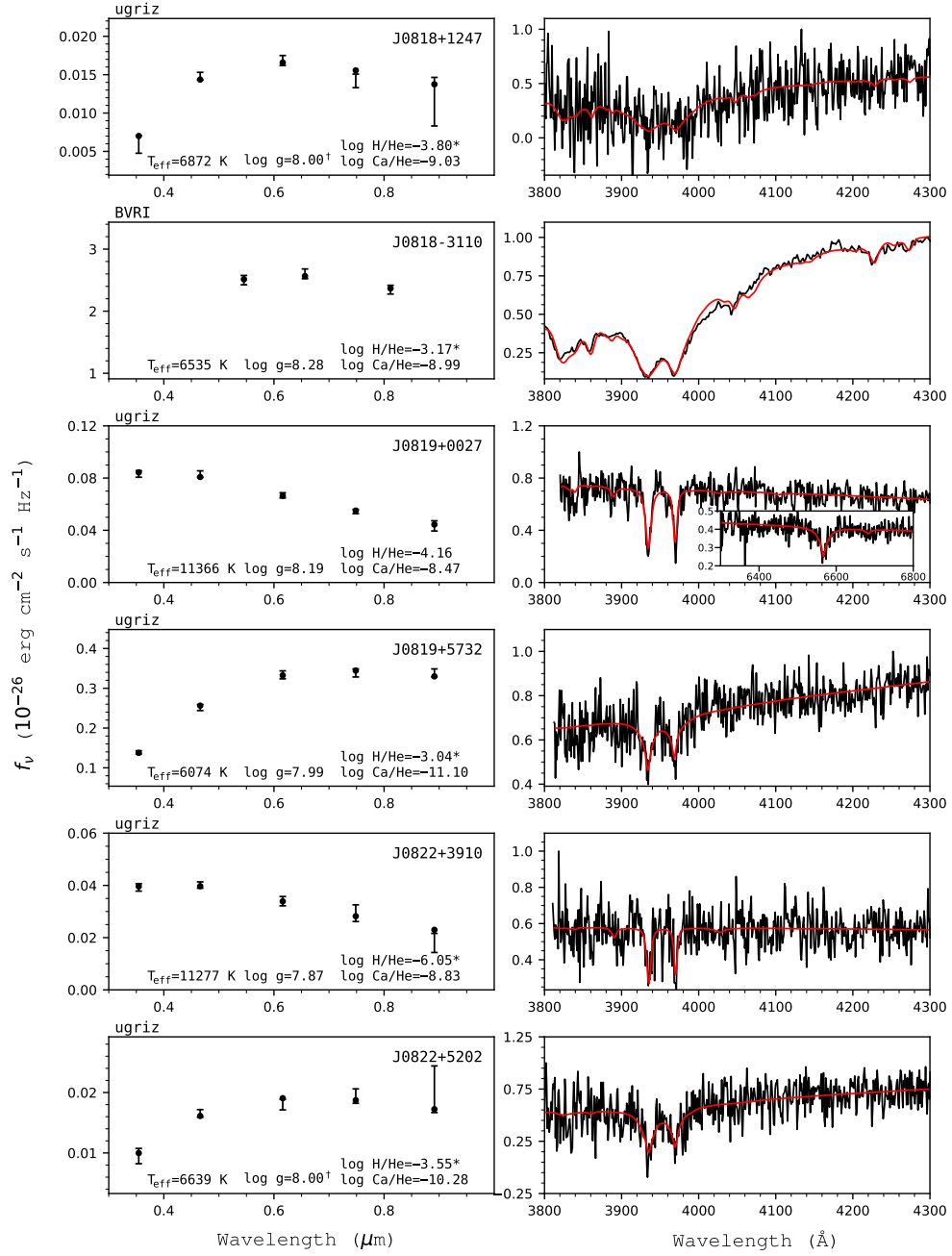


Figure 52. Fits to the DBZ/DZ(A) white dwarfs - continued.

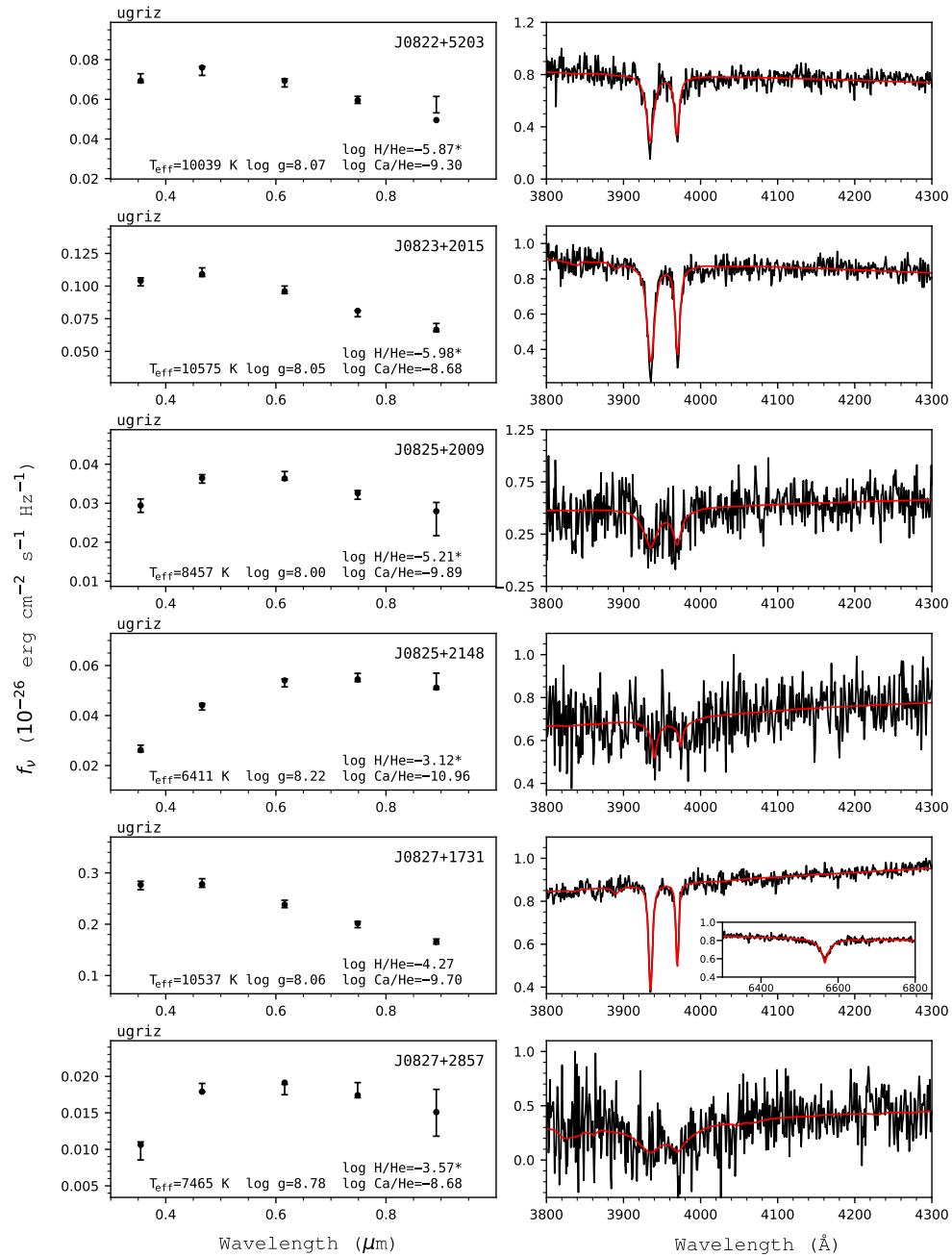


Figure 53. Fits to the DBZ/DZ(A) white dwarfs - continued.

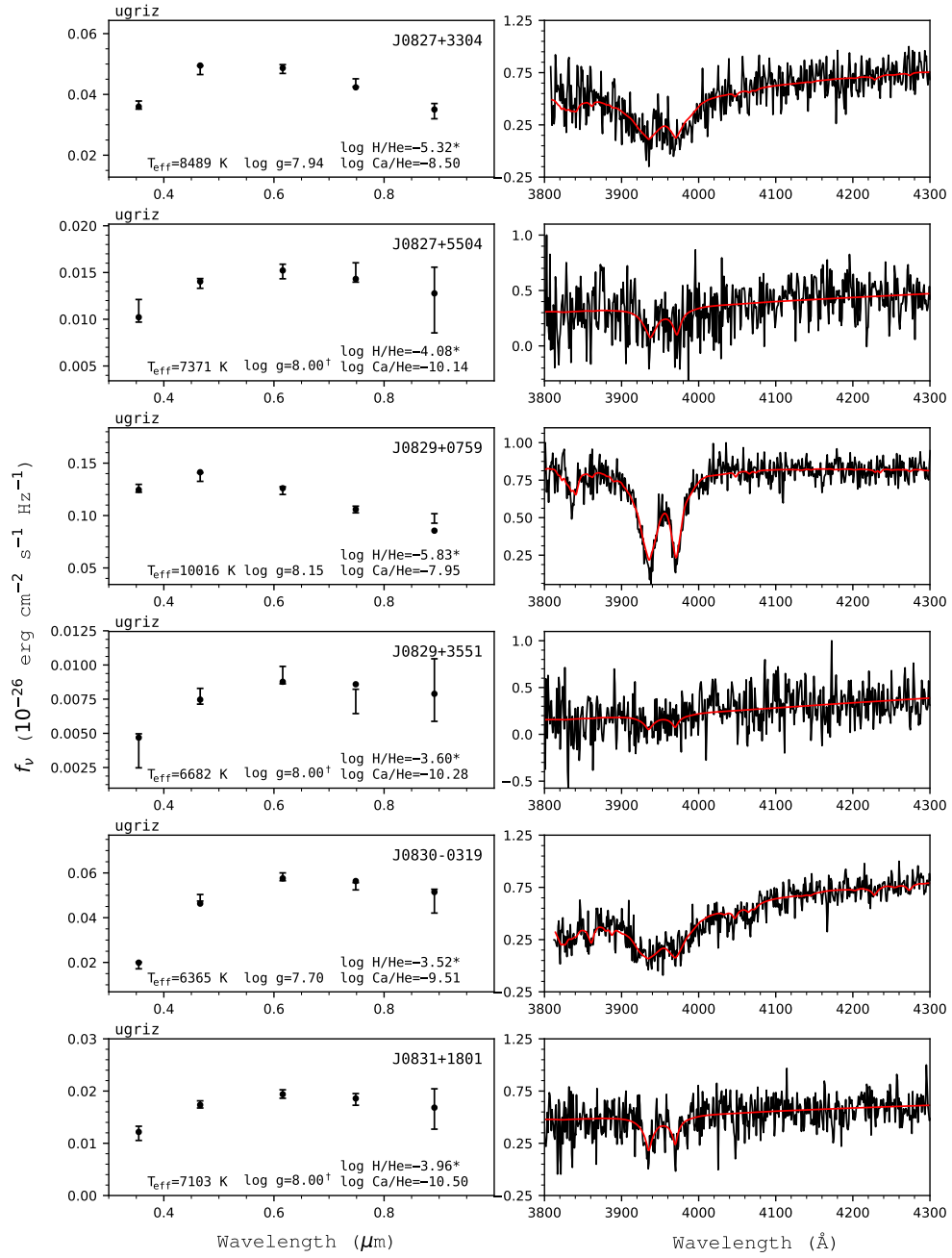


Figure 54. Fits to the DBZ/DZ(A) white dwarfs - continued.

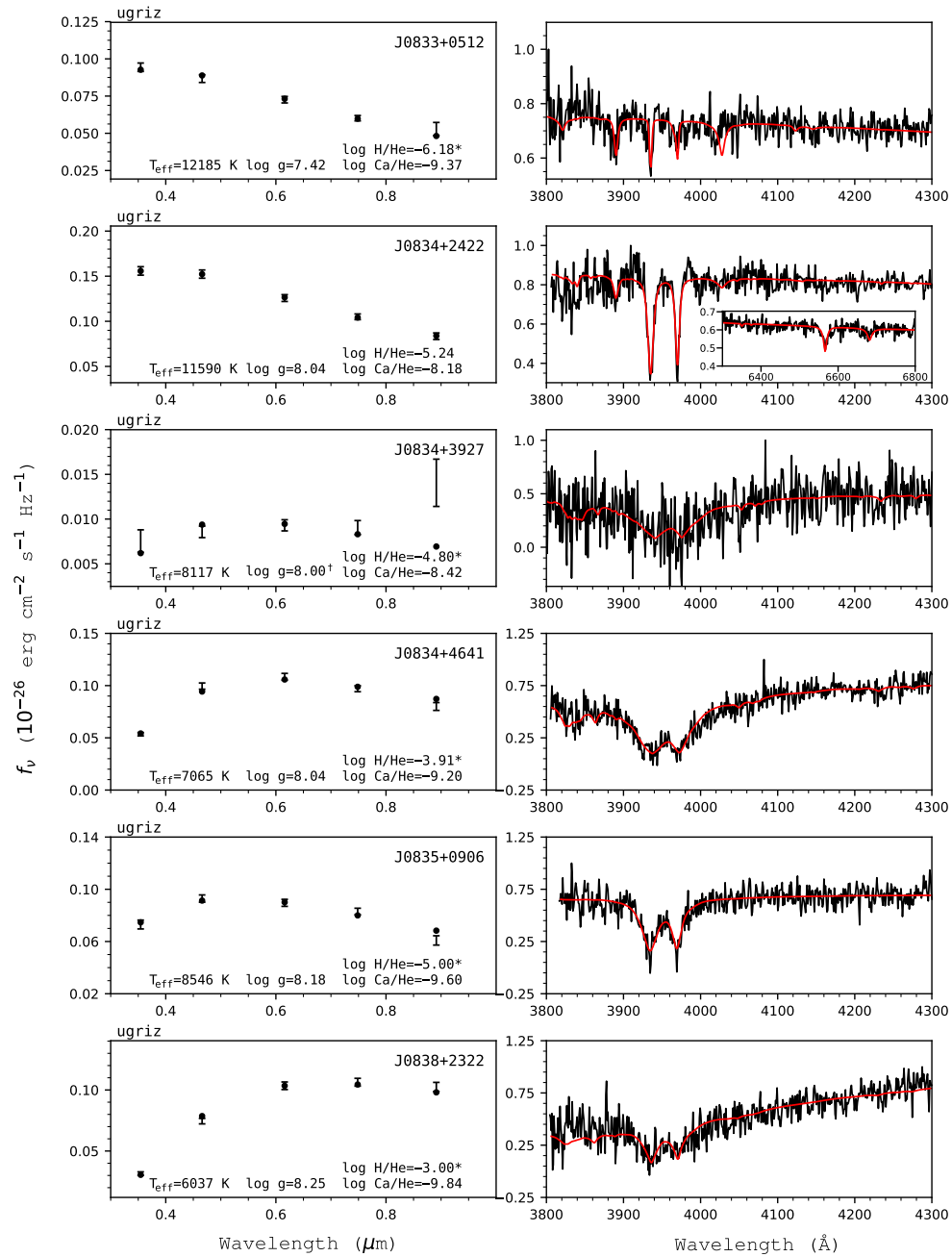


Figure 55. Fits to the DBZ/DZ(A) white dwarfs - continued.

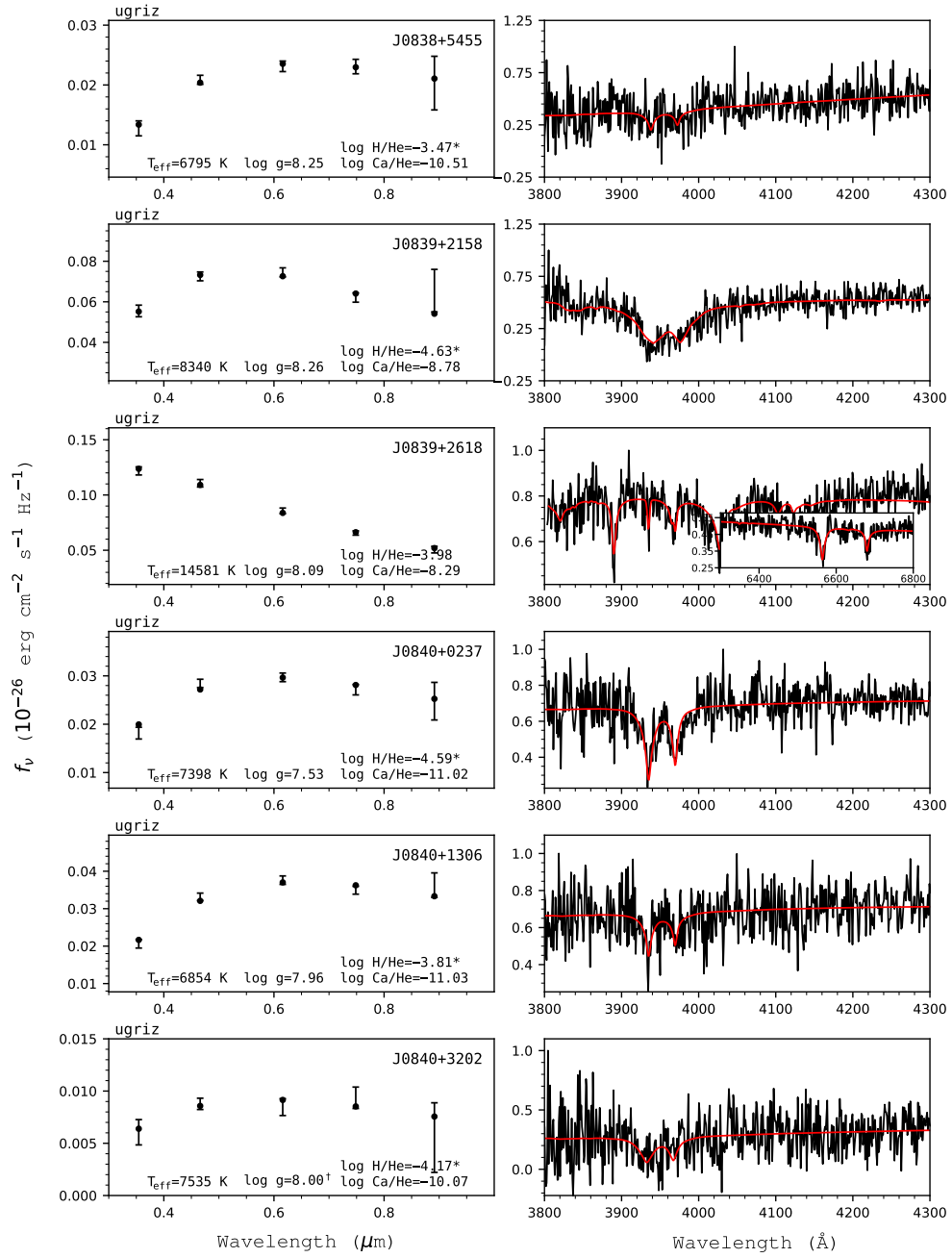


Figure 56. Fits to the DBZ/DZ(A) white dwarfs - continued.

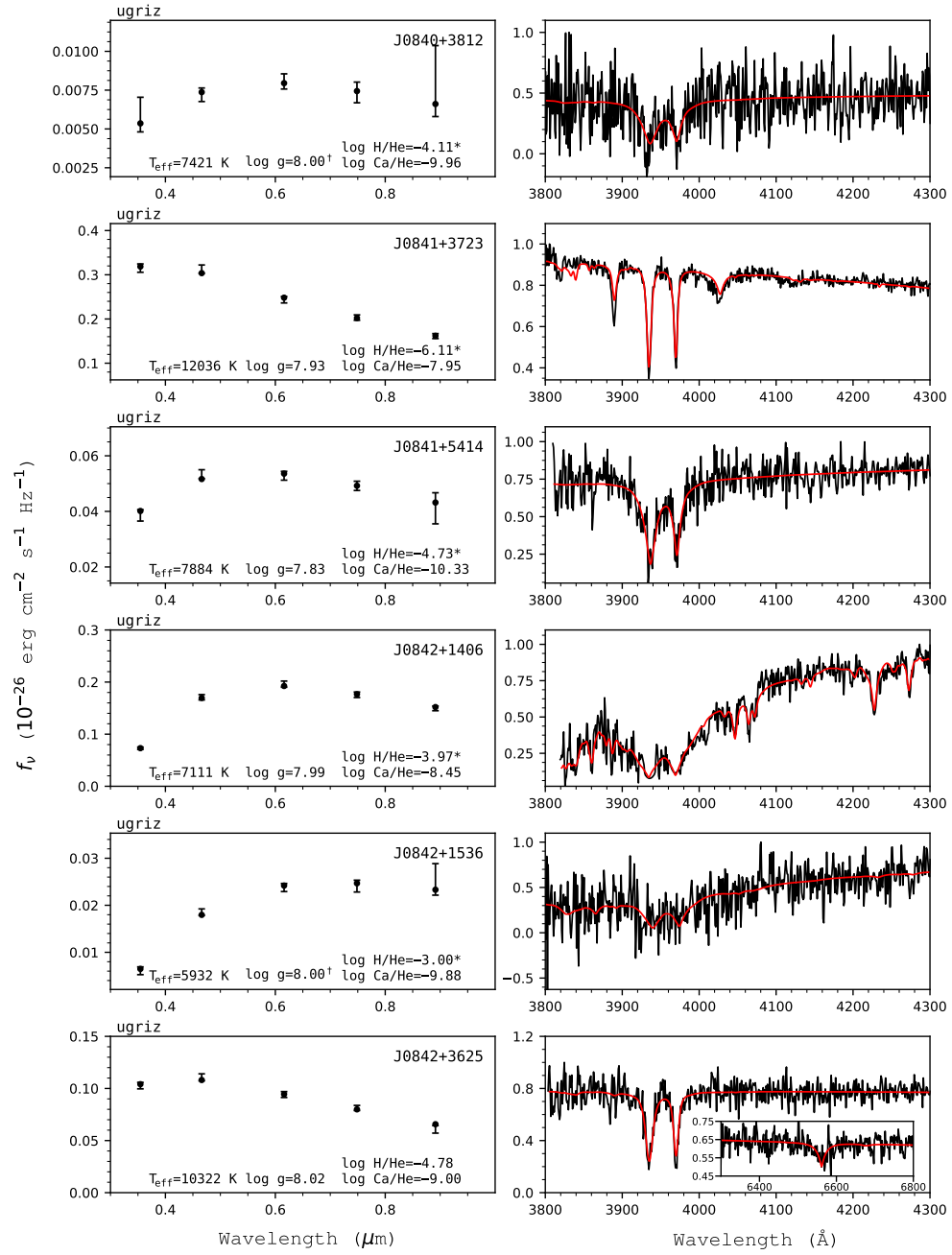


Figure 57. Fits to the DBZ/DZ(A) white dwarfs - continued.

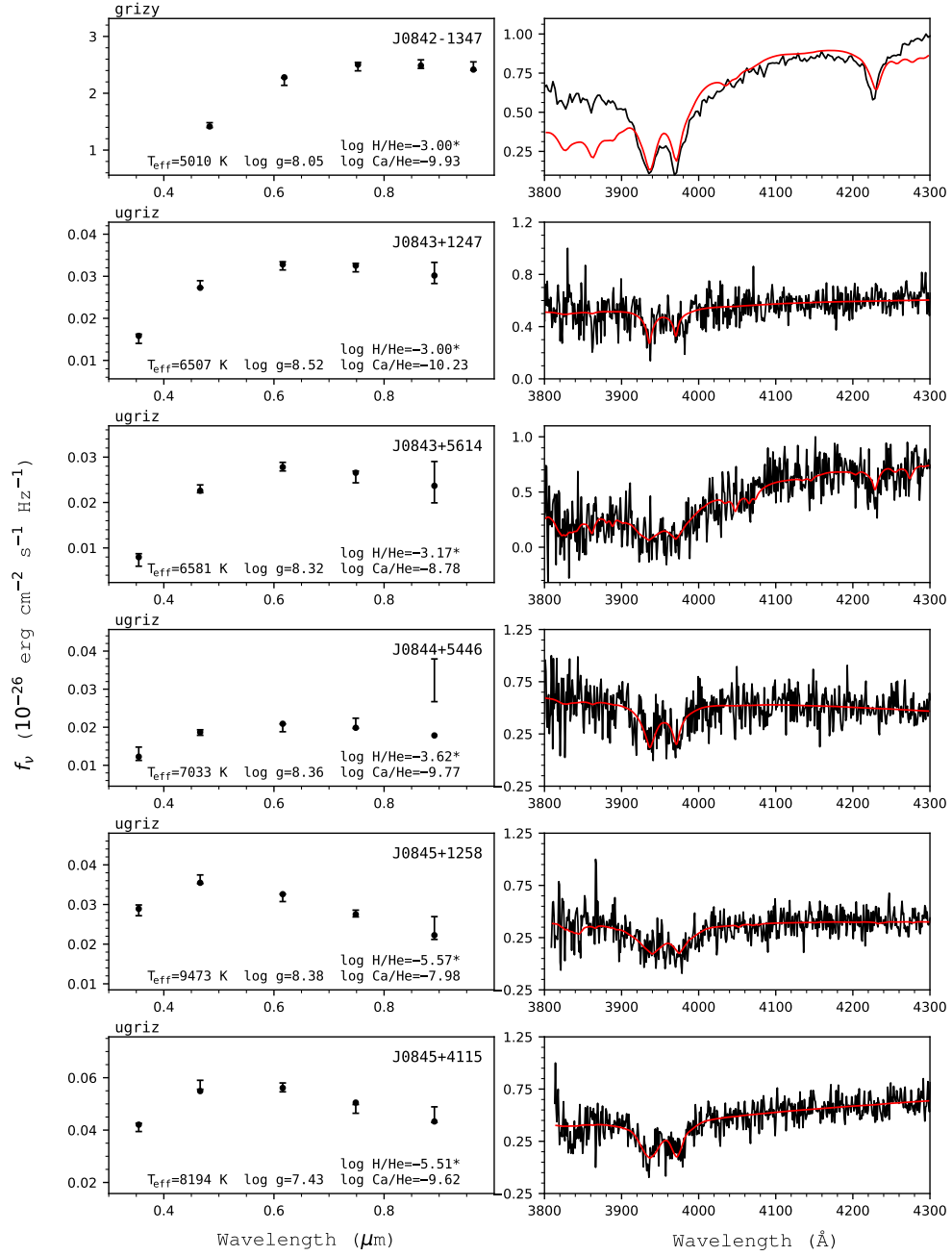


Figure 58. Fits to the DBZ/DZ(A) white dwarfs - continued.

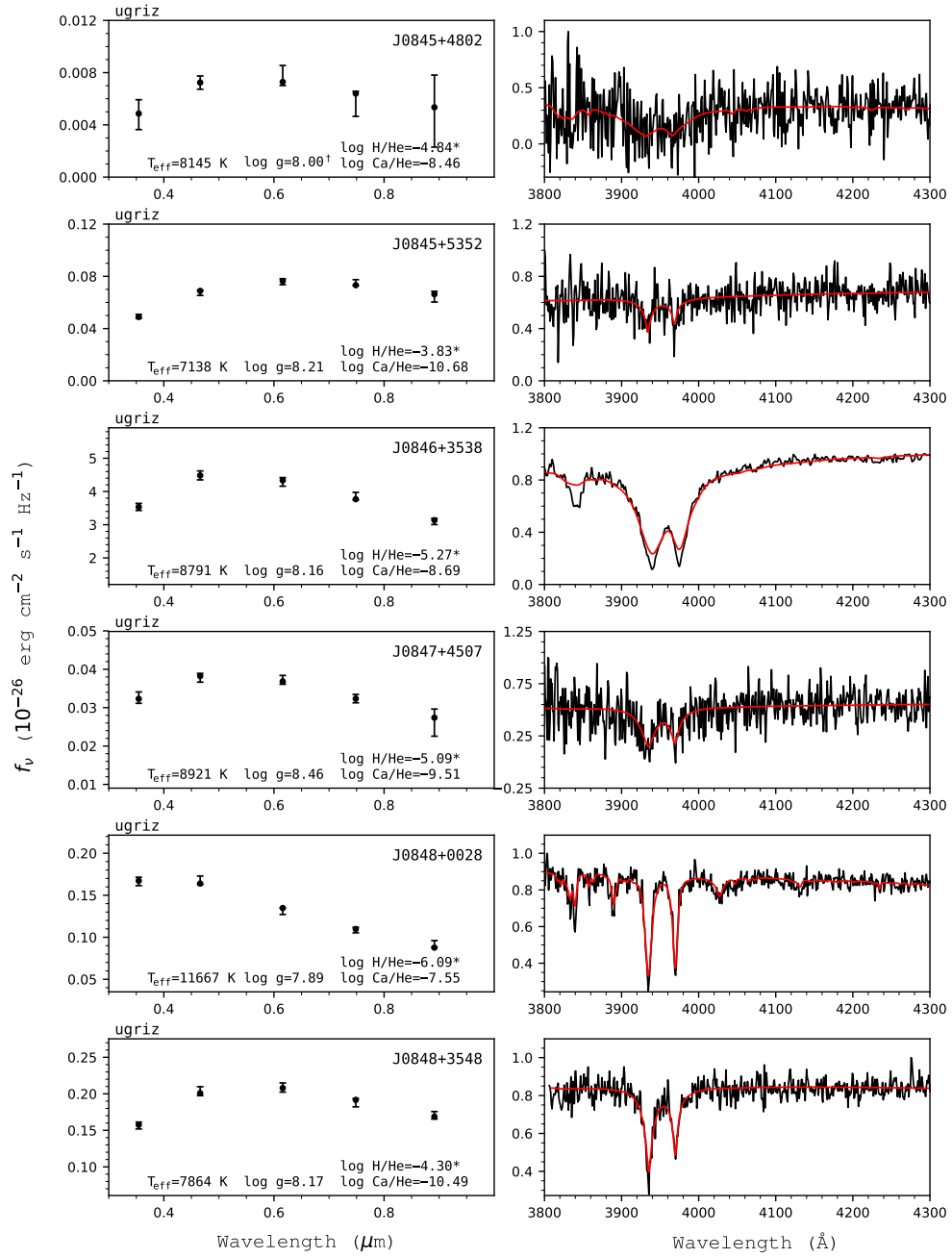


Figure 59. Fits to the DBZ/DZ(A) white dwarfs - continued.

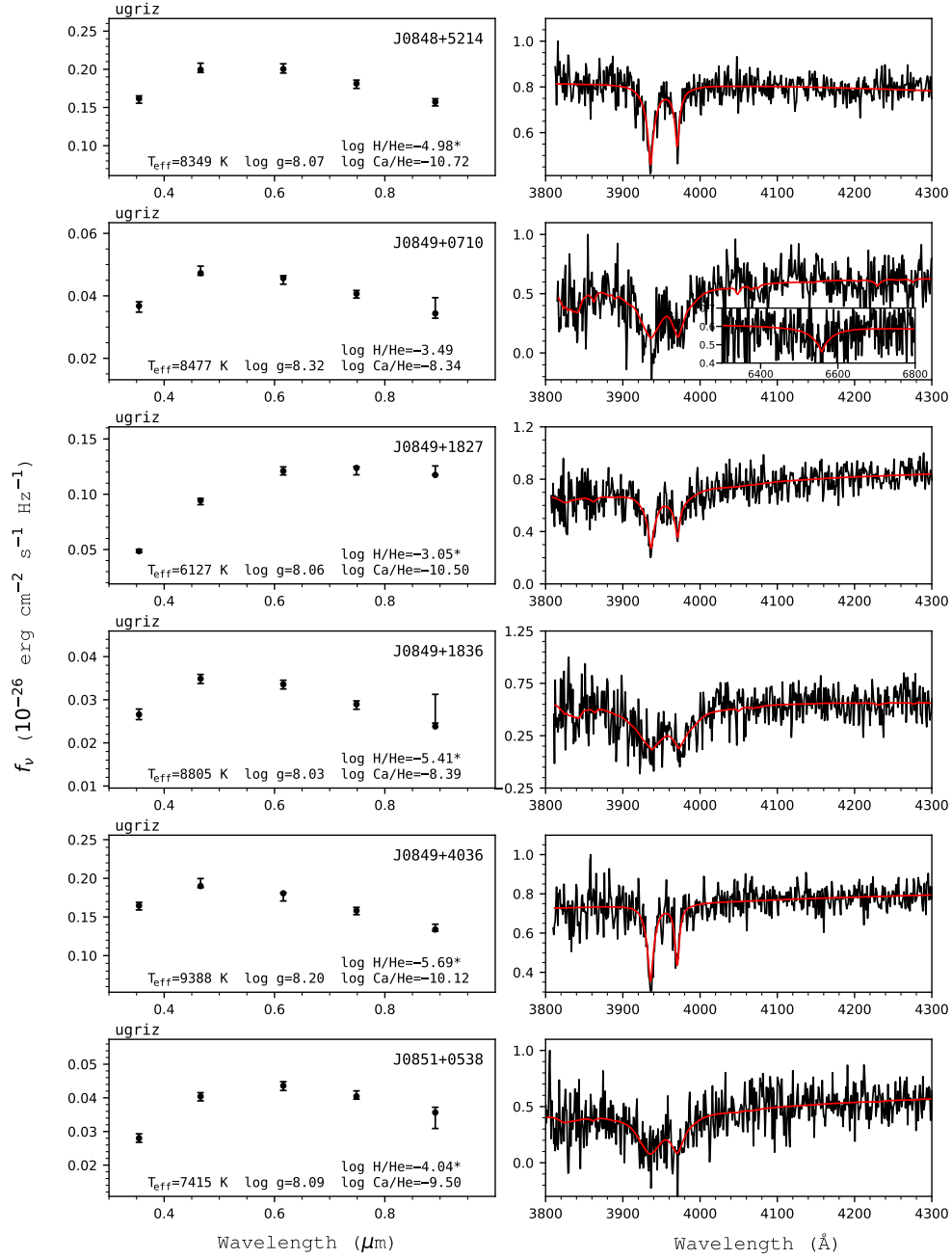


Figure 60. Fits to the DBZ/DZ(A) white dwarfs - continued.

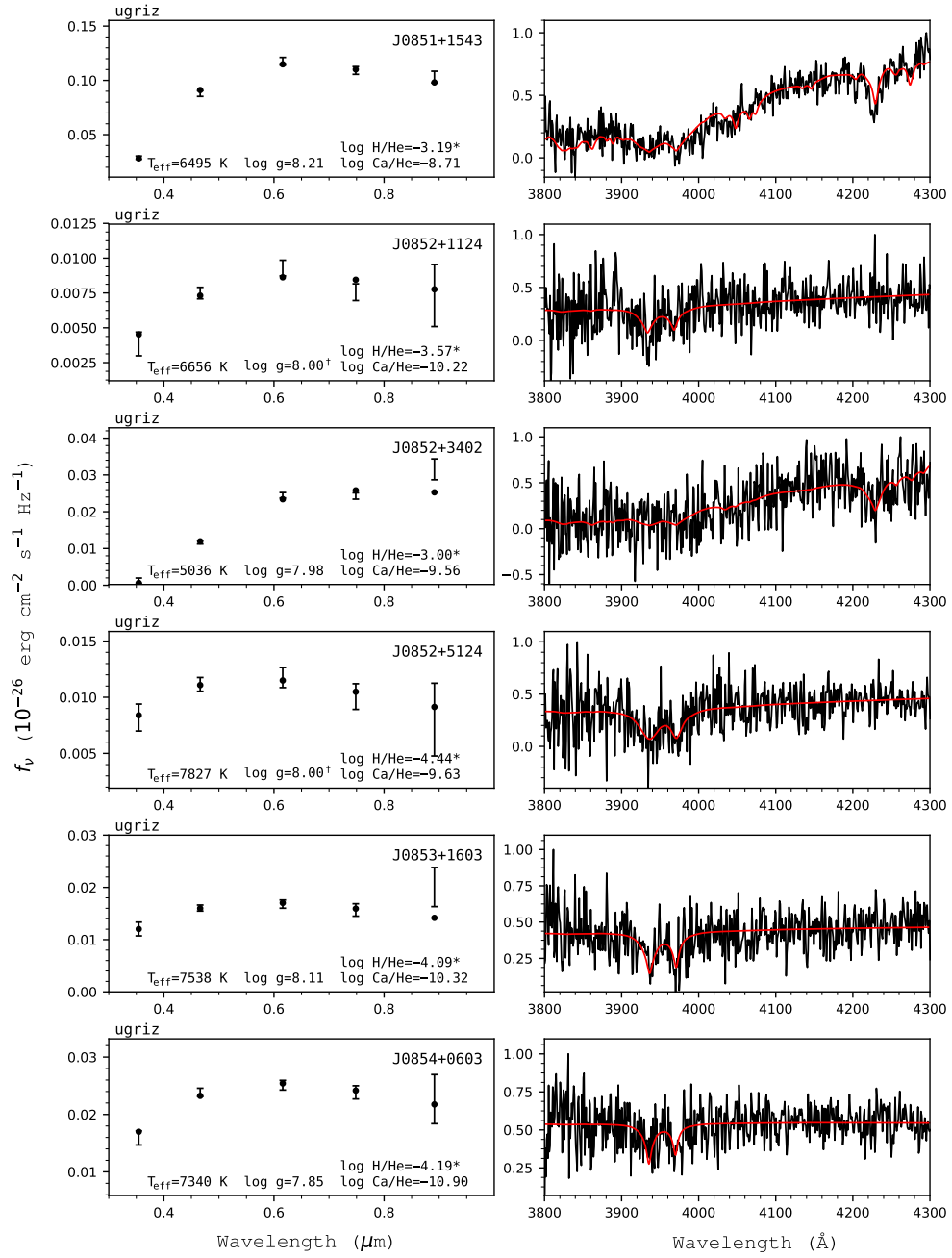


Figure 61. Fits to the DBZ/DZ(A) white dwarfs - continued.

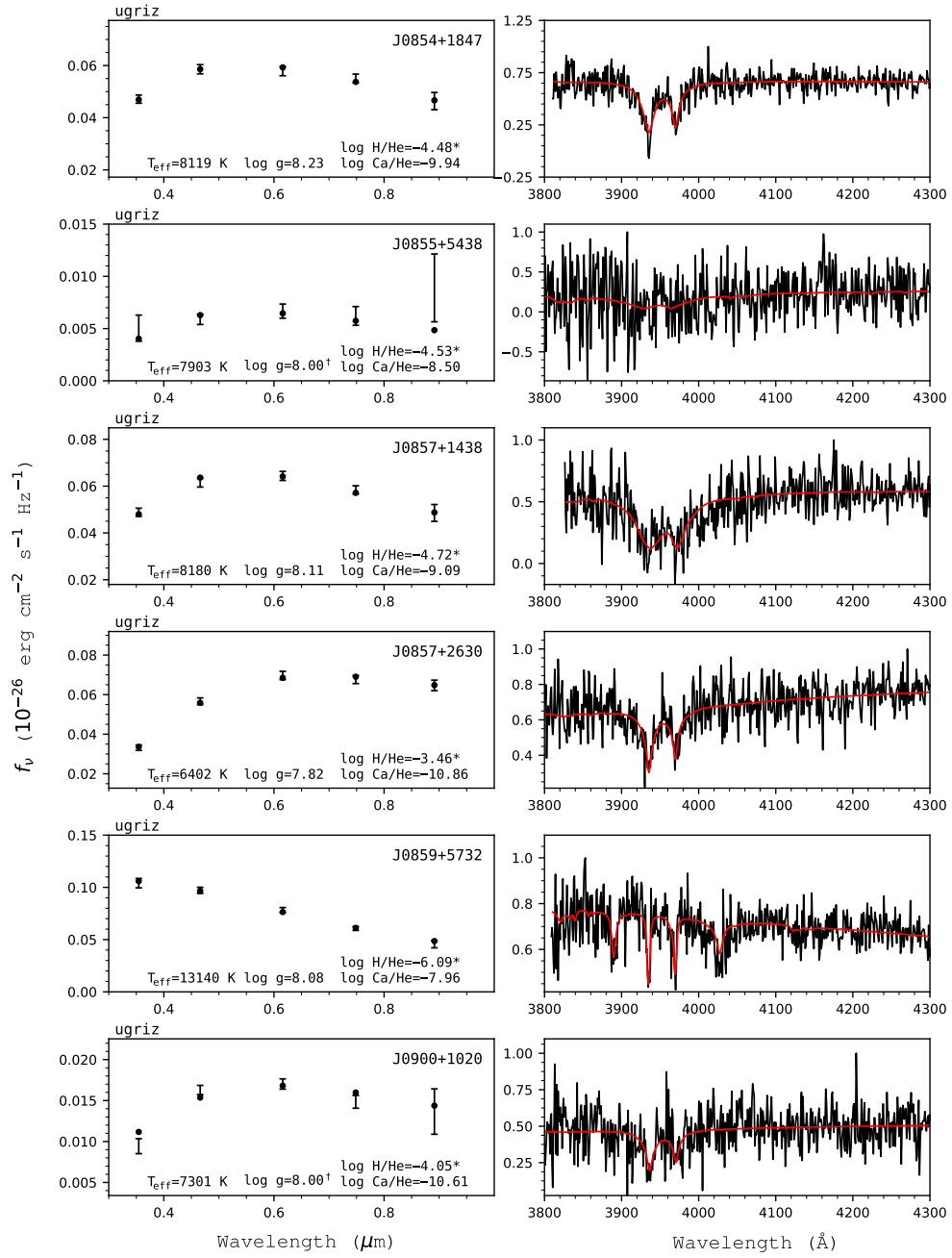


Figure 62. Fits to the DBZ/DZ(A) white dwarfs - continued.

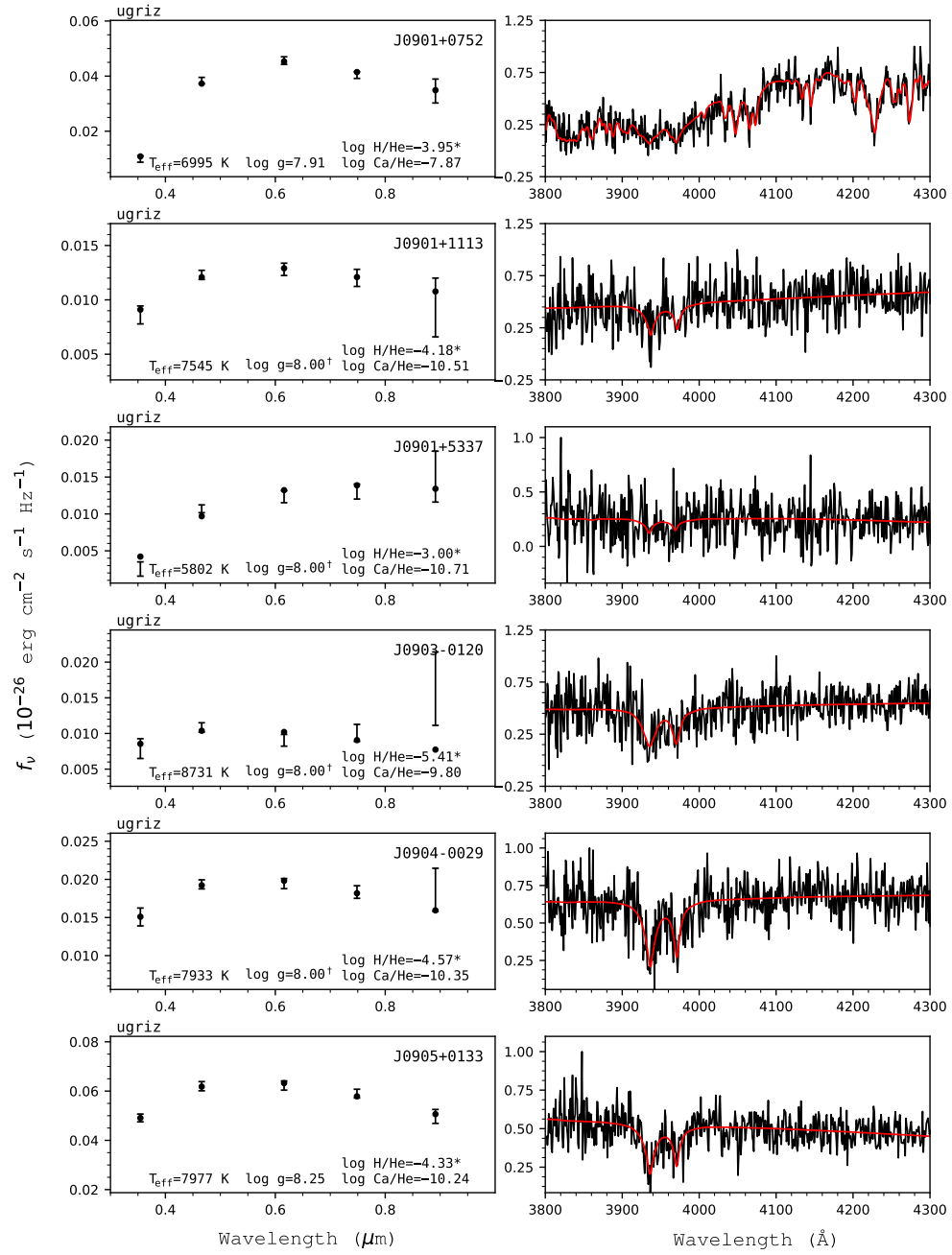


Figure 63. Fits to the DBZ/DZ(A) white dwarfs - continued.

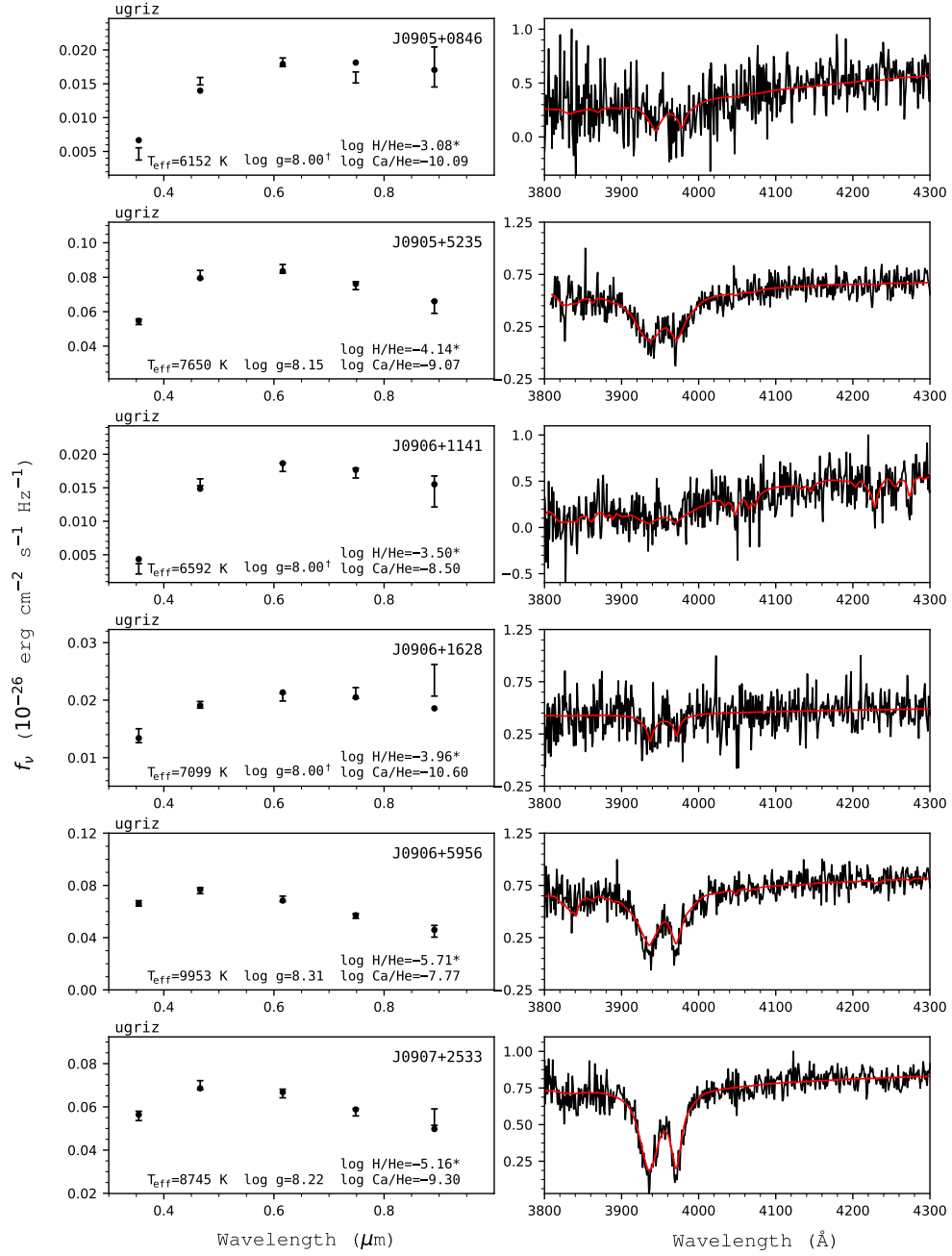


Figure 64. Fits to the DBZ/DZ(A) white dwarfs - continued.

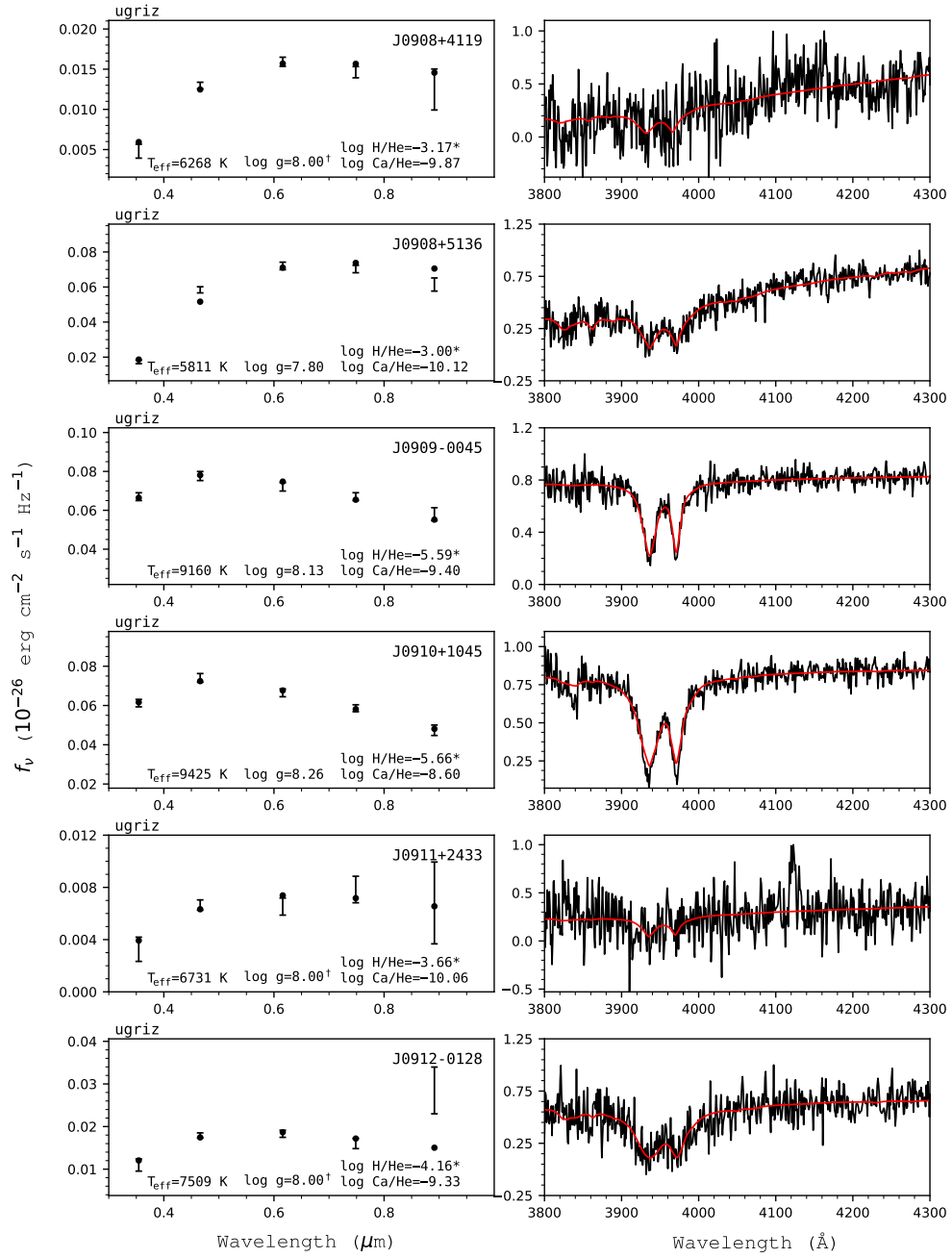


Figure 65. Fits to the DBZ/DZ(A) white dwarfs - continued.

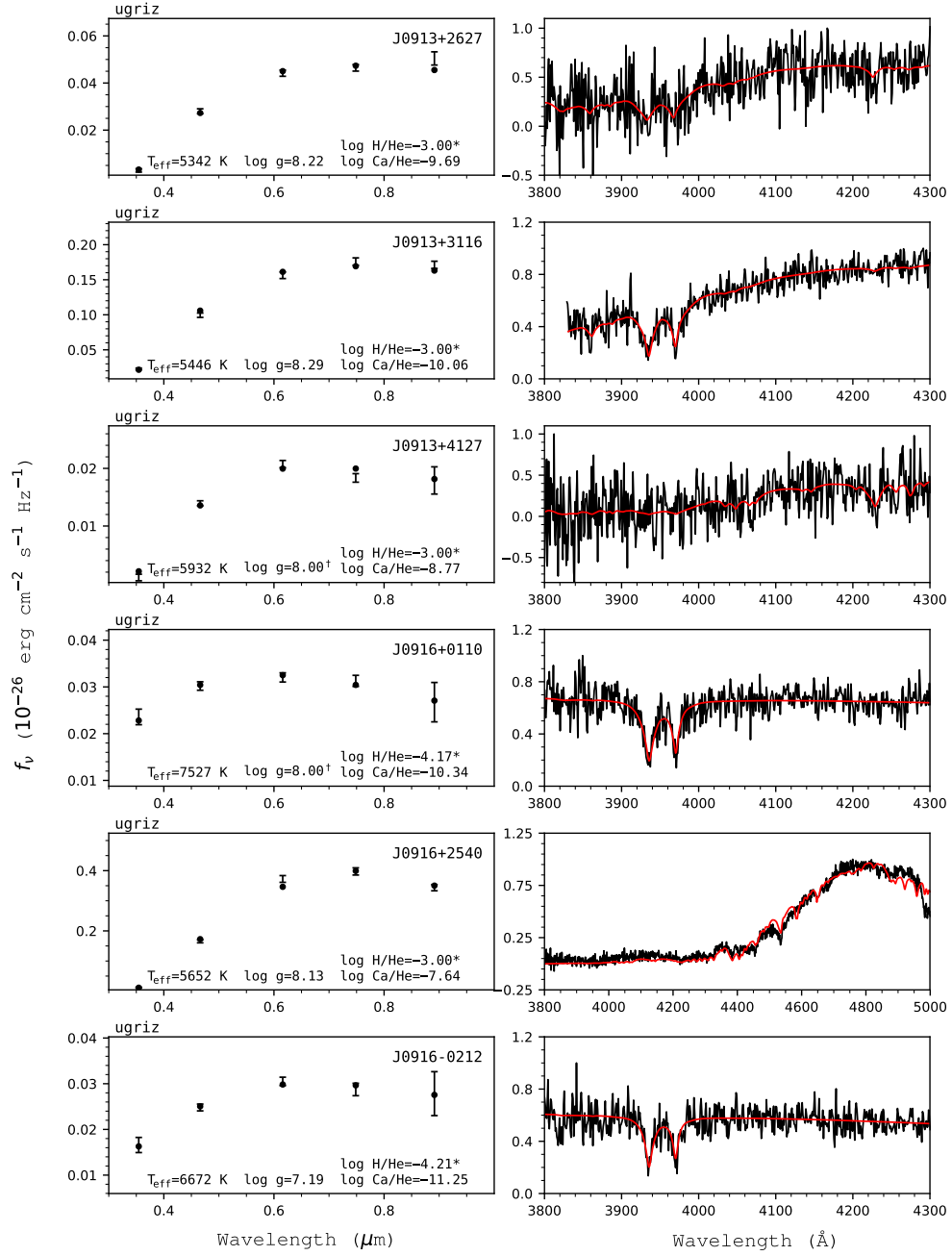


Figure 66. Fits to the DBZ/DZ(A) white dwarfs - continued.

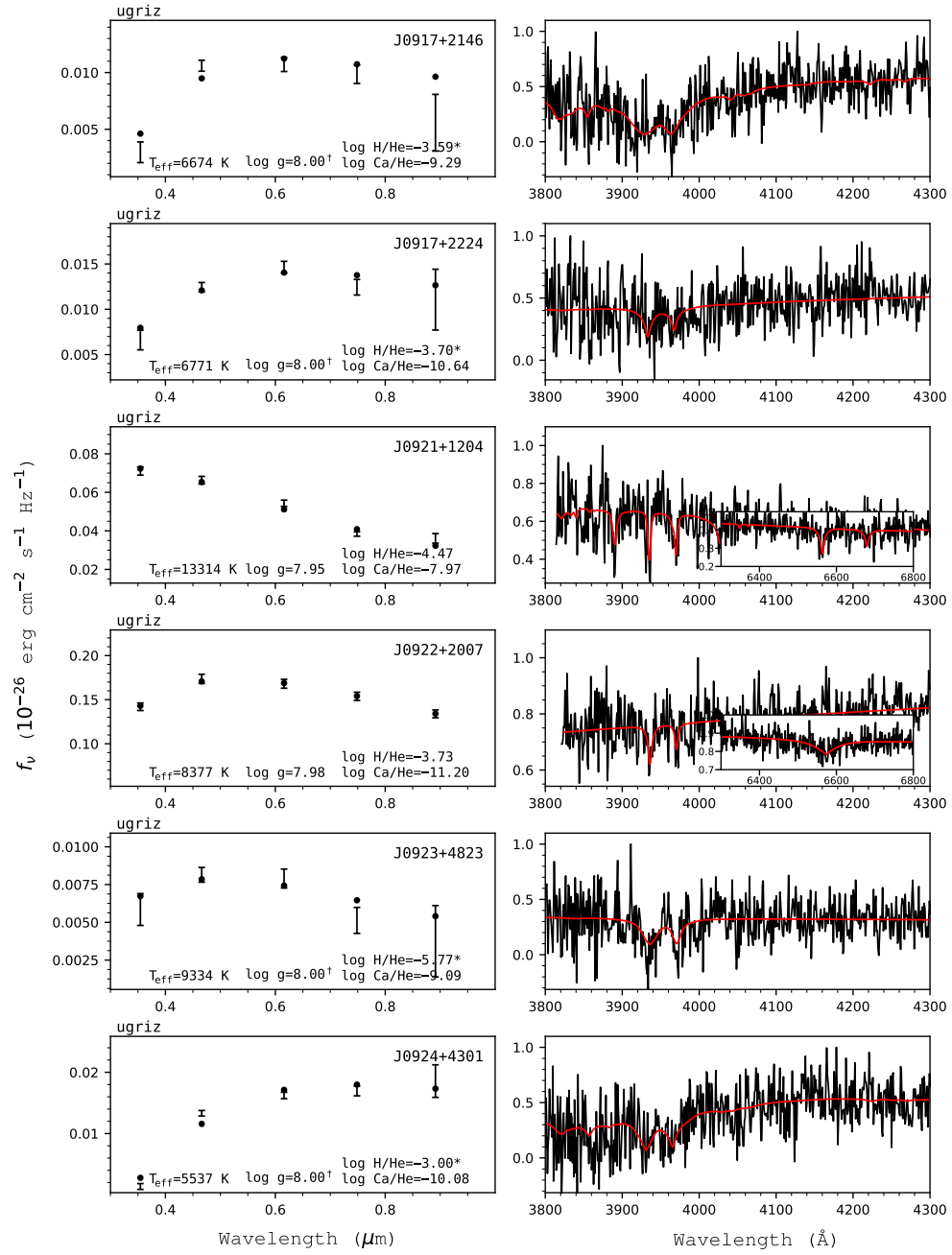


Figure 67. Fits to the DBZ/DZ(A) white dwarfs - continued.

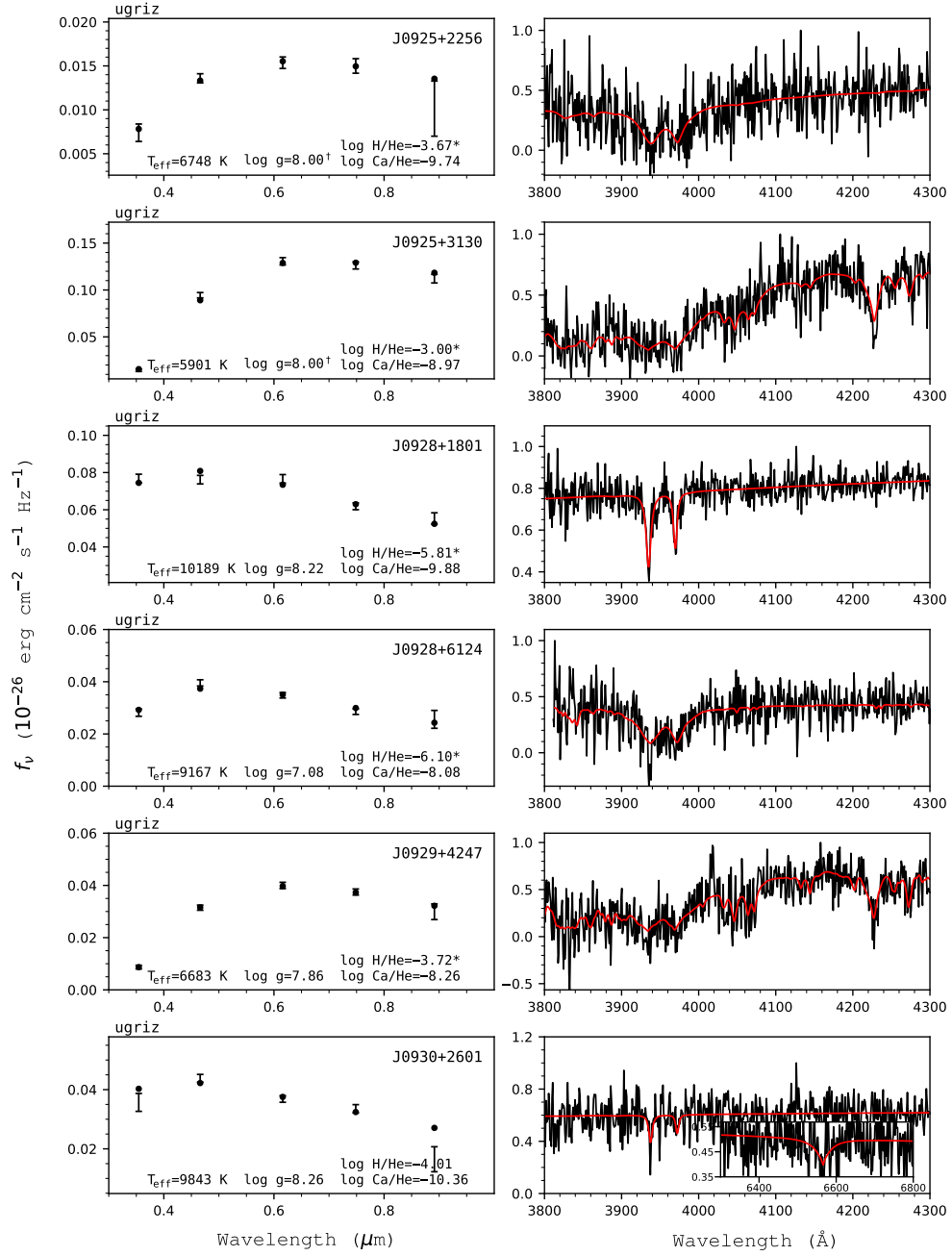


Figure 68. Fits to the DBZ/DZ(A) white dwarfs - continued.

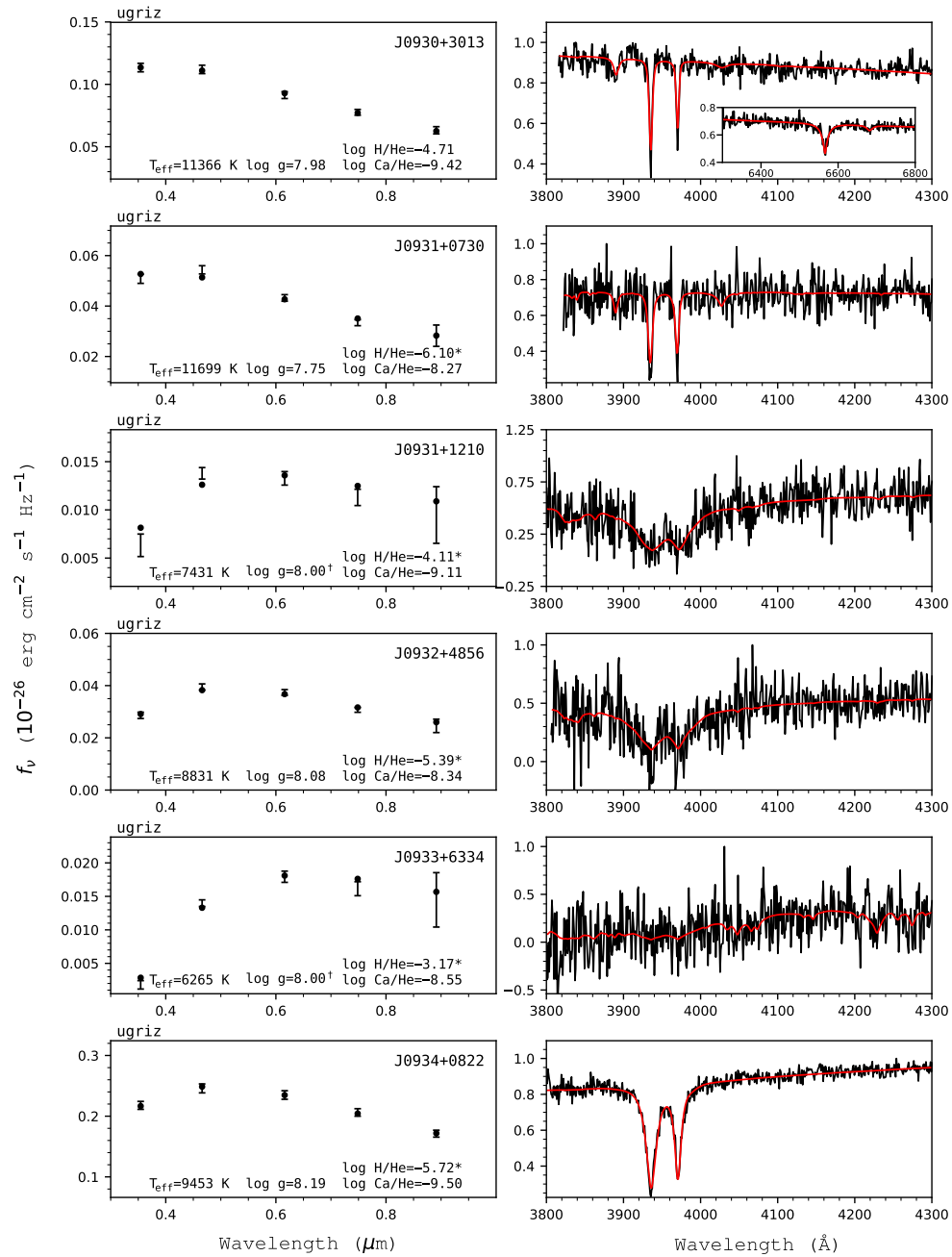


Figure 69. Fits to the DBZ/DZ(A) white dwarfs - continued.

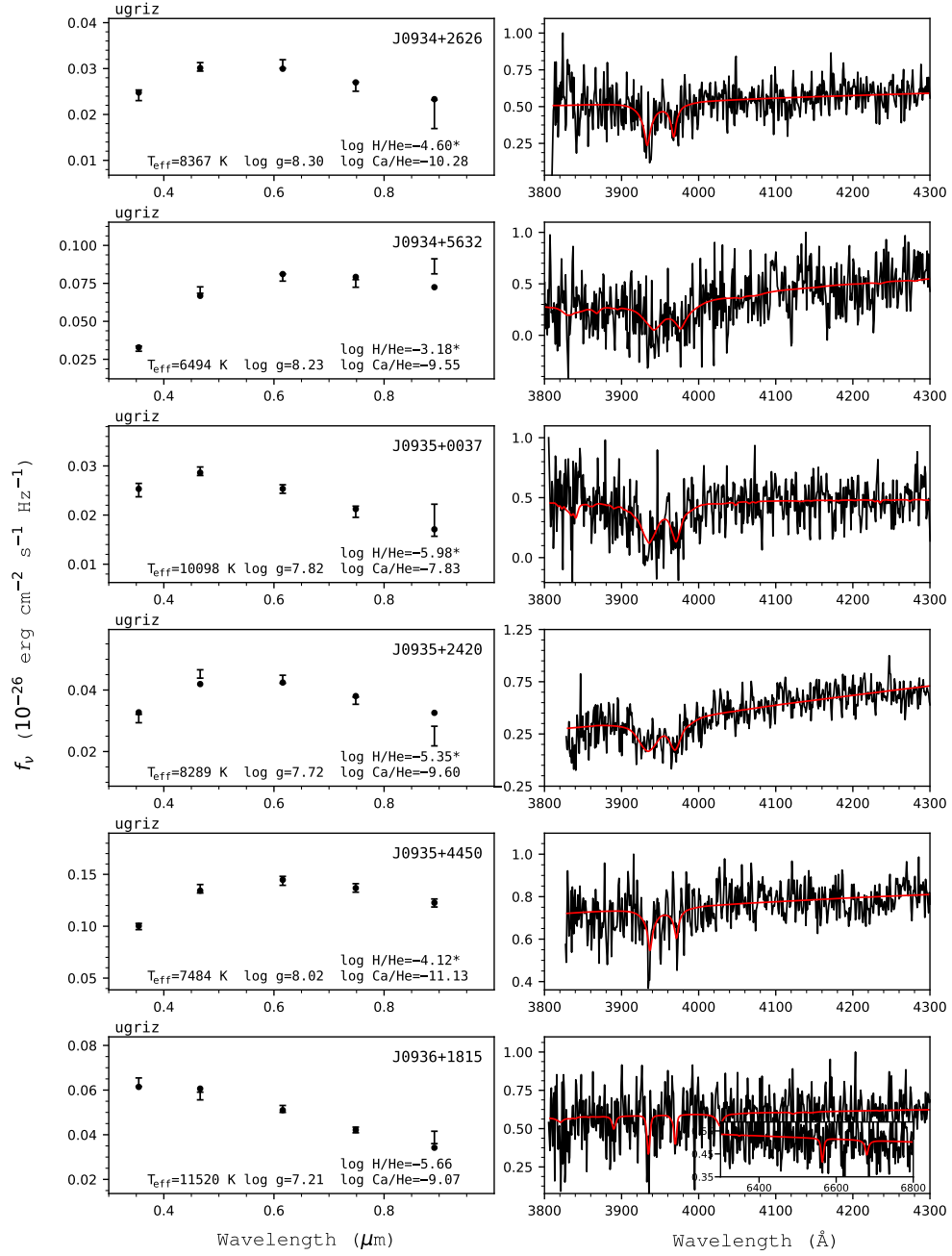


Figure 70. Fits to the DBZ/DZ(A) white dwarfs - continued.

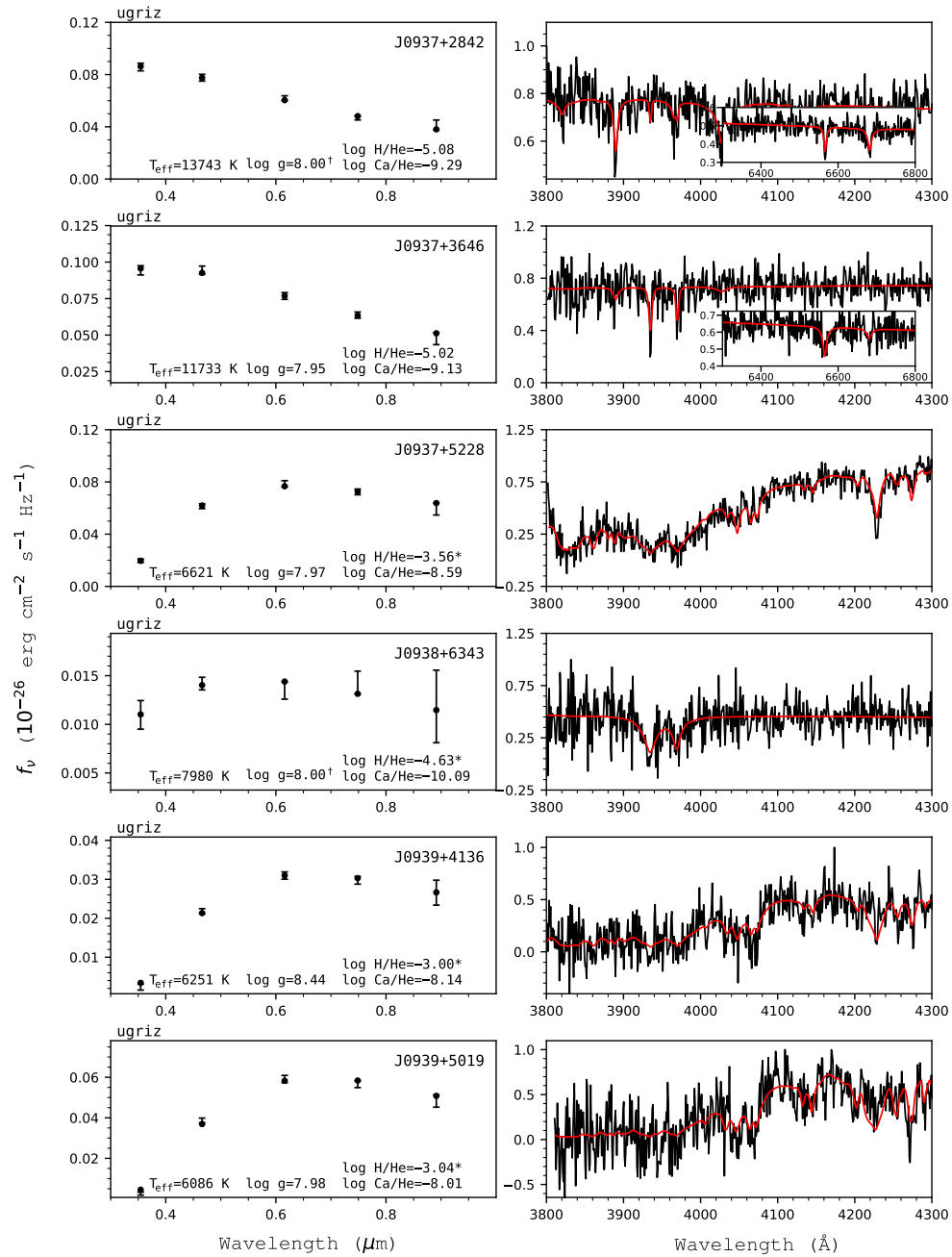


Figure 71. Fits to the DBZ/DZ(A) white dwarfs - continued.

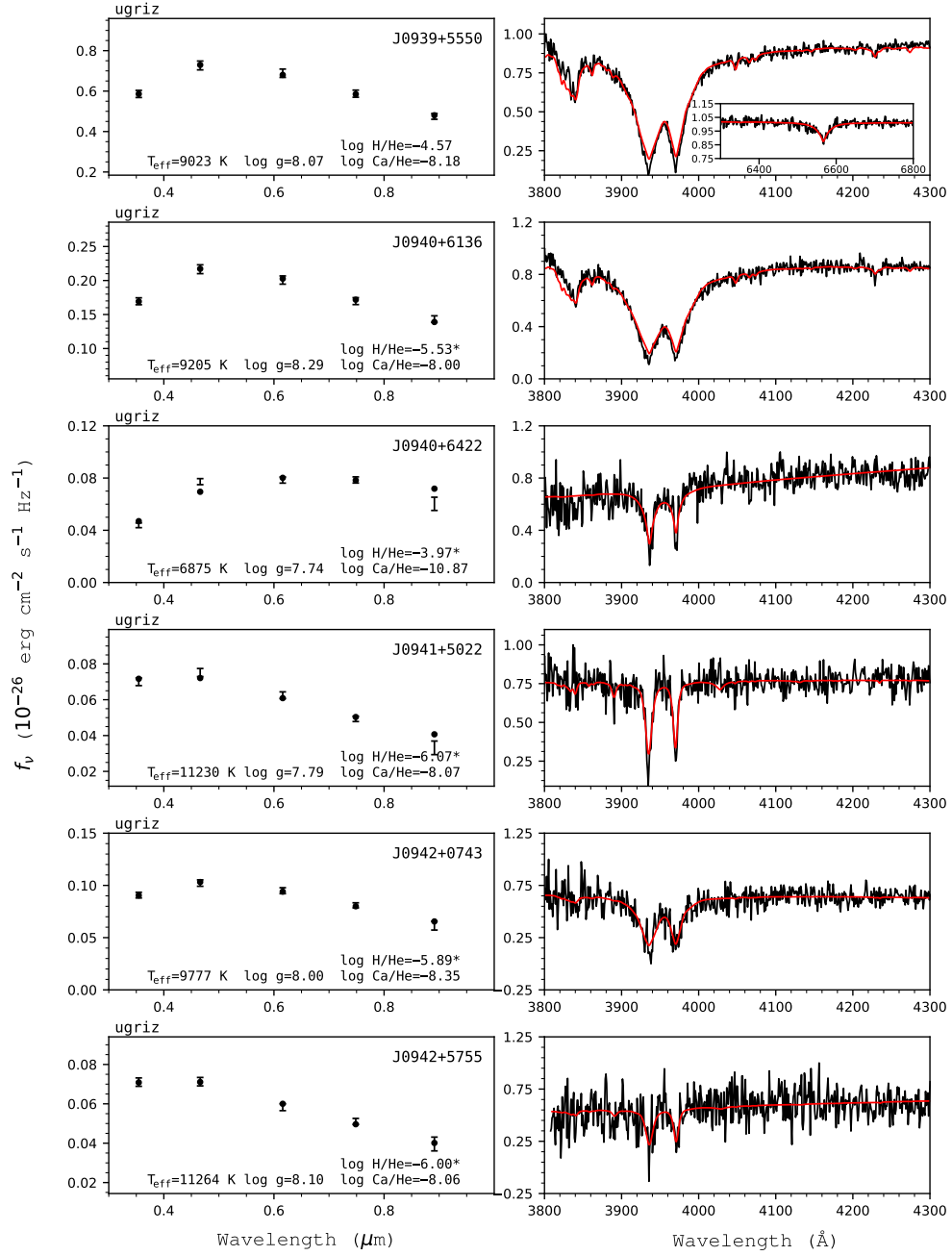


Figure 72. Fits to the DBZ/DZ(A) white dwarfs - continued.

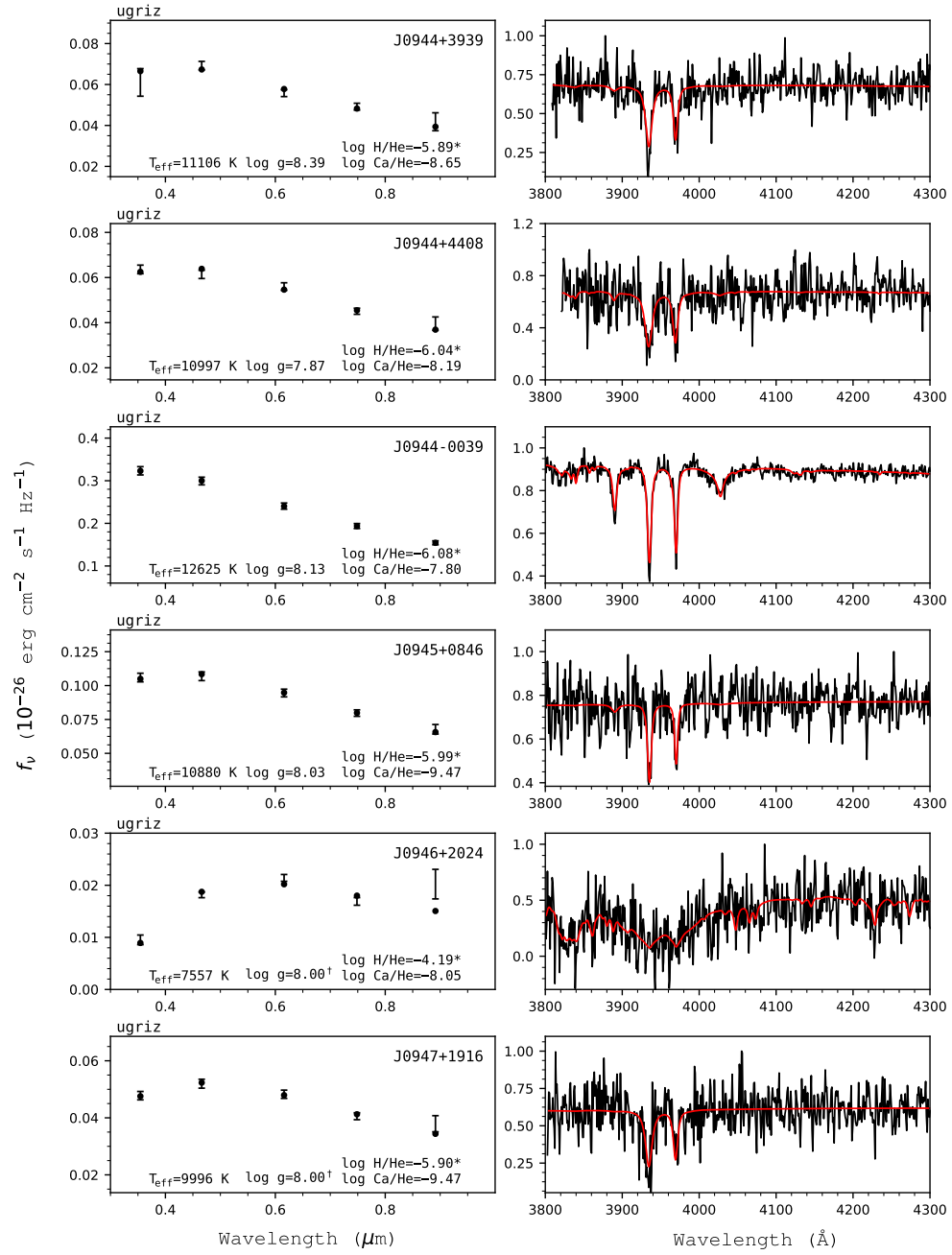


Figure 73. Fits to the DBZ/DZ(A) white dwarfs - continued.

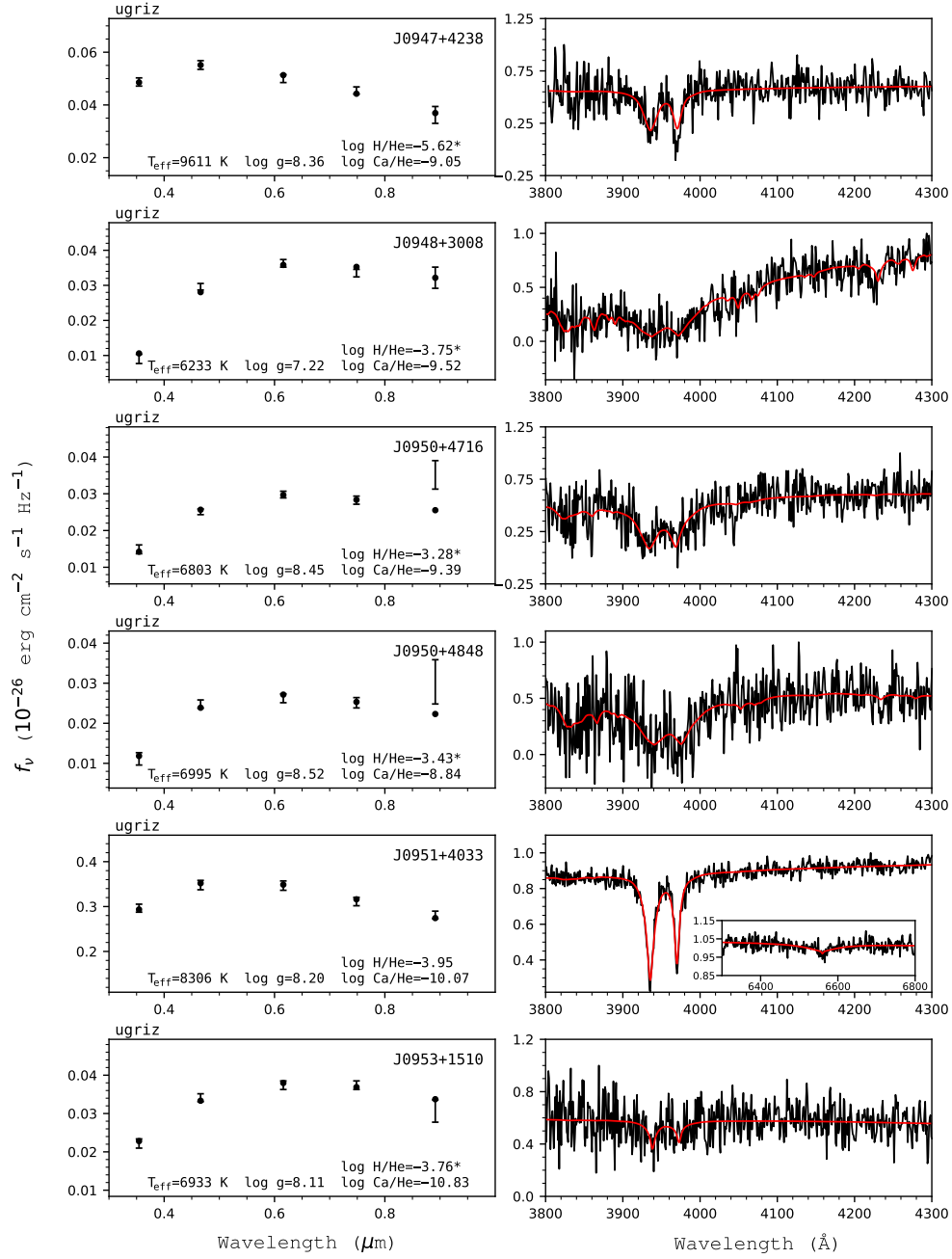


Figure 74. Fits to the DBZ/DZ(A) white dwarfs - continued.

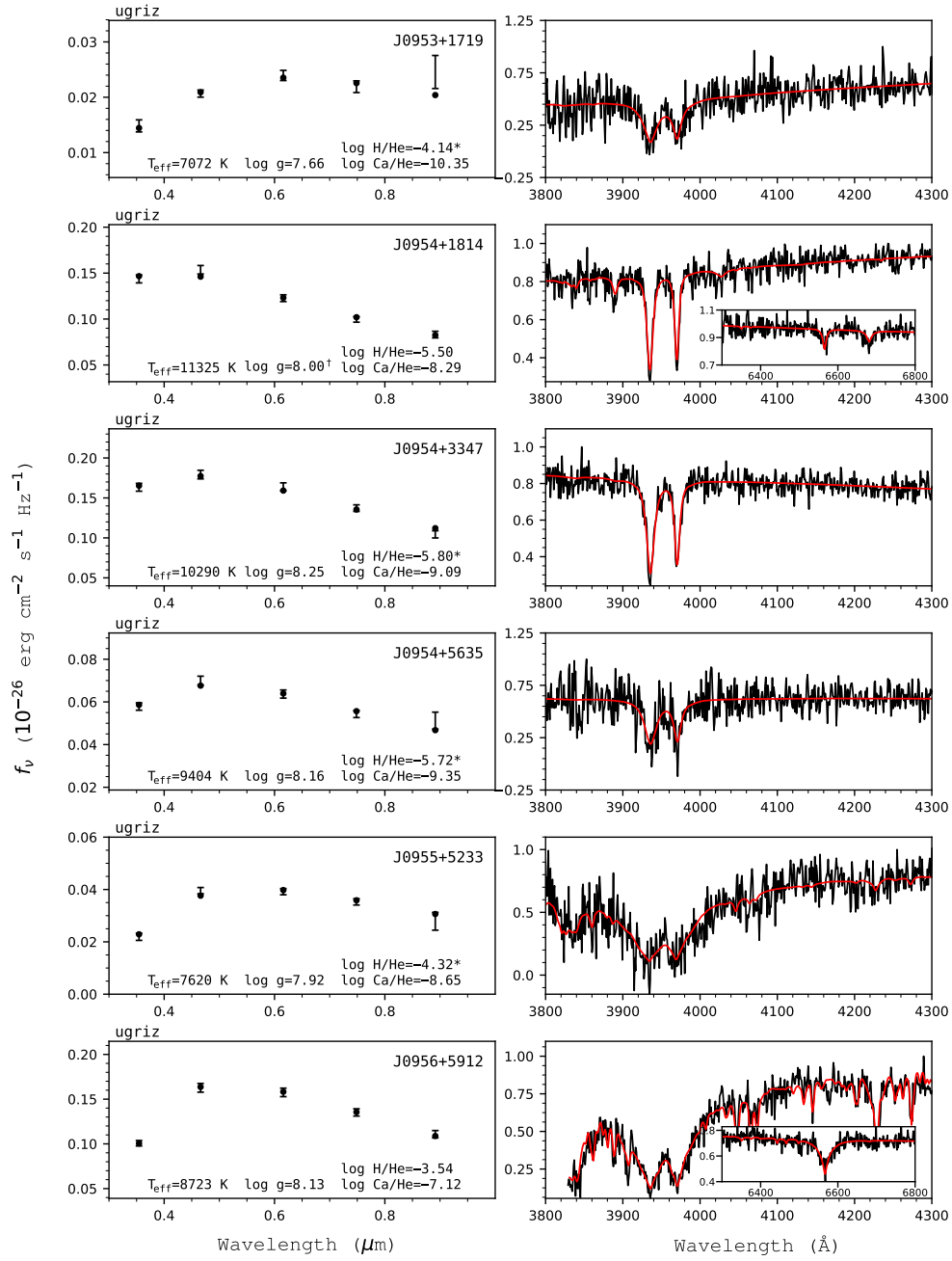


Figure 75. Fits to the DBZ/DZ(A) white dwarfs - continued.

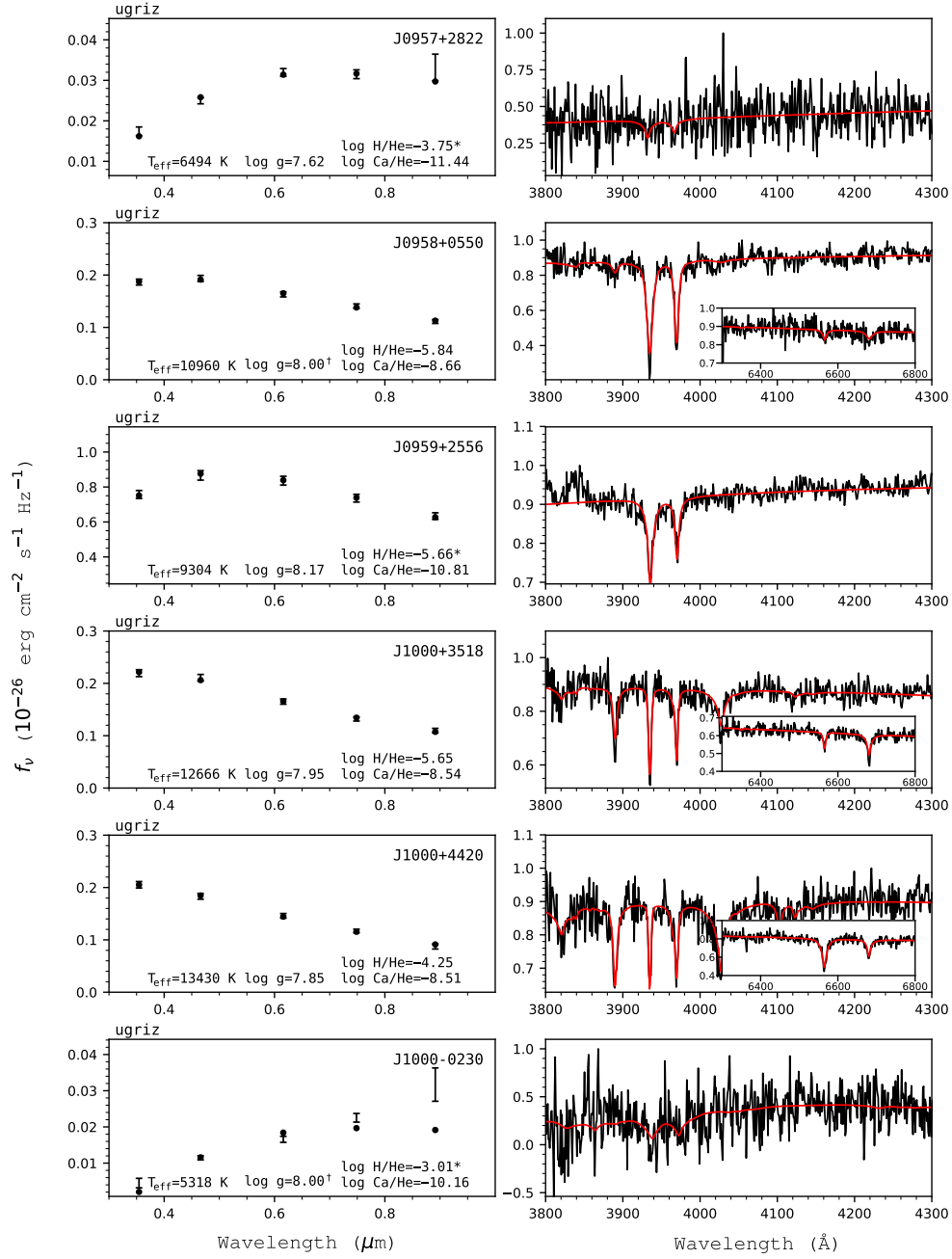


Figure 76. Fits to the DBZ/DZ(A) white dwarfs - continued.

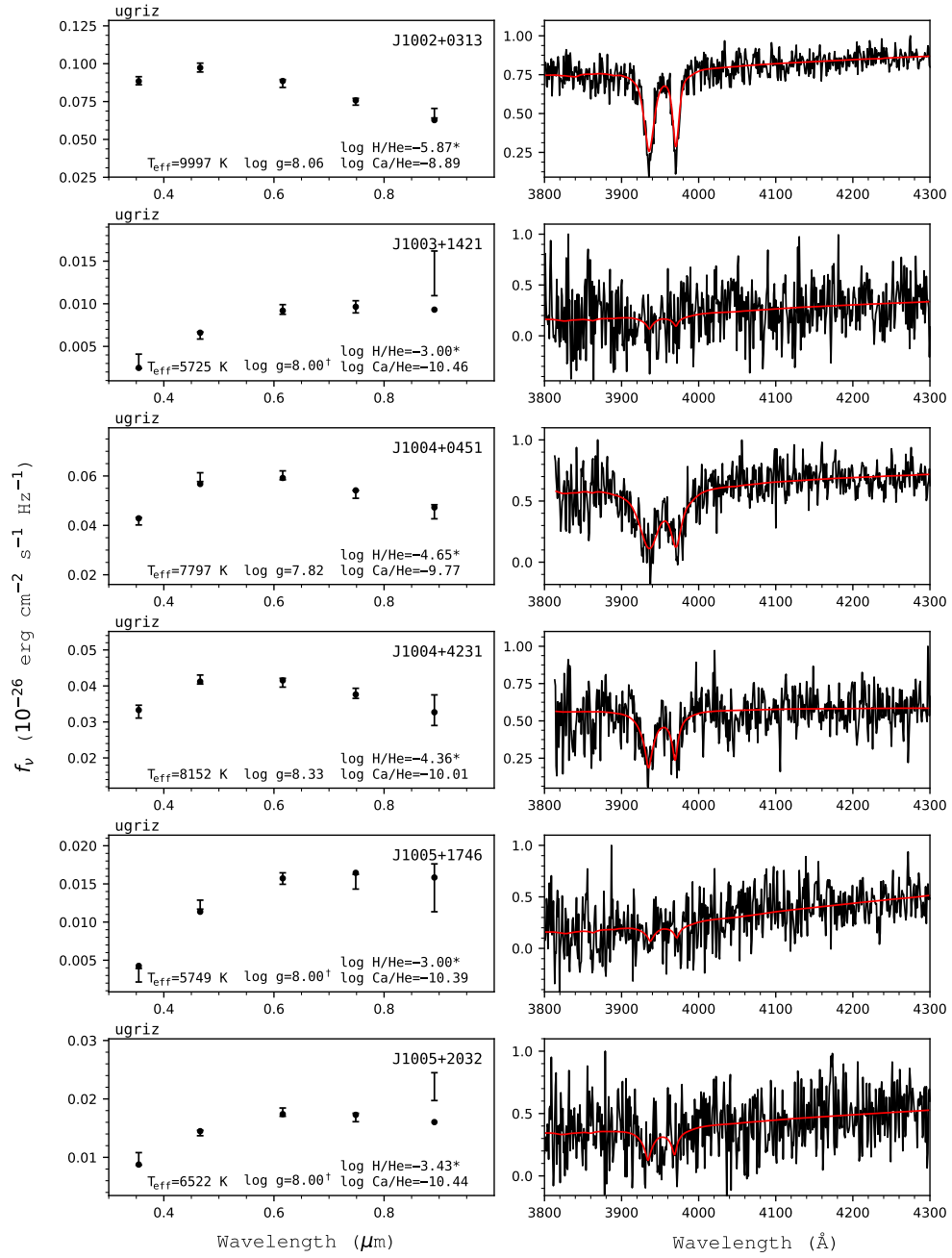


Figure 77. Fits to the DBZ/DZ(A) white dwarfs - continued.

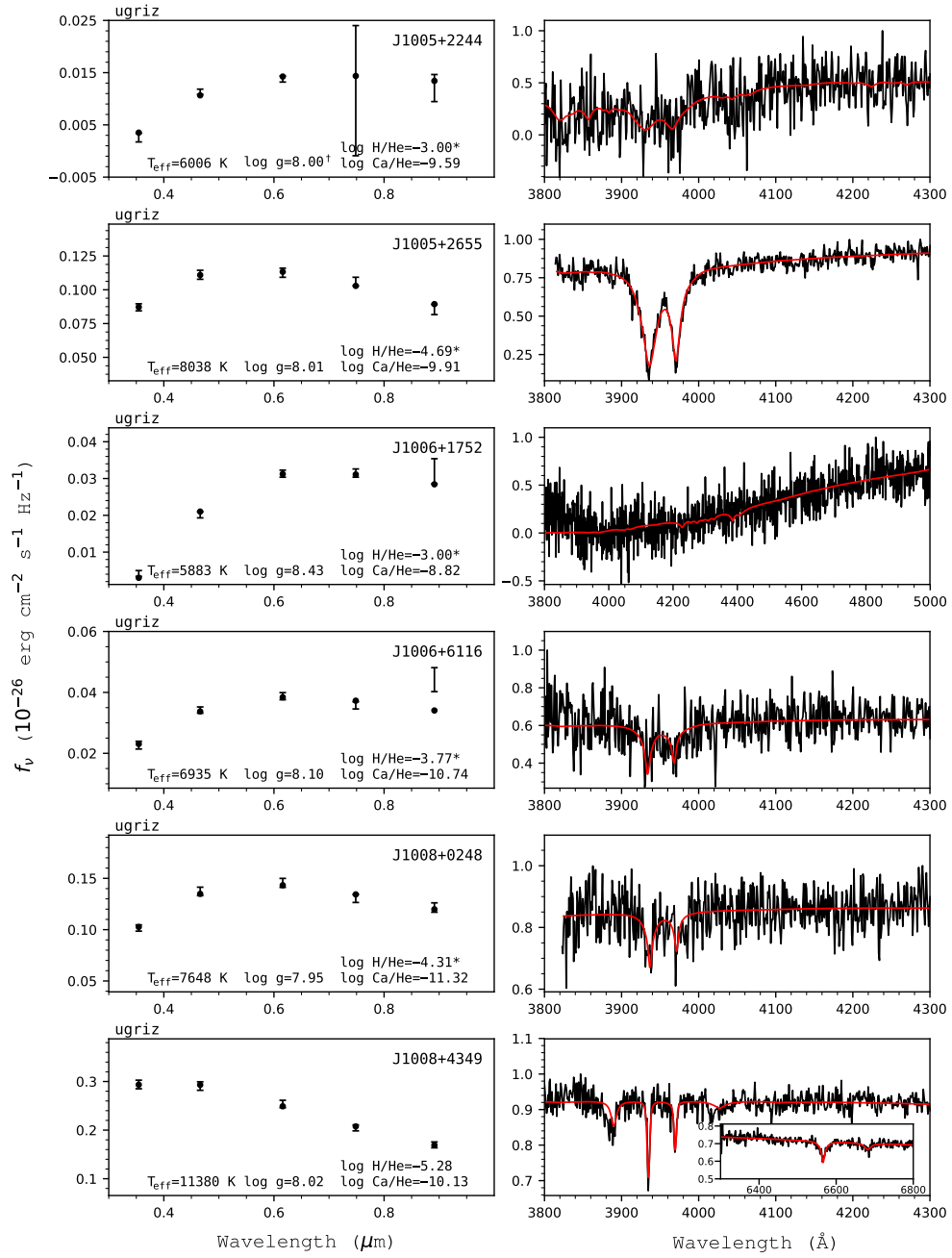


Figure 78. Fits to the DBZ/DZ(A) white dwarfs - continued.

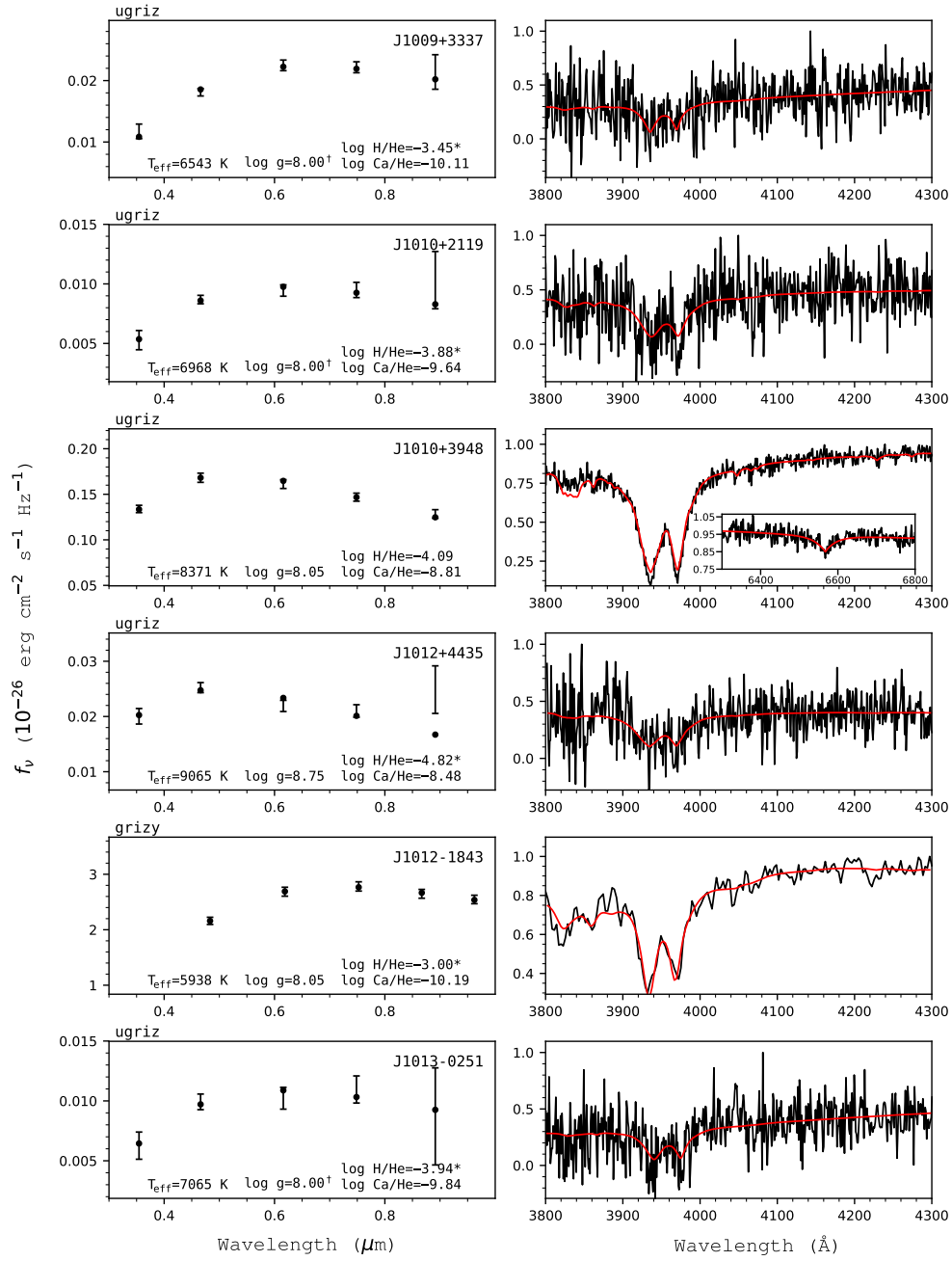


Figure 79. Fits to the DBZ/DZ(A) white dwarfs - continued.

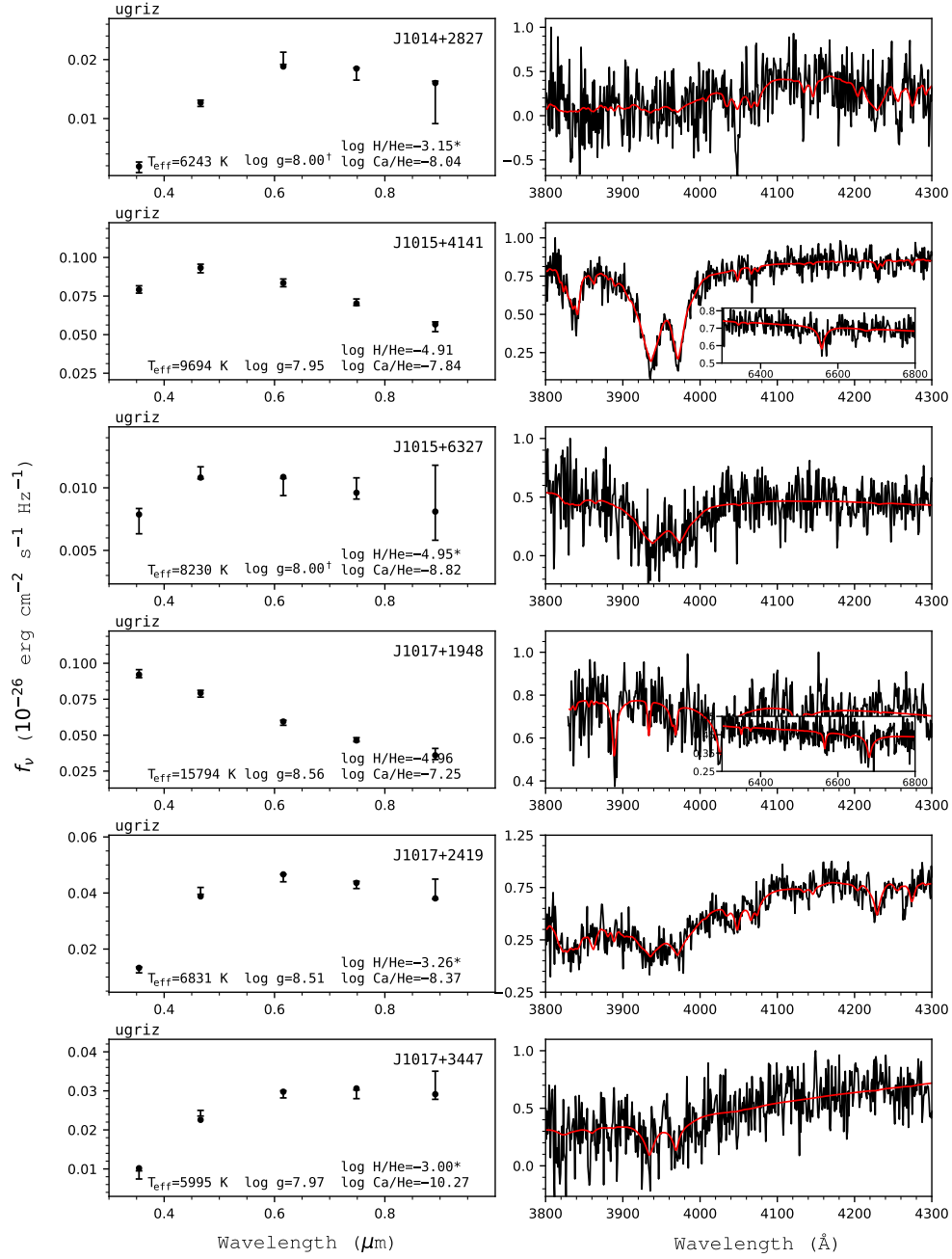


Figure 80. Fits to the DBZ/DZ(A) white dwarfs - continued.

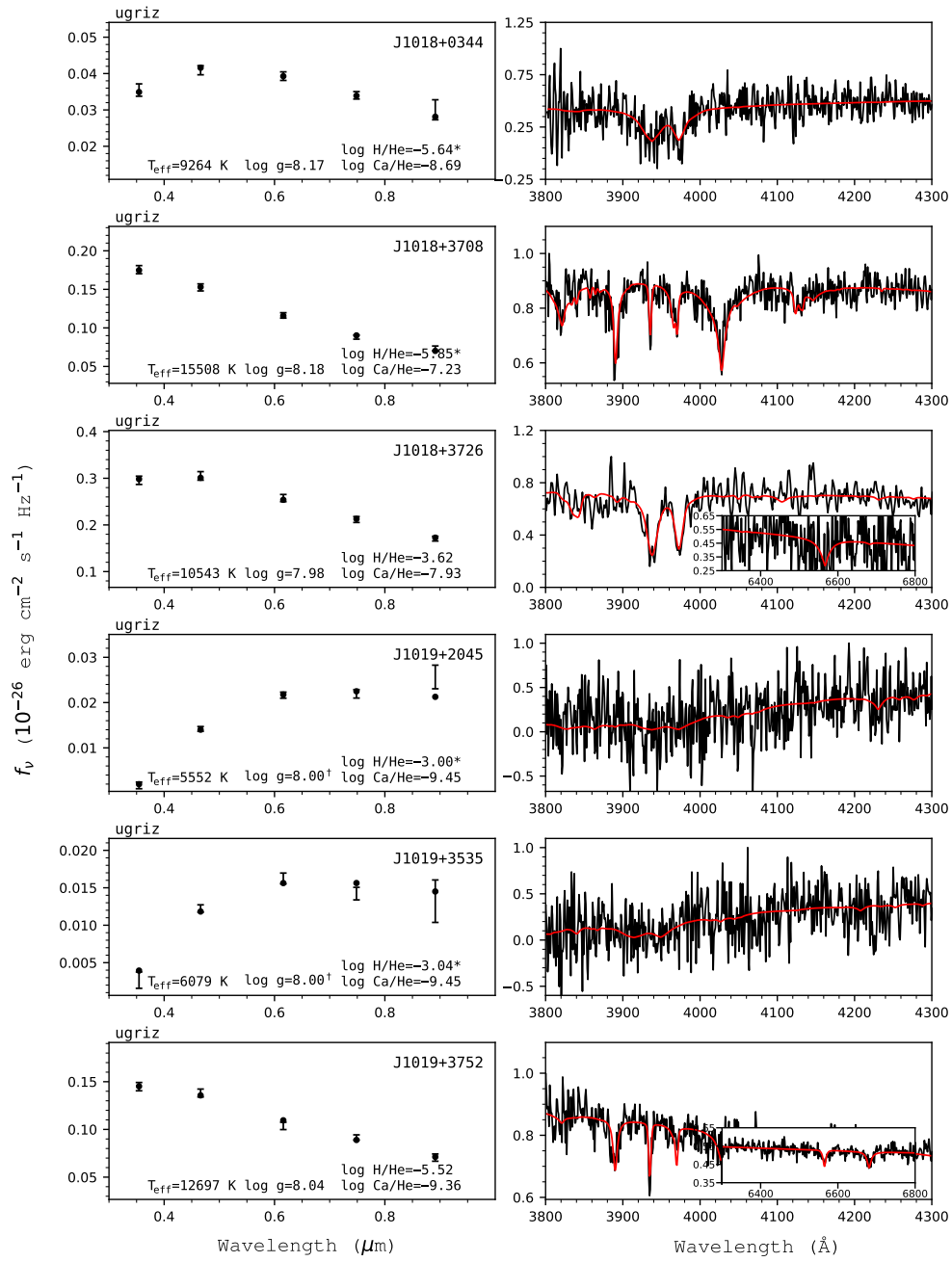


Figure 81. Fits to the DBZ/DZ(A) white dwarfs - continued.

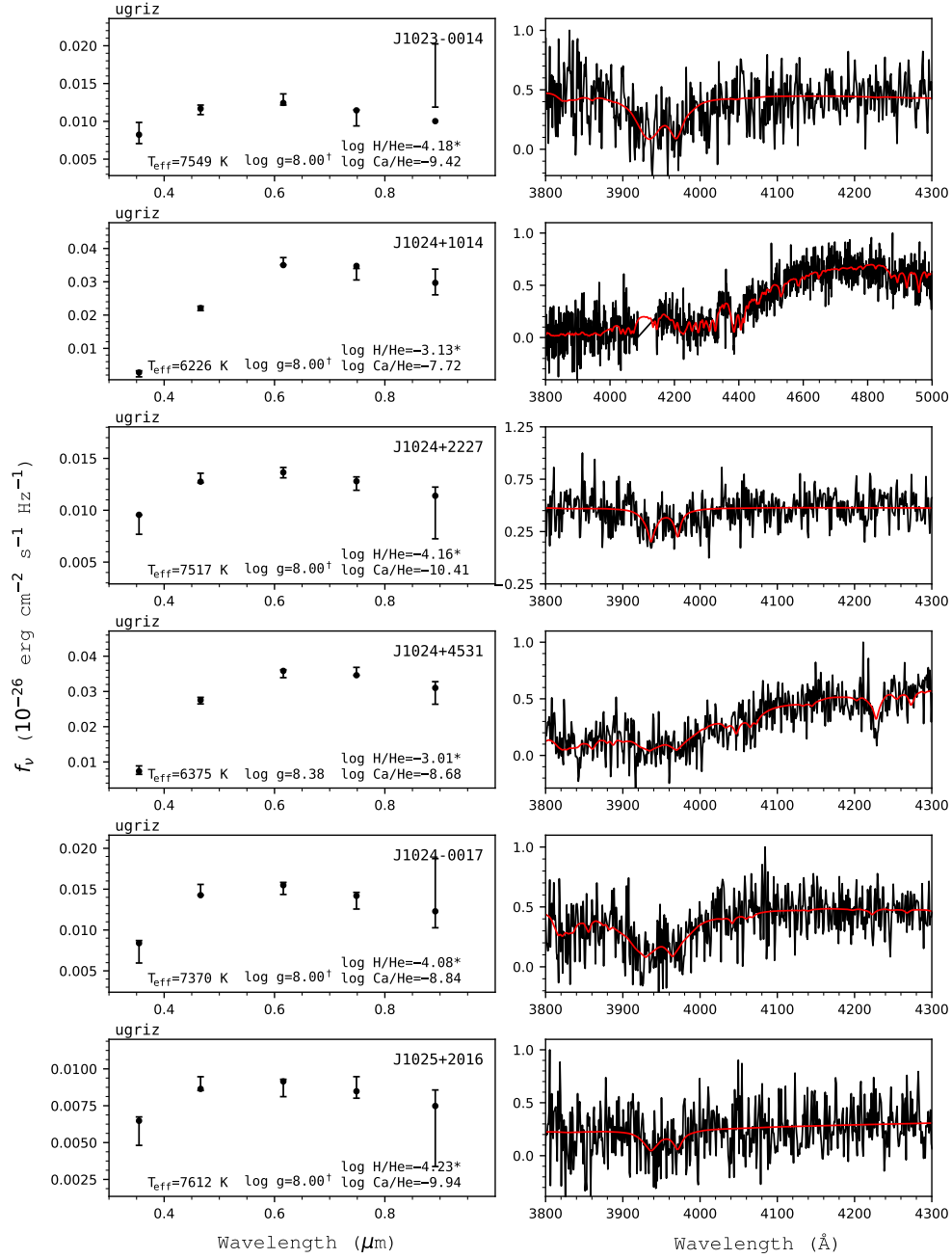


Figure 82. Fits to the DBZ/DZ(A) white dwarfs - continued.

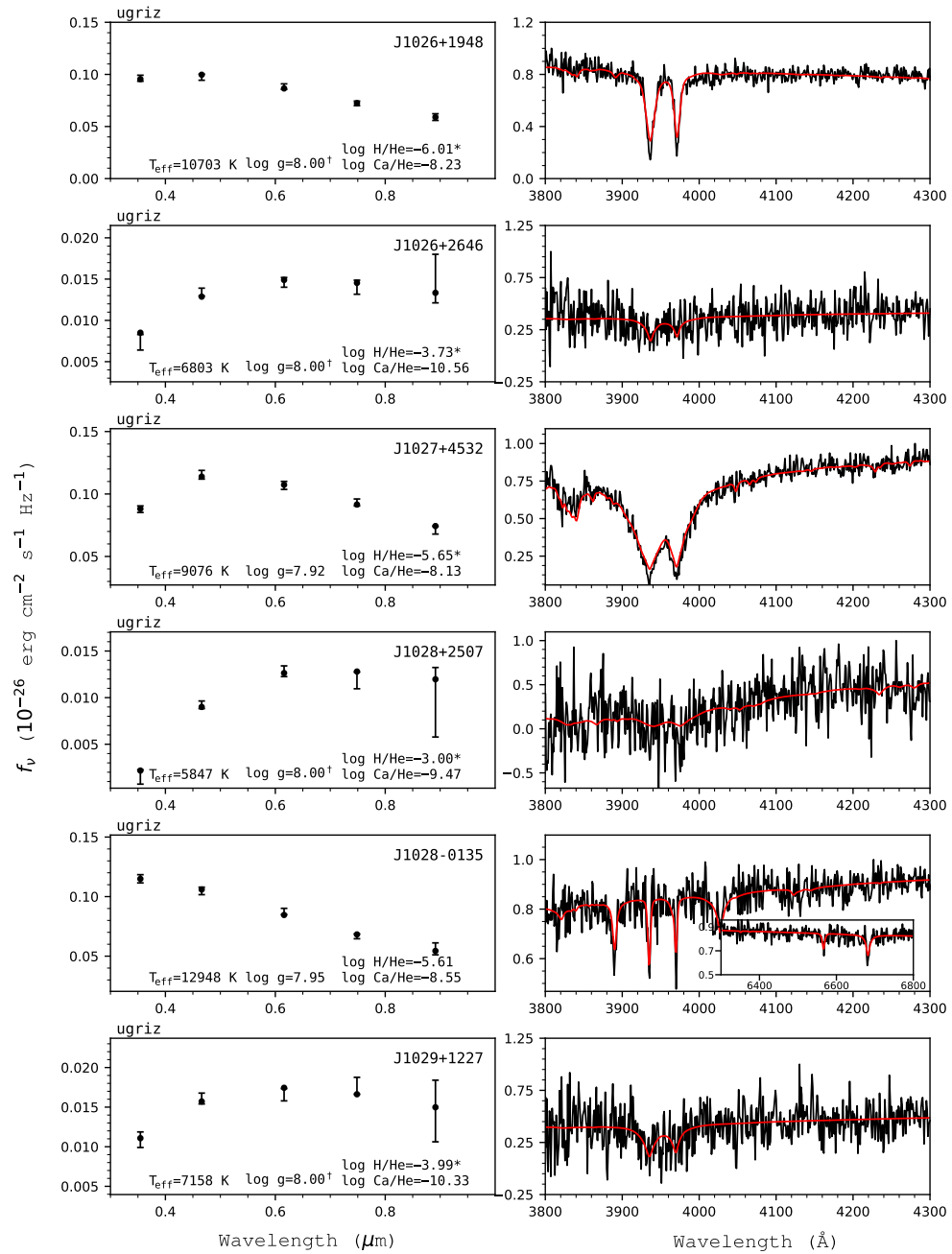


Figure 83. Fits to the DBZ/DZ(A) white dwarfs - continued.

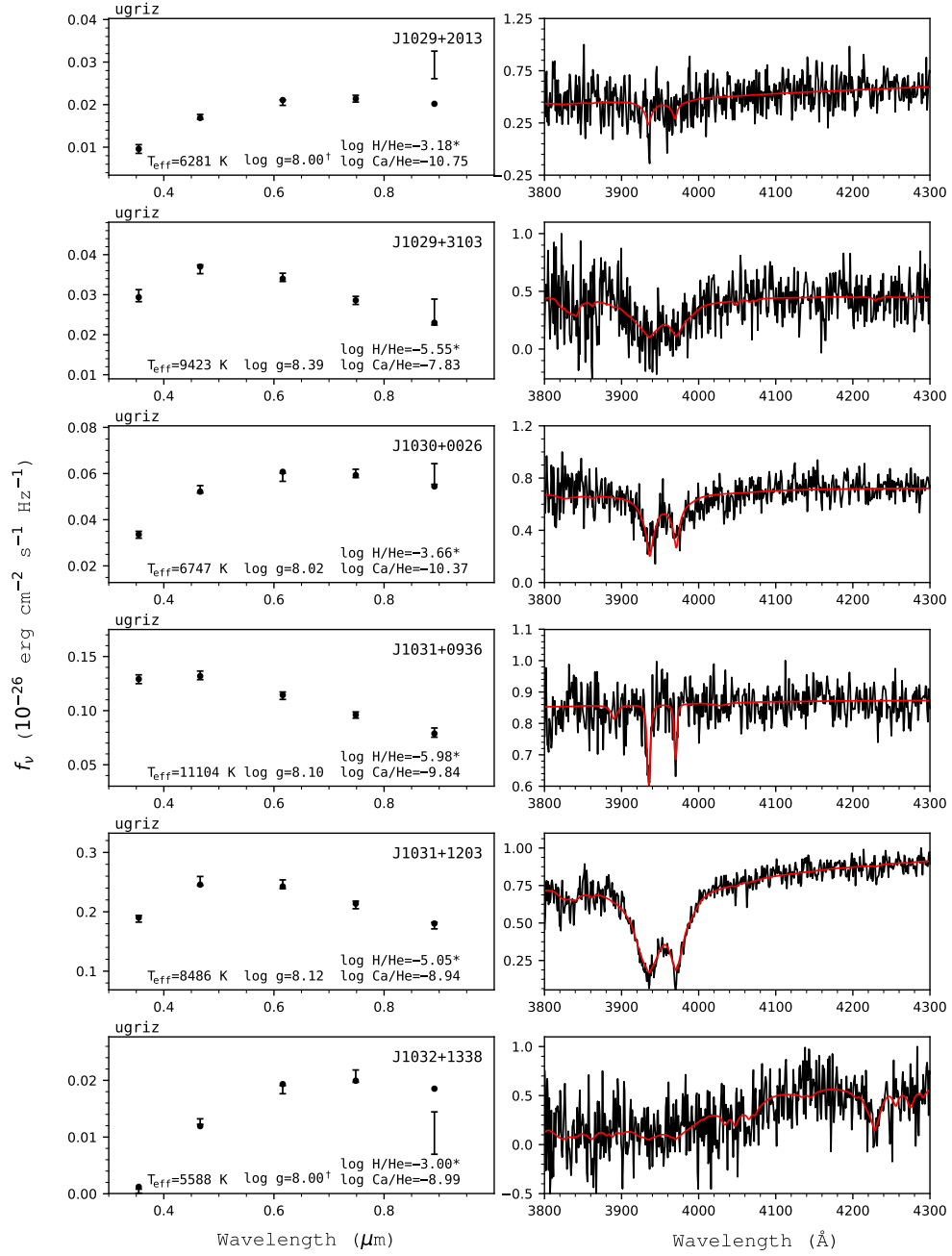


Figure 84. Fits to the DBZ/DZ(A) white dwarfs - continued.

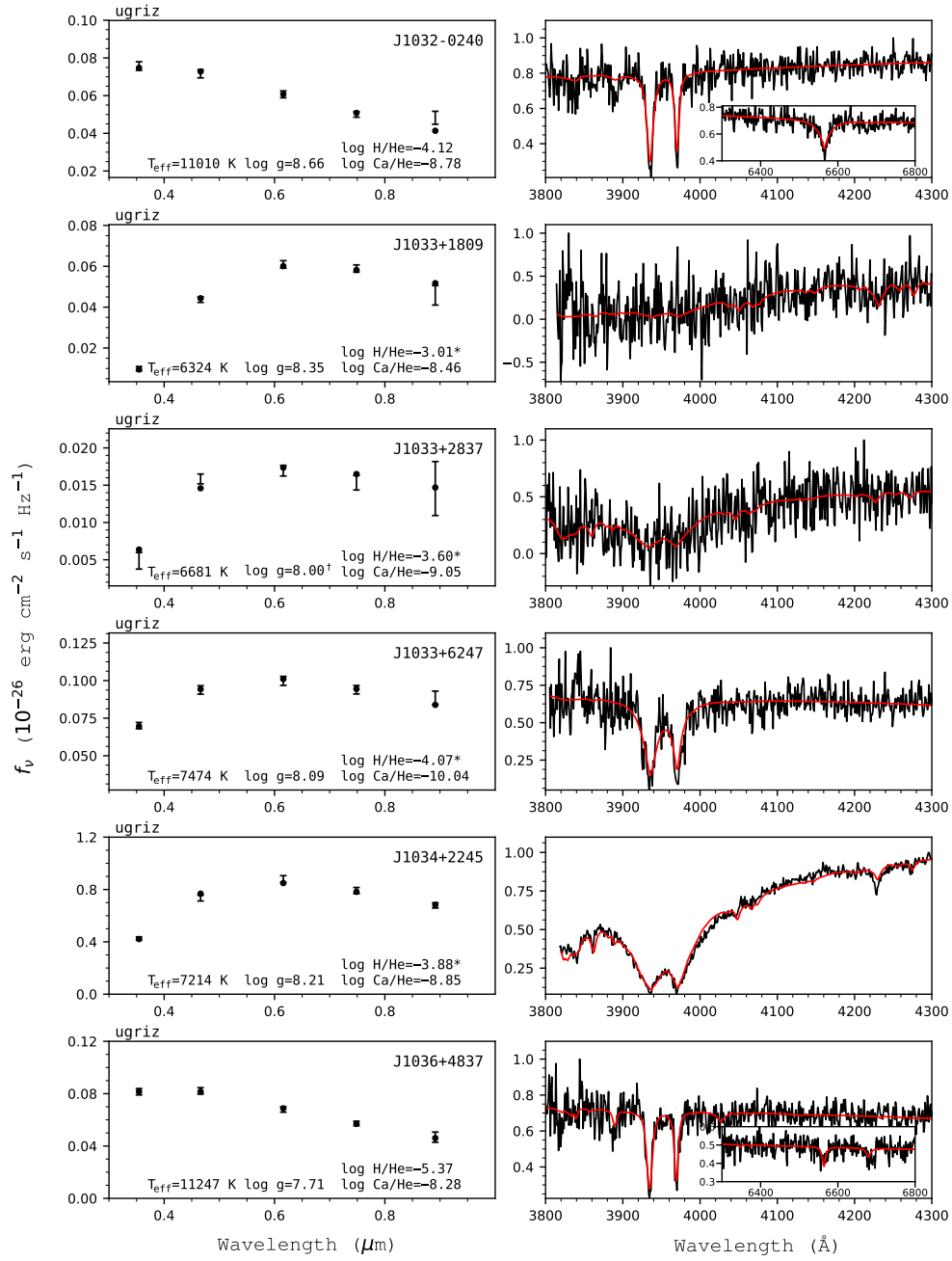


Figure 85. Fits to the DBZ/DZ(A) white dwarfs - continued.

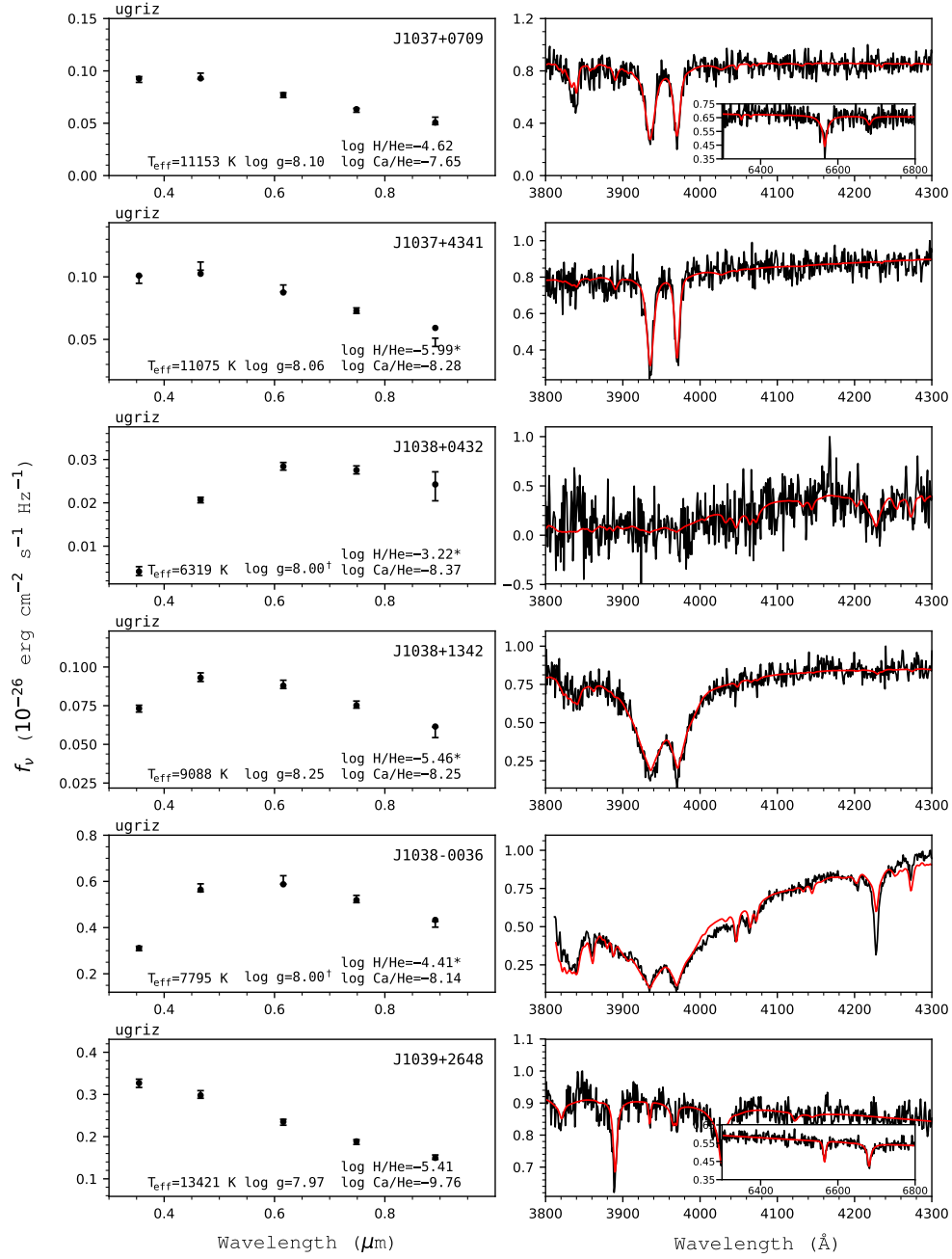


Figure 86. Fits to the DBZ/DZ(A) white dwarfs - continued.

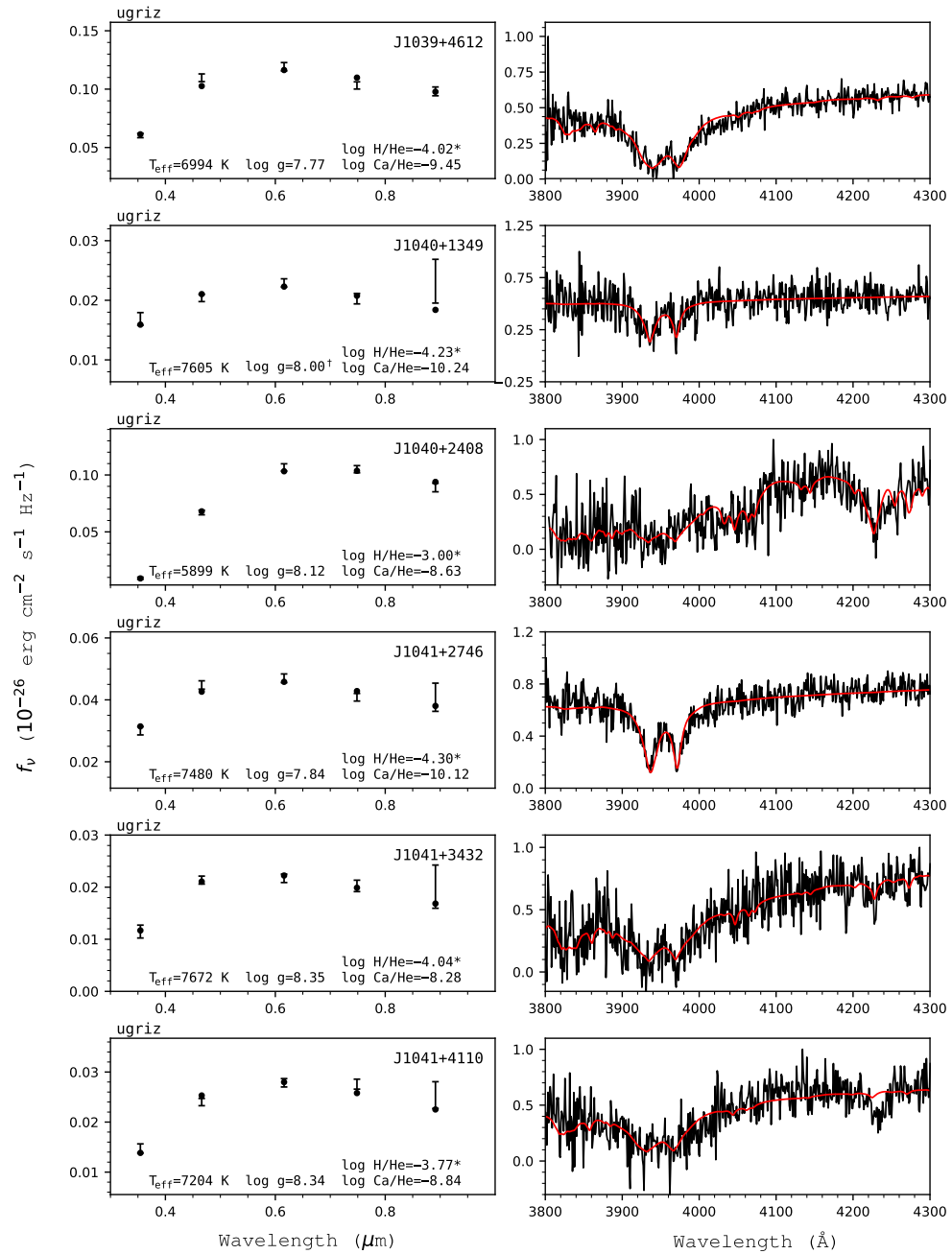


Figure 87. Fits to the DBZ/DZ(A) white dwarfs - continued.

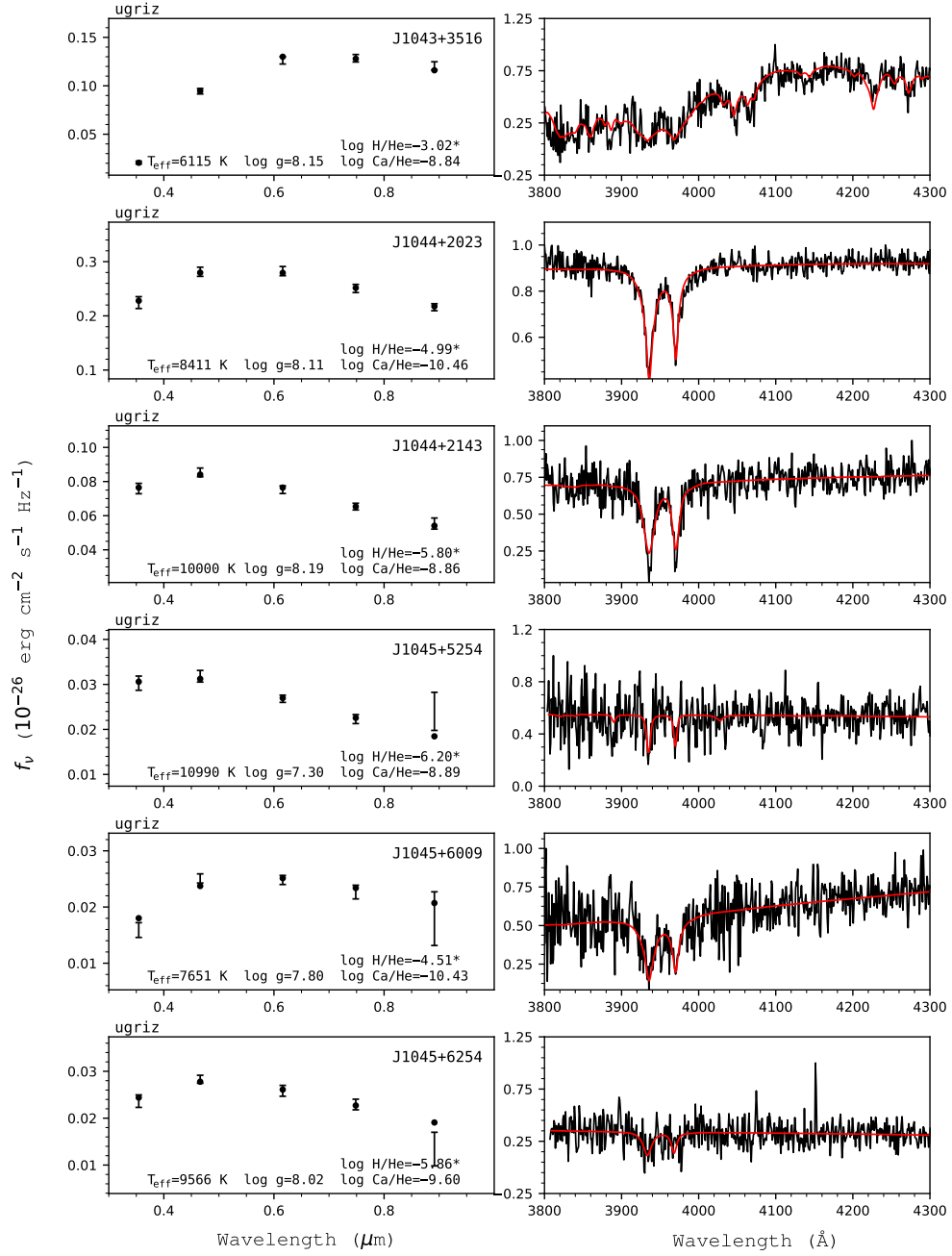


Figure 88. Fits to the DBZ/DZ(A) white dwarfs - continued.

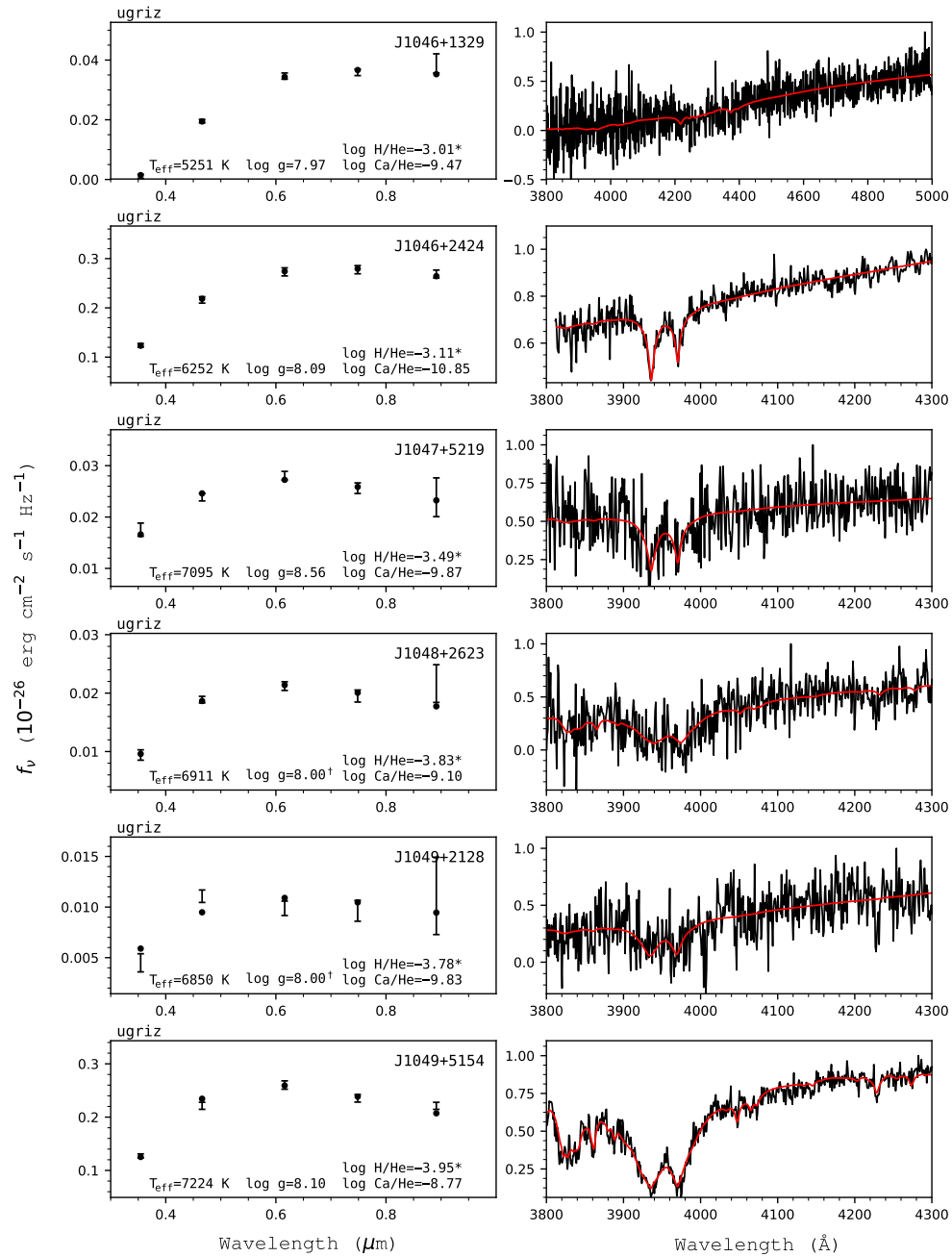


Figure 89. Fits to the DBZ/DZ(A) white dwarfs - continued.

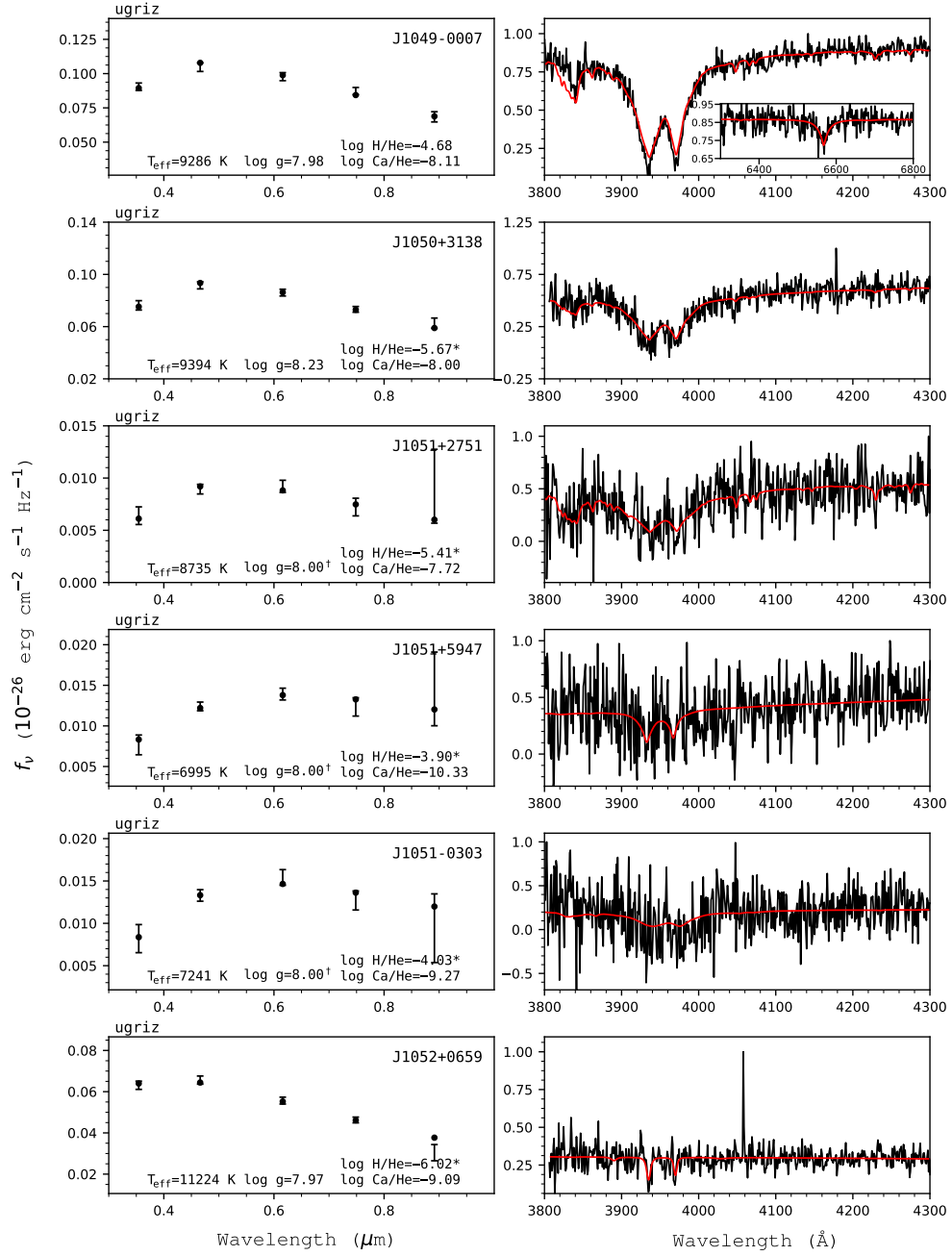


Figure 90. Fits to the DBZ/DZ(A) white dwarfs - continued.

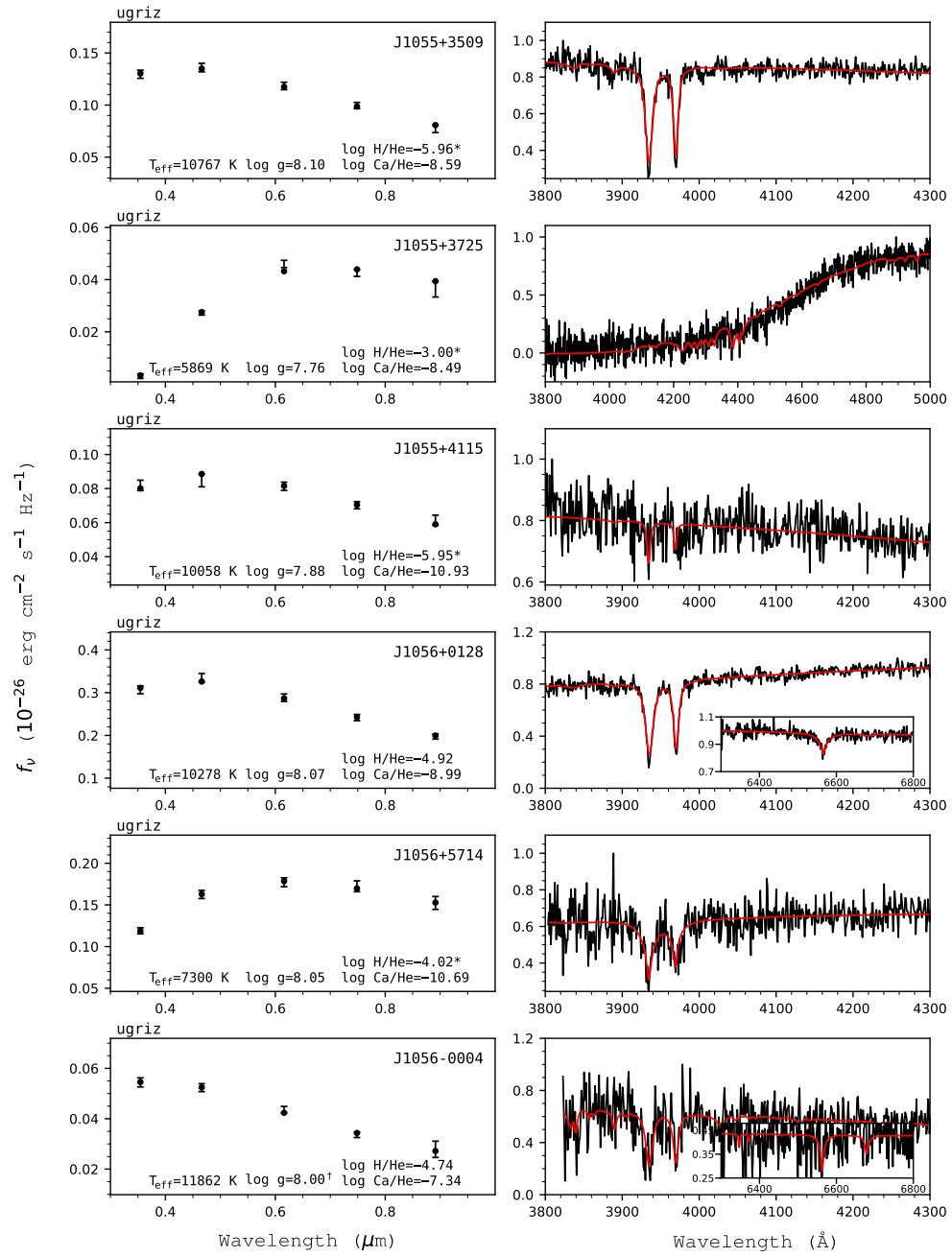


Figure 91. Fits to the DBZ/DZ(A) white dwarfs - continued.

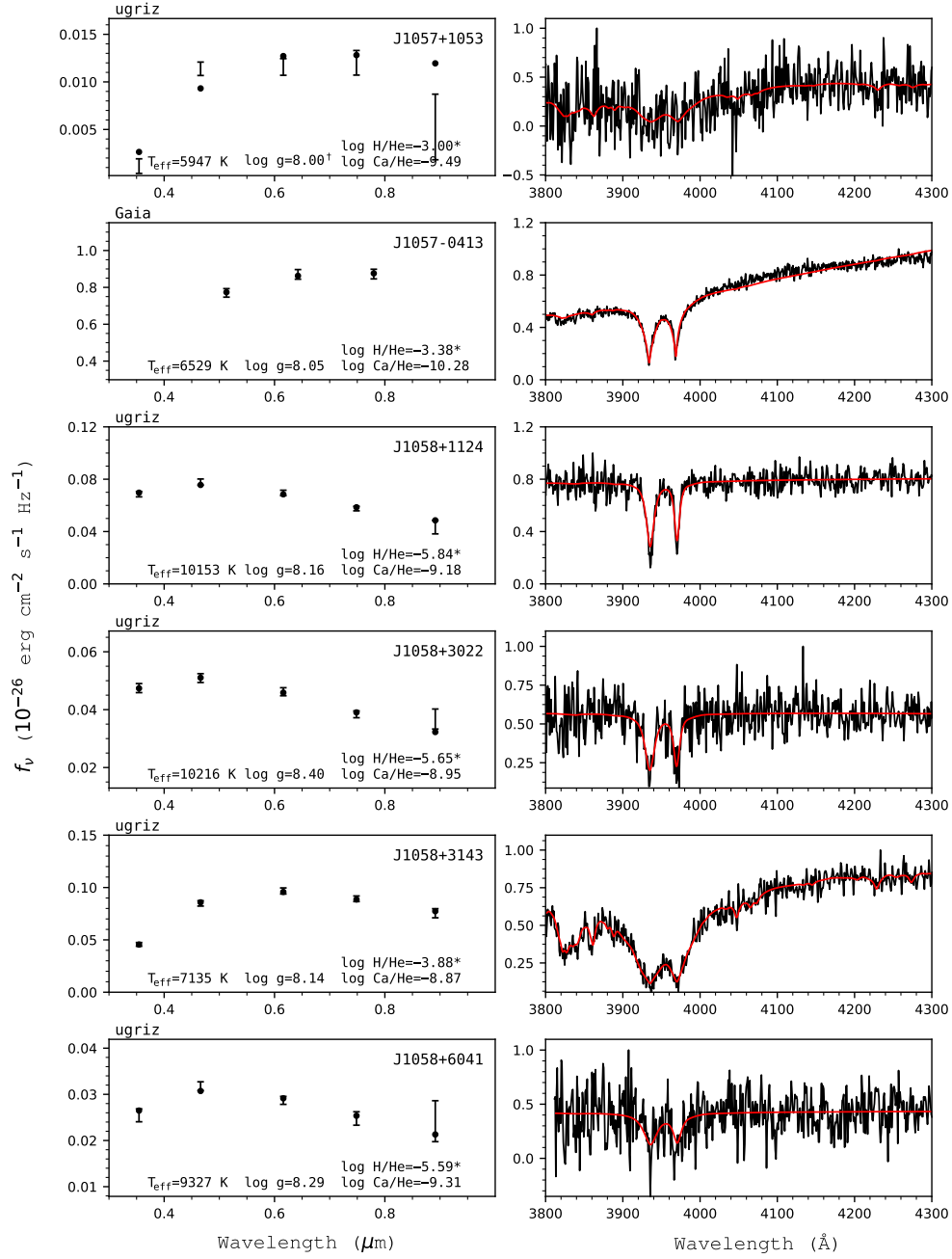


Figure 92. Fits to the DBZ/DZ(A) white dwarfs - continued.

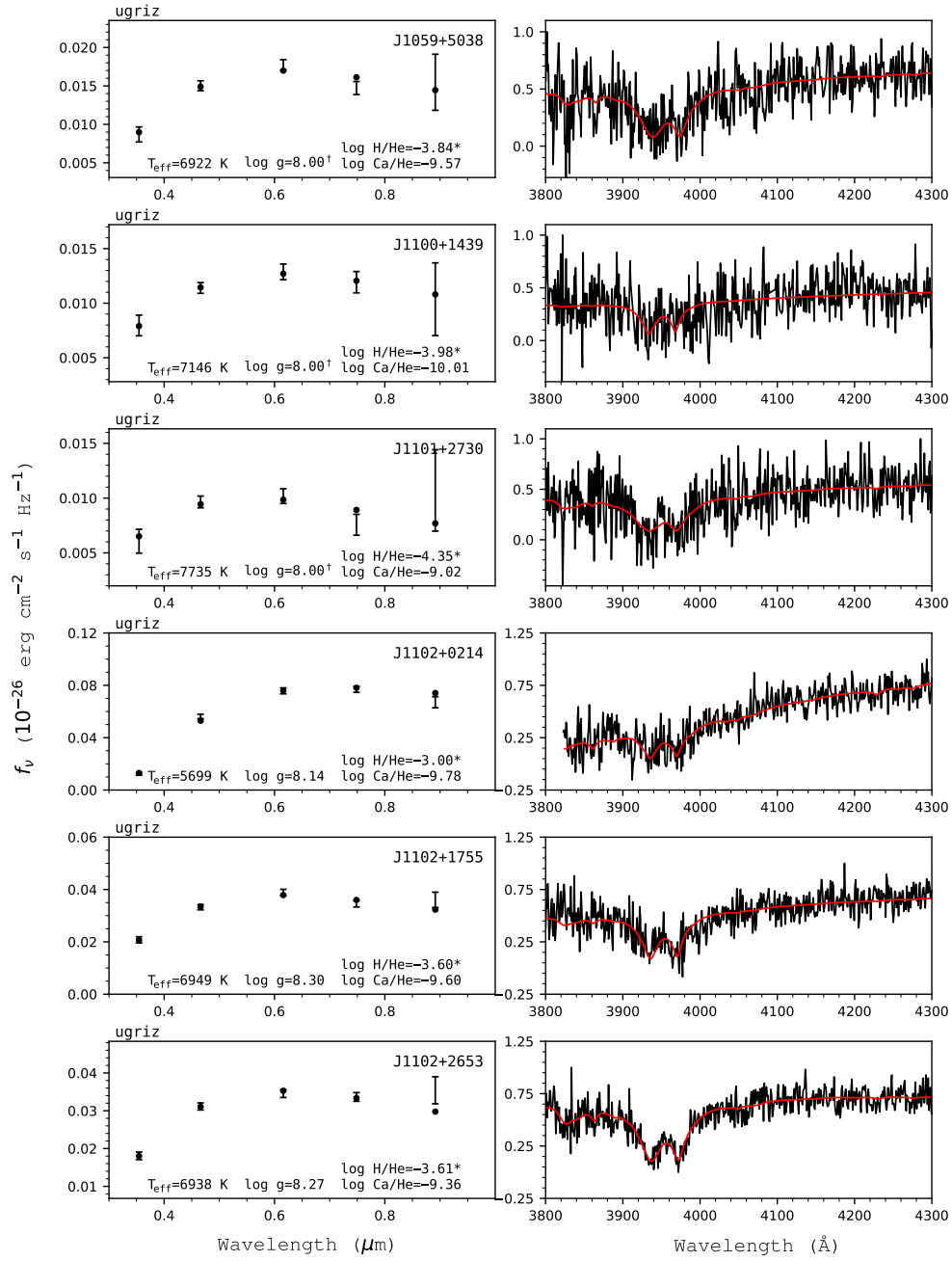


Figure 93. Fits to the DBZ/DZ(A) white dwarfs - continued.

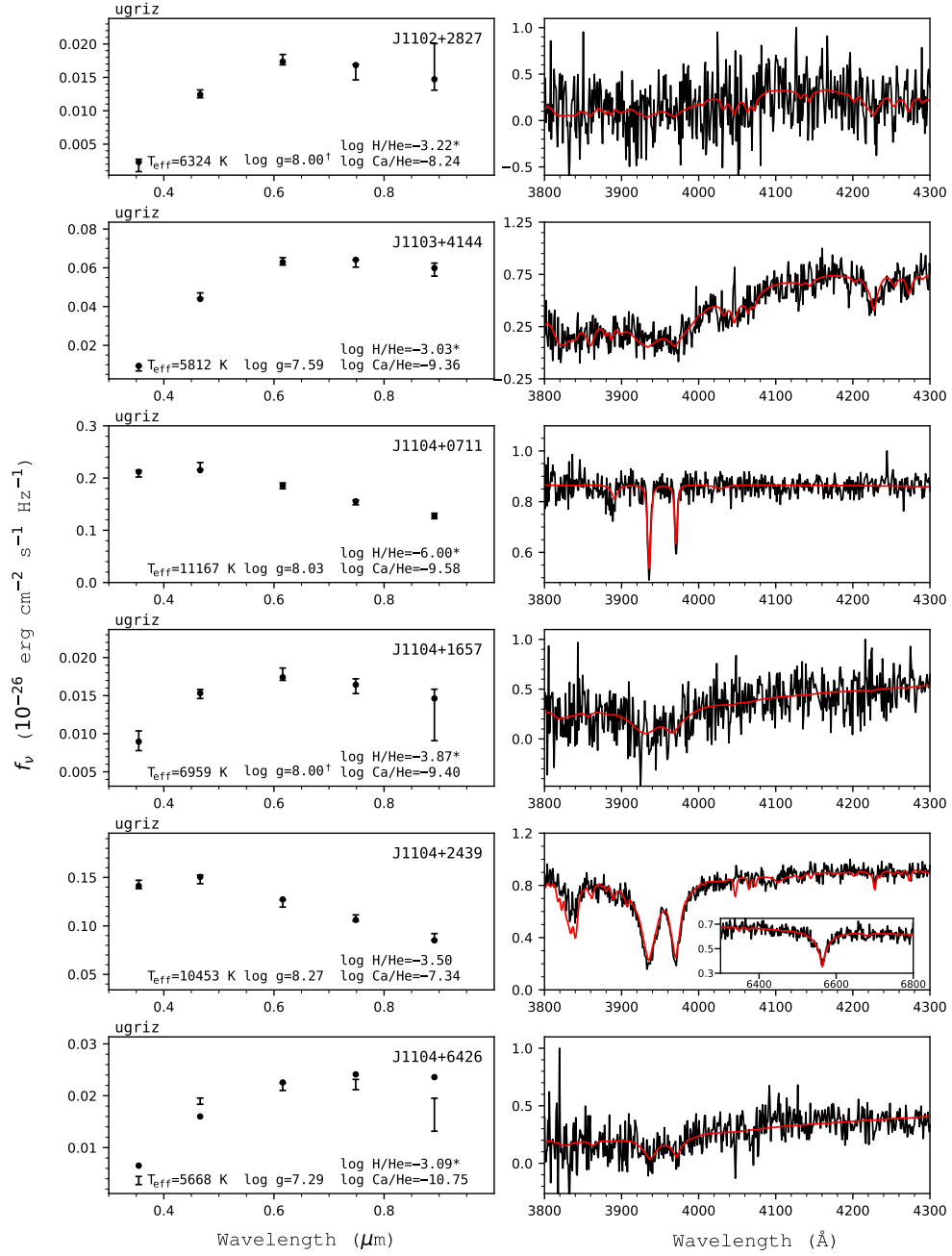


Figure 94. Fits to the DBZ/DZ(A) white dwarfs - continued.

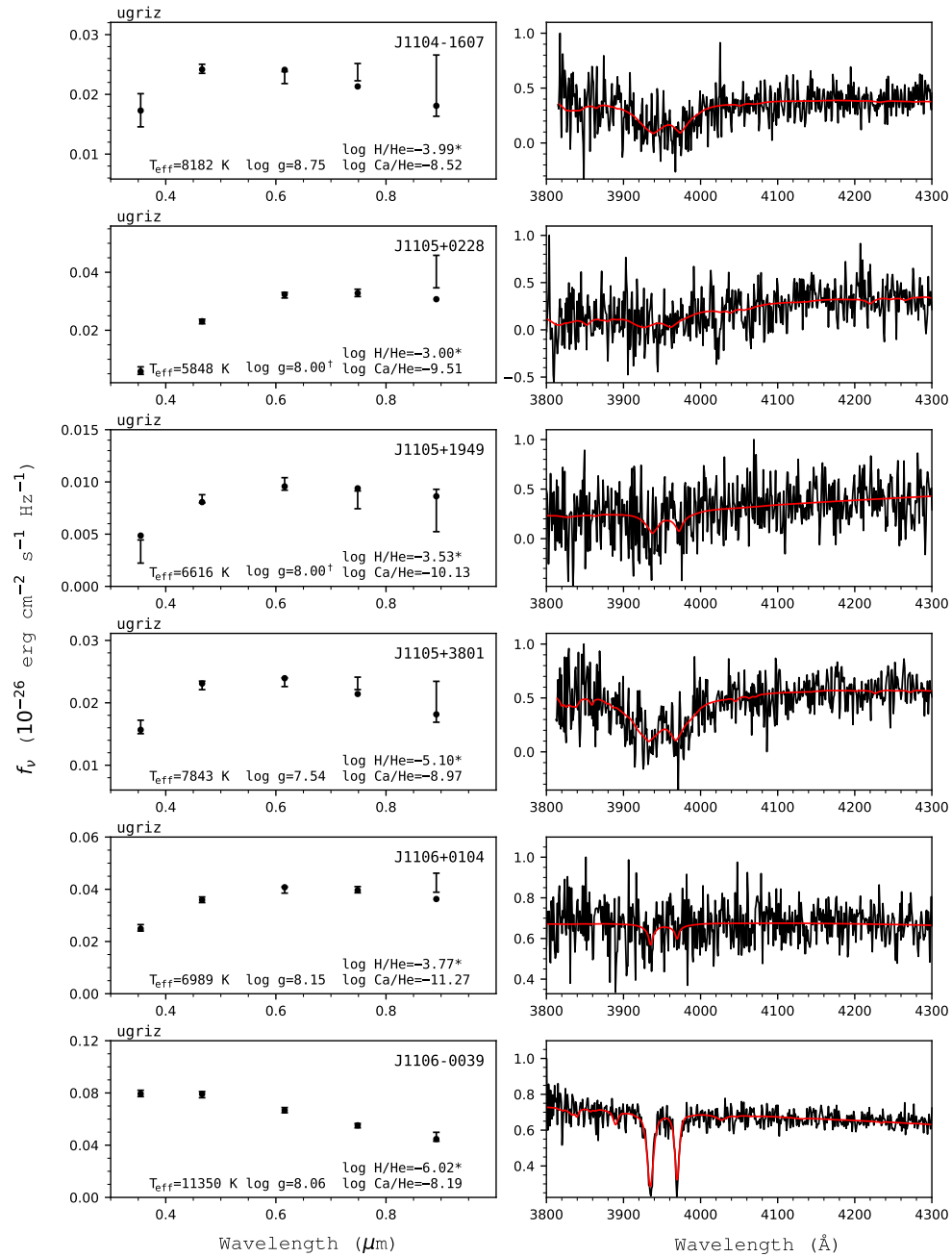


Figure 95. Fits to the DBZ/DZ(A) white dwarfs - continued.

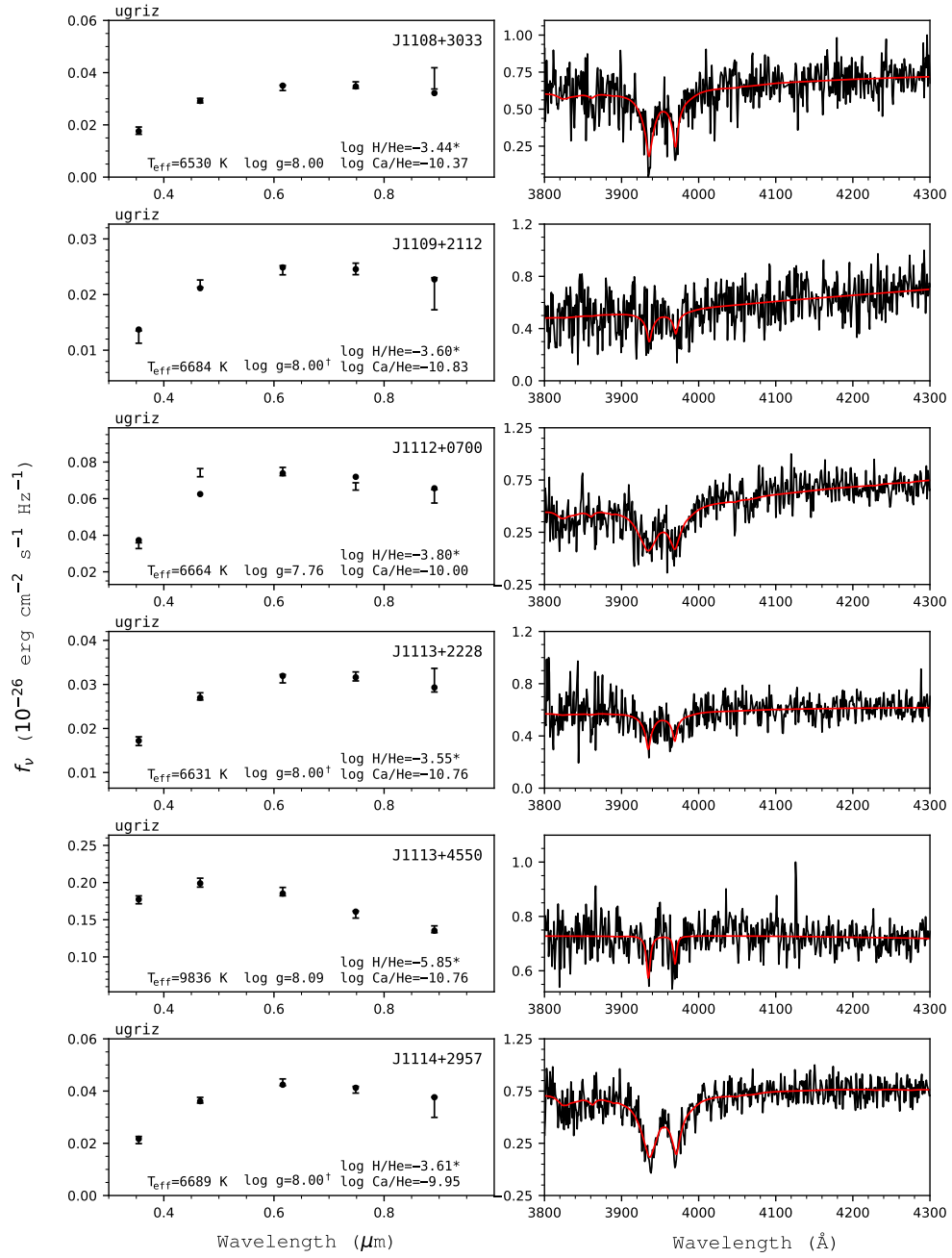


Figure 96. Fits to the DBZ/DZ(A) white dwarfs - continued.

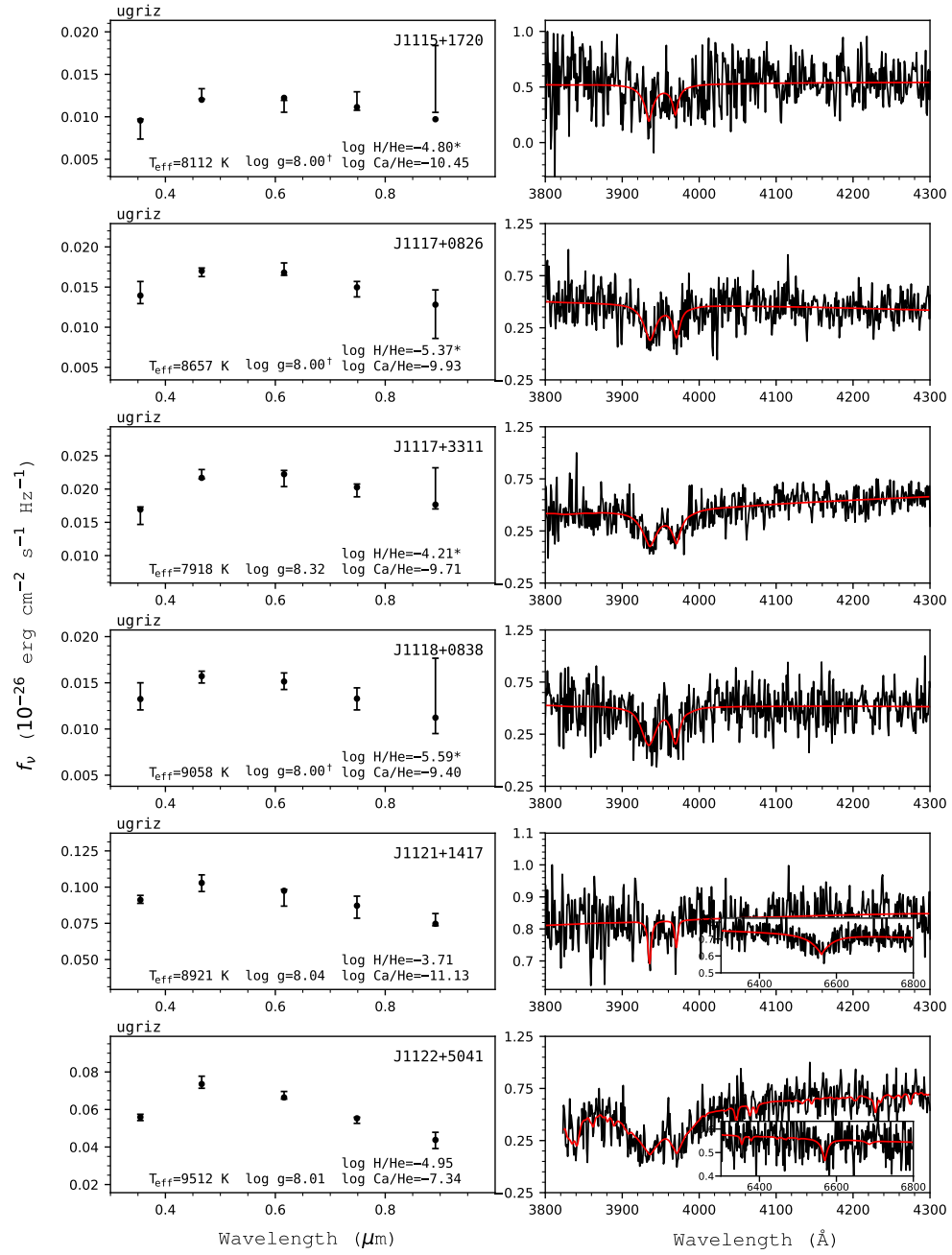


Figure 97. Fits to the DBZ/DZ(A) white dwarfs - continued.

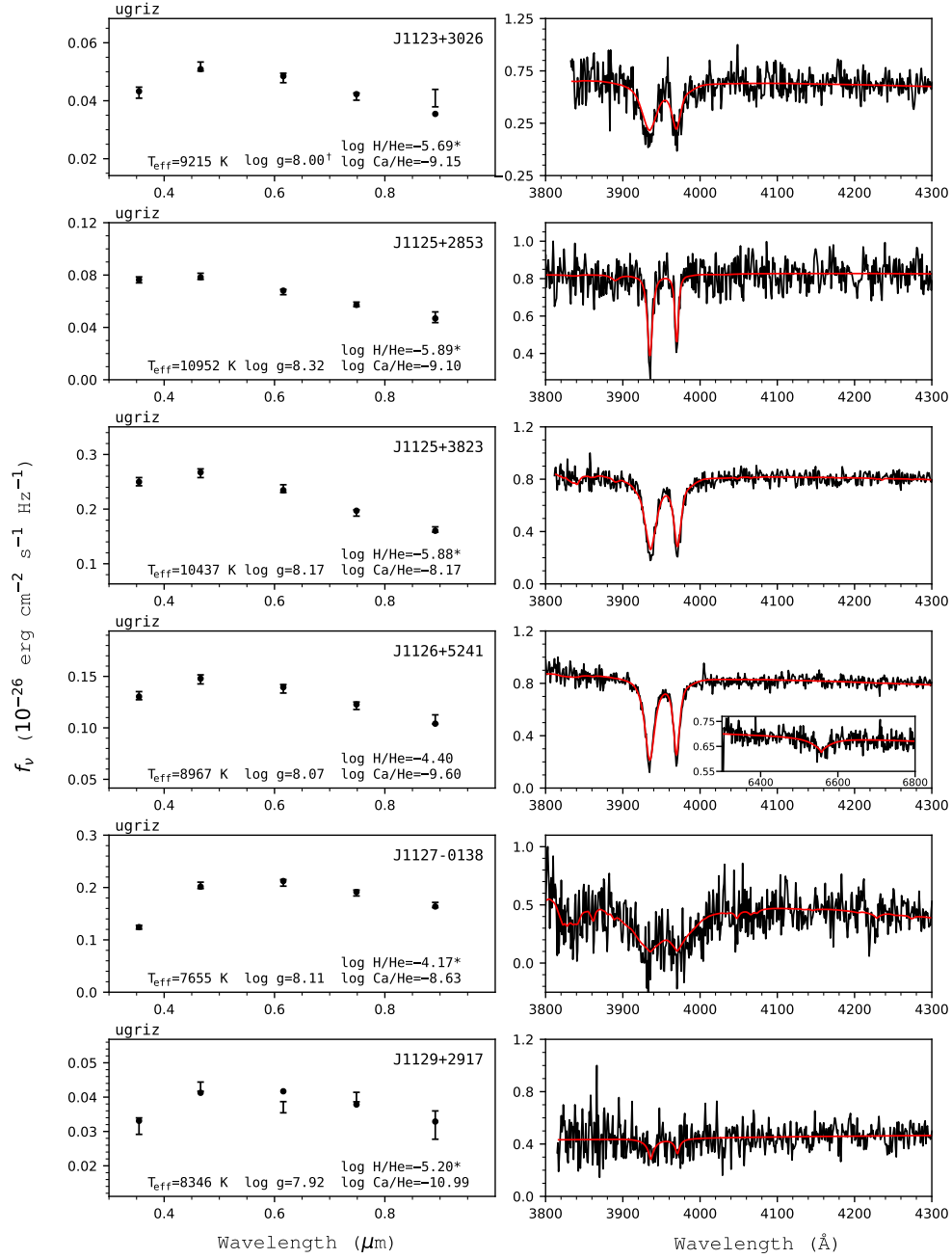


Figure 98. Fits to the DBZ/DZ(A) white dwarfs - continued.

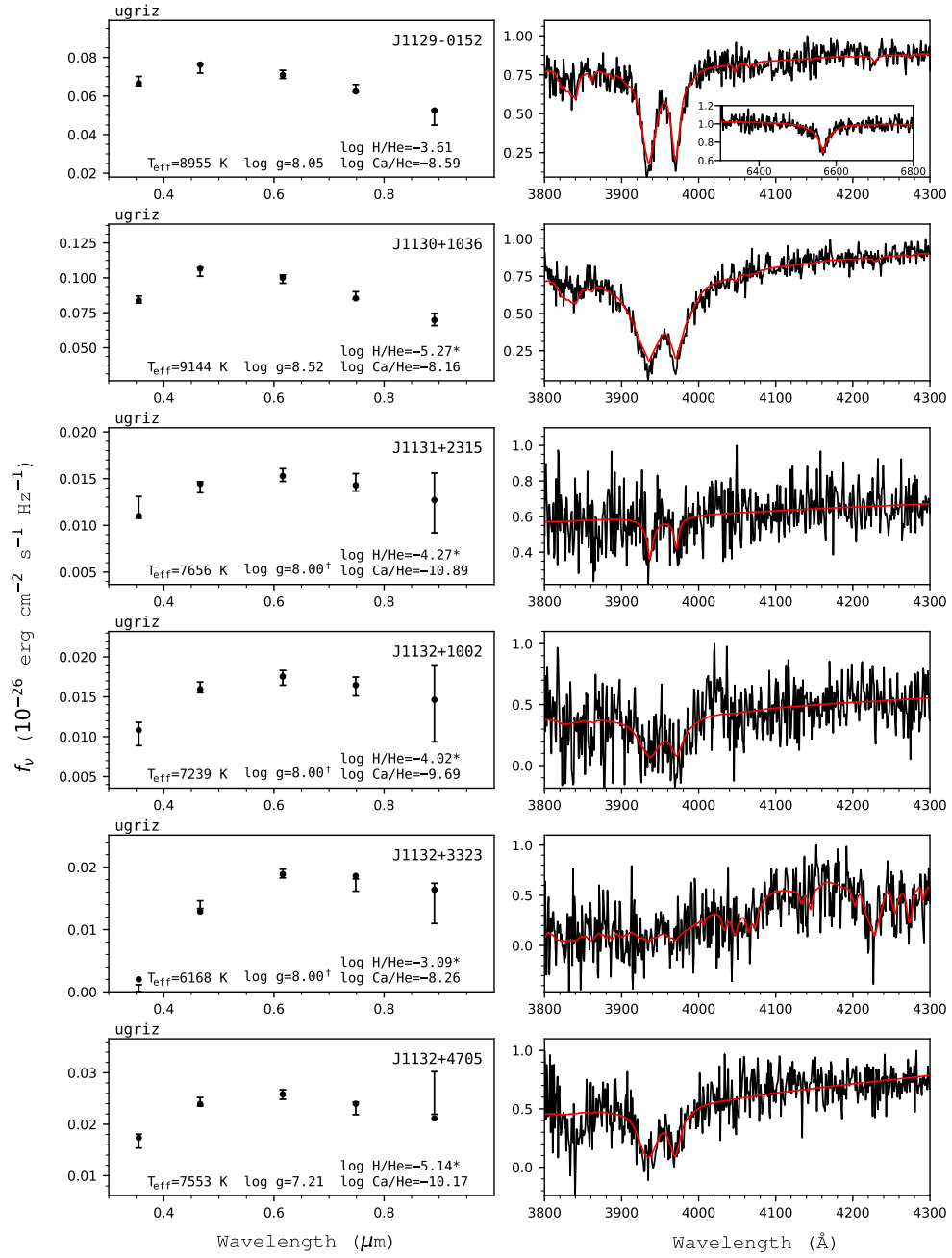


Figure 99. Fits to the DBZ/DZ(A) white dwarfs - continued.

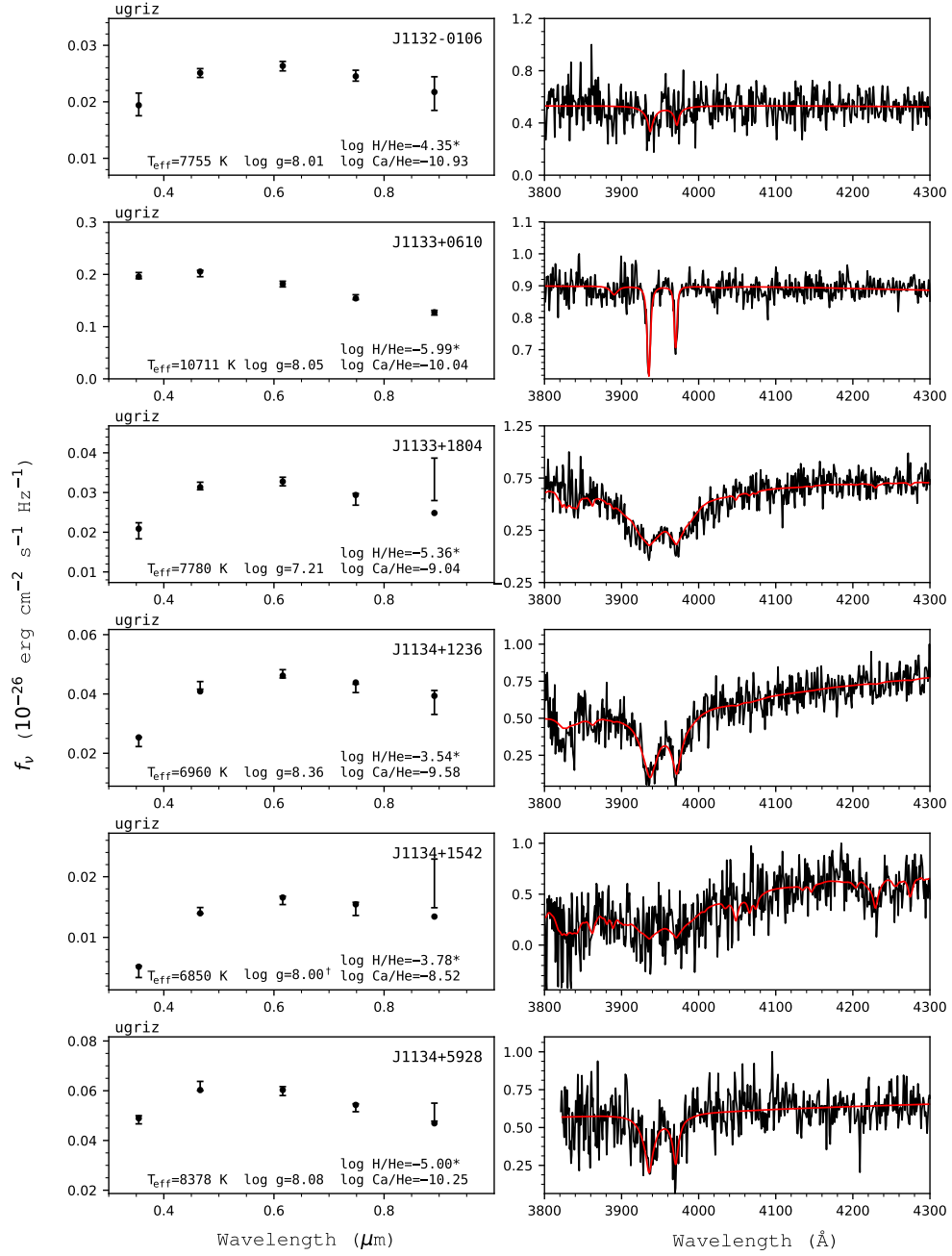


Figure 100. Fits to the DBZ/DZ(A) white dwarfs - continued.

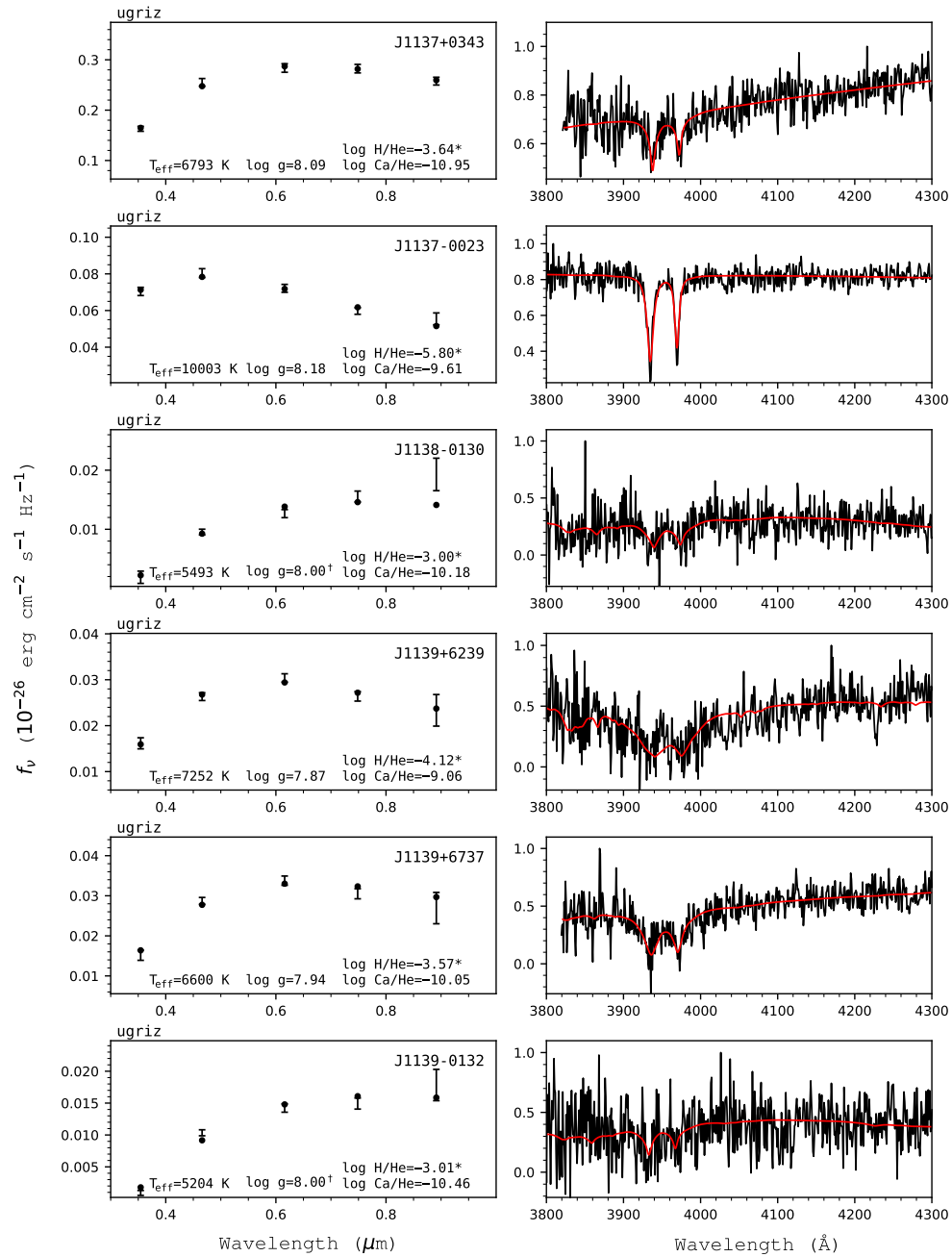


Figure 101. Fits to the DBZ/DZ(A) white dwarfs - continued.

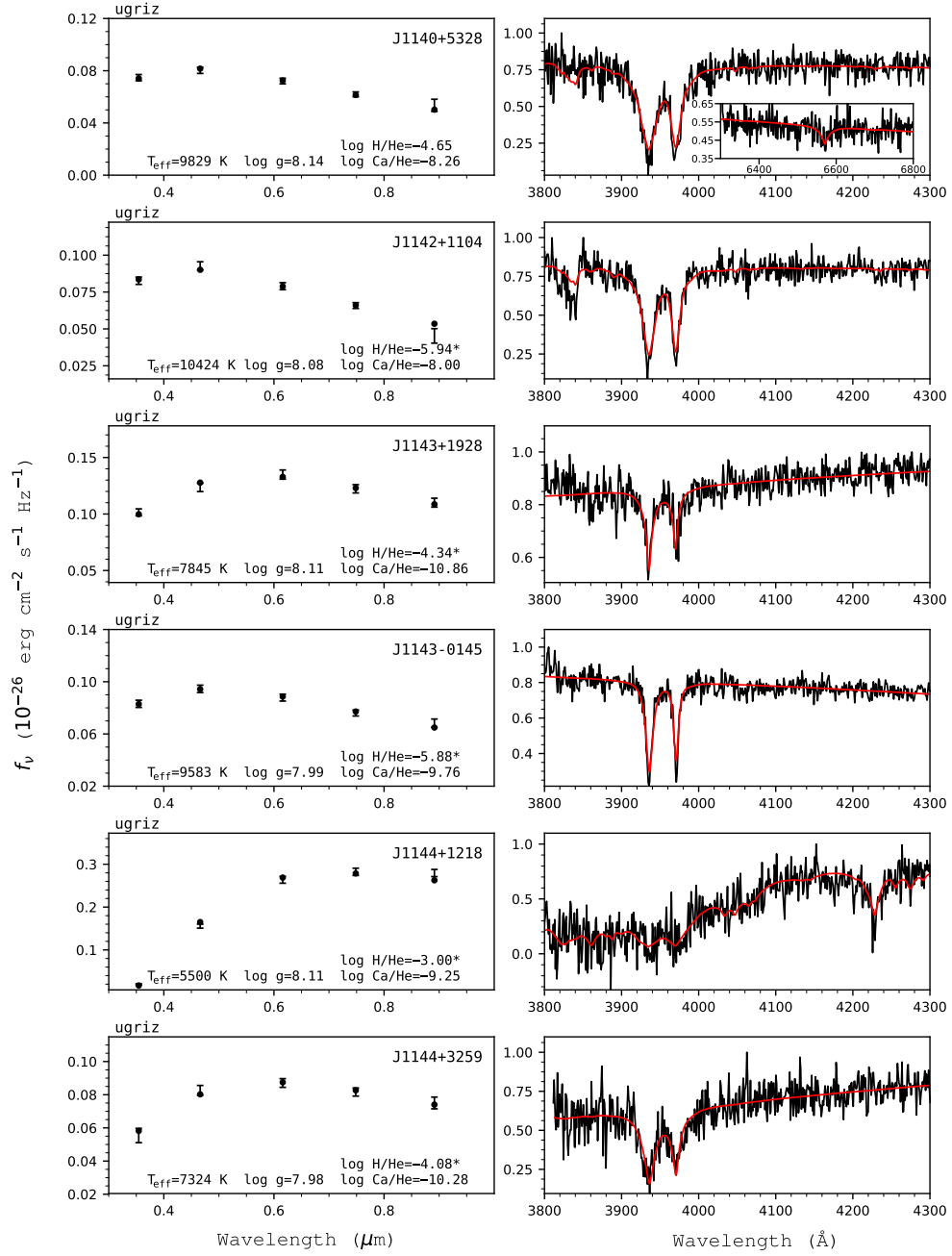


Figure 102. Fits to the DBZ/DZ(A) white dwarfs - continued.

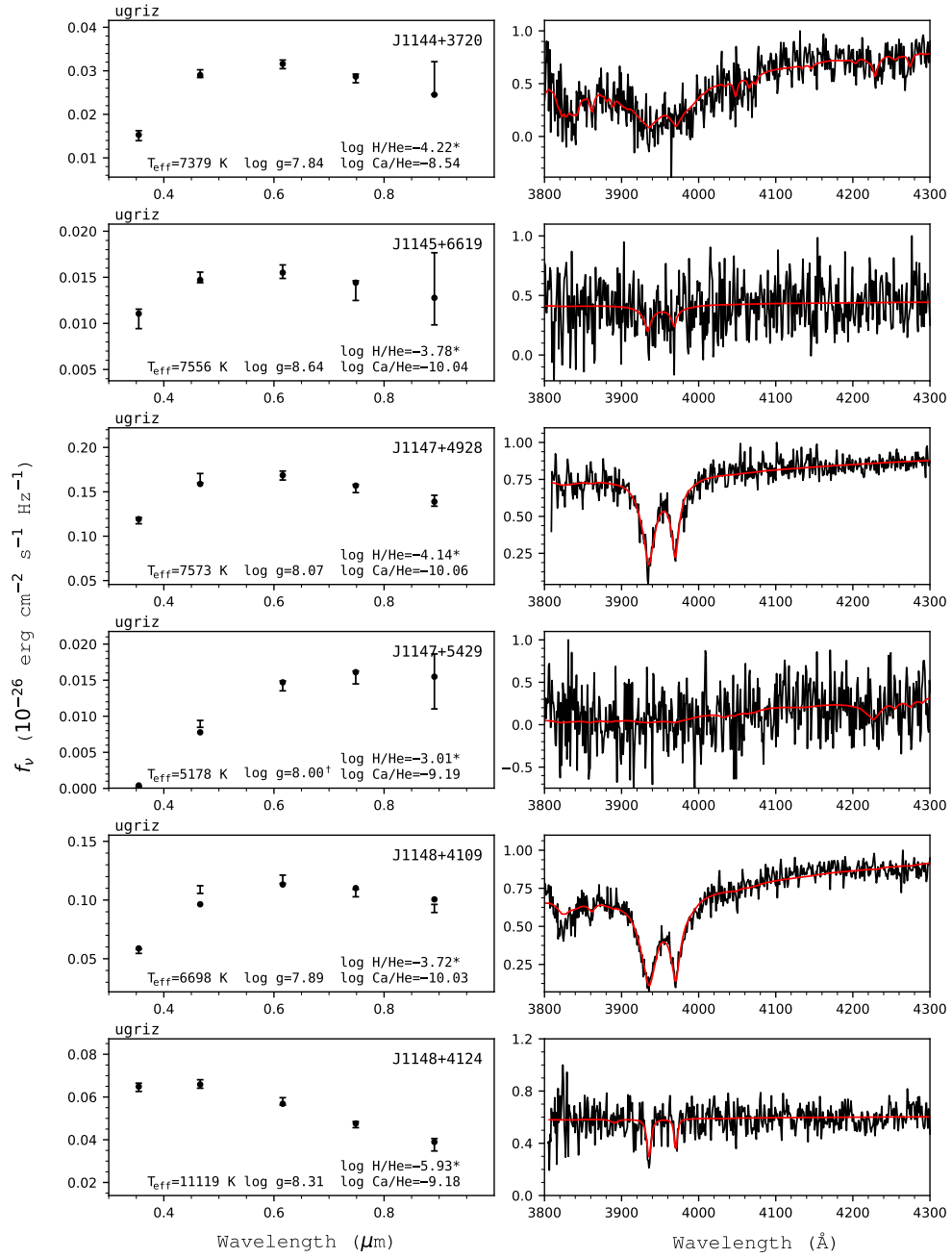


Figure 103. Fits to the DB/DZ(A) white dwarfs - continued.

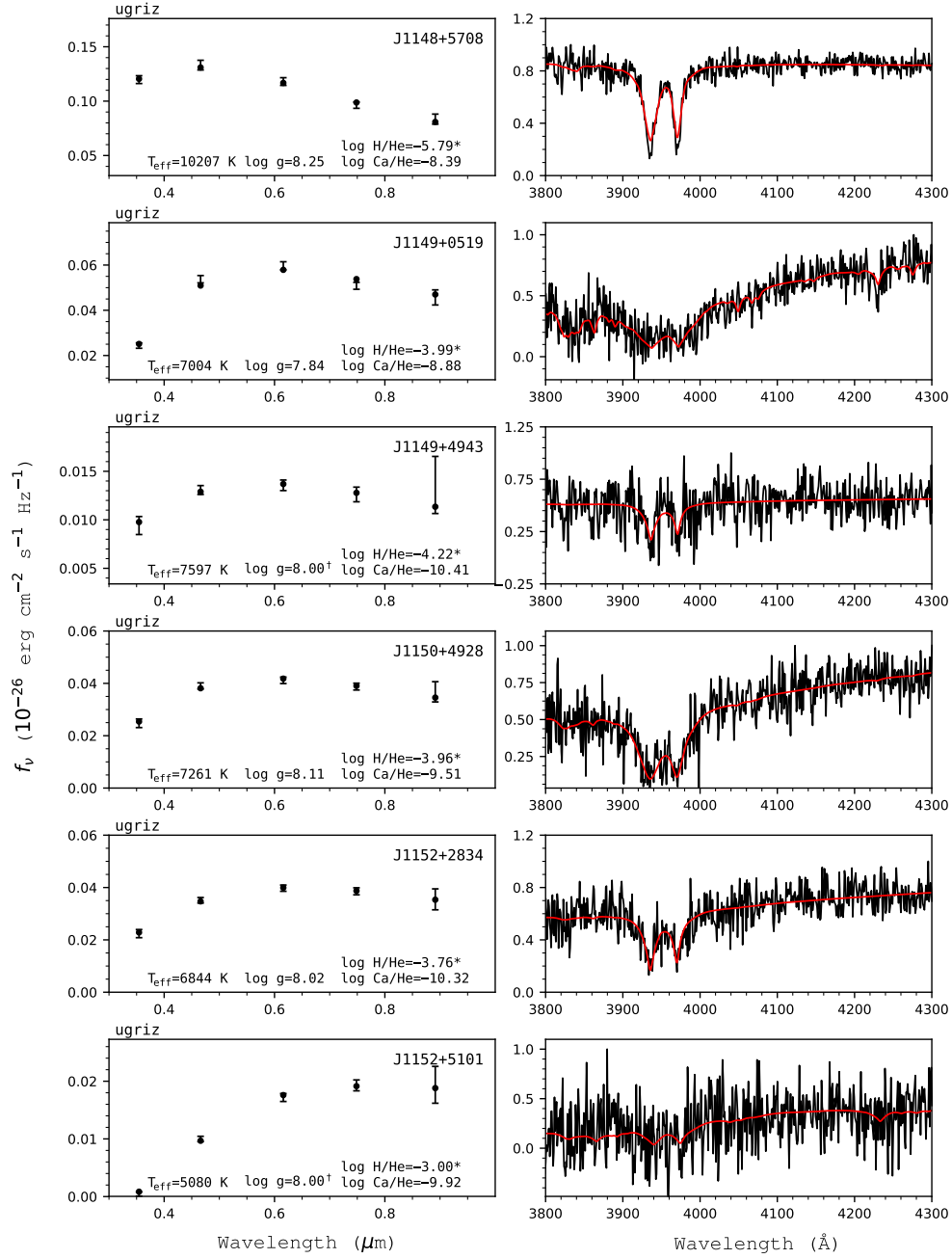


Figure 104. Fits to the DBZ/DZ(A) white dwarfs - continued.

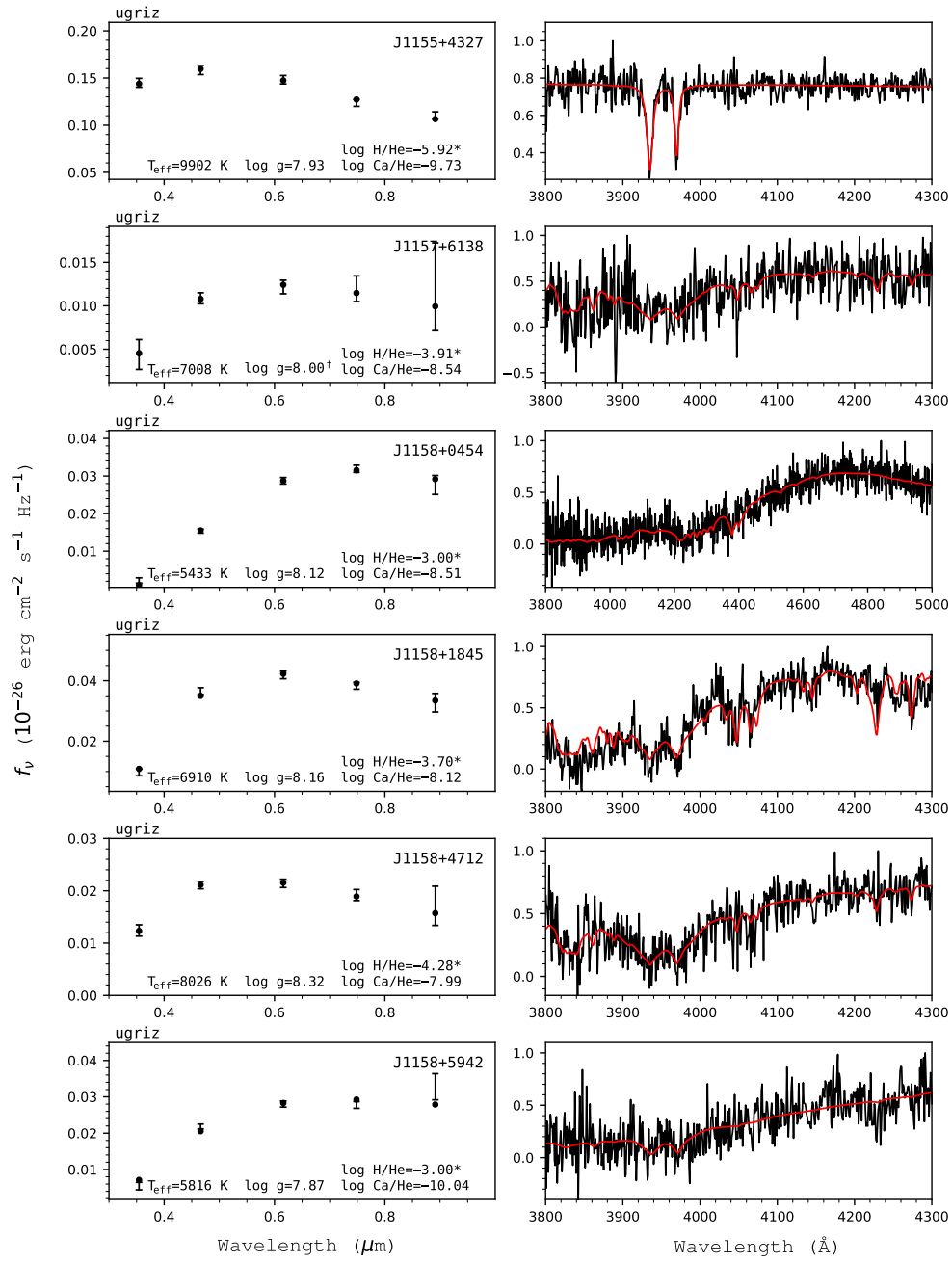


Figure 105. Fits to the DBZ/DZ(A) white dwarfs - continued.

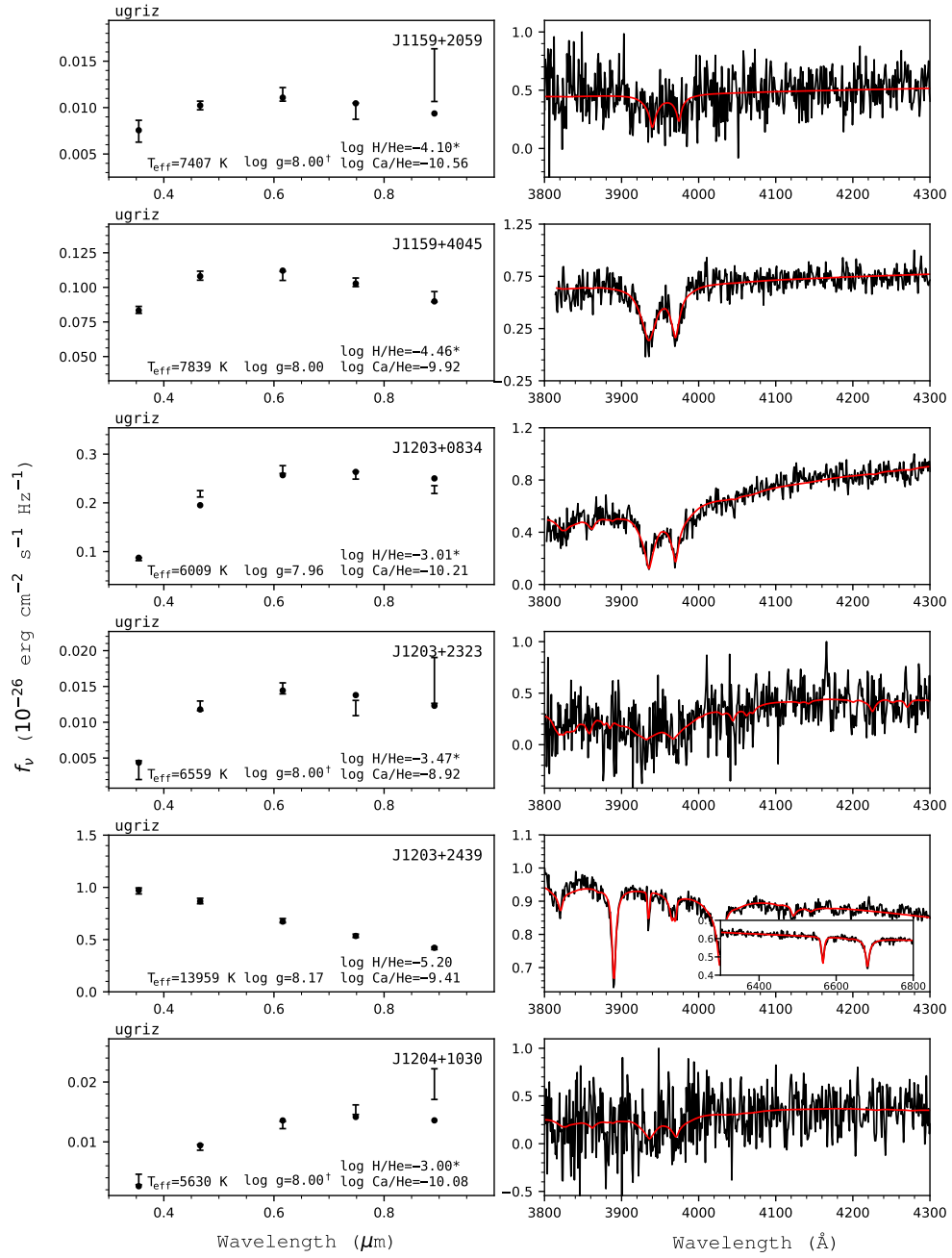


Figure 106. Fits to the DBZ/DZ(A) white dwarfs - continued.

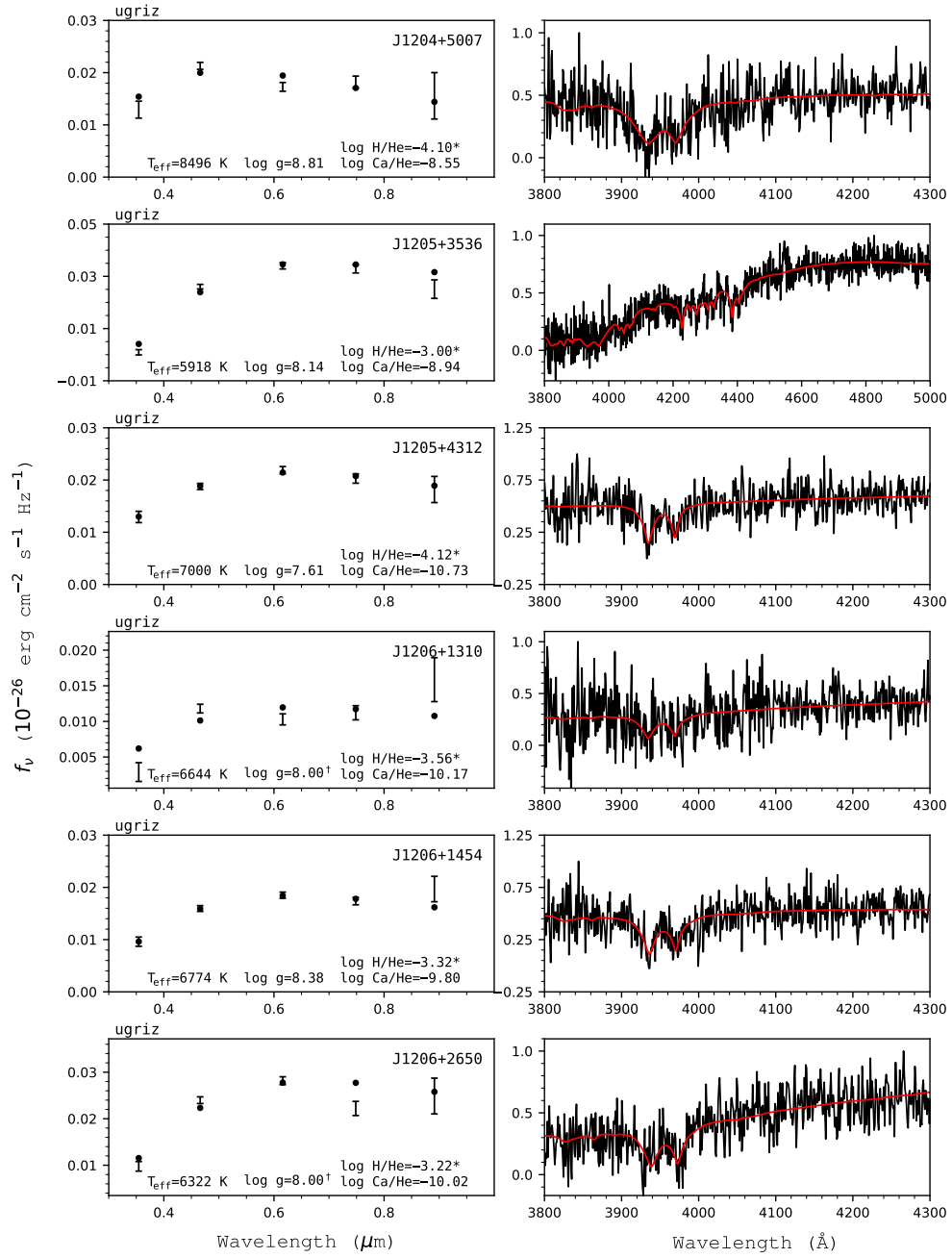


Figure 107. Fits to the DBZ/DZ(A) white dwarfs - continued.

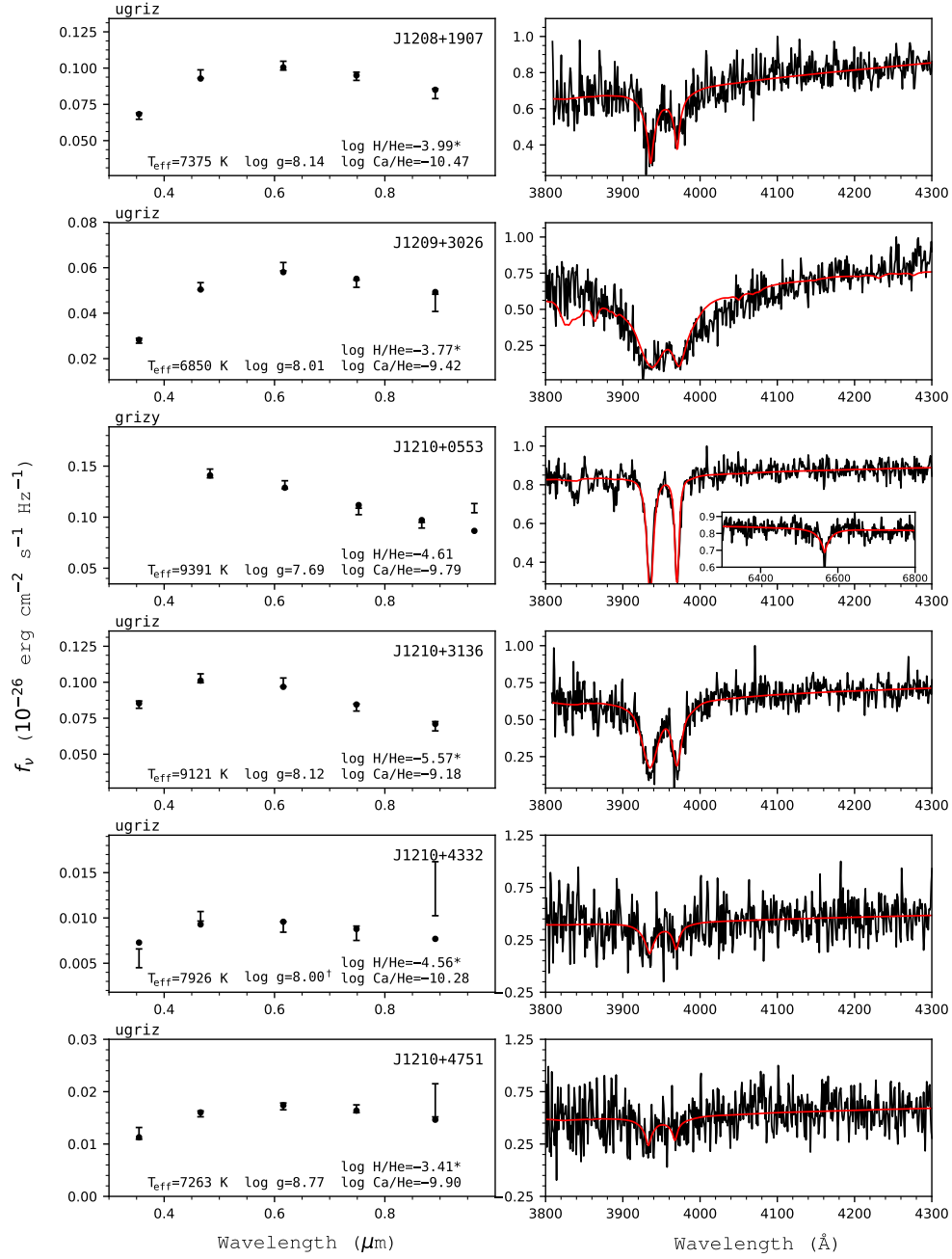


Figure 108. Fits to the DBZ/DZ(A) white dwarfs - continued.

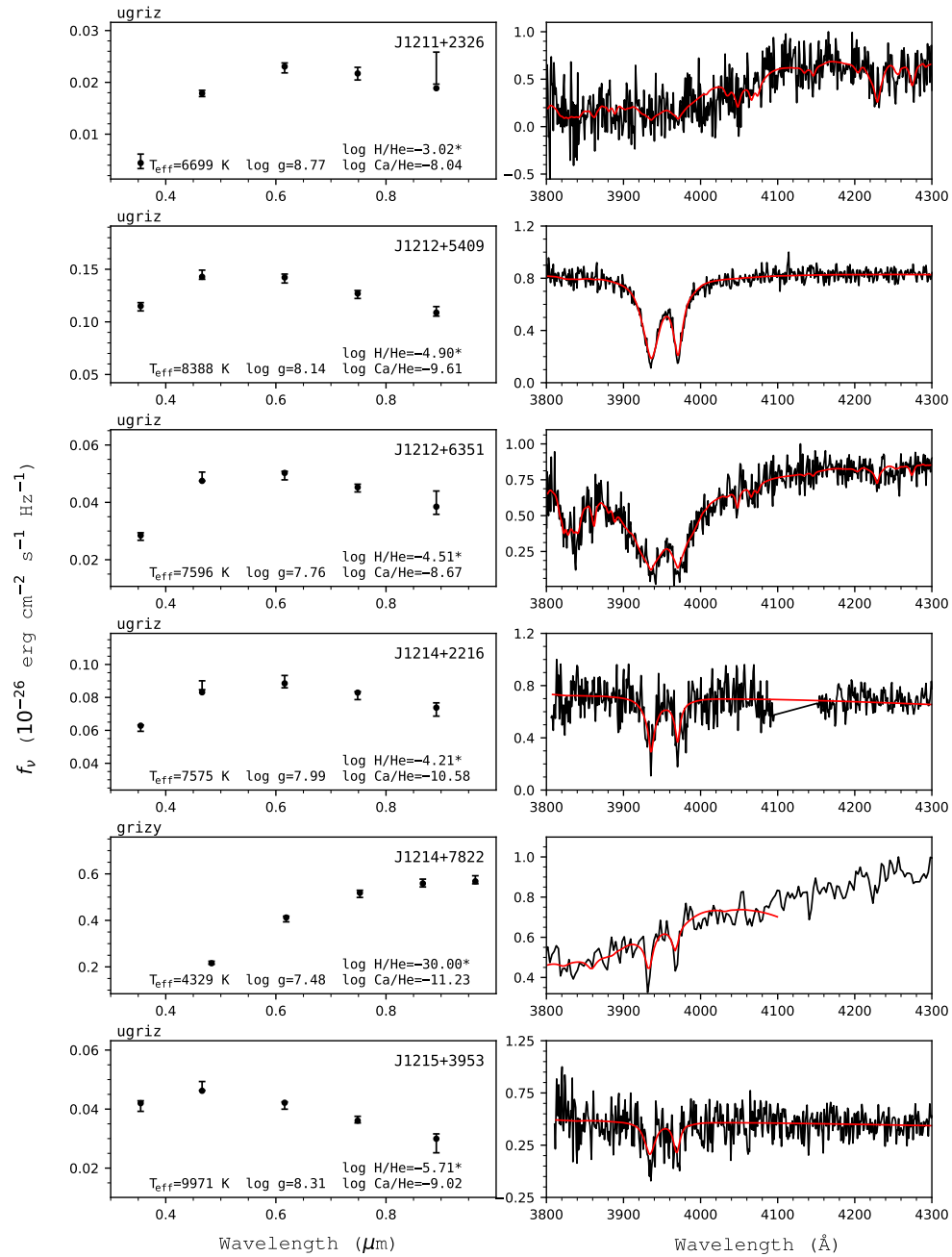


Figure 109. Fits to the DBZ/DZ(A) white dwarfs - continued.

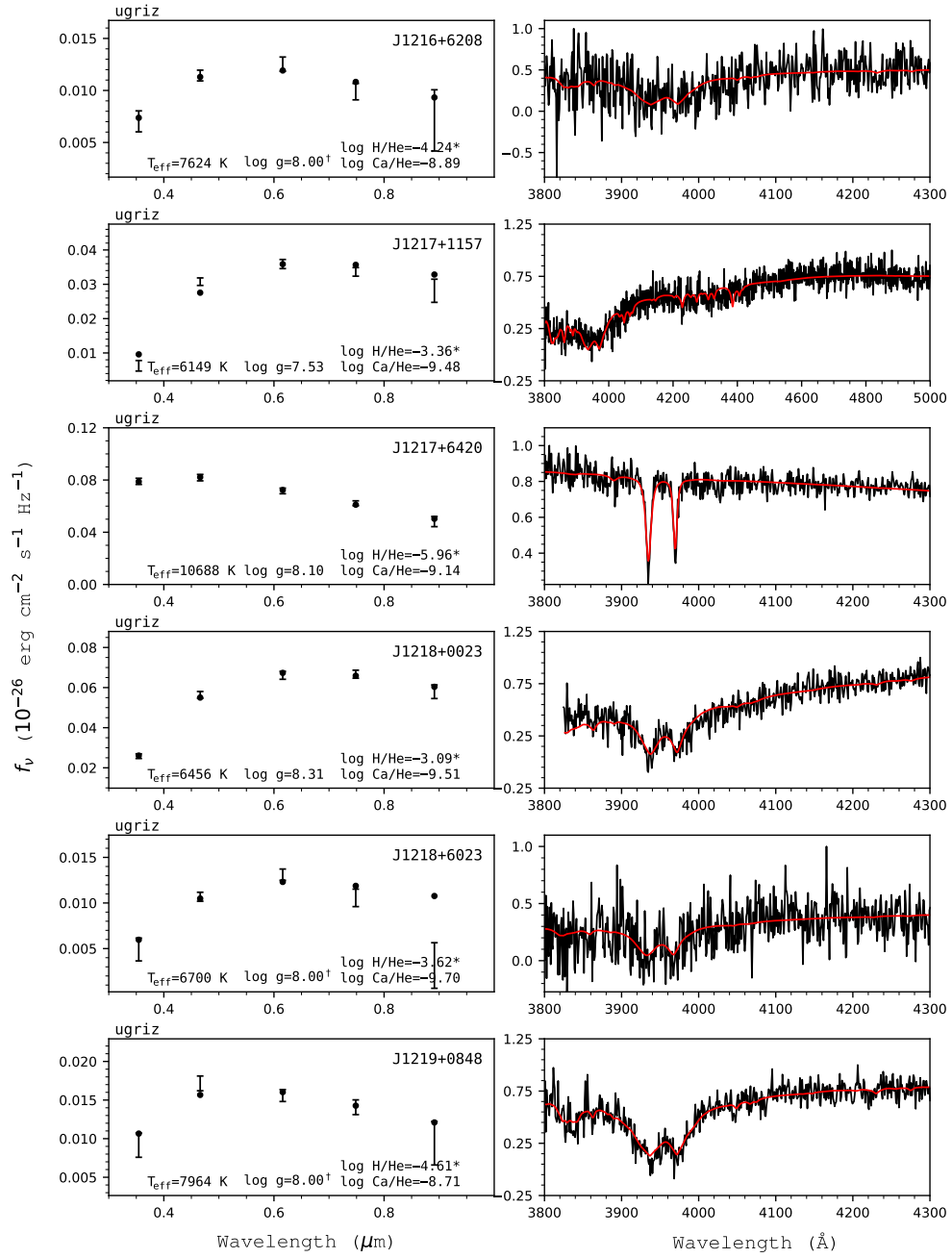


Figure 110. Fits to the DBZ/DZ(A) white dwarfs - continued.

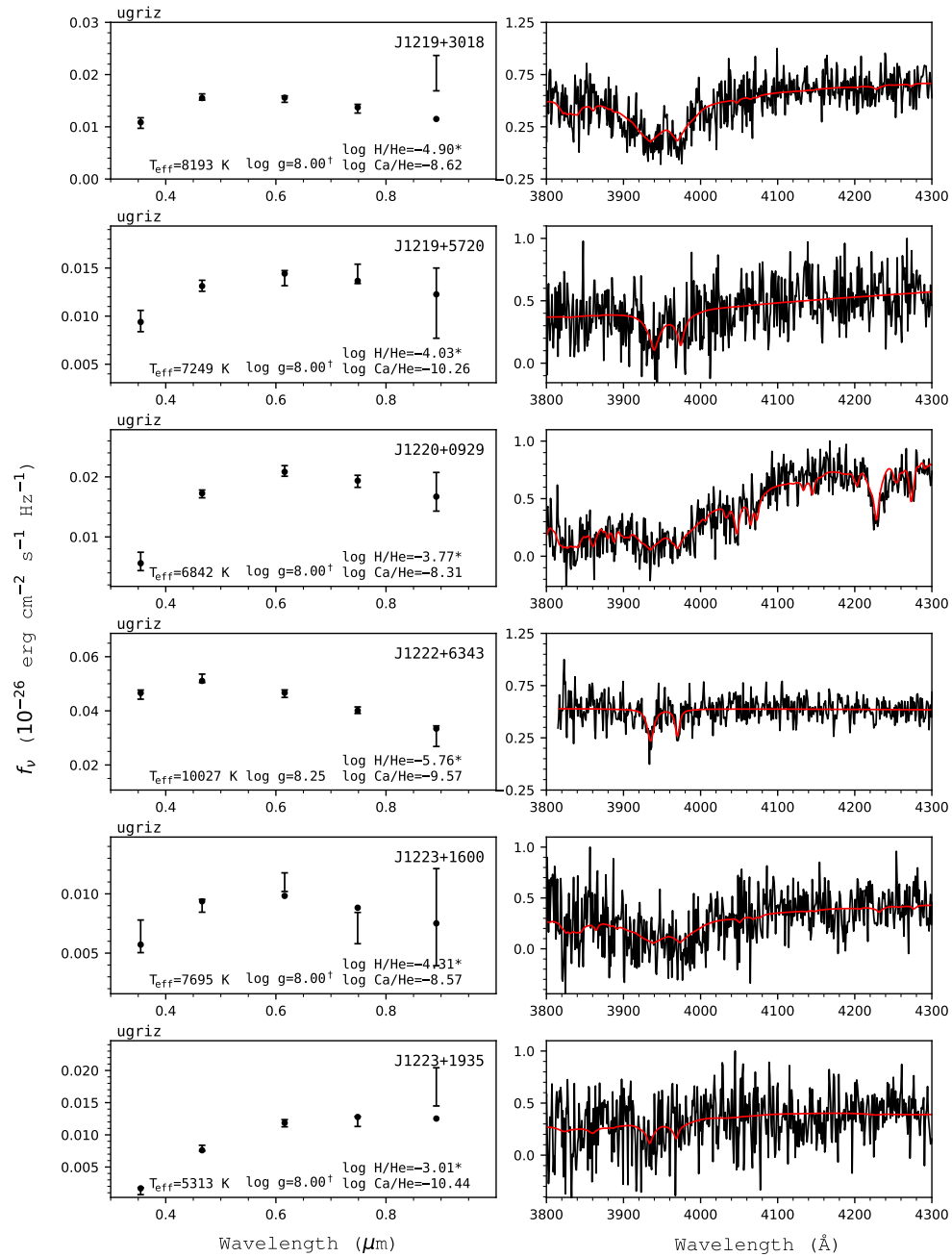


Figure 111. Fits to the DBZ/DZ(A) white dwarfs - continued.

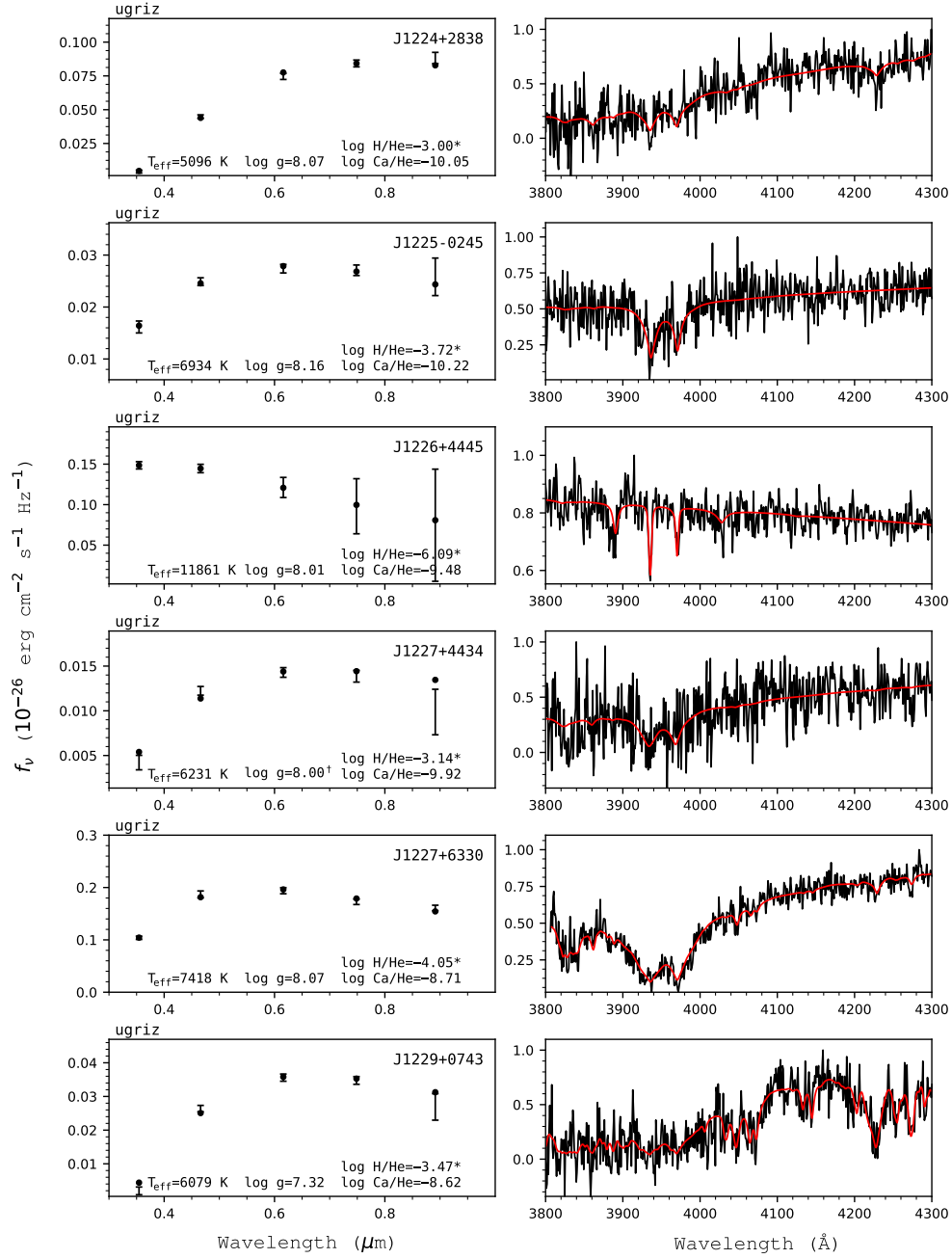


Figure 112. Fits to the DBZ/DZ(A) white dwarfs - continued.

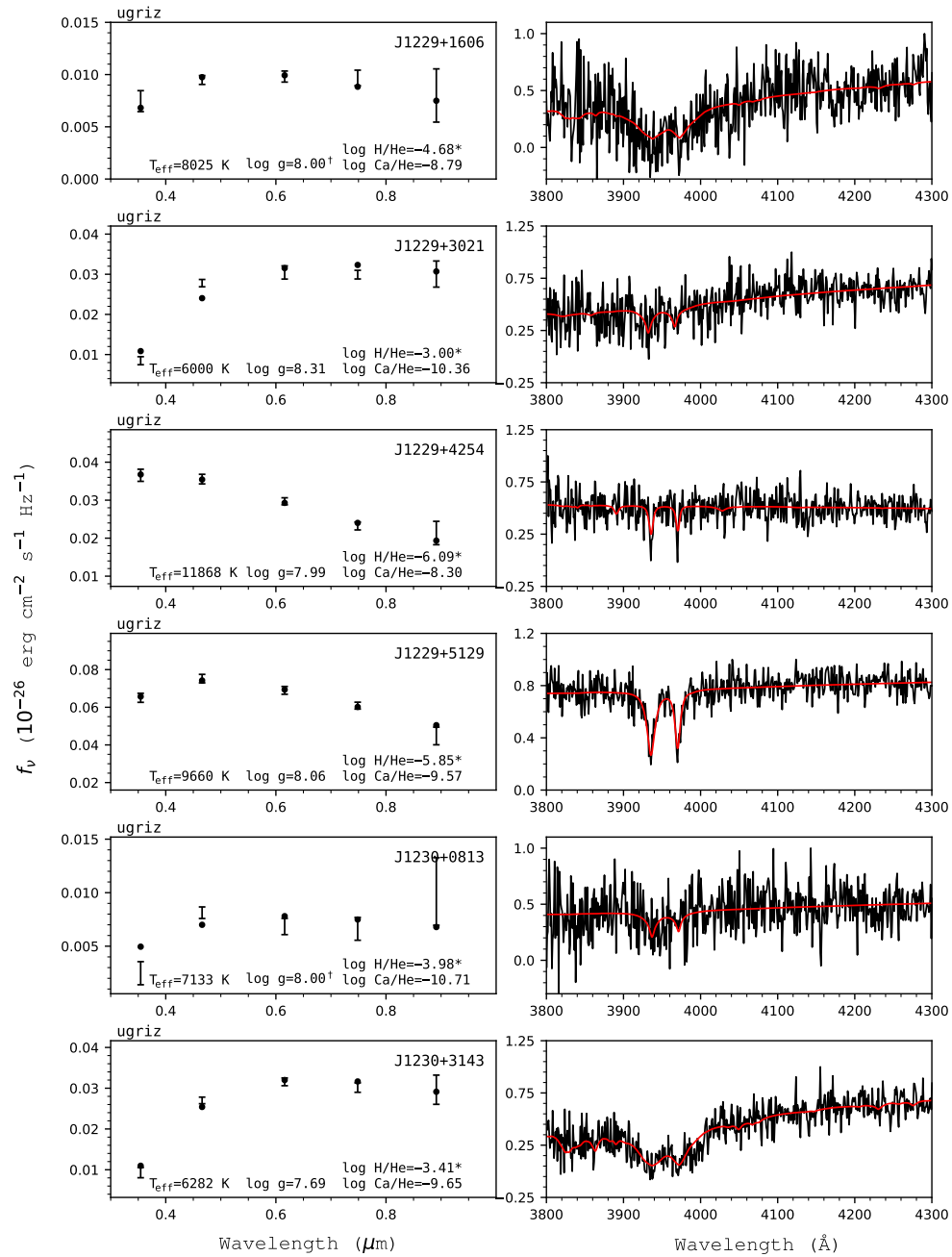


Figure 113. Fits to the DBZ/DZ(A) white dwarfs - continued.

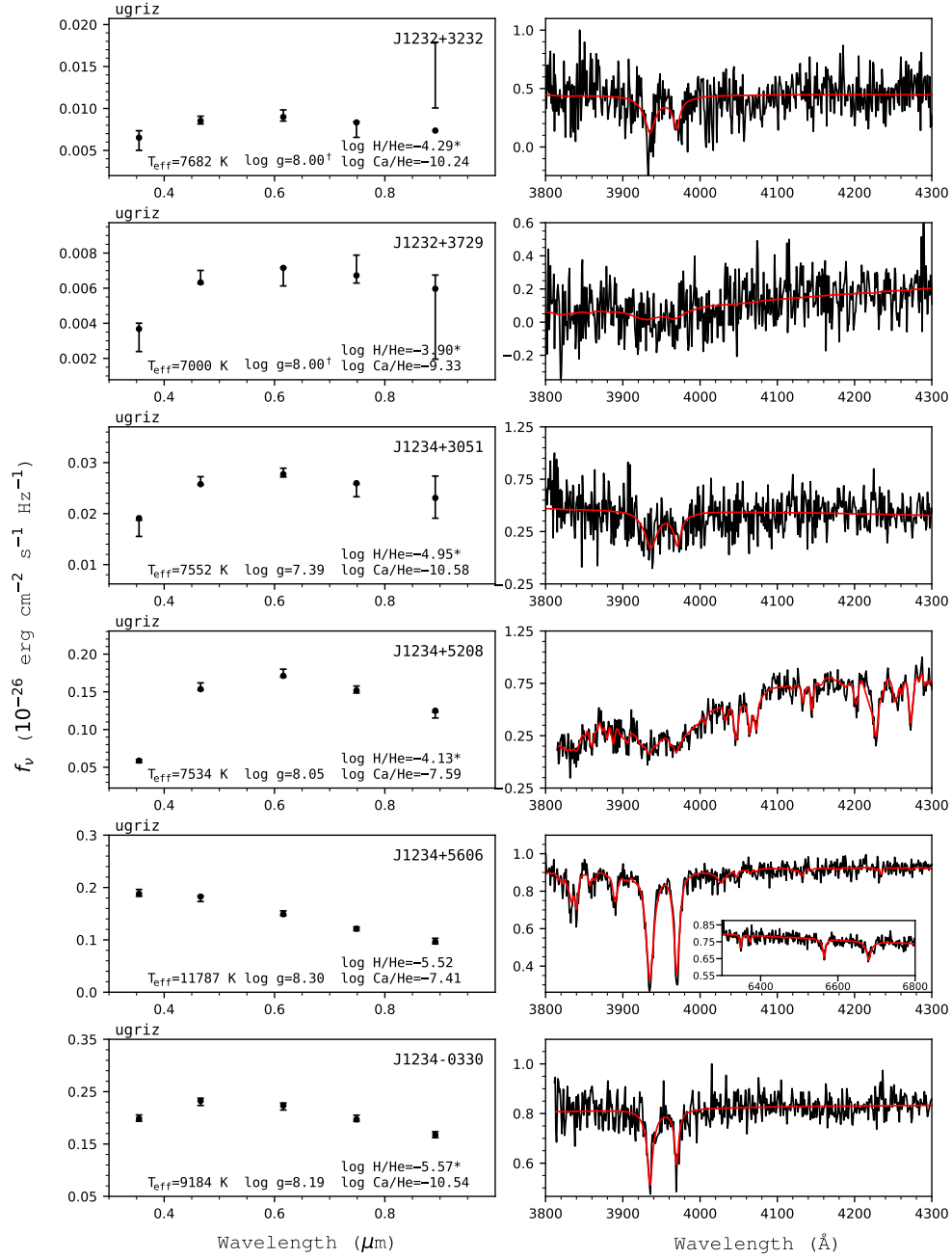


Figure 114. Fits to the DBZ/DZ(A) white dwarfs - continued.

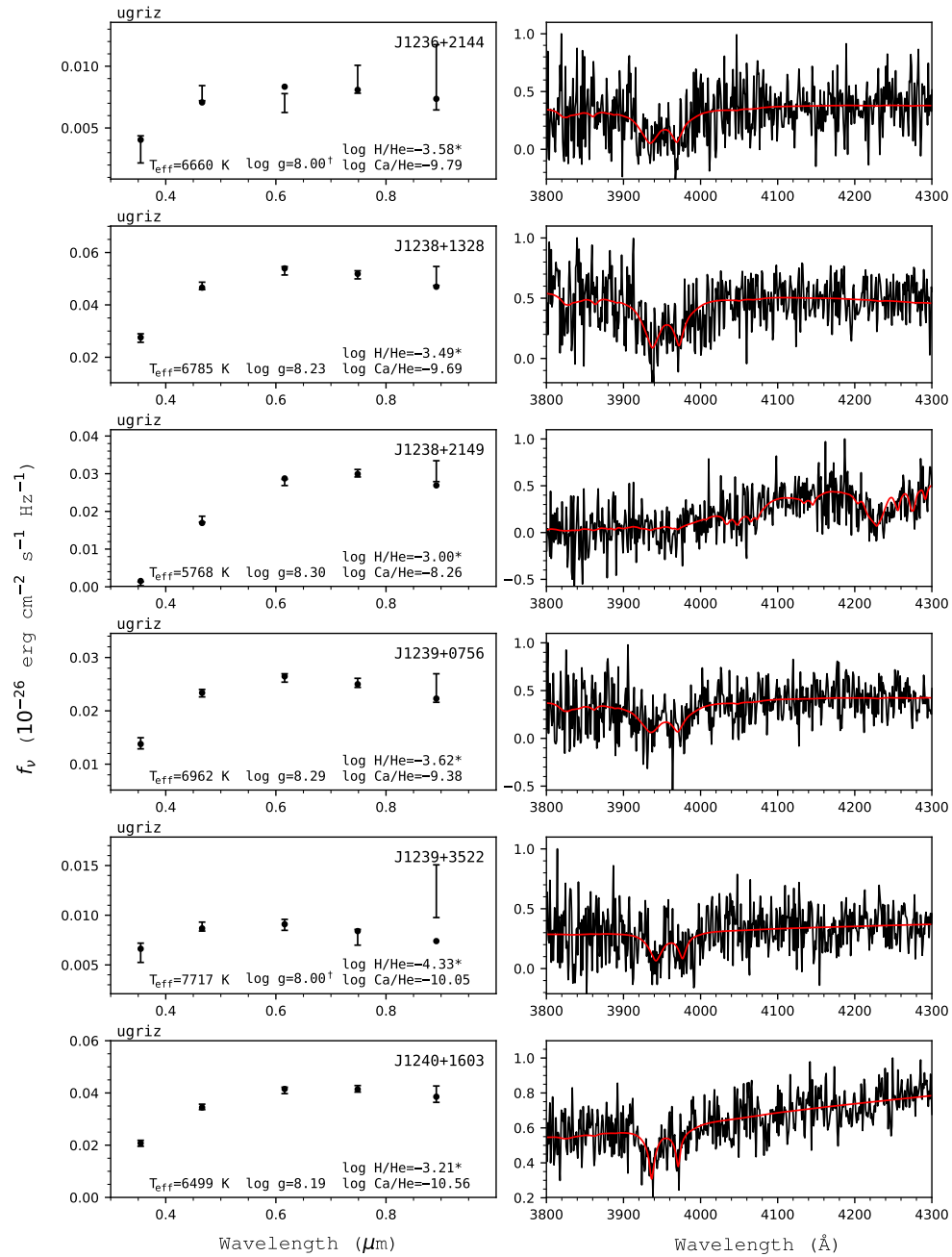


Figure 115. Fits to the DBZ/DZ(A) white dwarfs - continued.

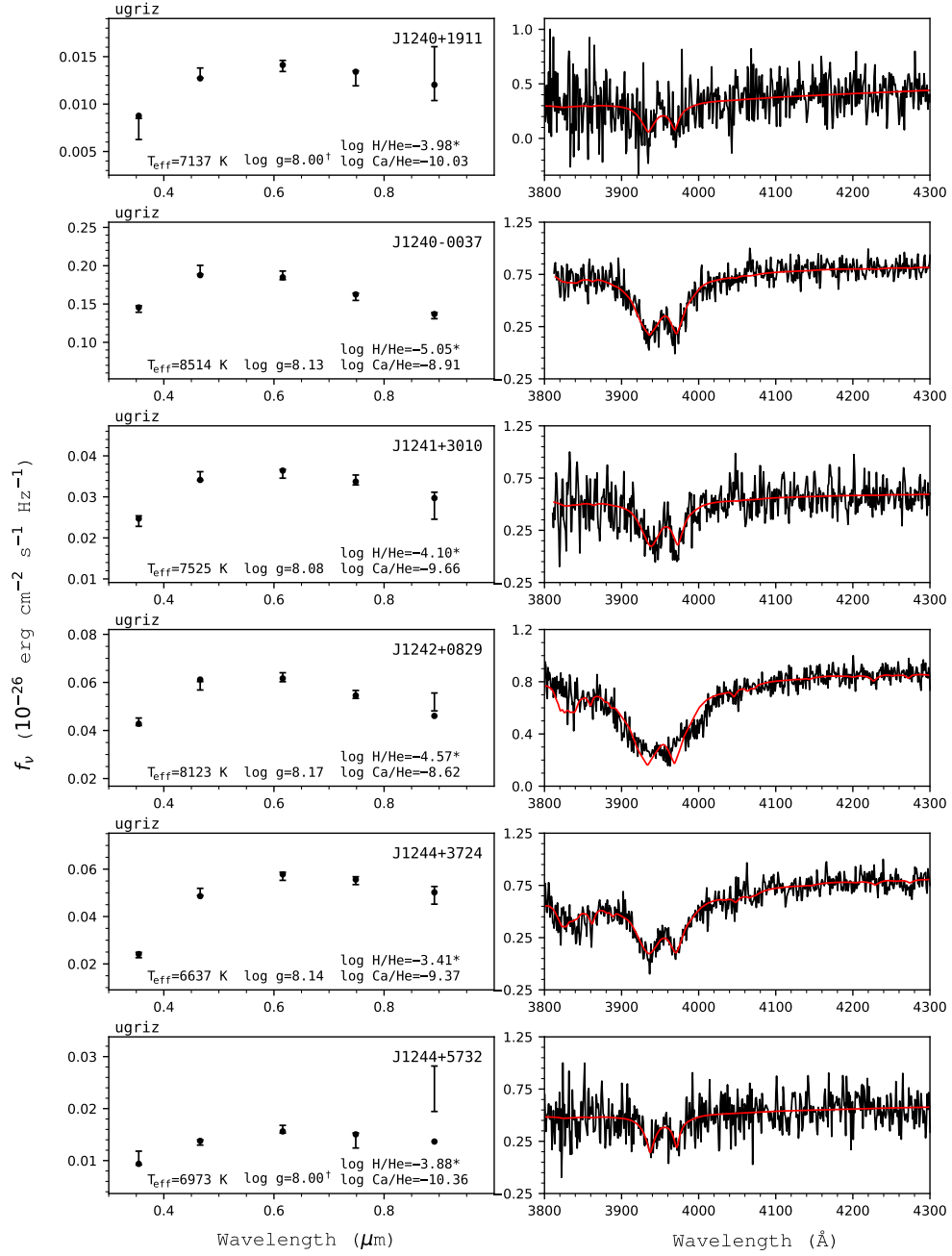


Figure 116. Fits to the DBZ/DZ(A) white dwarfs - continued.

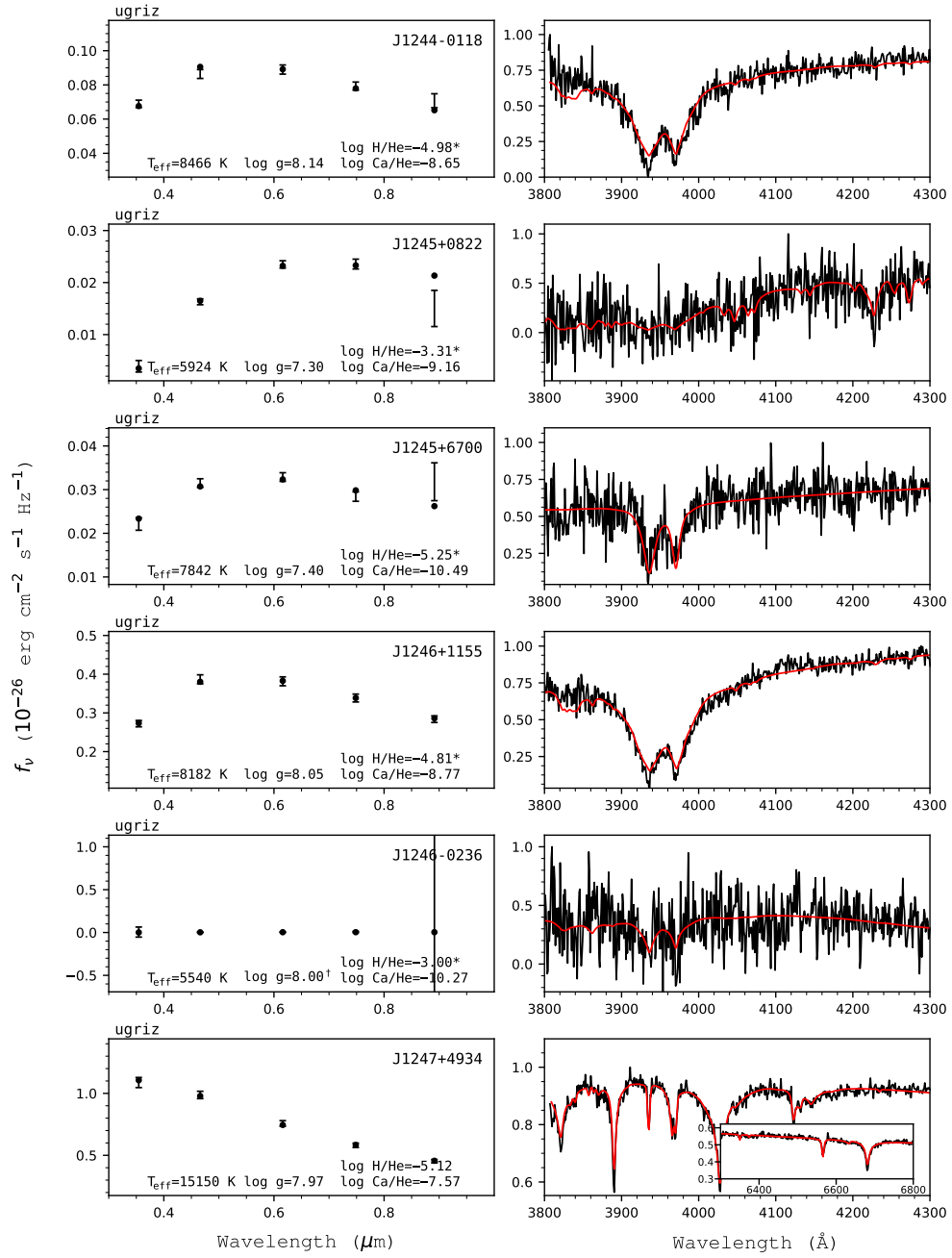


Figure 117. Fits to the DBZ/DZ(A) white dwarfs - continued.

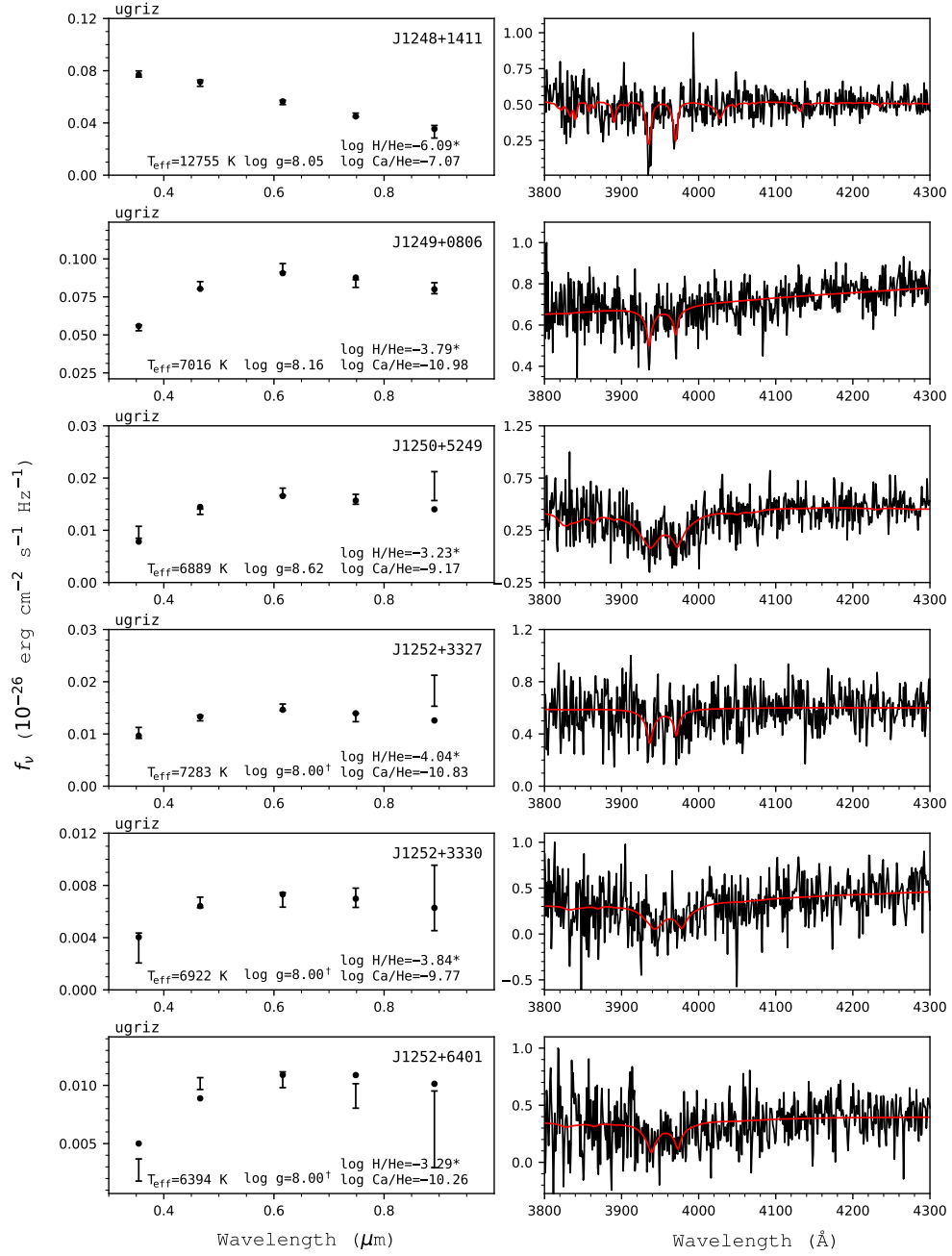


Figure 118. Fits to the DB/DZ(A) white dwarfs - continued.

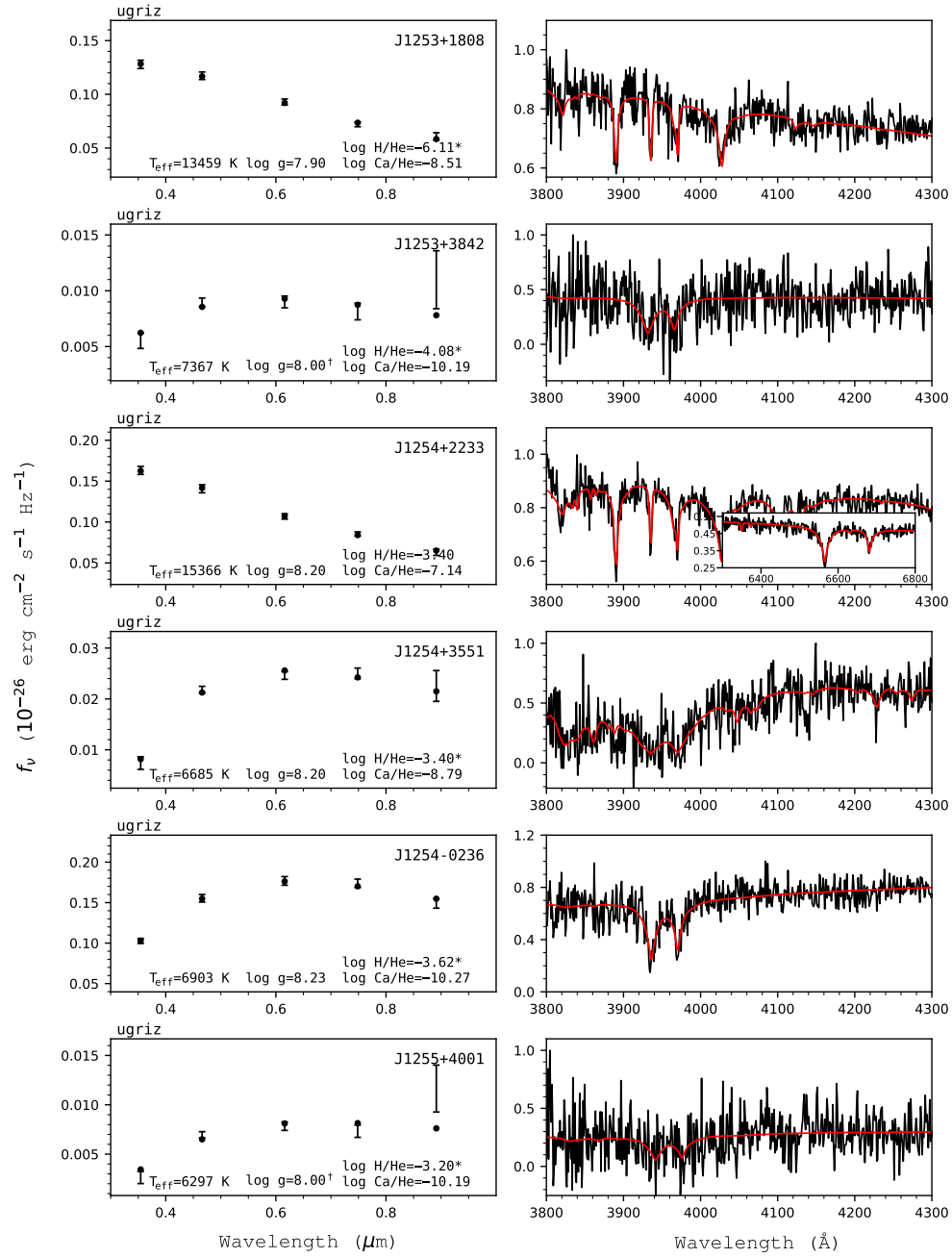


Figure 119. Fits to the DBZ/DZ(A) white dwarfs - continued.

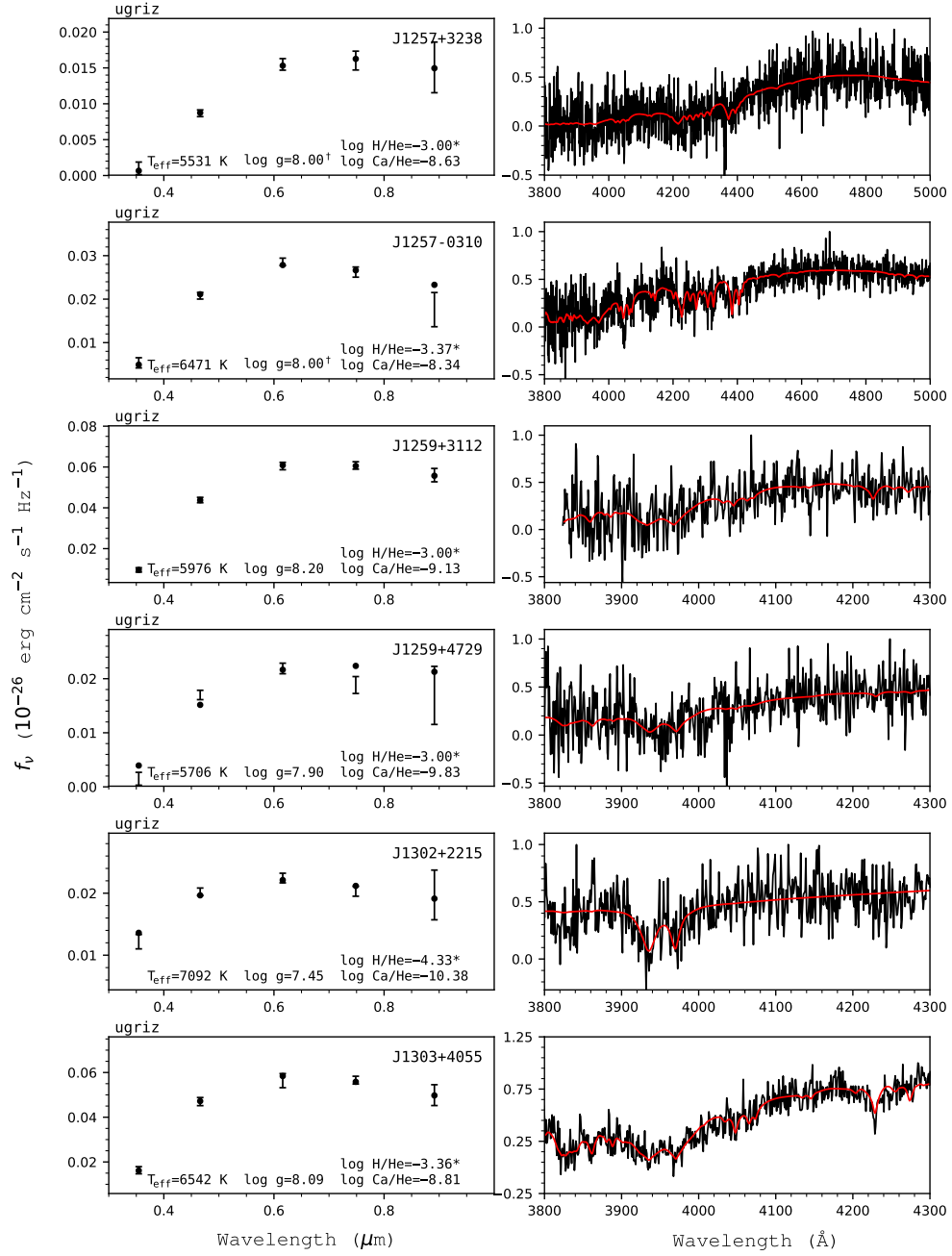


Figure 120. Fits to the DBZ/DZ(A) white dwarfs - continued.

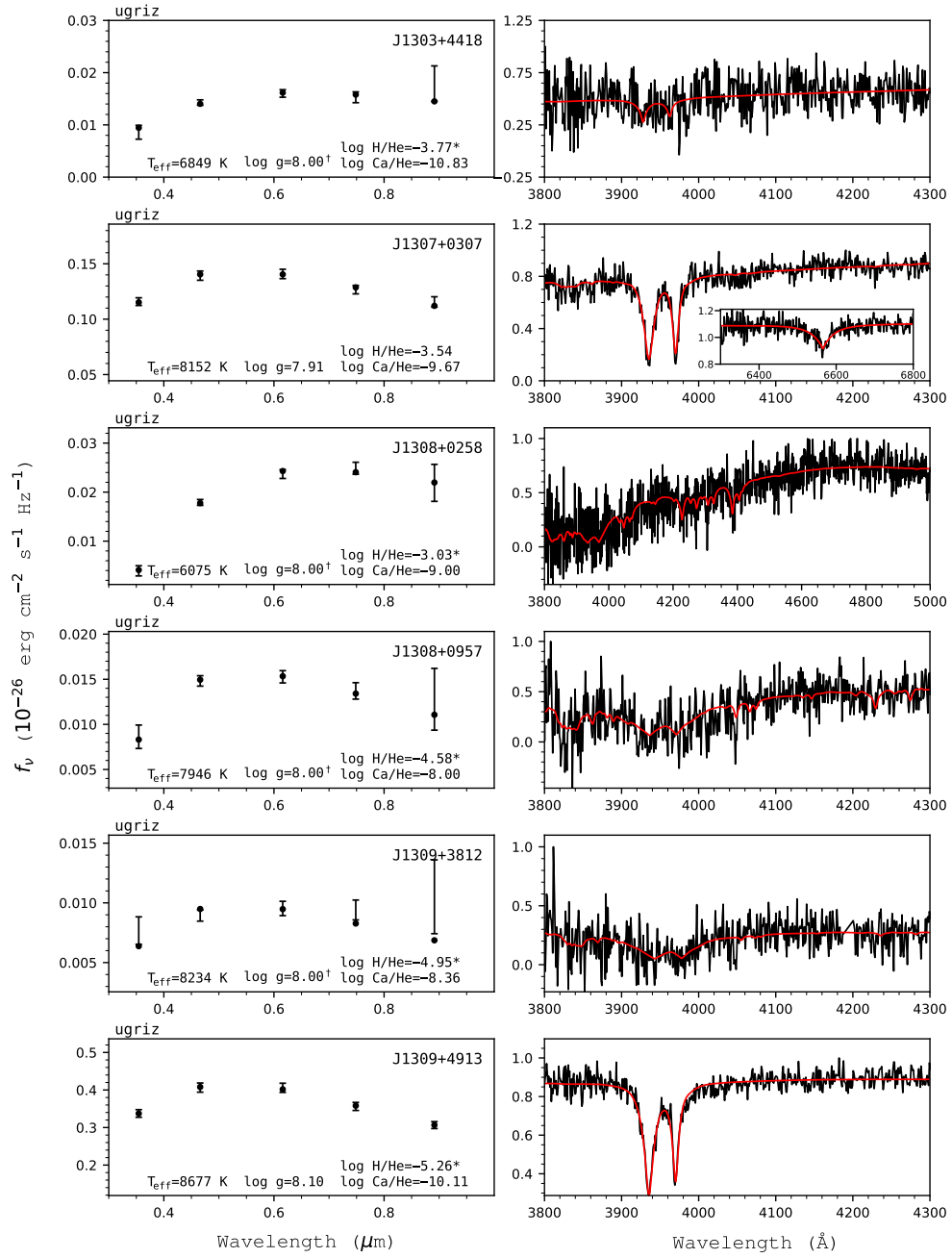


Figure 121. Fits to the DBZ/DZ(A) white dwarfs - continued.

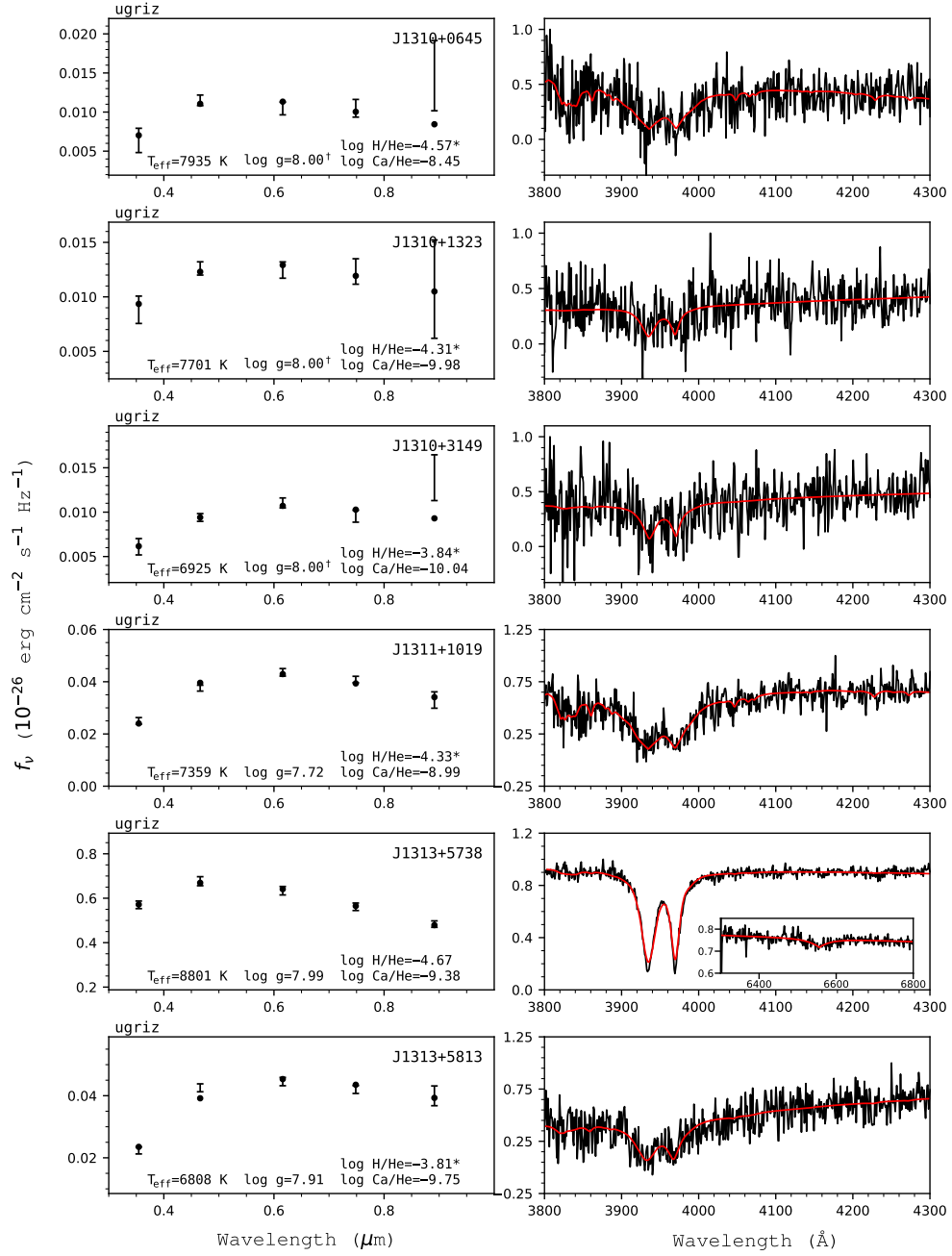


Figure 122. Fits to the DBZ/DZ(A) white dwarfs - continued.

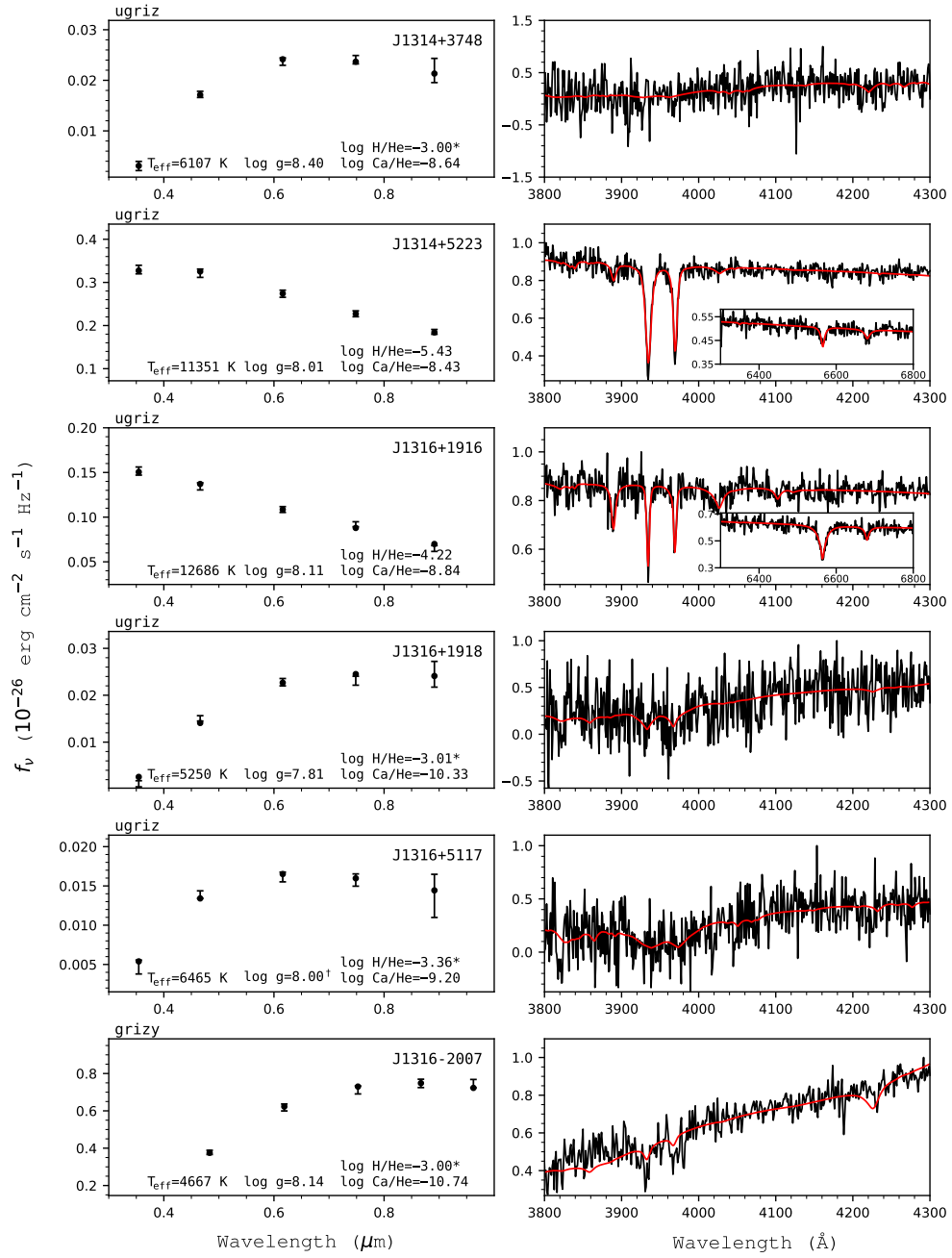


Figure 123. Fits to the DBZ/DZ(A) white dwarfs - continued.

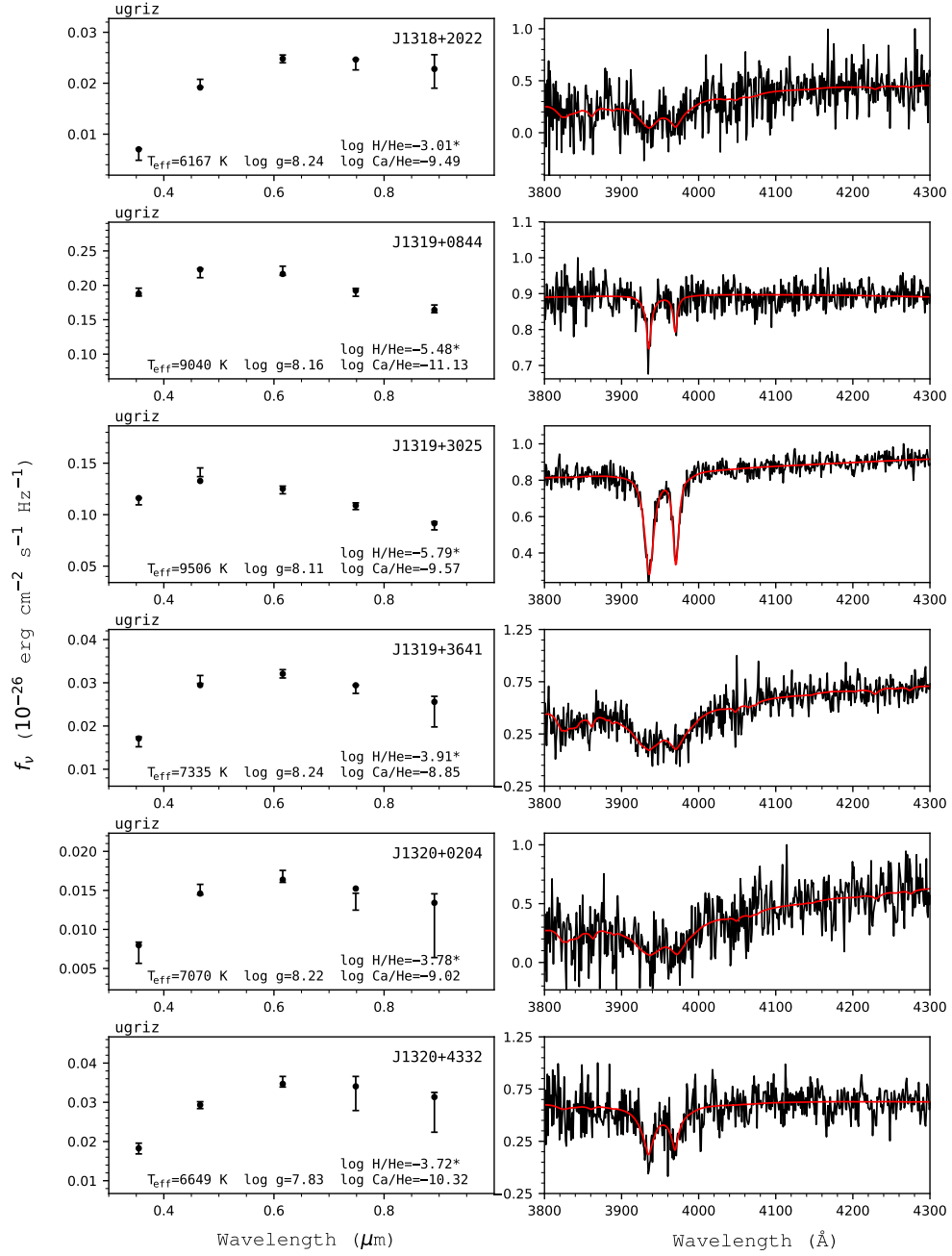


Figure 124. Fits to the DBZ/DZ(A) white dwarfs - continued.

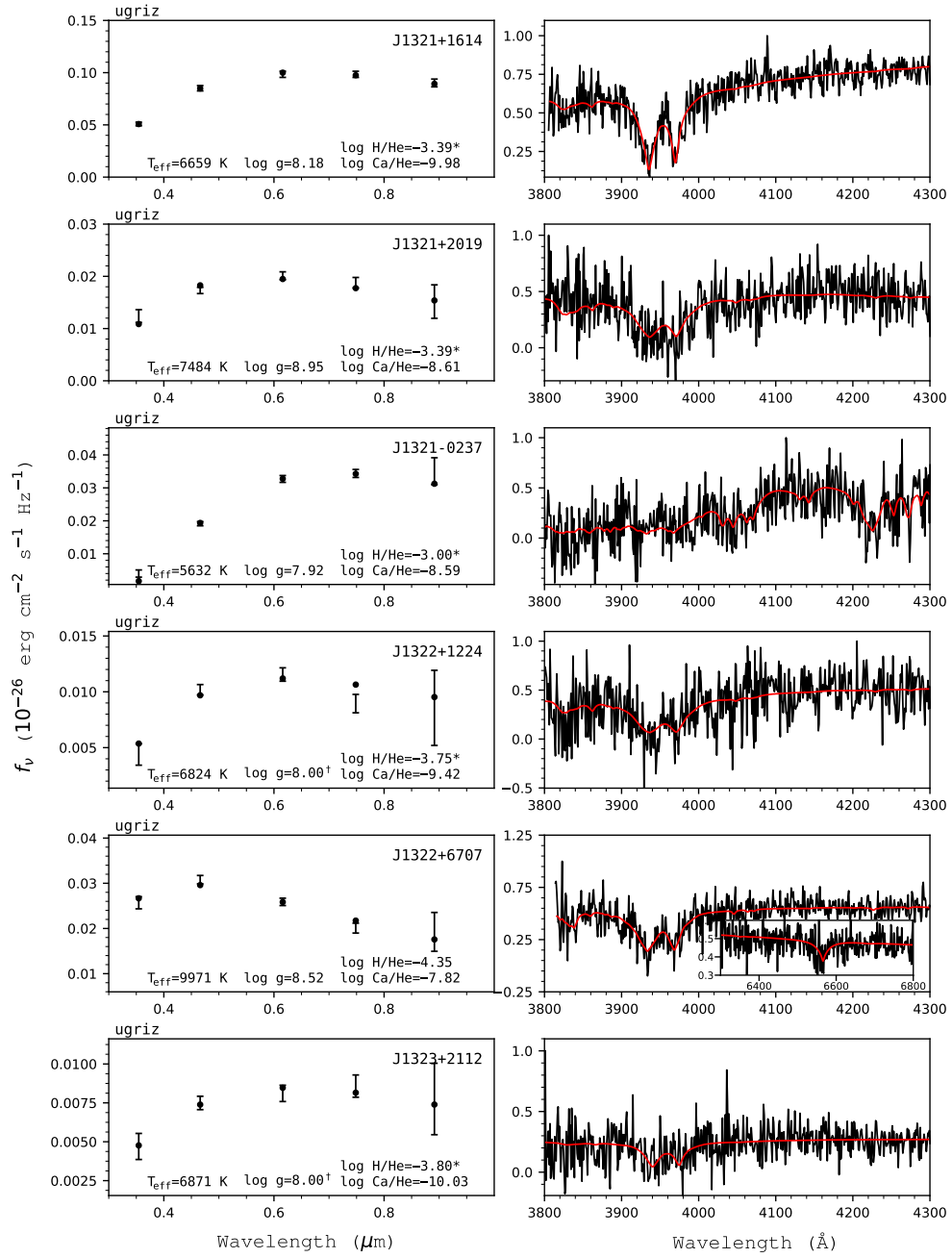


Figure 125. Fits to the DBZ/DZ(A) white dwarfs - continued.

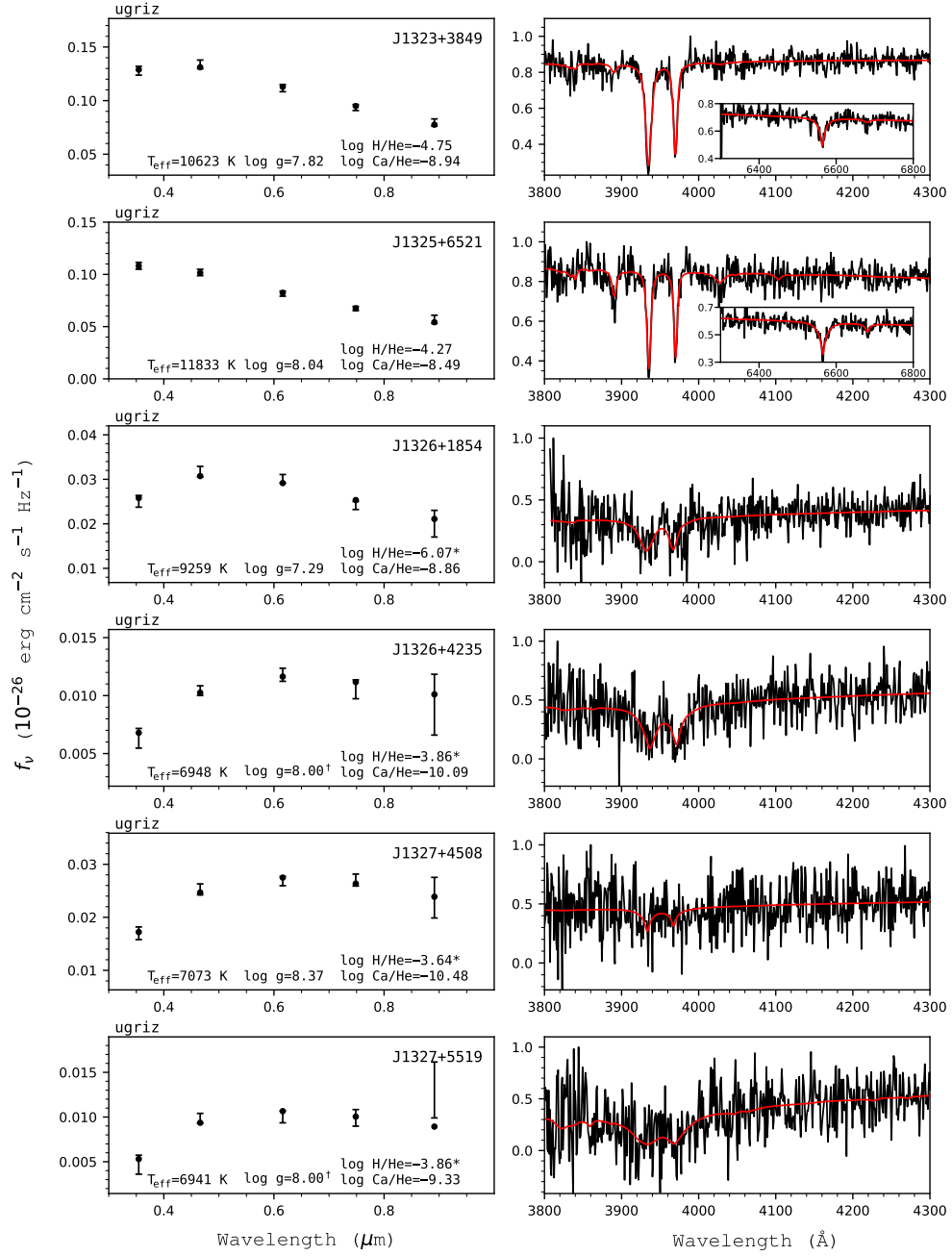


Figure 126. Fits to the DBZ/DZ(A) white dwarfs - continued.

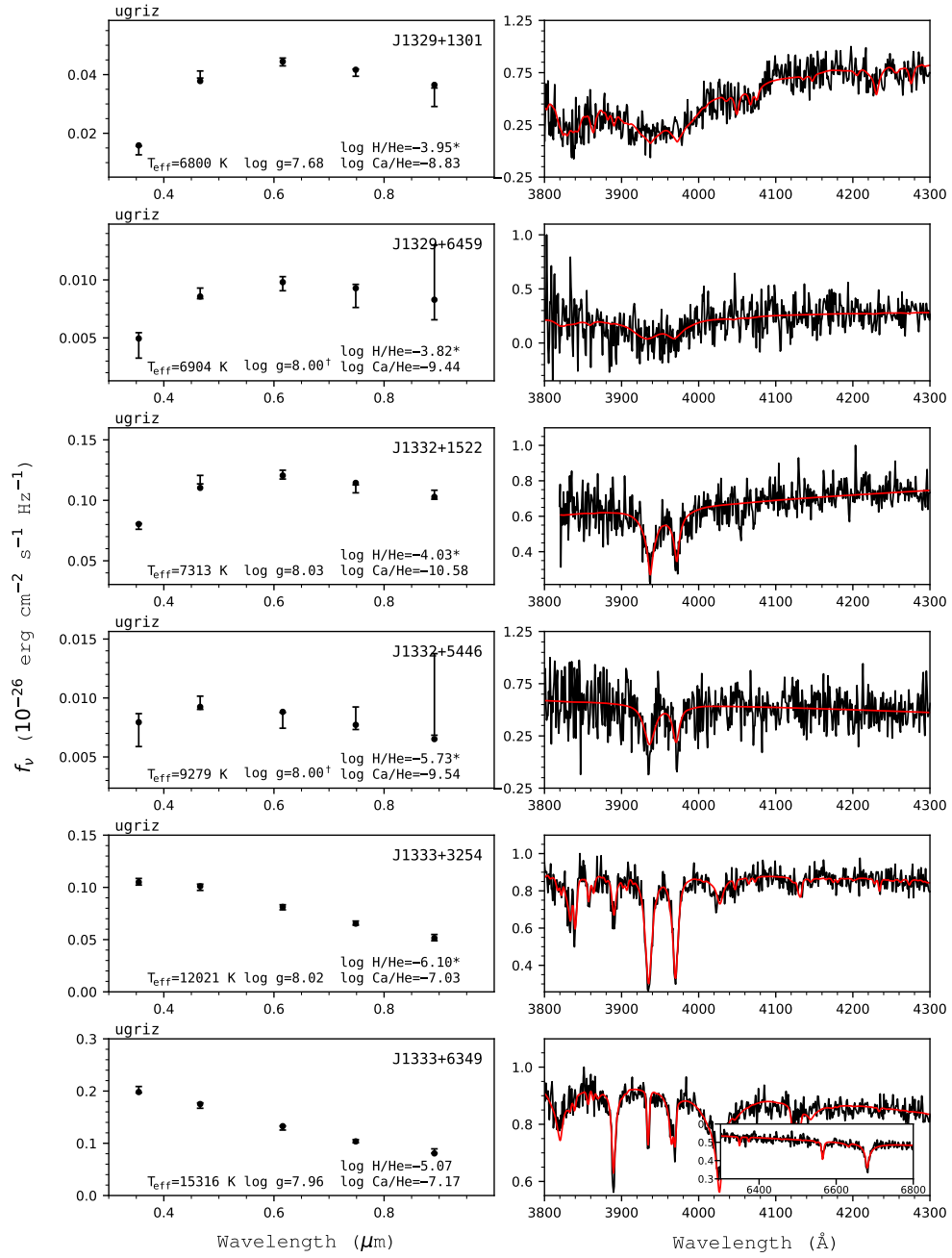


Figure 127. Fits to the DBZ/DZ(A) white dwarfs - continued.

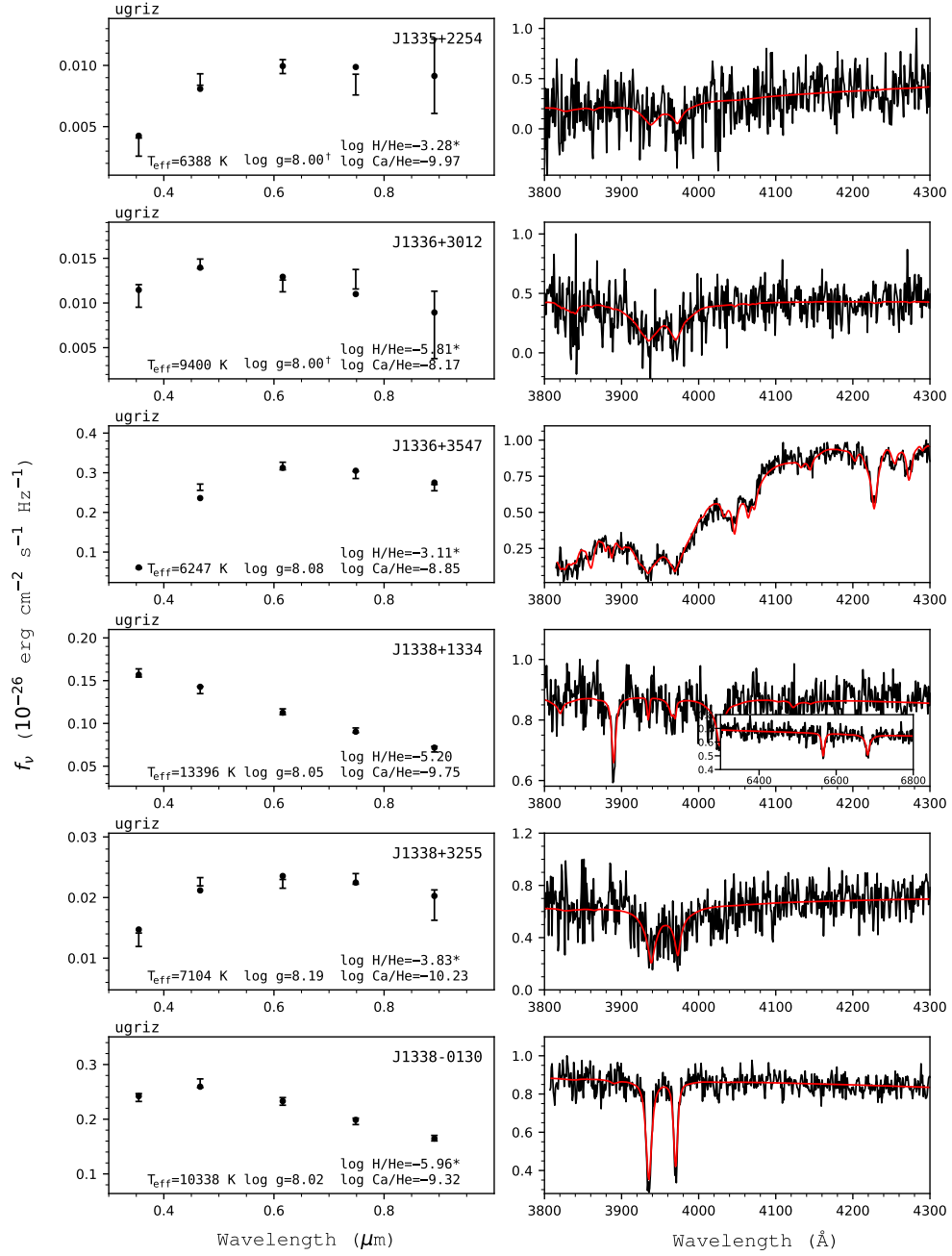


Figure 128. Fits to the DBZ/DZ(A) white dwarfs - continued.

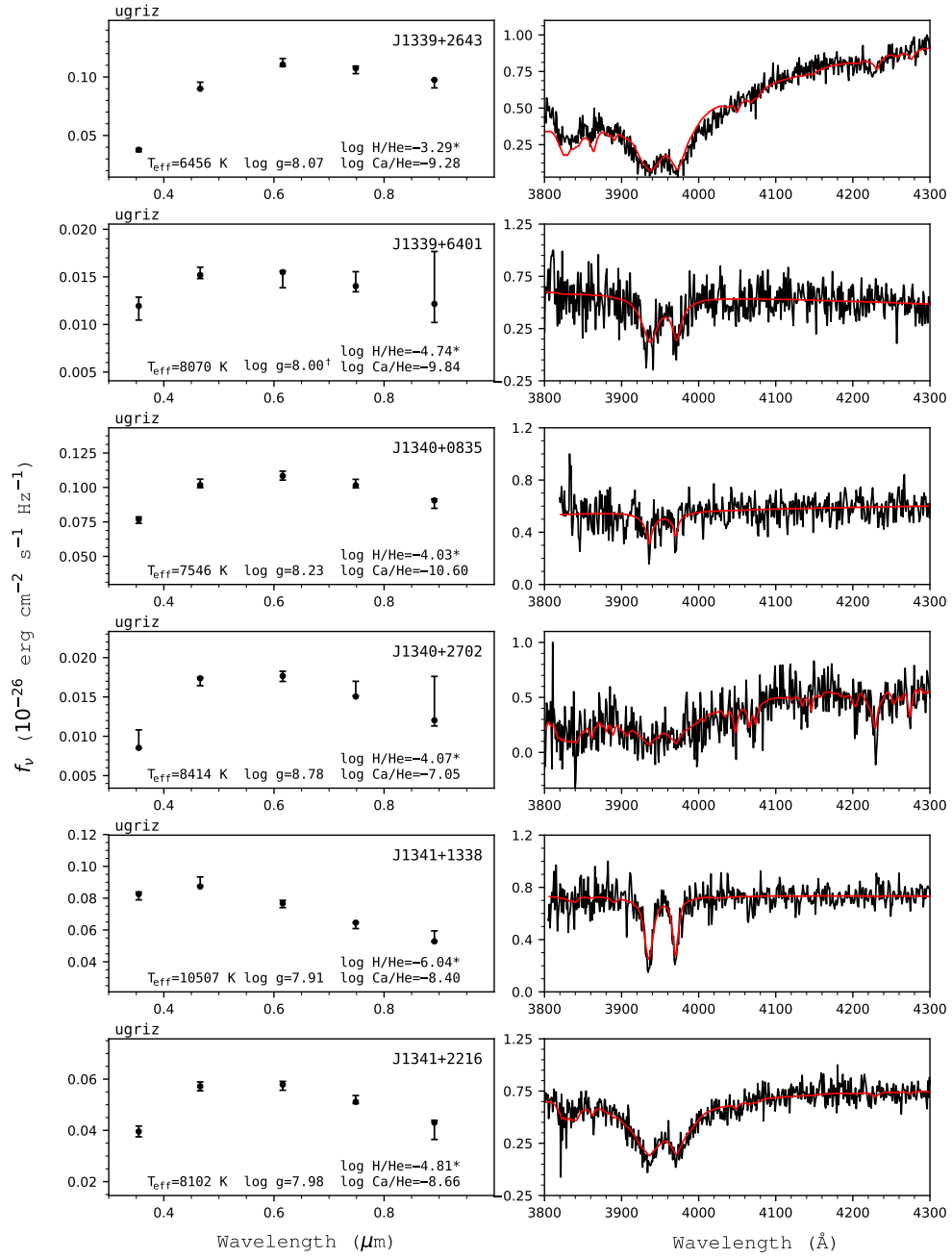


Figure 129. Fits to the DBZ/DZ(A) white dwarfs - continued.

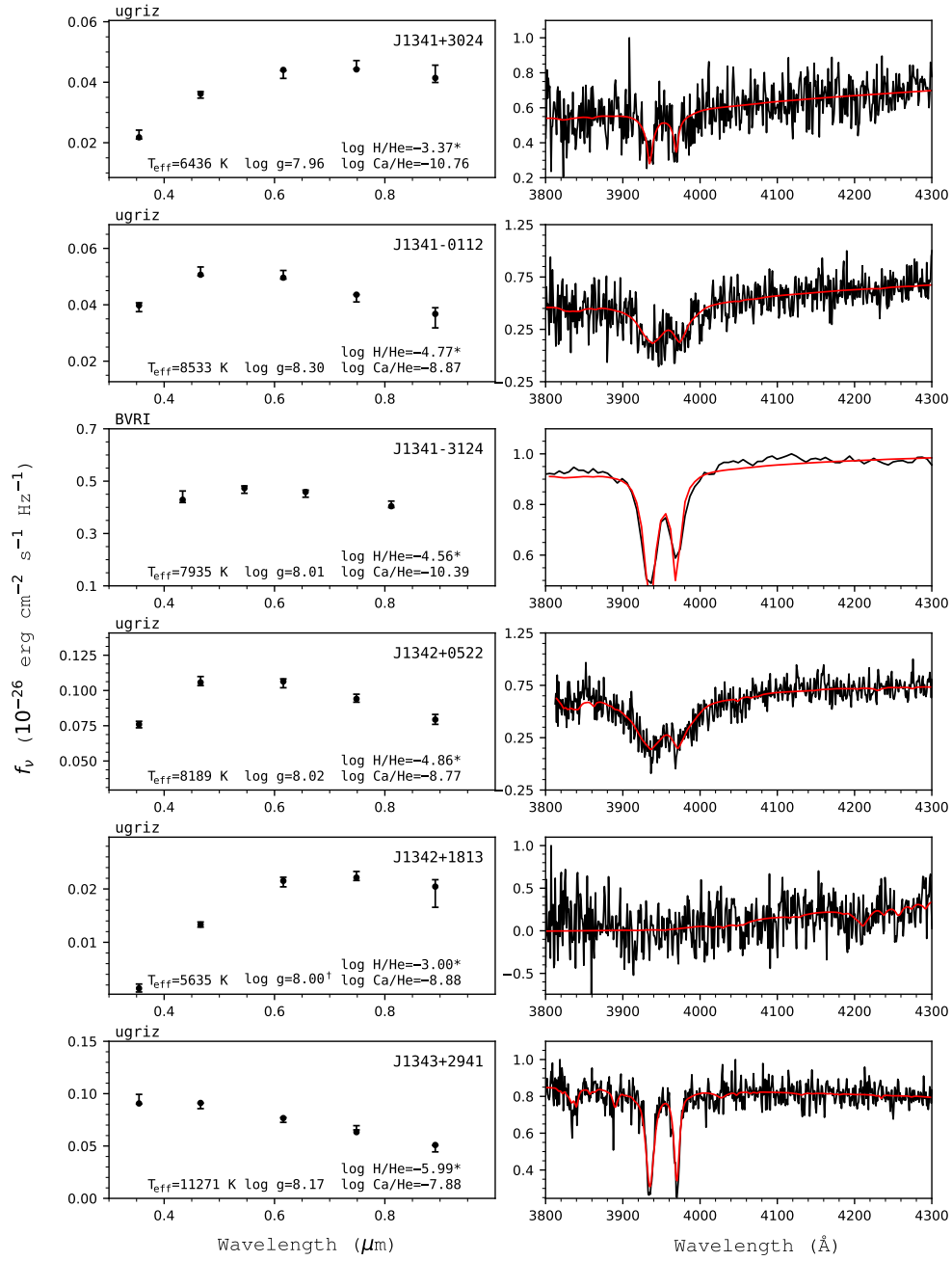


Figure 130. Fits to the DBZ/DZ(A) white dwarfs - continued.

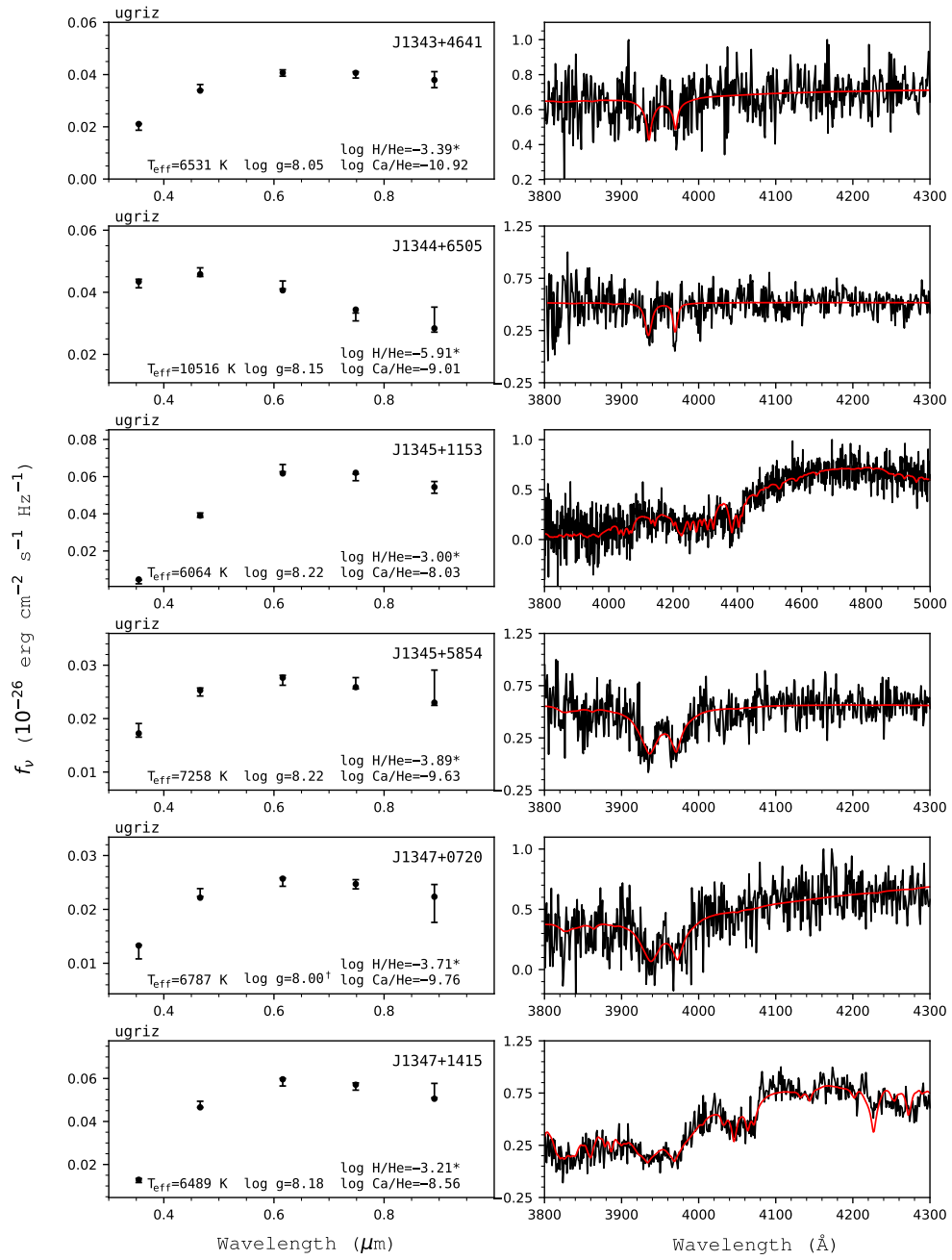


Figure 131. Fits to the DBZ/DZ(A) white dwarfs - continued.

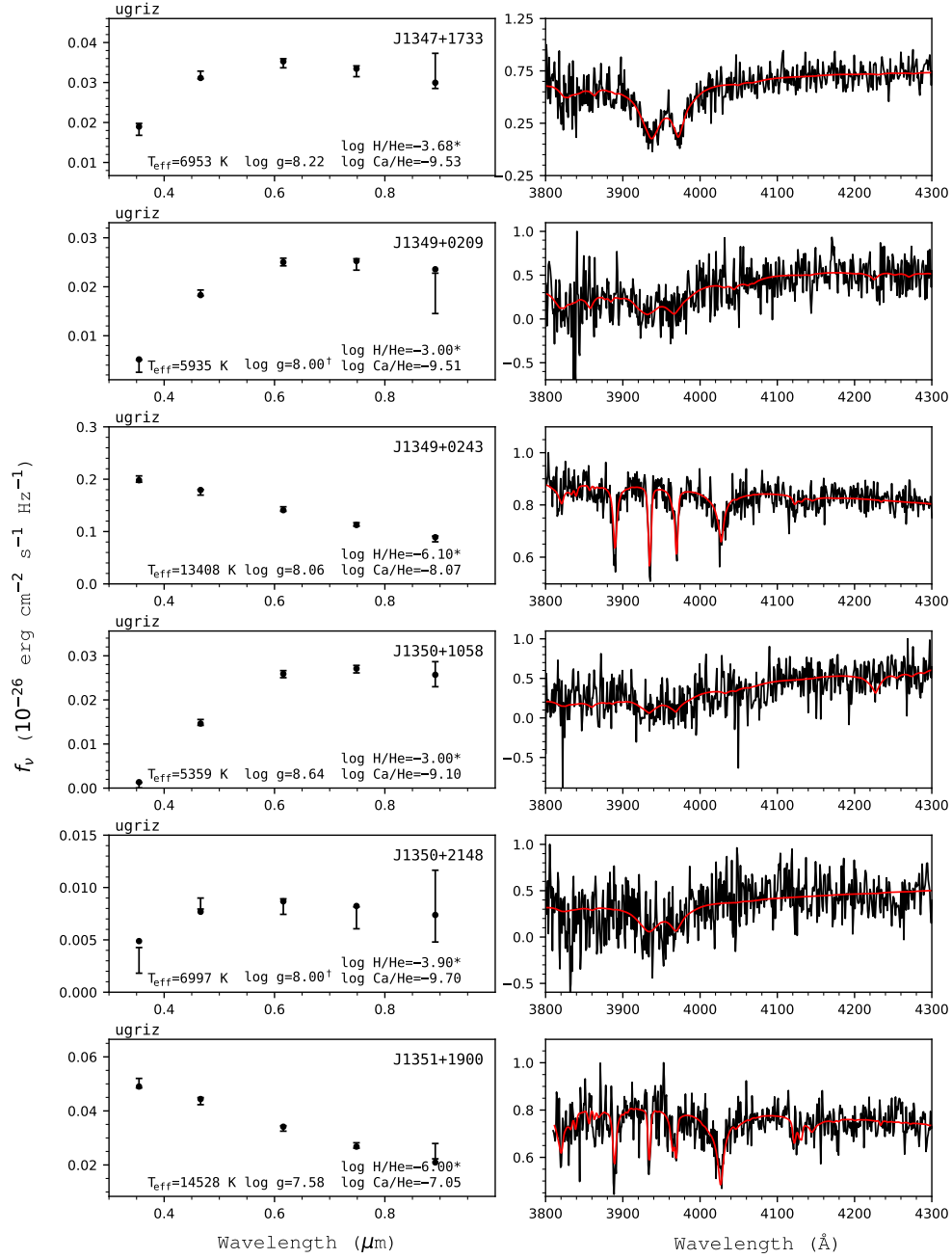


Figure 132. Fits to the DBZ/DZ(A) white dwarfs - continued.

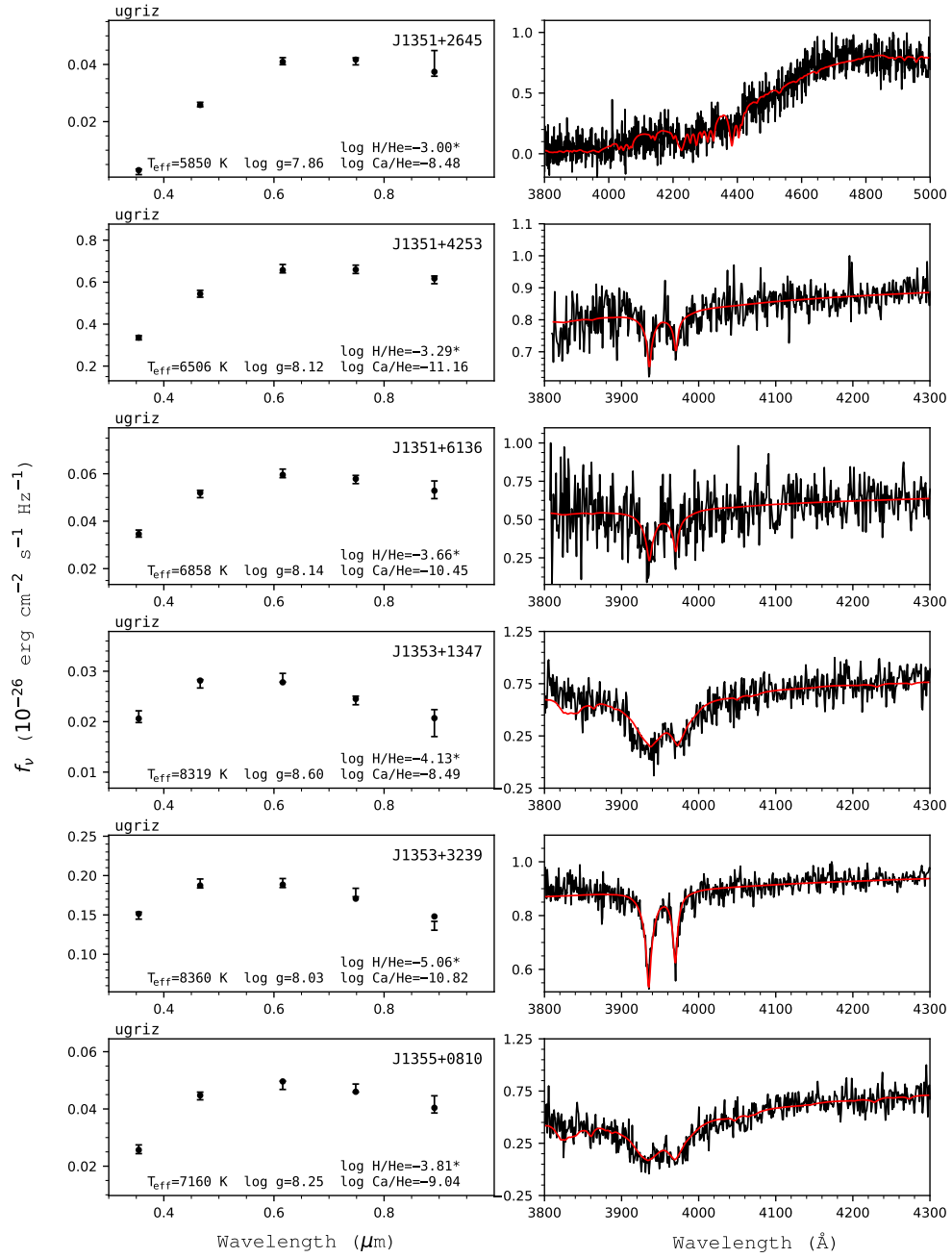


Figure 133. Fits to the DBZ/DZ(A) white dwarfs - continued.

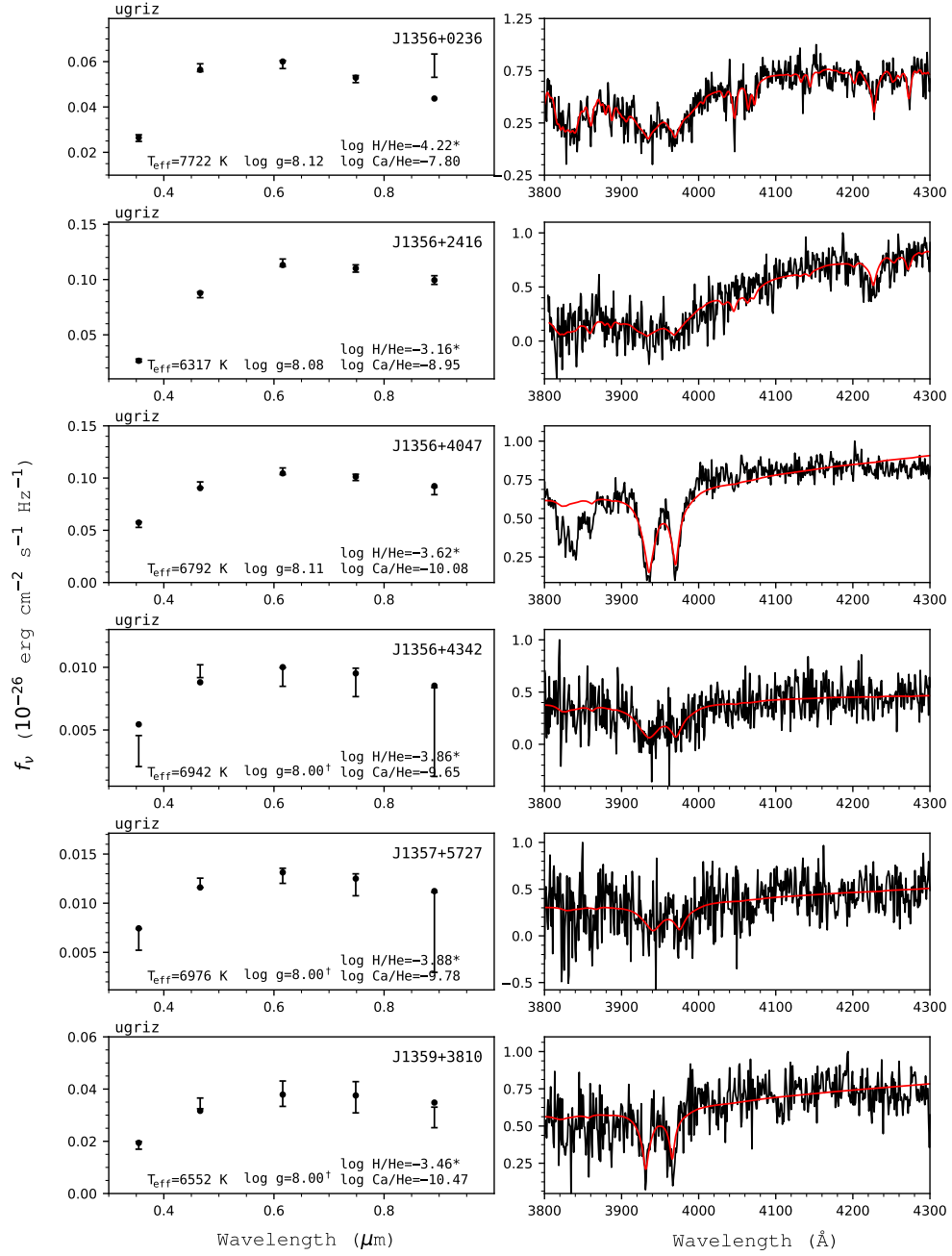


Figure 134. Fits to the DBZ/DZ(A) white dwarfs - continued.

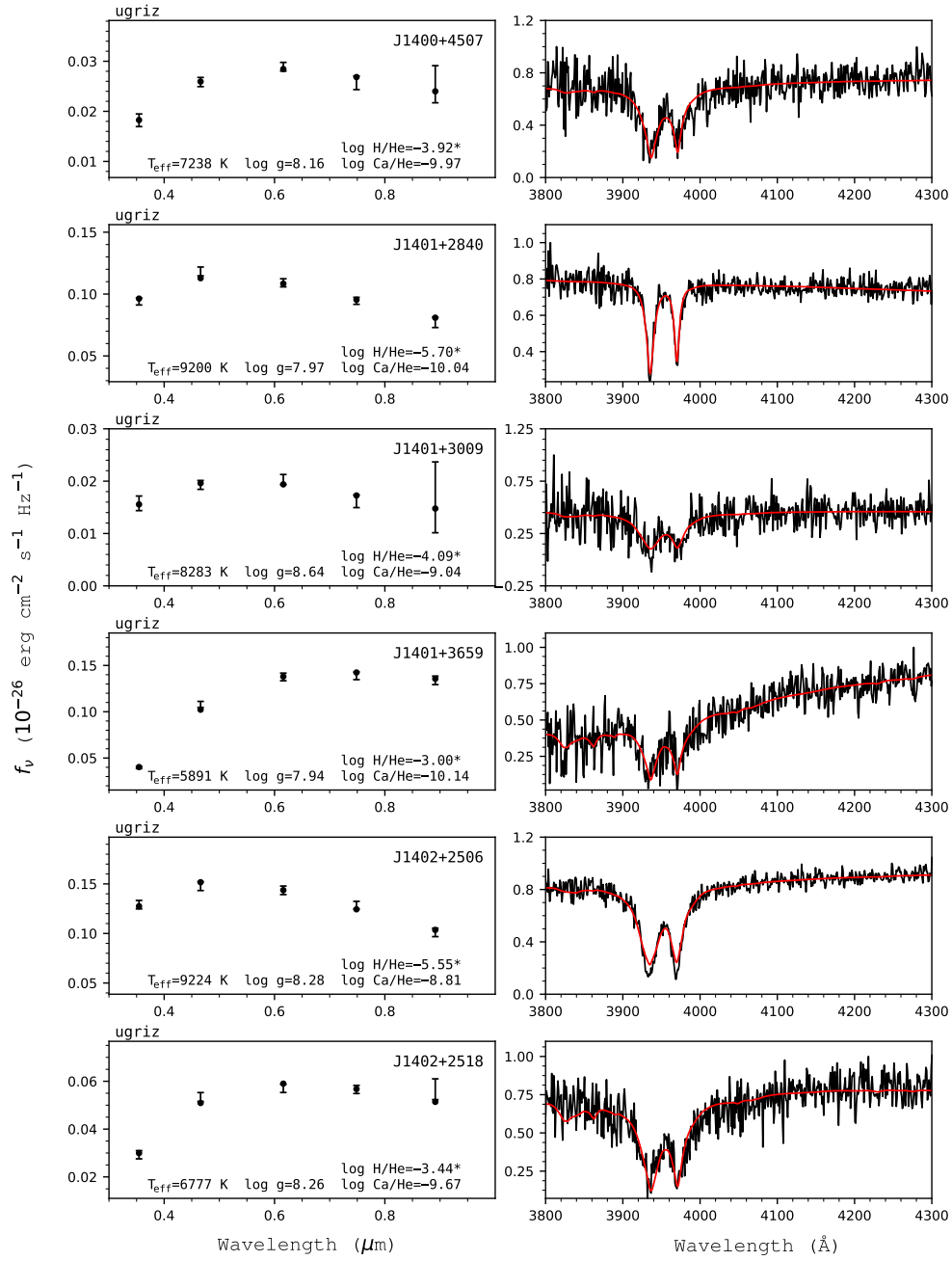


Figure 135. Fits to the DBZ/DZ(A) white dwarfs - continued.

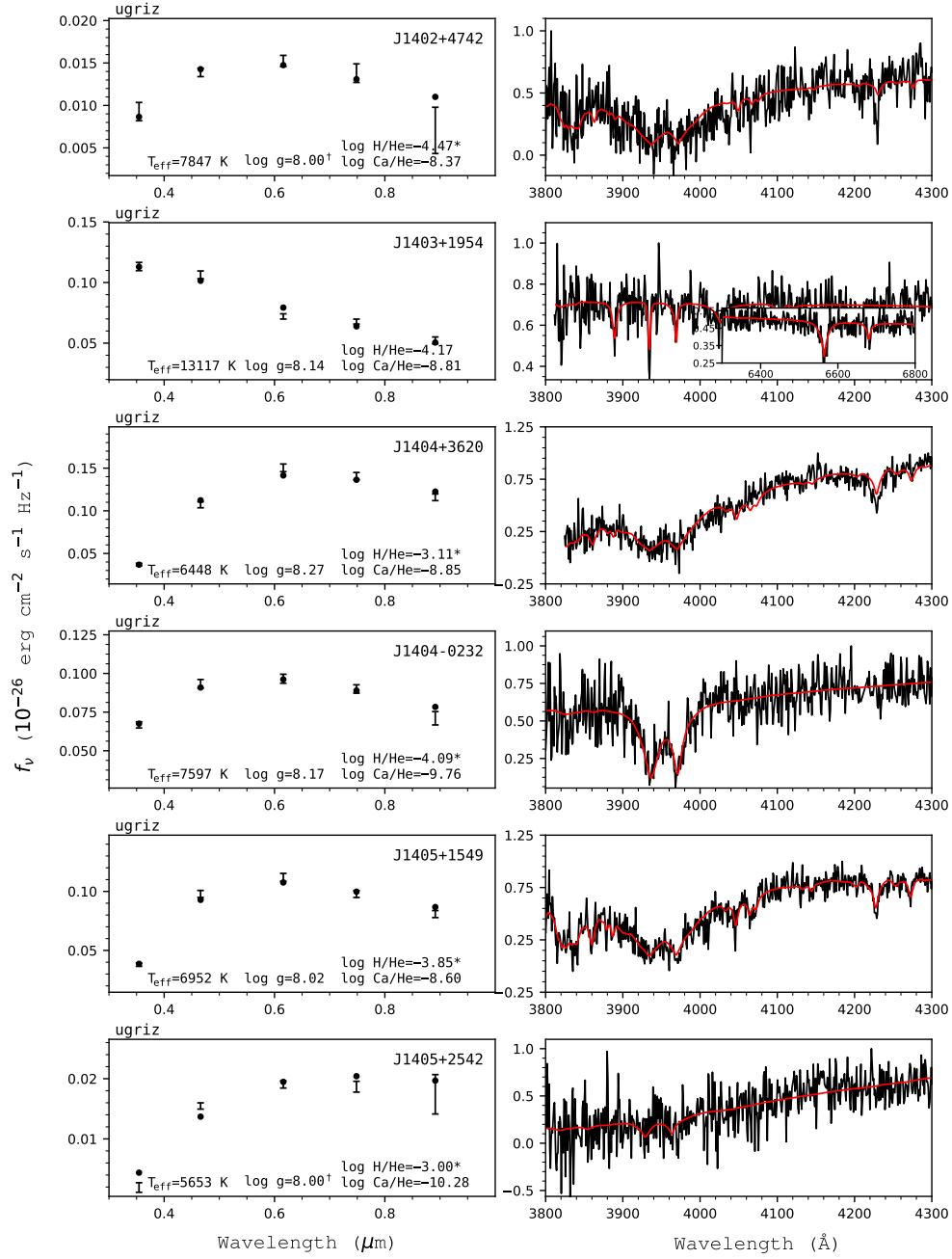


Figure 136. Fits to the DBZ/DZ(A) white dwarfs - continued.

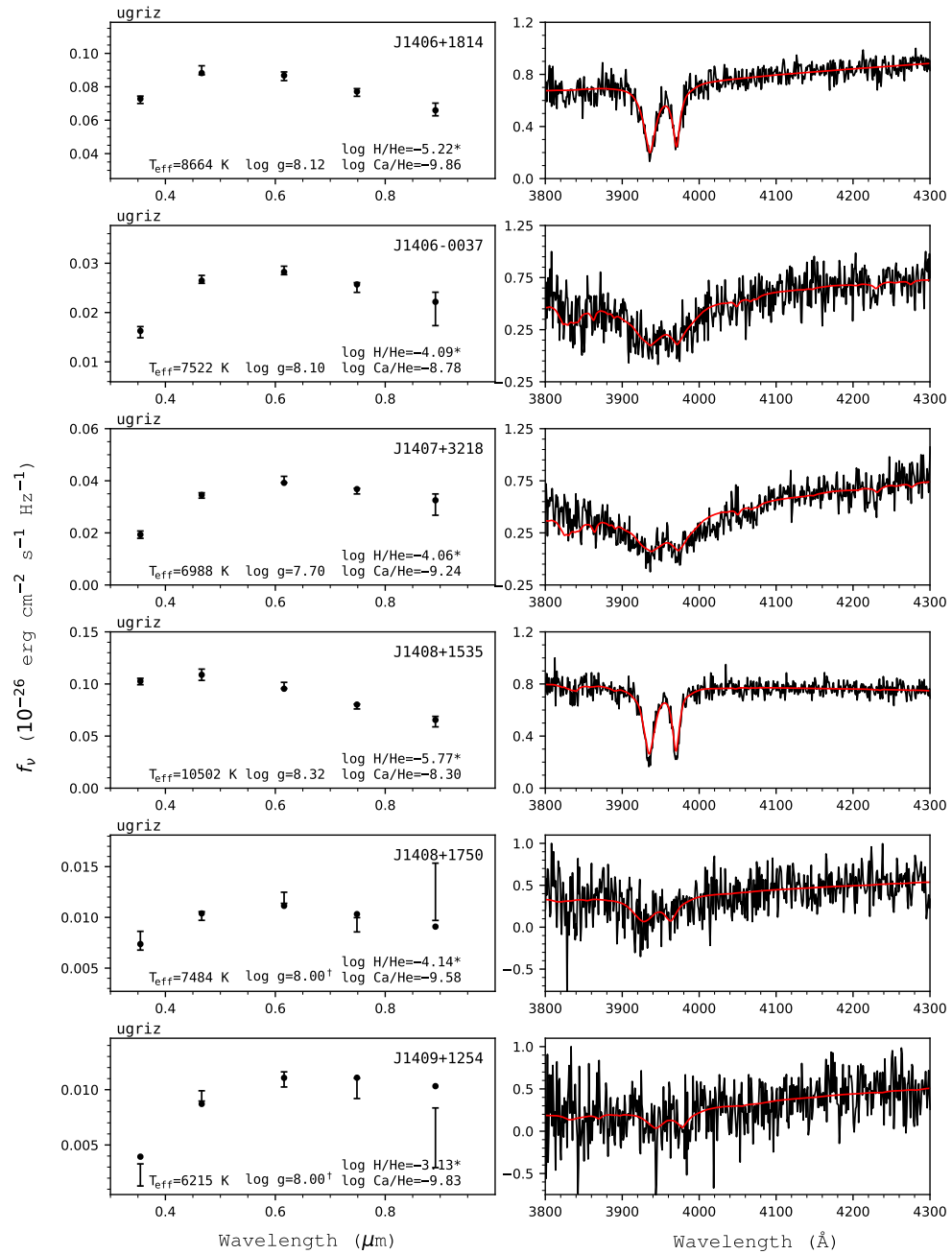


Figure 137. Fits to the DBZ/DZ(A) white dwarfs - continued.

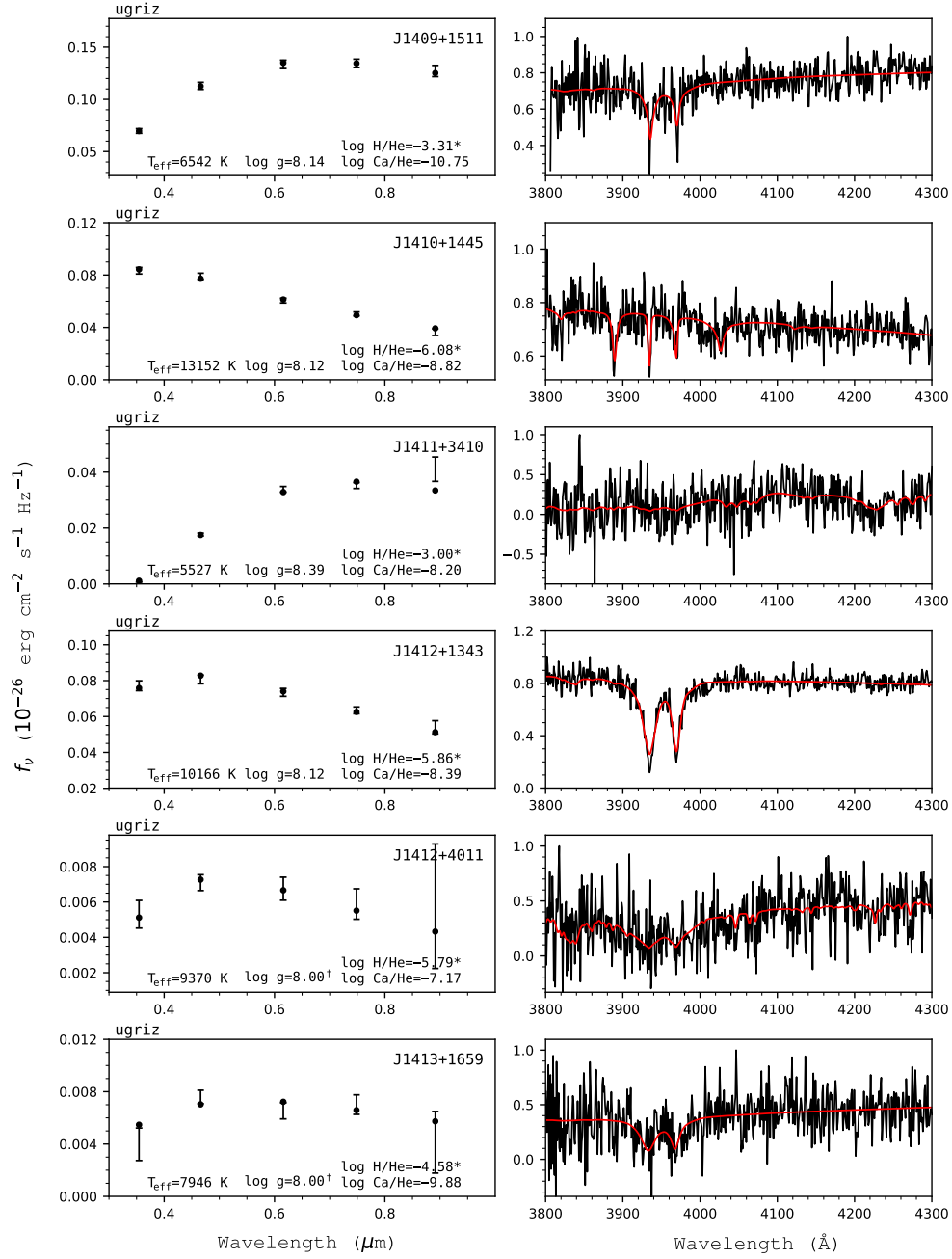


Figure 138. Fits to the DBZ/DZ(A) white dwarfs - continued.

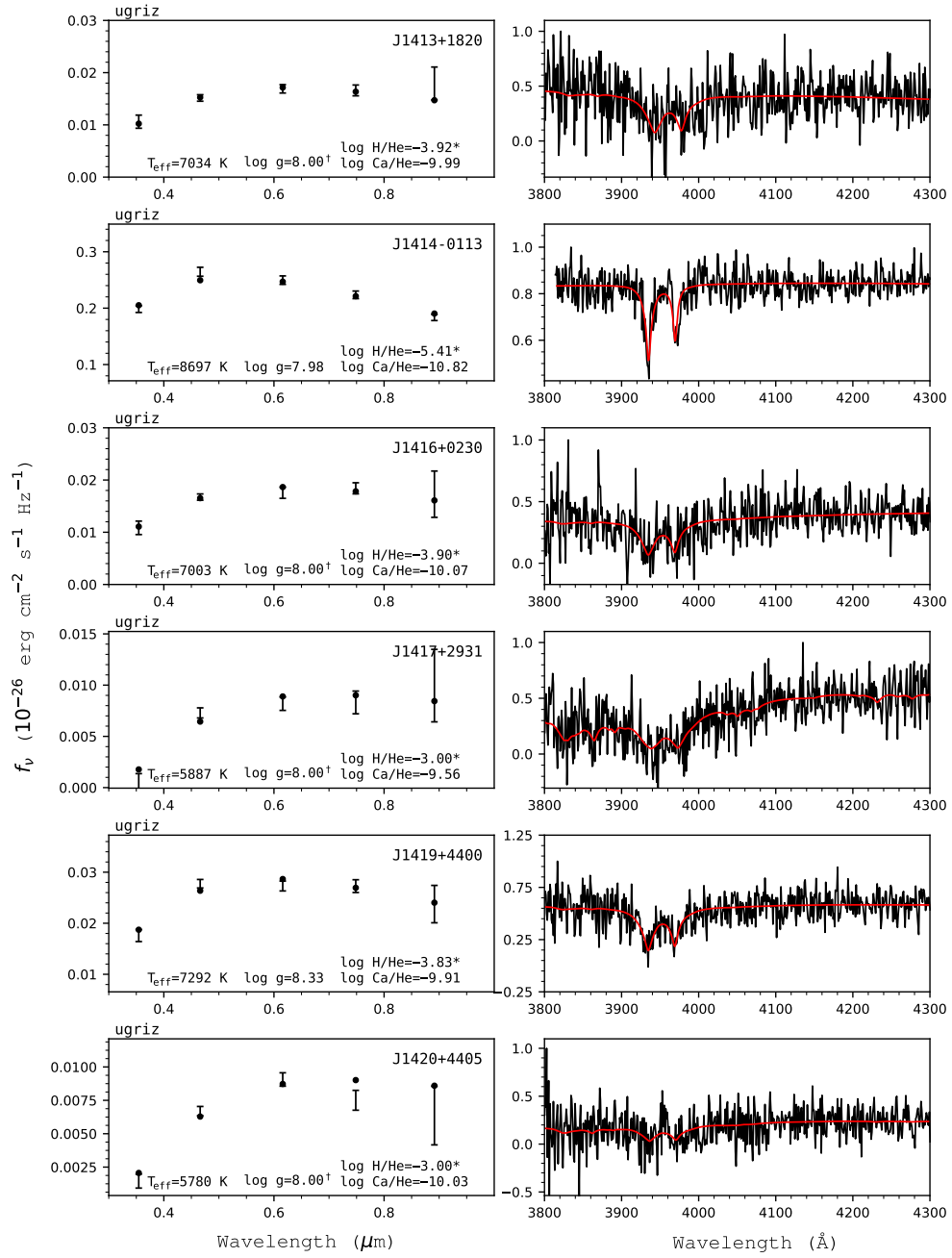


Figure 139. Fits to the DB/DZ(A) white dwarfs - continued.

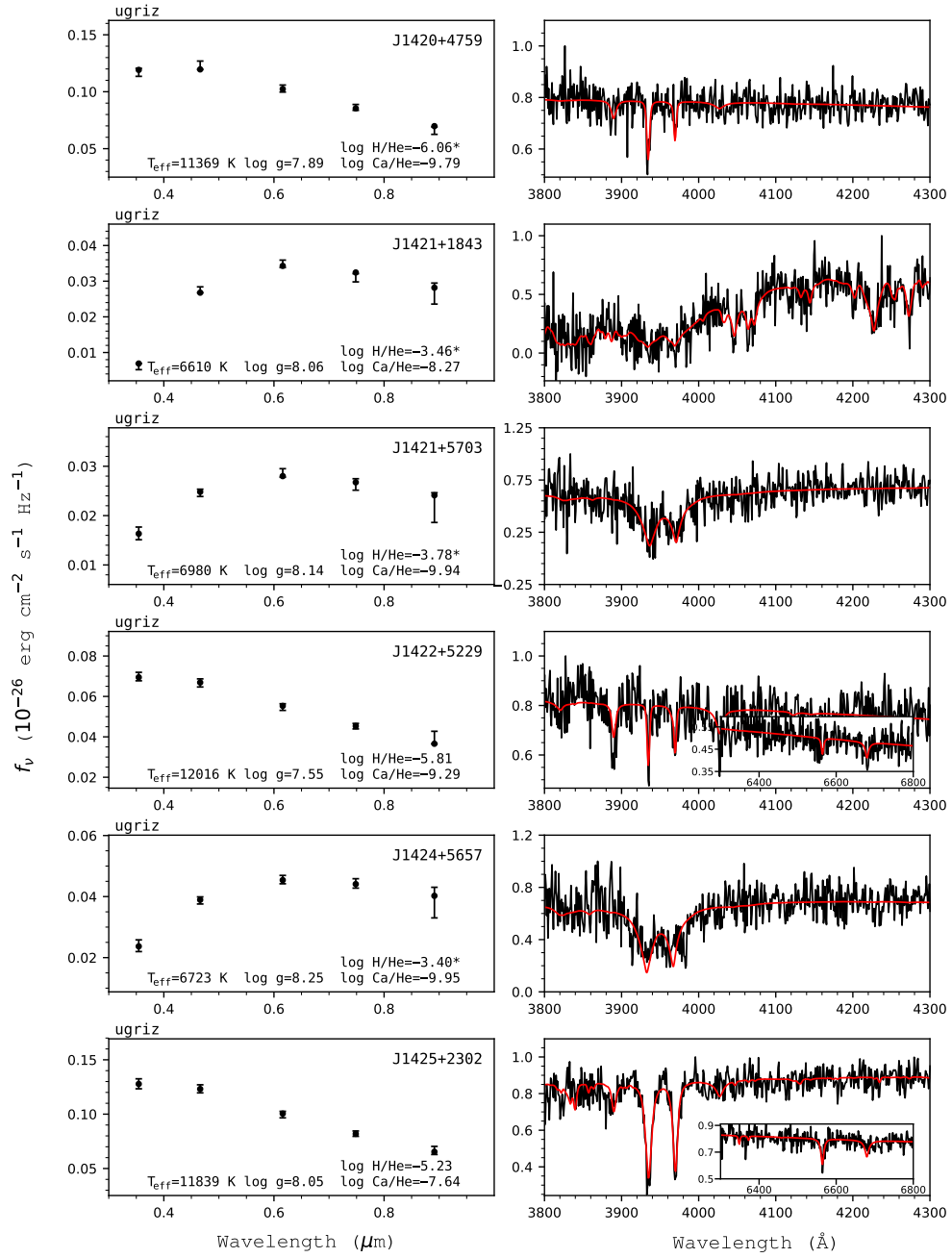


Figure 140. Fits to the DBZ/DZ(A) white dwarfs - continued.

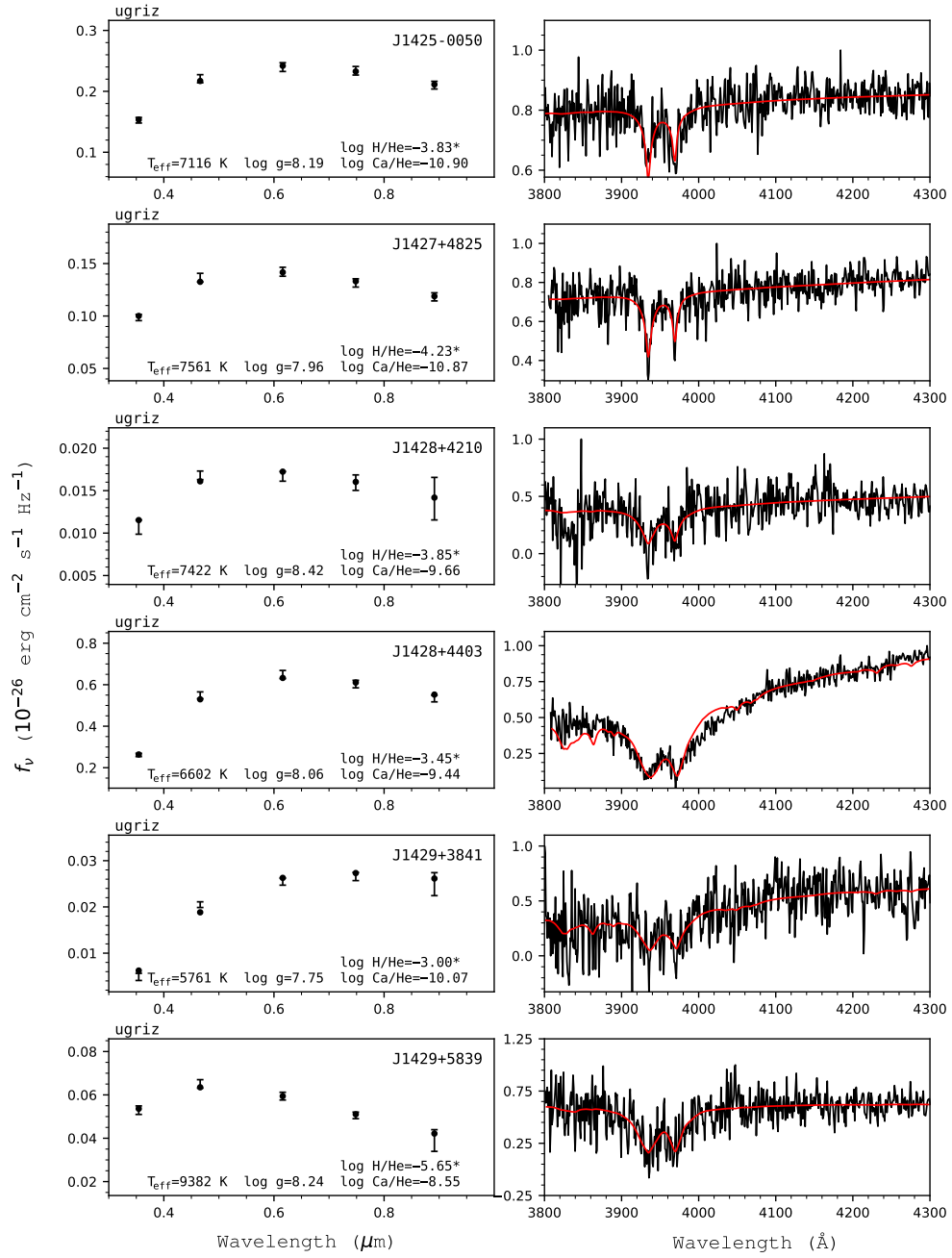


Figure 141. Fits to the DBZ/DZ(A) white dwarfs - continued.

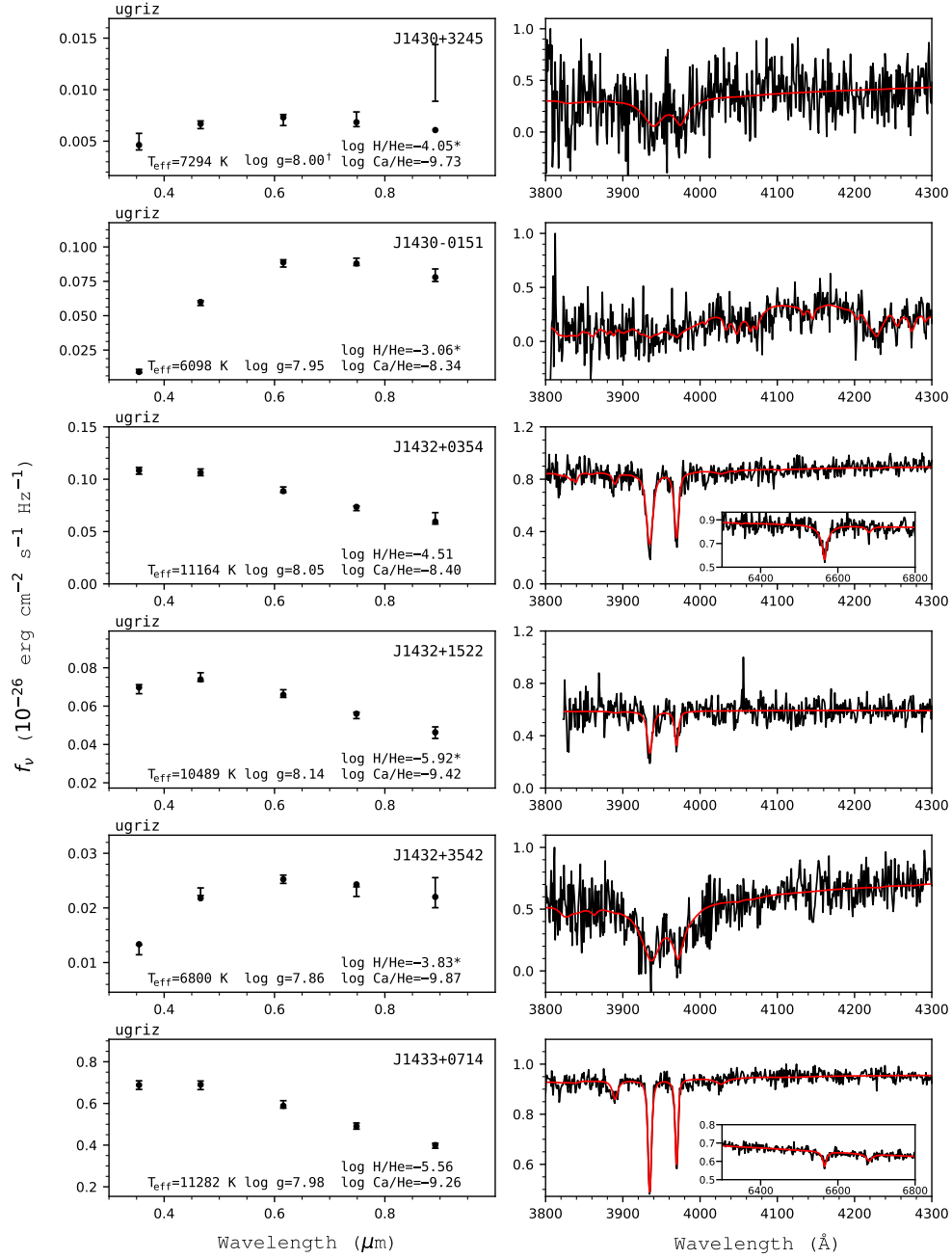


Figure 142. Fits to the DBZ/DZ(A) white dwarfs - continued.

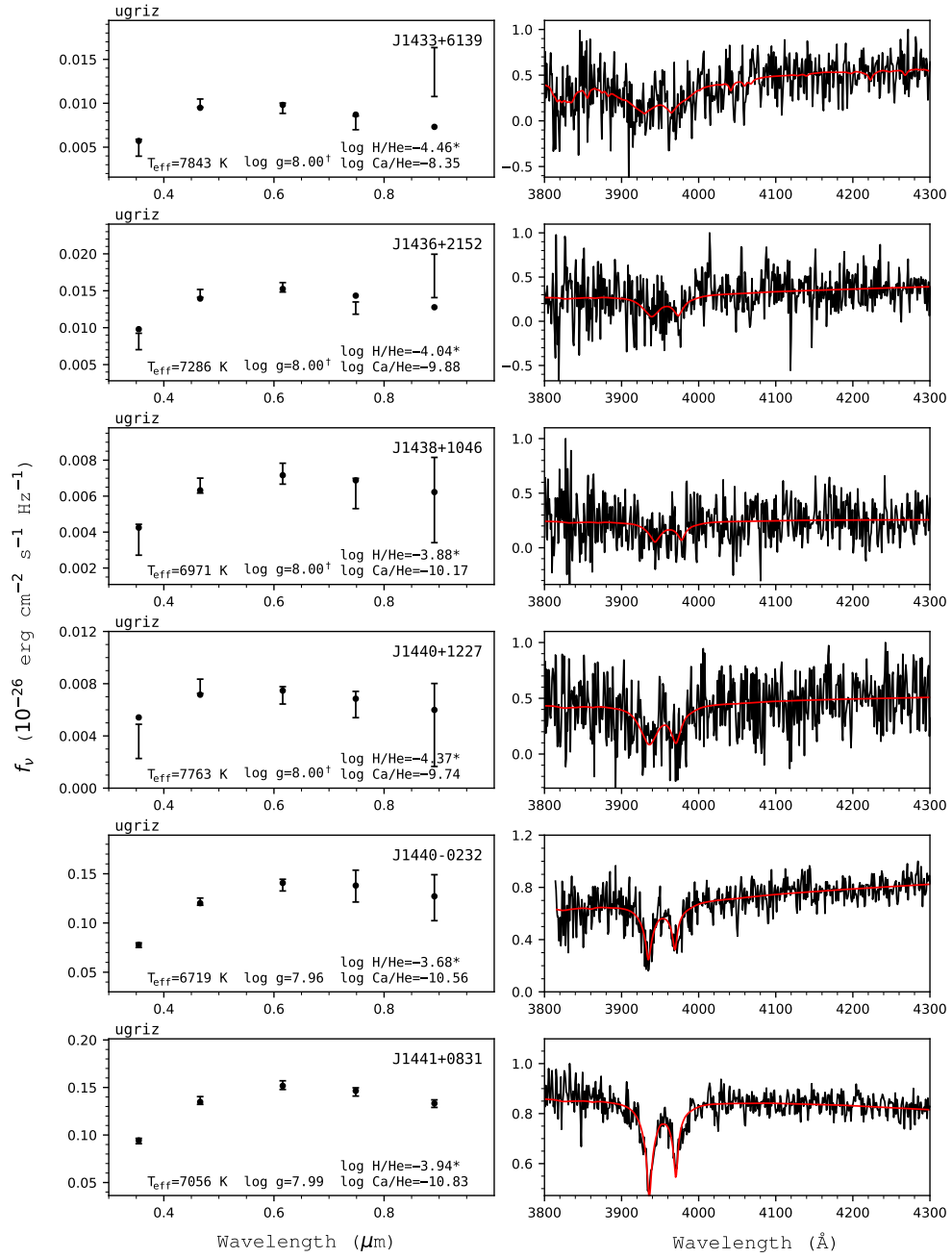


Figure 143. Fits to the DBZ/DZ(A) white dwarfs - continued.

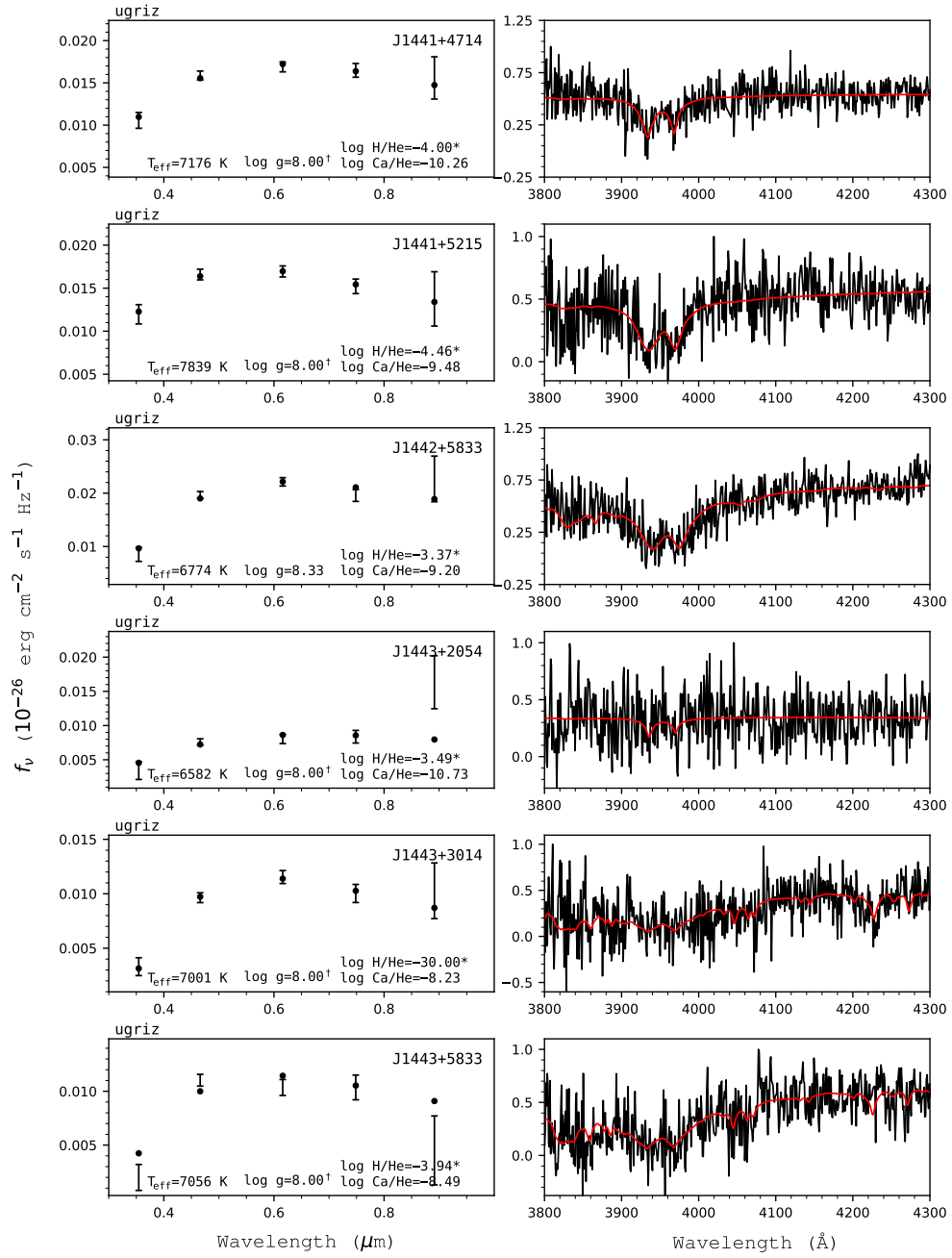


Figure 144. Fits to the DBZ/DZ(A) white dwarfs - continued.

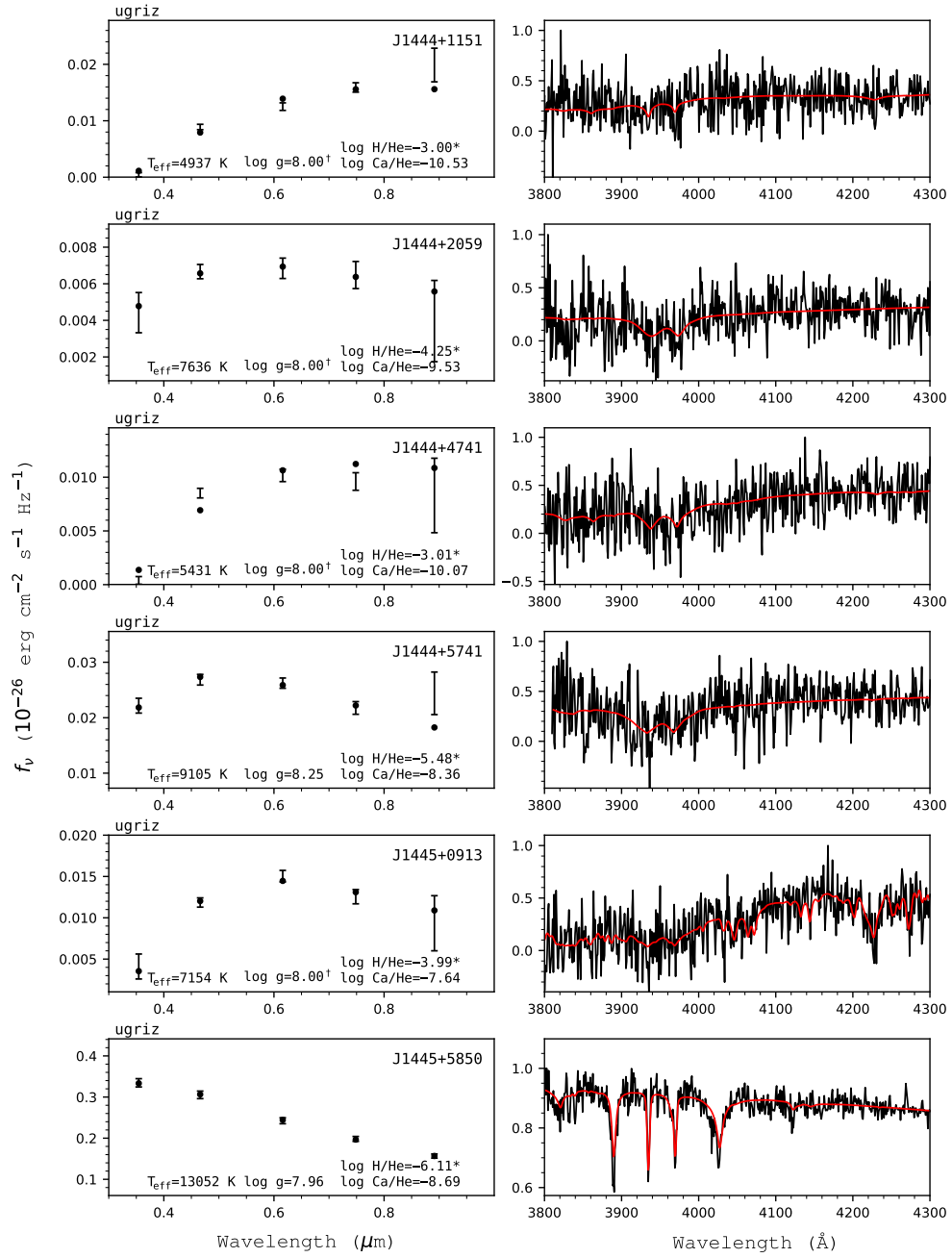


Figure 145. Fits to the DBZ/DZ(A) white dwarfs - continued.

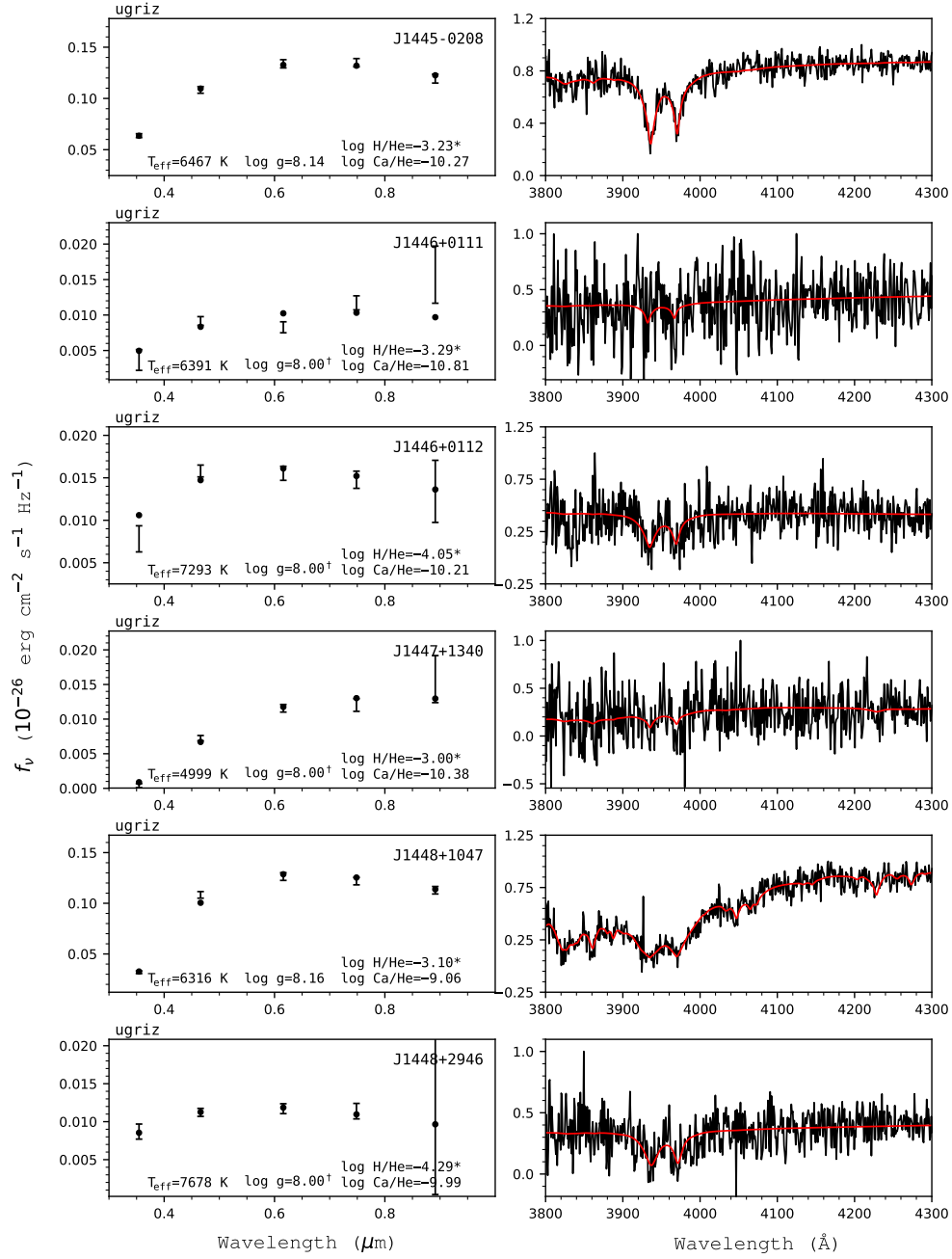


Figure 146. Fits to the DBZ/DZ(A) white dwarfs - continued.

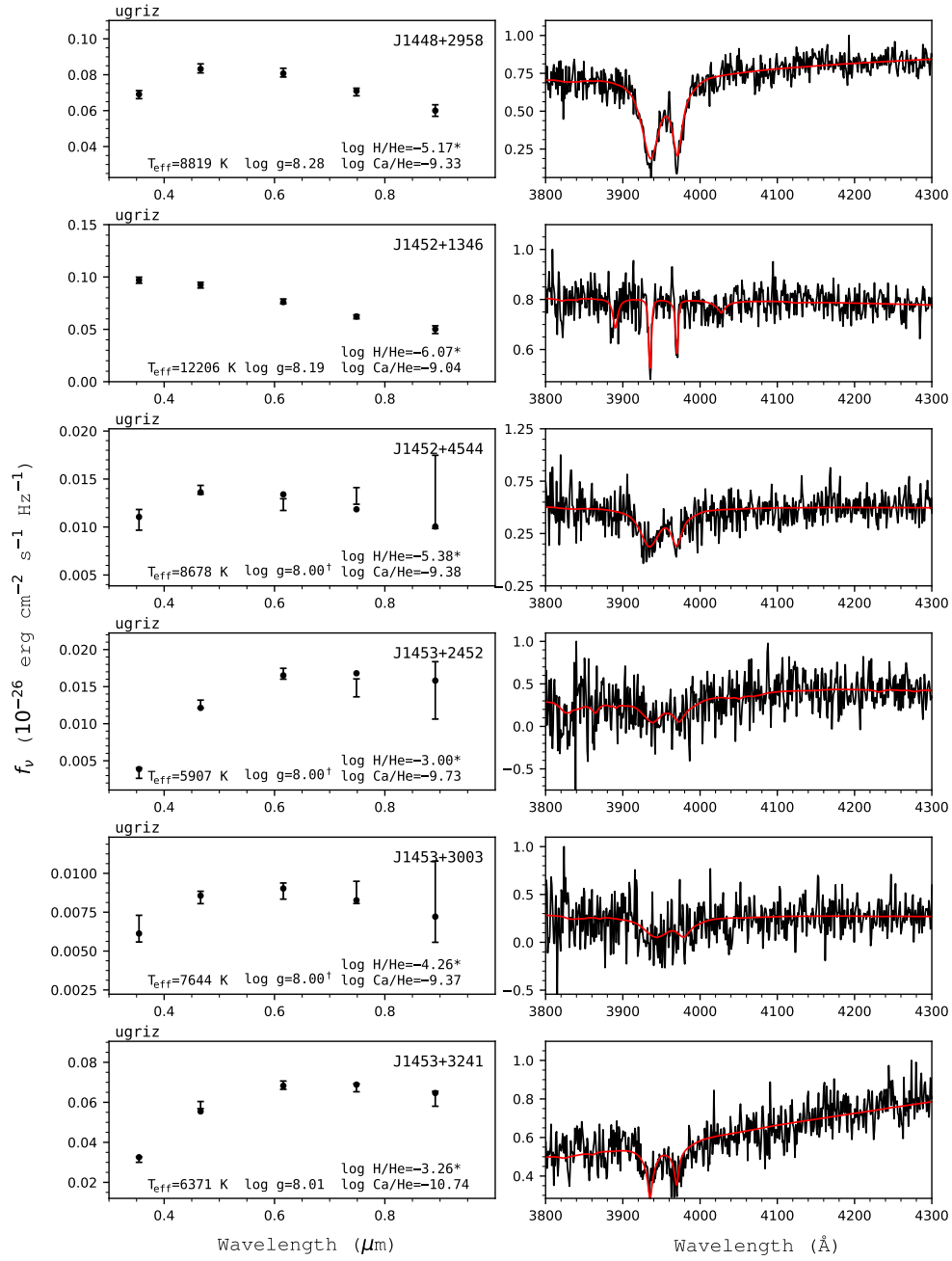


Figure 147. Fits to the DBZ/DZ(A) white dwarfs - continued.

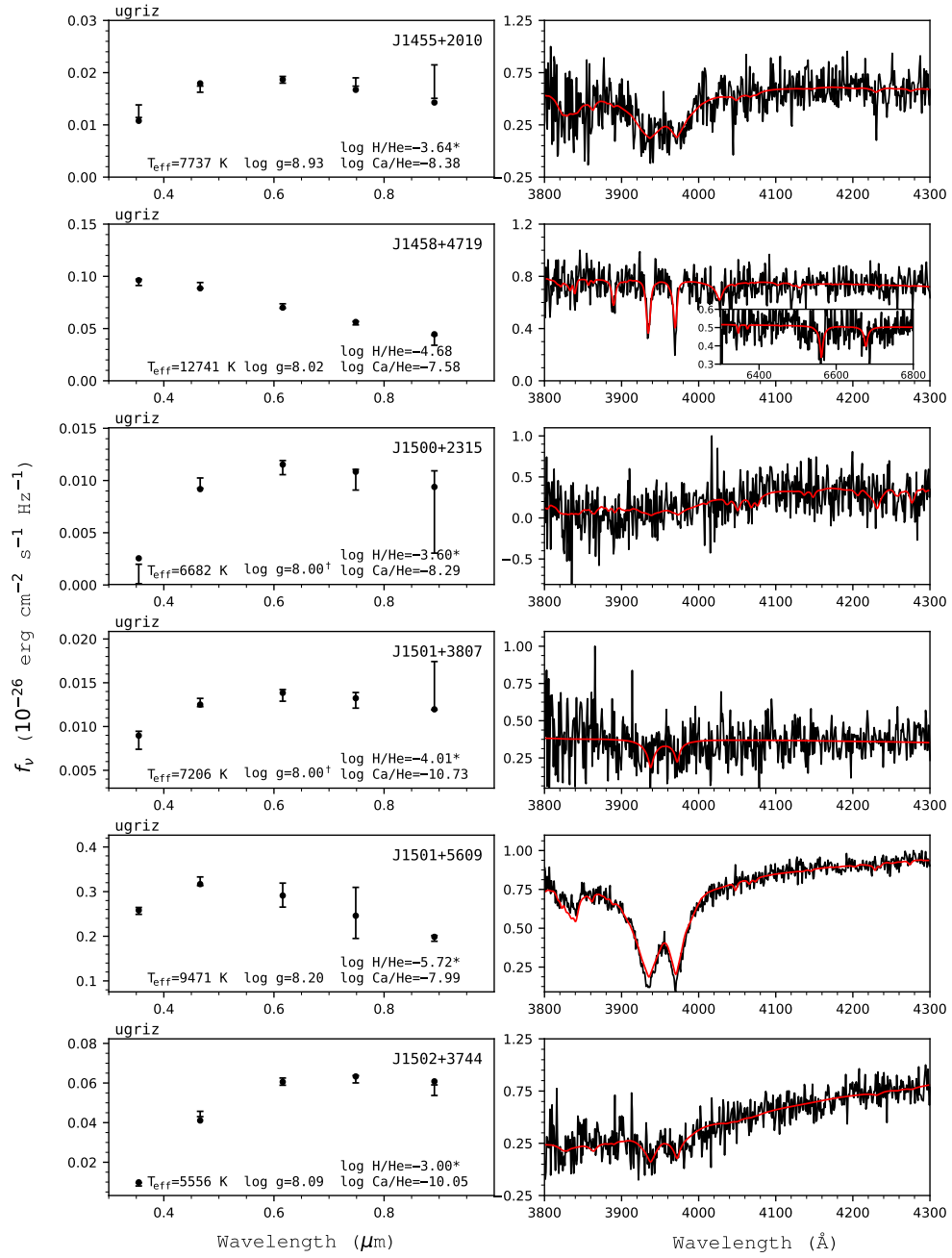


Figure 148. Fits to the DBZ/DZ(A) white dwarfs - continued.

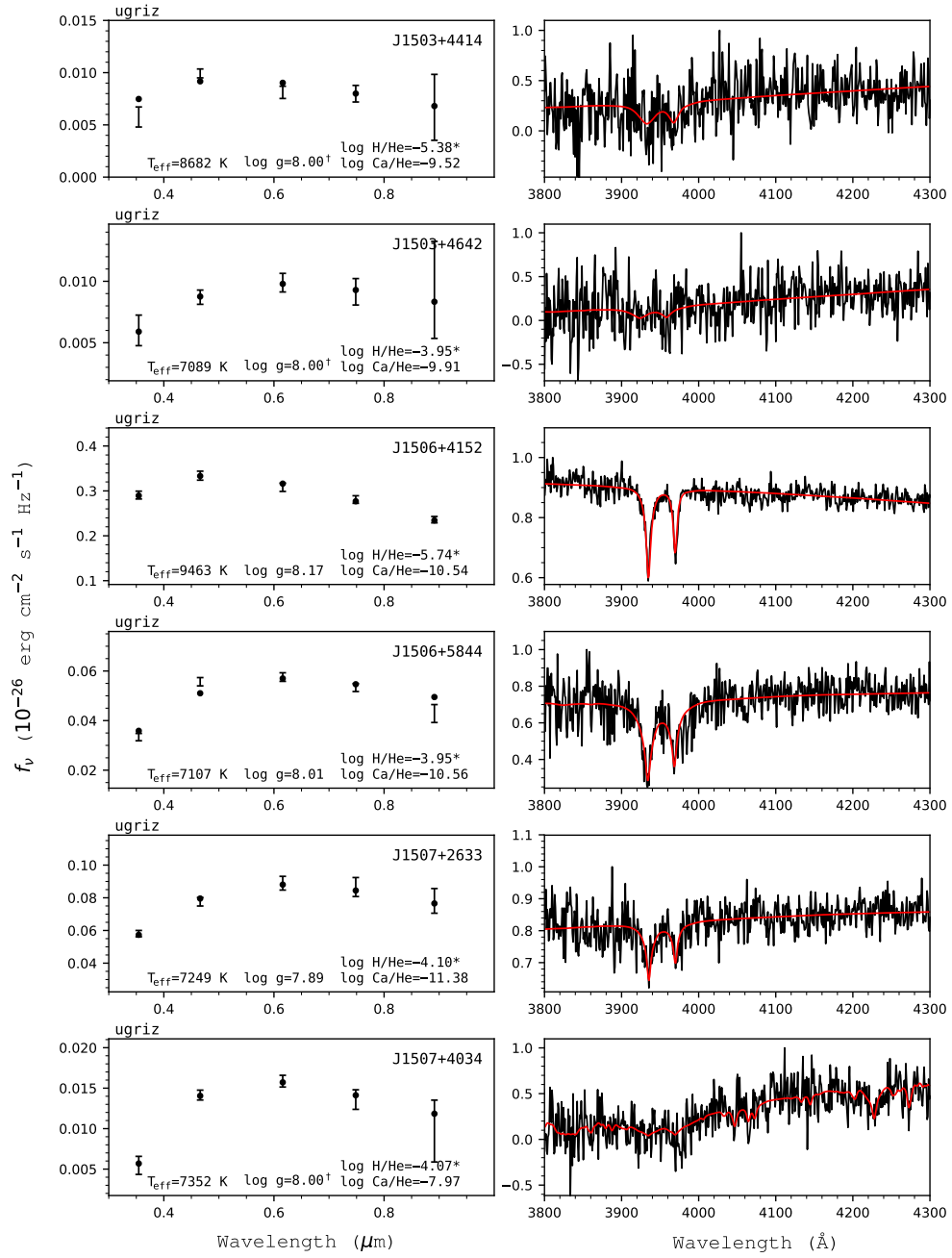


Figure 149. Fits to the DBZ/DZ(A) white dwarfs - continued.

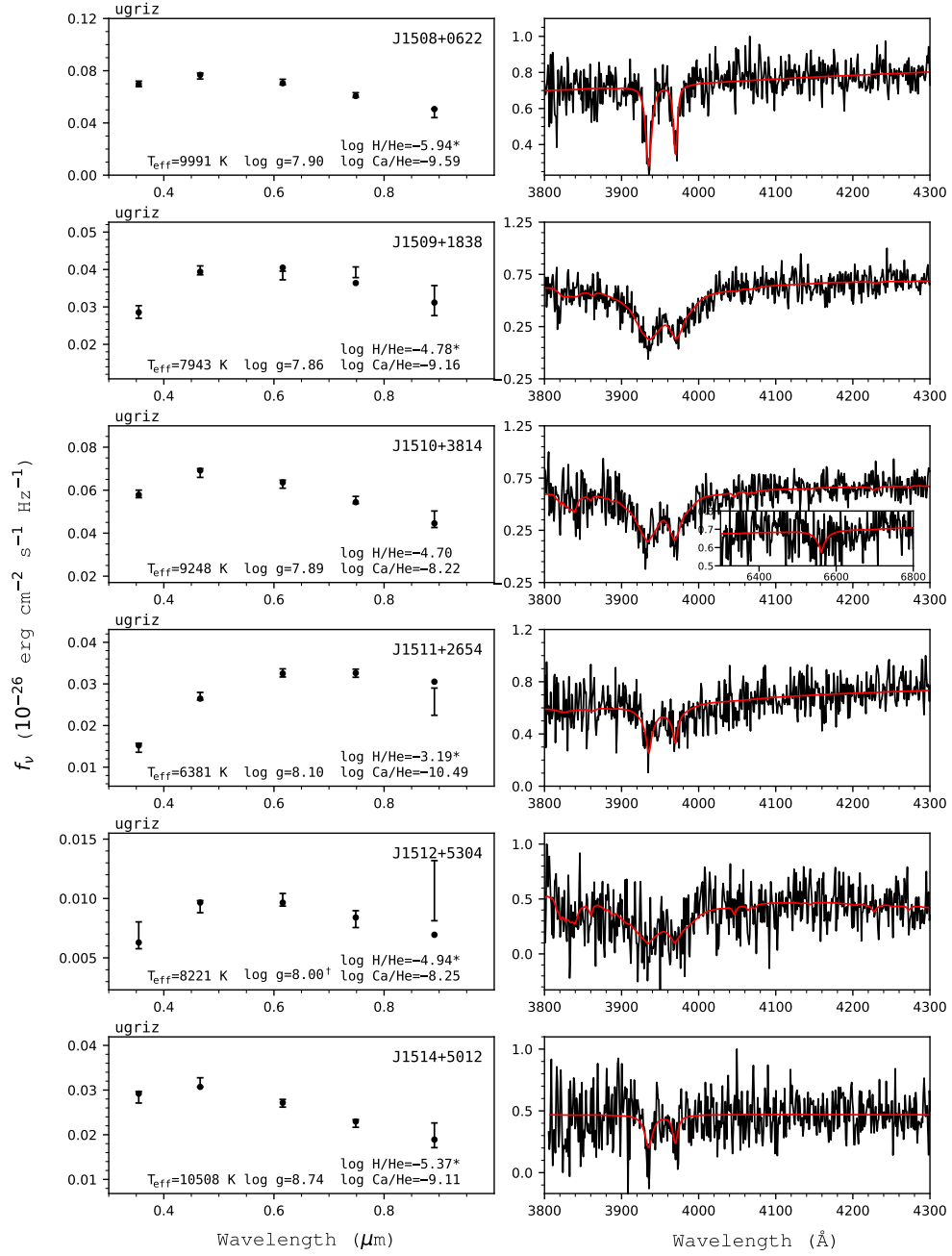


Figure 150. Fits to the DBZ/DZ(A) white dwarfs - continued.

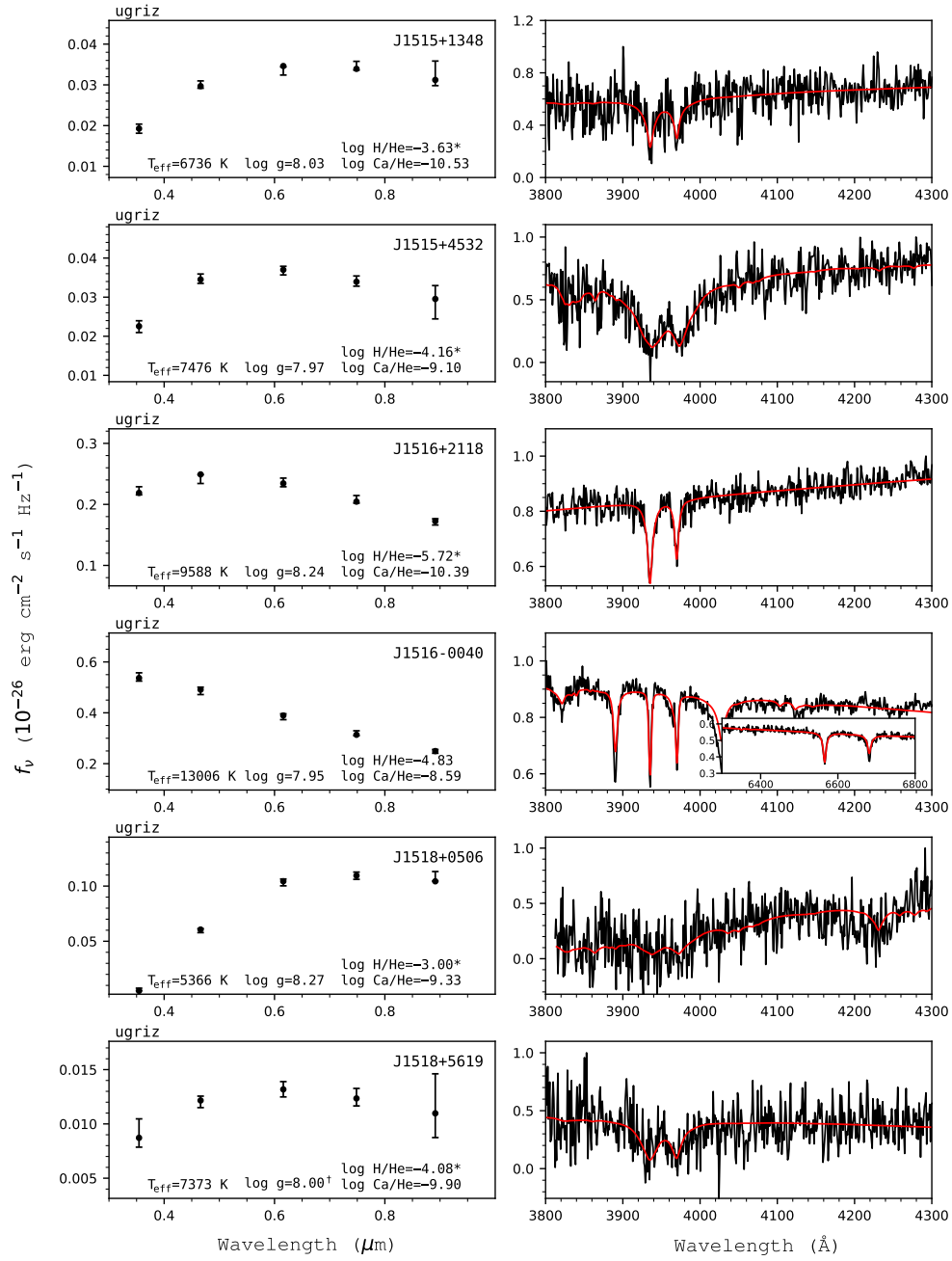


Figure 151. Fits to the DBZ/DZ(A) white dwarfs - continued.

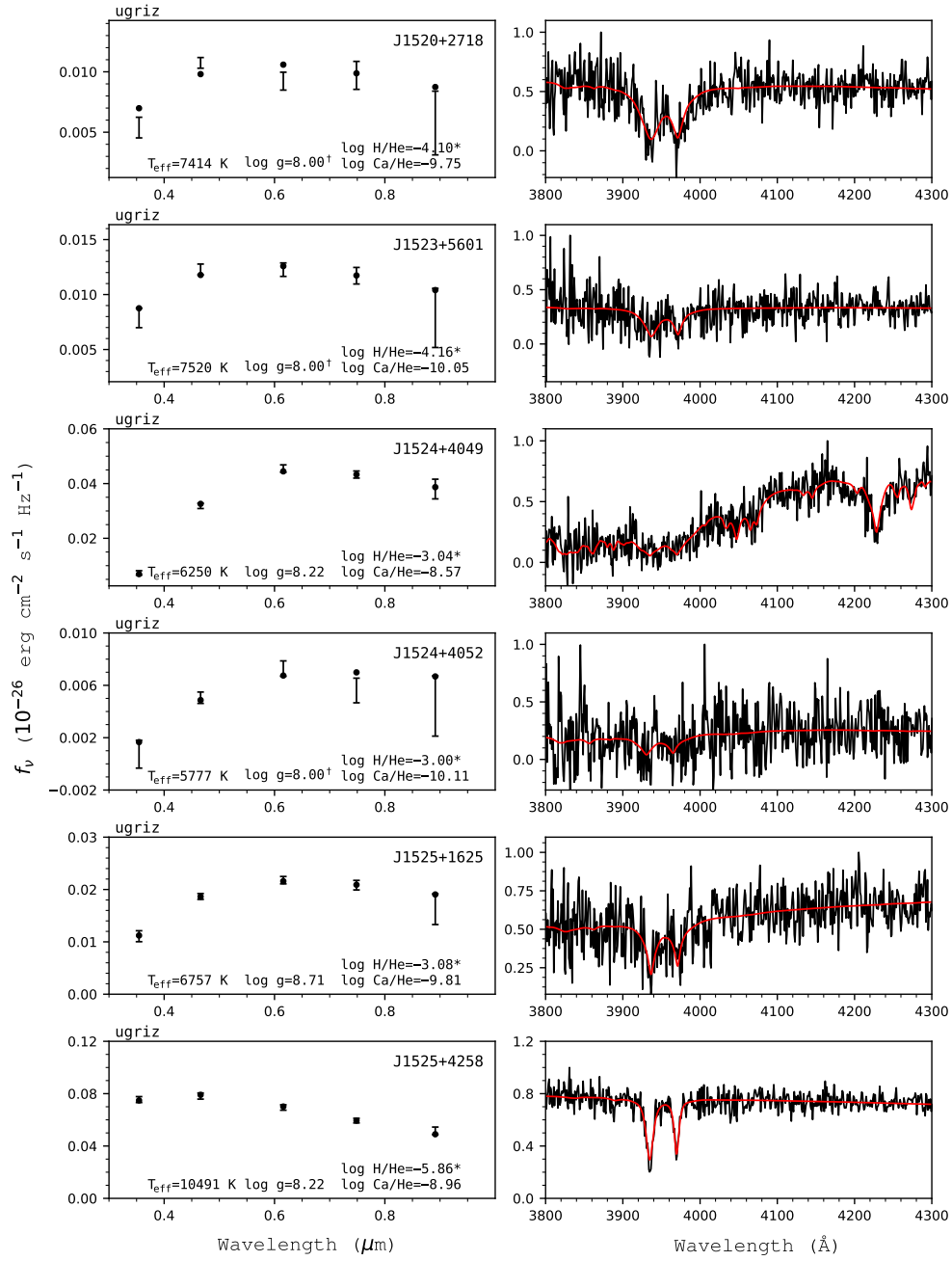


Figure 152. Fits to the DBZ/DZ(A) white dwarfs - continued.

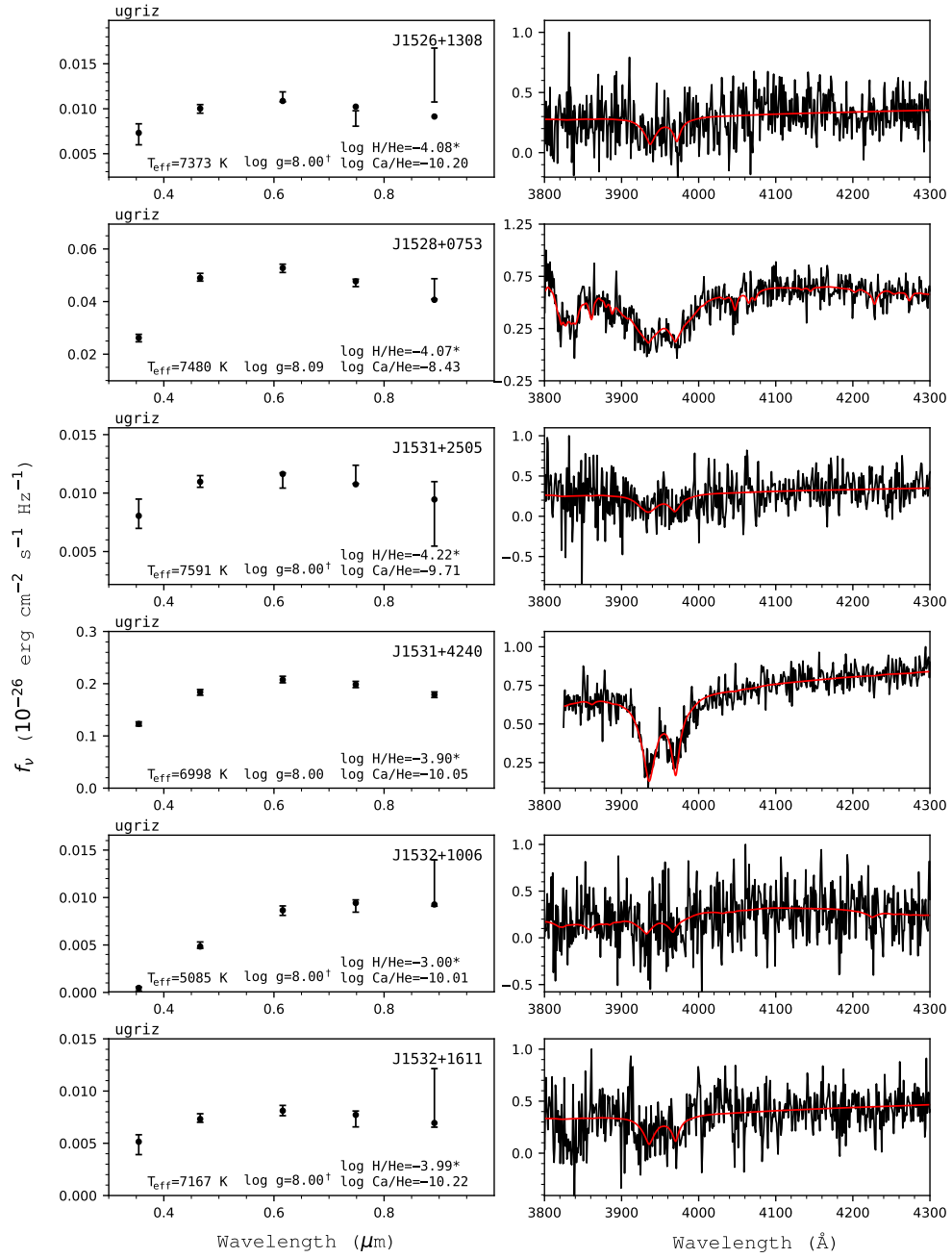


Figure 153. Fits to the DBZ/DZ(A) white dwarfs - continued.

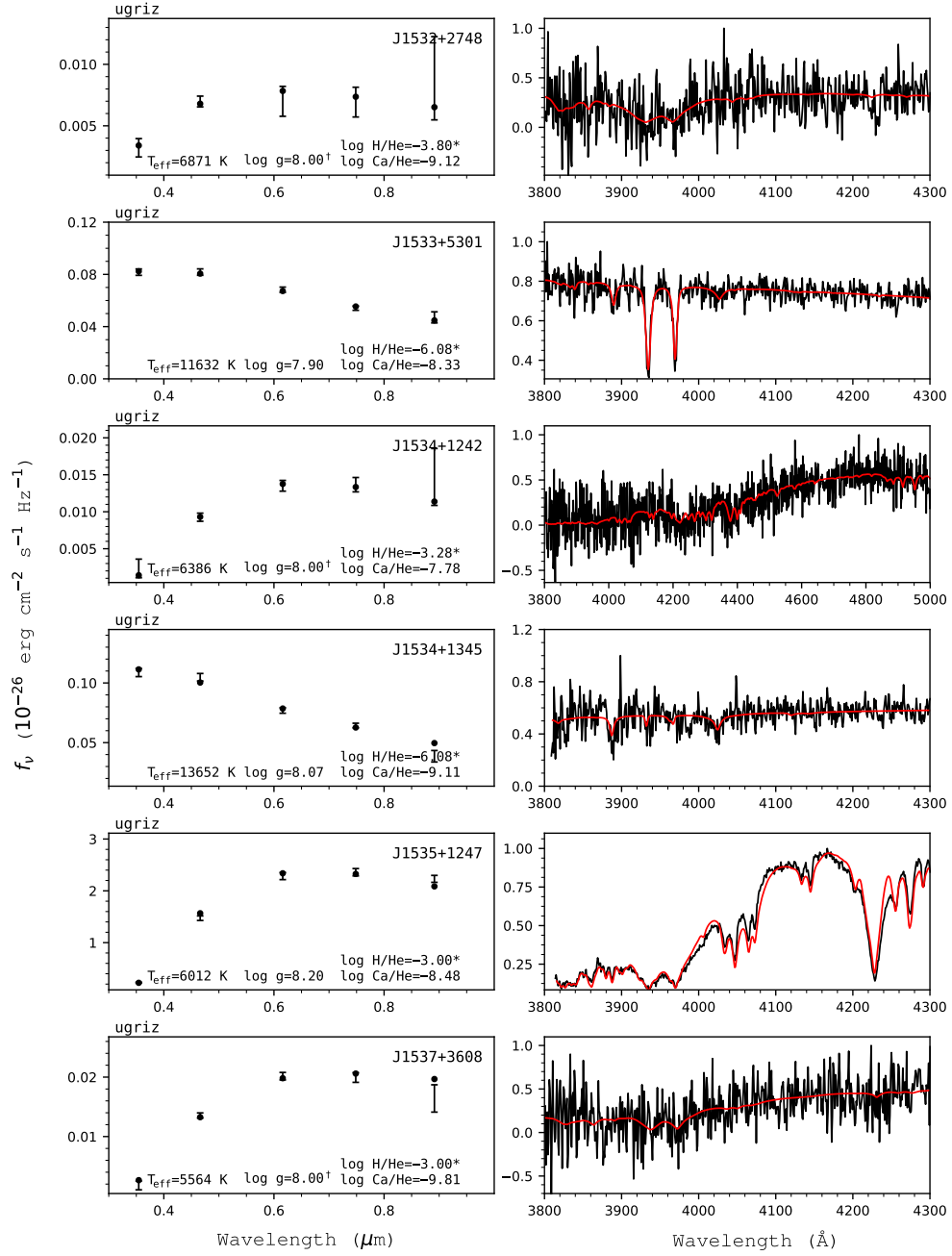


Figure 154. Fits to the DBZ/DZ(A) white dwarfs - continued.

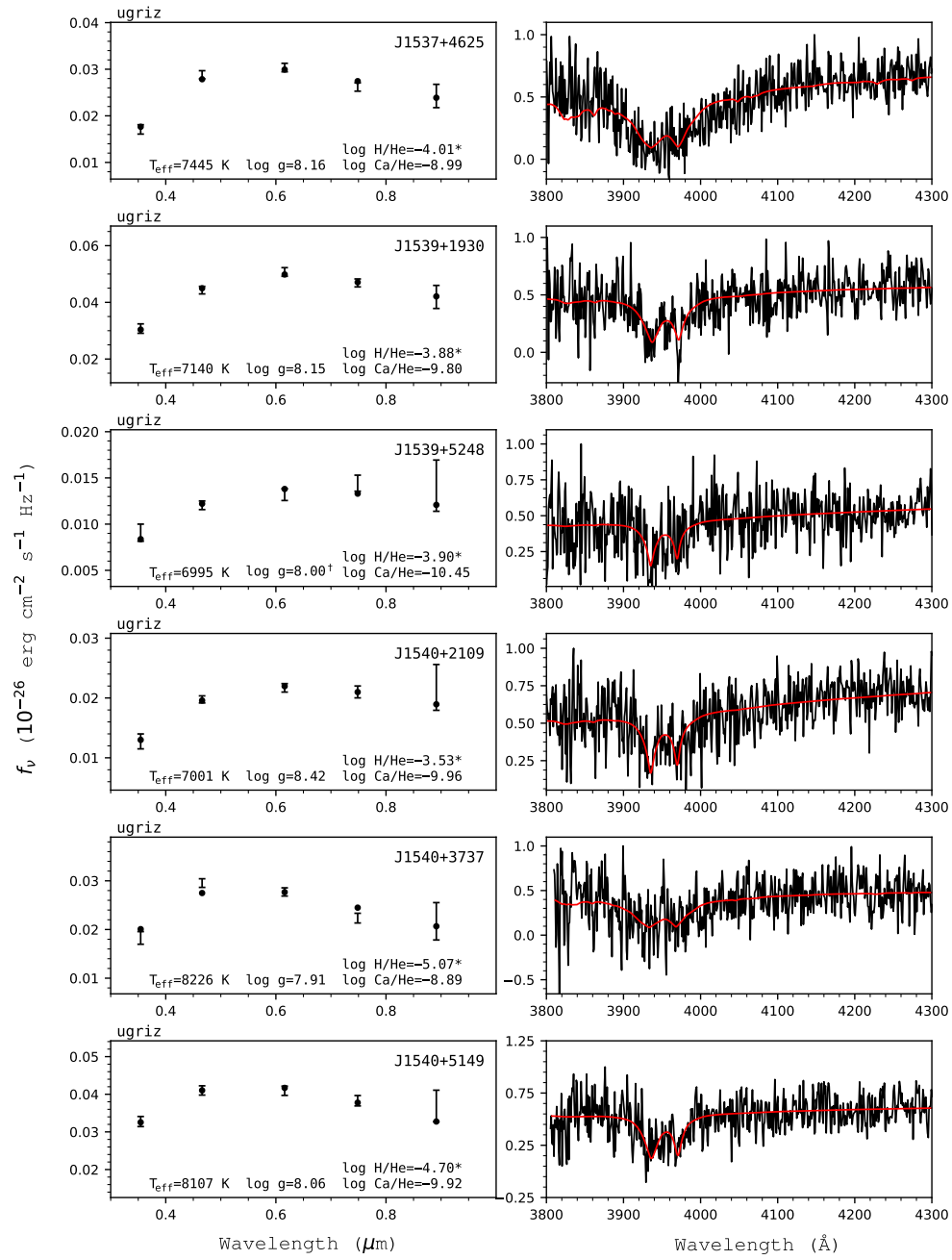


Figure 155. Fits to the DBZ/DZ(A) white dwarfs - continued.

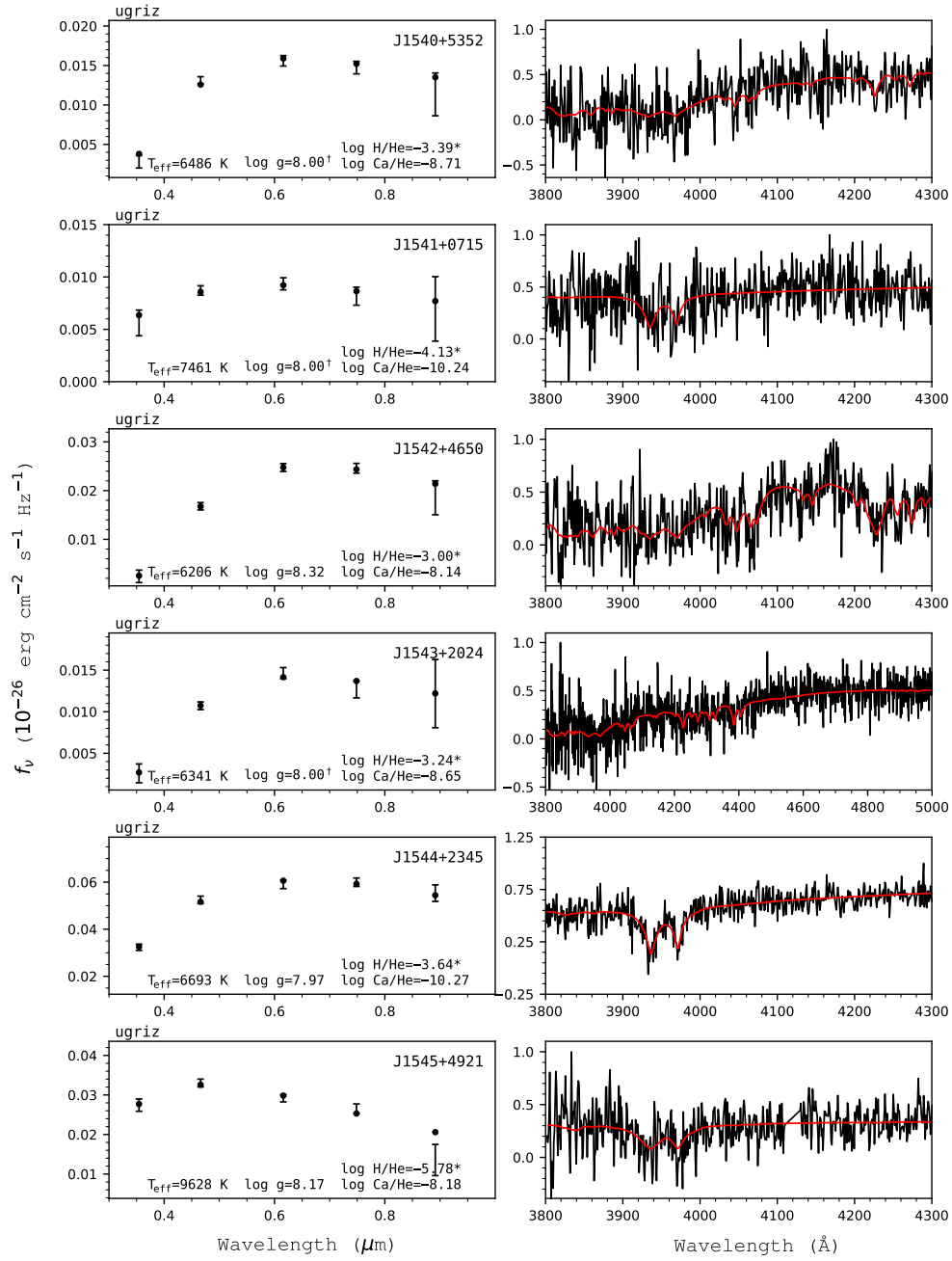


Figure 156. Fits to the DBZ/DZ(A) white dwarfs - continued.

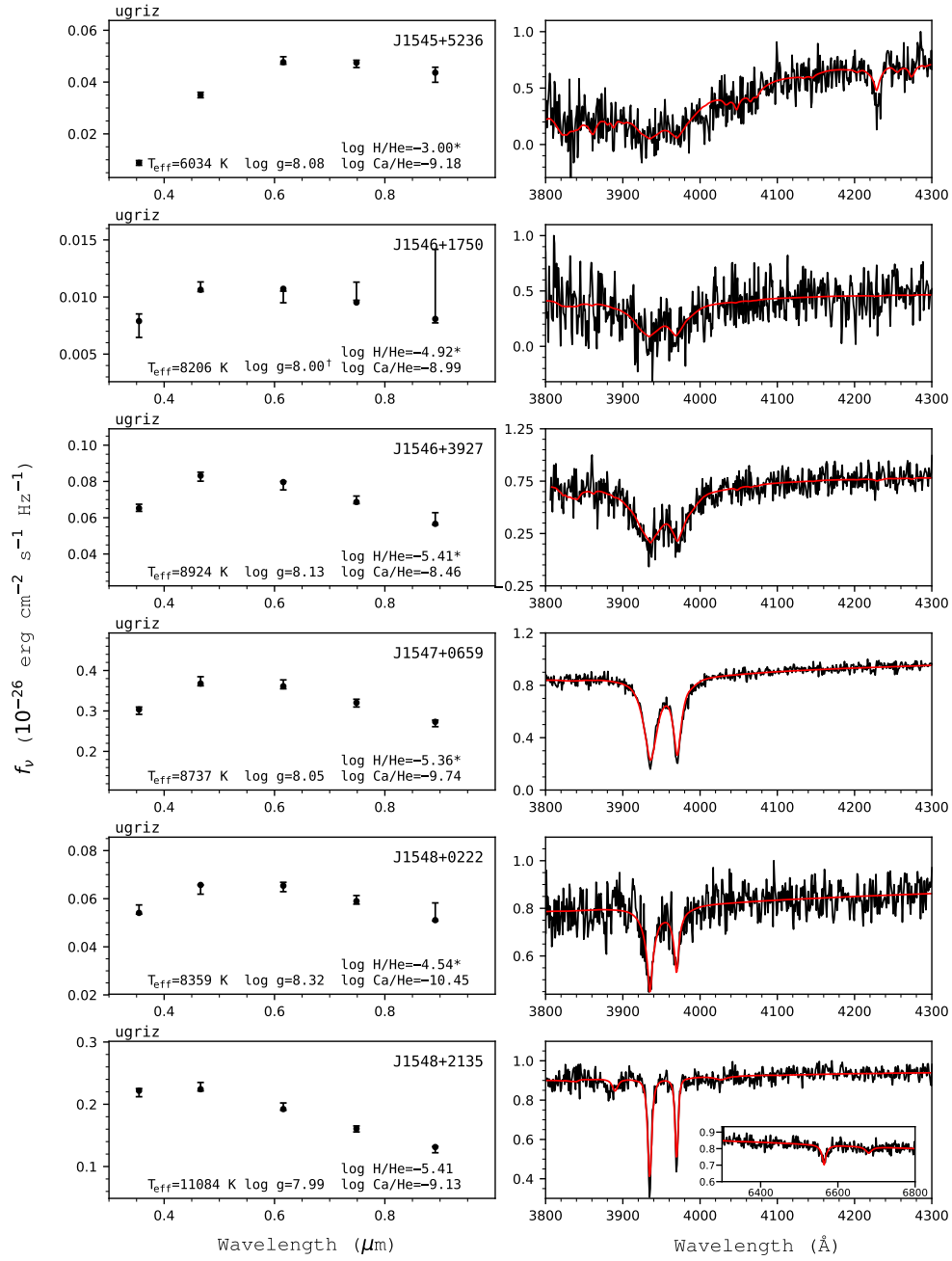


Figure 157. Fits to the DBZ/DZ(A) white dwarfs - continued.

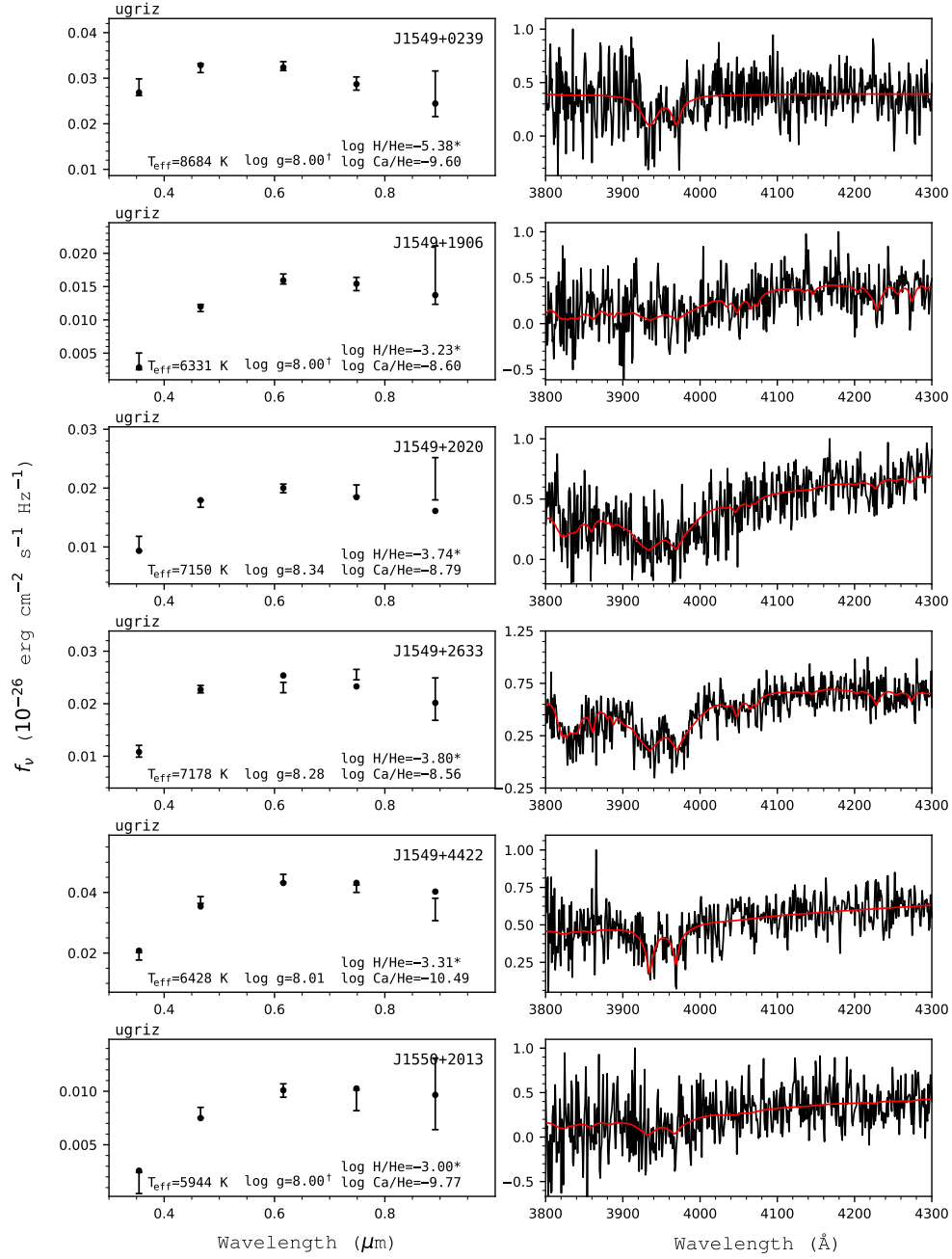


Figure 158. Fits to the DBZ/DZ(A) white dwarfs - continued.

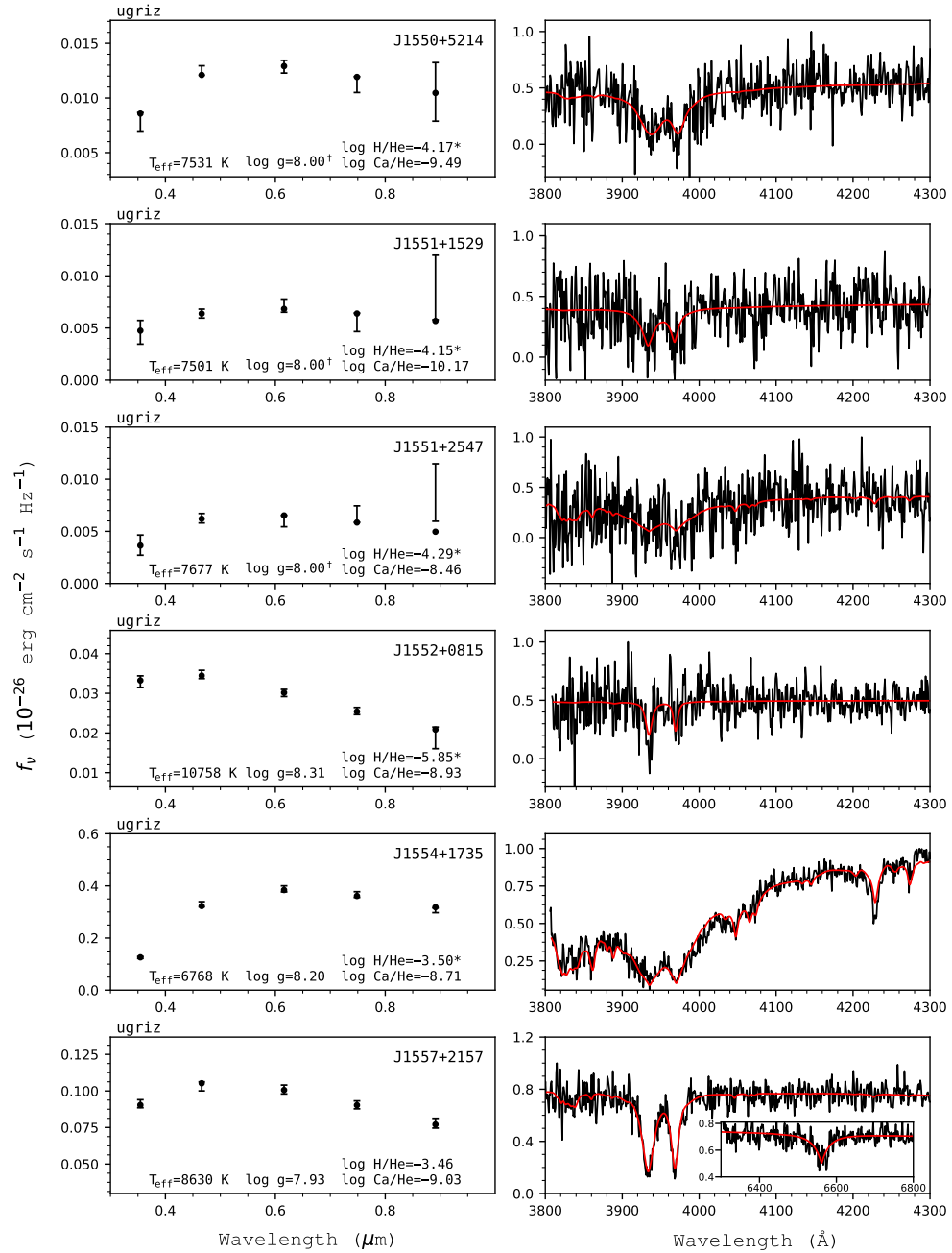


Figure 159. Fits to the DBZ/DZ(A) white dwarfs - continued.

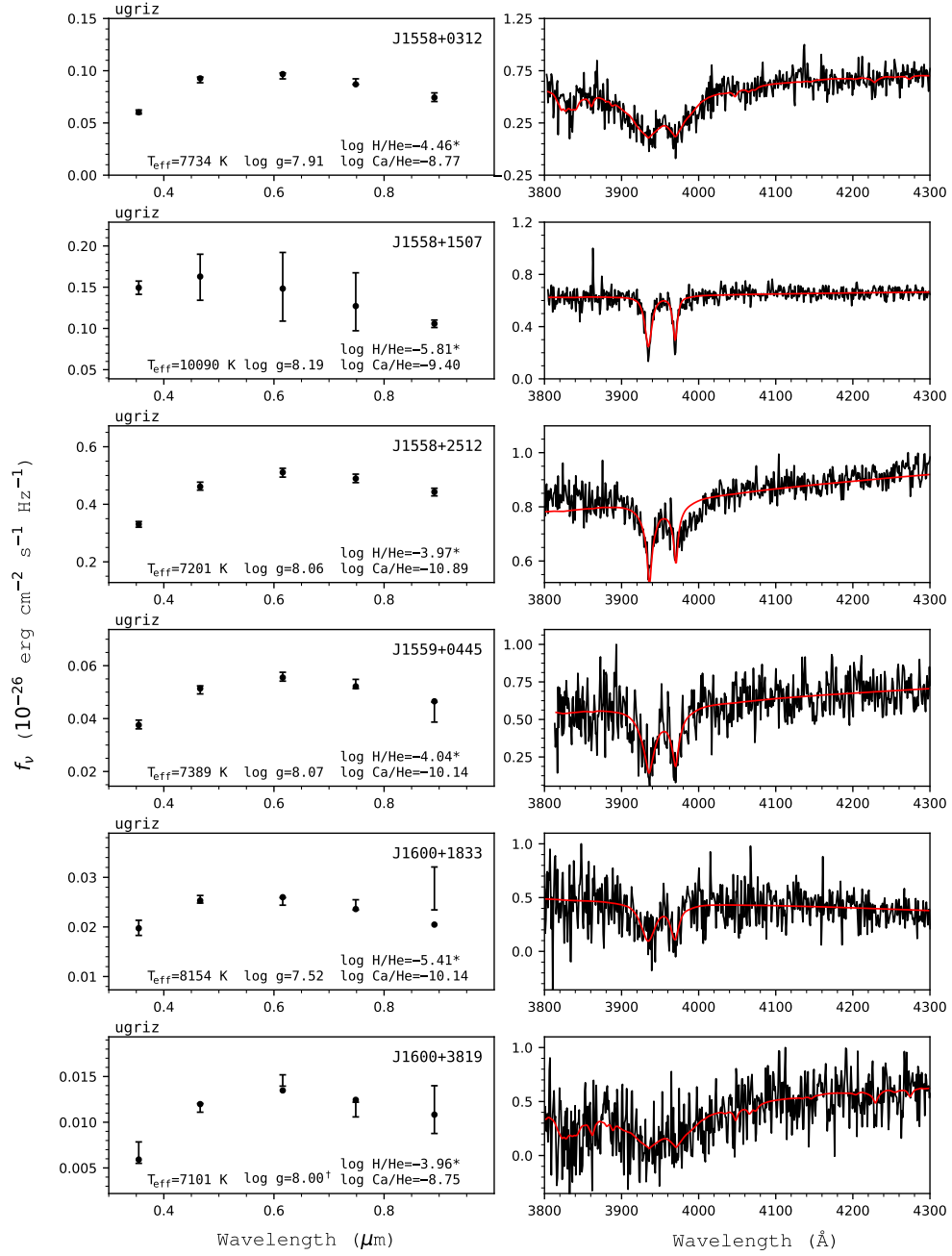


Figure 160. Fits to the DBZ/DZ(A) white dwarfs - continued.

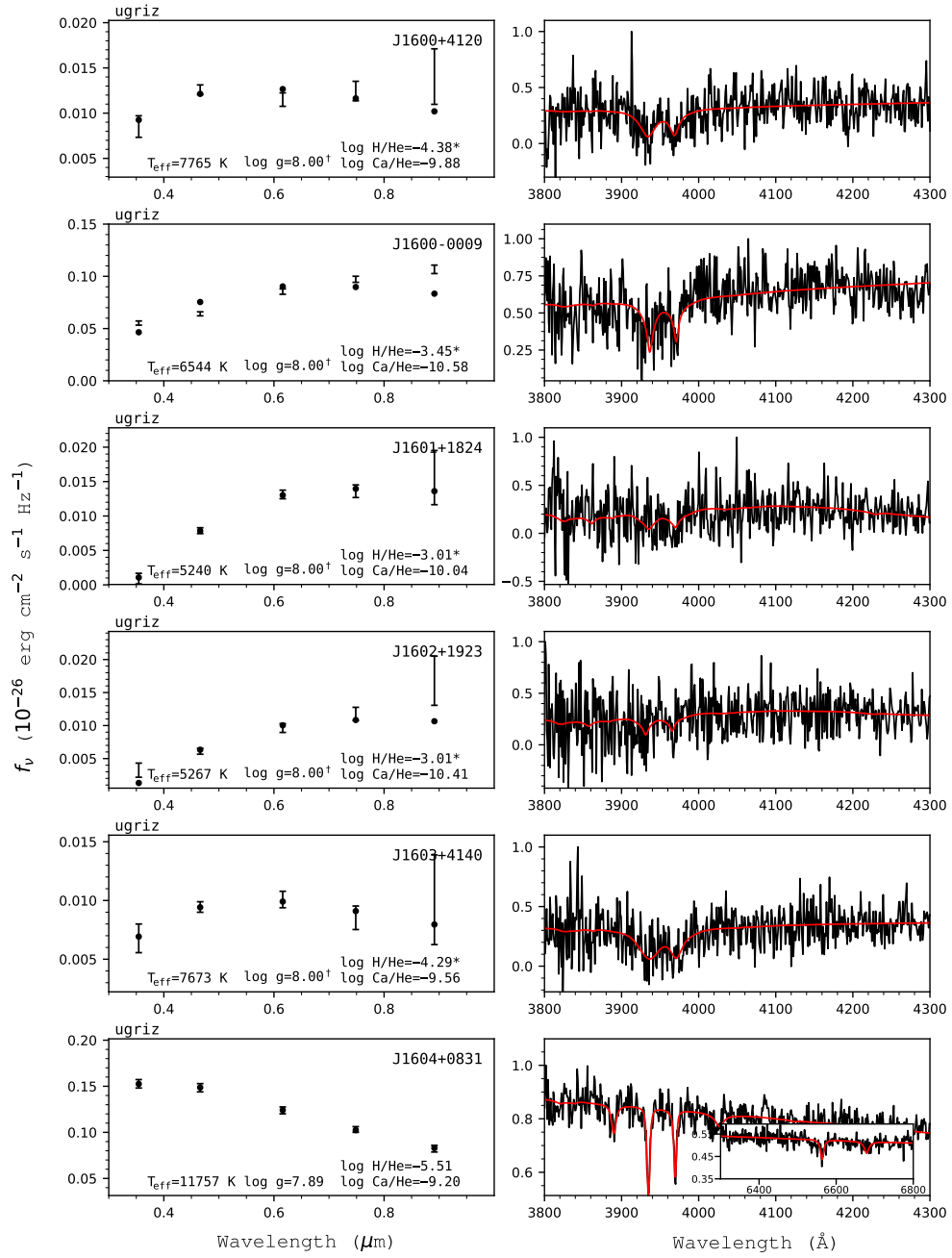


Figure 161. Fits to the DBZ/DZ(A) white dwarfs - continued.

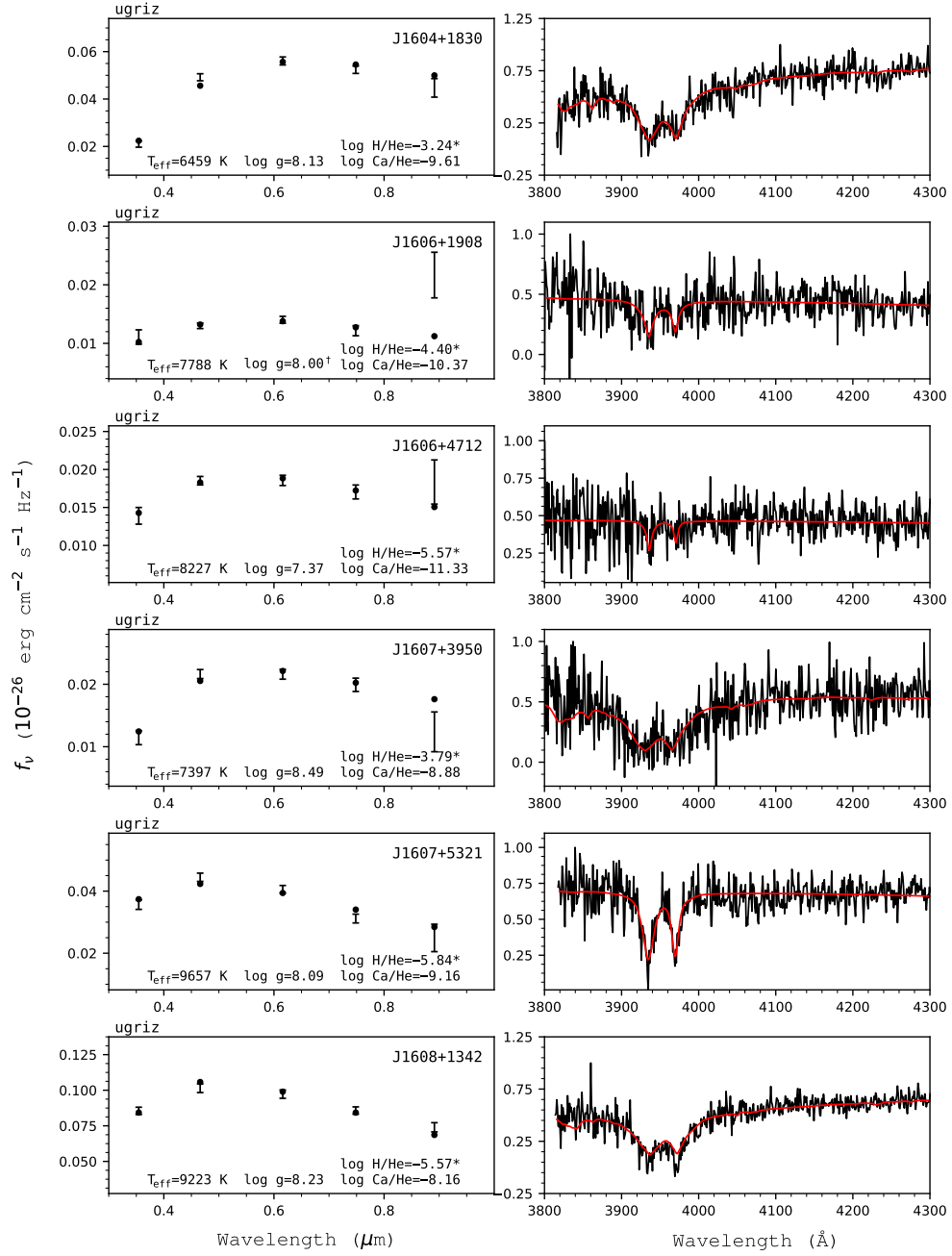


Figure 162. Fits to the DBZ/DZ(A) white dwarfs - continued.

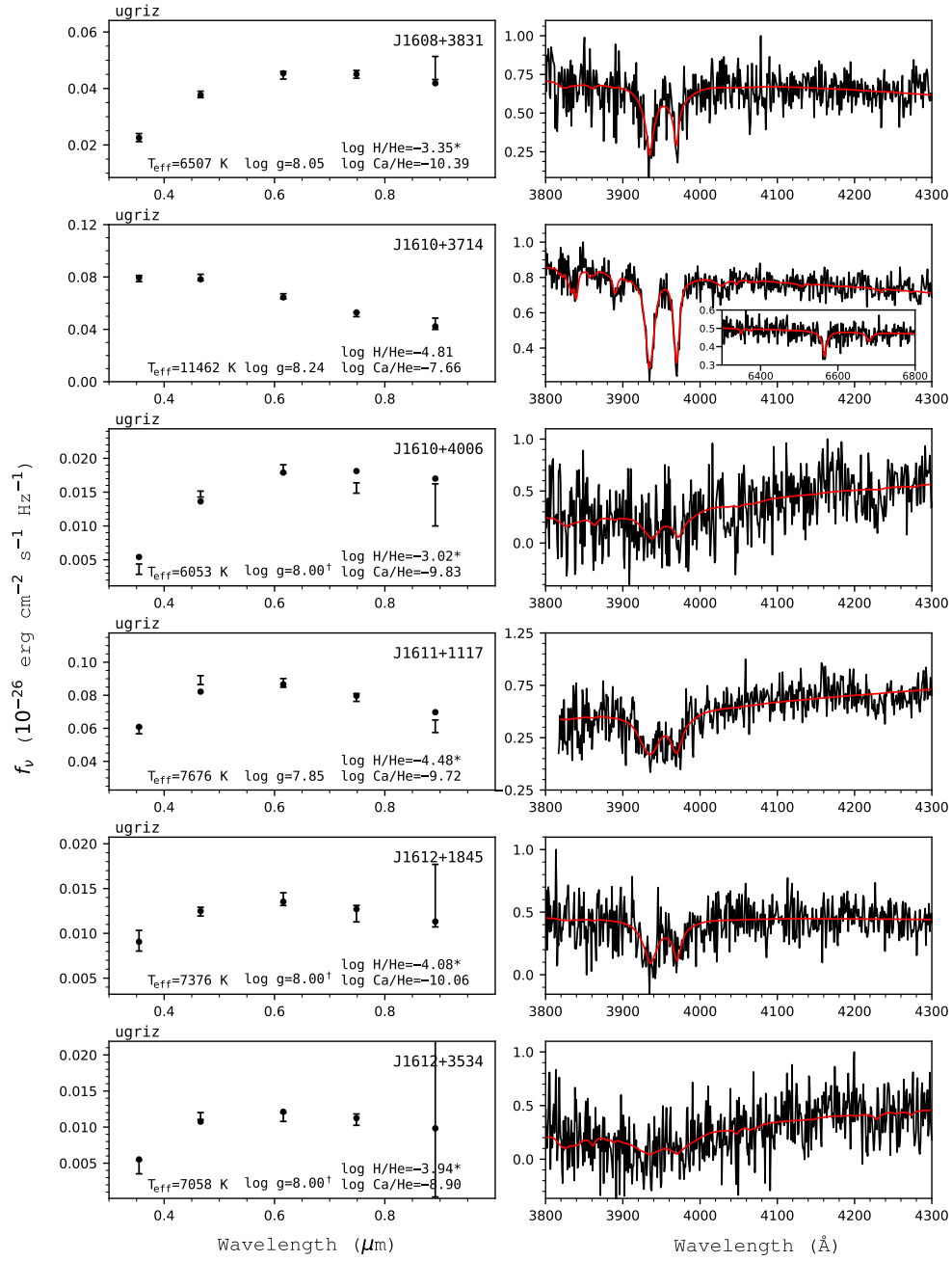


Figure 163. Fits to the DBZ/DZ(A) white dwarfs - continued.

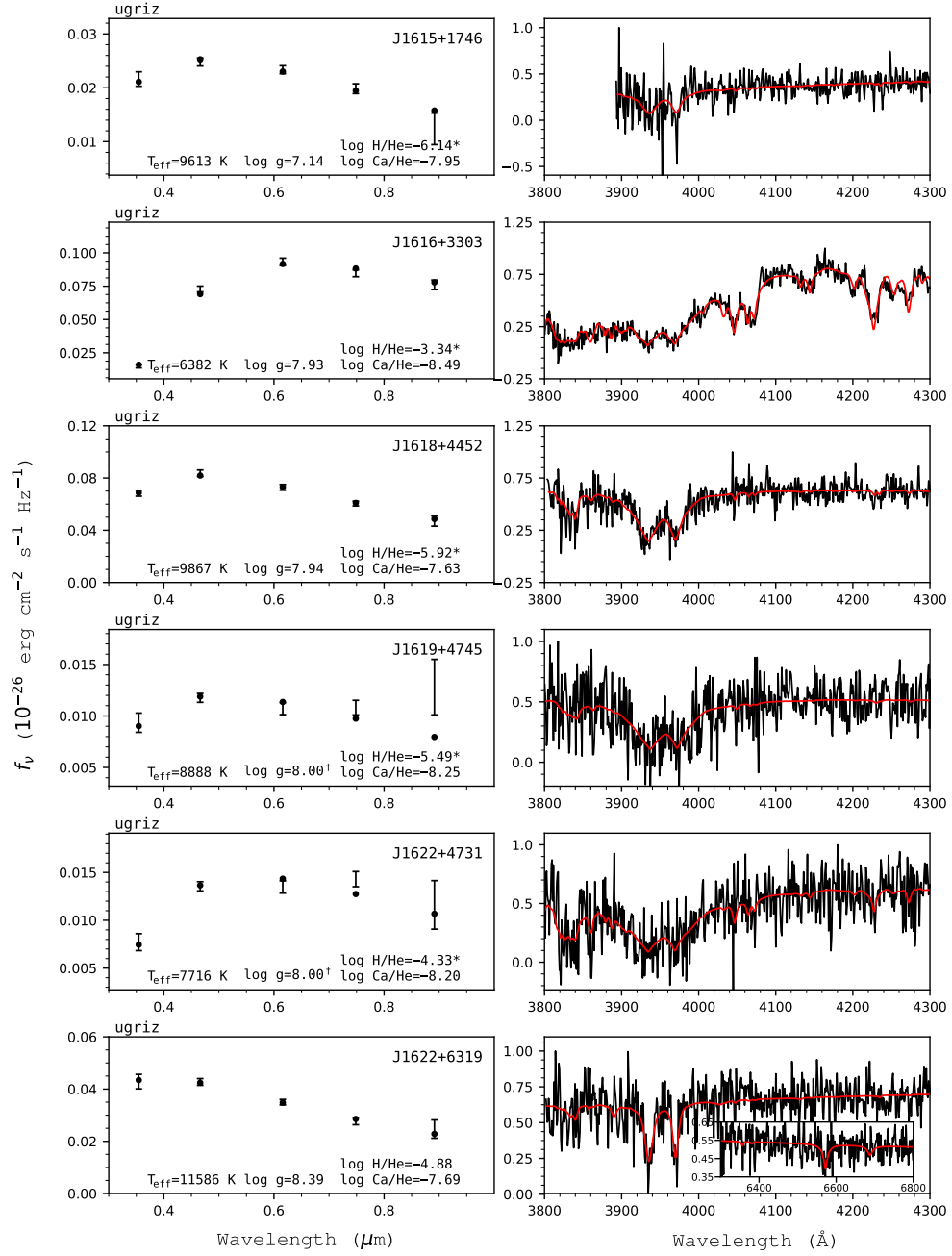


Figure 164. Fits to the DBZ/DZ(A) white dwarfs - continued.

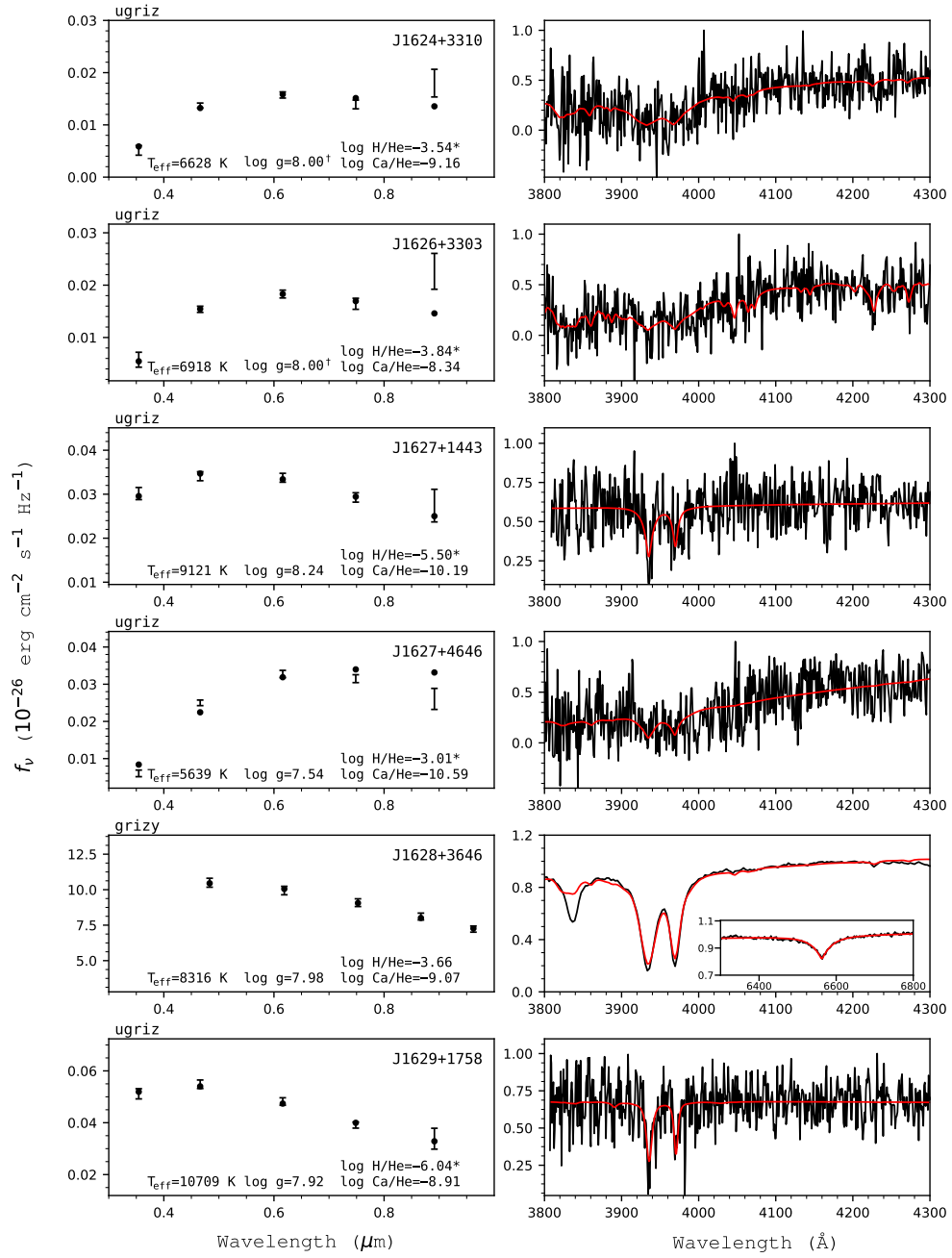


Figure 165. Fits to the DBZ/DZ(A) white dwarfs - continued.

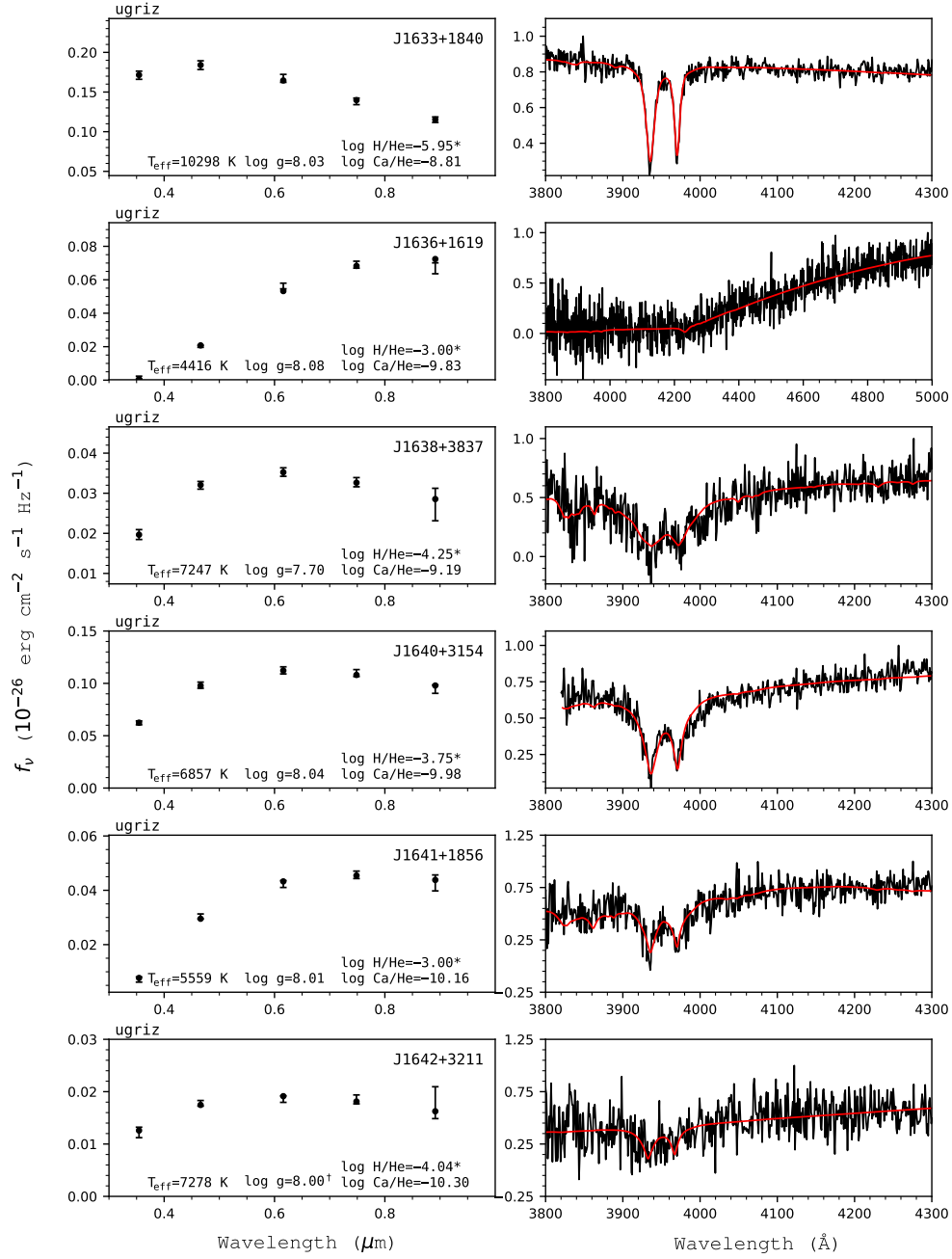


Figure 166. Fits to the DBZ/DZ(A) white dwarfs - continued.

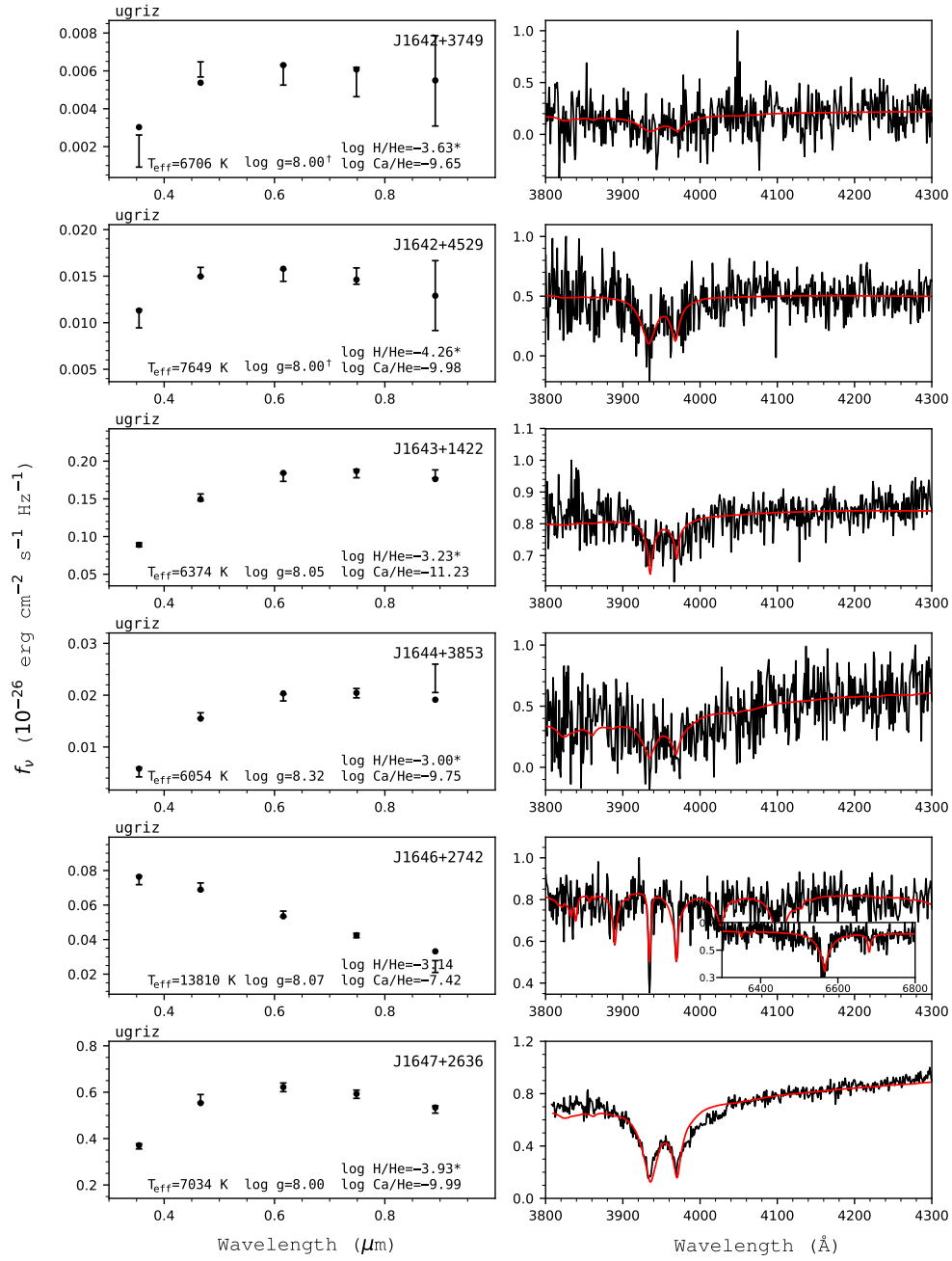


Figure 167. Fits to the DBZ/DZ(A) white dwarfs - continued.

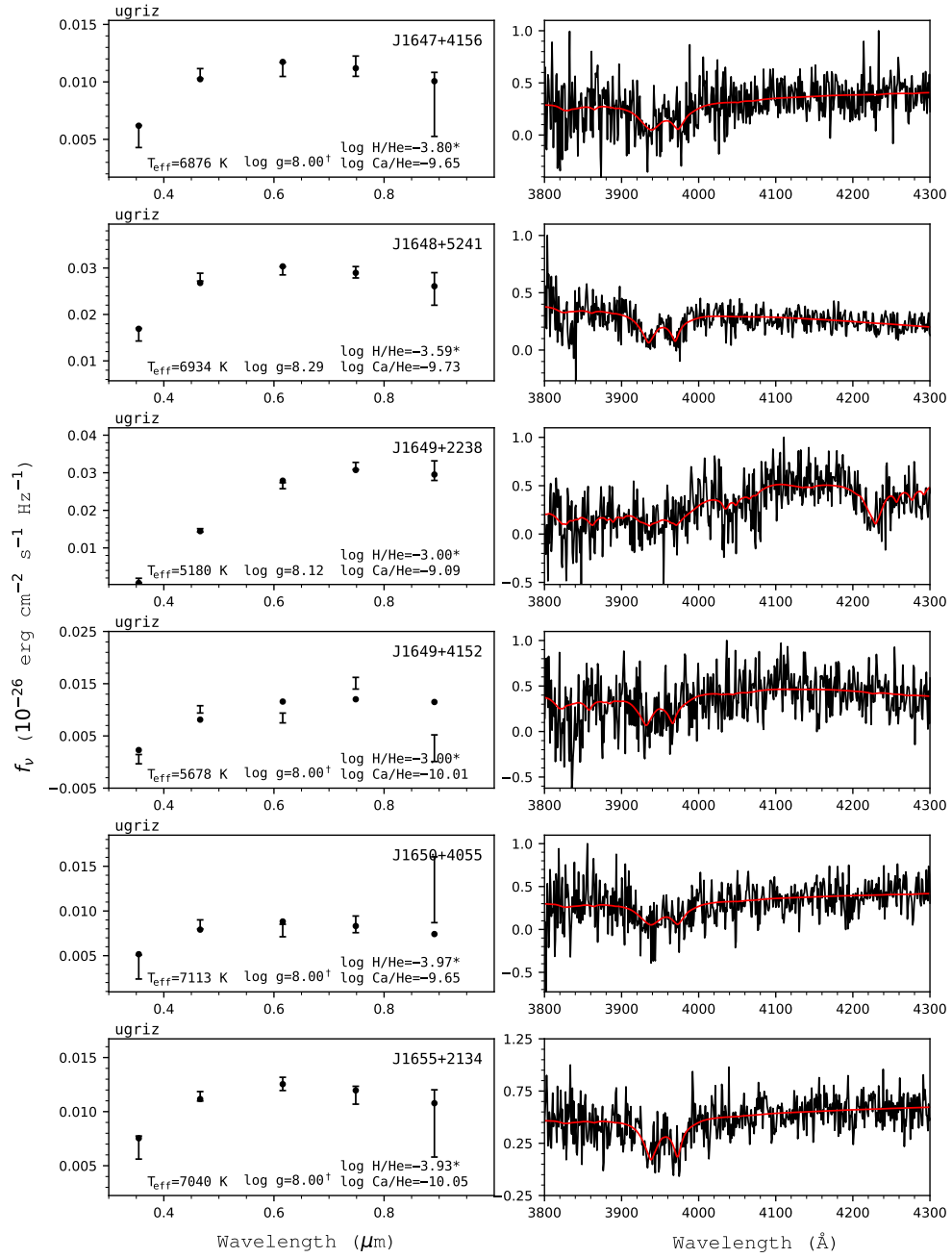


Figure 168. Fits to the DBZ/DZ(A) white dwarfs - continued.

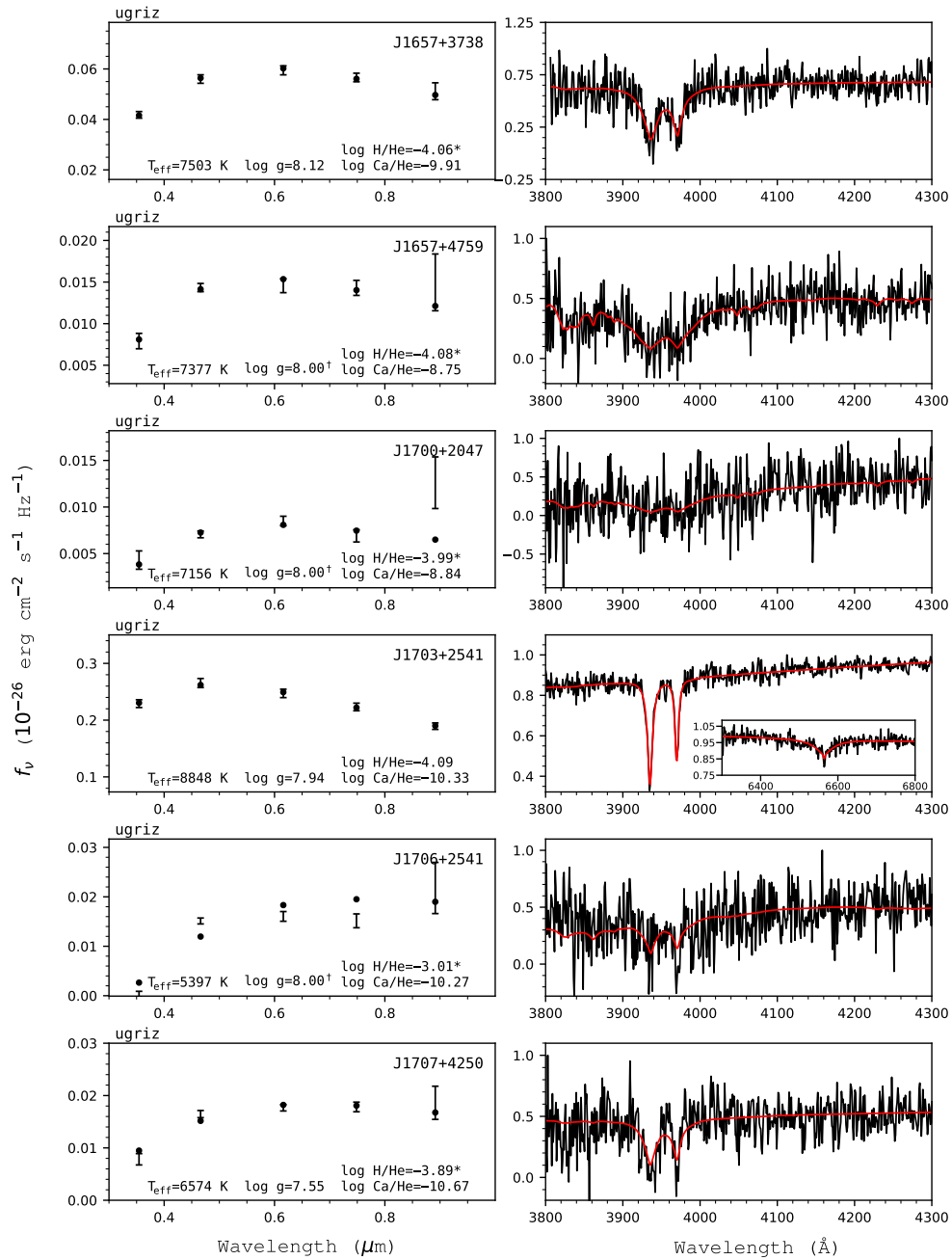


Figure 169. Fits to the DBZ/DZ(A) white dwarfs - continued.

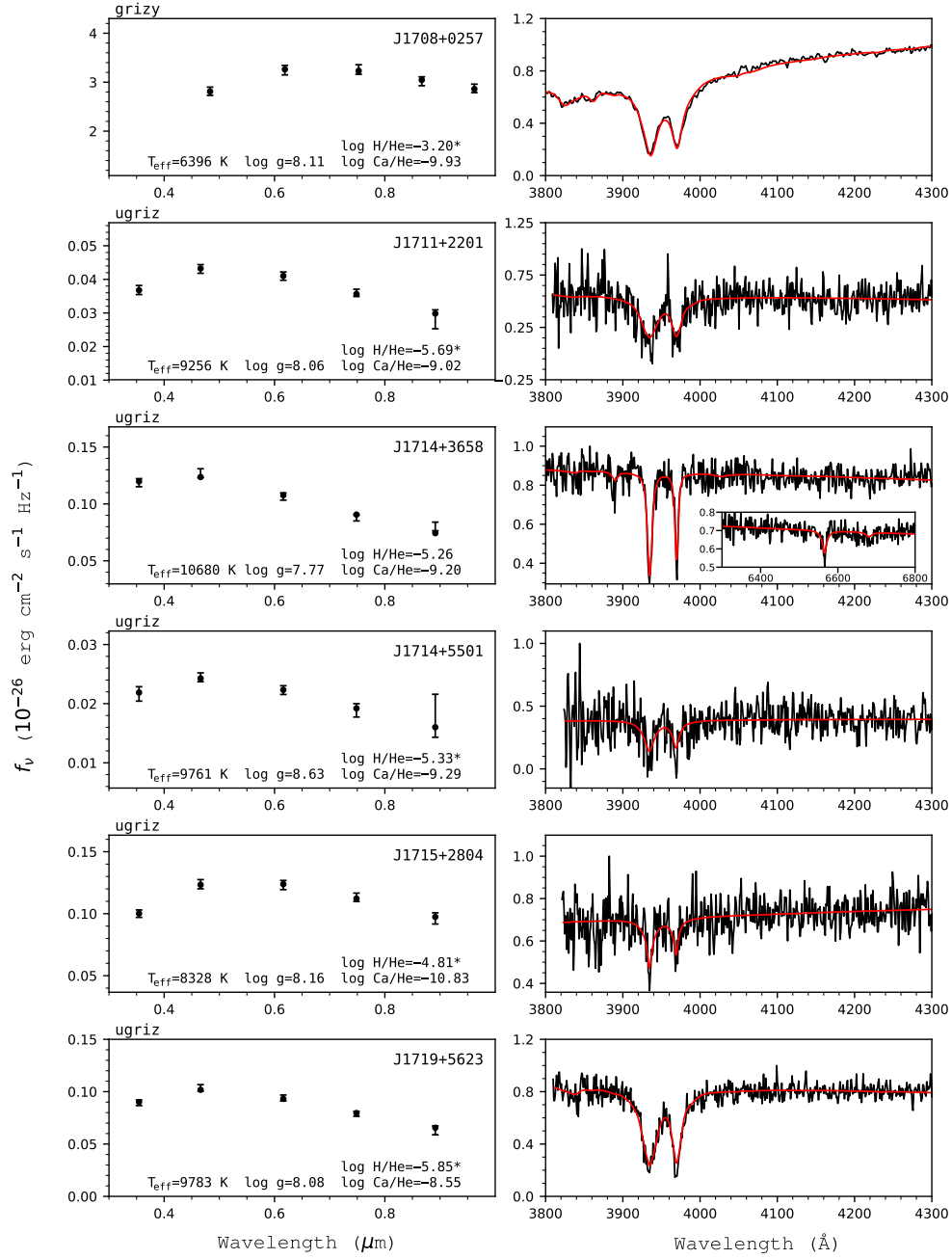


Figure 170. Fits to the DBZ/DZ(A) white dwarfs - continued.

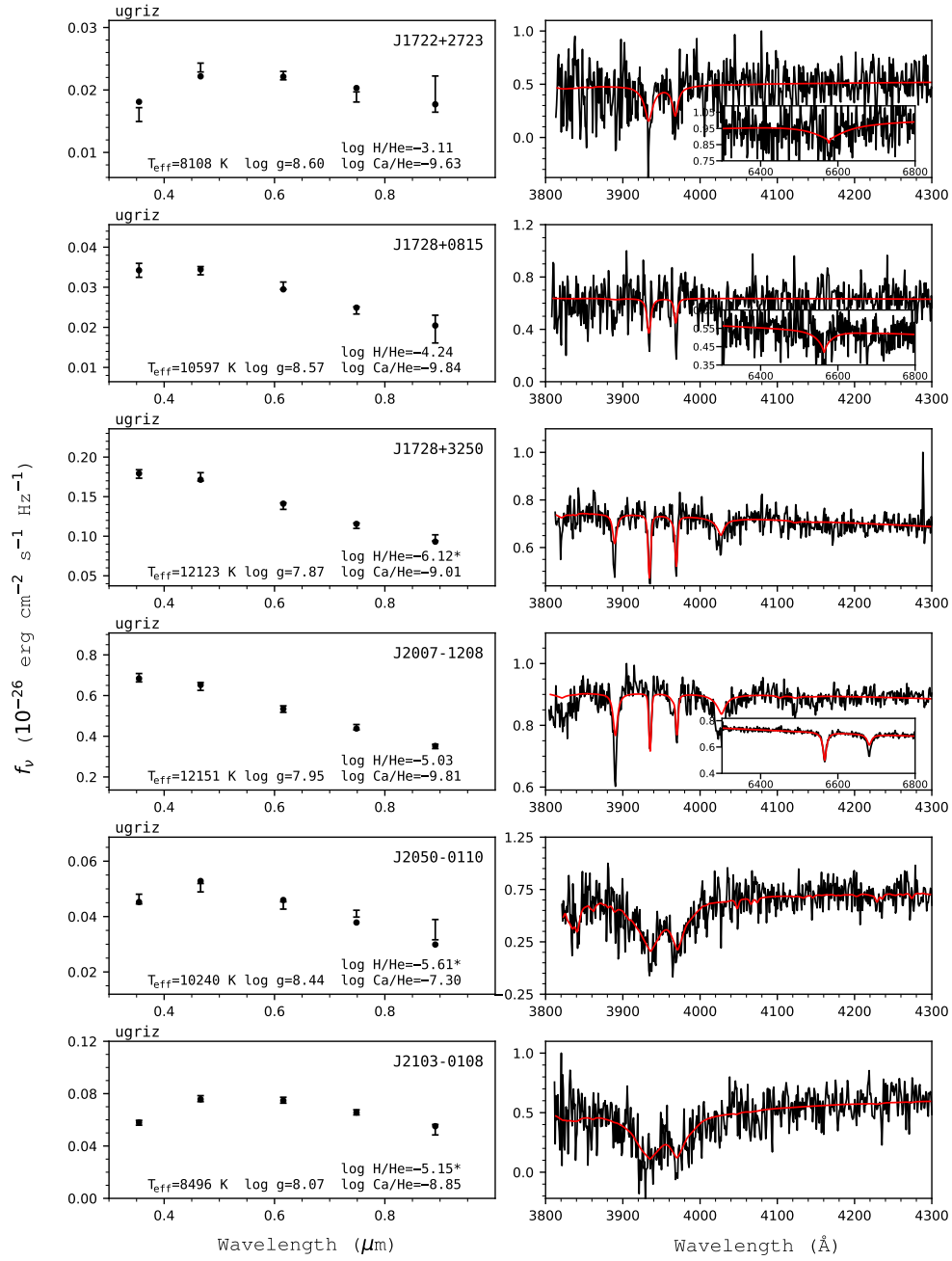


Figure 171. Fits to the DBZ/DZ(A) white dwarfs - continued.

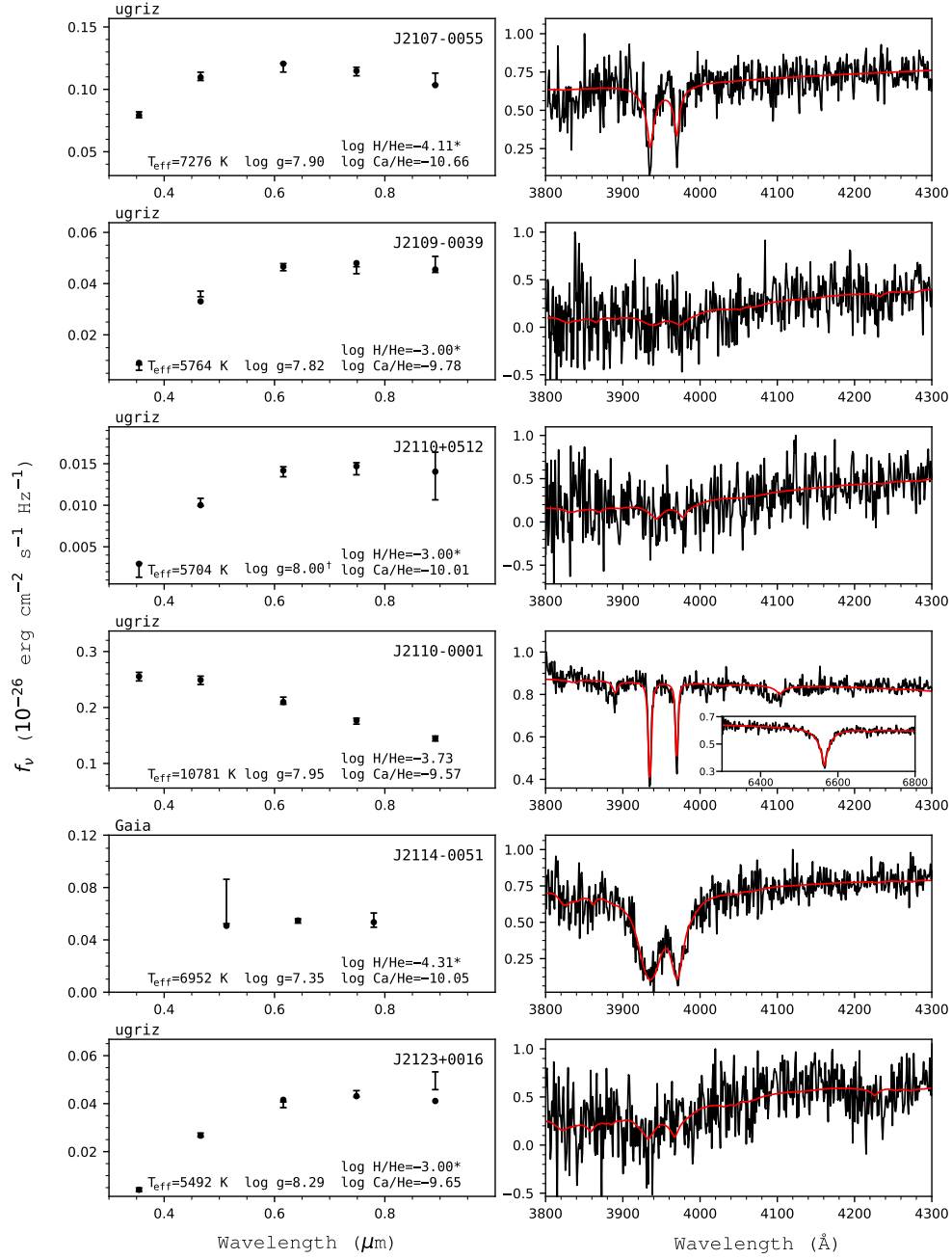


Figure 172. Fits to the DBZ/DZ(A) white dwarfs - continued.

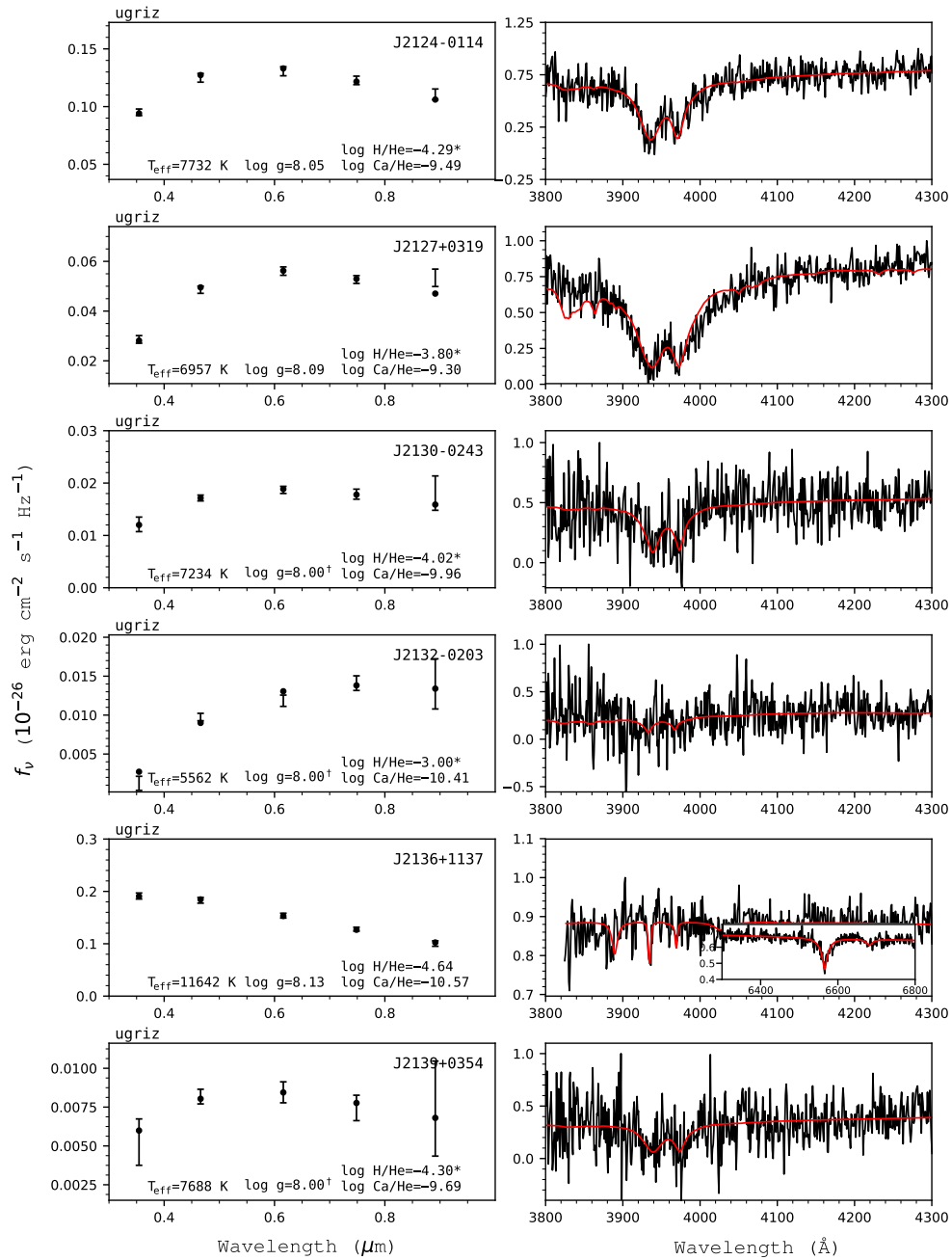


Figure 173. Fits to the DBZ/DZ(A) white dwarfs - continued.

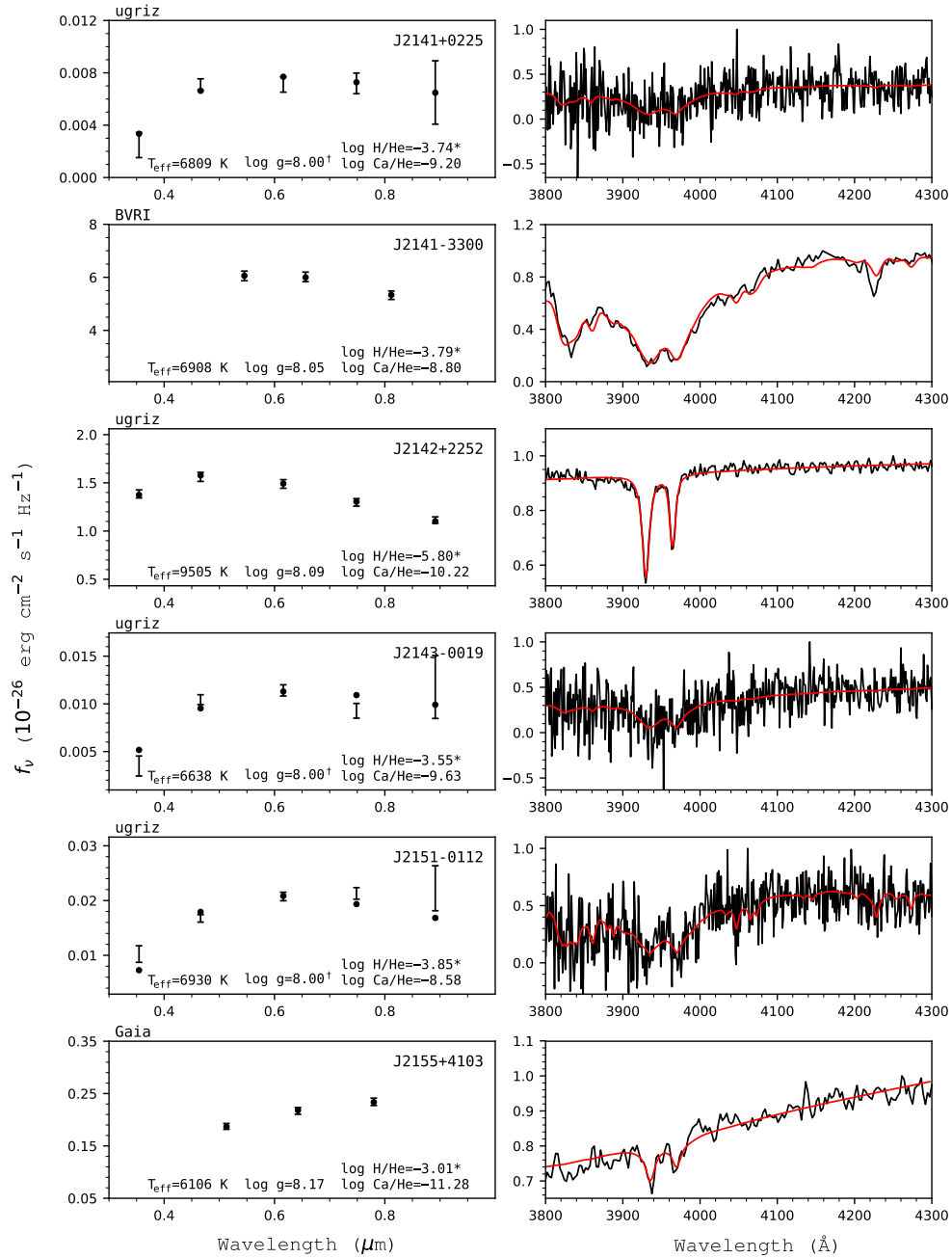


Figure 174. Fits to the DB/DZ(A) white dwarfs - continued.

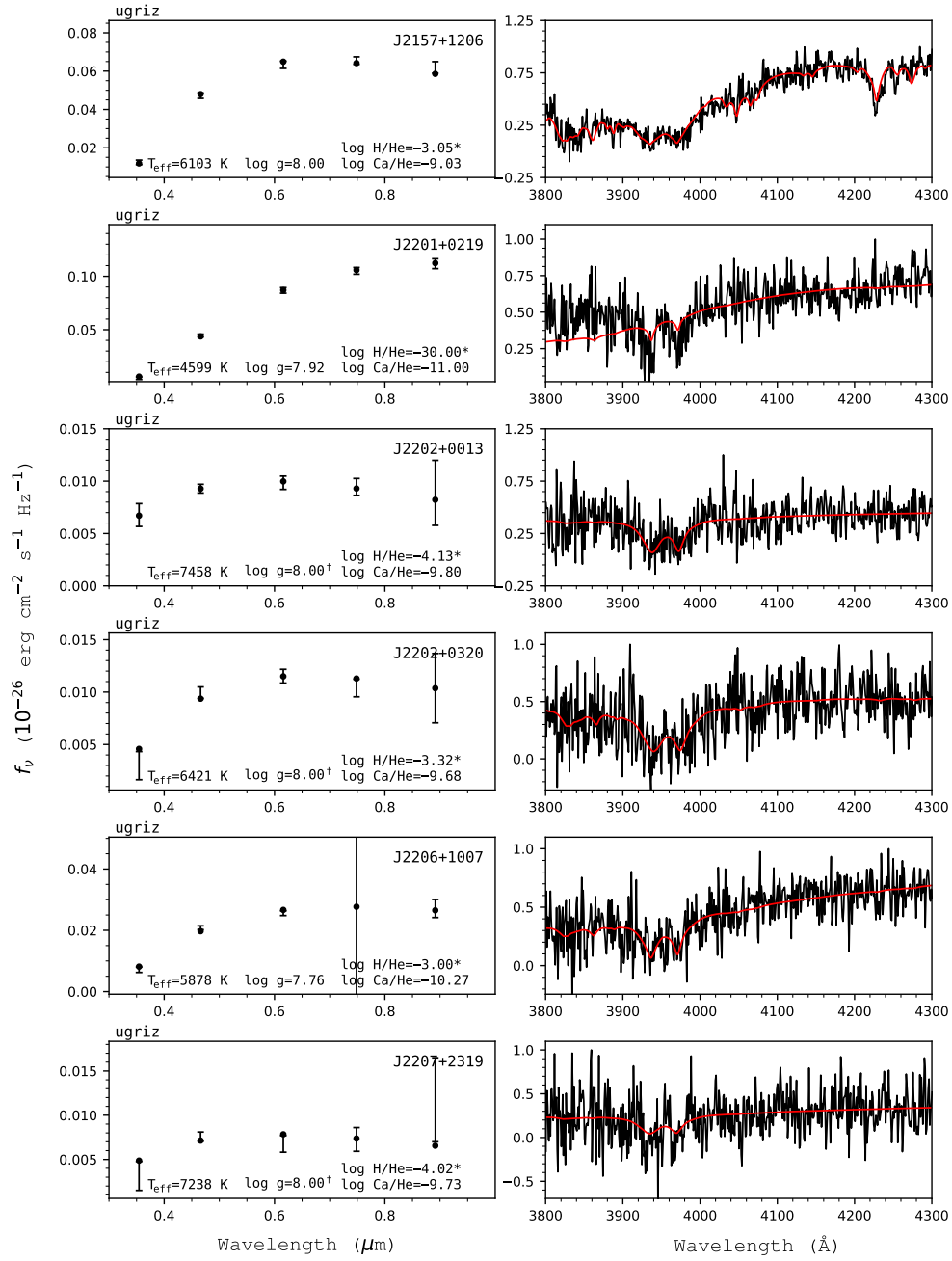


Figure 175. Fits to the DBZ/DZ(A) white dwarfs - continued.

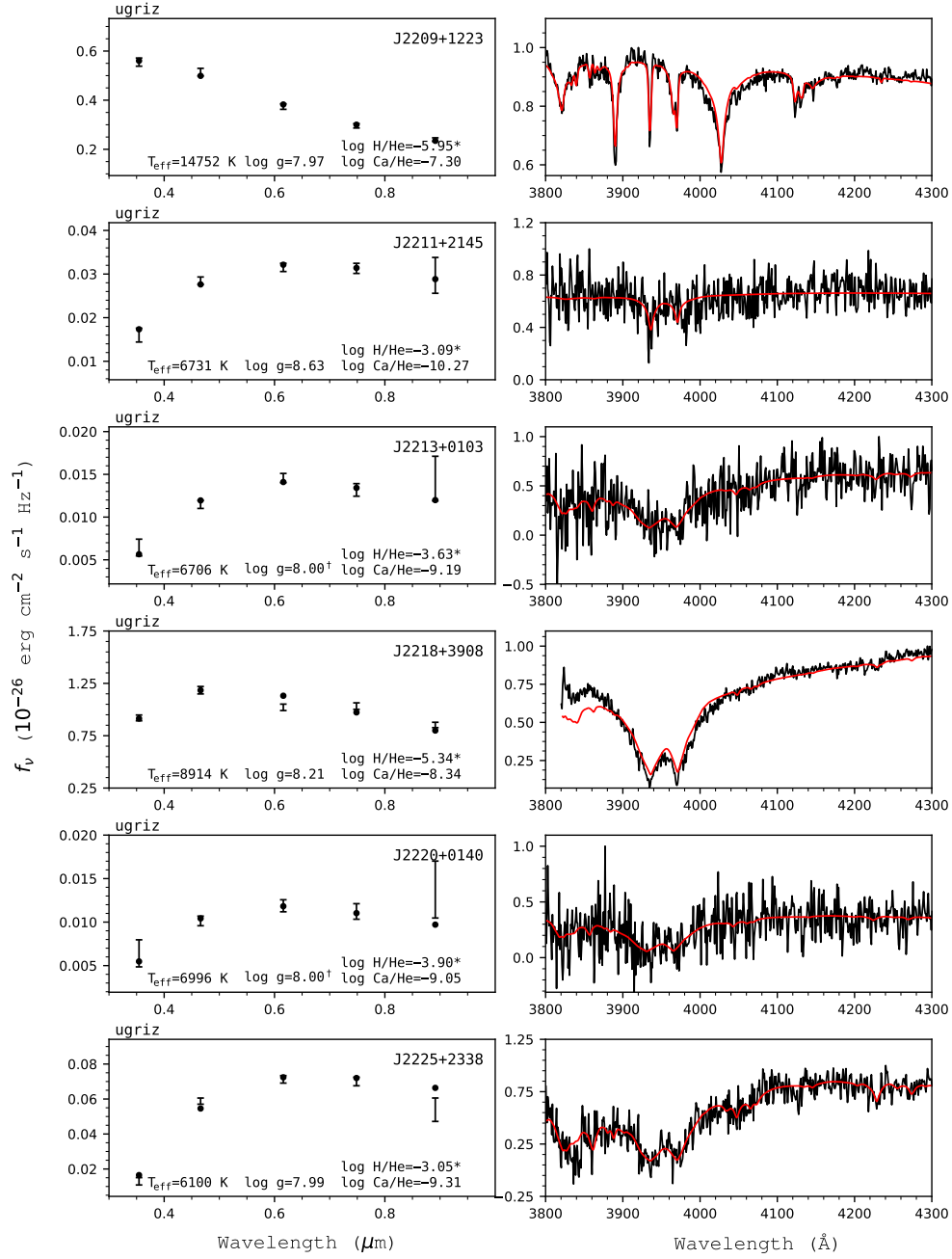


Figure 176. Fits to the DBZ/DZ(A) white dwarfs - continued.

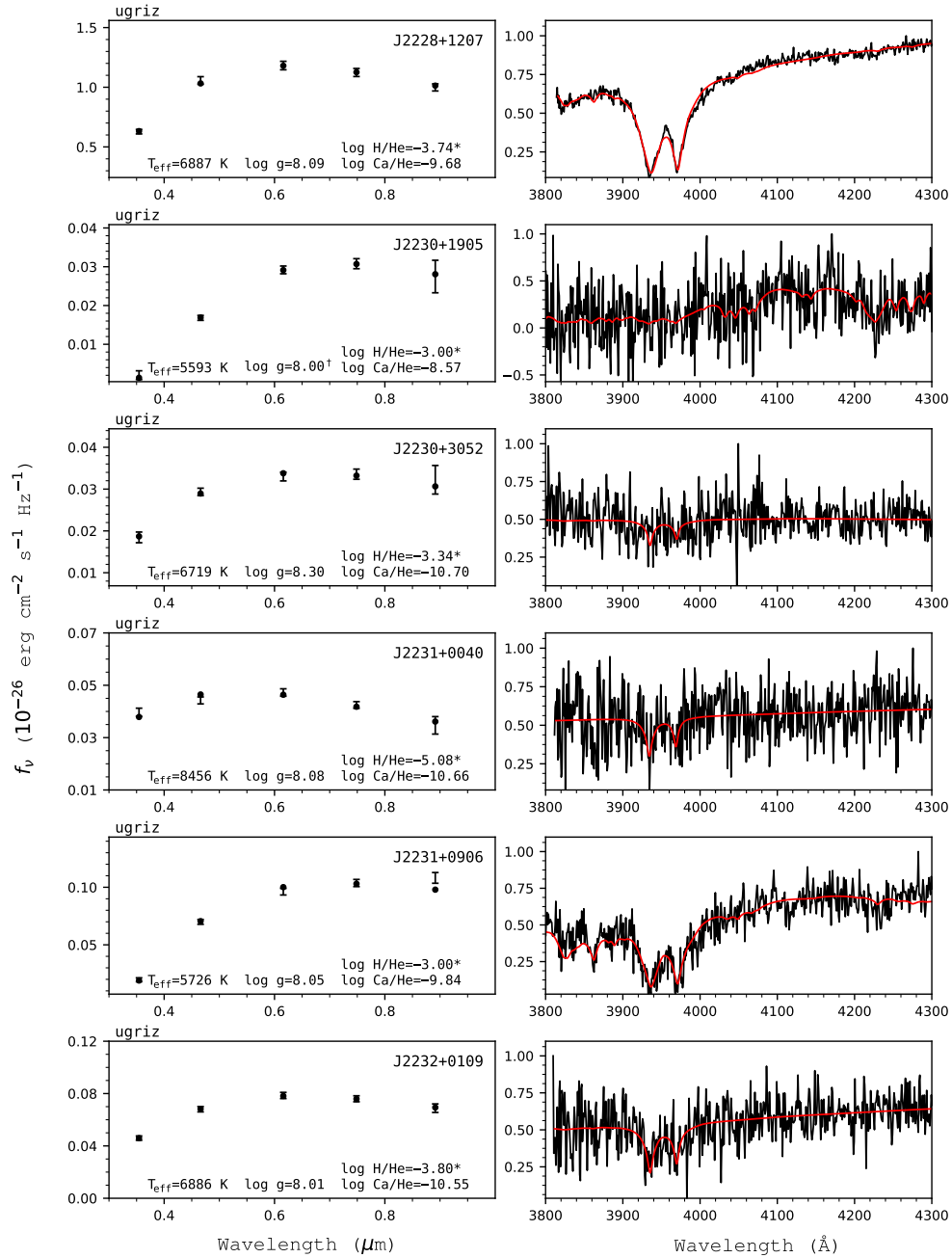


Figure 177. Fits to the DBZ/DZ(A) white dwarfs - continued.

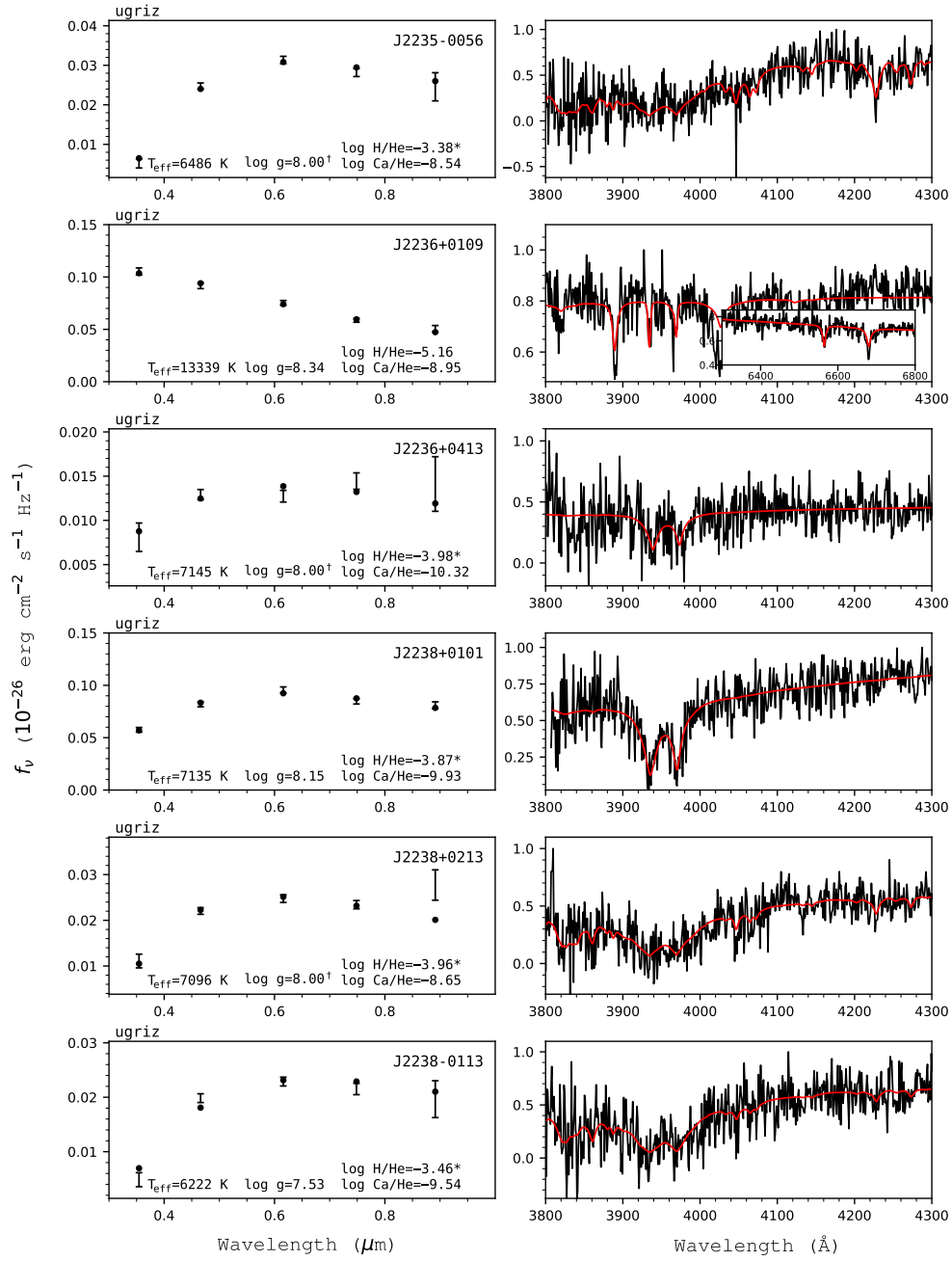


Figure 178. Fits to the DBZ/DZ(A) white dwarfs - continued.

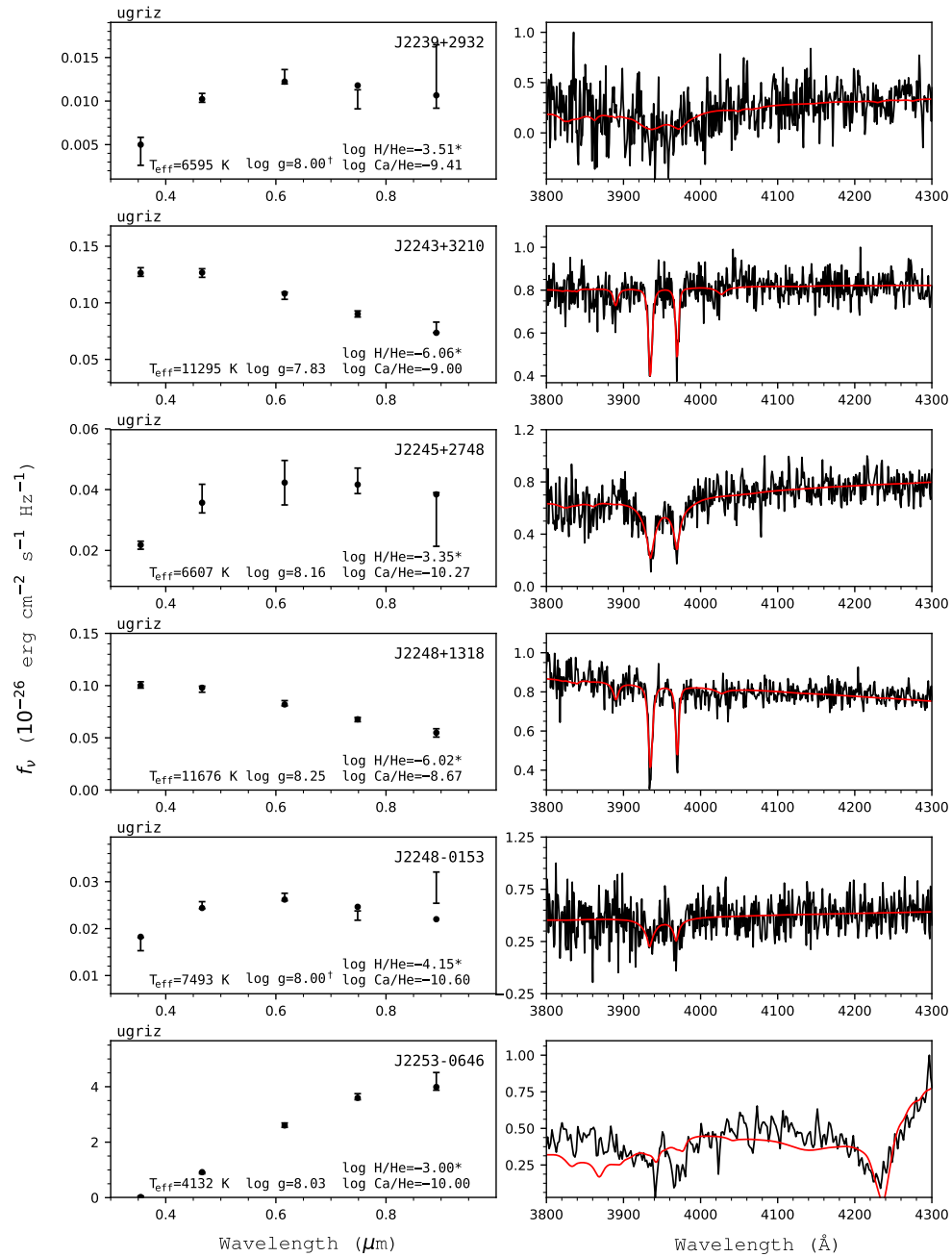


Figure 179. Fits to the DBZ/DZ(A) white dwarfs - continued.

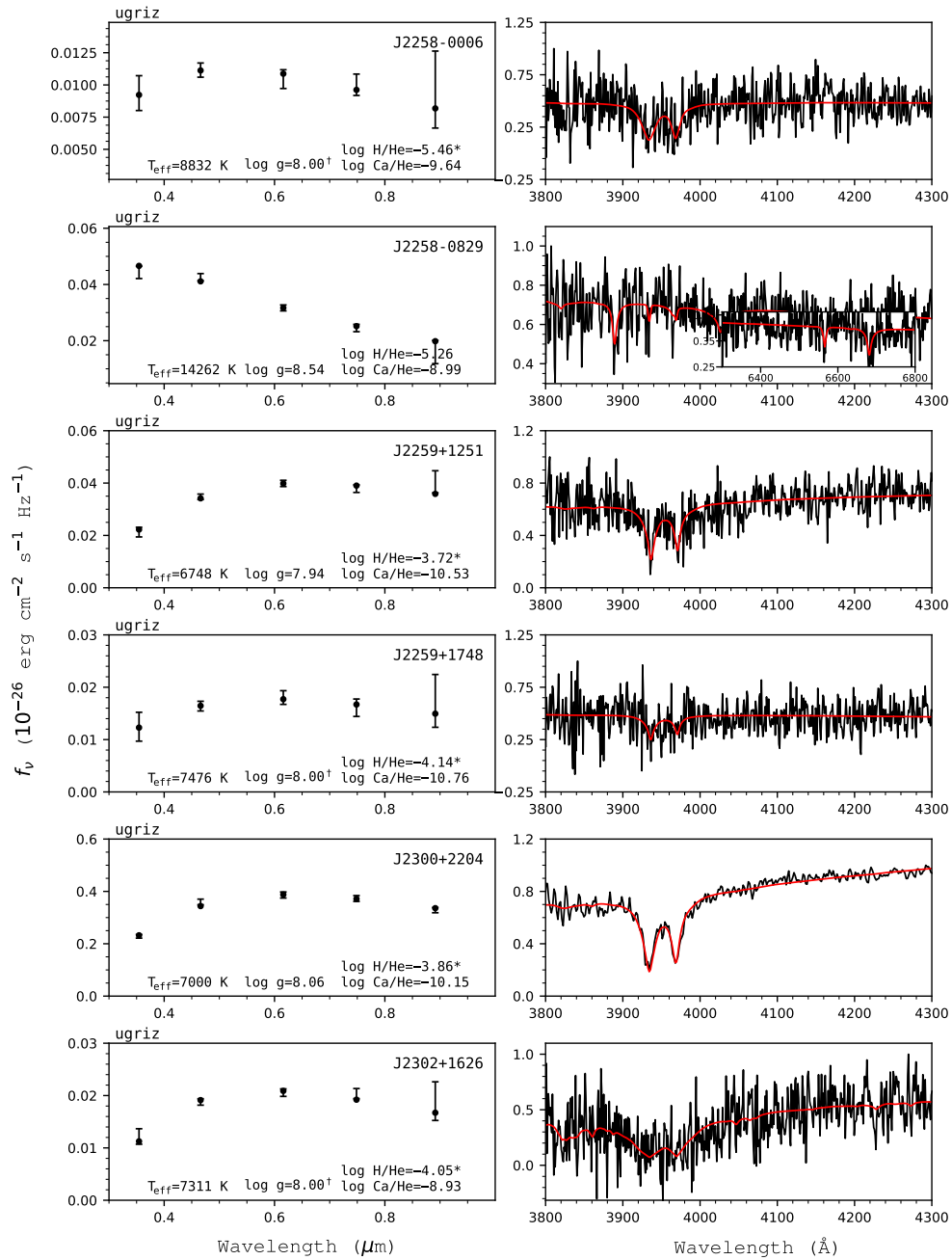


Figure 180. Fits to the DBZ/DZ(A) white dwarfs - continued.

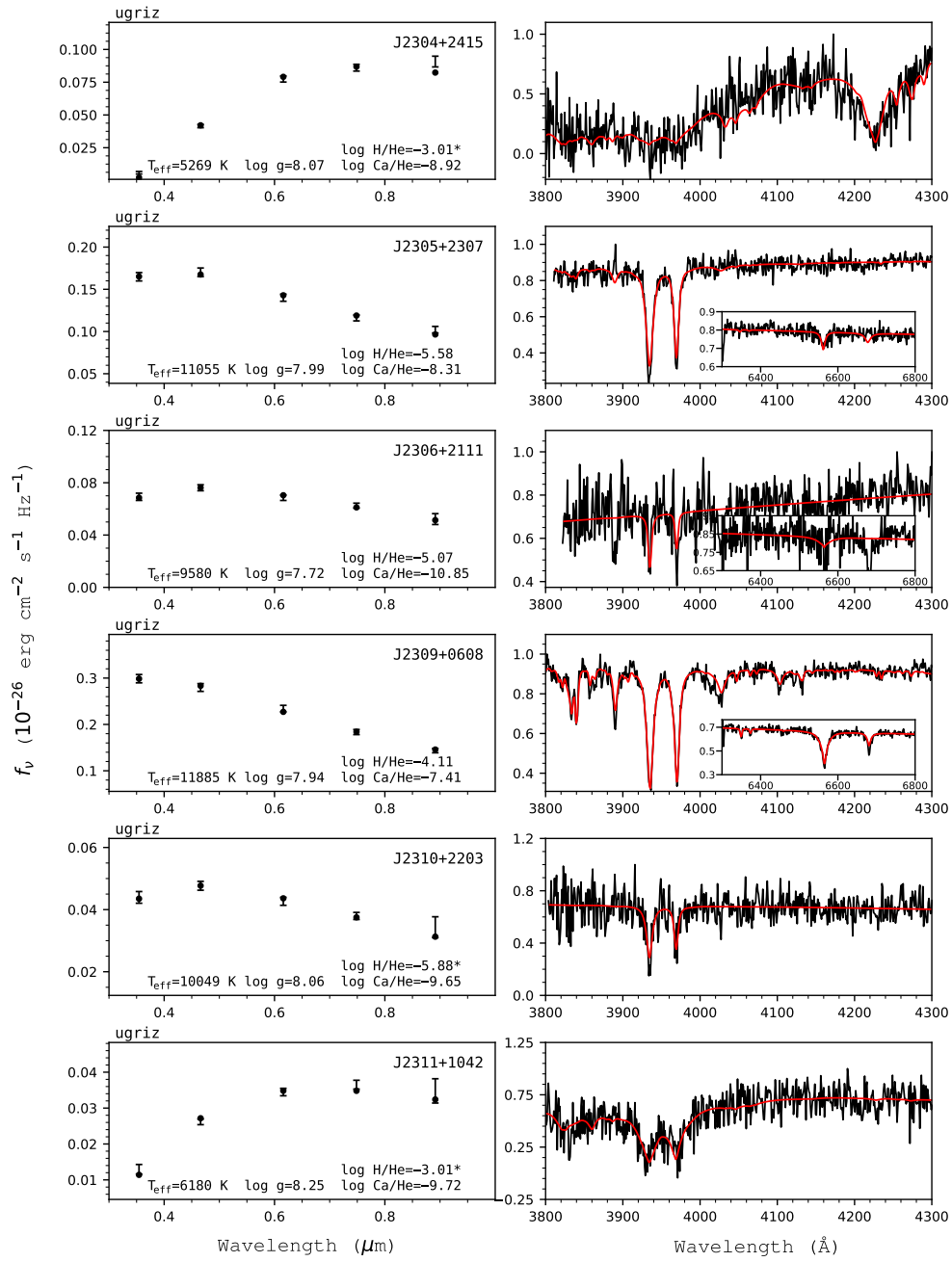


Figure 181. Fits to the DBZ/DZ(A) white dwarfs - continued.

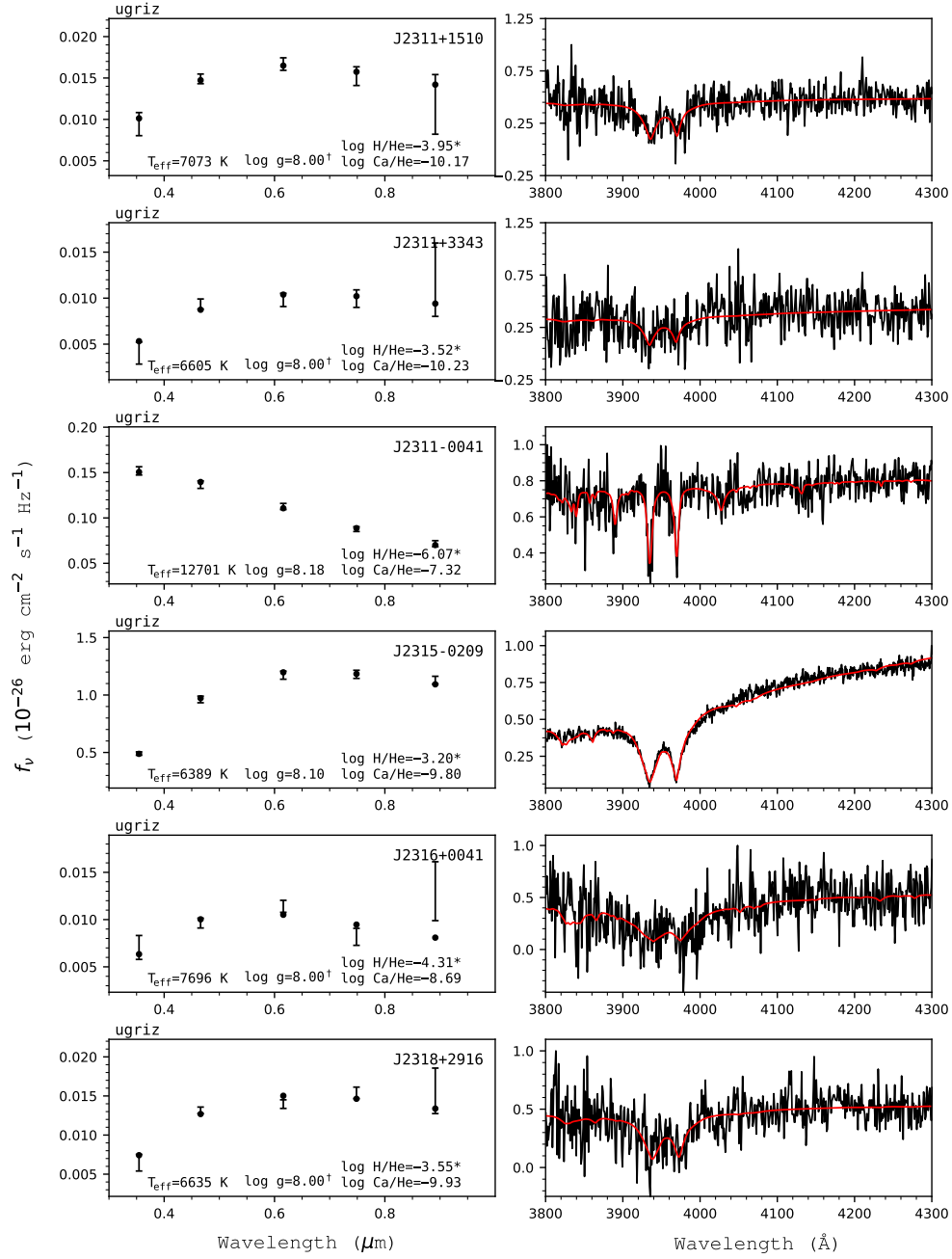


Figure 182. Fits to the DBZ/DZ(A) white dwarfs - continued.

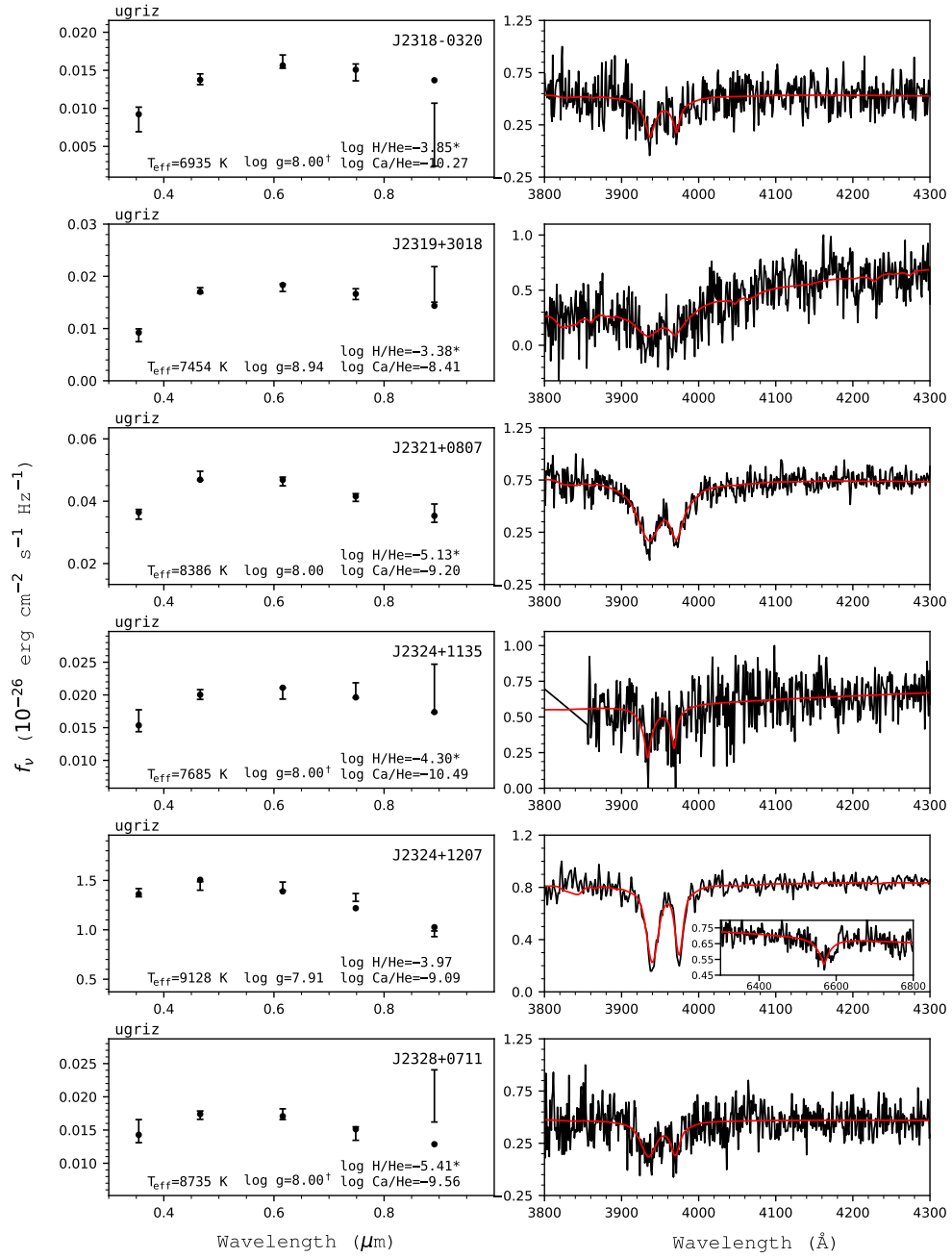


Figure 183. Fits to the DBZ/DZ(A) white dwarfs - continued.

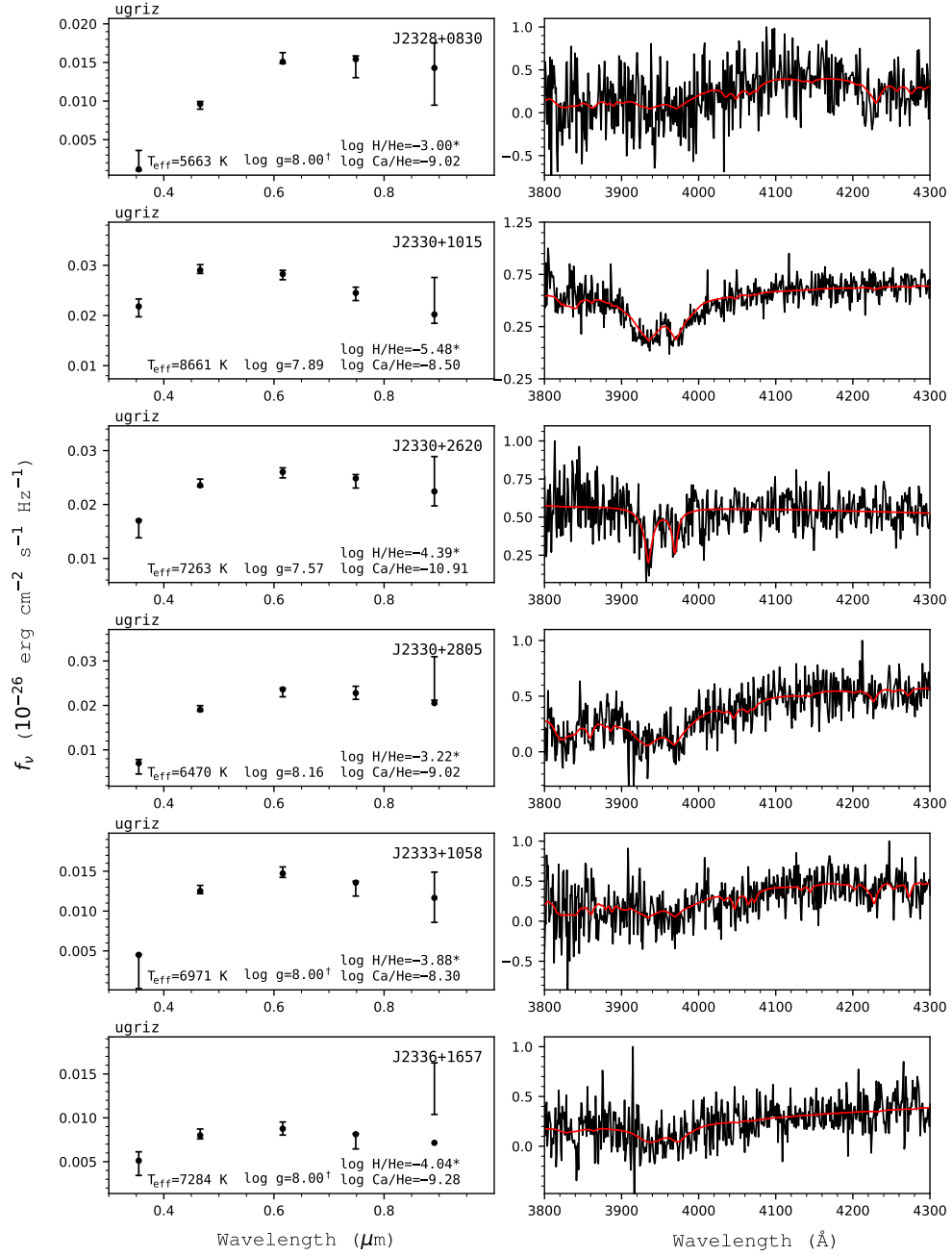


Figure 184. Fits to the DBZ/DZ(A) white dwarfs - continued.

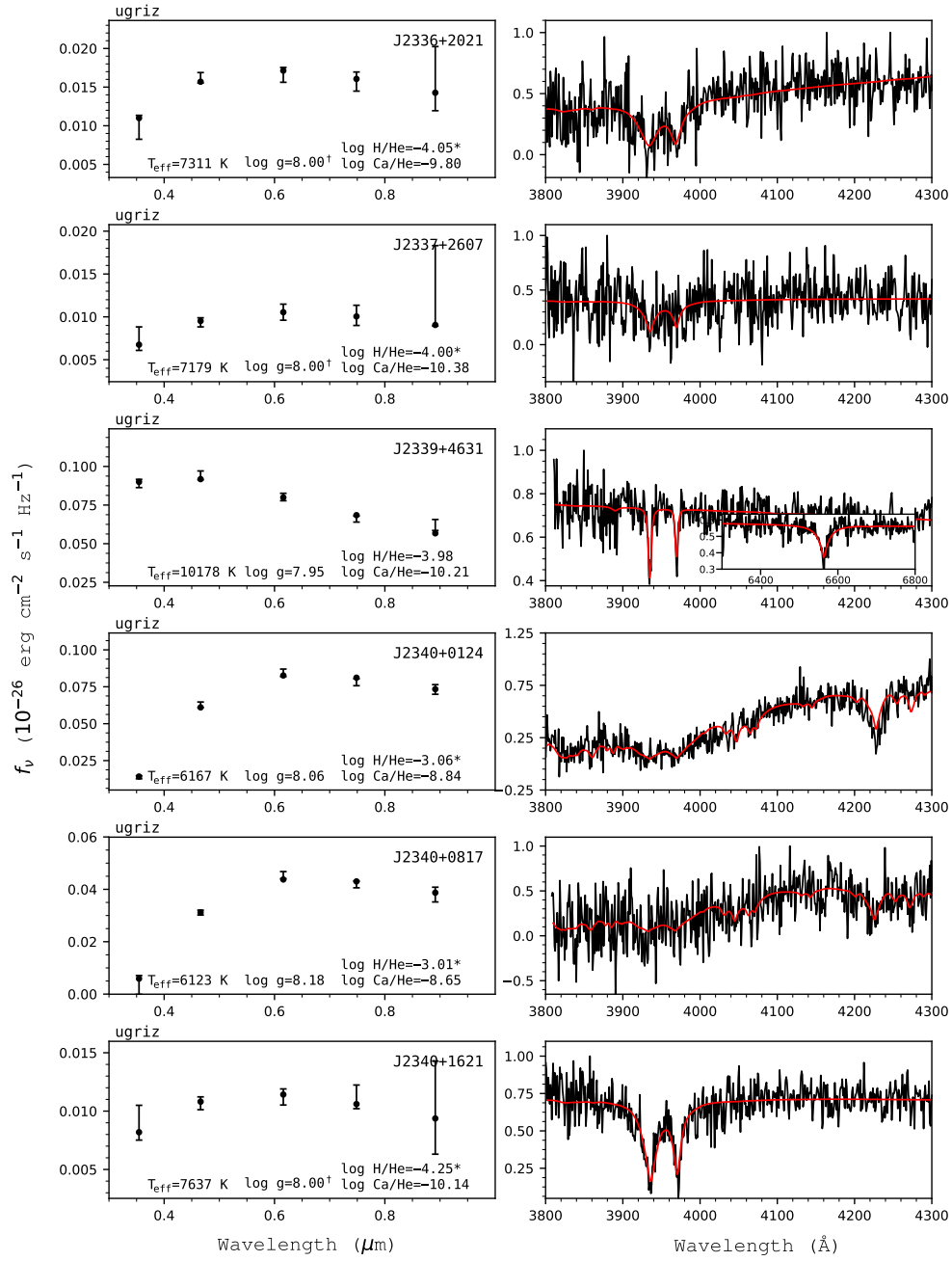


Figure 185. Fits to the DBZ/DZ(A) white dwarfs - continued.

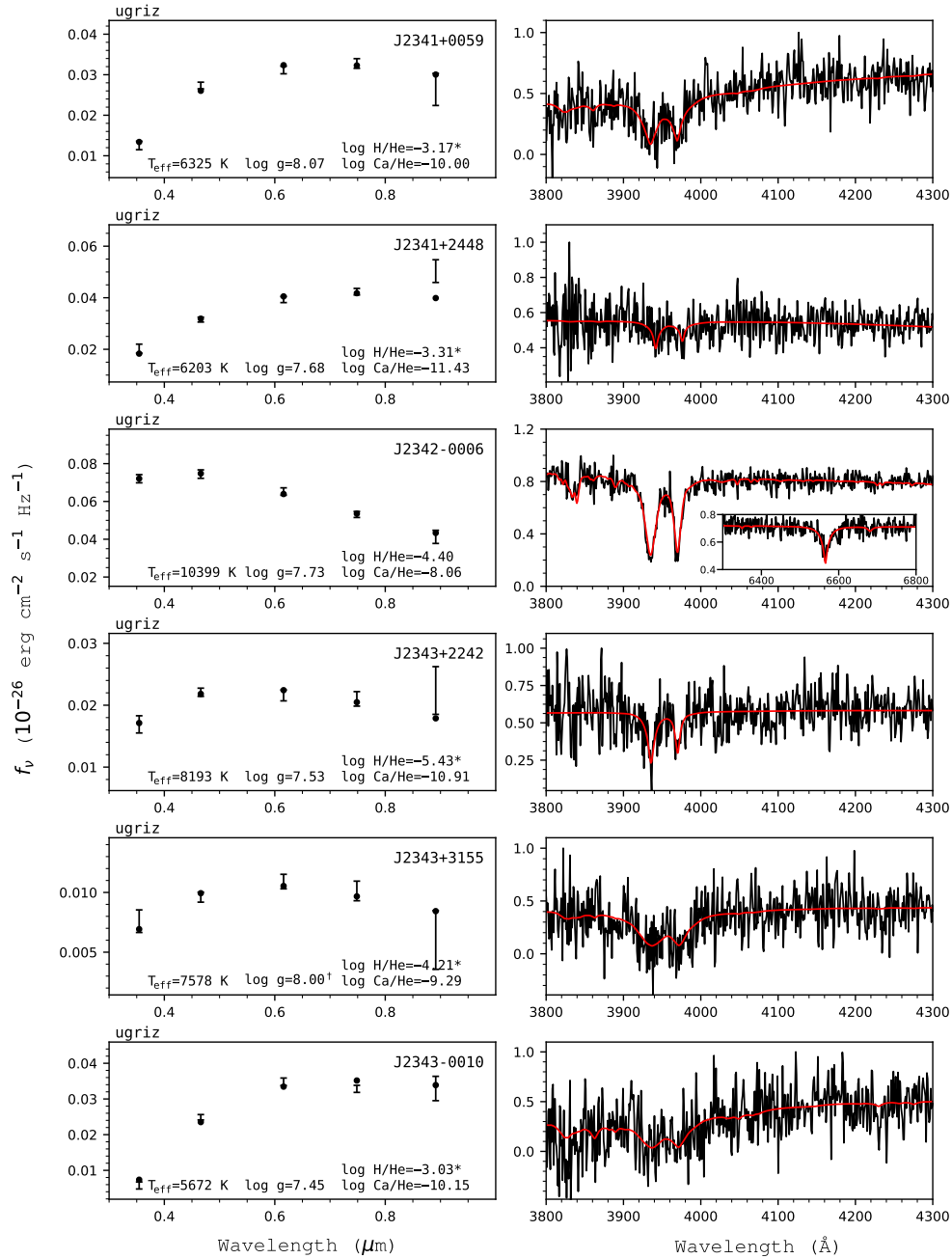


Figure 186. Fits to the DBZ/DZ(A) white dwarfs - continued.

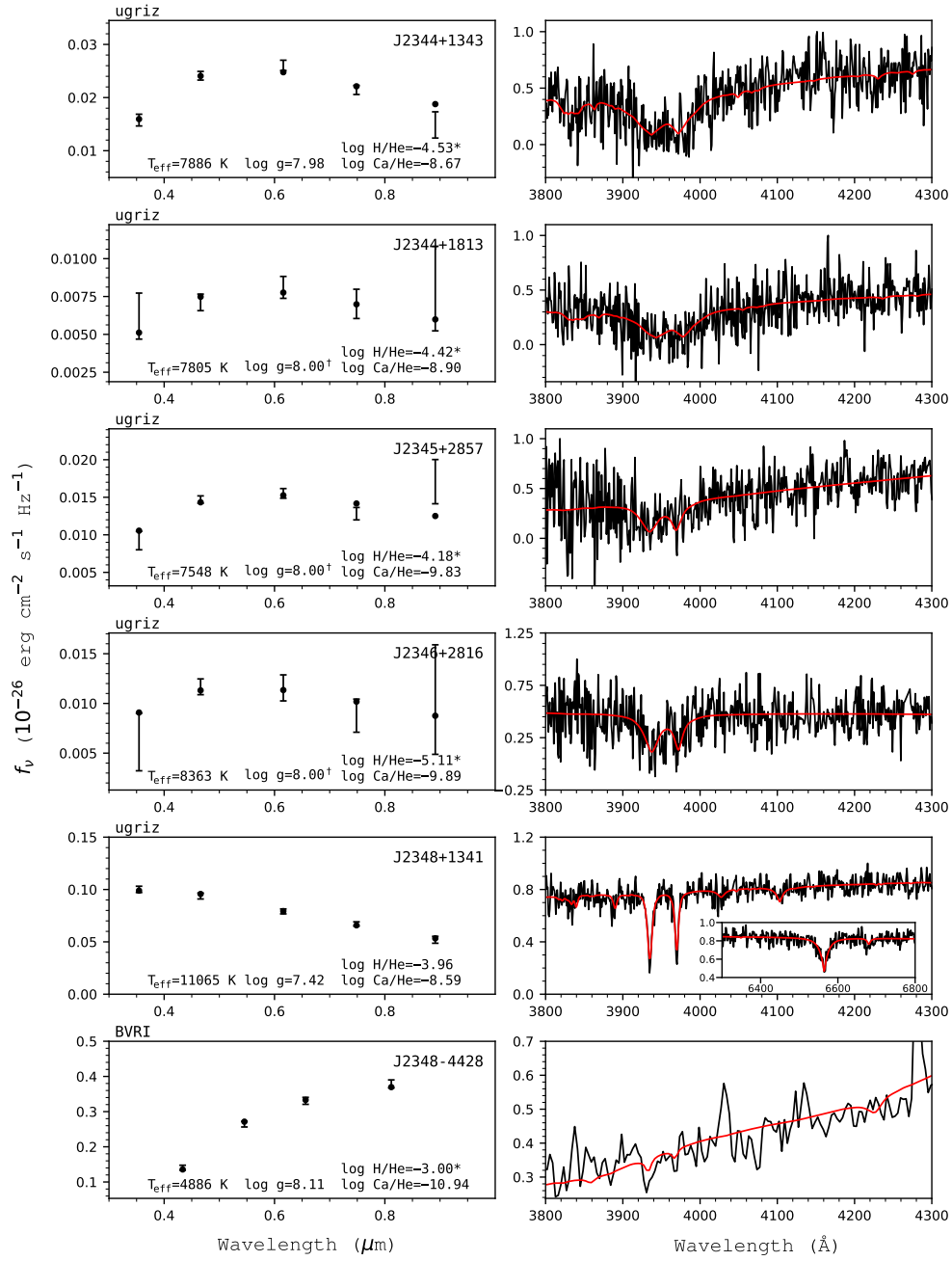


Figure 187. Fits to the DB/DZ(A) white dwarfs - continued.

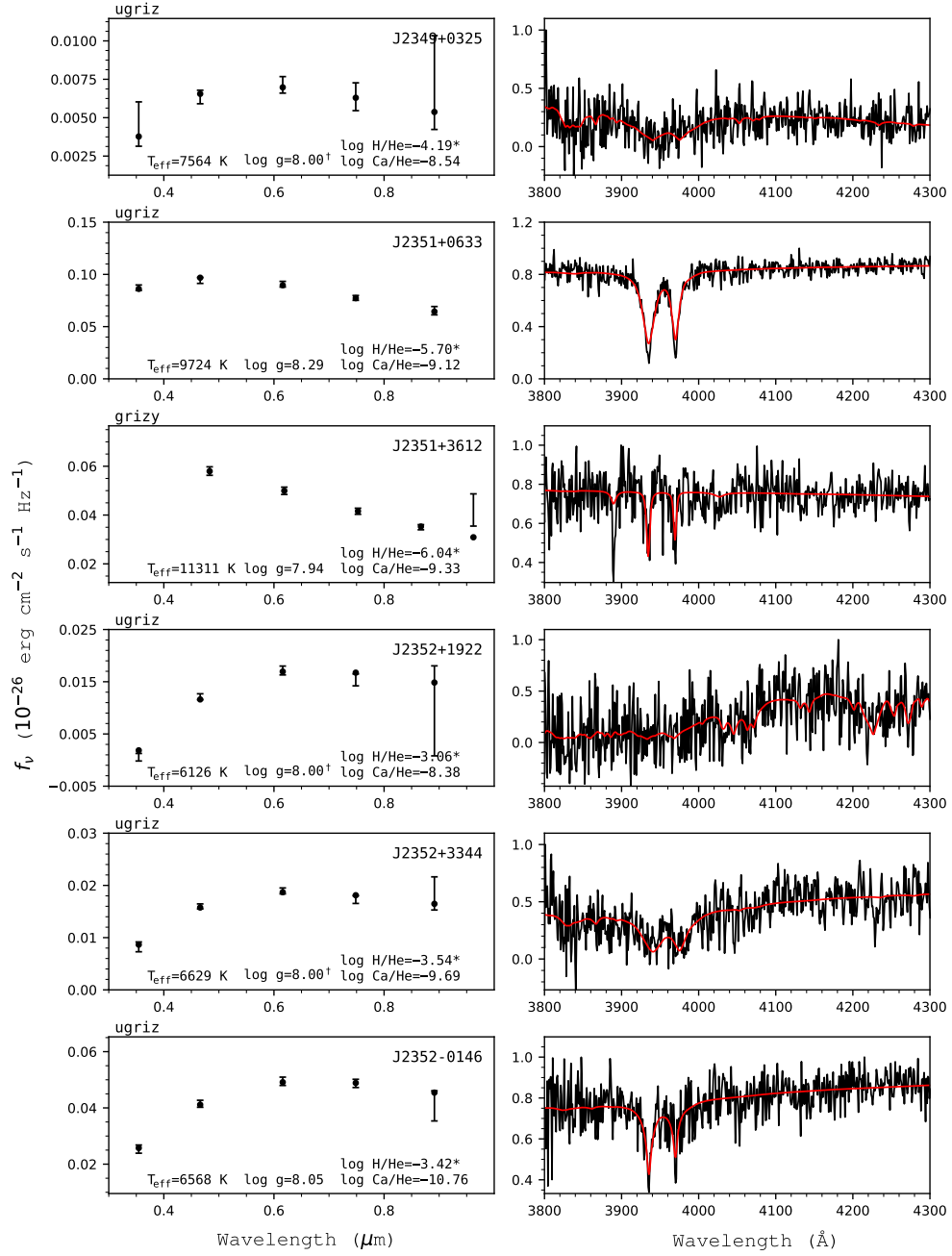


Figure 188. Fits to the DBZ/DZ(A) white dwarfs - continued.

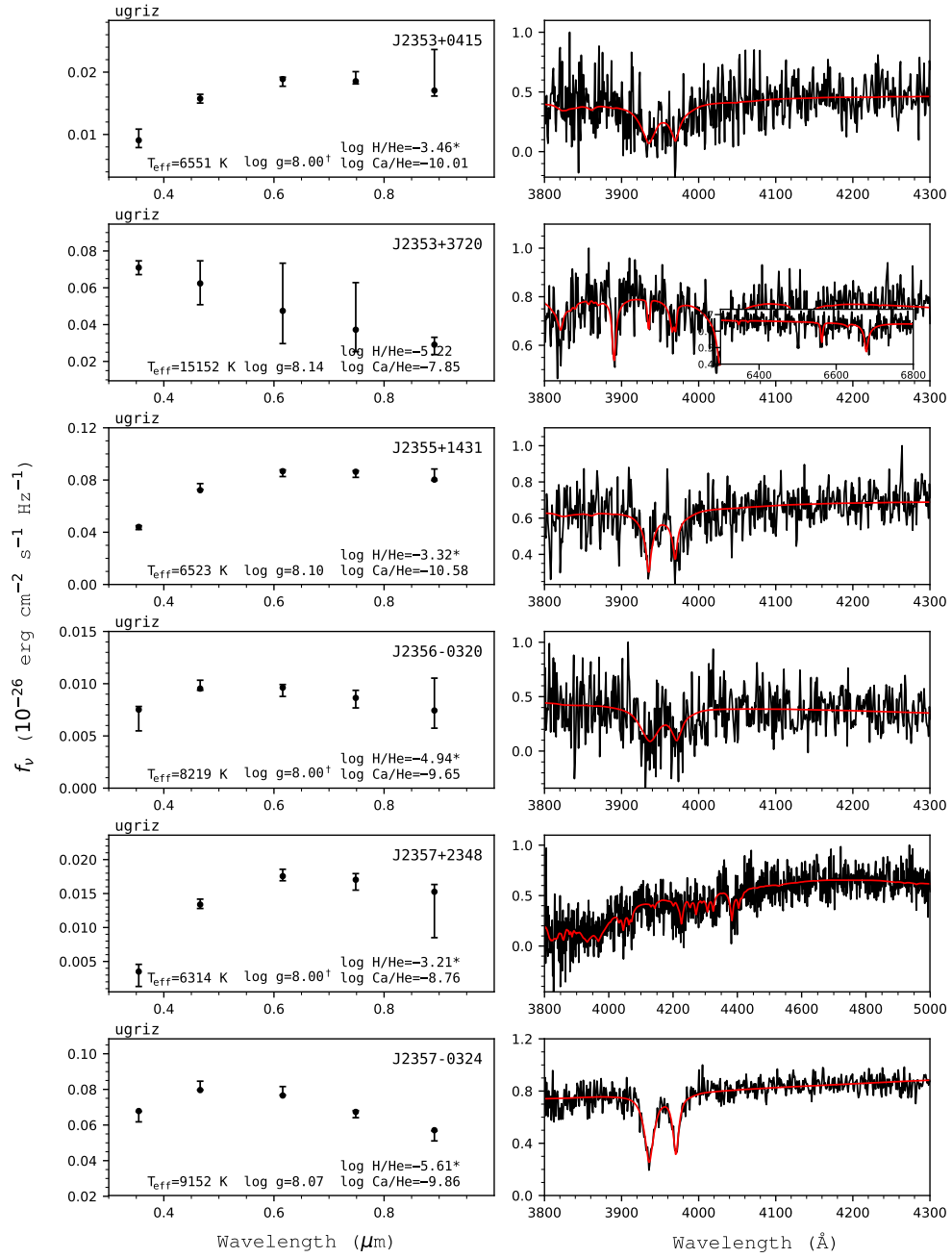


Figure 189. Fits to the DBZ/DZ(A) white dwarfs - continued.

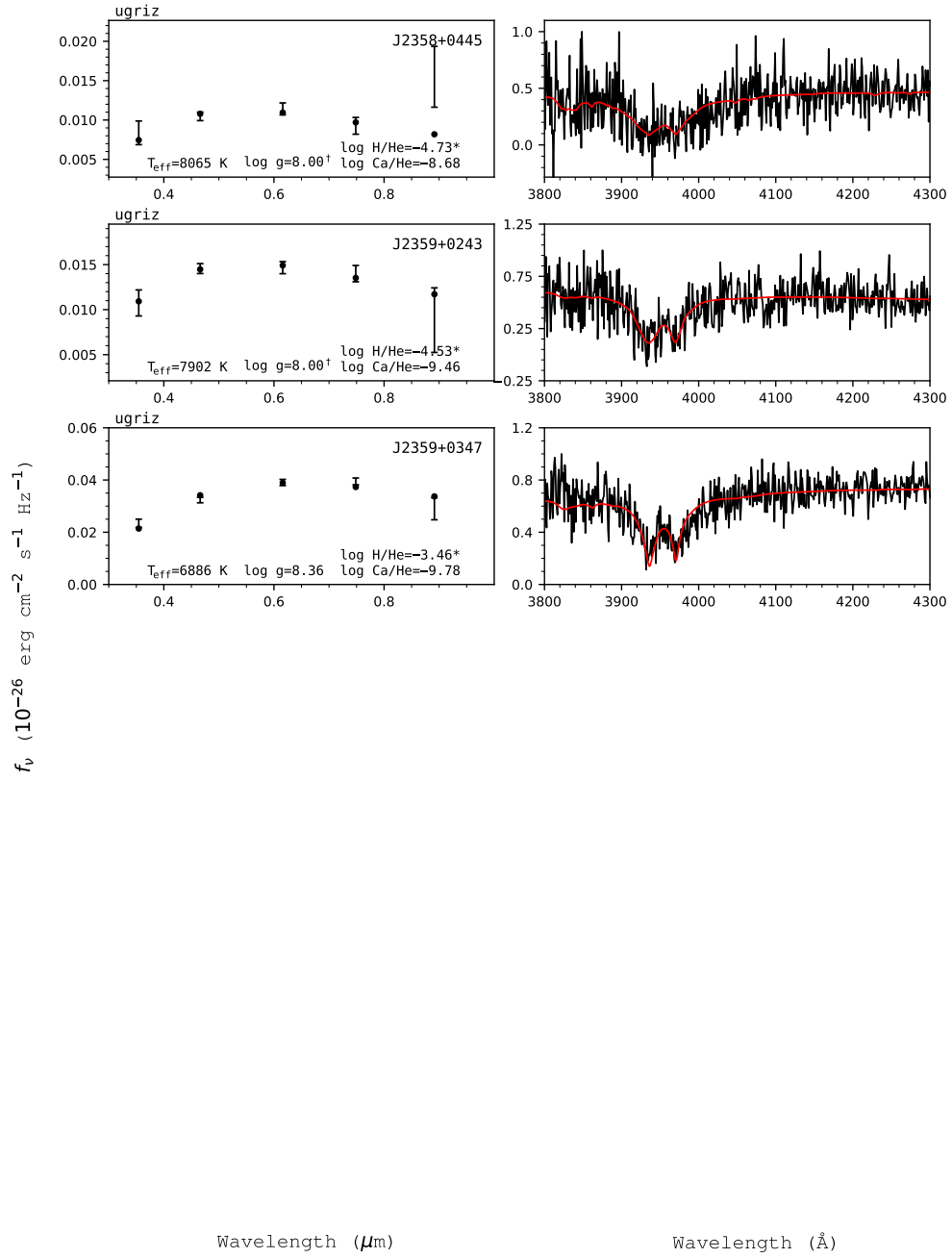


Figure 190. Fits to the DBZ/DZ(A) white dwarfs - continued.

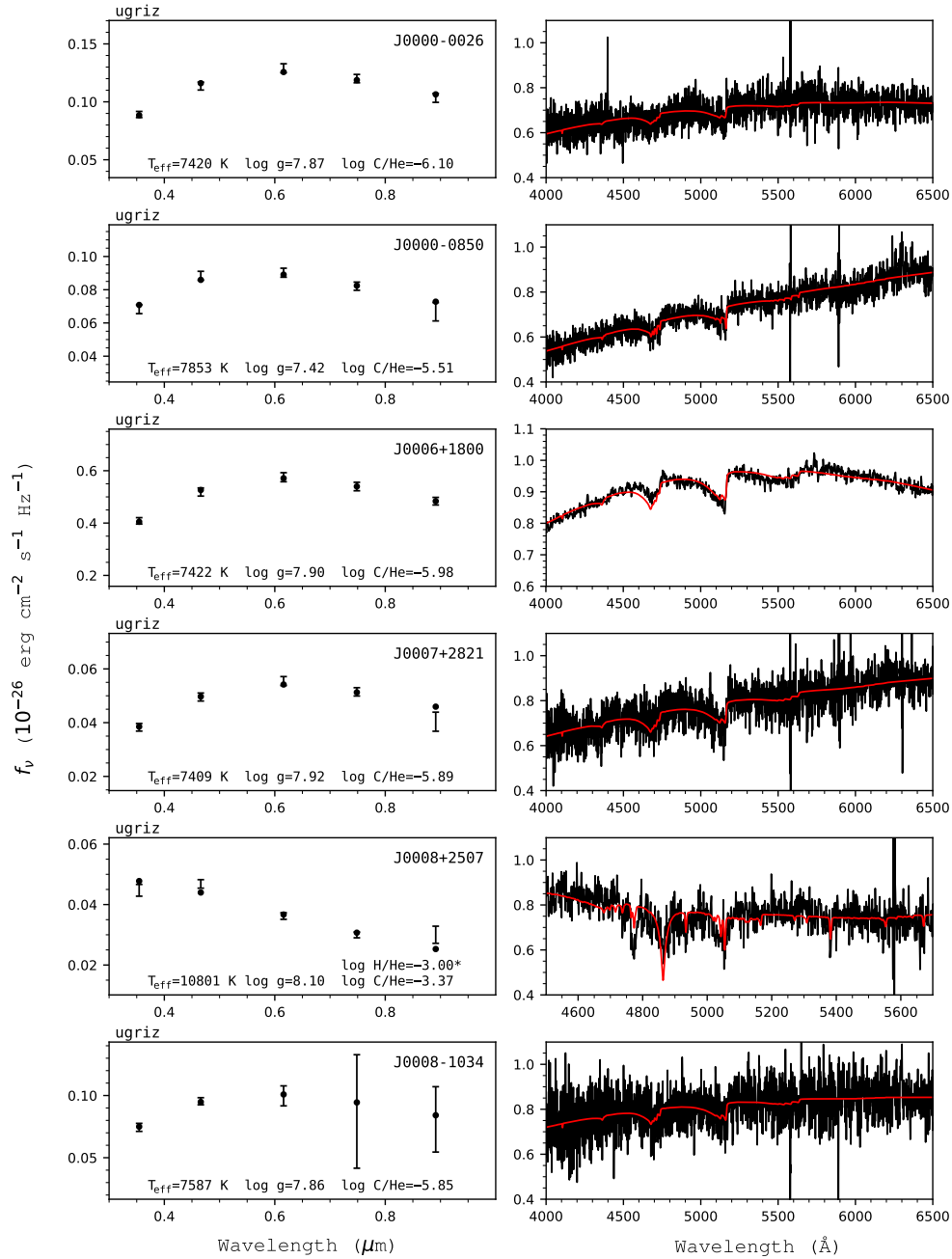


Figure 191. Fits to DQ white dwarfs in our sample. In the left panels, error bars represent the observed data, while filled circles correspond to our best fit model, with the atmospheric parameters given in each panel. The photometry used in the fit is indicated at the top left of each panel. A dagger symbol indicates that the $\log g$ value has been fixed at 8.0, when no trigonometric parallax is available. A star symbol indicates that the value of $\log \text{H/He}$ has been fixed rather than fitted. The right panels show our spectroscopic fits (red) to the normalized observed spectra (black).

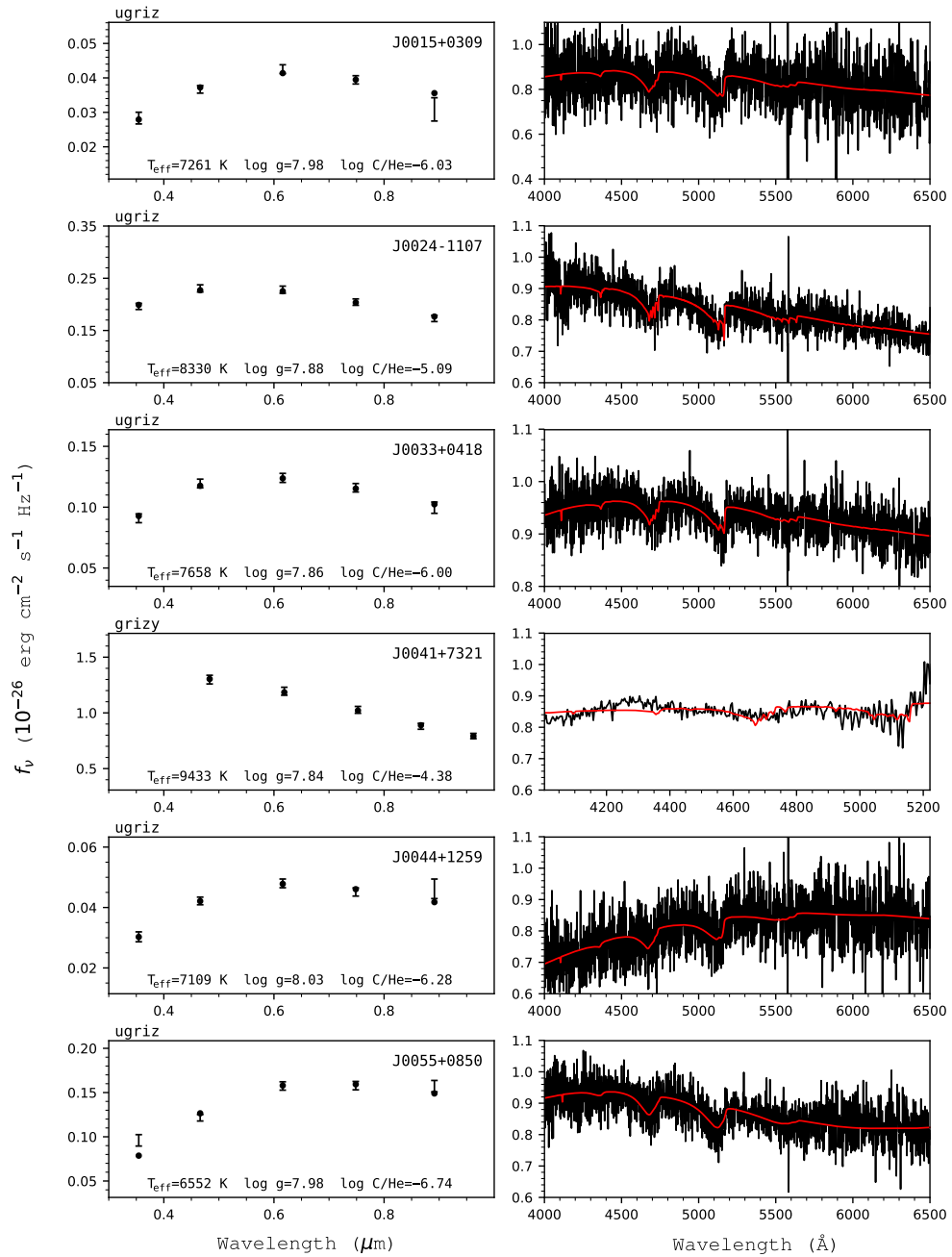


Figure 192. Fits to the DQ white dwarfs - continued.

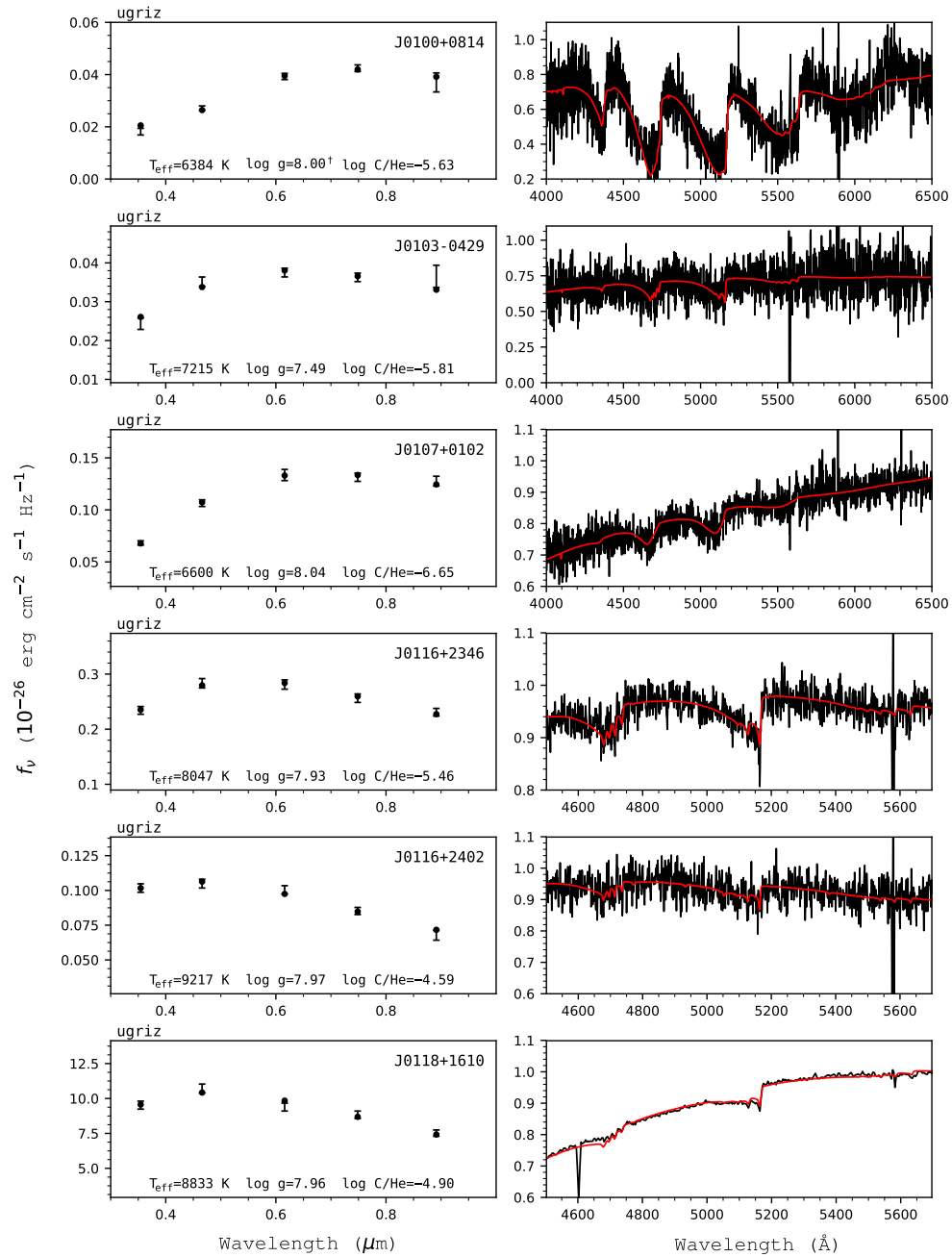


Figure 193. Fits to the DQ white dwarfs - continued.

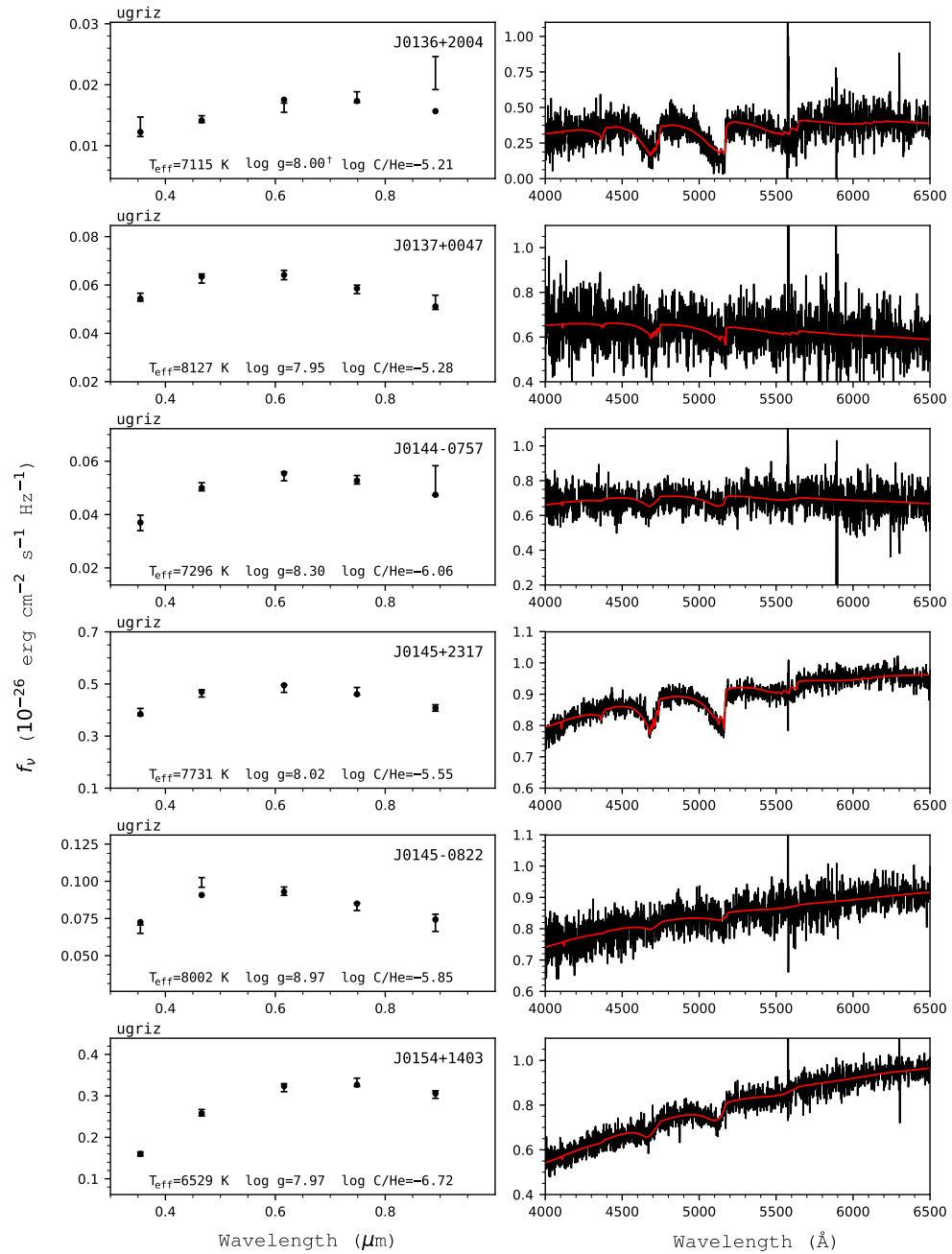


Figure 194. Fits to the DQ white dwarfs - continued.

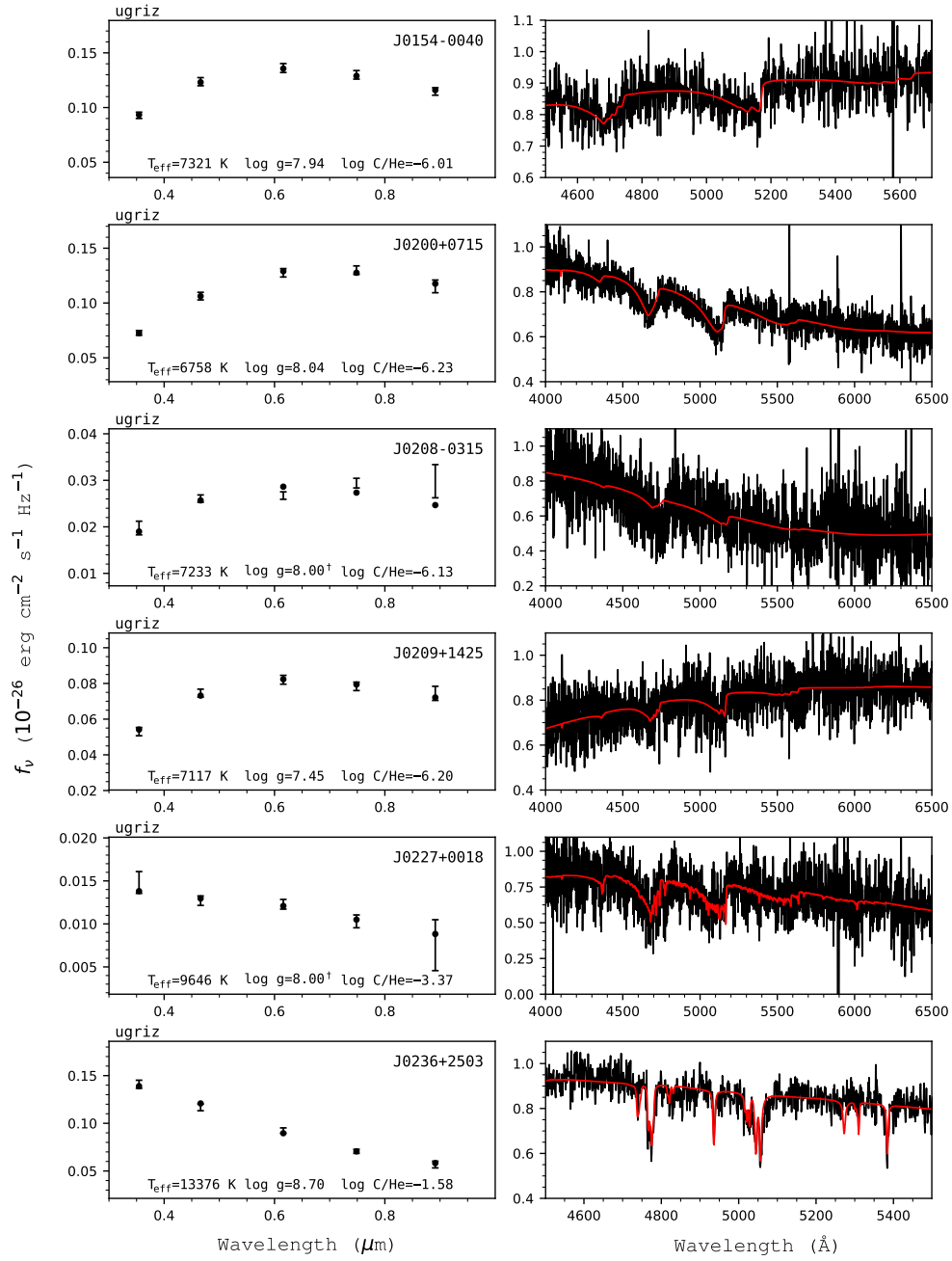


Figure 195. Fits to the DQ white dwarfs - continued.

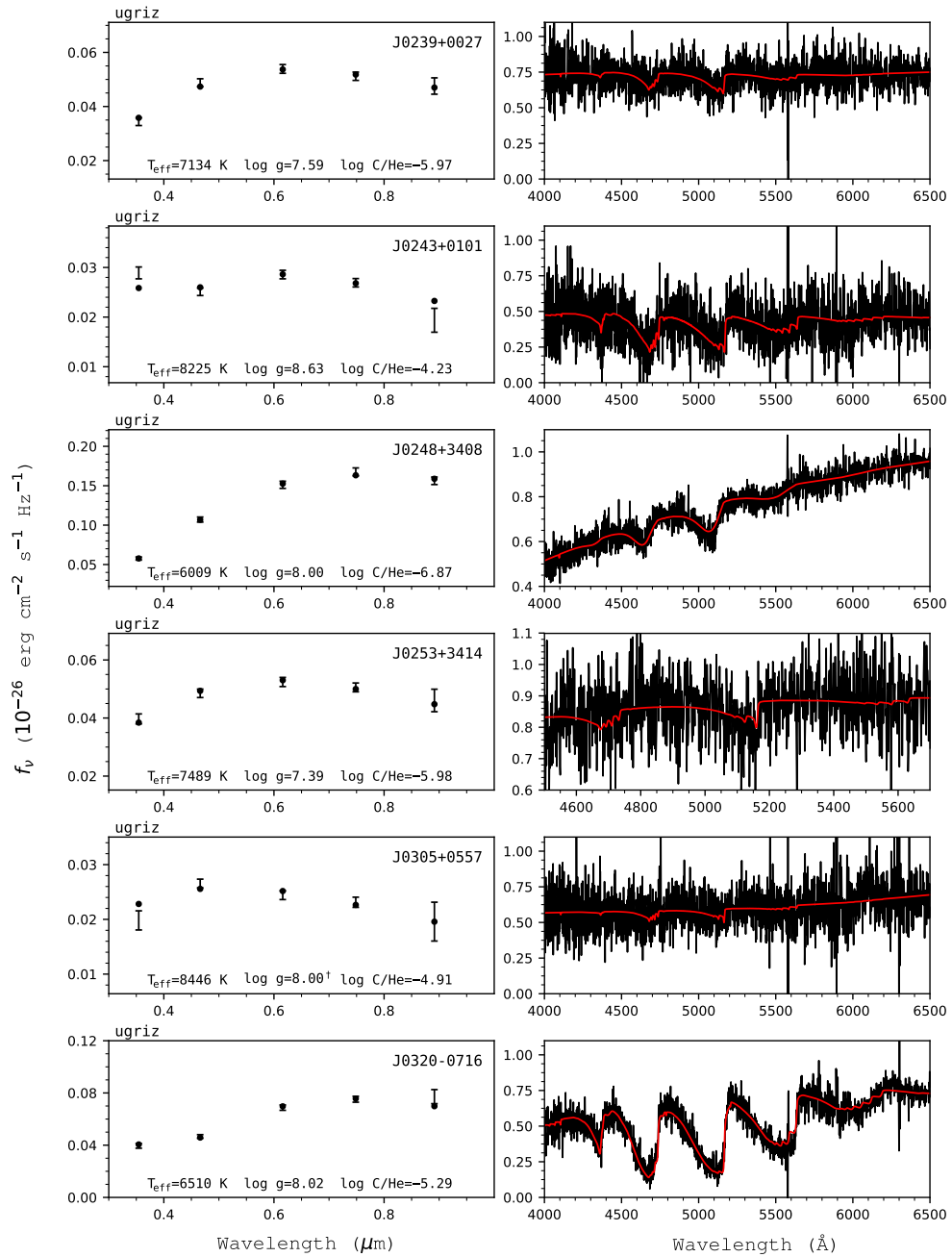


Figure 196. Fits to the DQ white dwarfs - continued.

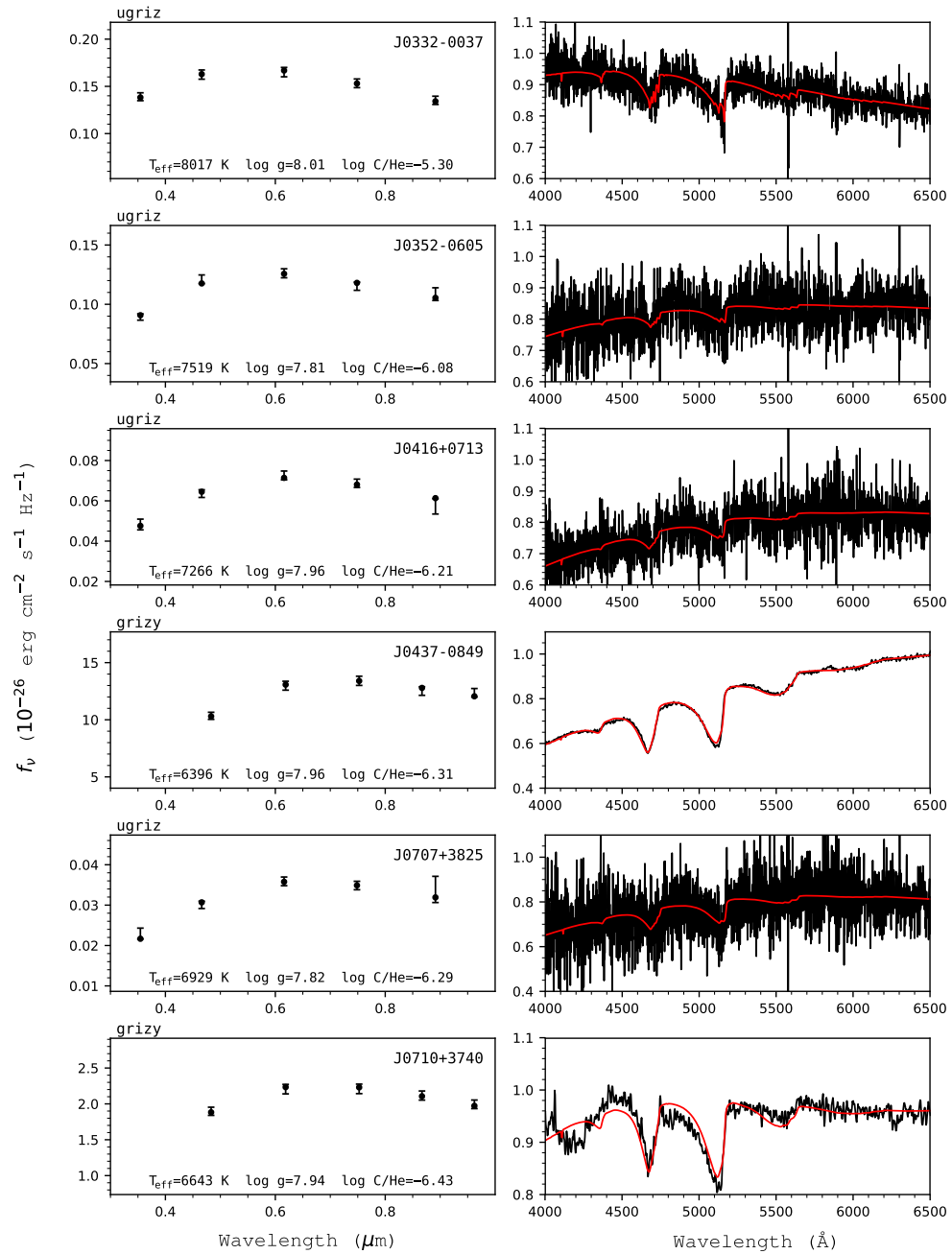


Figure 197. Fits to the DQ white dwarfs - continued.

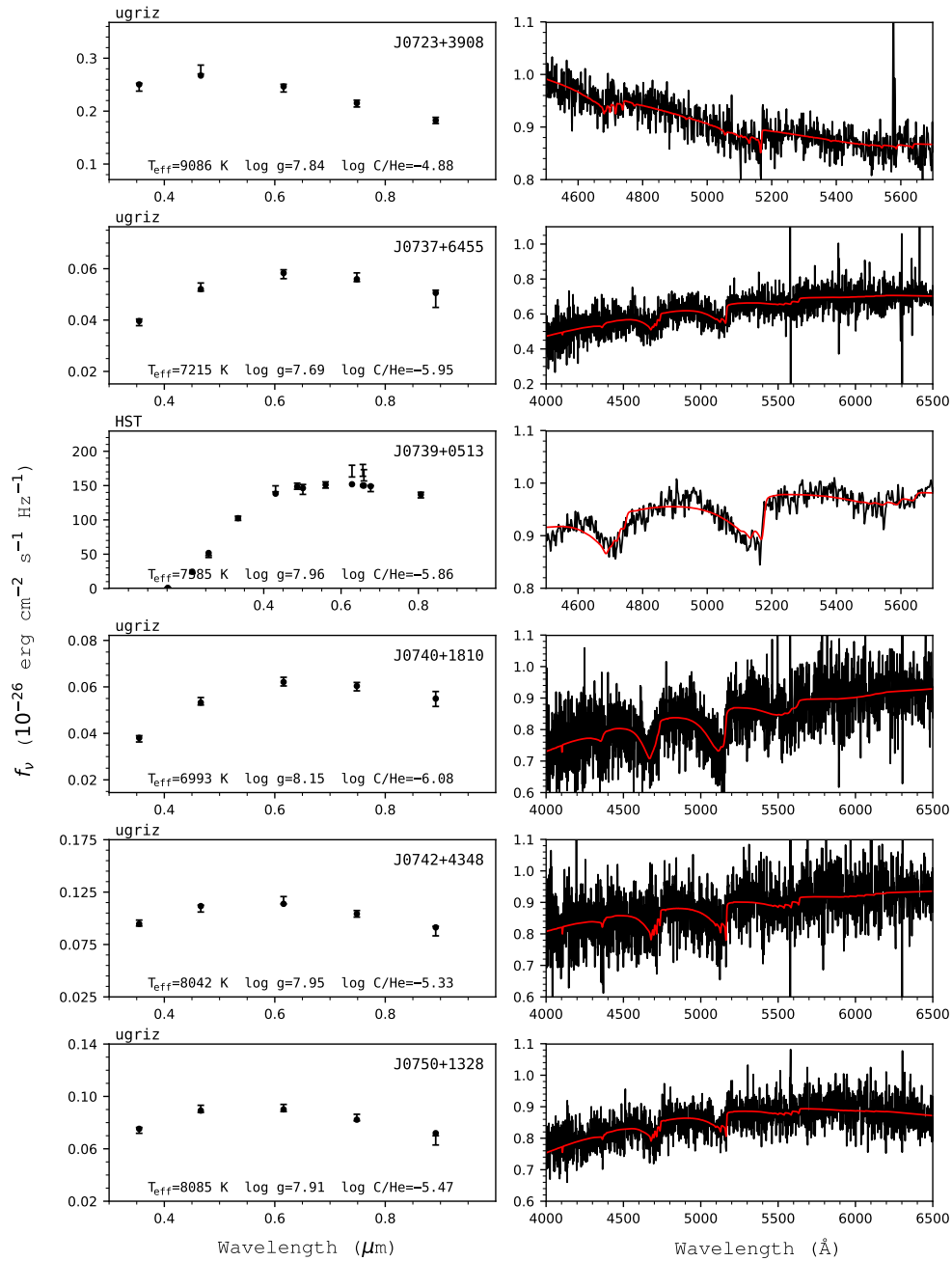


Figure 198. Fits to the DQ white dwarfs - continued.

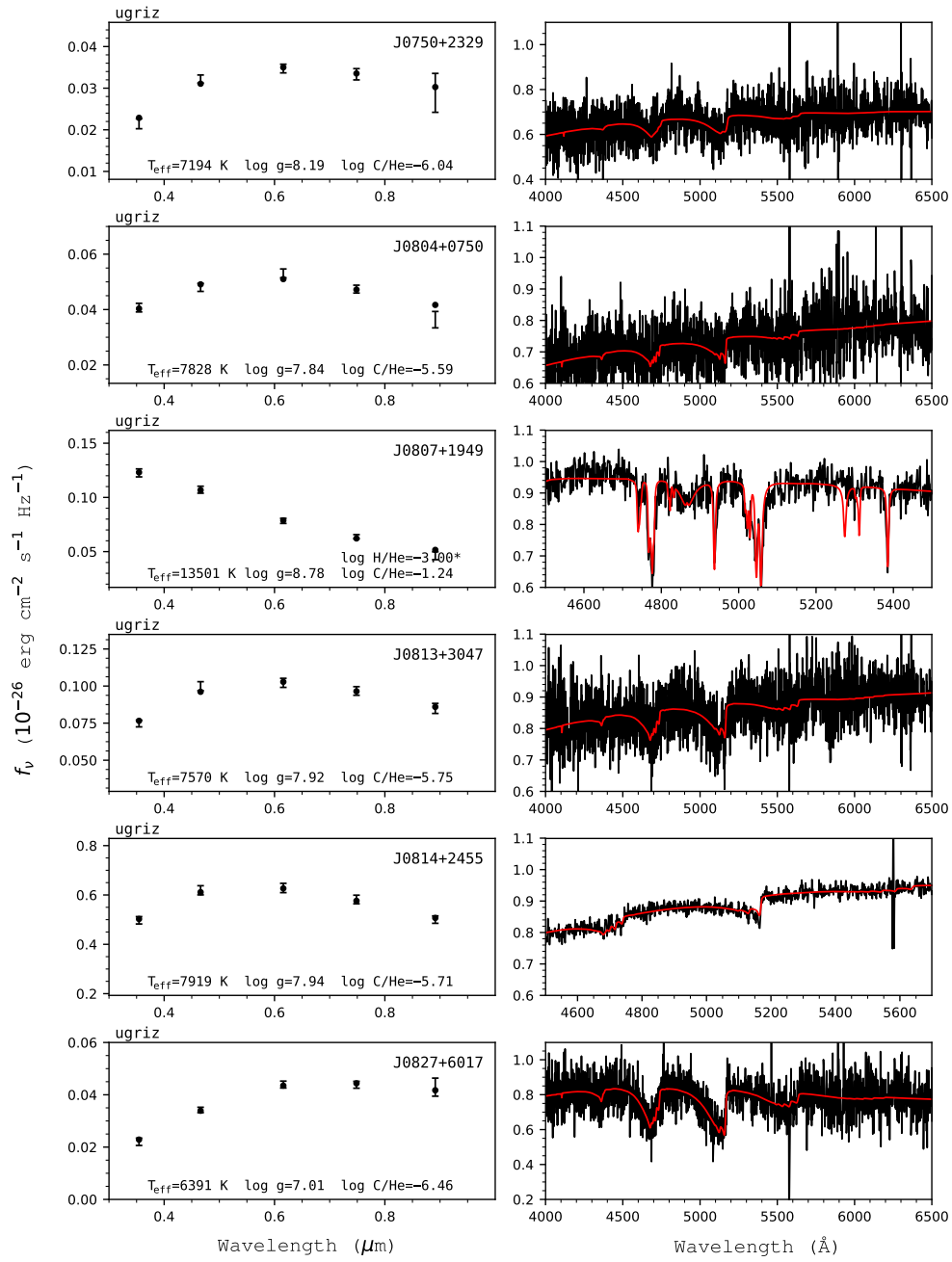


Figure 199. Fits to the DQ white dwarfs - continued.

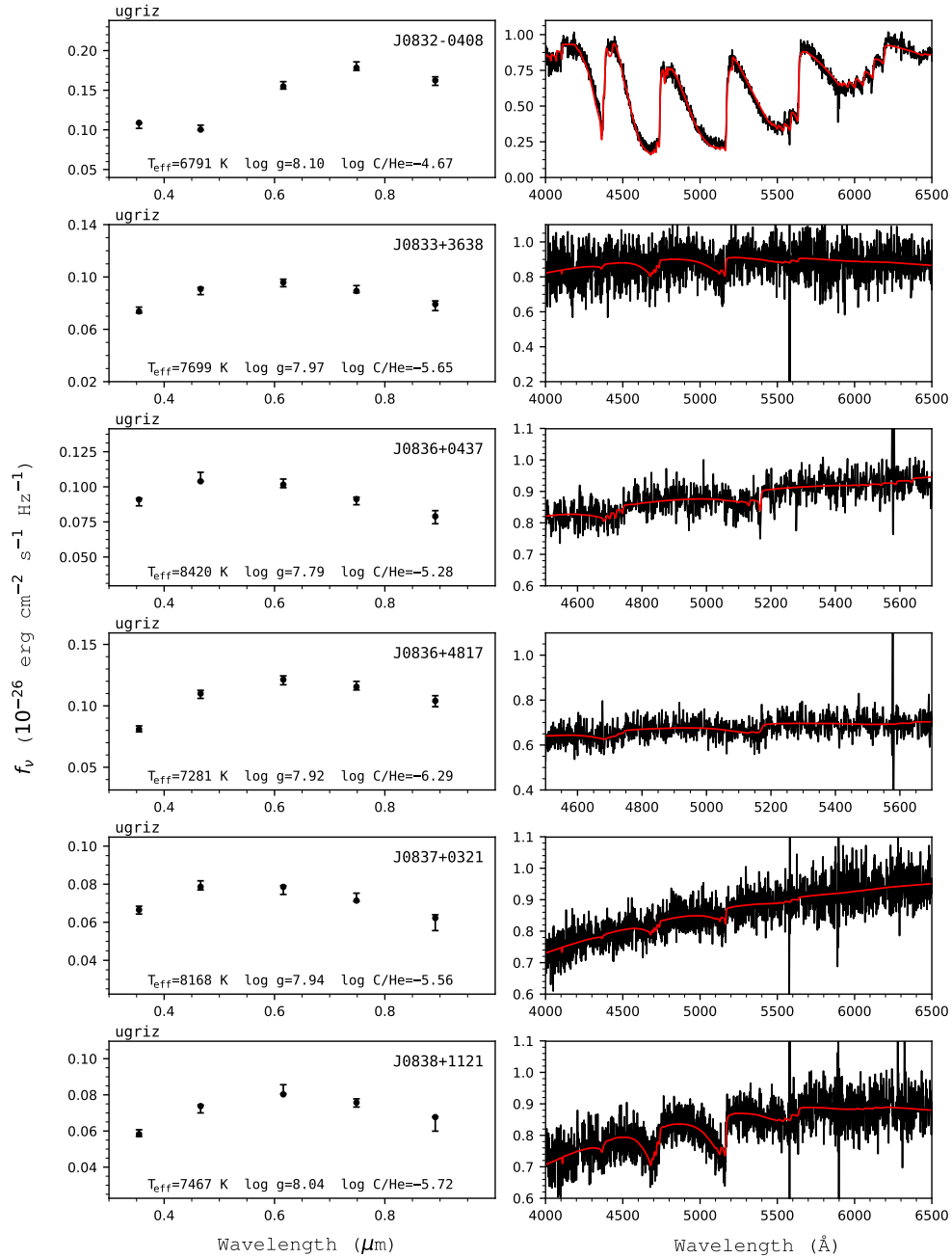


Figure 200. Fits to the DQ white dwarfs - continued.

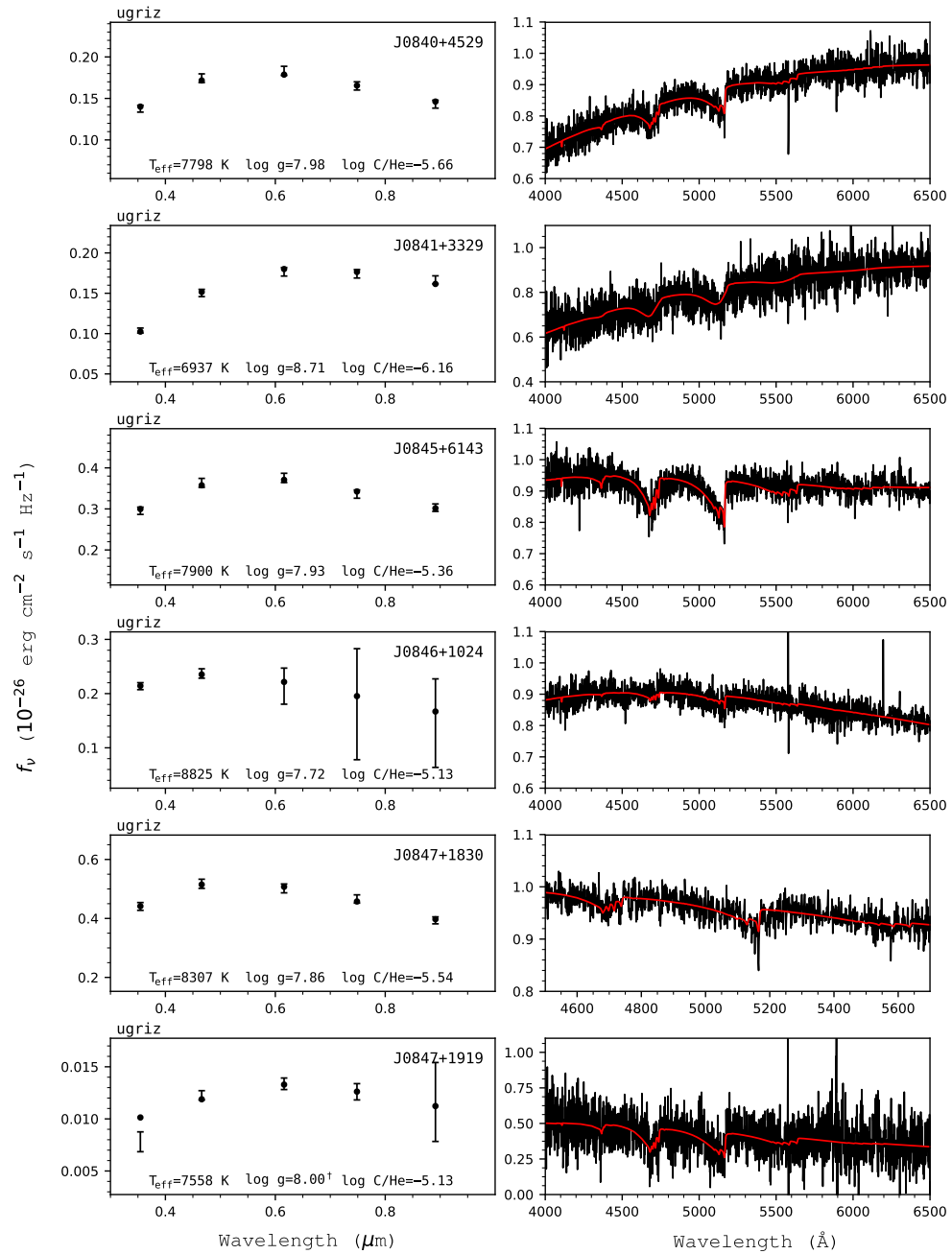


Figure 201. Fits to the DQ white dwarfs - continued.

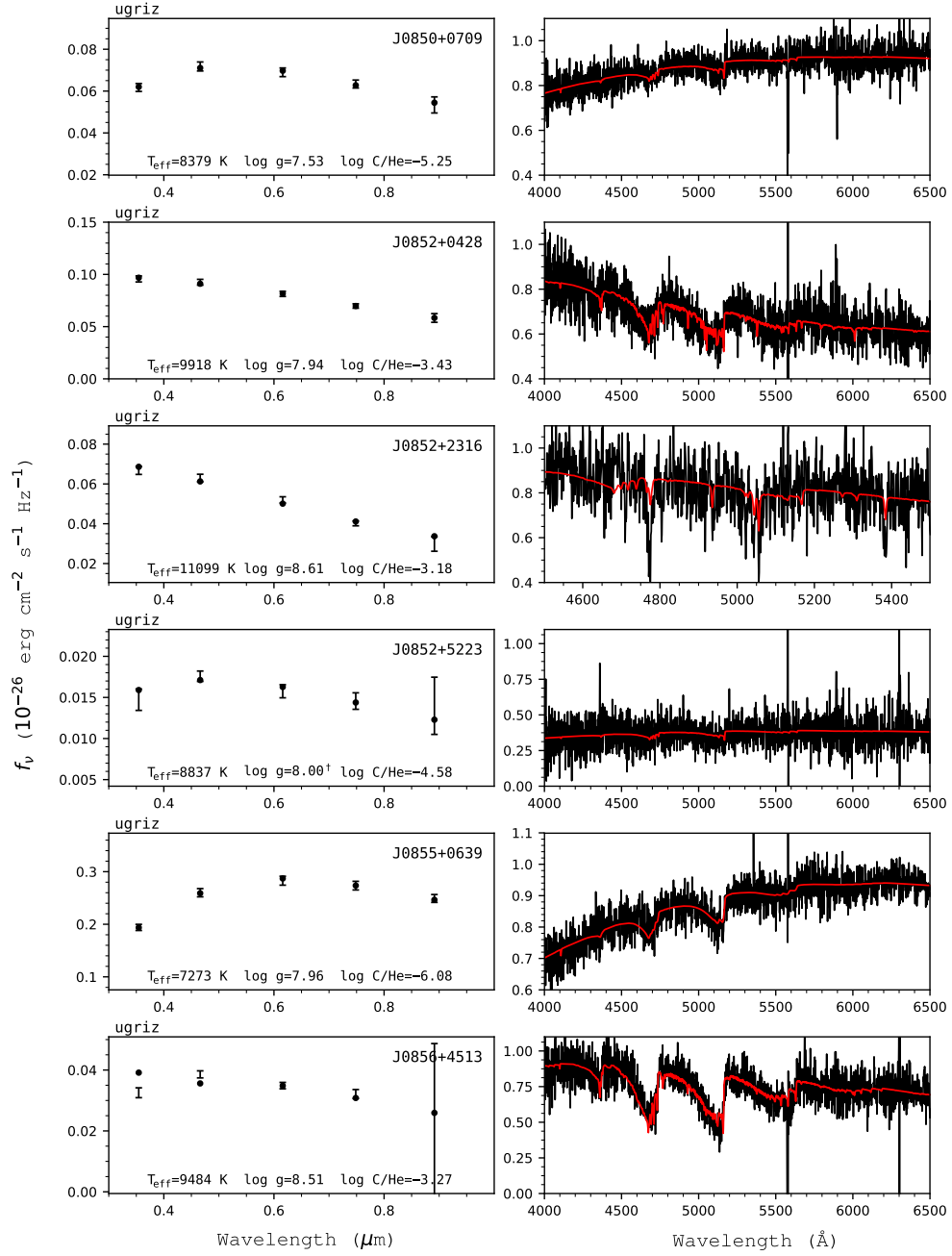


Figure 202. Fits to the DQ white dwarfs - continued.

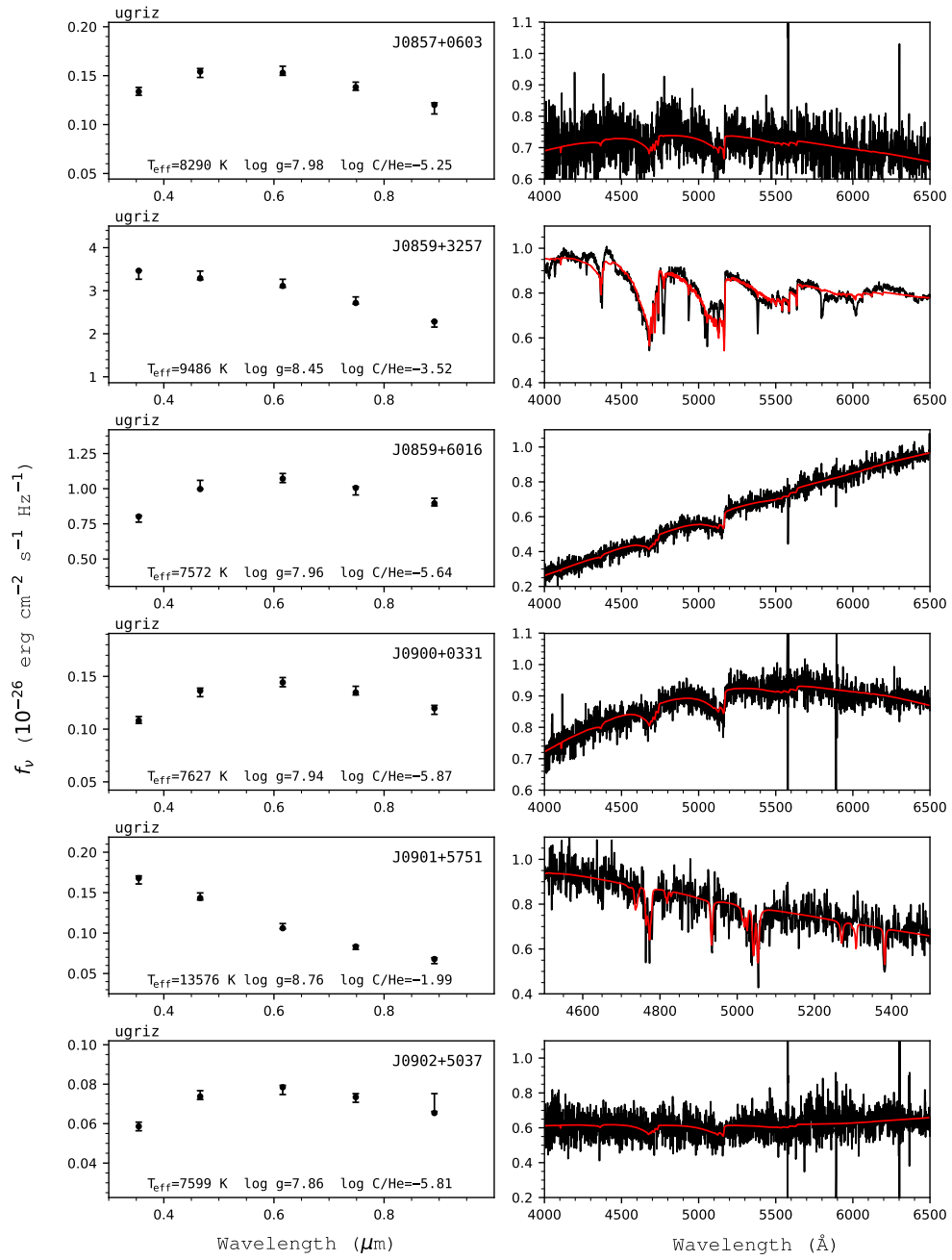


Figure 203. Fits to the DQ white dwarfs - continued.

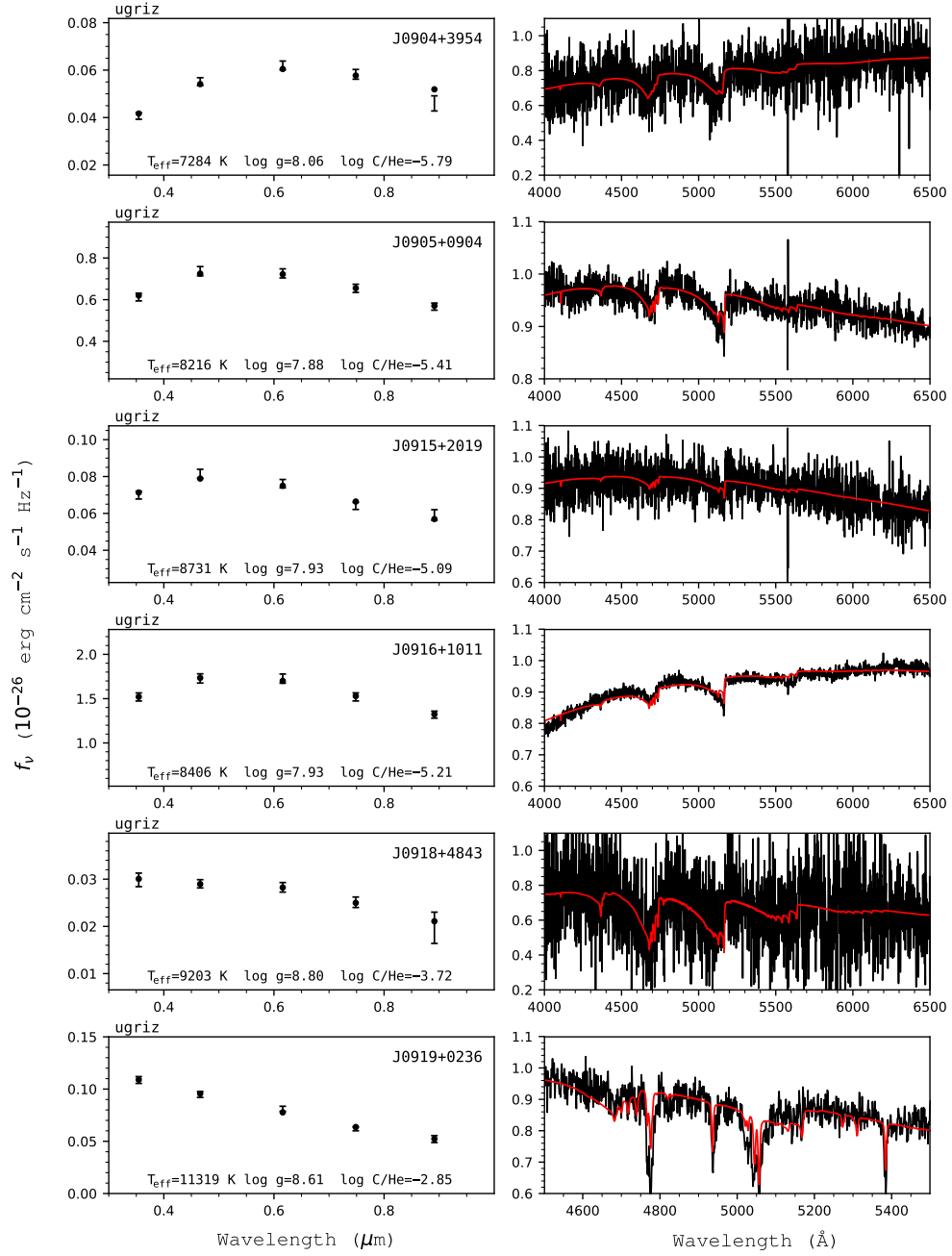


Figure 204. Fits to the DQ white dwarfs - continued.

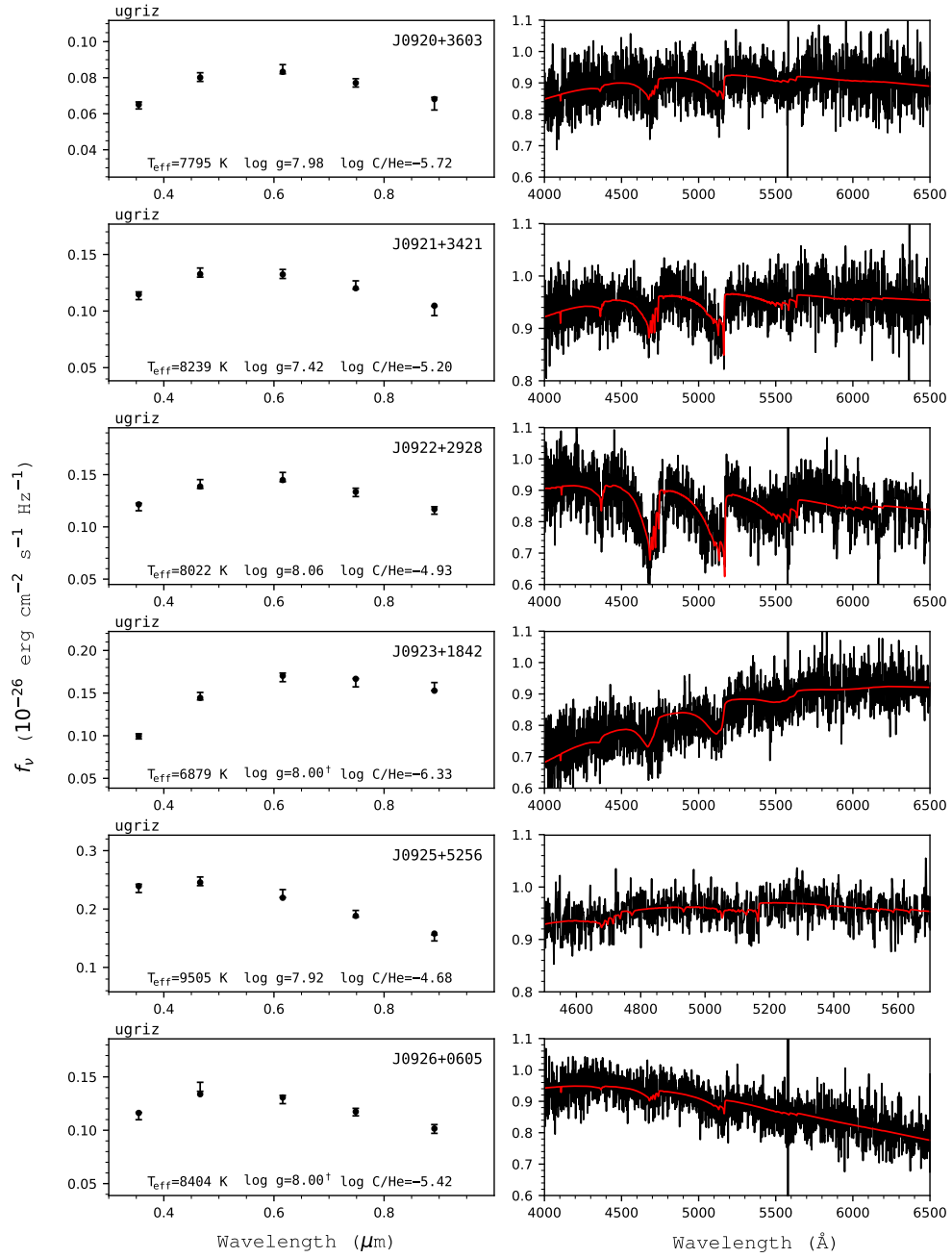


Figure 205. Fits to the DQ white dwarfs - continued.

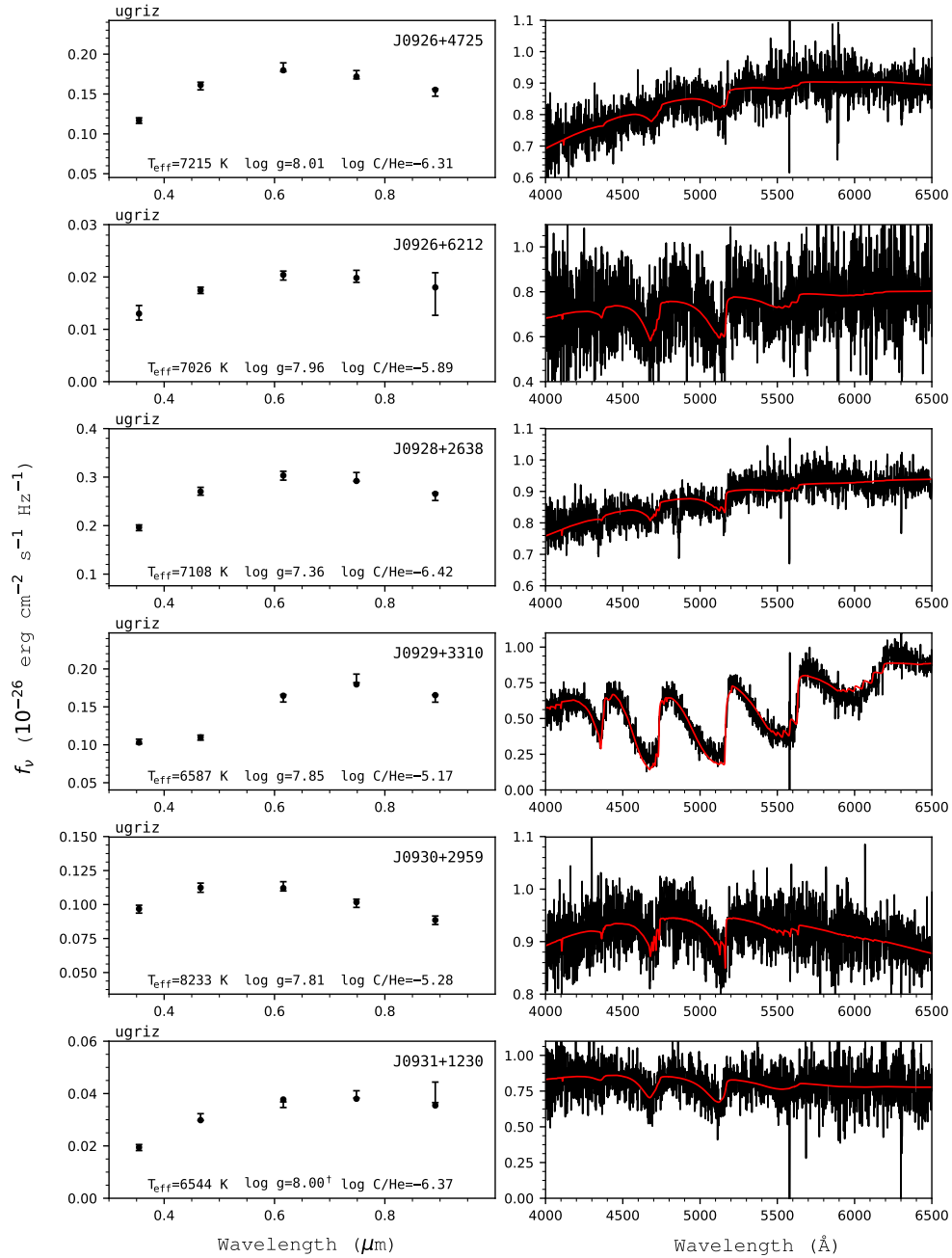


Figure 206. Fits to the DQ white dwarfs - continued.

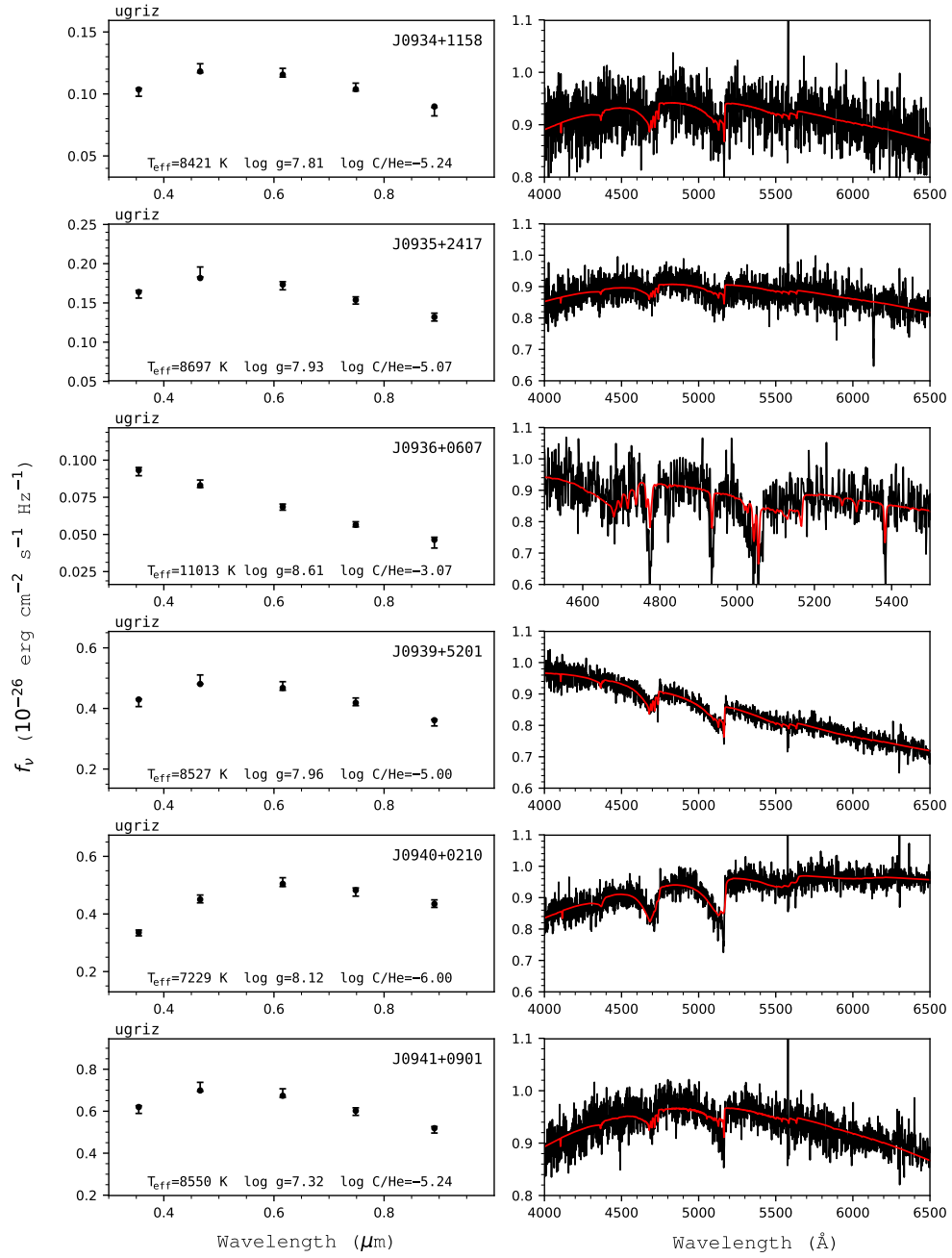


Figure 207. Fits to the DQ white dwarfs - continued.

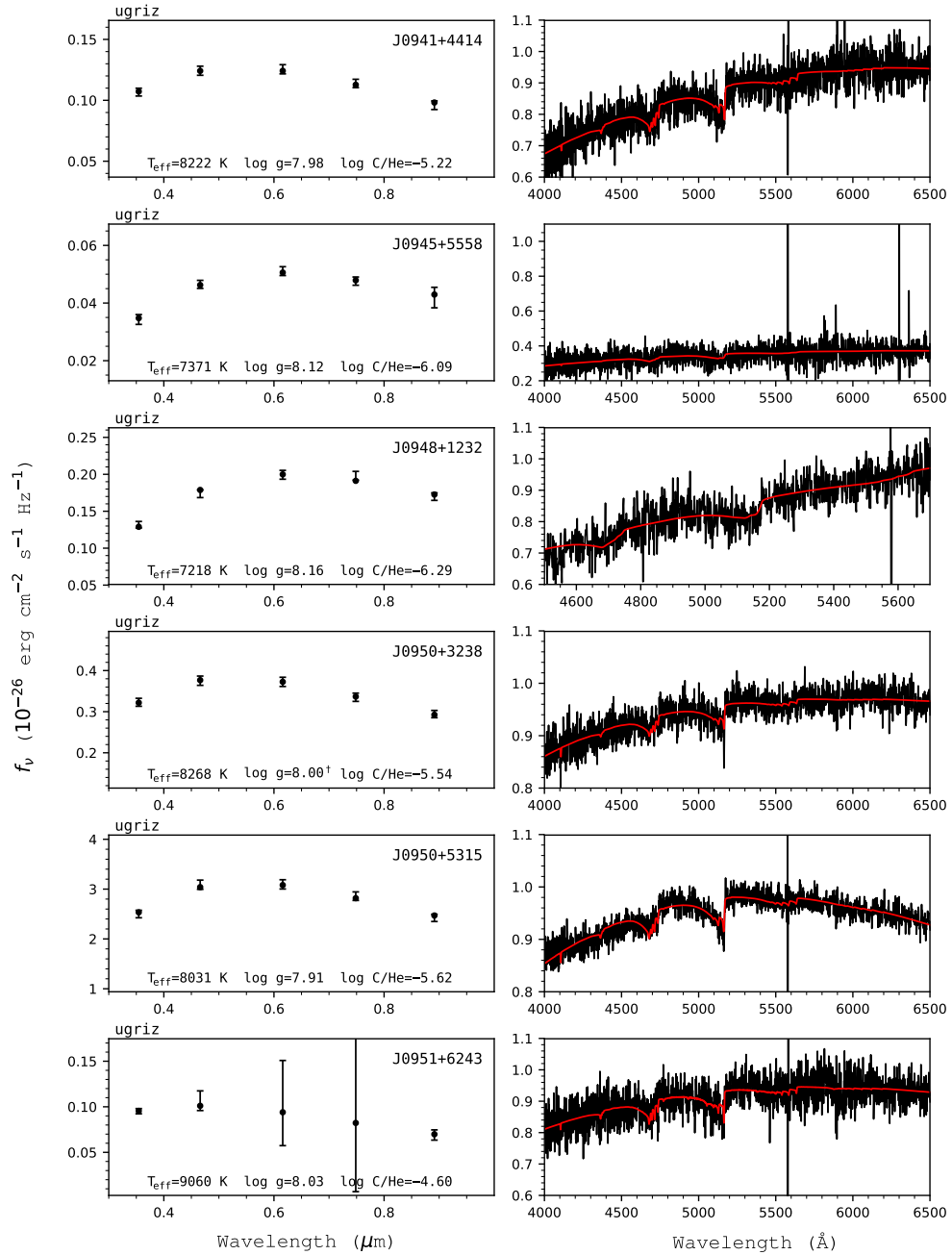


Figure 208. Fits to the DQ white dwarfs - continued.

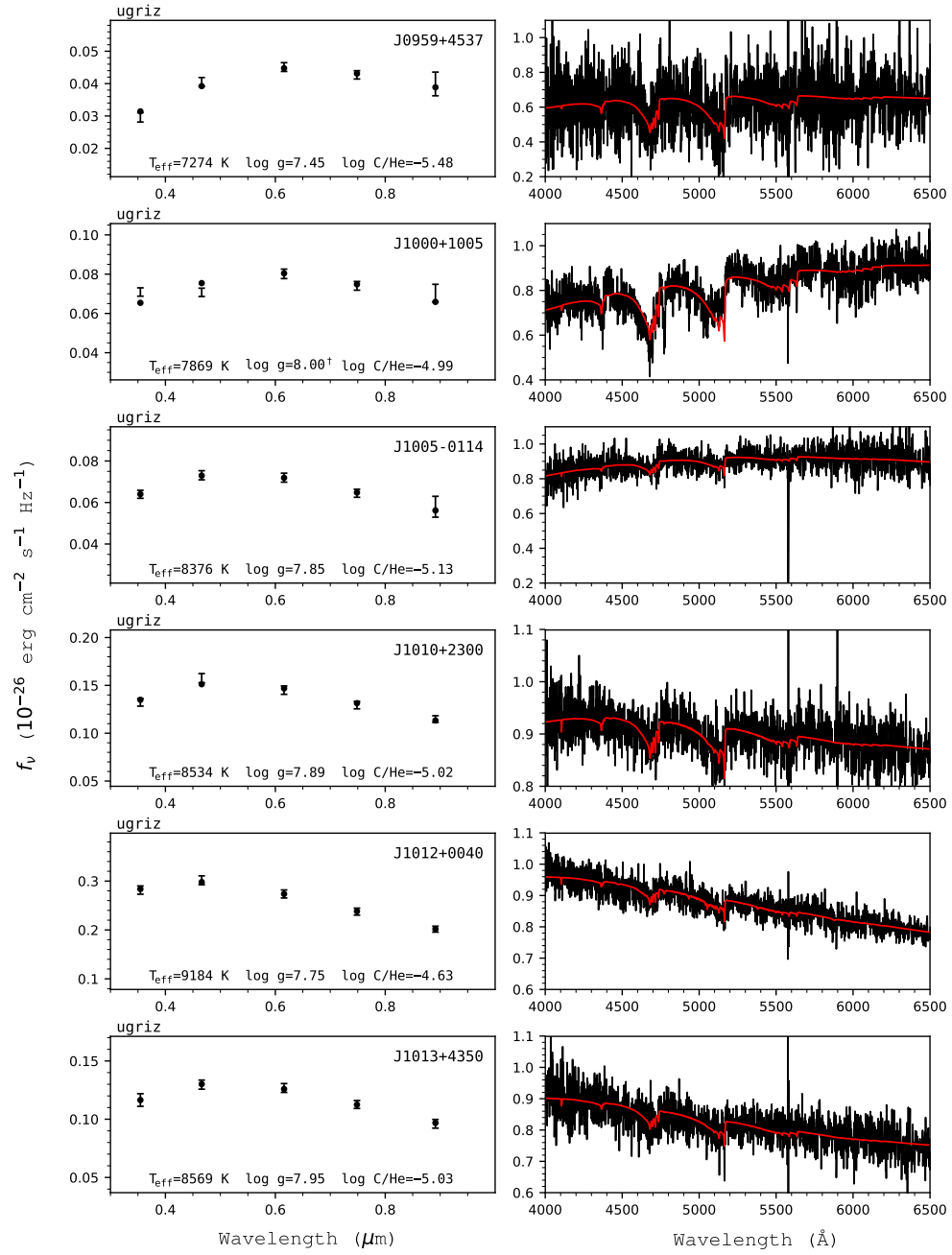


Figure 209. Fits to the DQ white dwarfs - continued.

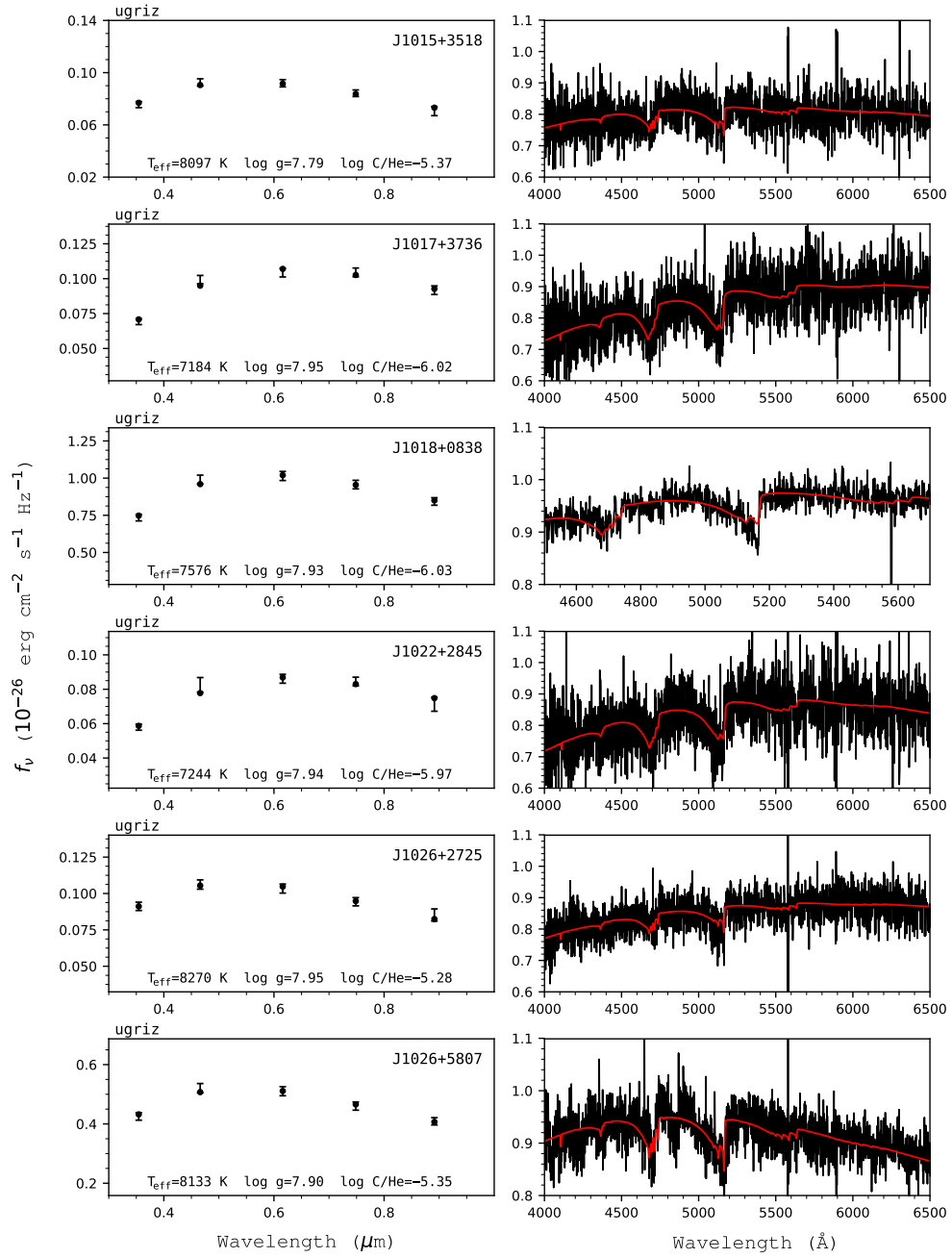


Figure 210. Fits to the DQ white dwarfs - continued.

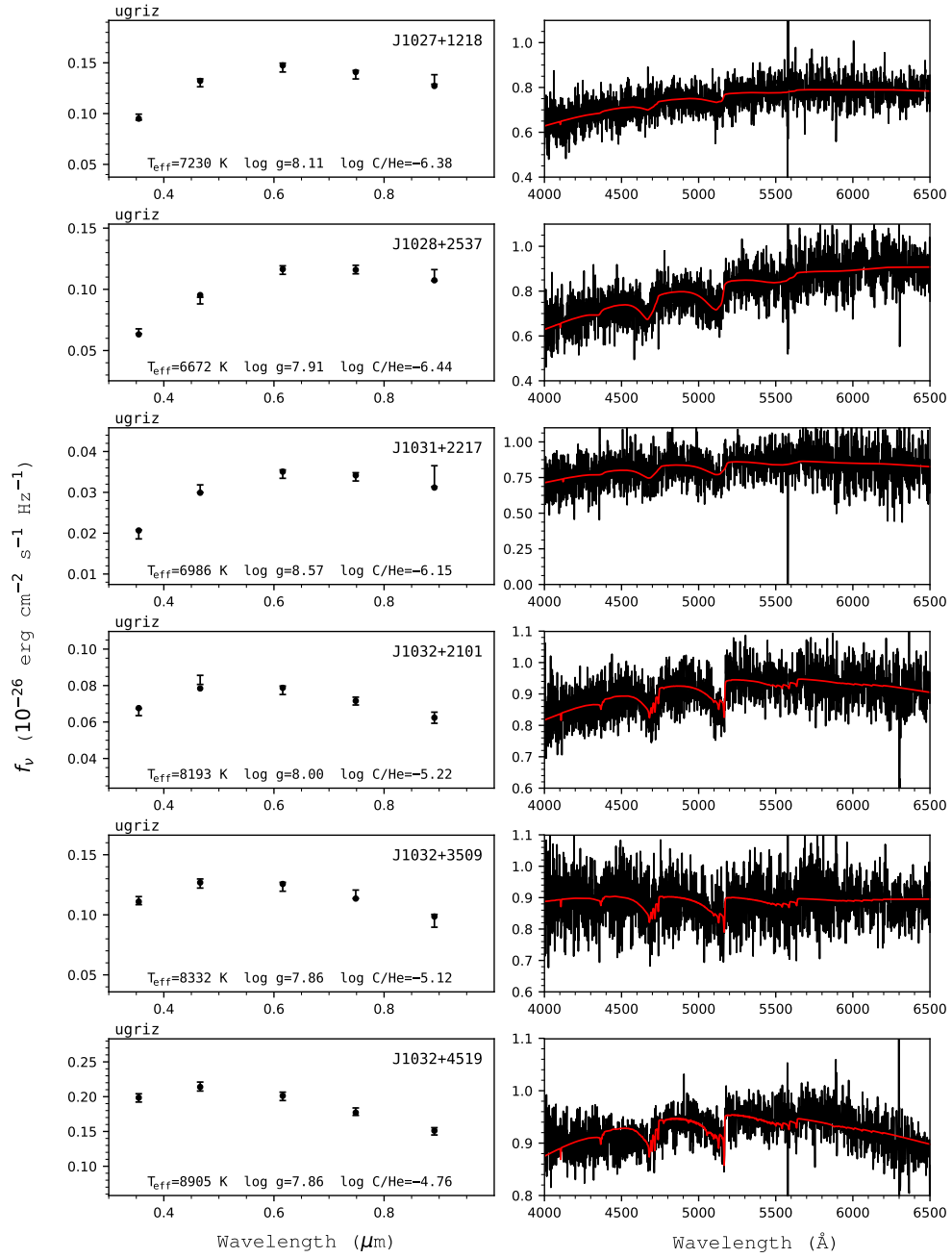


Figure 211. Fits to the DQ white dwarfs - continued.

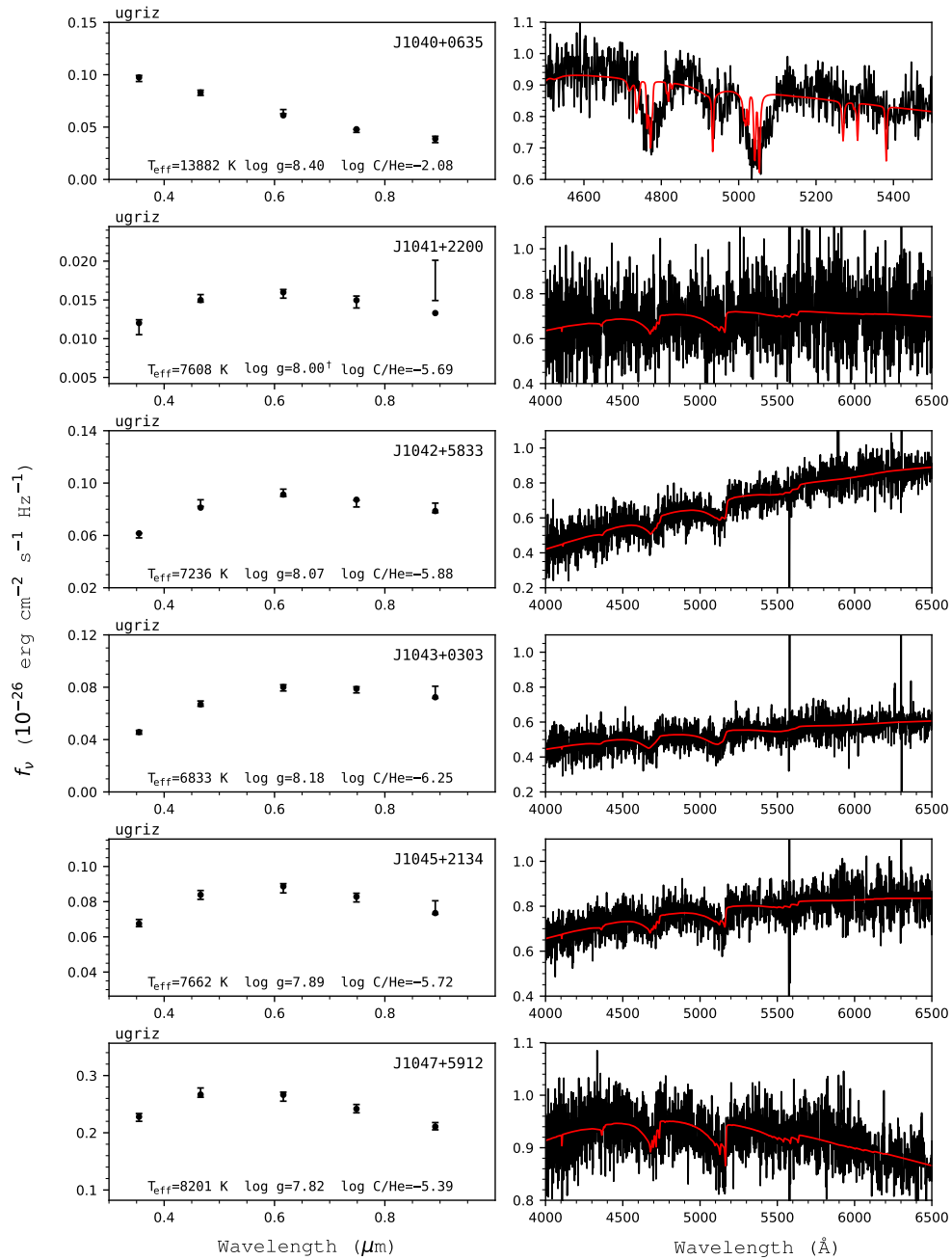


Figure 212. Fits to the DQ white dwarfs - continued.

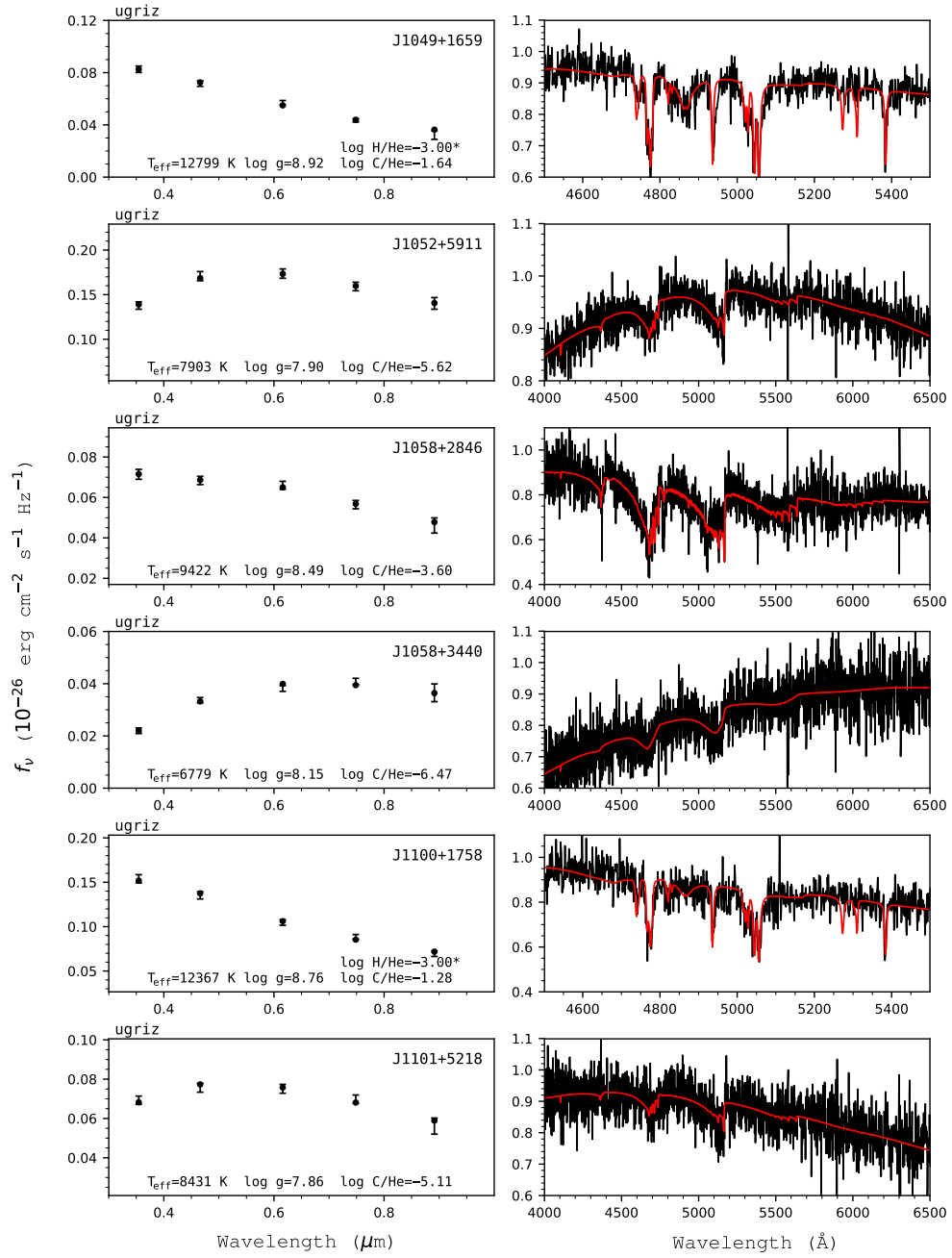


Figure 213. Fits to the DQ white dwarfs - continued.

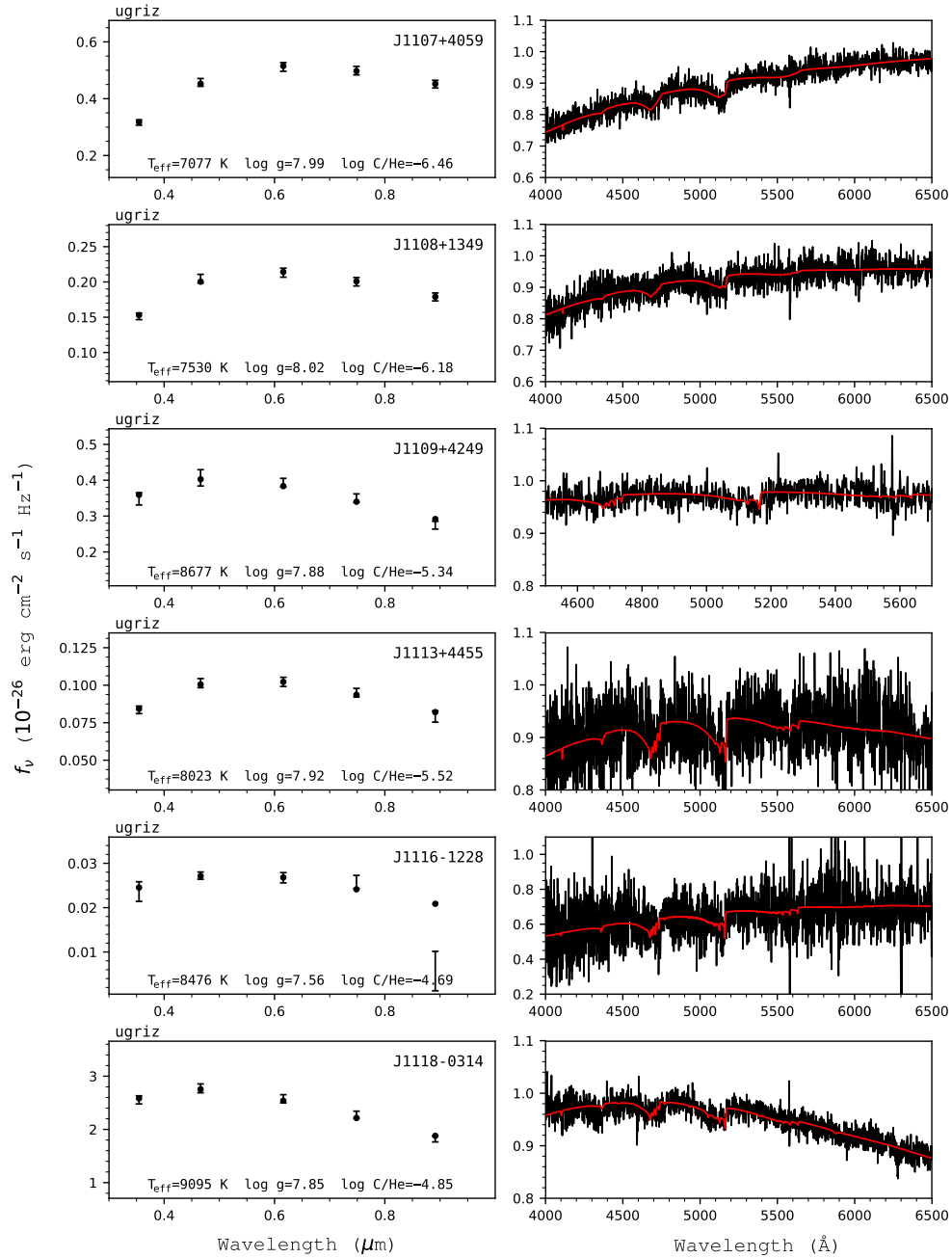


Figure 214. Fits to the DQ white dwarfs - continued.

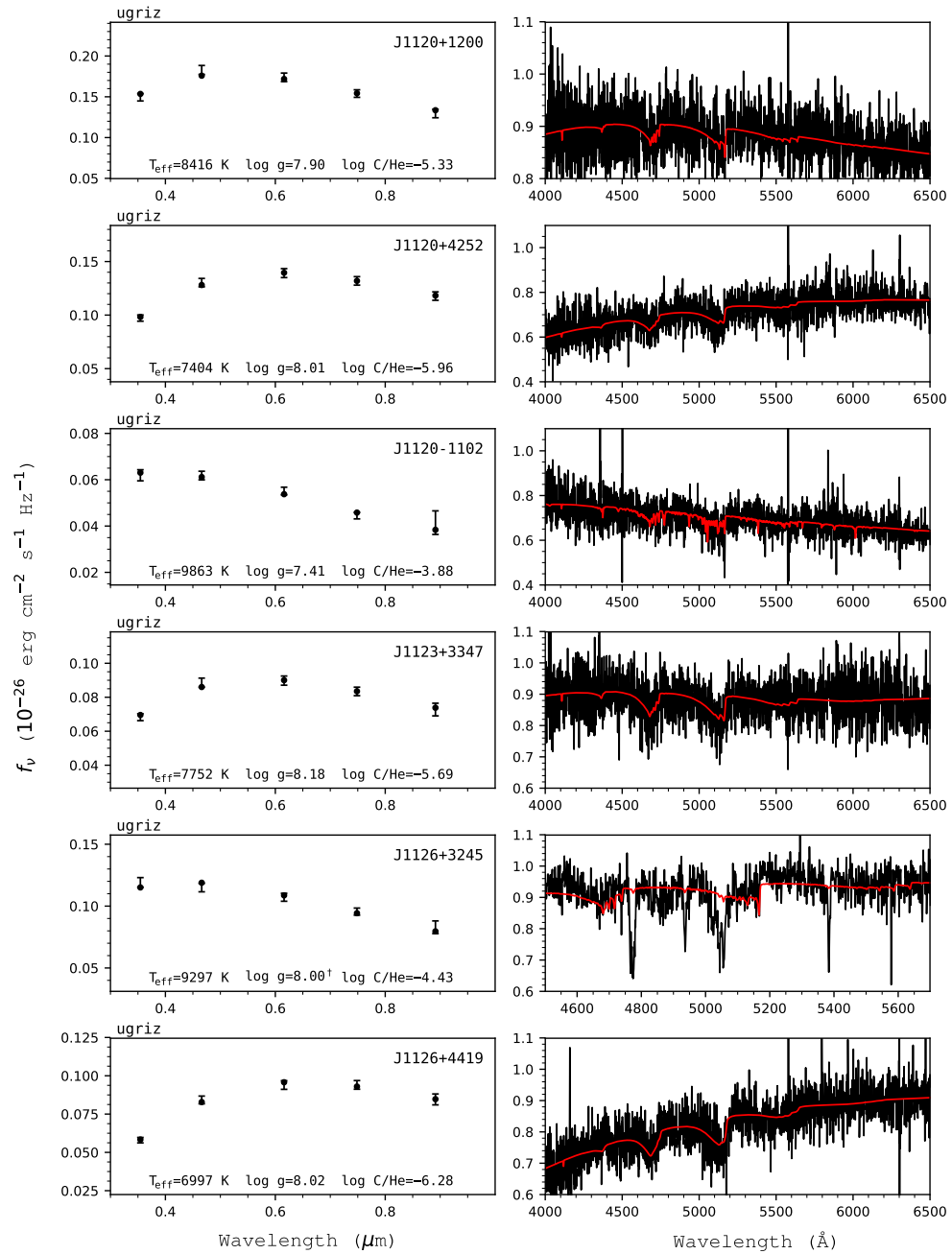


Figure 215. Fits to the DQ white dwarfs - continued.

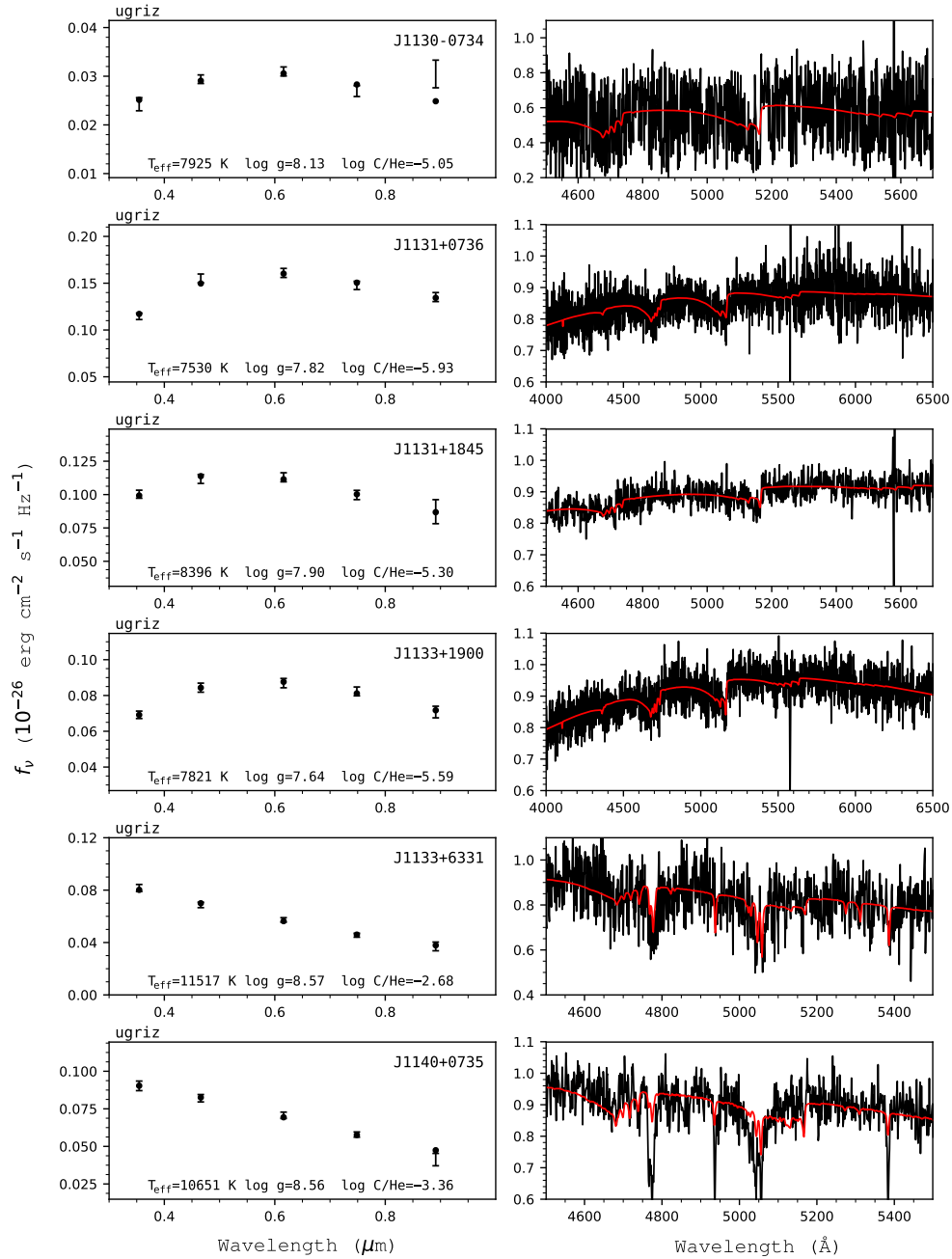


Figure 216. Fits to the DQ white dwarfs - continued.

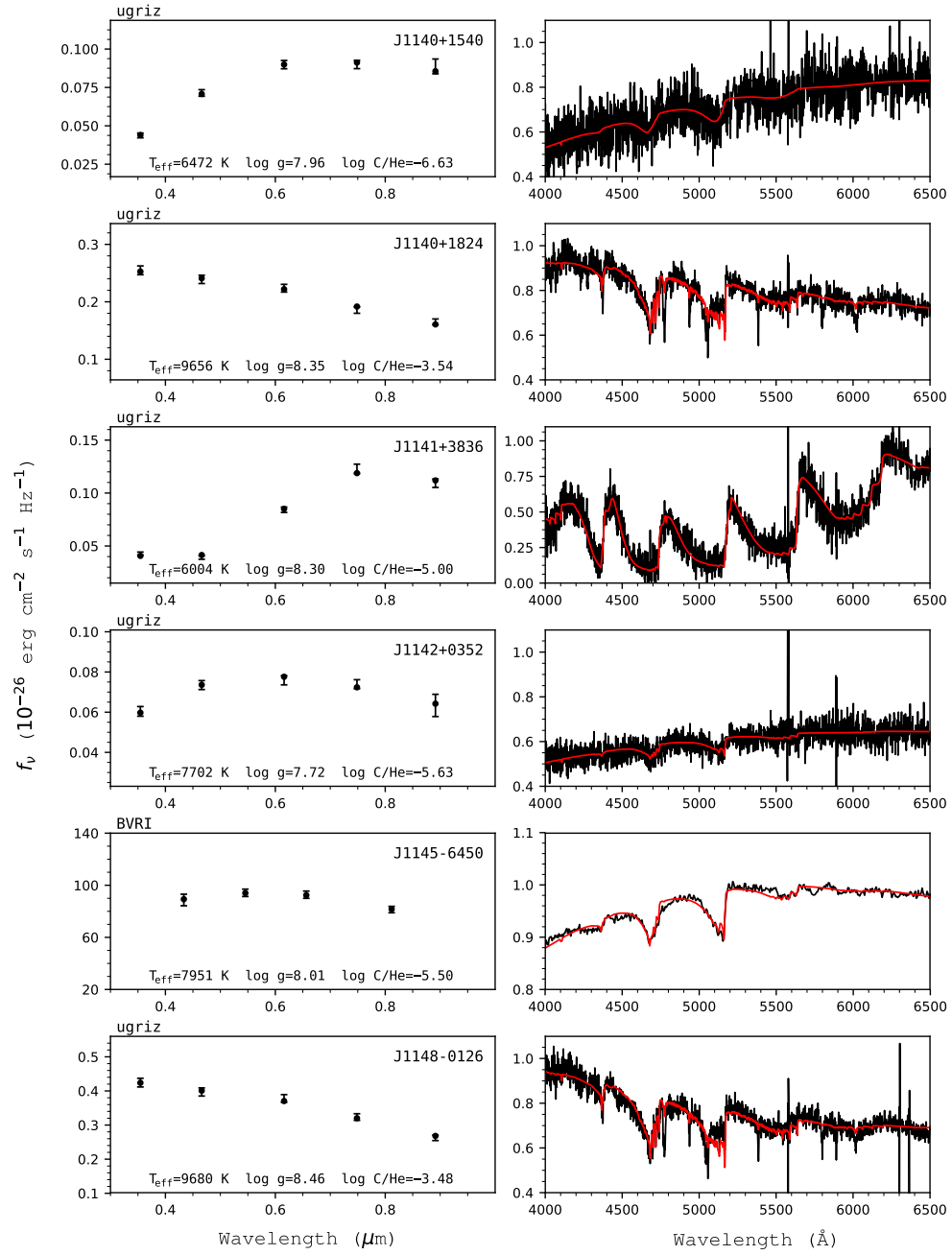


Figure 217. Fits to the DQ white dwarfs - continued.

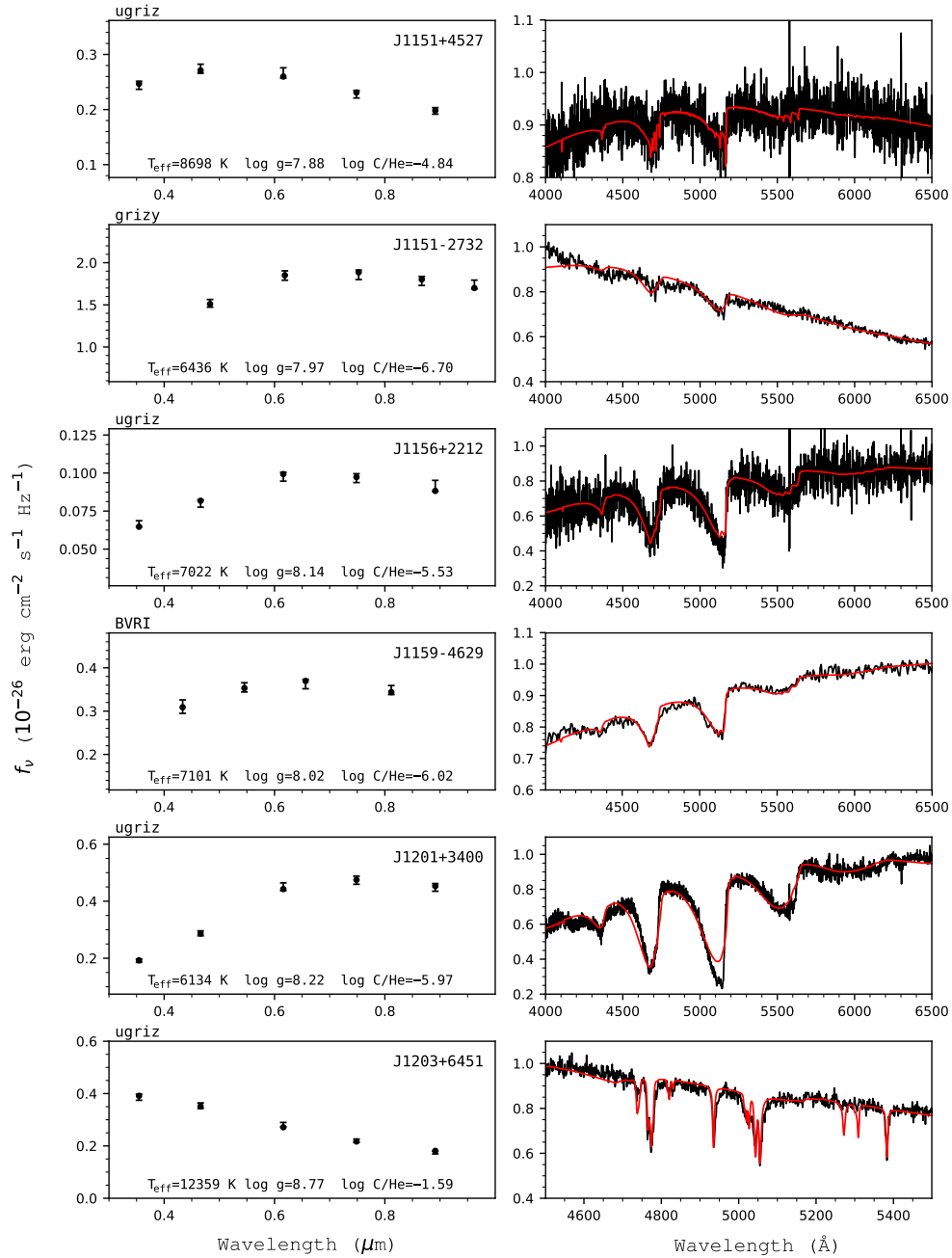


Figure 218. Fits to the DQ white dwarfs - continued.

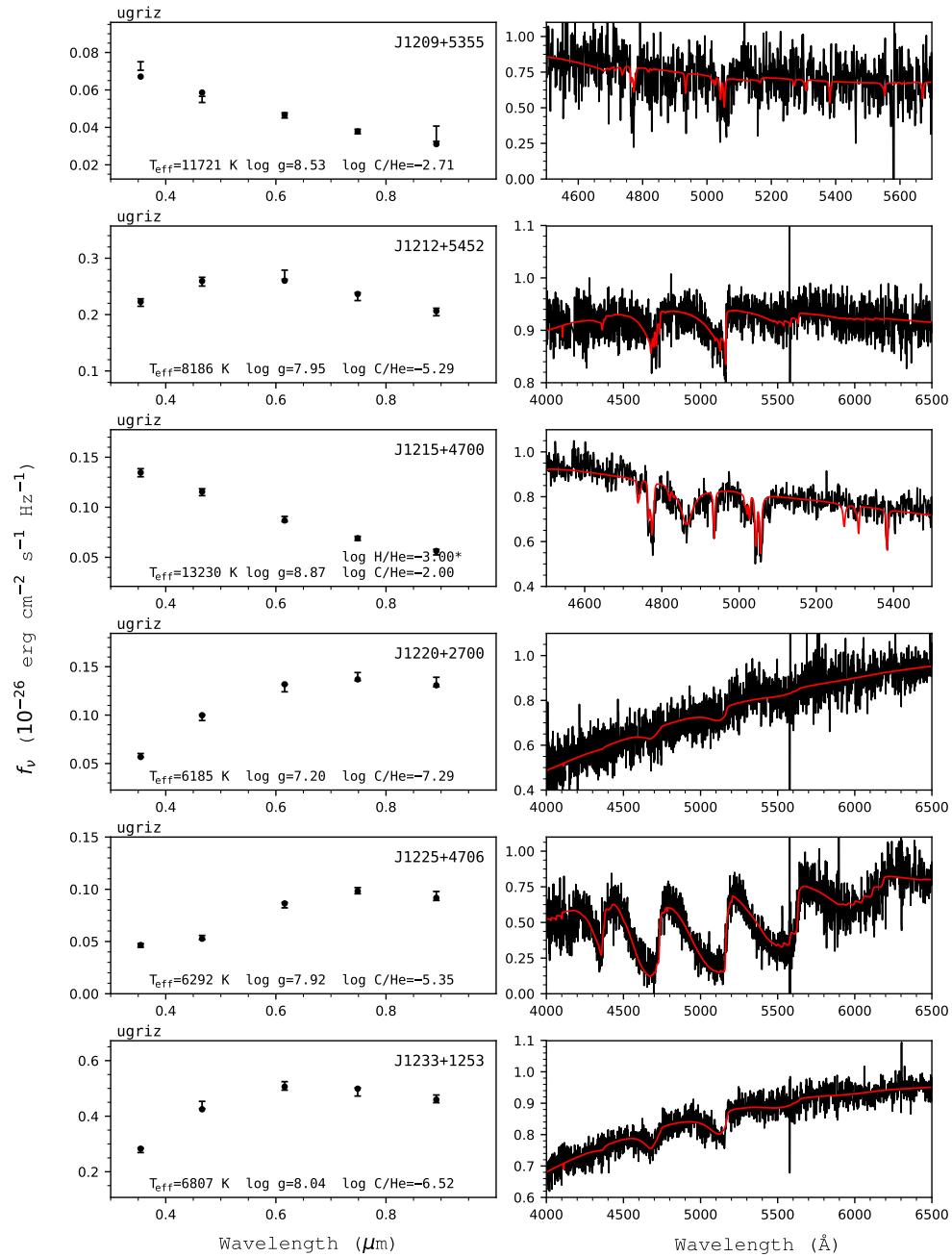


Figure 219. Fits to the DQ white dwarfs - continued.

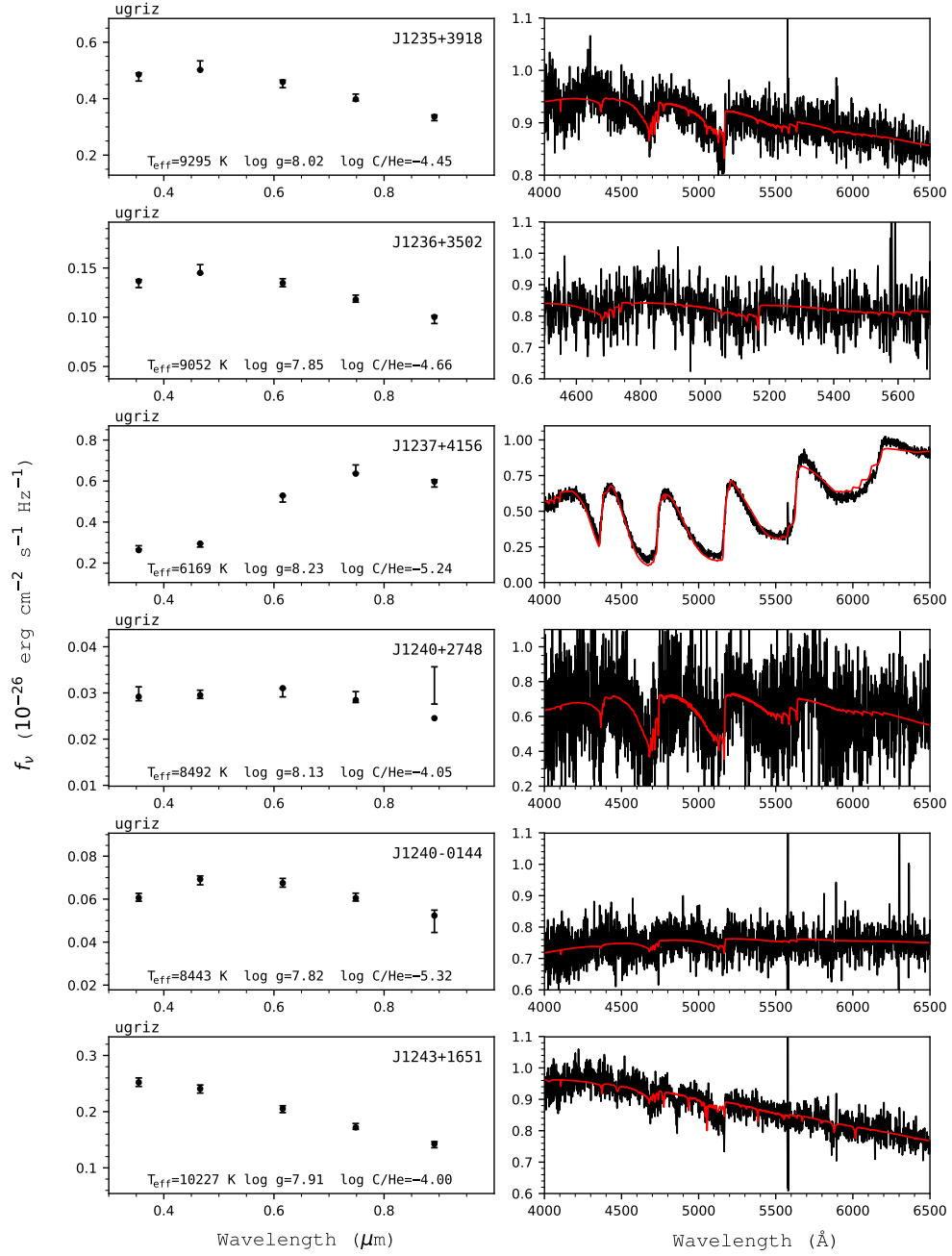


Figure 220. Fits to the DQ white dwarfs - continued.

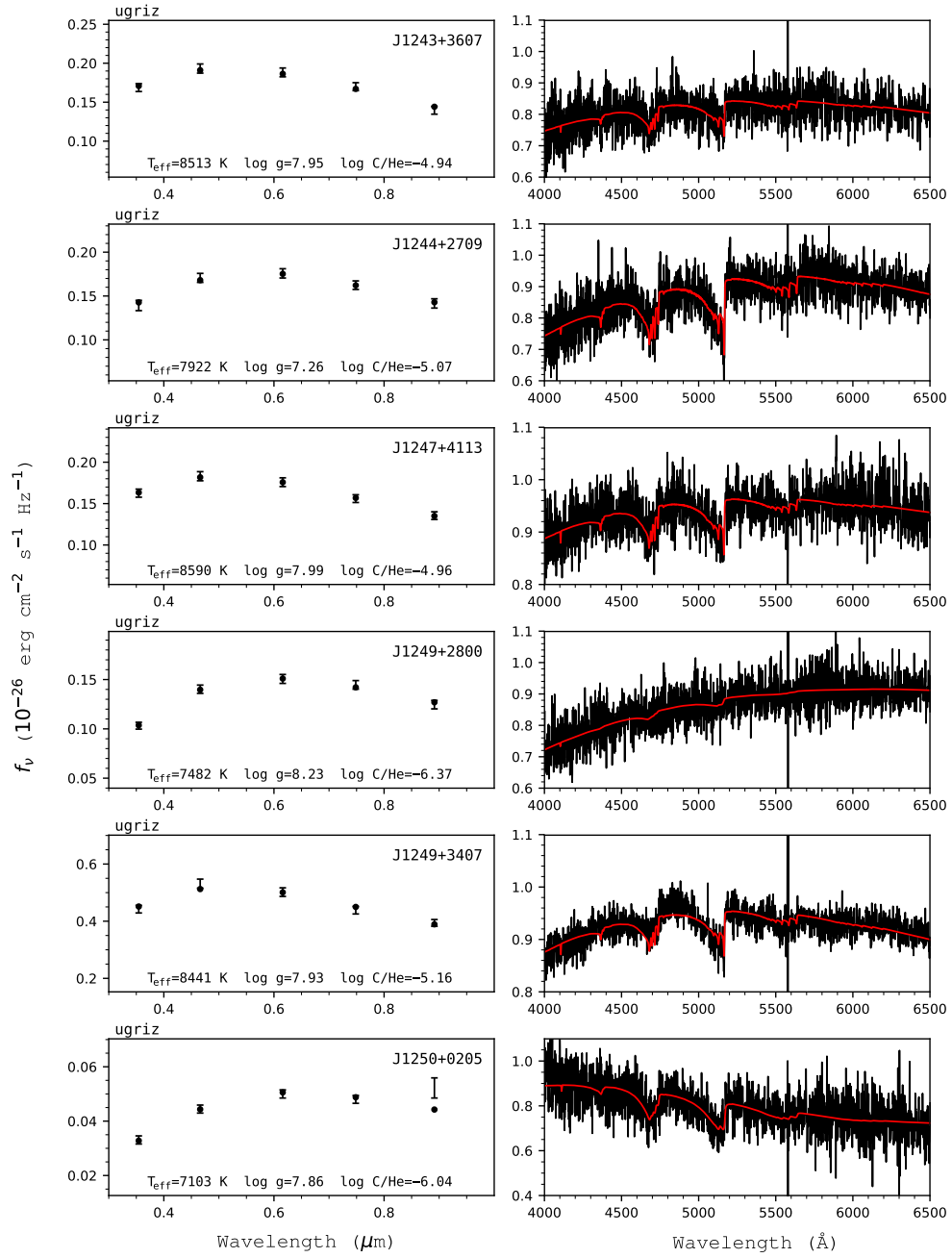


Figure 221. Fits to the DQ white dwarfs - continued.

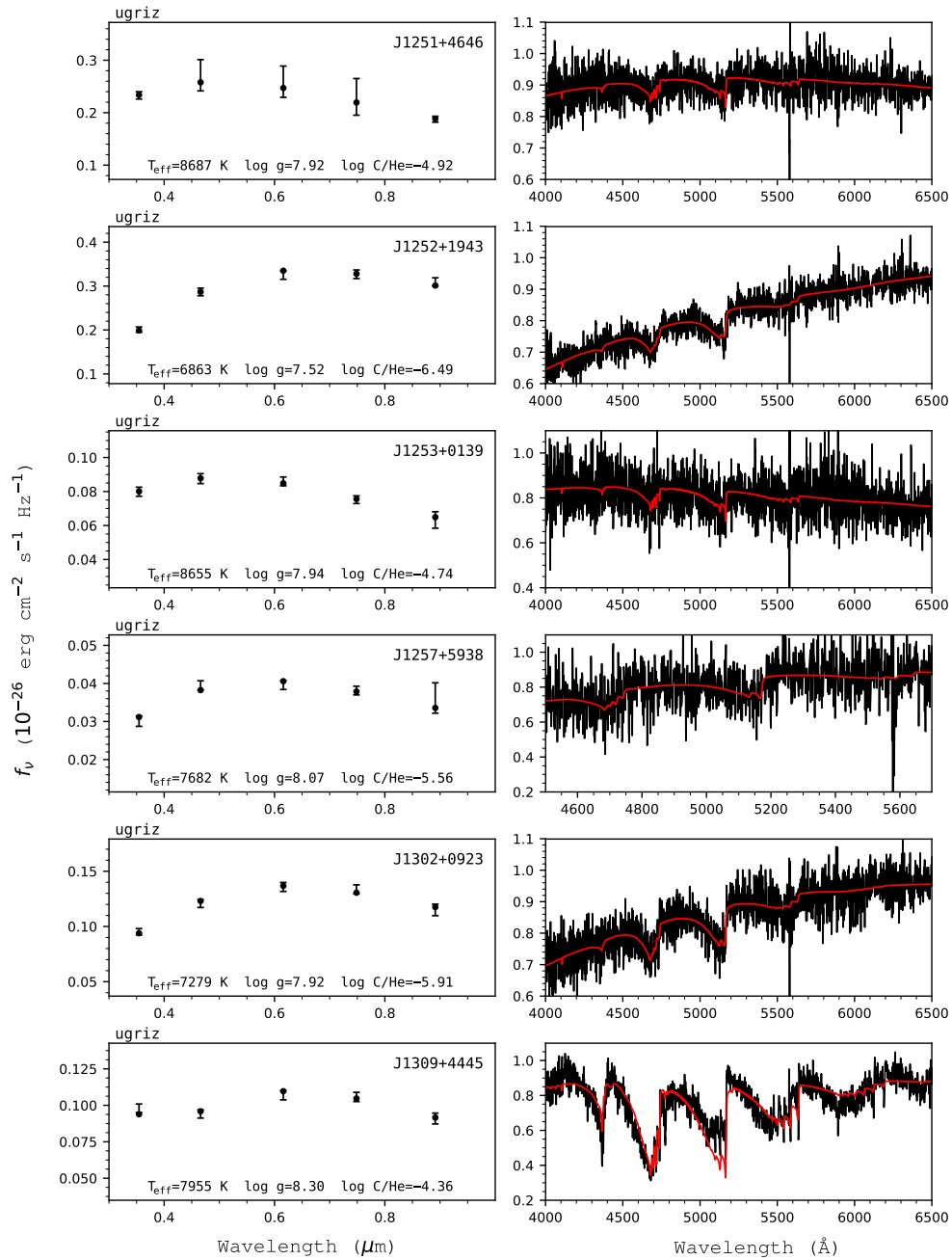


Figure 222. Fits to the DQ white dwarfs - continued.

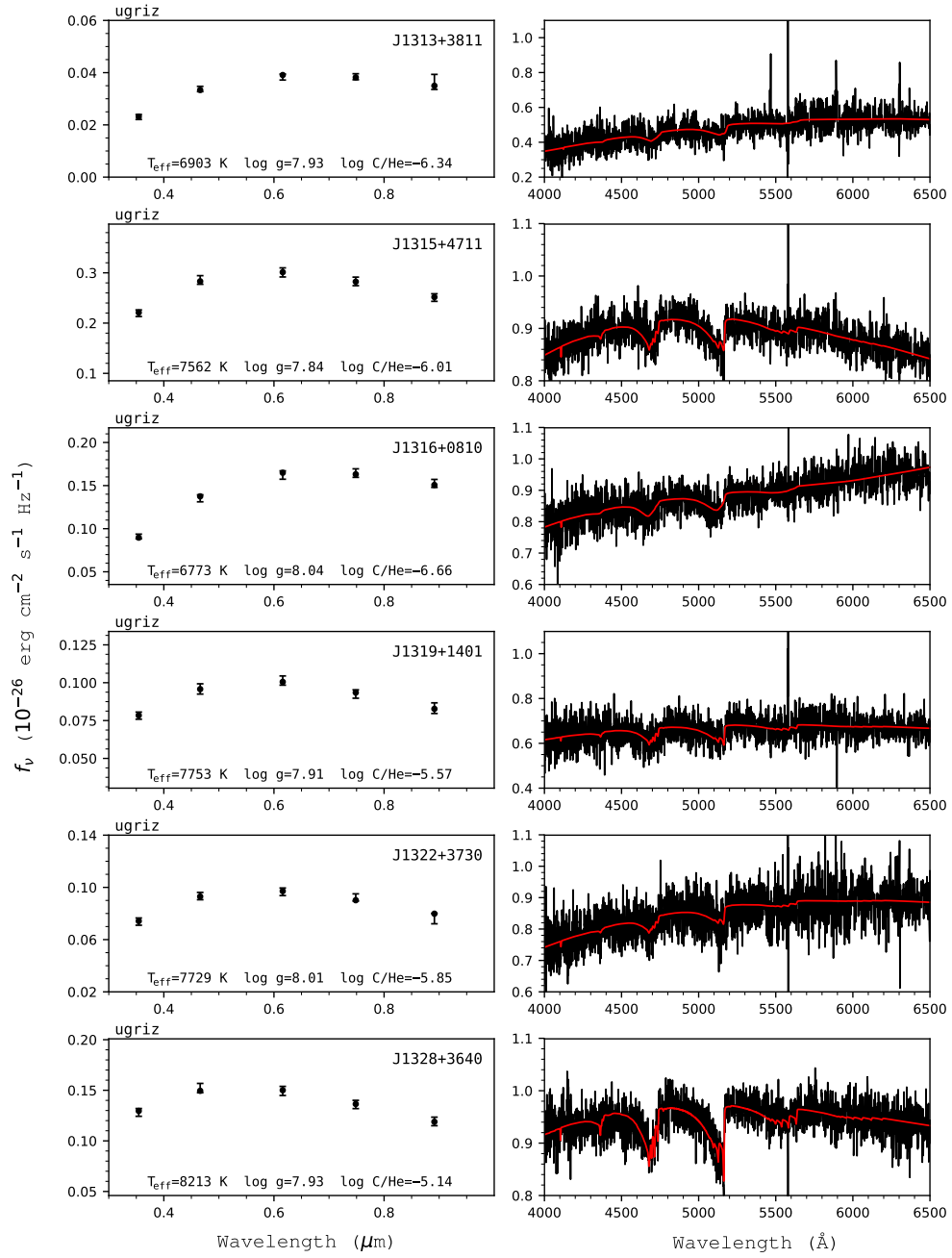


Figure 223. Fits to the DQ white dwarfs - continued.

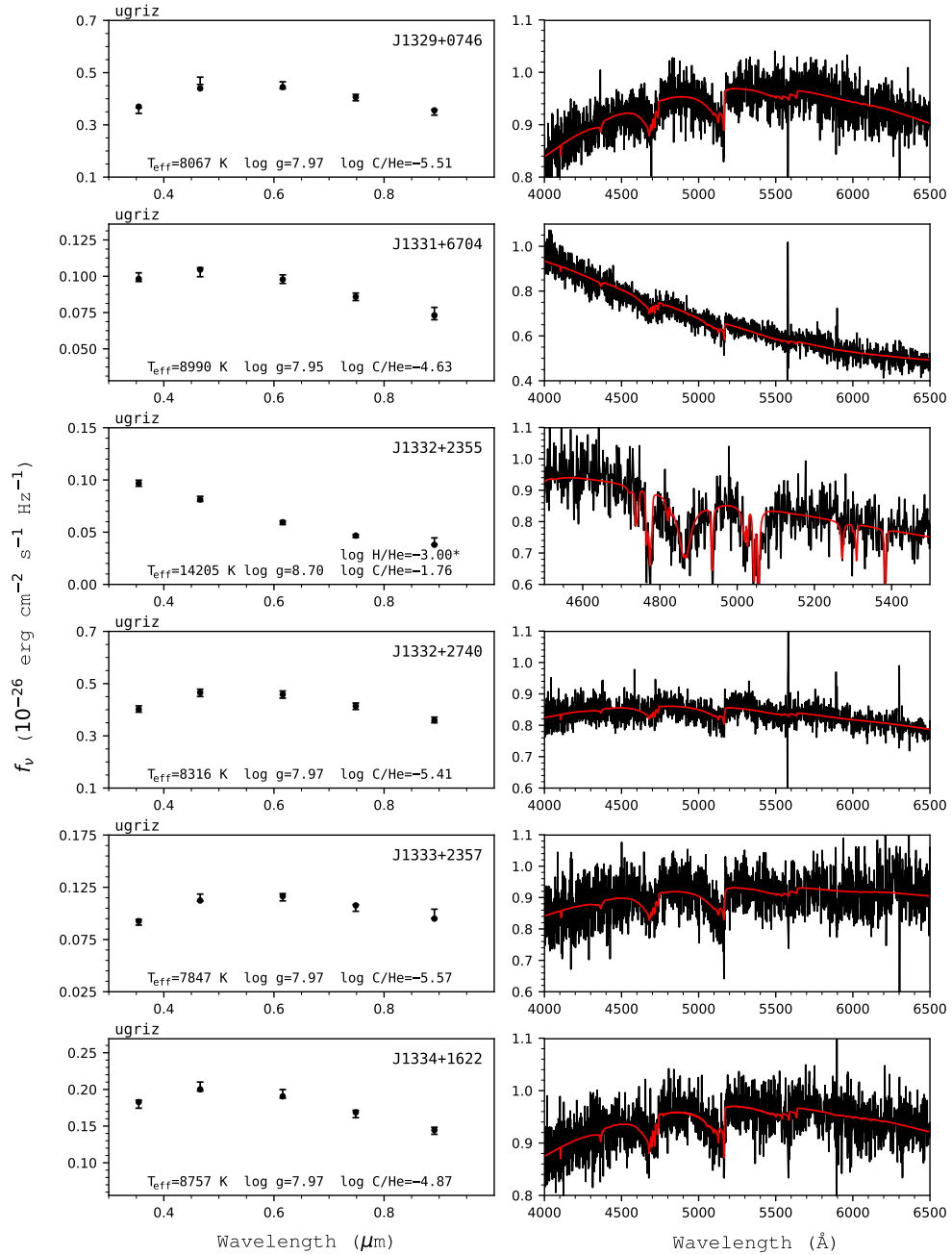


Figure 224. Fits to the DQ white dwarfs - continued.

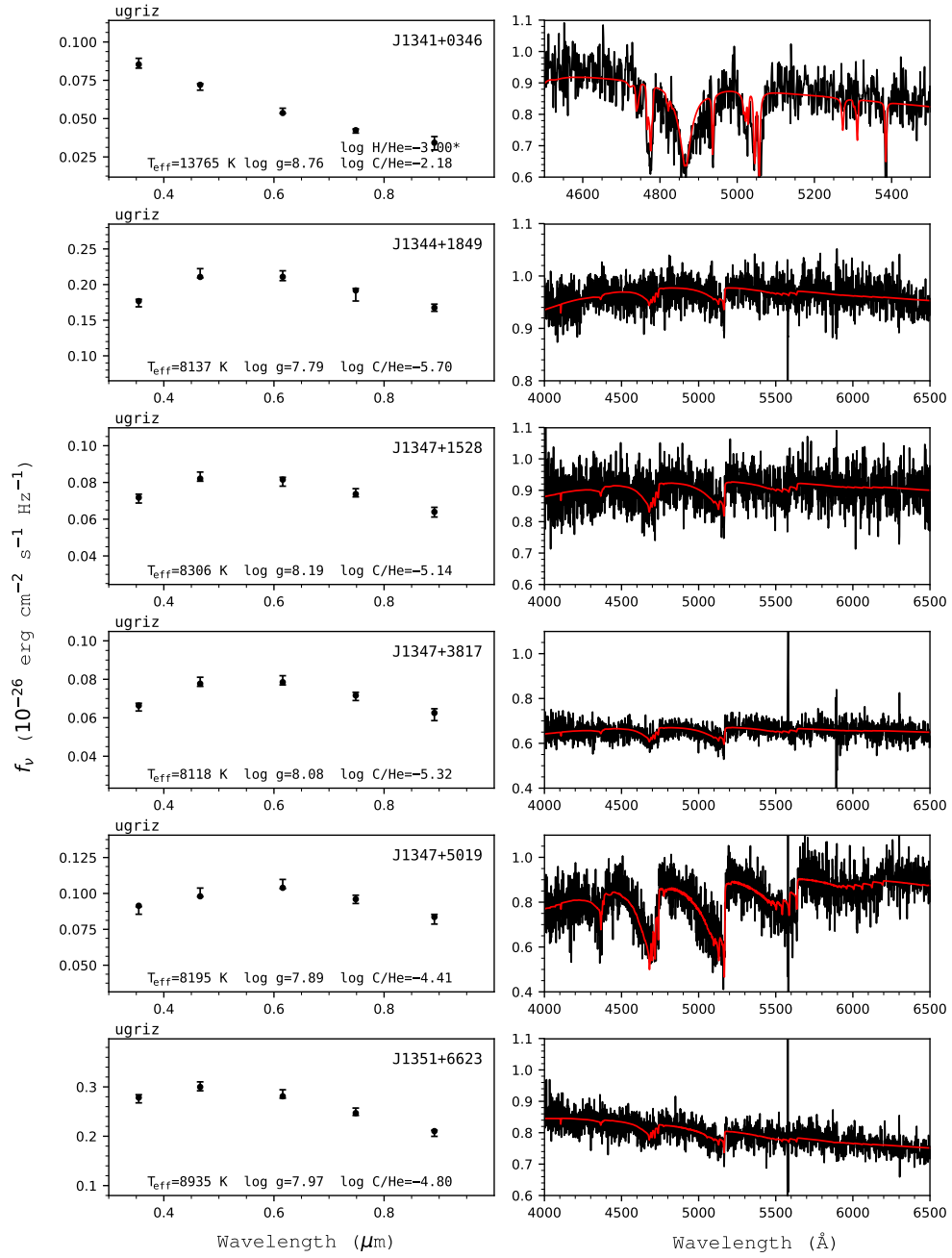


Figure 225. Fits to the DQ white dwarfs - continued.

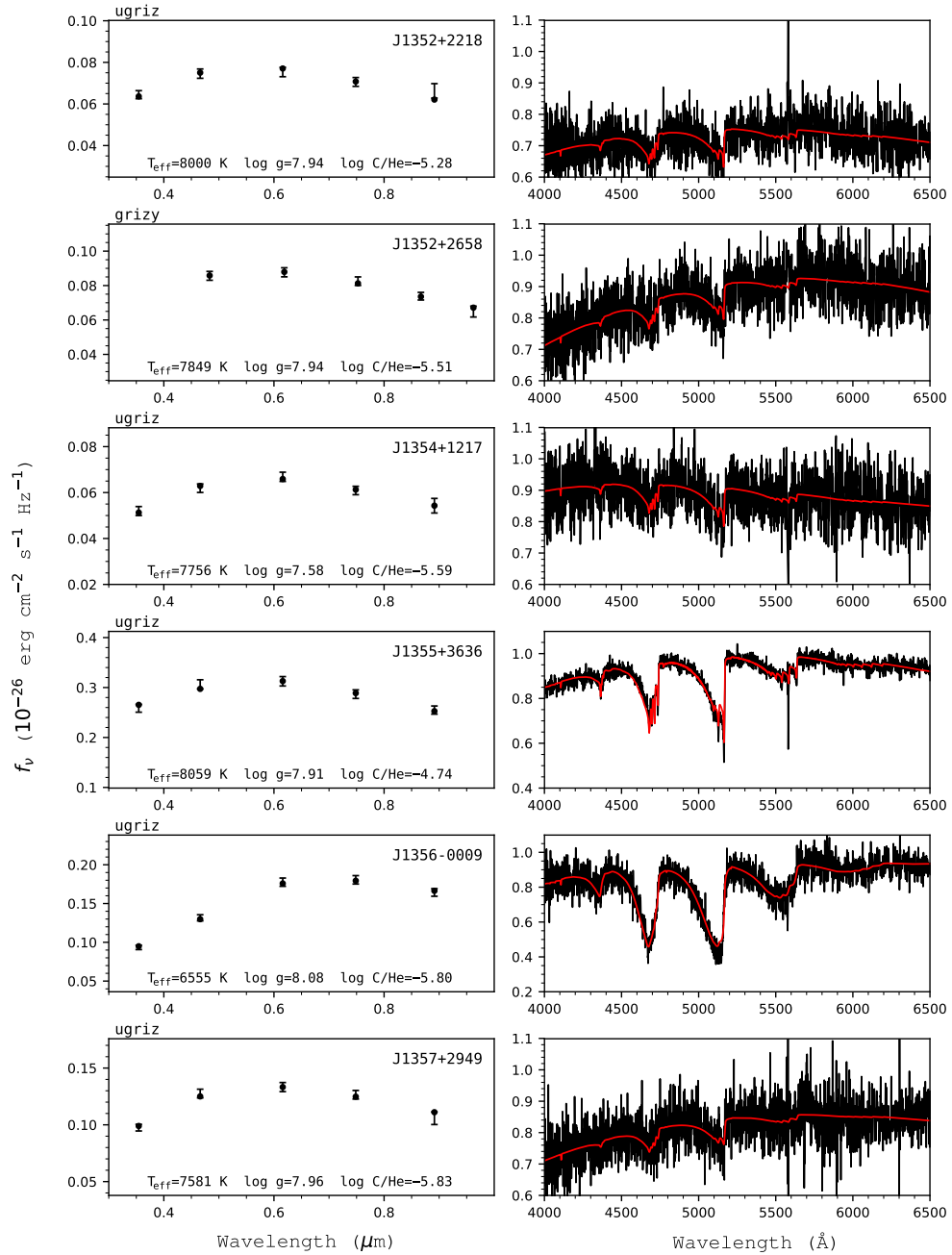


Figure 226. Fits to the DQ white dwarfs - continued.

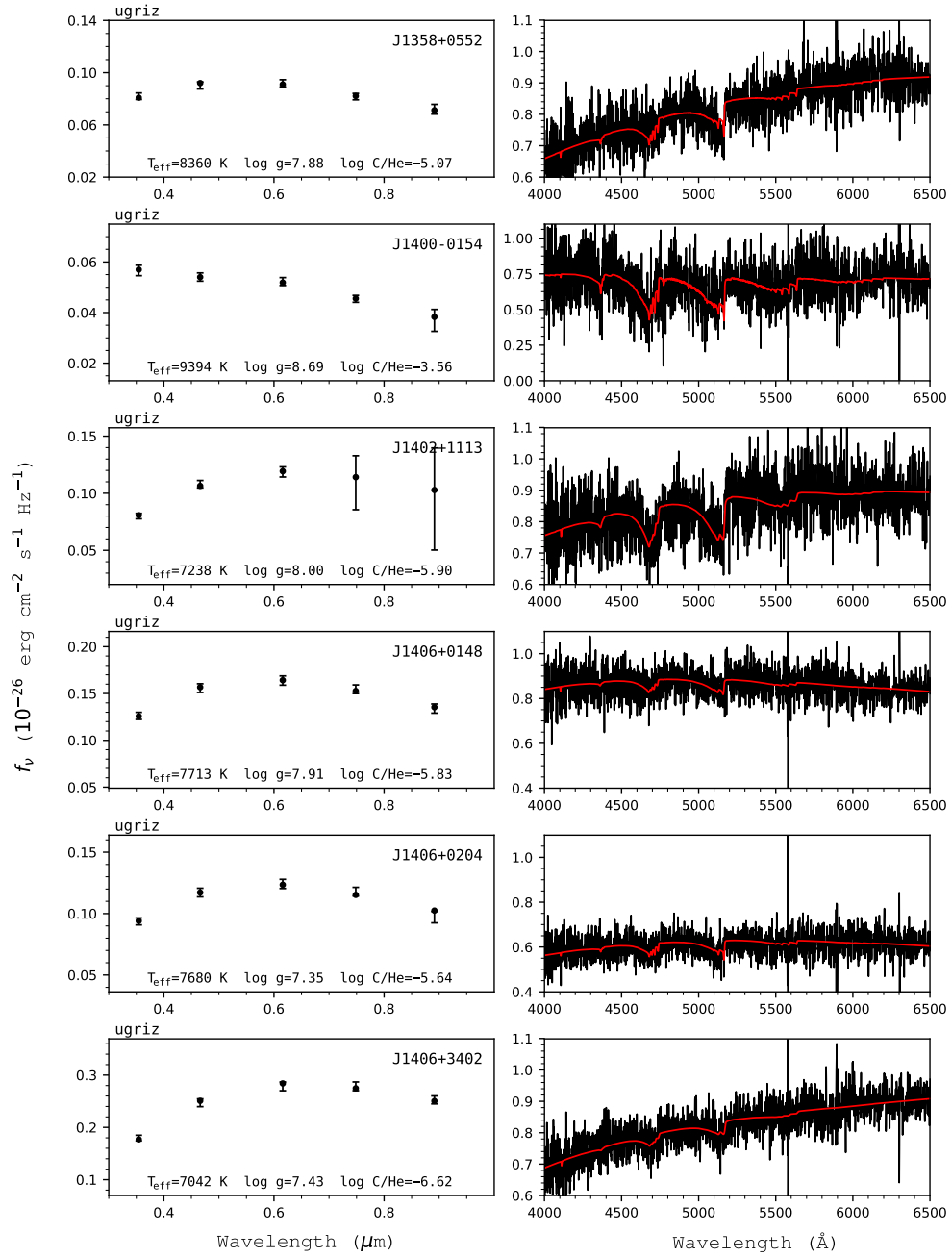


Figure 227. Fits to the DQ white dwarfs - continued.

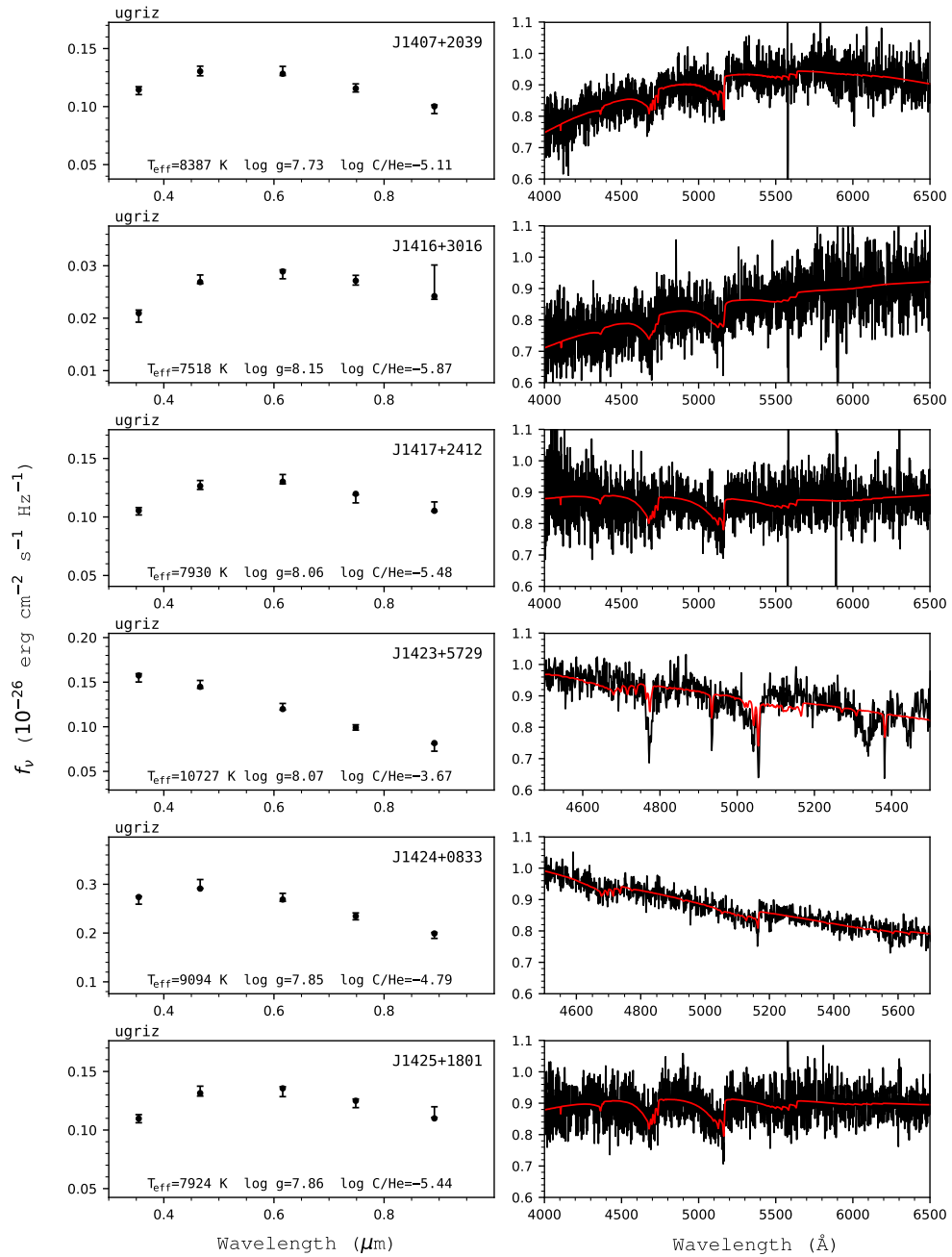


Figure 228. Fits to the DQ white dwarfs - continued.

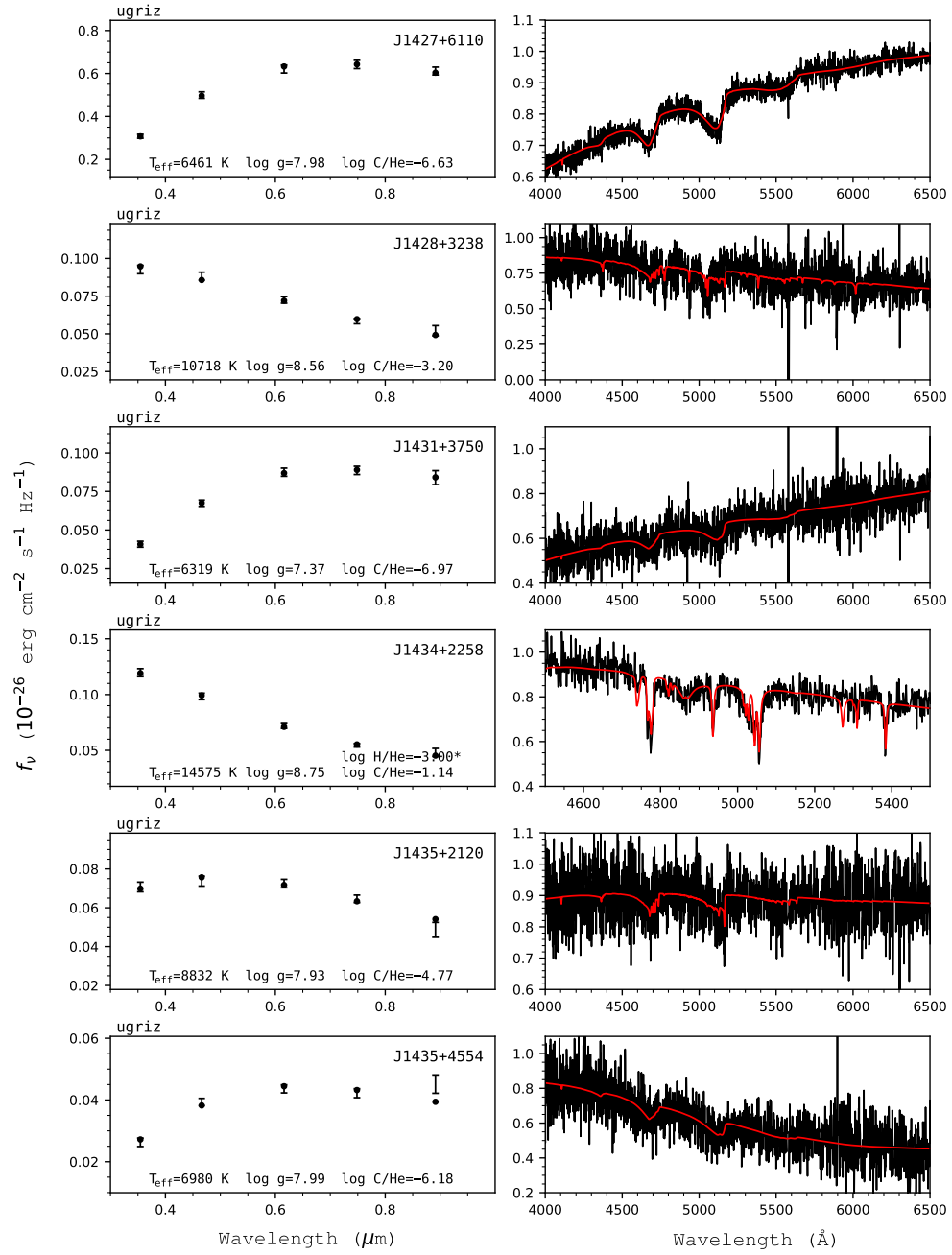


Figure 229. Fits to the DQ white dwarfs - continued.

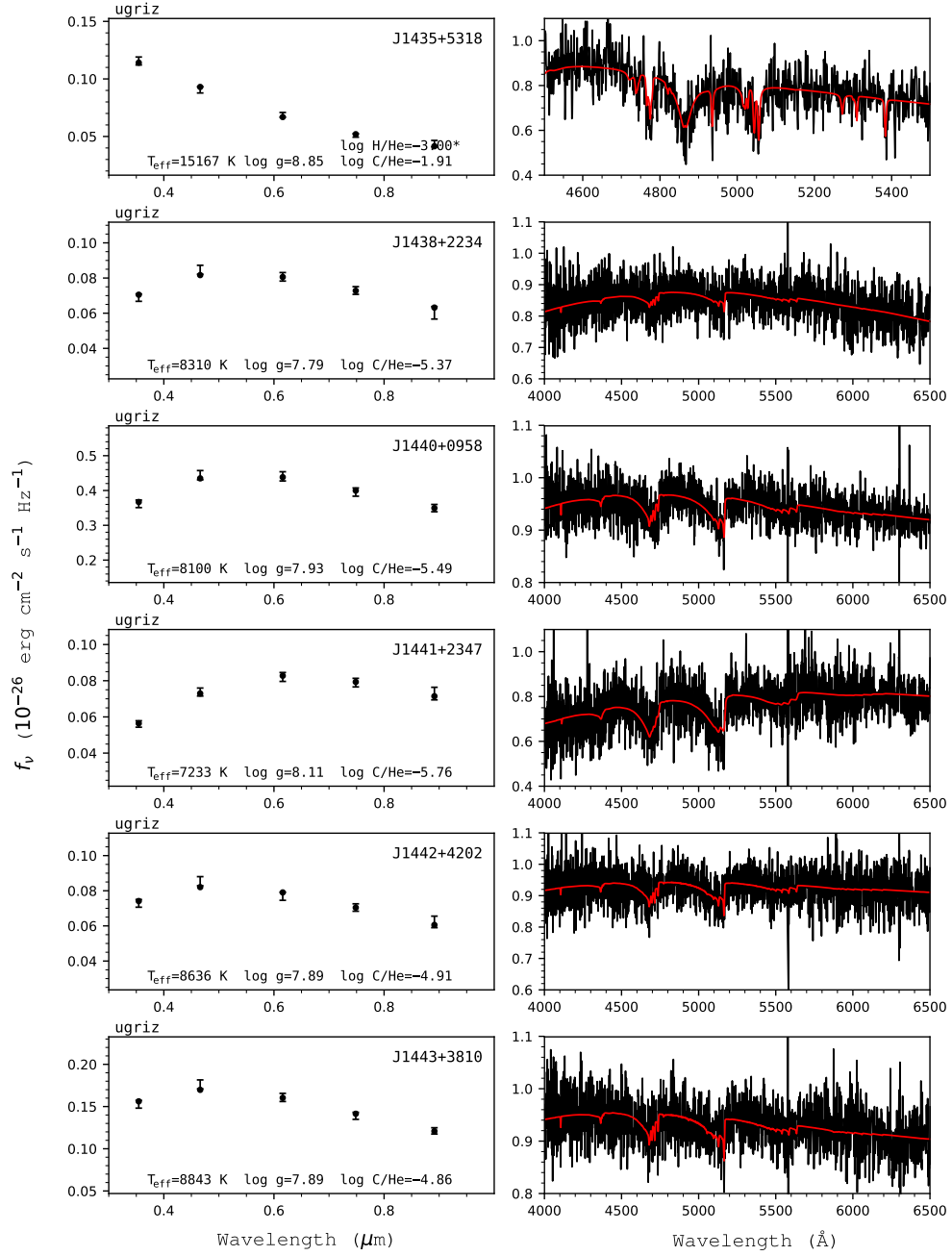


Figure 230. Fits to the DQ white dwarfs - continued.

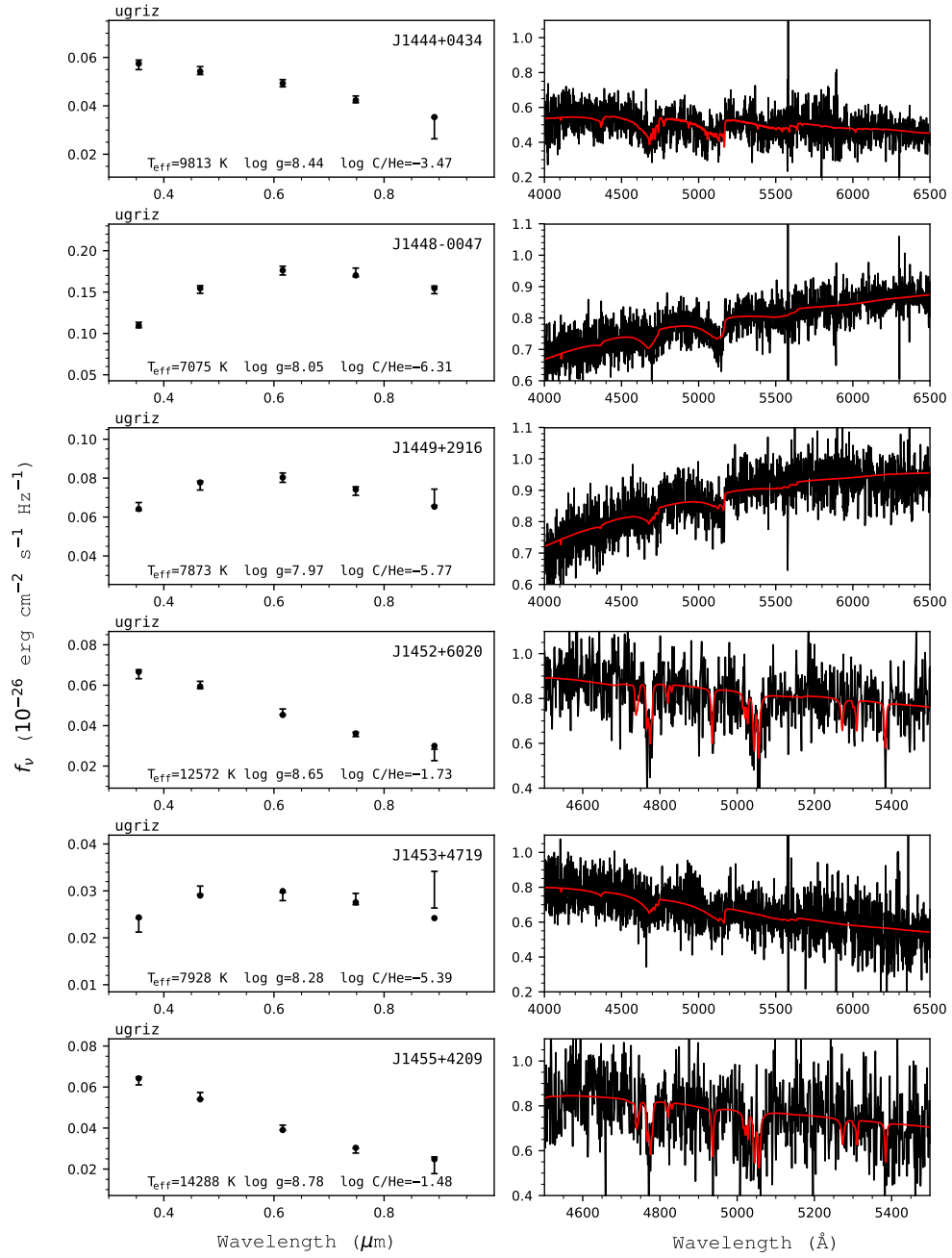


Figure 231. Fits to the DQ white dwarfs - continued.

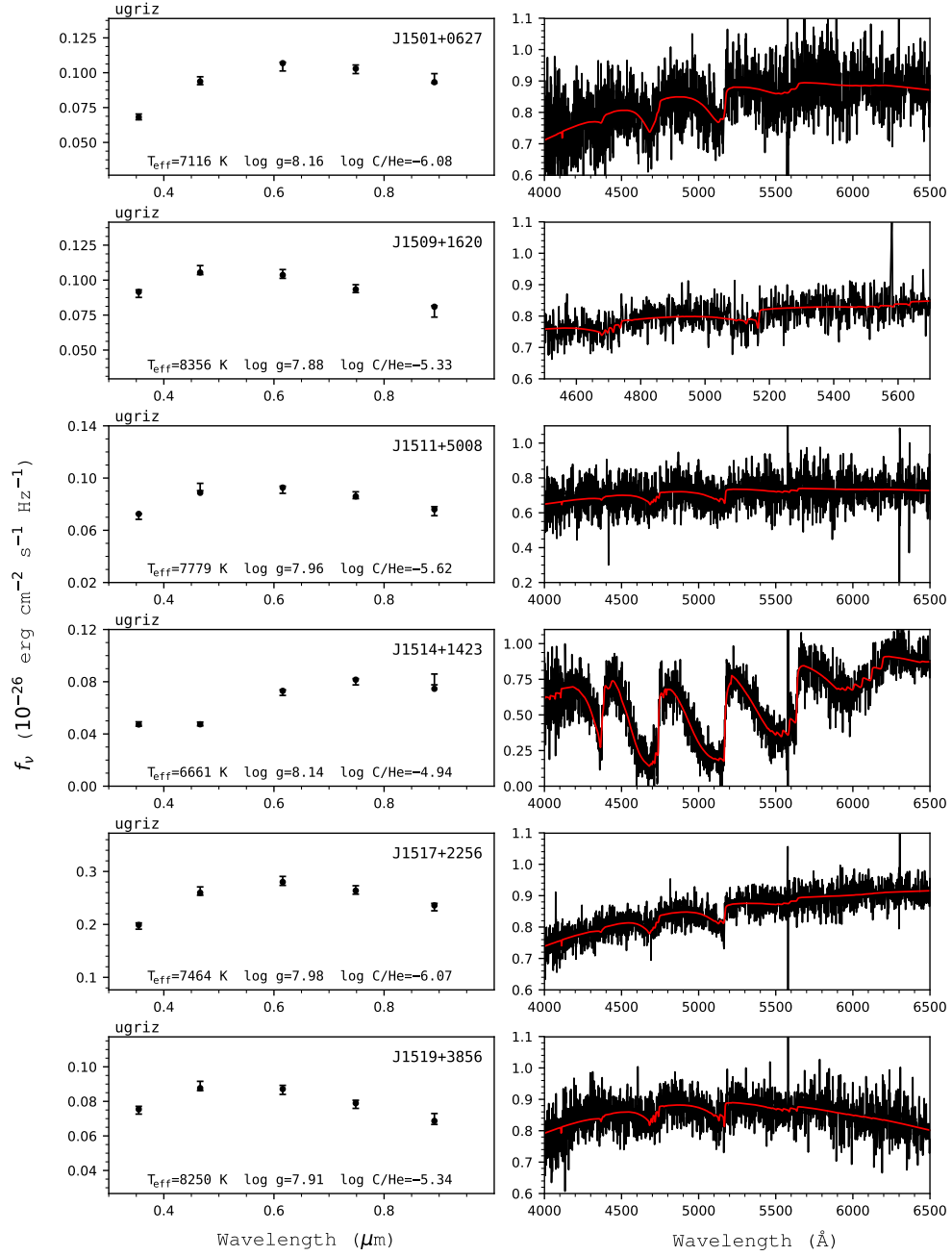


Figure 232. Fits to the DQ white dwarfs - continued.

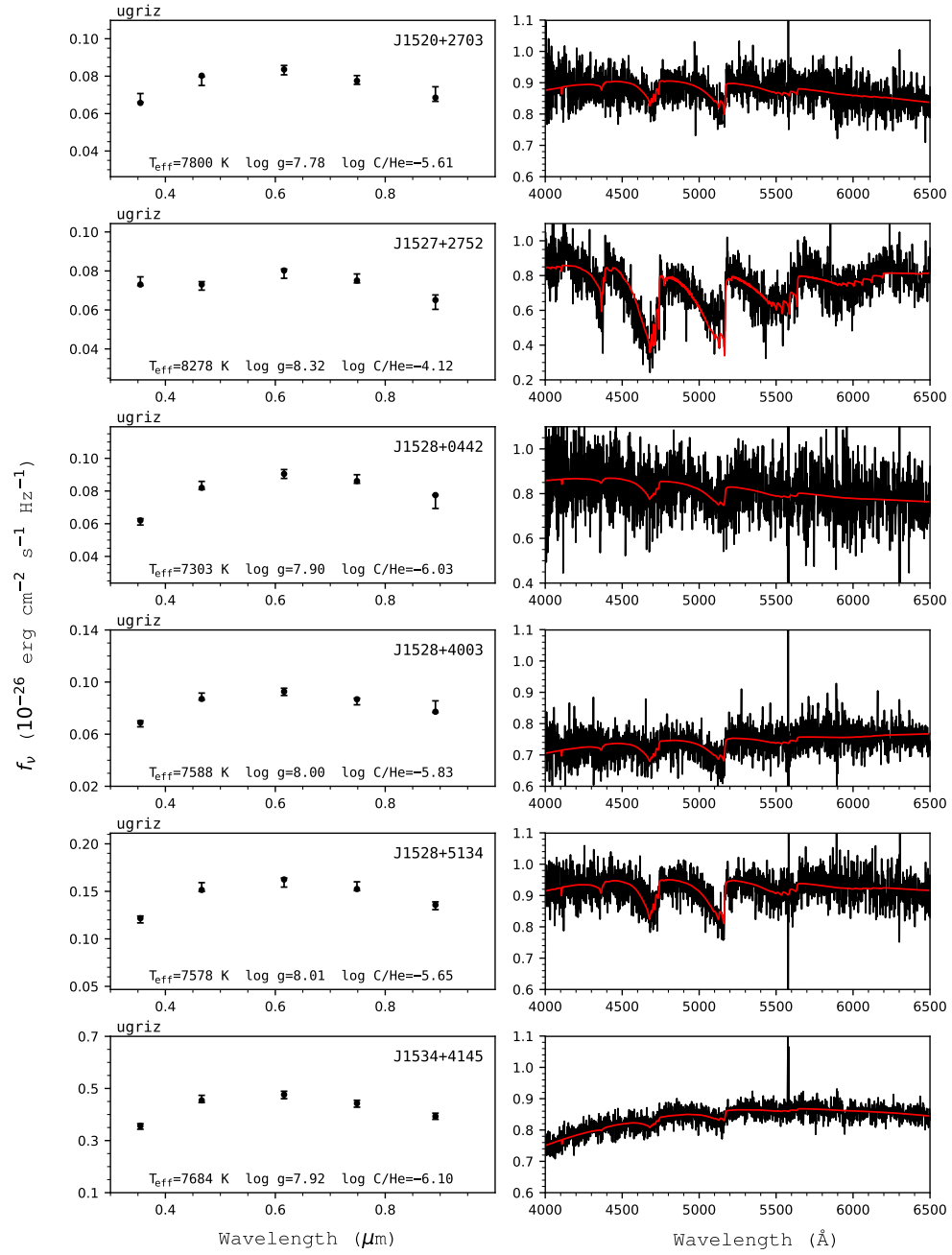


Figure 233. Fits to the DQ white dwarfs - continued.

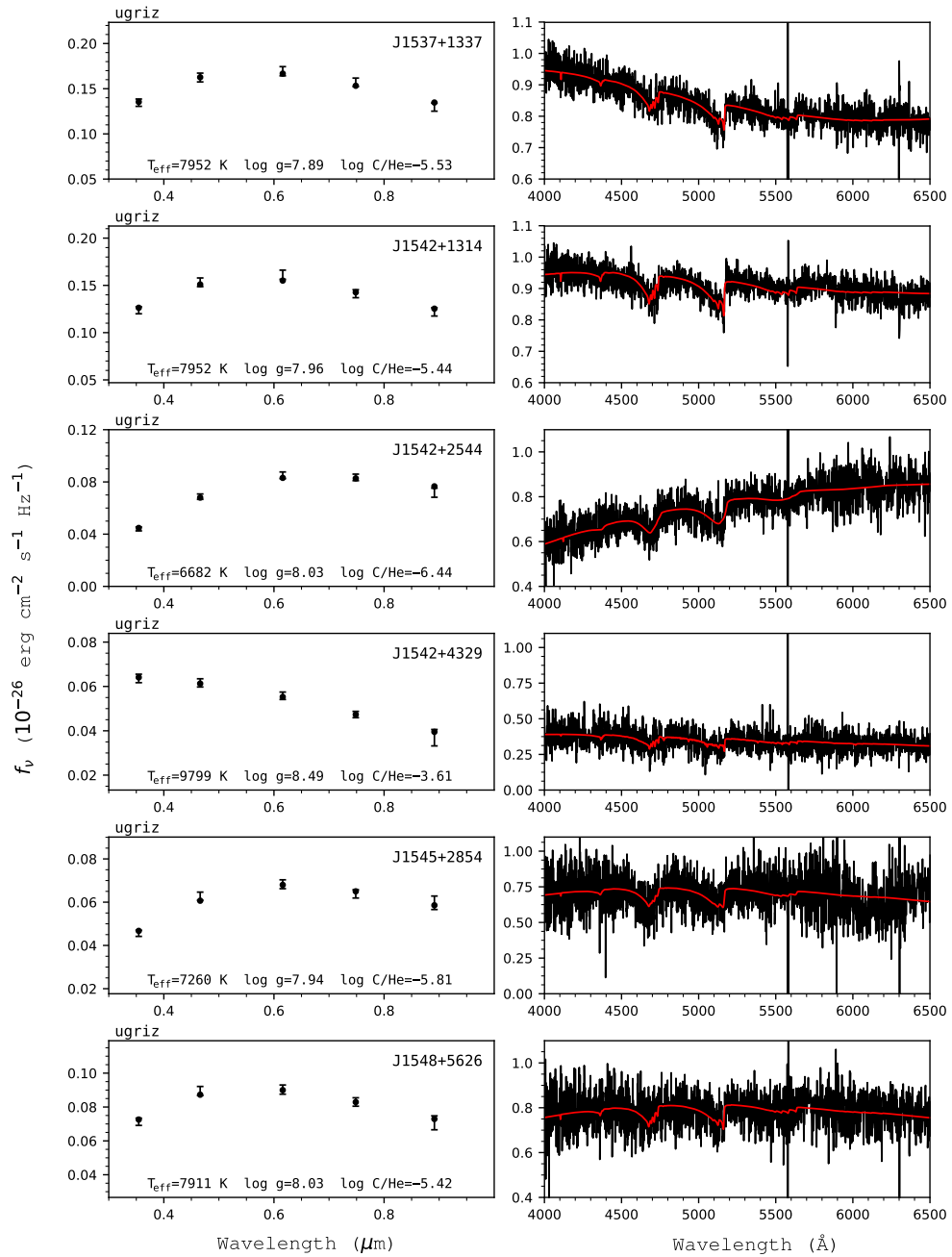


Figure 234. Fits to the DQ white dwarfs - continued.

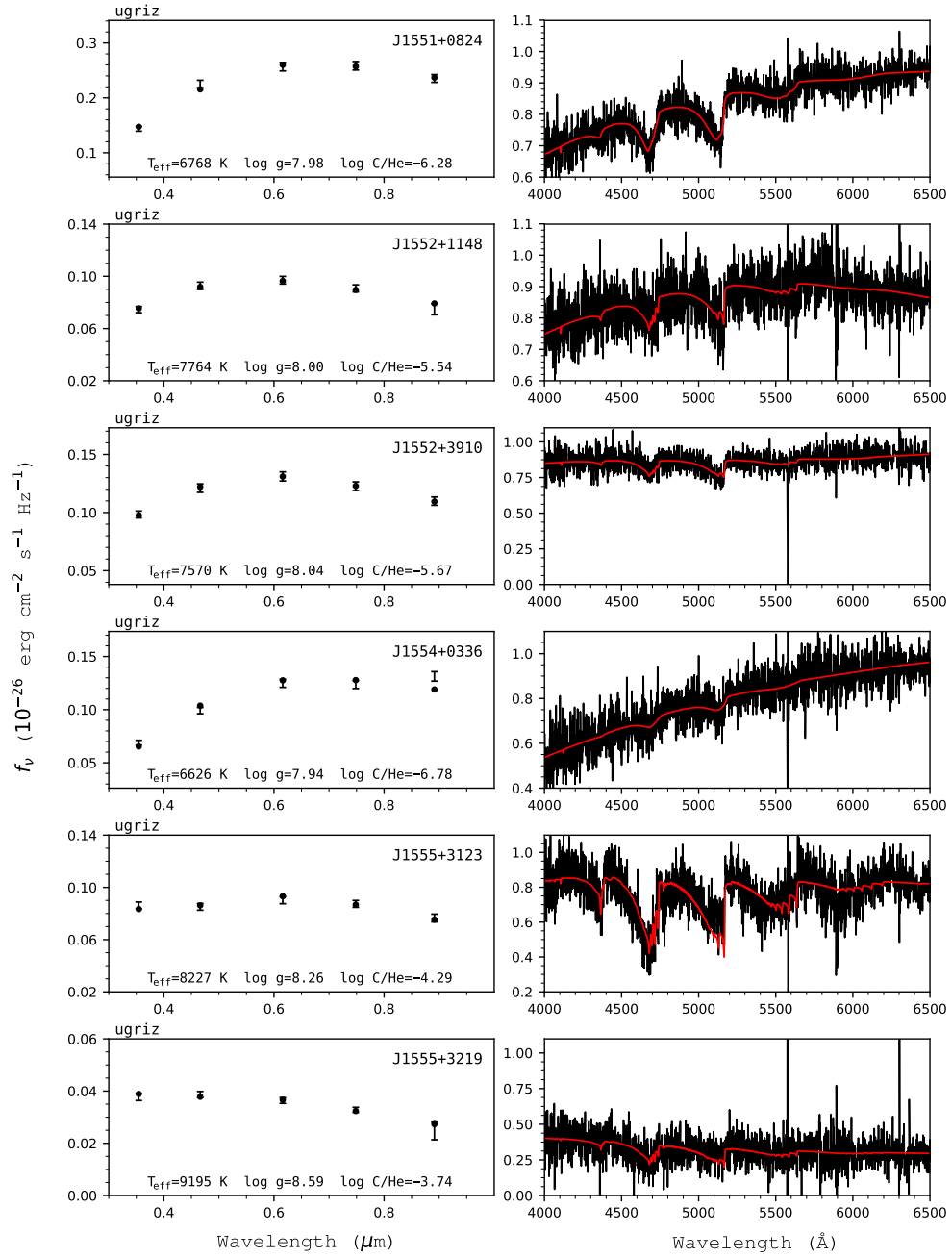


Figure 235. Fits to the DQ white dwarfs - continued.

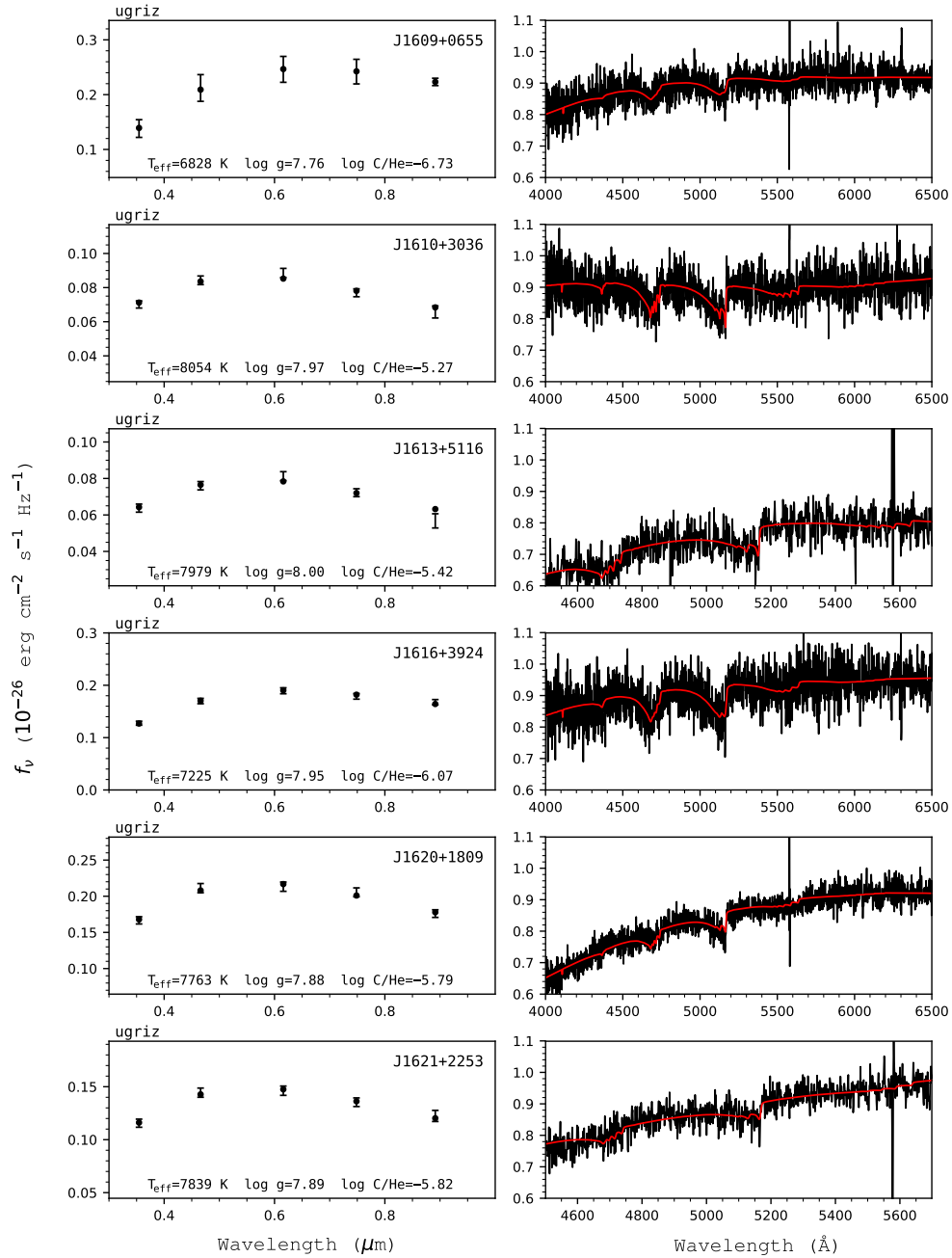


Figure 236. Fits to the DQ white dwarfs - continued.

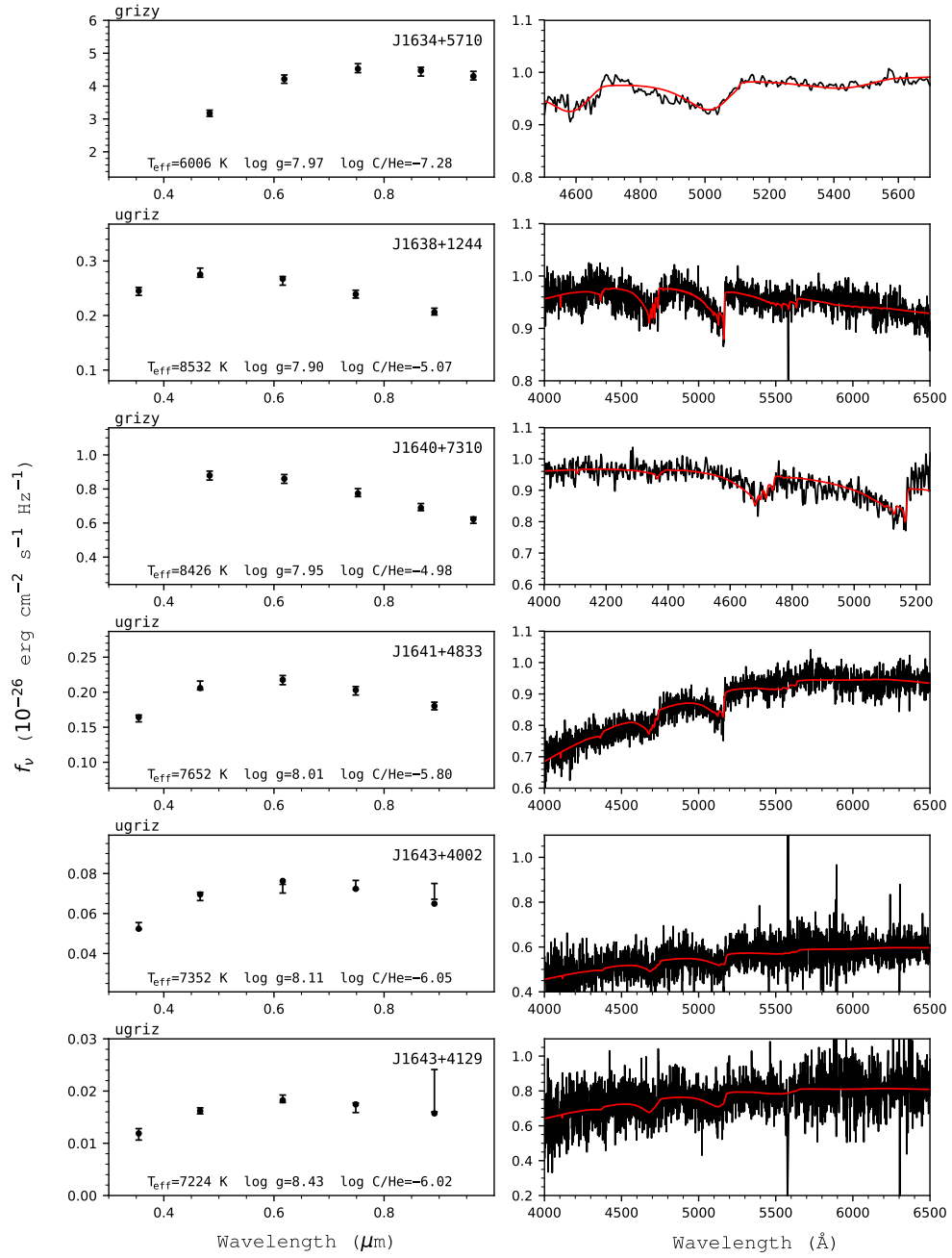


Figure 237. Fits to the DQ white dwarfs - continued.

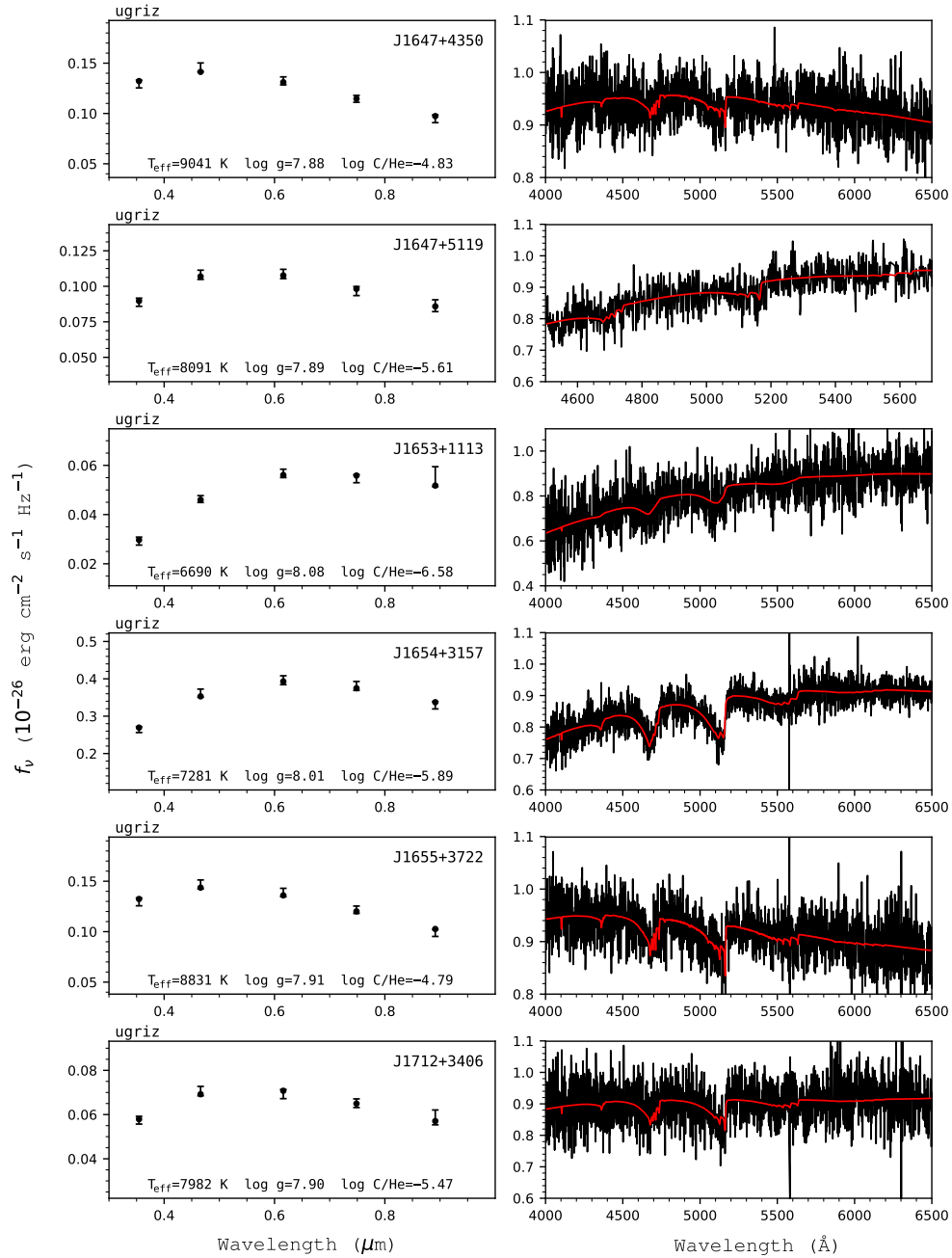


Figure 238. Fits to the DQ white dwarfs - continued.

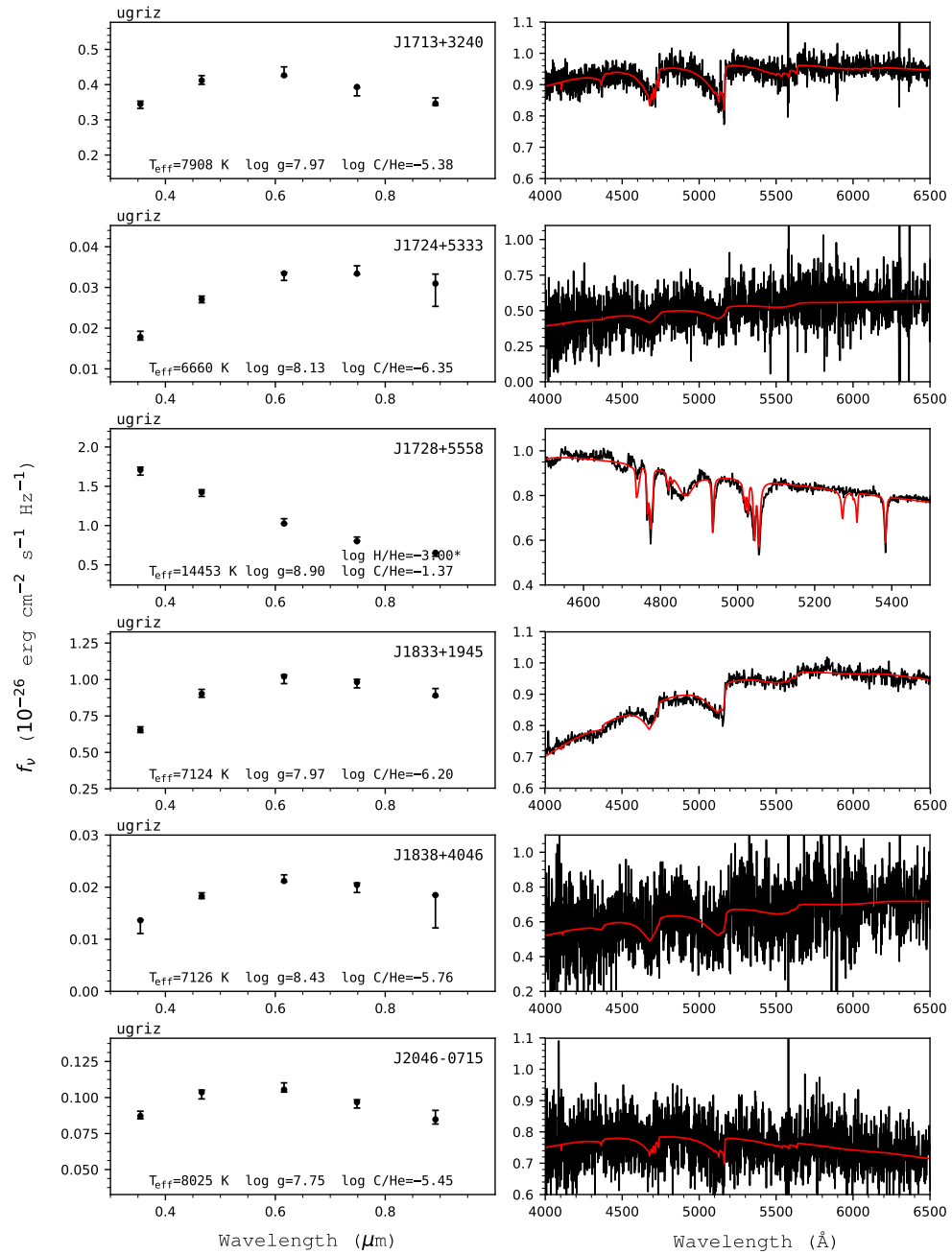


Figure 239. Fits to the DQ white dwarfs - continued.

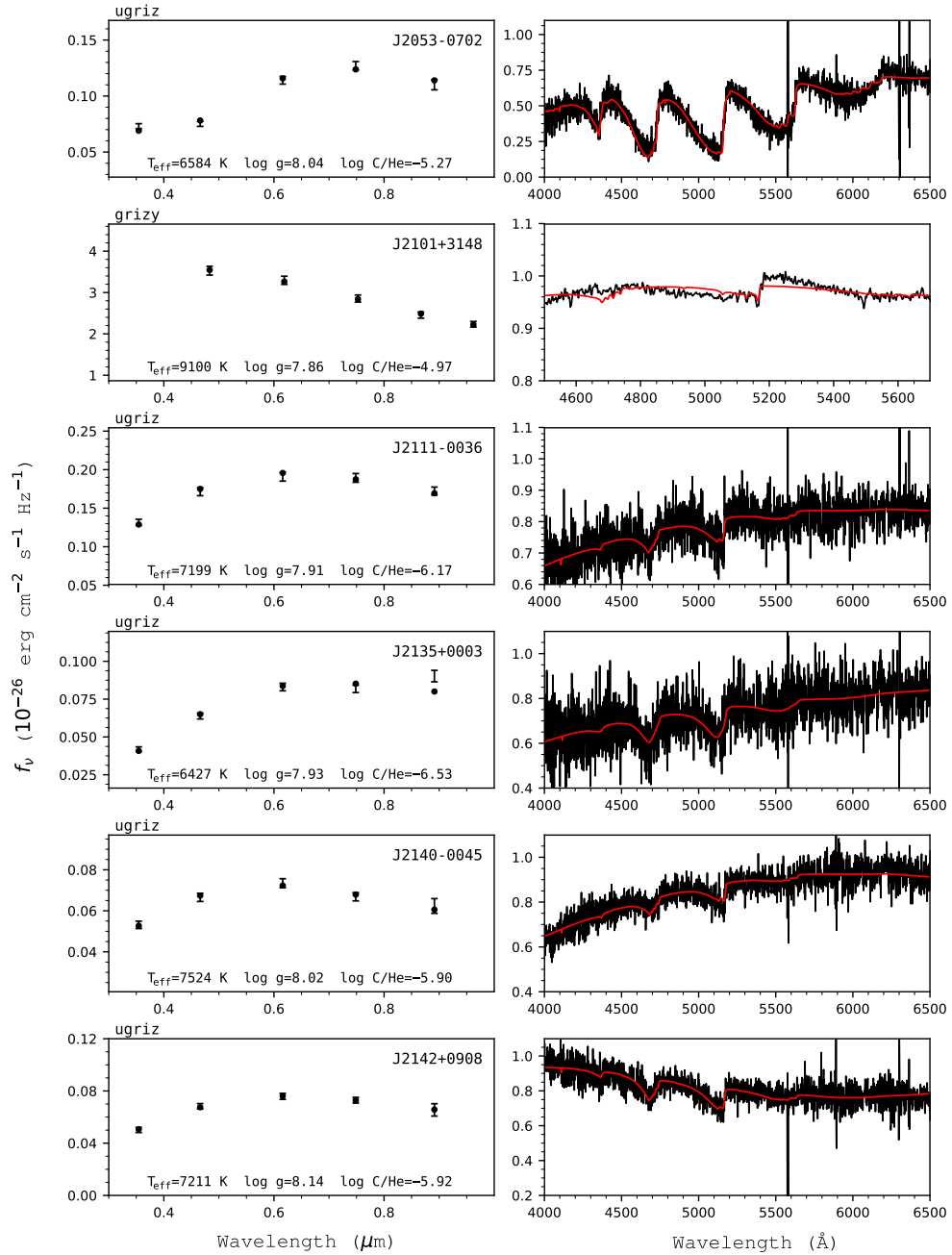


Figure 240. Fits to the DQ white dwarfs - continued.

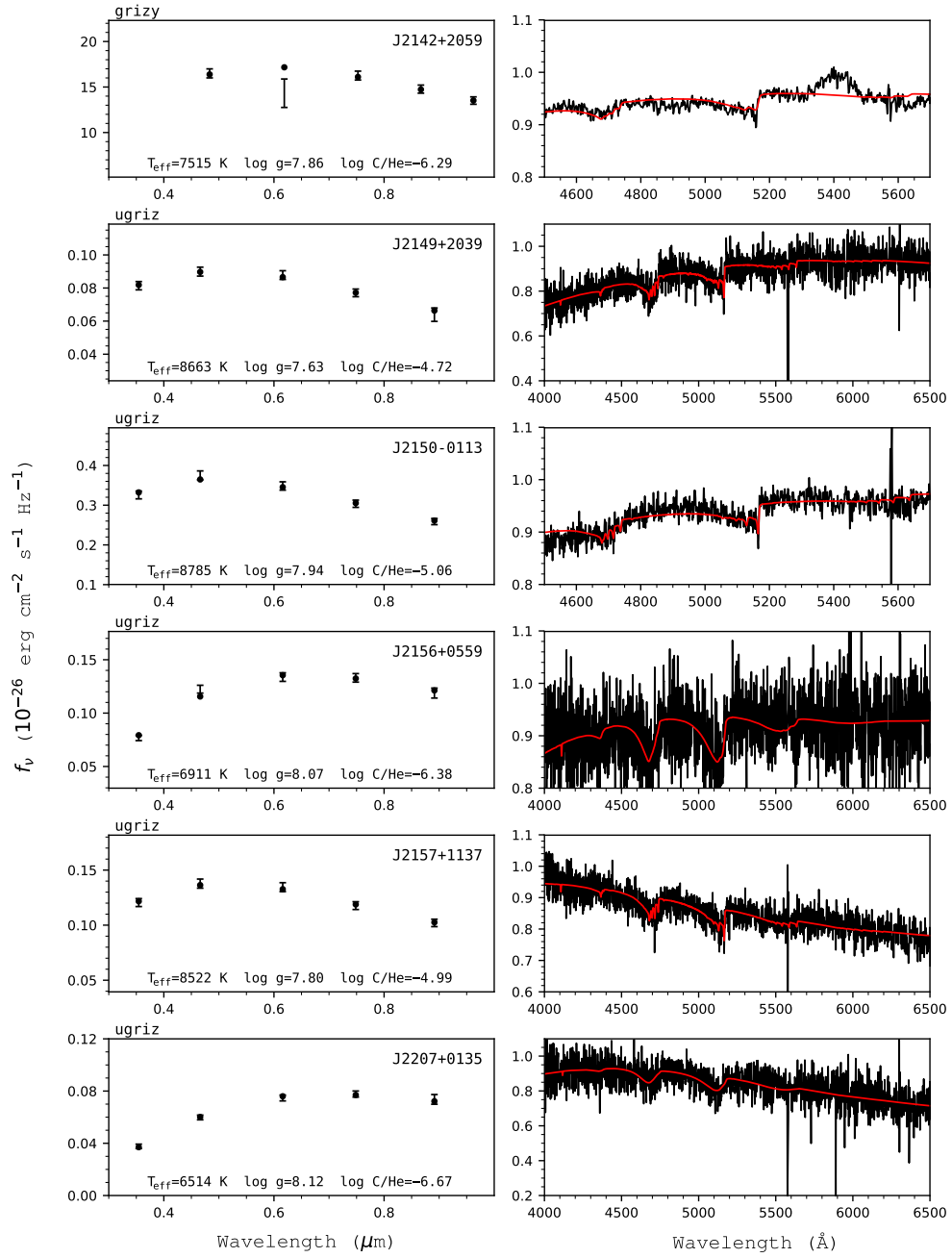


Figure 241. Fits to the DQ white dwarfs - continued.

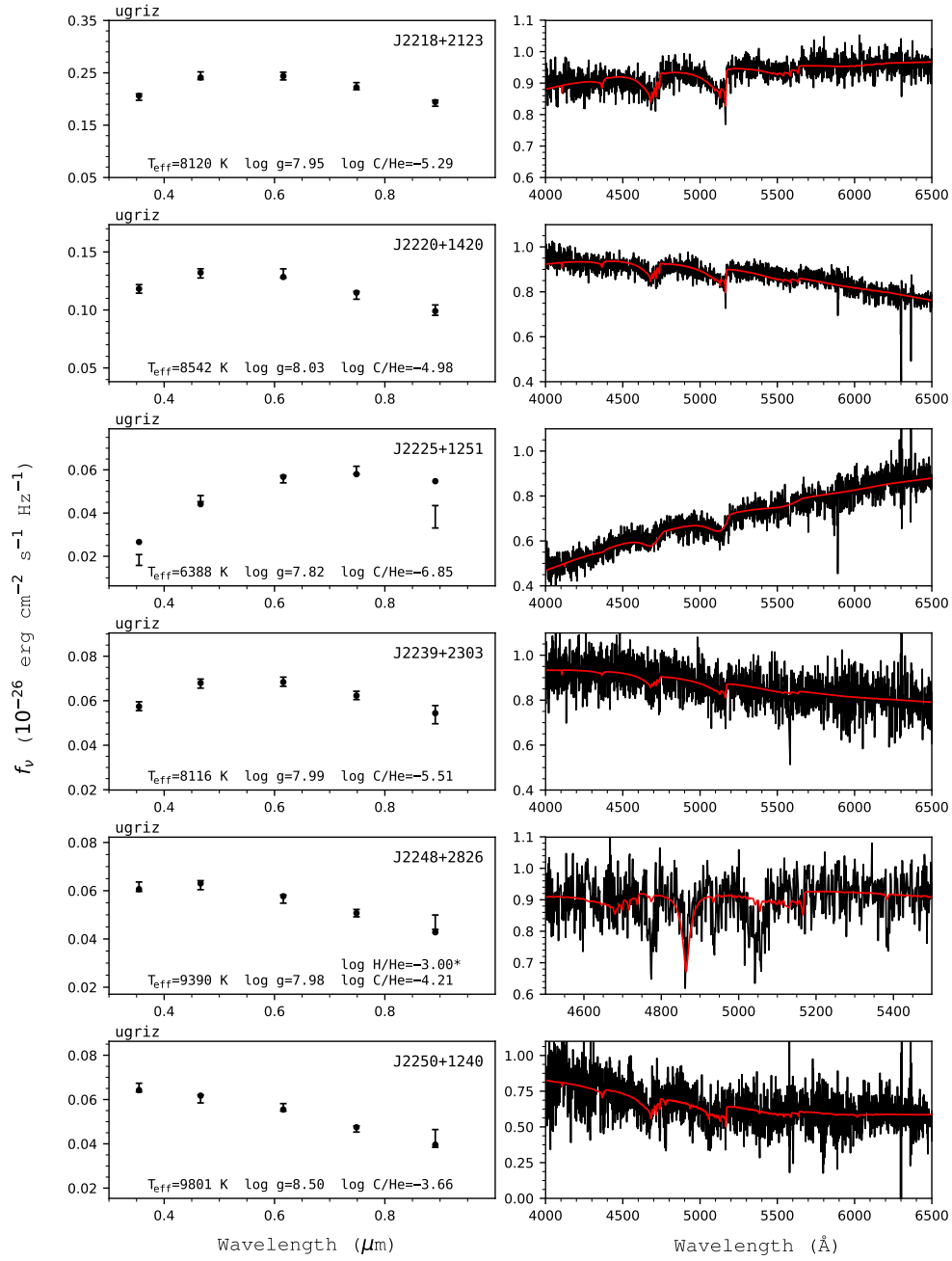


Figure 242. Fits to the DQ white dwarfs - continued.

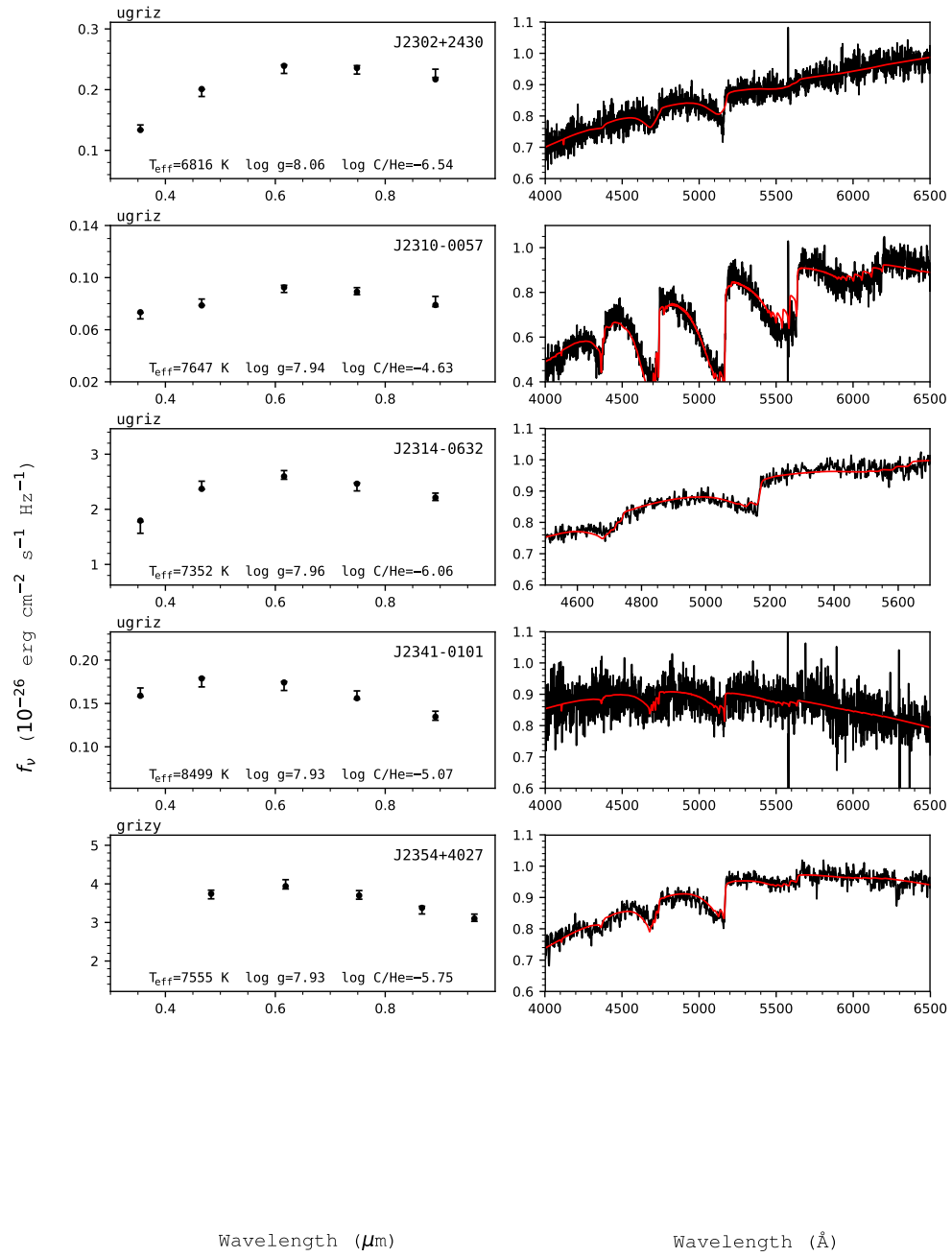


Figure 243. Fits to the DQ white dwarfs - continued.